Studies on host protective response to *Salmonella* infection

The thesis submitted for the Degree of Doctor of Philosophy (Science) in Life Science and Biotechnology, Jadavpur University (2024)

By

SUPARNA CHAKRABORTY

JU Index No: 51/20/Life Sc. /27

Department of Life Science and Biotechnology
Jadavpur University
Kolkata, India

2024

icmr | NICED
INDIAN COUNCIL OF MEDICAL RESEARCH | NATIONAL INSTITUTE OF CHOLERA AND ENTERIC DISEASES

आई. सी. एम. आर. – राष्ट्रीय कॉलरा और आंत्र रोग संस्थान
ICMR - NATIONAL INSTITUTE OF CHOLERA AND ENTERIC DISEASES
स्वास्थ्य अनुसंधान विभाग, स्वास्थ्य और परिवार कल्याण मंत्रालय, भारत सरकार
Department of Health Research, Ministry of Health and Family Welfare, Govt. of India

WHO COLLABORATING CENTRE FOR RESEARCH AND TRAINING ON DIARRHOEAL DISEASES

CERTIFICATE FROM THE SUPERVISOR

This is to certify that the thesis entitled "**Studies on host protective response to *Salmonella* infection**" Submitted by **Smt. Suparna Chakraborty** who got her name registered on **04.11.2020** for the award of **Ph. D. (Science) Degree** of **Jadavpur University**, is absolutely based upon her own work under the supervision of **Dr. Santasabuj Das** and that neither this thesis nor any part of it has been submitted for either any degree / diploma or any other academic award anywhere before.

Santasabuj Das

23.07.2024

सान्तासबुज दास, एस. डि.
SANTASABUJ DAS, M.D.
वैज्ञानिक (एफ) / Scientist (F)
आइ.सि.एम.आर. - राष्ट्रीय कॉलरा और आंत्र रोग संस्थान
ICMR National Institute of Cholera & Enteric Diseases
पी-३३,सी.आइ.टी. रोड, स्किम-१०एम, बेलियाघाटा, कोल-१०
P-33, C.I.T. Road, Scheme-XM, Beliaghata, Kol-10
E-mail : santasabujdas@yahoo.com

(Signature of the Supervisor, Date, with Official seal)

DECLARATION

I do, hereby declare that the work embodied in the thesis entitled '**Studies on host protective response to *Salmonella* infection**' submitted for the award of Doctoral of Philosophy (Science) in Life Science and Biotechnology, is the completion of work carried put under the supervision of **Dr. Santasabuj Das, Scientist F** at the division of Clinical Medicine, ICMR-National Institute of Cholera and Enteric Diseases, Kolkata. Neither this thesis nor any part of it has been submitted for either any equivalent degree/diploma or any other academic award elsewhere.

Date- 23.07.24

Place- Kolkata

Suparna Chakraborty
.....

(Signature of the candidate)

SUPARNA CHAKRABORTY

I Dedicate this thesis to
Maa, Baba and Snehanjan.

Without their endless love, patience, understanding, mental support and encouragement, this venture would never have been possible.

Acknowledgement

I would like to express a deep sense of gratitude, and humbly acknowledge all those people, who have contributed in meaningful ways to the organized completion and execution of this thesis work. It has indeed been a wonderful journey.

First and foremost, I would like to convey my heartfelt gratitude to **Dr. Santasabuj Das, my Supervisor,** for providing me with the opportunity to work in the Clinical Medicine laboratory, as a part of his research group. His relentless enthusiasm, support and guidance have been my source of motivation. I have learnt to logically question the study findings, and troubleshoot my experimental problems. His insightful ideas have helped me to analyze my data efficiently, thoroughly and have made it possible to achieve my goals. His unflinching encouragement, farsightedness, relevant advice and wisdom were instrumental in creating a proactive environment in the laboratory. This has in turn provoked my independent and scientific thought process; to positively contribute towards the overall direction of my research work and enrich my growth as a researcher.

I want to express my sincere thanks to **'Innovation in Science Pursuit for Inspired Research (INSPIRE)'** program by the Department of Science and Technology (**DST-INSPIRE**); for providing me with the financial platform in the form of Junior and Senior Research Fellowship, which helped my financial stability during my doctoral studies.

I am immensely grateful to **Dr. Shanta Dutta**, **Director, ICMR-National Institute of Cholera and Enteric Diseases (ICMR NICED),** for permitting me to work in this institute, equipped with state-of-the-art research facilities, for carrying out experimental research works during my doctoral studies.

I gratefully acknowledge **Dr. Ashish Mukhopadhyay,** from ICMR NICED, for his valuable comments, mentoring and encouragement throughout my research advisory committee meetings.

I am thankful to **Dr. Hemanta Koley** from ICMR NICED, for his enlightenment on animal experiments and **Dr. Nabendu Sekhar Chatterjee** from ICMR NICED for his advices in protein purification techniques.

I would like to thank **Dr. Moumita Bhowmick,** from ICMR NICED, for providing me with her valuable time to clear my confusions regarding immunology work, and **Dr Amlanjyoti Dhar** from International Institute of Innovation and Technology (I3TK), for counselling me on the FPLC techniques and sequence analyses.

I would like to acknowledge the Department of Biotechnology, Government of India and Japan Initiative for Global Research Network on Infectious Diseases (**J-GRID**), from Ministry of Education, Culture, Sport, Science & Technology in Japan, and Japan Agency for Medical Research and Development (**AMED**), for funding my research work. I specially thank **Dr. Julian Parkhill** of Wellcome Trust Sanger Institute and **Dr. Rupak Kumar Bhadra**, CSIR-IICB for providing our lab with bacterial strains, which I utilized in my study.

I am incredibly grateful to Science and Engineering Research Board (**SERB**) and **Indian Immunology foundation,** for providing me with the international travel support covering my registration fee, travel and visa charges to attend the Gordon Research Seminar and Conference on Salmonella Biology and Pathogenesis 2023, in Lucca Barga, Italy. I am forever grateful to **Bill and Melinda Gates Foundation** alongside with the **Sabin Vaccine Institute** for bearing the entire travel expenses, for attending the 13th International conference, on Coalition against Typhoid and other invasive salmonellosis, in Kigali, Rwanda to elucidate my research work.

All my **lab members-** Dr. Pujarini Dutta, Dr. Asim Biswas, Dr. Sayan Das, Dr. Bhupesh Kumar Thakur, Dr. Atri Ta, Dr. Rimi Chowdhury, Dr. Debayan Ganguli, Dr. Sneha Mitra, Dr. Shreya Dasgupta, Mrs. Swarnali Chakraborty, Ms. Risha Haldar, Mr. Sudip Dey, Dr. Jaya Verma, Dr. Lena Dhara, Mr. Udipto Sarkar, Mr. Khokan Roy, Mr. Animesh Gope, Ms Sagarika Mali; have played a significant role in the successful completion of my doctoral study. It is a pleasure to pay tribute to **Mr Ananda Pal,** Technical officer for his constant support and cooperation in the experimental work. I would also like to mention and thank, Dr. Ranjan Barman, Dr. Rahul Subhra Mandal, Dr. Sreeja Shaw, Dr. Ishani Banerji, Dr. Mainak Chakraborty, Mr. Prolay Haldar, Mr. Anupam Adhikari, Mr. Safirul Islam, Dr. Titli Nargis, Mr. Niraj Nag, Dr. Bani Mallick, Dr. Bipul Karmakar, Dr. Suman Das, Mrs. Sampurna Biswas, Mr. Partha Mondal, Mr. Devendra Tiwari, Mr. Prasenjit Samanta, Mrs. Susmita Pal, Mr. Saibal Saha- for their support. Their cooperation and love made working in lab very relaxing and comfortable A special round of applause goes to my dear friends Dr. Prerona Dutta, Dr Anushka Khasnobish, Ms. Purnima Kovuri, Dr. Senjuti Halder, Mr. Pawan Kumar Sharma; who encouraged me throughout.

I would also like to thank my **teachers** Puspita Chakraborty, Dr. Aditi Nag Chowdhury, Mr. Samrat Chatterjee, Dr. Maheswaran Mani, Dr. Busi Sidhhartha, Dr. Regina Sharmila Dass, Dr. Sharmili Jagtap, Dr. Joseph Selvin, for kindling a passionate desire to pursue further research work.

My deepest gratitude goes to **my family** at 58 Khelat babu lane for their unflagging love and support throughout my life; this research work would have been simply impossible without them. My endless love goes to beloved Mithia, Bittu and Rupsi for keeping me sane during my leisure time.
My sincere gratitude also to my **parents-in-laws and naran da** for constantly motivating me.

I am forever indebted to my **husband Snehanjan** for always standing by my side, motivating me all the possible ways.

I can never ever thank enough to Maa and Baba for their endless love, patience. mental support, encouragement and motivation. Without them it would have been impossible for me to have come this far in life.

My PhD has been a labour of love, patience, perseverance, dedication and ambition. It has witnessed a global pandemic and survived the test of time. I am incredibly grateful to the **Almighty** for endowing me with the divine blessings.

Suparna Chakraborty

July, 2024.

Abbreviations

µg	microgram
µL	microliter
µM	micromolar
M	Molar
APCs	Antigen Presenting Cells
ATCC	American Type Culture Collection
BMDC	Bone Marrow-derived Dendritic cell
BSA	Bovine Serum Albumin
CD	Circular Dichroism
CFU	Colony-forming units
DCs	Dendritic Cells
DMEM	Dulbecco's Modified Eagle Medium
DMSO	Dimethyl sulfoxide
DNA	Deoxyribonucleic acid
dNTP	Deoxynucleotide triphosphates
DTT	Dithiothreitol
e.g.	Exempli Gratia / For Example
ELISA	Enzyme-linked immunosorbent assay
FBS	Fetal Bovine Serum
FITC	Fluorescein isothiocyanate g Gram
GAPDH	Glyceraldehyde-3-Phosphate Dehydrogenase
GFP	Green Fluorescence Protein
HRP	Horseradish peroxidase
IEC	Intestinal Epithelial Cell
IL	Interleukin
in vitro	latin for within glass
in vivo	latin for within living
iNOS	Inducible Nitric Oxide Synthase
IPTG	Isopropyl β-D-Thiogalcopyranoside

Kb	Kilo base
kDa	Kilodalton
kg	Kilogram
L	Liter
LA	Luria Bertani Agar
LB	Luria Bertani Broth
LD50	Lethal Dose 50%
LPS	Lipopolysaccharide
M cell	Microfold cells
m	Minute
MDR	Multi Drug Resistance
MFI	Mean Fluorescence Intensity
mg	milligram
MHC	Major Histocompatibility Complex
MIC	Minimum Inhibitory Concentration
mL	milliliter
MLNs	Mesenteric lymph nodes
MOI	Multiplicity of Infection
NCBI	National Centre for Biotechnology Information
ng	nanogram
NTS	Non typhoidal *Salmonella*
OMP	Outer Membrane Protein
PAGE	Poly Acrylamide Gel Electrophoresis
PAMP	Pathogen associated Membrane Protein
PBS	Phosphate-buffered saline
pBSK	pBluescriptSK
pH	Negative logarithmic measure of hydrogen ion concentration
PMN	Poly Morpho Nuclear Leukocytes
PP	Peyer's Patches
PVDF	Polyvinylidenedifluoride

qPCR/qRT-PCR Quantitate/ Quantitate real-time polymerase chain reaction

RAS	Rabbit Anti Serum
ROS	Reactive Oxygen Species
RPMI	Roswell Park Memorial Institute Medium
RT-PCR	Real-time polymerase chain reaction
SCV	*Salmonella* Containing Vacuole
SD	Standard Deviation
SDM	Site-Directed Mutagenesis
SDS	Sodium Dodecyl Sulfate
Sec	Second
SEM	Standard Error Mean
SPI	Salmonella Pathogenicity Island
T3SS/ TTSS	Type 3 Secretion System
TBS	Tris-Buffered Saline
TCR	T cell Receptor
TEMED	Tetra methyl ethylene diamine
Th1	Type 1 T helper
TLR	Toll-like receptor
TNF-α	Tumor necrosis factor alpha
TT	Tetanus Toxoid
Vi	Vi capsular Polysaccharide viz namely
WB	Western blot
WHO	World Health Organization

Symbols

%	Percentage
°C	Degree Celsius
±	plus-minus
α	Alpha
β	Beta
γ	Gamma

Table of contents

List of Tables.

List of Figures.

ABSTRACT

Title: Studies on host protective response to *Salmonella* infection

Submitted by: Suparna Chakraborty; JU Index No: 51/20/Life Sc./27

Typhoid and paratyphoid fevers, collectively known as enteric fever are caused by *Salmonella enterica* serovar Typhi (*S.* Typhi) and *S. enterica* serovar Paratyphi A and B (*S.* Paratyphi), and remain major threats to public health in the developing world. Although improved food and water hygiene with proper sanitation is the key to the permanent solution of this problem, vaccination of the high-risk population would result in immediate reduction of morbidity and mortality. Commercially available, injectable typhoid vaccines are modestly effective and work through the induction of systemic Vi antibody response, whereas the efficacy of the licensed oral vaccine is compromised owing to oral tolerance. These vaccines are ineffective against Vi negative salmonella strains. Additionally, no commercial vaccines against paratyphoid fever exist to-date. A broad-spectrum vaccine that is safe to use at all age groups, and can provide long term protection against both these serovars is urgently required. A major bottleneck in developing a broad-spectrum vaccine is the limited knowledge on the correlates of vaccine-induced protection against enteric fever. Despite serum antibody titres being widely used for this purpose, they are often poorly correlated with the secretory antibodies in the intestine and the cell mediated immune response, both of which are required for long term protection against typhoid fever.

The studies undertaken for my PhD thesis has several components. Firstly, I established an iron overloaded murine model to study the pathogenesis of *S.* Paratyphi A infection. Second, A chimeric antigenic formulation, called rCTB-T2544 was developed by conjugating a somatic antigen, rT2544 of *S.* Typhi and *S.* Paratyphi A and the B subunit of the cholera toxin (CTB) from *Vibrio cholerae*. Intranasal immunization with rCTB-T2544 evoked strong and sustained systemic and intestinal mucosal immunity and conferred with the protection against *S.* Typhi and *S.* Paratyphi A infection in iron overloaded mice model. Thirdly, another mucosal adjuvant FliC was co-administered systemically with rT2544 that showed considerable protection with a smaller dose of the individual components and provided with a platform for designing a multivalent vaccine against enteric diseases in the future. Both the vaccine formulations substantiated the potentiality of the mucosal antibodies to inhibit bacterial motility and bacterial attachment to the host epithelial cells by *in vitro* studies. The role of follicular helper T cells, gut homing lymphocytes, cytotoxic T lymphocytes in the circulation was underappreciated prior to this study. The current study focused on the contribution of mucosal antibodies in the intestine and cell mediated immune response that might significantly contribute to the overall vaccine outcome. A prime-boost regimen with intranasal followed by systemic immunization may be ideal for typhoid and paratyphoid vaccination and demands further elucidation. This study has special implications for India to reduce the burden of both acute enteric fever cases and the asymptomatic carrier stage, the latter being the reservoir of infection and responsible for future development of gall bladder adenocarcinoma.

Candidate's Sign:
Suparna Chakraborty
23.7.24

सान्तासबुज दास, एस. डि.
SANTASABUJ DAS, M.D.
वैज्ञानिक (एफ)/Scientist (F)
आइ.सि.एम.आर. राष्ट्रीय कॉलरा और आंत्र रोग संस्थान
ICMR National Insurance of Cholera & Enteric Diseases
पी-३३,सी. आई. टी. रोड, स्कीम-७०एम, बेलियाघाटा, कोल-१०
P-33, CIT Road, Scheme-XM, Beliaghata, Kolkata-10

23.07.2024.

Chapter 1.

General Introduction

and

Review of Literature

1.1. Background.

Enteric fever, encompassing Typhoid and Paratyphoid fevers, are caused by Gram negative pathogens, *Salmonella enterica* serovar Typhi (*S*. Typhi) and *S*. *enterica* serovar Paratyphi A, and rarely *S*. Paratyphi B and C. They pose significant threats to public health in the developing countries. Antibiotic treatment is generally prescribed to infected individuals. But increasing incidents of antimicrobial resistance further complicates the situation. Additionally, *Salmonella* infections contribute to the economic burden of industrialized and also the underdeveloped countries through the costs associated with surveillance, control measurements and treatment of disease (Crump, Luby, and Mintz 2004). Vaccination of susceptible population of endemic areas coupled with ongoing programs to improve water, sanitation and hygiene (WASH) are the only effective means to control the disease spread.

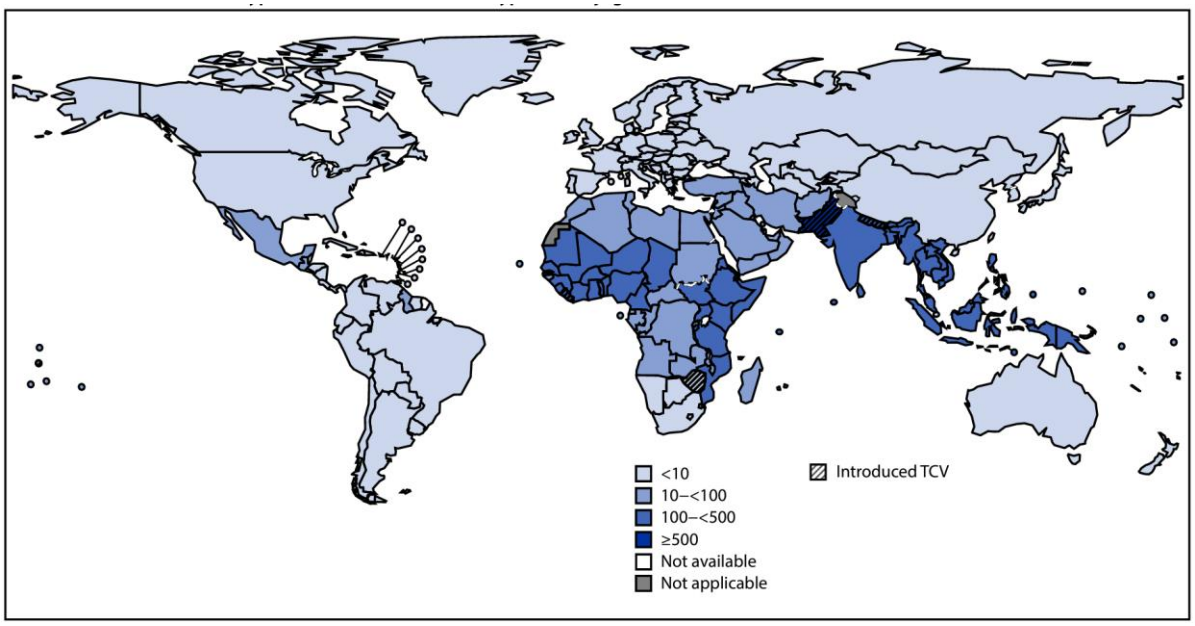

Fig 1.1. Incidences of typhoid fever cases worldwide and introduction of typhoid conjugated vaccine. Adapted from (Hancuh et al. 2023).

1.2. Epidemiology.

14.3 million cases of typhoid and paratyphoid fever were reported globally every year till 2017. Later on, in 2018, WHO recommended usage of typhoid conjugate vaccine in endemic areas to control typhoid. Additionally, multisectoral typhoid fever prevention program to improve water, sanitation and hygiene (WASH) further reinforced the surveillance and eventually resulted in reduced morbidity and mortality in those areas. Around 9.24 million new typhoid

fever cases with 110,000 deaths occurred worldwide in 2019, according to Global Burden of Disease data (Hancuh et al. 2023) (**Fig. 1.1**). Nevertheless, typhoid fever still poses a considerable threat to global health. With increasing antimicrobial resistance, *S.* Paratyphi A expedited global disease burden of enteric fever, causing one quarter of cases with 19.1 million deaths annually in South Eastern Asia, including India.

1.3. Looking back in Time- History of *Salmonella* Infection.

The history of Typhoid dates back to 430 BC, when an extensive plague, in Athens, Greece, affected one third of the entire population fatally. Typhoid fever emerged as the most likely reason, in a study, examining the ancient dental pulp microbial DNA, obtained from cadaveric remains of burial grounds at Kerameikos, Athens (Papagrigorakis et al. 2006). Another deadly epidemic affected the Mexican highlands in 1545 and 1576 respectively, leading to 7 to 17 million casualties. Later, a study in 2018, utilized a metagenomic analyzer tool MALT, to identify *Salmonella enterica,* procured from dental tissues, from cadaveric remains, in an epidemic cemetery at Teposcolula-Yucundaa, Oaxaca in southern Mexico. *S.* Paratyphi C was proposed to be one of the strongest offenders (Vagene et al. 2018). Another incident from Jamestown, which was an English colony in Virginia, USA, was thought to be affected severely by Typhoid fever. The fever brutally affected the settlers between 1607 and 1624. To the Native Americans, typhoid fever was a "virgin soil disease," indicating absence of any prior immunity to these microbes (Earle 1979). William Budd was a pioneer in observing the typhoid landscape in England during 1838. He found that the offending agent was present in the excreta of the affected persons, and was transmitted through consumption of contaminated water. To control the typhoid outbreaks, Budd advised isolation and proper disposal of fecal matter. In England the condition was known as typhoid fever, owing to specific similarities to typhus. The disease demonstrated rapid onset of fever, headache and nausea, being accompanied by diarrhea or constipation. The causative agent, *Salmonella typhi*, was finally isolated in 1880 (Moorhead 2002).

The Mary Mallon episode- Mary Mallon (1869-1938) was born in Ireland in 1869 and came to the United States in 1884. She used to work as a cook for wealthy families at New York. Mary was nicknamed as "Typhoid Mary", when persons of many households were found to become ill with Typhoid fever', after consuming food cooked by her (Marineli et al. 2013). Later she was found to be a healthy and silent carrier of *Salmonella Typhi*, by the health authorities (**Fig. 1.2**) , responsible for endangering the lives of at least one hundred and twenty

two persons (Marineli et al. 2013). Further, During the Spanish-American war, soldiers succumbed to typhoid, in addition to yellow fever, due to poor sanitation systems (Byerly 2010). Another prominent typhoid outbreak occurred at Crowdon, Surrey in 1937, leading to 341 typhoid cases. It had occurred due to water contamination of a well. In 1964, at Aberden, Scotland, typhoid outbreak occurred to selling of contaminated canned meat, leading to three deaths ('Aberdeen typhoid outbreak of 1964' 1966).

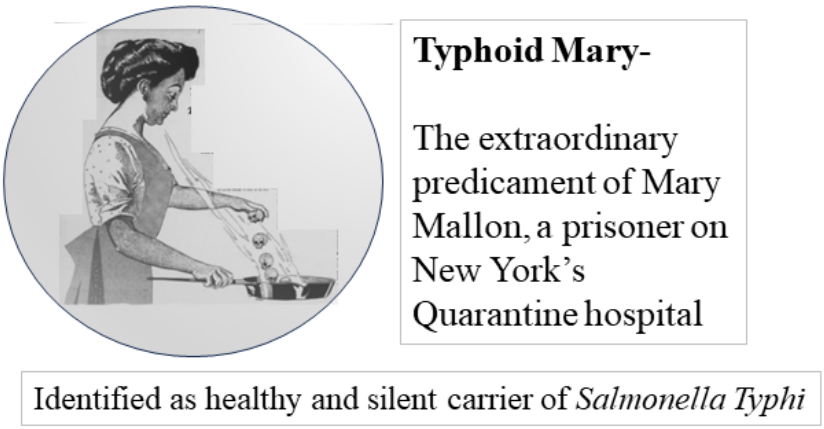

Fig 1.2. A picture of Mary Mallon (Created with BioRender).

1.4. Discovery of the contagion- *Salmonella.*

Karl Joseph Eberth was the first to describe the bacillus that was thought to cause typhoid fever in 1880. Four years later, pathologist Georg Gaffky confirmed this link, terming the bacillus as *Eberthella typhi,* which is now known as *Salmonella typhosus, (also called as Bacillus typhosus).* Sometimes later, Daniel Elmar Salmon and his aide, Theobald Smith, an American bacteriologist, isolated *Salmonella Choleraesuis* from pigs, implying that the agent was responsible for cholera in swine. However, later research proved that the causative agent was a virus, instead of the proposed bacterium (Schultz M. 2010). Later, Joseph Lignières, a French bacteriologist, proposed the genus name *Salmonella* in recognition of Salmon's efforts, which encompasses a spectrum of motile, non-spore bearing, aerobic or facultative anerobic bacteria of the Enterobacteriaceae group.

1.5. Classification.

The genus '*Salmonella'* belongs to the family *Enterobacteriacea,* which is a Gram-negative rod-shaped facultative anaerobe, ranging from 0.7 to 1.5 µm in diameter with a length of 2 to

5 µm in size and show predominant peritrichous motility. This genus refers to primary intracellular pathogens, leading to different clinical manifestations in the development of infection in humans (Coburn, Grassl, and Finlay 2007).

Initially, classifying different serovars of *Salmonella* was complex and necessitates a uniformity in nomenclature for easy communication between scientists, health officials and public. At the beginning, Kauffmann proposed 'one serotype-one species' concept on the basis of the serologic identification of O (somatic) and H (flagellar) antigens leading to more than 2600 species of *Salmonella* (Kauffmann F 1966). Later, *Crosa et al.* proposed another nomenclature using DNA-DNA hybridization techniques. But, the name of *Salmonella choleraesuis* for both species and serotypes initiated another debate. Owing to biochemical distinction, scientists preferred using the name of "choleraesuis" as species name over serotype (Crosa et al. 1973).

To avoid all the confusions and debates, currently the World Health Organization (WHO) Collaborating Centre for Reference and Research on *Salmonella* at the Pasteur Institute updated the classification of *Salmonella* based on the Kauffman-White scheme. According to this, the genus *Salmonella* was divided in two major species, *S. enterica* and *S. bongori* (Fabrega and Vila 2013). Further, *S. enterica* can be sub-grouped into six subspecies owing to biochemical difference and genetic relatedness and are referred by name and number (**Fig. 1.3**).

S. enterica subsp. enterica (I),
S. enterica subsp. salamae (II),
S. enterica subsp. arizonae (IIIa),
S. enterica subsp. diarizonae (IIIb),
S. enterica subsp. houtenae (IV), and
S. enterica subsp. indica (VI).

Initially *S. bongori (V)* was classified as another subspecies, which was later corrected to a distinct lineage from *S. Enterica*. *S. bongori* and the subspecies II, IIIa, IIIb, IV, and VI, rarely isolated from clinical specimens are predominately found in cold-blooded vertebrates and in the environment (Fabrega and Vila 2013). Hence, majority of the *Salmonella* organisms leading to disease in humans and domestic animals belong to *S. enterica subspecies enterica (I)*. Prior to this classification, serovar names were treated as species and were italicized, which was later corrected with this updated classification*(Achtman et al. 2012).*

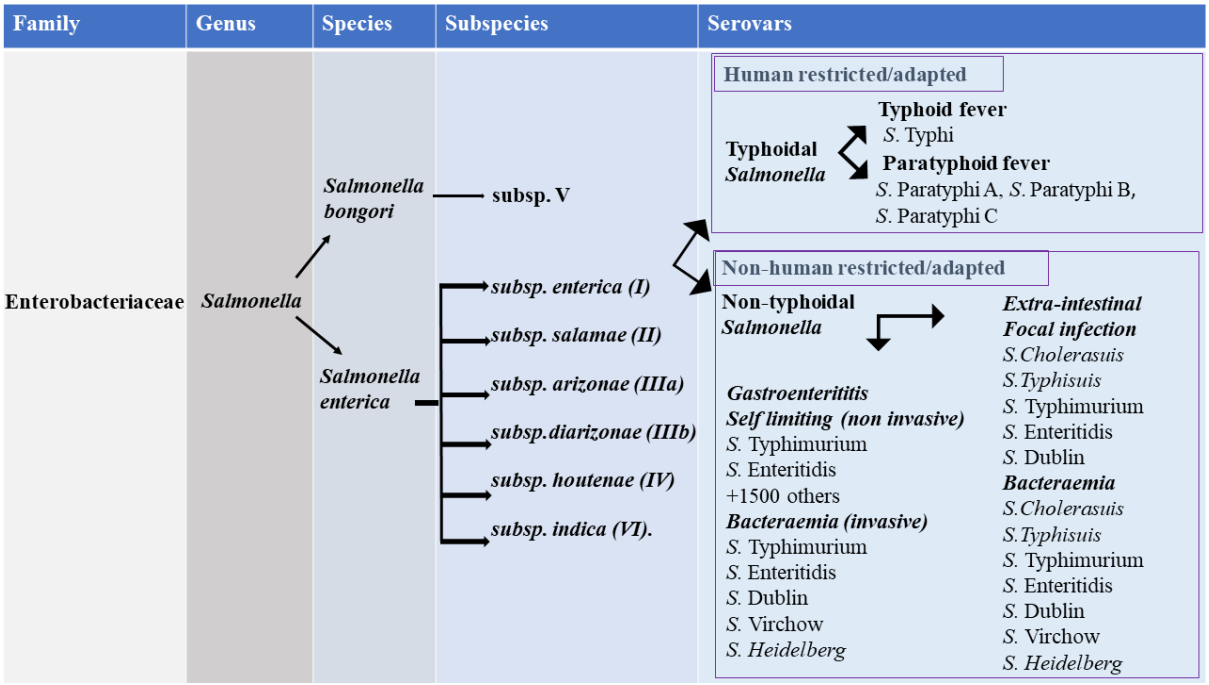

Fig 1.3. Updated classification of *Salmonella* (Created with BioRender).

1.6. Outline of clinical syndromes of *Salmonella* infection and pathophysiology.

In humans, *Salmonella* infections can cause self-limiting gastroenteritis which is linked with nontyphoidal *Salmonella* (NTS), whereas typhoidal strains are responsible for life threatening enteric fever. Both types of salmonellosis results into significant morbidity and mortality in both humans and other animals and responsible for a significant global socioeconomic impact. Enteric fever encompassing typhoidal and paratyphoid fever is protracted systemic illness. Clinical conditions include gradual onset of fever, hepatosplenomegaly, abdominal pain and occasionally characterized by rash, anorexia, nausea, transient diarrhea, or constipation, headache with relative bradycardia (Stuart and Pullen 1946). Usually, the bacteria enter into human host through oral mucosal route by ingestion of contaminated food or water or simply by contacting with a carrier. Immediately after ingestion, *Salmonella* employs adaptive acid tolerance strategy to withstand the lower pH milieu of stomach to survive effectively and reaches to the intestine (Garcia-del Portillo, Foster, and Finlay 1993). The incubation period of *Salmonella* usually ranges from 3 to 21 days. The typhoidal fever can be fatal without effective treatment. The problem of *S.* Typhi infection is further complicated by the emergence and spread of multi-drug resistant and extensively drug resistant (XDR) strains across continents (Carey, McCann, and Gibani 2022). If left untreated, the mortality rate reaches approximately 20%, whereas an incompletely cured infection, followed by an asymptomatic chronic carrier

state leads to the significant risk of developing adenocarcinoma of the gall bladder (Gonzalez-Escobedo, Marshall, and Gunn 2011).

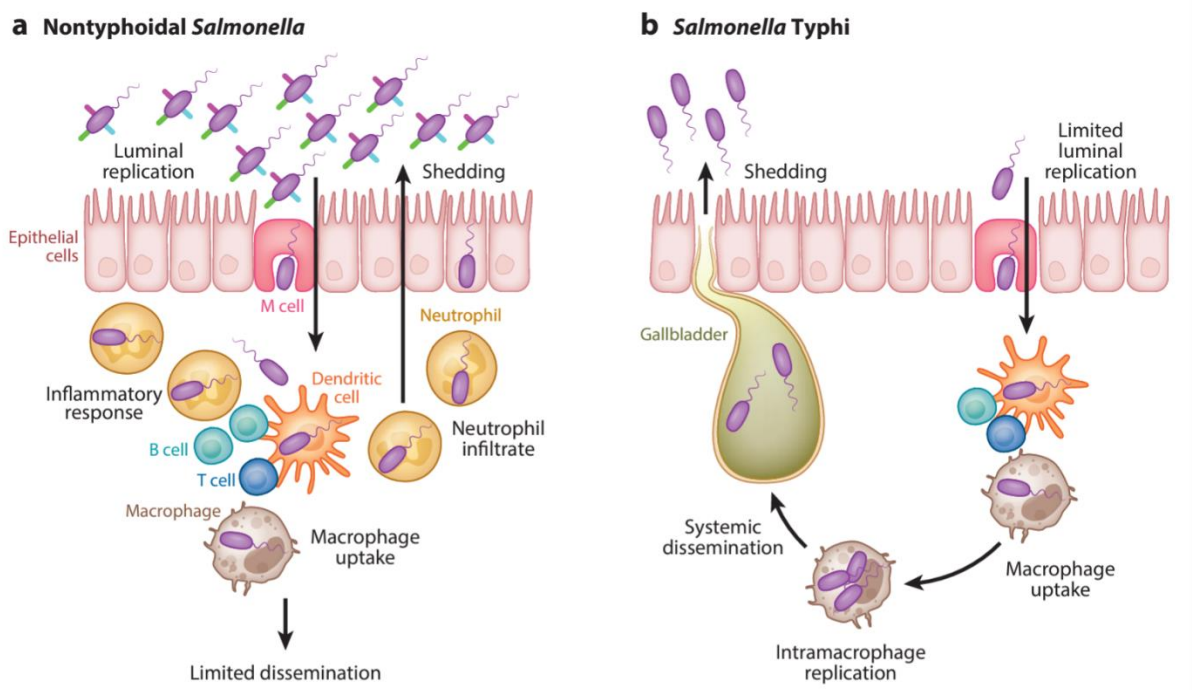

Fig 1.4. A schematic comparison of infection associated with Non-Typhoidal *Salmonella* and Typhoidal *Salmonella,* Adapted from (Dougan and Baker 2014).

After entering the small intestinal mucosa, the bacteria adheres to the intestinal epithelial cells with adhesins. Primarily, *salmonella* induces membrane ruffling by profound cytoskeleton rearrangements and thereby promoting its own uptake into the non-phagocytic cells that lies at the border linings of intestinal lumen – A physiologically active process named bacteria induced endocytosis (**Fig. 1.4**). Literature suggested that few *Salmonella* can translocate passively through intestinal mucosa by exploiting the microfold (M) cells, which sample the antigenic content of the intestine (Haraga, Ohlson, and Miller 2008). Next, *salmonella* gains access to infect phagocytes of the lamina propria. Consequent activation of virulence mechanism supports their replication in intracellular environment. Finally, it disseminates into lymphatics and blood stream, allowing the bacteria to spread to the visceral organs such as liver and the spleen and persist in the gall bladder (Ruby et al. 2012).

1.7. Mechanism of pathogenesis of *Salmonella*.

The ability of *Salmonella* to endure in a variety of host cells style it up to a successful intracellular pathogen. The genomes of prokaryotes are highly mosaic and dynamically structured. The genomic content of bacterial species is continually changing, with genome size varying among different strains or even clinical isolates within a species. Genetic recombination events such as point mutations, gene conversion, rearrangements, and the insertion or deletion of foreign DNA elements modify the organization of genetic information over time. The gain or loss of genetic elements can significantly alter a bacterium's lifestyle and enable it to adapt to new ecological niches. A group of mobile genetic elements that include virulence-associated genes are clustered in specific regions across the chromosome, known as Pathogenicity Islands (PAIs) (van Asten and van Dijk 2005). There are more than 300 genes which are responsible to contribute to several aspects of virulence mechanisms undertaken for successful colonization and replication in the host. Majority of these virulence genes are clustered in the regions which are distributed over the chromosomes '***Salmonella* pathogenicity islands (SPI)**'(van Asten and van Dijk 2005). These pathogenicity islands contain higher GC rich regions, often flanked by genes which are contiguous in closely related non-pathogenic bacteria. Transposon insertion sequences and remnants of bacteriophage are often found at the borders of these island. All these findings indicated that these gene clusters are reportedly assimilated through horizontal gene transfer. Genes located in SPI-1, a 40kb region, encode for protein important for invading epithelial cells by mediating cytoskeletal rearrangements. These molecules are reported to be further translocated into the host via type3 secretion system (T3SS), which is again encoded by SPI-1. T3SS acts as a needle like surface appendage which aids in injecting bacterial effector molecules into the host cells to ease its invasion into the nonphagocytic cells. In addition to these, few effector proteins (SopA, SopB, SopD) crucial to cause diarrhea were also encoded by SPI-1 genes.

Another 40kb region, named SPI-2 locus, contains genes necessary for the survival and replication of *Salmonella* in phagocytic cells facilitating its dissemination into the systemic organs. SPI-2 mutants showed reduced virulence and failed to cause systemic disease in mice (Hensel et al. 1995). SPI-2 encodes T3SS-2, crucial for protecting SCV from the anti-bacterial immunity of host (Uchiya et al. 1999). It also empowers the pathogen to colonize warm blooded hosts (Baumler 1997).

SPI-3 locus contains two IS elements. It encodes one of the crucial virulence factor, MgtCB, a magnesium trasporrt system, which aid bacteria to adapt in the microbicidal and nutrient deficient milieu of phagosomes, regulating metabolic pathways and transport system (Blanc-Potard and Groisman 1997).

SPI-7, encoding viaB gene pivotal for biosynthesis of capsular Vi polysaccharide is exclusively reported in *S.* Typhi (Hansen-Wester and Hensel 2002). A gene cluster encoding Type 4 pili is also encoded by the genes of this locus which aid in invading epithelial cells (Zhang et al. 2000).

However, several other SPIs are also reported from the genome sequences from *S*. Typhi and *S.* Typhimurium, but their functions still need to be investigated (Wang et al. 2020).

Effector molecules as Adhesins and invasins- Various adhesion molecules bestow bacteria with the ability to attach to host cell or ECM to ease their entry and facilitate subsequent pathogenesis. There are 13 predicted fimbrial loci reported yet, many of which are induced in vivo and necessary for biofilm formation, attachment to host cells and colonization (Humphries et al. 2001). Several other non fimbrial adhesins, including outer membrane proteins (eg, PagN/T2544) that binds to laminin and enables epithelial attachment of the bacteria (Ghosh et al. 2011) and auto transporter adhesins (MisL, ShdA) that bind to fibronectin for successful intestinal colonization (Dorsey et al. 2005; Kingsley et al. 2002). Rck, reported as an outer membrane protein of *S. Enteritidis* promotes epithelial invasion (Rosselin et al. 2010). T2942 of *S*. Typhi was reported to mediate T3SS-1 independent invasion (Chowdhury et al. 2015).

1.8. Treatments.

1.8.1. Antimicrobial therapy.

Currently emerging and global distribution of drug resistant *S.* Typhi strains need intense attention for implementing effective treatment of typhoid fever. The mortality related to typhoid fever strictly went down from 30% to 1% due to the introduction of first line antimicrobials such as chloramphenicol, sulfamethoxazole and ampicillin. Resistance to these antibiotics gradually developed in different regions worldwide, evoking a threat of multi drug resistant strains, especially in south east Asian countries in late 1900s and early 2000 (Wain et al. 1999; Sheorey et al. 1993; Kumar, Rizvi, and Berry 2008). The alternative approaches introduce Fluoroquinolones and cephalosporins as treatment options (Buckle, Walker, and

Black 2012). Later, the SEAP (Surveillance of Enteric fever in Asia Project) reported very few cases of multidrug resistant strains from India, Bangladesh and Nepal. However, Pakistan showed a different scenario with majority of the multidrug resistant strains (Barkume et al. 2018). In areas with higher rates of MDR strains with fluroquinolone resistance, application of azithromycin and newer antibiotics such as carbapenams were recommended. However, disease incidence with strains resistant to cephalosporine also have been reported in Germany, Philippines, India and Pakistan (Ahmed et al. 2012).

Hence, expensive antimicrobial therapy to treat typhoid faced a further challenge in the low resource setting of developing countries. To overcome this grave situation, urgent development of a low cost, safe and efficacious typhoid vaccine is needed.

1.8.2. Typhoid and Paratyphoid Vaccines.

The most cost-effective means to control the spread of any disease in endemic zone is vaccination. It directly acts on specific targets and evoke a cascade of immune responses against the pathogen.

Currently licensed purified Vi polysaccharide (Vi-PS) parenteral vaccine and the oral live-attenuated *S.* Typhi Ty21a vaccine against *S.* Typhi are moderately immunogenic and exert protective efficacy of 55-72%. Owing to the large size of the capsules, it is difficult to swallow for the children below 6 years of age, hence it is not recommended for them (Guzman et al. 2006). Considering difficulty in administering multiple booster doses, and, aiming to escalate their immunogenicity with a single dose several research groups have developed attenuated *S.* Typhi Ty2 stains which are summarized in the **Table 1.1**

Table 1.1. Vaccines against Typhoid fever.

Vaccine and Developer	**Genetic changes**	**Current status**	**Reference**
Ty21a Vivotif (Crucell)	gal E mutant.	Commercially available	(Levine et al. 1999)
Vi-PS Typherix (GSK), Typhim Vi (Sanofi), Typbar Vi (Bharat Biotech),	Purified Vi polysaccharide.	Commercially available	(Sur et al. 2009)

Typbar-TCV: Bharat Biotech	Vi polysachharide is conjugated with the Tetanus toxoid.	Recommended by WHO.	(Kim et al. 2022)
Vi-DT: International Vaccine Institute (IVI)/Shanta Biotech	Vi polysaccharide is conjugated with diphtheria toxoid	Phase III clinical trial.	(Medise et al. 2019; Shakya, Neuzil, and Pollard 2021)
Vi-CRM197 Novartis Vaccines Institute for Global Health (NVGH)	Vi polysachharide is conjugated with the CRM197, a nontoxic mutant of diphtheria toxin.	Phase I and II clinical trials.	(van Damme et al. 2011; Bhutta et al. 2014)
Vi-rEPA National Institutes for Health	Pseudomonas aeruginosa exotoxin A as a carrier protein, the resultant conjugates (Vi-rEPA	Phase III clinical trial.	(Thiem et al. 2011; Shakya, Neuzil, and Pollard 2021)
CVD 908 University of Maryland	Deletion in the aroC and aroD	Showed bacteremia in clinical trial.	(Tacket et al. 1992)
CVD 908-htrA University of Maryland	Deletion in the aroC, aroD and htrA genes	Phase II study with 80 human volunteers.	(Tacket et al. 2000)
CVD 909 University of Maryland	Continuous expression of Vi polysaccharide	Phase I clinical trial.	(Wahid et al. 2011; Tacket et al. 2004)
Ty800 Avant Immunotherapeutics	Deletion in the phoP/phoQ virulence regulatory genes.	Phase II clinical trial.	(Hohmann et al. 1996)
M01ZH09 emergent Biosolutions	Deletion in the aroC and ssaV genes	Phase II clinical trial.	(Kirkpatrick et al. 2006; Tran et al. 2010)

Various live attenuated vaccine candidates are in clinical trial phase. However, CVD 908 resulted in vaccinemia with a single oral dose of 10^7 viable organisms, and was later on

modified by the deletion of another stress protein, htrA that prevented vaccinemia, but retained both humoral and cellular immune responses (Tacket et al. 2000). To ensure more consistent serum anti-Vi antibodies, Vi was constitutively expressed in CVD 908 strain, generating CVD909 (Wahid et al. 2011; Tacket et al. 2004). A prime boost regimen with orally administered CVD 909, followed by an injection of Vi-polysaccharide vaccine failed to induce strong Vi-specific antibody response, but instead, significantly raised Vi-specific IgA+ B memory cells. However, the need for pre-administration of buffer to neutralize stomach acid renders a potential delivery challenge for live attenuated vaccines (Syed et al. 2020). Purified Vi polysaccharide vaccine, being a T cell independent antigen, did not induce cell mediated immunity, but was verified to exert moderate protective efficacy and (Sur et al. 2009). Chemical conjugation of a carrier protein to Vi Polysaccharide augments the immunogenicity of the vaccine by converting Vi polysaccharide to a T cell dependent antigen. Bharat biotech in India has launched 'Typbar TCV', (Vi polysaccharide conjugated to Tetanus toxoid) that nay be administrated to infants as young as 6 months of age (Kim et al. 2022). Several recombinant proteins such as recombinant *Pseudomonas aeruginosa* exotoxin A (rEPA) (Thiem et al. 2011), CRM197 (van Damme et al. 2011; Bhutta et al. 2014) and diphtheria toxoid (Medise et al. 2019), conjugated to purified Vi-polysaccharide showed improved efficacy, but the conjugate vaccines are still under investigations.

None of the vaccine strains was shown to be effective against Paratyphoid infection. Vi-polysaccharide based vaccines against *S*. Typhi, which are more popular across the world are ineffective in protecting against non-capsulated *S*. Paratyphi A. Since epidemic areas of *Salmonella* Typhi and Paratyphi infections largely overlap, bivalent vaccine candidates targeting both *S.* Typhi and the dominant Paratyphi A strain (*S.* Paratyphi A) have attracted significant attention for new vaccine development (Crump and Mintz 2010) and are listed in **Table 1.2.** *S.* Paratyphi A vaccines are principally based on either whole-cell live attenuated strains such as CVD1902 or comprising of repeating units of the O:2 (O-antigen of lipopolysaccharide), conjugated to several protein carriers such as TT and CRM-197. Currently, vaccination with Ty21a strain has reported to elicit humoral immunity with in vitro cross-reactivity against both *S*. Paratyphi A and B infection but need more studies to further assessing the protective efficacy. Additionally, with the help of chemical conjugation of O antigen of lipopolysachharide of *S.* Paratyphi A with tetanus toxoid (O2:TT), CRM197 (O2: CRM197) and diptheria toxoid (O2: DT) separately, scientists across the world had developed vaccine candidates which showed immunogenicity against *S.* Paratyphi A infection and further

were proposed to administered with Vi-TT, Vi-CRM197 and Vi-DT respectively for improved protective efficacy against both the typhoidal *Salmonella* serovar Typhi and Paratyphi A infection (Martin et al. 2016). An advanced approach including the Multiple Antigen Presenting System (MAPS) uses the affinity pair biotin-rhizavidin to formulate a complex of polysaccharide (Vi and OSP) and proteins (CRM197, rEPA of Pseudomonas, and a pneumococcal fusion protein SP1500-SP0785) which showed durable bactericidal immune response (Zhang et al. 2022). The GSK Vaccines Institute for Global Health (GVGH) has formulated a system by disrupting Tol pal apparatus leading to over production of outer membrane vesicles (OMVs) which is also referred to as Generalized Modules for Membrane Antigens and engineered to produce heterologous *S*. Typhi Vi antigen and the homologous O:2 O antigen. (Meloni et al. 2015; Gasperini et al. 2021)

Table 1.2. Bivalent vaccines against Typhoid and Paratyphoid fever.

Vaccine and Developer	**Genetic changes**	**Current status**	**Reference**
CVD 1902 alone or with CVD 909 University of Maryland	Deletions in the guaBA and clpX regions	Clinical trial phase 1 study. Technology licensed to Bharat Biotech where a combination with CVD909 will be studied.	(Wahid et al. 2019; Konadu et al. 1996)
O:2 TT with Vi-TT NIH	O antigen from *S.* Paratyphi A chemically conjugated with tetanus toxoid delivered with Vi-TT.	Clinical trial phase 1 and 2 study. Technology transfer from NIH to Lanzhou Institute (China)	(Konadu et al. 1996; Martin et al. 2016)
O:2-CRM197 with Vi-CRM197 Novartis Vaccines	O antigen from *S.* Paratyphi A chemically linked with CRM197, combined with Vi-CRM197.	Pre-clinical study. Technology transferred to Biological E, India where a combination study with Vi-CRM197 was proposed	(Shakya, Neuzil, and Pollard 2021; Martin et al. 2016)

Institute for Global Health (NVGH)			
O:2 DT with Vi-DT IVI	O antigen from *S.* Paratyphi A chemically linked with diptheria toxoid	Clinical testing awaiting	(Martin et al. 2016)
The Multiple Antigen Presenting System (MAPS) Vaccine	affinity pair biotin-rhizavidin to formulating a complex of polysaccharide (Vi and OSP) and proteins (CRM197, rEPA of Pseudomonas, and a pneumococcal fusion protein SP1500-SP0785)	Pre-clinical	(Zhang et al. 2022)
Generalized Modules for Membrane Antigens (GMMA)	Tol pal apparatus leading to over production of outer membrane vesicles (OMVs)	Pre-clinical	(Meloni et al. 2015; Gasperini et al. 2021)

1.9. Animal models to study bacterial pathogenesis.

Animal models portray a significant role in understanding the bacterial pathogenesis. It also provides an indispensable platform to investigate the immunogenicity, efficacy and to evaluate the pre-clinical safety data prior to clinical trials of the vaccine candidates. Since, both the *Salmonella* Typhi and *Salmonella* Paratyphi A are the human restricted pathogen, their interactions with the human host and subsequent pathogenesis study are poorly understood. However, there are few animal models tabulated in **Table 1.3** which provide an insight into those investigations.

Table 1.3. Experimental use of animal models to study *S.* Typhi and *S.* Paratyphi A

Model	***Salmonella* serovar**	**Advantages and disadvantages**	**Reference**

Humanized mouse model	*S*. Typhi	Useful to study colonization and systemic spread but not for vaccine efficacy.	(Song et al. 2010; Libby et al. 2010)
Chimpanzee	*S*. Typhi	Oral infection with *S*. Typhi was established but with milder symptomatology of typhoid fever. Owing to smaller sample size due to higher cost and broad biological variation made this model difficult to determine the endpoint titer for assessing vaccine efficacy	(Edsall et al. 1960; Higginson, Simon, and Tennant 2016)
Neonatal mice oral infection model	*S*. Typhi, *S*. Paratyphi A	Useful for protection studies but not for immunogenicity studies of the vaccine candidates.	(Santander and Curtiss 2010)
Intraperitoneal infection model	*S*. Typhi, *S*. Paratyphi A	Useful for evaluating the protective efficacy of the vaccine candidates but not recommended for studying the immunogenicity of those vaccine.	(Zhu et al. 2015; Xiong et al. 2017)
Rabbit model	*S*. Typhi, *S*. Paratyphi A	Useful for studying reacto-genecity and immunogenicity of vaccine candidates but an heavily elevated antibody titer value complicate the correlation studies with human data.	(Roland et al. 2010)
CHIM (Control human infection model) studies	*S*. Paratyphi A, *S*. Typhi,	Very much useful for evaluating the immunogenicity of the vaccine candidates and provides a useful insight to clinical trial with the potential vaccines. This study showed promising result with some limitations. Strict regulation and guidelines with enrolment of healthy individual from developed countries raise an issue as they	(Sztein and Booth 2022; Raymond et al. 2019)

		are different in their genetic background, nutritional status and subsequent microbiome, age and co-morbidities and co-infections associated with background immunity with the young individual from disease predisposed areas.	

Our lab had previously demonstrated an iron overloaded mouse model to study *S.* Typhi infection (Ghosh et al. 2011). This model is based on the studies suggesting iron as one of the critical micronutrients for bacteria including *Salmonella* (O'Brien 1982; Powell et al. 1980). Studies previously showed that systemic overload with iron (administered through the parenteral route) renders mouse susceptible to *S*. Typhi infection (Powell et al. 1980; O'Brien 1982). However, large dose requirement for iron that markedly suppresses the immune system could be circumvented by co-administration of iron chelator desferoxamine that makes iron available to the phagosomal bacteria and inhibits NADPH oxidase activity, promoting intracellular survival and growth and significantly reducing the lethal dose. Given that systemic infection could be established in wild type mouse after oral administration, which affected the same visceral organs as humans following natural infection, this iron overloaded murine model can probably be considered a physiological model of infection (Das et al. 2017; Ghosh et al. 2011).

1.10. Host immune responses against infection.

For battling against an intracellular pathogen like *Salmonella*, host needs to employ both the humoral and cell mediated immune responses. Antibodies impart a major role in defense against extracellular bacteria. On the other hand, cell mediated immune response (CMI) is projected towards elimination of *S*. Typhi-infected cells. Based on the data available from the various investigations with attenuated typhoid vaccines, it is well verified that cumulative effort from serum antibodies, sIgA, T-cell subsets, and the interaction between T, B, and antigen-presenting cells accord an acquired immune response (Sztein, Salerno-Goncalves, and McArthur 2014). Although, the relative contribution from each of the immune arms remains to be elucidated (**Fig. 1.5)**.

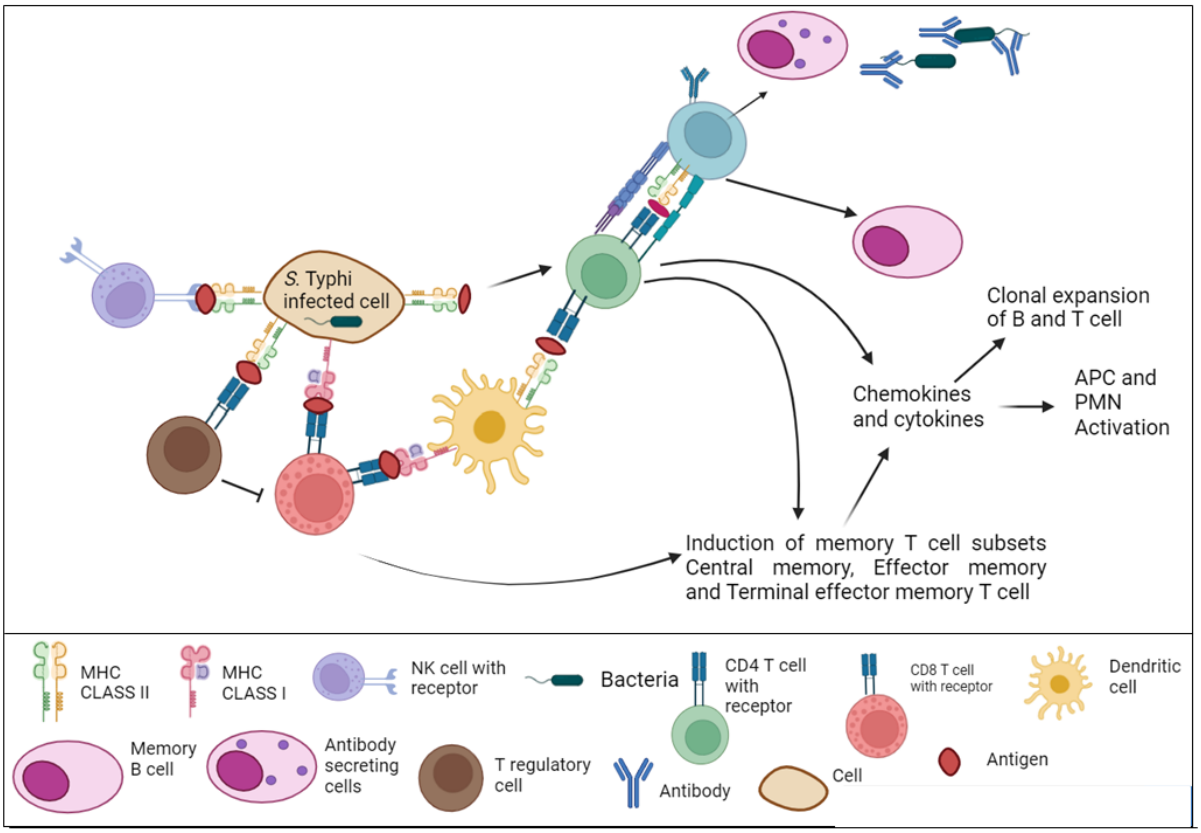

Fig. 1.5. Immunity to Typhoidal *Salmonella* in humans. Multiple antigens presenting cells involved in contributing protection against Typhoidal *Salmonella*. (Created with BioRender).

1.10.1. Humoral responses.

1.10.1.1. Antibodies.

Several studies had reported generation of serum antibodies specific to the O antigen present in the *S.* Typhi LPS, the Vi antigen, and the H antigen upon *S.* Typhi immunization (Tacket et al. 2000; Tacket et al. 2004; Hohmann et al. 1996). Despite presence of high antibody titer, reports confirmed susceptibility of those recovered patients towards typhoidal reinfection (Dupont et al. 1971; Hornick et al. 1970). In a human challenge study with *S.* Typhi, volunteer who developed typhoid or remain uninfected showed little differences in their IgG, IgM, and IgA to LPS and H antigens (Waddington et al. 2014). However, throughout the study, their anti Vi titers were continued to be unchanged (Waddington et al. 2014). A different investigation reported a defined amount of serum anti-Vi antibodies (1.4–2.0µg/ml) as a serological surrogate of protection (Szu, Klugman, and Hunt 2014). However, a study with Ty21a vaccine which lacks the Vi antigen in its formulation, imparted similar protection with those of the Vi polysaccharide vaccine (Ivanoff, Levine, and Lambert 1994), signifying multiple adaptive

immunological responses, leading to a protective response against typhoid. Another field study with Ty21a, seroconversion, which was measured by anti-O IgG, correlated with protection (Levine, Tacket, and Sztein 2001) and had been used as a marker of immunogenicity with several other live-attenuated vaccine candidates (Tacket et al. 2000; Tacket et al. 2004; Hohmann et al. 1996). Additionally, studies with natural infection or immunization with Salmonella Typhi reported generation of bacteria specific IgA in saliva, intestinal fluids, and stools (Cancellieri and Fara 1985; Pakkanen et al. 2010; Herath 2003). However, no single studies reported avidity, which measure the strength of the antibody-antigen interaction. Despite several studies using antibodies as markers of immunogenicity with different vaccine candidates, very few study focused on the functional properties of these the antibodies generated. A study with Ty21a immunization verified that bacteria specific IgA aid in antibody dependent cellular cytotoxicity (ADCC) (Tagliabue et al. 1986). Again, another investigation found no significant correlation between bactericidal titer and anti-Vi titer (Pulickal et al. 2009). More detailed study for better understanding of the functional role of induced antibodies is the need of the hour.

1.10.1.2. B cells.

B cells were previously reported to be crucial for protection against *S.* Typhimurium (Mittrucker et al. 2000). However, their contribution in conferring protection from typhoidal salmonella remains to be elucidated. B cells help in antibody production, antigen presentation, cytokine secretion and also T cell activation (Sztein, Salerno-Goncalves, and McArthur 2014).

1.10.1.2.1. Antibody secreting cells.

B cells were reported to undergo differentiation and become antibody secreting cells (Tarlinton et al. 2008). Bacteria specific ASCs were reported to peak in systemic circulation between 7 to 10 days post-*Salmonella* infection and further home to mucosal effector sites (Tacket et al. 2004; Tacket et al. 2000; Levine, Tacket, and Sztein 2001; Kantele et al. 2013; Kantele et al. 1999). Interestingly patients with continuing diarrhea reported to maintain circulating ASCs throughout the infection (Kantele 1996). This study also established presence of predominantly bacteria-specific IgA ASCs in the circulation, followed by IgM and IgG ASCs (Kantele 1996). Three factors viz. nature of the antigen, number of immunization doses and the formulation primarily modulate the magnitude of the immune response generated. Live oral vaccine boosted more ASCs compared to the killed vaccine (Kantele et al. 1991). Three dosed vaccine

prompted higher number of ASCs compared to two or single dosed vaccine (Kantele 1996). Suspension formulation of live attenuated vaccine generated greater ASCs compared to gelatin and enteric coated capsule version of the same live attenuated vaccine (Kantele 1996).

1.10.1.2.2. Memory B cells.

Memory B (B_M) cells, the long-lived antigen primed cells, which upon antigenic stimulation undergo rapid terminal differentiation into plasmablasts and plasma cells are the utmost important cells to retain long term protective efficacy of any vaccine candidates (Takemori et al. 2014). A study with attenuated typhoid vaccines elicits memory B cells (CD19+ CD27+) specific for flagella (T-cell-dependent) and also LPS, Vi (T-cell-independent antigen) of *S.* Typhi which persisted upto 1 year (Wahid et al. 2011). Another study confirmed induction of robust B memory cell responses in individual receiving CVD 909 (Salazar-Gonzalez et al. 2004). Additionally, they reported a predominantly LPS-specific IgA B_M response over IgG $B_{M,}$ predicting a strong association between antigen-specific memory B cells with the antibody levels (Salazar-Gonzalez et al. 2004). Mice immunized with porins had been observed with IgM memory B cells, indispensable for long-term production of bactericidal IgM antibodies (Perez-Shibayama et al. 2014). This study also found an induction of T follicular helper (Tfh) cells secreting IFN-γ critical for generation of memory B cells (Perez-Shibayama et al. 2014). However, further characterizations of these cell subsets are required for better understanding of the relative contribution of the memory B cells and Tfh subsets.

1.10.1.2.3. B cell homing.

In addition to circulatory antibodies of the host, the effector immune response in the gut is another critical factor that needs to be addressed for better understanding of protection against *S*. Typhi infection, considering its portal of entry through gut mucosa. Study with live attenuated oral typhoidal vaccine found mucosally derived circulating IgA ASCs (Pasetti et al. 2011), which further homed to the lamina propria (Bouvet, Decroix, and Pamonsinlapatham 2002), driven by the expression of the gut homing markers (integrin α4β7 and chemokine C–C motif receptor CCR-9) (Mora et al. 2006). Upon Ty21a immunization, a significant number of bacteria specific IgM and IgA ASCs were observed to migrate towards chemokine (C–C motif) ligand (CCL)25 and CCL28, which is known as the ligand for CCR9 (Sundstrom et al. 2008). On the other hand, tetanus-specific ASC generated after immunization with systemic immunization with typhoidal vaccine failed to migrate toward CCL25. Only oral Ty21a, but not the parenteral Vi immunization recapitulates the homing receptor expression in ASCs

(Kantele et al. 2013). Moreover, both the IgG and IgA cells were reported to express integrin α4β7 + CD62L+, indicating their ability to migrate to the gut mucosa and also to peripheral lymph nodes. However, more insights into the homing potential need to be explored for better understanding of the underlying mechanism.

1.10.2. Cell mediated immune responses.

In addition to the humoral responses, studies verified that relevant contribution from the cellular arm is also critical to impart protection against *Salmonella* infection. Both T cell subsets (CD4+ and CD8+ T-cells) were detected in the volunteers, immunized with attenuated typhoidal vaccine or naturally infected with typhoidal *Salmonella* (Salerno-Goncalves, Pasetti, and Sztein 2002; Salerno-Goncalves et al. 2004; Kirkpatrick et al. 2005; Wahid et al. 2008).

1.10.2.1. T-cells.

CD4+ T cells were observed to be more responsive to soluble antigens, whereas CD8+ T cells were chiefly activated by bacteria infected targets (Salerno-Goncalves, Wahid, and Sztein 2010; Salerno-Goncalves et al. 2003). Upon immunization with attenuated typhoidal vaccines, CD4+ and CD8+ T-cells secreting IFN-γ was observed up to 56 days (Salerno-Goncalves, Wahid, and Sztein 2010),(Salerno-Goncalves et al. 2003; Sztein et al. 1994). Cytotoxic CD8+ T-cells cast two different mechanisms for facilitating apoptosis of the target cells. One involves granular exocytosis by perforin and granzyme (Kagi et al. 1996) and the other induces recruitment of FAS or APO-1 (Hanabuchi et al. 1994). Investigations with PBMC from Ty21a (Salerno-Goncalves et al. 2004) and CVD 909 (Wahid et al. 2007) immunized individuals showed that the specific CD8+ T-cells killed *S*. Typhi-infected targets by a granule-dependent pathway. Another concern was raised when no correlation between antibody titer and cellular response could have been established even after several thorough investigations on the basis of volunteer with varied attenuated vaccine strains (Sztein et al. 1994; Salerno-Goncalves et al. 2003). These strongly suggest multifactorial influences targeting both the arms of the immune response in individuals having different genetic makeups and gut microbiome composition.

1.10.2.2. Memory T cells.

Memory T cells can be divided into central memory T-cells (TCM) expressing CD45RO, and CCR7 and CD62L (L-selectin), and effector memory T-cells (TEM) expressing CD45RO with thea downregulation in the expression pattern of CCR7 and CD62L (Sallusto, Geginat, and Lanzavecchia 2004; Sallusto et al. 1999), which circulate and further migrate to non-lymphoid

tissues and spleen. TEMRA or "terminal memory", is another T cell subset, which expresses CD45RA instead of CD45RO (Sallusto, Geginat, and Lanzavecchia 2004; Sallusto et al. 1999). A study observed induction of all these memory T cells which persisted up to 2 years post-immunization with Ty21a (Salerno-Goncalves, Wahid, and Sztein 2010). CD8+ TCM secreting IL-2 and IFN-γ was further found to lead the development of a larger pool of memory T cell subsets, which is indispensable for contributing towards improved protection against re-infection (Salerno-Goncalves, Wahid, and Sztein 2010). CD8. This was further confirmed using multichromatic flow cytometric data, which measured six cytokines concurrently, namely IL-17A, IFN-γ, TNF-α, IL-2, IL-10 and MIP-1β (McArthur and Sztein 2012).

1.10.2.3. Dendritic cell cross-presentation and CD8+ T-cells.

Animal studies with dendritic cells (DCs) showed elicitation of bacteria-specific CD8+ T-cells, involving either direct uptake and processing of antigens or the use of bystander mechanisms indirectly (Sundquist, Rydstrom, and Wick 2004). Upon *S.* Typhi infection, human DC induced significant levels of pro-inflammatory cytokines, IL-8, IL-6, and TNF-α with lower levels of IFN-γ and IL-12 p70 (Salerno-Goncalves and Sztein 2009), whereas, co-culturing DC with Salmonella infected cells prompted induction of strong IFN-γ, TNF-α and IL-12 p70 (Salerno-Goncalves and Sztein 2009), supporting the critical role of IL-12 and IFN-γ in imparting protection against *Salmonella* infection.

1.10.2.4. T cell homing.

Investigations with Ty21a immunization had shown memory CD4+ and CD8+ T-cells, expressing integrin β7 that produced 10-fold higher IFN-γ (Lundin, Johansson, and Svennerholm 2002). Another study with CVD909 showed central, effector memory T populations expressing gut homing markers secreting IFN-γ (Wahid et al. 2008)). Central memory CD4+ T cells express integrin α4β7+ whereas, effector memory CD4+ T cells express integrin α4β7+ and integrin α4β7− cells. On the contrary, IFN-γ secreting CD8+ TEM expresses both α4β7 and α4β7, whereas, CD8+ TEMRA expresses only α4β7 + (Wahid et al. 2008). CD8+ T-cells isolated from the PBMC of the healthy subject co-express higher levels of integrin α4β7 with intermediate expression of CCR9 and lower levels of CD103 (Salerno-Goncalves, Wahid, and Sztein 2005), bearing various TCR Vβ specificities (Salerno-Goncalves, Wahid, and Sztein 2005) that supports long-term persistence of bacteria-specific effector CD8+ T memory cells in the circulation. The above data together indicated multiphasic

kinetics of cell-mediated immune response involving various subset of T and dendritic cells. Upon expression of gut homing markers, these *Salmonella* specific T cells migrate from the circulation to the gut and lymphoid tissues.

1.11. Cross-reactive immune responses among *S.* Typhi, *S.* Paratyphi A.

Owing to the lack of animal models for studying pathogenesis of *Salmonella* Paratyphi A, very few information related to host immune responses to *S*. Paratyphi A infection, is available till date. Majority of the suggestive mechanisms regarding immune responses against *S*. Paratyphi A were inferred from the studies with *S*. Typhi. Induced IgA antibodies upon Ty21a immunization showed T-cell-dependent ADCC against most of the serovars such as *S*. Typhi, *S.* Paratyphi A, and B, but not C (Tagliabue et al. 1986). IgA ASC expressing homing potential, induced after Ty21a immunization, had shown a lesser propensity towards LPS of *S*. Paratyphi A and B compared to *S*. Typhi (Wahid et al. 2012). Similarly, an increased induction of antibodies and memory B cells, specific to *S.* Typhi antigens (LPS and OMP) had shown to cross-react with *S.* Paratyphi A and B, but with a lesser magnitude. All these cross-reactive responses were induced due to the presence of a trisaccharide (mannose–rhamnose–galactose) – "O:12" repeating unit. This structure is preserved in *S*. Typhi, *S.* Paratyphi A, and B. Another surprising finding is the presence of cross reactivity of ASCs induced in Vi-PS recipients towards *S.* Paratyphi A and B, possibly due to lower level of *S*. Typhi LPS contamination with Vi-PS as *S.* Paratyphi A, and B do not possess Vi polysaccharide in their structure (Tacket et al. 1986; Pakkanen, Kantele, and Kantele 2014). Further investigations are required to unveil the basis of the cross-reactive immune responses (humoral and cell mediated immune mechanism) and also to formulate bivalent vaccine to protect against enteric fevers.

1.12. Adjuvants used for augmenting the immune response.

The foremost goal of vaccination includes generation of a strong immune response to the antigen of interest, which further contributes to long-term protection against the infection. However, subunit-based vaccines are reported to be inherently less immunogenic as compared to the whole cell inactivated vaccines or live attenuated vaccines. Hence, inclusion of an immunological adjuvants in the vaccine formulation is increasingly happening in recent approaches (Tritama et al. 2018). The Latin word 'Adjuvants' means to help. Adjuvants modulate the cellular and humoral immune responses against co-administered antigens (Tritama et al. 2018)**.** Adjuvants were being used for improving efficacy of the vaccines since

early 1920's and led to develop a better vaccination schedule. Adjuvants such as aluminium hydroxide, water-in-oil emulsions, bacterial toxins and liposomes were being used in several vaccines, measuring and maintaining the degree of adjuvanticity and the acceptable level of safety. Several other adjuvants including ISCOMS, QS-21, monophosphoryl lipid A and Advax-CpG are being investigated. Interestingly, none of the widely used, commercially available typhoidal vaccines use adjuvants. Licensed Vi capsular polysaccharide vaccine, (Typhim Vi) and Ty21a strain of *Salmonella* serotype typhi, both require multiple doses for generating optimum immune response against typhoid infection (Guzman et al. 2006)**.** Moreover, maintaining precise dosing intervals along with cold chain requirements for storage further add compliance and logistic hurdles. Addition of an appropriate adjuvant ensures re-vaccination at longer time intervals and also reduces the vaccine dose, leading to the increase the cost effectivity of the vaccine candidate (Tritama et al. 2018). Report claimed that the immunogenicity of polysaccharide subunit typhoidal vaccines such as VI-PS (Typhim Vi) and conjugate vaccine VI-TT (Typbar TCV) was exhibited owing to the presence of TLR4 ligands (such as bacterial endotoxin) in these vaccines formulation (Alugupalli 2024). The vaccine antigen, purified Vi polysaccharide, reported to contain trace amount of bacterial polysaccharide during the preparation phase. As being a TLR4 ligand, bacterial polysaccharide further contributed to immunogenicity (Alugupalli 2024). The author assessed Turbo, a monophosporyl lipid A based TLR4 ligand, as vaccine adjuvant for Typhoid vaccine and observed an increased and durable immunogenicity. In another investigation where Vi conjugate vaccines (Vi-DT and Vi-TT) were formulated in alum-based adjuvants either in aluminium hydroxide (AlOH) or aluminium phosphate (AlPO4) confirmed a significantly improved and sustained immunogenicity with AlOH formulation (Tritama et al. 2018). Another study with aluminium phosphate adjuvanted Typhax where Vi polysaccharide is non-covalently entrapped into a glutaraldehyde catalyzed and further cross-linked with a-poly-L-lysine and CRM197 protein matrix, induced immunogenicity but encountered a lesser magnitude of immune response (Cartee et al. 2020). Later, Advax-CpG adjuvant (inulin polysaccharide with TLR agonist) further improved the immunogenicity exerted by the Typhax specifically against Vi polysaccharide (Honda-Okubo et al. 2022). Another study explored multi epitope properties of outer membrane proteins of *S.* Typhi adjuvanted with nanoporous chitosan particles and has been found to significantly augment the protective efficacy of the vaccine candidate (Ayub et al. 2022). Flagellin, being the self-adjuvanting protein, significantly improved the protective efficacy of the lipid A free polysaccharide conjugate vaccine against non-typhoidal salmonella

infections (Chiu et al. 2020). All these investigations concluded that the presence of an adjuvant resulted in improved and durable immune response.

1.13. Unaddressed issues.

All the available typhoidal Vi conjugate vaccines work through circulating antibodies as no intrinsic protein of *Salmonella* antigen is present in this formulation (Simon and Levine 2012). Live attenuated oral vaccines require multiple booster doses for generating optimum response but often reported bacteraemia. Despite that sufficient number of reports suggest production of antibodies against *Salmonella* infection, the relative contributions of humoral and mucosal antibodies and functional attributes of these antibodies are not known yet. Considering the entry of the pathogen through the intestinal route, mucosal immune response in the intestine is highly desirable but not yet addressed with conjugate vaccines. Oral immunization of Ty21a recapitulates gut homing receptor profile of ASC from natural infection, but parenteral Vi conjugate vaccine failed to do so (Kantele et al. 2013). Additionally, no commercial vaccines against paratyphoid fever exist due to the dearth of animal models, coupled with conceptual design lacunae regarding bacterial pathophysiology and host response. Therefore, studies which aim to formulate a bivalent vaccine candidate effective against both *Salmonella* Typhi and Paratyphi with protective mucosal, humoral and cell mediated immune response are the need of this hour.

Chapter 2.

Rationale of Study Objectives

2. Rationale of my study objectives-

According to WHO, high prevalence of enteric fever occurs in the south and south-east Asia and affects primarily children under 5 years of age. There are cases of asymptomatic carriers who develop adenocarcinoma of the gall bladder. Safe drinking **wa**ter, proper maintenance of **s**anitation and food **h**ygiene -**WASH** strategies are considered indispensable for elimination of *S.* Typhi and *S*. Paratyphi A (Kim et al. 2023). Moreover, mass vaccination in the susceptible populations plays the best option to reduce the disease burden in the near future. Commercially available licensed oral vaccines require multiple doses to boost optimum systemic and intestinal secretory antibodies with T cell mediated response. However, large size of the capsules makes it difficult for the children below 6 years of age to swallow. Hence it is not recommended for them (Guzman et al. 2006). Additional risk of bacteremia sometimes reported with live engineered typhoid vaccine which are in clinical trial phase (Guzman et al. 2006). Systemically injectable Vi polysaccharide vaccine showed poor immunogenicity especially in children as it could not evoke T cell dependent immune response. Further, chemical conjugation of a carrier protein, such as tetanus toxoid, to Vi Polysaccharide (called Vi-TT), augments the immunogenicity of the vaccine by converting it to a T cell dependent antigen (Cross et al. 2020). Although, Vi-TT reported to induce higher and sustained immune response by generating memory B and T cells, the induced T cell response is not specific to *Salmonella* antigen. Recent TyVac trials with Typbar TCV in Nepal, Bangladesh and Malawi showed 79%, 85% and 84% protective efficacy (Shakya et al. 2021; Khanam et al. 2023; Liang et al. 2023). However, they exclusively work through the circulating anti-Vi antibodies as no intrinsic *salmonella* proteins are present in this formulation (Simon and Levine 2012). Although current TyVac trials showed protection from salmonella infection in the endemic populations of Nepal, Malawi and Bangladesh, a protective antibody titer was not established yet. Despite of sufficient number of reports suggesting production of antibodies by the glycoconjugate vaccine against *Salmonella* infection, functional attributes of these are not known much. Vi-based vaccines failed to generate gut homing antibody (IgA) secreting cells.
In addition to all these, lack of suitable animal model is a major bottleneck for studying pathogenesis of human restricted pathogen *S.* Paratyphi and assessing protective efficacy of potential vaccine candidates. The increasing incidence of multi-drug resistant typhoid fever has accentuated the burden on the global health sector. Additionally, cases with Vi negative multi drug resistant and extensive drug resistant *salmonella* strains further complicate the situation. This had happened owing to the spontaneous mutations in the regulatory region of the

polysaccharide used. A possible threat associating with the mass immunization program with vi conjugate vaccine employ a selection pressure on the existing Vi negative salmonella strains (Simon and Levine 2012). Vi conjugate vaccine utilize anti-Vi antibodies, hence it did not confer any protection to such Vi negative *S.* Paratyphi A infection. Aiming to develop future vaccines conferring protection against both the serovars, *S.* Typhi and *S.* Paratyphi A, somatic antigens like rT2544, which is conserved across serovars, provide the best opportunity to work with.

Dr Das's laboratory previously reported that systemic administration of T2544, a highly immunogenic outer membrane adhesion protein of *S*. Typhi, confers protection to immunized mice against subsequent challenges with *S*. Typhi. T2544-specific antibodies were detected in both acute as well as convalescent sera of naturally infected humans and strong IgG response was observed in antiserum collected from children younger than five years. This is especially significant because currently licensed vaccines are less effective in young children (Ghosh et al. 2011).

However, considering the entry of the pathogen through the intestinal route, mucosal immune response in the intestine is highly desirable. Here in this study, we further boosted and optimized the mucosal and systemic immune response by conjugating or coadministering it with widely used mucosal adjuvants like CTB and FliC, respectively. Additionally, we developed an animal model to study pathogenesis of *Salmonella* Paratyphi A infection. Our formulated vaccine candidates showed bivalent potency in conferring protection against *Salmonella* Typhi and *Salmonella* Paratyphi A infection.

Here in our study will investigate the followings.

1) **Studies on the adaptive immune response after mucosal and systemic immunization with Salmonella antigens;**
2) **Augmentation of the immune response by adjuvants;**
3) **Exploration of the mechanisms underlying the augmentation of immune response by adjuvants.**

Chapter 3.

Materials And Methods

3. Materials and Methods.

3.1.Materials.

3.1.1. Cells.

HT-29, RAW 264.7, THP-1 cell lines were obtained from American Type Culture Collection (ATCC). Murine intestinal epithelial cells were kind gift from Dr. Philips Tsichlis,Tufts Medical Center, Boston, MA, USA. HT-29, RAW 264.7 and muIECs were maintained in DMEM supplemented with 10% FBS. THP-1 cells were grown in RPMI 1640 supplemented with 10% FBS and 0.05mM 2-mercapto ethanol (Sigma) for 48 h to differentiate them to macrophages. Media was replaced with RPMI-1640 without antibiotics for 24 hr. All cell culture reagents were purchased from Invitrogen. All the cell lines were cultured in presence of 100 U/ml of Penicillin/Streptomycin (Invitrogen) in a 37°C humidified incubator with 5% CO2.Cells near confluence. They were incubated overnight in serum-free medium before experiments.

3.1.2. Bacteria Strains and growth conditions.

S. Typhi strains Ty2, Salmonella Typhimurium LT2 and *E. coli* strain BL21 were generous gifts from J. Parkhill (Sanger Institute, Hinxton, United Kingdom) and Dr. Rupak K. Bhadra (Indian Institute of Chemical Biology, Kolkata, India). *E. coli* strain BL21 DE3 and E. coli strain BL21 DE3 pLysS were purchased from Invitrogen. All the clinical isolates of *S.* Paratyphi A were obtained from Dr. Shanta Dutta (ICMR-NICED, Kolkata). The reference strain of *S.* ParatyphiA 9150 were purchased from ATCC. All *Salmonella* strains were grown in Hektoen enteric agar (BD Difco), whereas other bacterial strains were maintained in Luria–Bertani agar at 37°C. Liquid cultures were grown in Luria–Bertani (LB) broth (BD Difco). All the bacterial strains used are listed in Table 3.1.

Table 3.1. Sources of Bacterial strains used in this study.

Strain	Genotype and Source	Refereence
Salmonella Typhi Ty2	Commercial	ATCC #700931

Salmonella Typhi Ty2 expressing GFP	GFP+ Plasmid electroporated in commercial strain	(Chakraborty et al. 2024)
Salmonella Typhimurium LT2	Commercial	ATCC #25870
Salmonella Paratyphi A	Commercial	ATCC #9130
Salmonella Paratyphi A C1	Vi- ; Clinical	Unpublished
Salmonella Paratyphi A C2	Vi- ; Clinical	Unpublished
Salmonella Paratyphi A C3	Vi- ; Clinical	Unpublished
Salmonella Paratyphi A C4	Vi- ; Clinical	Unpublished
Salmonella Paratyphi A C5	Vi- ; Clinical	Unpublished
Salmonella Paratyphi A C6	Vi- ; Clinical	Unpublished
Salmonella Paratyphi A C7	Vi- ; Clinical	Unpublished
Salmonella Paratyphi A C8	Vi- ; Clinical	Unpublished
Salmonella Paratyphi A C9	Vi- ; Clinical	Unpublished
Salmonella Paratyphi A C10	Vi- ; Clinical	Unpublished
Vibrio Cholerae N16961	O1 El Tor; carRr Amps Strr PBr	(Samanta et al. 2020)
E. coli BL21 (DE3)	Commercial	Novagen #69387

3.1.3. Plasmids.

pTZ57R/T, pBSIIKS and pET28a were purchased from Thermo-Fisher, Addgene and Novagen respectively.

3.1.4. Reagents used in this study.

Molecular biology reagents were purchased as follows:
DNA restriction enzymes were purchased from New England Biolabs (NEB). cDNA synthesis reagents and SYBR Green Master Mix were procured from Fermentas and ABI. HRP-conjugated secondary antibodies were from Pierce. All other chemicals were purchased from Sigma-Aldrich unless otherwise mentioned.

3.1.4.1. Chemicals.

Streptomycin, Kanamycin, Ampicillin, Di-Thiothreitol (DTT), Isopropyl β-D-1-thiogalactopyranoside (IPTG), 5-Bromo-4-chloro-3-indolyl β-D-galactopyranoside (X-Gal), Lipopolysaccharide, Lectin from pokeweed, Protein A from *Staphylococcus aureus*, BCIP/NBT substrate, LDH assay kit, Bovine serum albumin (BSA) and Gentamicin were purchased from Sigma Aldrich, USA. AEC (3 amino 9 ethyl carbazole) were from Calbiochem. ODN 1826, Murine recombinant GM-CSF and IL-2 proteins were purchased from Invivogen and R&D systems, USA respectively. Vi-TT was procured from Bharat Biotech. All the ELISA and ELISPOT kits used, are listed below in Table 3.2.

Table 3.2. ELISA and ELISPOT kits used in this study.

ELISA kit (mouse)		
Kit name	Cat #	Manufacturer
IL2	555148	BD Biosciences
IL-4	555232	BD Biosciences
IL-5	555236	BD Biosciences
IL-6	555240	BD Biosciences
IL-10	555252	BD Biosciences
IL-12	555256	BD Biosciences
IFNγ	DY485-05	BD Biosciences
TNFA	558534	BD Biosciences
ELISPOT kit (mouse)		
Kit name	Cat #	Manufacturer
IFNγ	EL485	R&D
IL-17	EL421	R&D

3.1.4.2. Antibodies.

All the antibodies used, are listed below in Table 3.3.

Table 3.3. Antibodies used in this study.

ANTIBODY (flow cytometry)				
Antigen (mouse)	Flurochrome	Origin	Cat #	Manufacturer
CD4	APC H7	Rat	560181	BD biosciences

CD4	PE	Rat	553048	BD biosciences
CD3	perCPcy5.5	Rat	560527	BD biosciences
B220	PeCy7	Rat	552772	BD biosciences
CD11C	FITC	Mouse	557400	BD biosciences
MHC II (I-A^d)	BIOTIN-STREPTAVIDIN PE	Mouse	553546 554061	BD biosciences BD biosciences
CD103	APC	Rat	562772	BD biosciences
A4B7 (LPAM)	PE CF594	RAT	562668	BD biosciences
CCR9 (CD199)	PE	Mouse	565576	BD biosciences
PD1 (CD279)	PE	Hamster	561788	BD biosciences
CxCR5	FITC	RAT	561989	BD biosciences
CD44	APC	Rat	561862	BD biosciences
CD62L	PeCy7	Rat	560516	BD biosciences

ANTIBODY (western blot)				
Antigen (mouse)	Flurochrome	Origin	Cat #	Manufacturer
HIS-tag (western blot)	Nil	Rabbit	2365S	Cell Signaling Technology

ANTIBODY (ELISA)				
Antigen (mouse)	Flurochrome	Origin	Cat #	Manufacturer
Anti mouse IgG – HRP		Goat	31432	Thermo
Anti rabbit IgG –HRP		Goat	31464	Thermo
Anti mouse IgA- HRP		Goat	A4789-1ML	Sigma
Anti mouse IgG1 – HRP		Rabbit	SAB3701171-1MG	Sigma

Anti mouse IgG 2a– HRP		Rabbit	SAB3701178-1MG	Sigma
ANTIBODY (ELISPOT)				
Antigen (mouse)	Flurochrome	Origin	Cat #	Manufacturer
IgG-HRP (human adsorbed)	HRP	Goat	1030-05	Southern biotech
IgA-AP	AP	Goat	1040-04	Southern biotech

3.1.4.3. Oligos.

Oligos were custom-synthesized from IDT, USA and listed in Table 3.4.

Table 3.4. Oligonucleotides used in the study.

Sequence	Description	Application
CTB fus Prot FP	CGCGGATCCACACCTCAAAATATTACT GATTTGTG	Cloning of ctxB in pET28a
CTB fus Prot RP	GCCGTCGACATTTGCCATACTAATTGCG GC	Cloning of ctxB in pET28a
Fus T2544 FP	GCCGTCGACGGACCAGGACCAGAAGG GATCTATATCACCGGG	Cloning of t2544 in pET28a
FusT2544RP	GCCCTCGAGTTAAAAGGCGTAAGTAAT GCCGAG	Cloning of t2544 in pET28a
FliC FP	GAATTC AAGATCATGGCACAAGTCATT	Cloning of fliC in pET28a
FliC RP	CTCGAG TCAATCGCCGGATTAACGCA	Cloning of fliC in pET28a
fliC com-s	AATCAACAACAACCTGCAGCG	Confirming *Salmonella* Paratyphi A strain.
fliCa-as	TAGTGCTTAATGTAGCCG AAGG	Confirming *Salmonella* Paratyphi A strain.

3.2. Methods.

3.2.1. Cloning of rCTB, rT2544, rCTB-T2544 and rFliC.

Open reading frame (ORF) of *ctxb gene* without signal peptide region was PCR amplified from *V. Cholerae* and cloned in pET28a vector between BamHI and SalI restriction sites (listed in Table 3.4**.**). Next, ORF of t2544 (total sequence length of 663bp) including an upstream linker sequence (ggaccaggacca - gene codon of a non-furin linker containing glycine and proline amino acids) was PCR amplified and cloned between SalI and XhoI restriction enzymes of pET28a-CTB plasmid**.** Simultaneously, ctxb and t2544 gene was cloned separately in pET28a plasmid. This recombinant clone was further validated by DNA sequencing. Similarly, ORF of fliC was cloned between EcoRI and XhoI pET28a plasmid and validated by DNA sequencing.

3.2.2. Expression of the recombinant proteins (rCTB, rT2544 and rCTB-T2544, rFliC).

These threes newly developed constructs were transformed into the bacterial expression host *E. coli* BL21 (DE3) and the recombinant fusion protein expressions were induced with 1mM IPTG by culturing the bacteria in Luria Broth medium at 37°Cs. All the proteins were extracted as an insoluble protein from inclusion bodies by sonication and solubilized with 8M urea in denaturing condition. Next, these denatured proteins were subjected to affinity chromatography using Ni2+conjugated agarose (Qiagen) and then renatured by gradual removal of urea by dialysis using a 10kD membrane. and the purity was confirmed by SDS-PAGE, stained with Coomassie Brilliant Blue. The Proper folding renatured protein was confirmed by Circular Dichroism. Purified proteins were next quantified using Bradford Reagent and the size of the recombinant proteins were confirmed by SDS-PAGE stained with Coomassie Brilliant Blue.

Similarly, expression of the rFliC protein was induced using 1mM IPTG (Isopropyl β-D-1-thiogalactopyranoside). Next, the induced and uninduced (prior to IPTG induction) bacterial cells were harvested by centrifugation at 5000rpm for five minutes at 4°C. The pellet was resuspended in binding buffer (20 mM Tris pH 8.0, 500 mM NaCl, 10 mM Imidazole) and lysed with sonication on ice. Next the sonicated solution was clarified by centrifugation at 15000 rpm for 20 min at 4°C. The supernatant containing the fliC was added onto the Ni-NTA agarose loaded column followed by washing with 30 column volume of binding buffer. Further the recombinant protein, rFliC, was eluted using elution buffer (20 mM Tris pH 8.0, 400 mM

NaCl, 400 mM imidazole) and dialyzed against PBS (pH=7.4) using three buffer changes. The purity and specificity of purified protein, r FliC was determined by 10% SDS-PAGE and quantified using Bradford Reagent.

3.2.3. Circular Dichroism (CD Spectra).

CD spectra were recorded on Jasco-1500 spectrophotometer. 1.0 ml aliquotes of sample (150µg/ml) of each protein was loaded into a quartz cell and minimum of three spectra for each of the sample were recorded in the wavelength ranging from 200 to 300 nm at 25°C. Finally, the recorded spectra were smoothed, corrected, and analyzed.

3.2.4. Immunoblot and pentamer analysis assay.

Aliquotes of each of the protein samples were subjected to SDS-PAGE and later electro-transferred to PVDF membrane (Millipore). After blocking with 5% BSA in PBS containing 0.05% Tween 20 for 1h, membranes were incubated overnight with anti-His antiserum (1:2500 dilution) at 4°C. Next, the membrane was washed and incubated with HRP conjugated anti-rabbit IgG (1:10,000) for another 1 hour. Then, the membrane was developed by adding chemiluminescent substrates (Super Signal West Pico, Thermo Scientific) and images were captured in Chemi Doc.

To assess whether our recombinants protein rCTB-T2544 folds into pentameric state during SDS-PAGE, samples were subjected to non-denaturing and denaturing conditions. For non-denaturing conditions, samples mixed with sample loading buffer devoid of β-mercaptoethanol and DTT and were not placed in boiling. Finally, samples were run on SDS PAGE and stained with Coomassie Brilliant Blue.

3.2.5. Endotoxin detection assay.

The endotoxin level present in purified proteins were quantified according to the Pierce™ Chromogenic Endotoxin Quant Kit. Briefly, 50µl of different dilutions of endotoxin standard and test samples (1mg/ml) were added to the plate which was preequilibrated with heat at 37°C. Next 50µl of Amebocyte lysate reagent was added to each well and gently mixed and was incubated for 30min. Later, 100µl of pre-warmed chromogenic substrate were added and incubated for 6min followed by addition of 50µl of stop solution (25% acetic acid) to each well and absorbance were measured at 405nm. A standard curve was prepared from the absorbance

of the endotoxin standard solutions. The endotoxin contaminations in each protein were calculated using the standard curve.

3.2.6. Animal experiments.

3.2.6.1 Animal housing.

All animal experiments were carried out as per the ethical approval (PRO/176/-MAY2023, dt. 14.05.2020) accorded by the animal ethical committee of ICMR-National Institute of Cholera and Enteric Diseases (NICED), Kolkata, India. All the animals were taken from in house animal facility of NICED (registration number. 68/GO/ReBi/S/99/CPCSEA) and maintained at 25°C and 45-55% humidity with 12-h alternate light and dark cycles.

3.2.6.2. Immunization schedule and sample collection.

3.2.6.2.1. Immunization and sample collection scheme.

Immunogenicity was studied by intranasal administration of 60µg of the recombinant proteins into female BALB/c mice (~5weeks old) for three times at 12 days intervals. Mice were bled from the tail vein to collect blood on days 0, 11, 23, 35, 108, and 120 without sacrificing them. Stool was also collected prior to each immunization dose and 12days after the last immunization dose. In a separate experiment, serum, stool, and intestinal wash were collected from the experimental mice twelve days after the last immunization. Another subcutaneous regimen with rT2544 admixed with rFliC (TF) uses 5ug and 12ug of rT2544 with 2.5ug of rFliC at seven days interval for consecutive four weeks. The blood was collected prior to each immunization and seven days after last immunization. The mice were euthanized in a euthanasia chamber following the gradual carbon dioxide filling method from a compressed CO2 gas cylinder followed by decapitation as per the American Veterinary Medical Association (AVMA) guidelines approved by IAEC. Samples were collected and stored at −20°C.

3.2.6.2.2. Preparation of Antiserum.

Blood samples were collected from mice of different immunized groups and incubated for 30 mins at 37°C. Next, the antiserum was separated from blood after centifugation at 1000g for 15 mins at 4°C. Feces were collected weighed, and suspended in100mg/ml of PBS containing 1% BSA, and vortexed for 30 mins at 37°C. Fecal wash containing antibodies were later

separated using centrifugation at 15,000×g at 4°C for 10min and stored at −20°C admixing with Protease inhibitor cocktails (Sigma-Aldrich). Simultaneously mice from different immunized groups were sacrificed and intestinal segments were isolated and washed with PBS containing 1%BSA (BSA, SRL). Next, intestinal lavage were separated using centrifugation at 10,000g at 4°C for 10min and mixed with protease inhibitor cocktails prior storing at -20°C.

3.2.6.3. Animal infection and protective efficacy.

3.2.6.3.1. Iron (Fe3+) Overload Mouse Model of *S*almonella infection.

An iron overload mouse model was used for oral *S*. Typhi and *S.* Paratyphi A infection (Chakraborty et al. 2024). Briefly, an iron-overload condition was created by administering injecting desferrioxamine (DFO; Novartis) (0.025 mg/g of body weight) and Fe3+ as FeCl3 (0.32 mg/g of body weight) intraperitoneally 5 h prior to the bacterial challenge. Log phase cultures of bacteria were re-suspended in sterile PBS buffer and were fed orally after neutralization of the gastric acid with 5% Sodium Bicarbonate. Mice were orally challenged with 5×10^7 *S.* Typhi and 5×10^5 *S.* Paratyphi A bacteria and monitored for 10 days.

To assess the virulence of *S.* Paratyphi A, 9-10 weeks old iron overloaded female Balb/c mice were challenged with different doses of *S.* Paratyphi A (5×10^4, 5×10^5, 5×10^6. The 50% lethal doses (LD_{50}) of the bacterial cultures were assessed by monitoring deaths within 12 days after infection.

3.2.6.3.2. Adult mice Ileal loop model.

In a separate experiment, mice from different immunized groups (rCTB, rT2544 and rCTB-T2544) were subjected to an ileal loop experiment. Briefly, mice were anaesthetized by intraperitoneal injection of a mixture of ketamine (35mgkg−1bodyweight; Sterfil Laboratories Pvt. Ltd, India) and xylazine (5mgkg−1bodyweight, AstraZeneca Pharma Ltd, India). A small abdominal incision was made and a loop (2–3cm in length) in the distal ileum was created by suture. The closed ileal loop was instilled with 100ng of cholera toxin (Sigma). After 8h of the surgery, mice were euthanized by gradual carbon dioxide inhalation. The loop weight/length ratio was quantified 8h later.

3.2.6.4. Bacterial load determination in intestinal tissues and visceral organs.

To study the bacterial load in the intestinal tissues and visceral organs, groups of mice (n=6/data points) were challenged with sub-lethal dose of *S.* Typhi Ty2 and *S.* Paratyphi A C1. Intestinal segments such as Ileum, Cecum and Colon and reticulo-endothelial organs viz liver and spleen were collected on different time points post infection (day 2, day 4, day 6) and weighed. Organs were homogenized and macerated to make single-cell suspensions in sterile PBS. Cell pellets were collected by centrifugation at 800X*g* for 5 m and were re-suspended in PBS containing 1% Triton-X, and serial dilutions were spread on LA plates with appropriate selection. In a separate study, mice were immunized and later infected with sublethal dose to investigate bacterial colonization in immunized mice post infection.

3.2.6.5. Bacterial shedding in feces.

Iron overloaded mice were orally infected with *S.* Paratyphi A. Day 2, 4 and 8 post infection, feces were collected, weighed, suspended in PBS and vortexed for 30 mins. Further, the vortexed fecal solutions were diluted and plated. Recovered bacterial colonies were counted and plotted.

3.2.6.6. Histological procedures for Macroscopic and microscopic evaluation.

Segments of the cecum, colon and ileum from all the experimental mice were collected, fixed in 4% paraformaldehyde and embedded in paraffin as per standard procedures. Next, they were cut in sections and stained with hematoxylin and eosin and mounted on slide for microscopic evaluation using Olympus AX70 Microscope. The pathological scoring system [adapted from (Erben et al. 2014)], is listed in Table 3.5.

Table 3.5. Histopathological scoring system.

Scoring system for small intestinal tissue section-					
Severity	Extent of Inflammatory cell infiltrate	Score A	Intestinal architecture-Epithelial changes	Mucosal architechture	Score B
Mild	Mucosa and sometimes submucosal	1	-	Mild villous blunting	1

Moderate	Mucosa and sometimes submucosal	2	Mild hyperplasia	Moderate villous blunting	2
Marked	Mucosa and submucosa, sometimes transmural	3	Moderate hyperplasia and goblet cell loss	Moderate villous blunting and broadening. Sometimes villous atrophy	3
Marked	Transmural	4	Marked hyperplasia and goblet cell loss	Villous atrophy, ulcerations	4
				Sum of score A and B	0 - 8
Scoring scheme for cecal and colonic tissue sections-					
Severity	Extent of Inflammatory cell infiltrate		Intestinal architecture-Epithelial changes	Mucosal architechture	Score
Mild	Mucosa and sometimes submucosal		Minimal Hyperplasia		1
Moderate	Mucosa and sometimes submucosal		Mild hyperplasia, minimal goblet cell loss		2
Marked	Mucosa and submucosa, sometimes transmural		Moderate hyperplasia, mild goblet cell loss		3
Marked	Transmural		Marked hyperplasia with moderate to marked goblet cell loss	Ulcerations, crypt loss	4
					Score 0 – 4

3.2.7. Enzyme linked immunosorbent assay (ELISA).

3.2.7.1 GM1 ELISA.

The binding affinity of the all the purified recombinant proteins (rCTB, rT2544, rCTB–T2544) for the GM1-ganglioside was analysed by GM1-ELISA**.** Briefly, ELISA plates were first coated with GM1 ganglioside at 4°C overnight (1µg/well). Next, after washing the wells with PBS-T (Phosphate buffer saline containing 0.05% Tween 20), blocking was performed with 5% BSA in PBS for 1h at 37°C. Further, the wells were incubated for 2h at 37°C with 100 µL of the recombinant proteins, serially diluted in PBS, and then washed again. Anti-His antibody (Cell Signaling Technology) (1:2500 dilution) was added to the plates and incubated for additional 1h at 37°C, followed by repeated washing with PBS-T. The wells were incubated with HRP-conjugated, goat anti-rabbit IgG for 1h at 37°C and later developed by adding tetramethylbenzidine (TMB) (BD) substrate at room temperature. The absorbance was measured at 450nm using a microplate reader.

3.2.7.2. ELISA for evaluating serum, fecal and intestinal antibody titer.

To evaluate antibody titers (on days 0, 12, 24, 36, 108, 120), 96 well microtitre plates were coated with purified proteins (10ng/ well) overnight at 4°C. Next, wells were blocked with 1%BSA in PBS for preventing non-specific binding. Further, the test samples (serum, fecal extract, or intestinal wash contents) were serially diluted in PBS and added to the wells for 2h. HRP-conjugated, goat anti-mouse IgG (1:10000) and goat anti-mouse IgA (1:5000) antibody were added to the respective wells and incubated for 1h at 37°C. Further, the plates were developed using TMB substrate and the absorbance was measured using a microplate reader at 450nm.

3.2.7.3. Avidity Assay.

To measure the generated avidity of IgG antibody against rT2544 in mice, the sera (diluted 1:100) from CTB-T2544 and T2544 immunized mice after primary and booster immunization were allowed to react with rT2544 coated wells for 2h at 37°C. The wells were washed thrice for 5 mins with PBS-Tween 20 with or without 4M urea. Next, HRP-conjugated, goat anti-mouse IgG antibody to the wells and incubating for 1h at 37°C.The plates were developed using TMB substrate and the absorbance was measured using a microplate reader at 450nm.The avidity index was represented as the ratio of the absorbance of the wells washed with and without 4MUrea containing buffer and multiplying the value by 100.

3.2.7.4. Quantification of Cytokines by ELISA.

Cytokines present in serum were quantified by ELISA kits (eBiosciences), following manufacturer instructions. For quantification, wells of ELISA plate were coated with 100 µL/well of diluted capture antibody overnight at 4°C. Next, wells were washed thrice with wash buffer and blocked with 200 µL/well of 1X ELISA diluent for 1 h. Further, wells were then incubated with 100 µL/well of diluted serum for 2 h at room temperature. Wells were next washed with wash buffer and incubated with 100 µL/well of diluted detection antibody at room temperature for 1 h. Wells were washed again with wash buffer, followed by incubation with 100 µL/well of diluted Avidin-HRP at room temperature for 30 m. Wells were again washed with wash buffer and were developed with 100 µL/well of 1X TMB solution for 15 m. 50 µL of stop solution was added to each well and absorbance was taken at 450 nm.

3.2.8. Enzyme-linked Immunospot (ELISpot) assay.

Mixed cellulose ester membrane-bottom plates (Millipore) were coated with rT2544 or anti-mouse total immunoglobulin overnight at 4°C. Coated wells were first blocked with 1%BSA for 2h at 37°C. Cells isolated from spleen, mesenteric lymph nodes (MLN), Peyer's Patches (PP) of immunized mice was added to blocked wells for 5h, followed by washing with PBST. The plate was incubated with enzyme-conjugated anti-mouse IgG and IgA (Southern Biotech) overnight at 4°C and developed with substrate. The number of spots was counted separately for each well. In a separate experiment, IFN-γ (ELISpot set from BD Bioscience) and IL-17 (ELISpot kit from R&D) pre coated mixed cellulose ester membrane-bottom plates were incubated with cells isolated from Peyer's Patches (PP) stimulated with rT2544 for 24h. The plate was incubated with enzyme-conjugated anti mouse IFN-γ and IL-17 antibodies and developed with substrate. The number of spots was counted separately for each well**.**

3.2.9. RNA Isolation and quantitative real-time PCR.

Dendritic cells (DCs) were separated from the rest of the cells present in the MLN of the PBS-immunized and experimental immunized mice using CD11c+ magnetic beads (Miltenyi Biotech). Total RNA was extracted from the DCs, and cDNA was prepared using a cDNA synthesis kit according to the manufacturer's instructions. Transcript levels were determined by quantitative real-time PCR, using SYBR Green PCR Master Mix (Applied Biosystem) on Step One Plus real time PCRsystem (Applied Biosystem).

3.2.9.1. RNA Isolation.

Total RNA from the isolated dendritic cells were i3solated using TRIZOL Reagent (Life Technologies). Briefly, cells were pelleted and lysed with 200 µL of TRIZOL and homogenized and collected in a centrifuge tube. 40 µL of chloroform was added to the cell lysate and later was vortexed and centrifuged at 12000X*g* for 15 m at 4°C. Post centrifugation 100 µL of 2-propanol was added to the aqueous phase (containing RNA) collected. Tubes were allowed to stand at room temperature for 15 min and further were centrifuged at 12000X*g* for 15 min at 4°C. RNA was precipitated in this step and washed with 200 µL of cold 70% ethanol, followed by centrifugation at 7,500X*g* for 10 min at 4°C. RNA pellet was further air dried and dissolved in nuclease-free water at 65°C for 15 min. Quantity of RNA was measured by absorbance at 260 nm and quality by ratio of absorbance at 260 and 280 nm using spectrophotometer.

3.2.9.2. cDNA synthesis.

cDNA was synthesized from the extracted RNA using SuperScript™ II reverse transcriptase (Life technologies) following manufacturer's manual. To this end, 1 µg of extracted RNA, Random hexamer or 100 pmol of Oligo(dT) and 1 µL of dNTP Mix (10 mM each) were mixed with sterile and nuclease-free water to make a final volume of 12 µL in sterile and nuclease-free tube. Tubes were incubated further at 65°C for 5 mim in thermocycler and immediately snap chilled on ice. Next, 4 µL of 5X First-Strand buffer, 2 µL of 0.1 M DTT, 1 µL of RNase Inhibitor (40 U) and 1 µL of SuperScript™ II reverse transcriptase (200 U) were added to each tube, mixed and centrifuged. Reverse transcription was performed by incubating the tubes for 10 m at 25°C followed by 50m at 42°C. Finally, the reaction was inactivated by heating the tubes for 10 m at 72°C.

3.2.9.3. SYBR-Green® Real Time PCR.

Real Time quantitative PCR (qPCR) was performed in Step One Plus System (Applied Biosystems) using Power SYBR®-Green master mix (Applied Biosystems).
qPCR sample assembly for single reaction: SYBR®-Green master mix, template, Forward and Reverse primer each and of sterile and nuclease-free water.
Thermal cycling parameters for qPCR: Step 1: Initial Denaturation at 95 °C for 5 mins; Step 2 (40 cycles): Denaturation at 95 °C for 20 sec, Annealing and Extension at 60°C for 1 min; Step 3: Melt Curve analysis (Included for the verification of specificity of the amplified products).

Relative quantitation was done by the comparative CT method (Chakraborty et al. 2009) and fold change was calculated using $2^{-\Delta\Delta}$**Ct**. GAPDH levels were taken for normalization, fold changes were calculated using $2^{-\Delta\Delta Ct}$.

3.2.10. Bone marrow-derived dendritic cells (BMDCs) generation.

Dendritic cells were generated from Bone Marrow (BM) cells collected from femurs and tibias of BALB/c mice as described in (Lutz et al., 1999). In brief, BM cells were collected from femurs and tibias of BALB/c mice by flushing out these cells using complete RPMI 1640 medium. About 5×10^6 BM cells were cultured in 90 mm culture dish in complete RPMI 1640 medium supplemented with murine recombinant GM-CSF (20 ng/mL). 60% of culture medium was replaced on every 3rd day with fresh complete RPMI 1640 medium containing GM-CSF. Cells were collected on day 7 (when CD11c positivity was found to be >90%) and seeded as per requirement.

3.2.11. Flow cytometry.

3.2.11.1. Dendritic cells.

CTB-T2544 and PBS immunized mice were euthanized by gradual carbon dioxide inhalation after 12days of three successful immunizations. $CD11c^{int}$ $MHCII^{hi}$ $CD103^{+}$ cells were stained with fluorochrome-tagged antibody and evaluated using flow-cytometer.

3.2.11.2. Gut homing B and T cell.

B and T cell subsets were isolated from the MLN and spleen of the all experimental mice and stained with fluorochrome-conjugated CD3+ CD4+ α4β7+ CCR9+ antibodies (BD Biosciences) against specific surface markers. After staining, the cells were washed and analyzed by flow cytometry (BD FACS ARIAII) following standard protocol.

3.2.11.3. Memory T cell assay.

Dendritic cells were generated from bone-marrow (BM) cells collected from the femurs and tibias of BALB/c mice as described in the 3.2.10. Cells were collected on day 7 and starved by culturing in RPMI 1640 containing 1% FBS for 12h, before treatment with rT2544 for 24h. To generate memory T cells, immunized mice were euthanized by gradual carbon dioxide inhalation. CD4+T lymphocytes were isolated from the immunized mice after 120 days and co-cultured for 5days with antigen-pulsed BMDCs at 37°C and in the presence of 5% CO2.

Memory T cells (CD4+CD62LlowCD44hi, CD4+CD62LhiCD44hi) were studied by flow cytometry and the culture supernatants were assayed for IFN-γ by ELISA.

3.2.12. In vitro serum bactericidal assay.

Sera were collected from the PBS, rT2544 and rT2544 + r FliC immunized mice on seven days after the fourth immunization and were heat inactivated for 1 h in a 65 °C. Next, 10^6 CFU of bacteria from log phase cultures (OD600=1.00) were opsonized by incubating them with various dilutions of the heat-inactivated sera containing 25% guinea pig complement in a 50 µL reaction for various durations. The reaction was stopped by adding Luria broth (950 µL) and various dilutions of the reaction mixtures were spread on Luria Agar plates containing streptomycin (50 µg/ml) for *S.* Typhi or on HEA plates for *S*. Paratyphi A. Reactions containing un-opsonized bacteria were used as the control.

Percent Lysis was quantified by the following formula: 100−100[(CFU of experimental wells)/(CFU of control wells without antisera)].

3.2.13. Cytotoxic T lymphocyte (CTL) assay.

For in vitro CTL assay, CD8+ T lymphocytes were isolated from the spleens of immunized C57BL/6 mice using Anti-Mouse CD8+ magnetic particles (BD Biosciences) according to the manufacturer's protocol. Isolated CD8+ T cells were activated by culturing them with rT2544 pulsed EL4 cells (EL4 cells incubated with 1 µg/ml rT2544 for 30 min) at the ratio of 20:1 (Hess et al. 1996). Viable T lymphocytes in the cocultures were separated by ficoll density gradient and used as effector cells. These cells were incubated with the target cells (rT2544 pulsed EL4vcells) at various ratios in 96 well plates for 5 h at 37 °C. LDH activity of the cell supernatants were measured by LDH assay kit (Takara, Japan) and the percentage specific lysis was calculated by the following formula: (ER – TS – ES)/ (MR – ES) X 100; Where, ER represents experimental LDH release (activity in the supernatants of the target cells, incubated with the effector cells), TS represents spontaneous LDH release from the target cells (activity in the supernatants of the target cells alone), ES represents spontaneous release from the effector cells (activity in the supernatants of the effector cells alone) and MR represents maximum release from target cells (activity in the supernatants of the target cells lysed with 1% Triton-X 100).

3.2.14. Myeloperoxidase (MPO) activity.

Colonic tissues were first Snap frozen, later homogenised in hexadecyl trimethyl ammonium bromide (HTAB) buffer (0.5% of HTAB, 50 mM potassium phosphate, pH 6.0; 50mg tissue/ml) followed by sonication. Protein was estimated using DC protein assay kit using manufacturer instructions (Bio-Rad). 100 µl of HTAB buffer containing equal amount of proteins were added into 2.9 ml of reaction buffer (50 mM potassium phosphate buffer, pH 6.0, containing 0.167 mg/ml o-Dianisidine and 0.0005% H2O2). Change in absorbance at 450 nm at regular time interval of 3 min was recorded. MPO activity was calculated and expressed in U/mg of protein. 1 U of activity was defined as change in absorbance of 1.0 per minute at 25 °C.

3.2.15. Quantitation of cell associated bacteria.

3.2.15.1. Invasion assay.

Murine IEC cell monolayers (5 x 10^5 cells/well) were infected with reference and clinical strains of *S.* Paratyphi A at 1: 100 MOI for 30 mins and then washed thrice with 1X PBS. The cells were further kept for additional 90 mins in a CO2 incubator min at 37°C with the media containing 100µg/mL gentamicin. Next, the cells were again washed thrice with 1X PBS and intracellular bacteria were released by the addition of 1% Trition X-100 in PBS. The cell lysate was gradually diluted and plated on HEA plate to determine viable bacterial counts. Intracellular CFU counts were plotted as percentage of bacteria recovered after 90 mins post infection with respect to the initial inoculum.

3.2.15.2. Intracellular survival assay.

RAW264.7 cells were seeded in 24 well plates at 2.5 × 10^5 cells per well for 24 hr. Cells were further infected with bacteria, at a bacterium to cell ratio of 10:1 for 60 mins. Thereafter, cells were washed thrice with 1X PBS, and extracellular bacteria were eliminated by incubating the cells in DMEM containing 100 ug/ml gentamicin for another 60 mins. Next, the medium was replaced with DMEM containing 10ug/ml gentamicin and was kept for 24 h. The cells were washed three times with 1X PBS. The intracellular bacteria were released by the addition of 1% Trition X-100 in PBS. Lysates were serially diluted and plated on HEA plate. Intracellular CFU counts were plotted as the number of recovered intracellular bacteria at 24h post infection divided by the number of invading bacteria after gentamycin treatment (100 ug/ml).

3.2.15.3. Bacterial adhesion inhibition assay.

Bacterial cell suspensions were pre-incubated for 30 min with 1:50, 1:500, 1:5000 dilutions of the heat-inactivated immune serum, fecal extracts or intestinal contents. HT-29 Cell monolayers (5×10^5 cells/ml) were infected with bacteria at 1:10 M.O.I (multiplicity of infection) and synchronized by centrifugation at 400×g for 5 min. Infected cells were incubated for 30 min and non-adhering bacteria were washed off with 1XPBS. Adherent bacteria were quantified by CFU counts after cell lysis with1% triton-X100 and spreading over the lysates on LA agar plates containing Streptomycin 50µg/ml. In parallel experiment, *S*. Typhi Ty2 was electroporated with pAK-GFP1 vector expressing GFP to enable visualization of the bacterium at 488 nm. *Salmonella* Typhi Ty2 expressing green fluorescent protein (appearing green) were pre-incubated for 30 mins with the serum, feces and intestinal lavage from different immunized groups and used for infection of HT-29 cell monolayer. Nucleus of the cell was stained with Hoechst (appearing blue) and the cells were viewed under confocal microscope. In a separate experiment, naïve mice were infected with or without bacteria pretreated with mucosal antibody present in fecal extract and intestinal wash. Mice were euthanized by gradual carbon dioxide inhalation on day 2, 4, 6 post-infection, and bacterial colonization was assessed in intestinal tissues and visceral organs.

3.2.15.4. Opsonophagocytosis assay.

Bacterial cell suspensions were pre-incubated for 30 min with 1:50 dilution of the heat inactivated immune serum, fecal extracts, or intestinal contents at 37°C to allow for opsonization. The opsonized bacteria were then added to the THP-1 cell-derived macrophage monolayers (5×10^5cells/ml), cultured in antibiotic free complete medium at a multiplicity of infection of 1:10(cell/ bacteria) and centrifuged at 400×g for 5 min to allow adhesion. The plates were incubated for 30min at 37°C. Following incubation, plates were washed three times with PBS. Extracellular bacteria were killed by incubating the plates with complete medium containing gentamicin (200µg/ml) for 60min. After washing the plates thrice with PBS, cells were lysed with1%Triton X-100 for 15minat 37°C. The lysates were diluted in PBS and plated onto LA agar plates containing Streptomycin 50µg/ml. In a parallel experiment, GFP-expressing *S*. Typhi Ty2 (appearing green) were pre-incubated with serum and fecal extracts or intestinal lavage. THP-1 cell monolayers were used for infection with the opsonized bacteria for 1h, followed by gentamicin protection assay. Nucleus of the cell was stained with Hoechst (appearing blue), followed by viewing under confocal microscope.

3.2.15.5. Motility assay.

10ul of the overnight grown *S*. Paratyphi A clinical and reference bacterial cultures were placed onto LB plate containing 0.3% agar. The plates were kept 8 h at 37°C without being inverted. The diameters of the concentrically growing bacterial cultures were measured and plotted.

3.2.15.6. Motility inhibition assay.

0.4% Bacto agar was mixed with 5% serum, fecal, or intestinal extracts were added to LB medium and poured on plates and allowed to dry at room temperature for 30min. Bacterial culture was inoculated on the center of the plate and placed at 37°C. The diameters of the concentrically growing bacterial cultures were measured for 6h and plotted.

3.2.16. Statistical Analysis.

Statistical analyses of data were performed using Graph Pad Prism 8.0.1.244. Log rank Mantel-Cox test was performed to analyze survival curves. Unpaired t test was used to compare between two groups, while one-way and two-way ANOVA with post hoc Tukey's multiple comparison tests were performed to compare amongst more than two groups. A P value of <0.05 was considered significant; *p:0.3332,**p:0.0021***p:0.0002,****p<0.0001. Data represented as mean ± SD. Error bars represent SD.

Chapter 4.

OBJECTIVE 1.

Studies on the adaptive immune response after mucosal and systemic immunization with Salmonella antigens

4.1. Introduction.

Commercialized Typhoid vaccines are modestly effective and work through the induction of systemic antibody response. Recent TyVac trials in Nepal, Bangladesh and Malawi with Typbar TCV showed 79%, 85% and 84% protective efficacy (Shakya et al. 2021; Khanam et al. 2023; Liang et al. 2023). However, these studies could not establish an absolute protective value for IgG and IgA titer in human. Reported literatures already showed that despite presence of elevated serum antibodies against *Salmonella* antigens, patients who recovered from typhoid fever, remain vulnerable to reinfection (Das et al. 2017). High anti Vi antibodies were also reported from the chronic biliary carriers, underscoring critical involvement of mucosal and cell mediated immune response for preventing typhoidal infection (Pulickal et al. 2009). On the other hand, licensed oral vaccine generates systemic and mucosal secretory antibodies with T cell response, but involves multiple doses for optimal protection. Further, difficulty in swallowing of larger sized capsules poses both risk and challenges for the children aged 6 years or below. Additionally, occasional reports of bacteremia raised safety issues with Live typhoid vaccine (Guzman et al. 2006).

A mucosal vaccine with easy administration and antigen specific serum and mucosal antibodies along with *Salmonella*-specific T cells are highly desirable for late clearance of *Salmonella* (MacLennan 2014) . This suggested that protection against typhoidal infection is not based on single component, rather necessitates a balanced cooperation between mucosal, humoral and cell mediated immune response.

In our previous studies with rT2544, we showed that when administered subcutaneously, antigen specific IgG and IgA secreting plasma cells were found in the spleen, MLN and PP and the antiserum is shown to lyse bacteria through antibody dependent cellular cytotoxicity (ADCC). It elicits cell mediated immune response by generating IFN-γ producing CTLs (Das et al. 2017). No typhoid subunit vaccine cross protect Paratyphoid infection. Since rT2544 was found to be present in multiple clinical isolates of *S*. Paratyphi A, we proposed an improved vaccine with somatic antigens like T2544 to cross protect against *S*. Paratyphi A infection. We, in this study, propose intranasal delivery of rT2544 by conjugating with widely used mucosal adjuvant CTB. Additionally, in a separate work, we improved the immunogenicity of this vaccine candidate, rT2544 after the addition of another vaccine adjuvant rFliC as an initial step

of a goal where we aim to optimize the minimum immunogenic dose of different antigens from different pathogen so that a multivalent vaccine can be developed.

This chapter is segmented in three different parts to **study the adaptive immune responses after mucosal and systemic immunization with *Salmonella* antigens (Objective 1).**

Part 1: Development of potential vaccine candidates against Typhoidal *Salmonella* infection.

Part 2: Development of an iron overloaded mouse model for studying *Salmonella* Paratyphi A infection.

Part 3: Assessing the immunogenicity and protective efficacy of the vaccine candidates against *Salmonella* infection.

Part I formulates two vaccine candidates against *Salmonella* infection. Both the adjuvant used in the study rCTB (Cholera toxin B subunit) and rFliC (Flagellin protein) are widely used for augmentation of immune responses. Mucosally delivered antigens are less immunogenic and induce tolerance. To overcome this, appropriate adjuvants are conjugated with the vaccine candidate or co-administered with the antigen to augment antigen specific immune responses for supporting the effective alliance between innate and adaptive immunity of the host (Rhee, Lee, and Kim 2012).

CTB delivered through non-oral mucosal routes significantly boosted antigen specific humoral and cell-mediated immunity, at both the local and distal mucosa, albeit to a variable degree. This phenomenon is called as "common mucosal immunity" (Holmgren and Czerkinsky 2005). Previous reports stated that intranasally immunized AIEC siderophore enterobactin conjugated to CTB elicited a strong mucosal antibody response in the small and large intestine and thereby reduced the bacterial colonization in the gut (Guo et al. 2014). Another study exhibited that intranasal CTB-siderophore administration induced intestinal mucosal antibodies which could significantly reduce *Salmonella* colonization of the inflamed gut (Sassone-Corsi et al. 2016). Here we constructed CTB genetically fused with rT2544 and co-expressed them and delivered into mice through intranasal route for studying adaptive immune responses after intranasal immunization with salmonella antigen.

In a separate study we explored bacterial flagellin (rFliC) as a self adjuvanting protein and admixed it with our protein antigen rT2544 and delivered into mice subcutaneously. rFliC, a structural protein of bacterial flagellar filament, is previously reported to trigger T cell dependent immune response through its intrinsic adjuvant characteristic exerting by toll like receptor (TLR5) and thereby act as potent immunomodulatory agent (Cui et al. 2018). Additionally, polymeric flagellin reported to cross-link with B-cell receptor (BCR) and stimulate B cell (Nossal, Ada, and Austin 1964). Thereby, rFliC can play dual function as the antigen and as adjuvant for TLR5 activation in vaccine formulation (Mizel and Bates 2010). FliC has been conjugated with low immunogenic antigens, viz mucoid exopolysaccharide (MEP) (Campodonico et al. 2011), O-antigens (Simon et al. 2013), and cocaine analogs (Lockner et al. 2015) and to assess its function against bacterial infection and also drug abuse. It was also reported to impart the protective efficacy when admixed with proteins but to a lesser degree compared to the conjugate vaccine (Asadi Karam et al. 2013; Bargieri et al. 2008).

Part II of this chapter deals with the development of the murine model to study pathogenesis of *S*. Paratyphi A. Non availability of suitable animal models of infection poses a major bottleneck regarding vaccine development, since *S*. Paratyphi A is a human restricted pathogen. Several preclinical vaccine candidates were assessed using neonatal mice oral infection model (Santander and Curtiss 2010), intraperitoneal infection model (Zhu et al. 2015; Xiong et al. 2017), or rabbit model (Roland et al. 2010). In few studies immunized mice were infected with the larger dose of wild type *S*. Paratyphi A strain solubilized in the hog gastric mucin to assess protective efficacy but failed to evaluate vaccine induced mucosal response. The newborn and infant mice may be useful for protection studies, but unsuitable for assessment of the immunogenicity of vaccine candidates due to their very early age (Santander and Curtiss 2010). Peroral rabbit models were used to evaluate the reactogenicity and immunogenicity of the vaccine candidates. However, the data showed much elevated antibody titer in rabbit possibly due to the coprophagic nature of rabbit which create a continuous exposure to the infection. Recently developed CHIM (Control human infection models) includes healthy individuals from developed countries, whereas young children of developing countries are the most susceptible to paratyphoid infection, which further reflects a greater difference in their genetic background, nutritional status and subsequent microbiome, age and co-morbidities and co-infections associated with background immunity of respective populations.

We proposed an iron overloaded model, based on the studies suggesting iron as one of the critical micronutrient for bacteria including *Salmonella* (O'Brien 1982; Powell et al. 1980). Studies previously showed that systemic overload with iron (administered through the parenteral route) renders mouse susceptible to *S*. Typhi infection (Powell et al. 1980; O'Brien 1982). However, large dose requirement for iron that markedly suppresses the immune system could be circumvented by co-administration of iron chelator desferoxamine that makes iron available to the phagosomal bacteria and inhibits NADPH oxidase activity, promoting intracellular survival and growth and significantly reducing the lethal dose. Given that systemic infection could be established in wild type mice after oral administration, which affected the same visceral organs as humans following natural infection, this iron overloaded murine model can probably be considered a physiological model of infection (Das et al. 2017; Ghosh et al. 2011).

Part III of this chapter assess the immunogenicity and protective efficacy of these vaccine candidates (generated in part I), utilizing the iron overloaded model developed in part II. Protective efficacy of rCTB-T2544 was assessed against *Salmonella* Typhi and *Salmonella* Paratyphi infection. Since CTB was cloned from *Vibrio cholerae* and expressed, we investigated whether CTB worked as antigen in addition to adjuvant and confer protection against *Vibrio cholerae* infection. Additionally, in a separate work, we investigated the immunogenicity imparted by the lower dose of rT2544 with or without the presence of rFliC and assessed protective efficacy for both the typhoidal *Salmonella* strains.

4.2. Method.

Part I: CTB was genetically fused with recombinant *Salmonella* Typhi outer membrane protein T2544, through a non-furin linker (GPGP) by cloning into pET28a. Later, it was co-expressed and purified using Ni2+affinity chromatography. Simultaneously, another protein rFliC from *Salmonella* Typhimurium was cloned in pET28a and transformed into BL21 DE3 cells. Later, it was induced using 1mM IPTG and purified. Similarly, rFliC was cloned into pET28a and purified using native condition. All the detailed methodology of cloning and purification is discussed in the method sections **3.2.1- 3.2.5.**

Part II: For both the vaccine candidates, iron overloaded mice were used as prototype. An iron overload murine model against *S*. Typhi infection is reported previously from our lab (Ghosh et al. 2011). Part II of the objective 1 discussed development of the iron overloaded model for studying pathogenesis of *Salmonella* Paratyphi. Briefly, an iron-overload condition was created

by administering desferrioxamine (DFO; Novartis) (0.025 mg/g of body weight) and Fe3+ as FeCl3 (0.32 mg/g of body weight) intraperitoneally 5 h prior to the bacterial challenge. Log phase cultures of bacteria were re-suspended in sterile PBS buffer and were fed orally after neutralization of the gastric acid with 5% Sodium Bicarbonate. Mice were orally challenged with 5×10^7 *S.* Typhi and 5×10^5 *S.* Paratyphi A bacteria and monitored for 10 days. All the detailed methodology of gradual development of an animal model of *S.* Paratyphi A infection is discussed in the method sections **3.2.6.4-3.2.6.6, 3.2.15.1, 3.2.15.2** and **3.2.15.5.**

Part III of the objective 1 focused on assessment of the immunogenicity and protective capacity of the formulations mentioned in part I against *Salmonella* infection. After purifying and ensuring the proper folding and conformation of the purified protein, rCTB-T2544, the immunogenicity and protective capacity of rCTB-T2544 was evaluated by administering 60 µg of CTB-T2544 through intranasal route in BALB/c mice. In a separate investigation, we subcutaneously co-administered 2.5ug rFliC with 5ug of rT2544 in the Balb/c mice for assessing the immunogenicity and protective capacity of the formulation against *Salmonella* infection. Immunized mice were infected with 10 times lethal bacterial dose and death was monitored for 10 days post infection. Further, Antigen specific antibody titer from serum, intestinal and fecal extract of another set of immunized mice were assessed using ELISA. All the detailed methodology of assessing immunogenicity of these vaccine candidates and protective efficacy against typhoidal salmonella infections are discussed in the method sections **(3.2.6,3.2.7.2,3.2.8).**

4.3. Results. Part I: Development of potential vaccine candidates against Typhoidal *Salmonella* infection.

4.4 Result- Part II. Development of an iron overloaded mouse model for studying *Salmonella* Paratyphi A infection.

4.5. Results- Part- III. The adaptive immune response and protective efficacy of these vaccine candidates against *Salmonella* infection.

4.3. Results. Part I: Development of potential vaccine candidates against Typhoidal *Salmonella* infection.

4.3.1. Cloning of Recombinant Proteins rCTB-T2544, rCTB and rT2544:

To construct a gene chimera of ctx-b and t2544, the open reading frame (ORF) of the ctx-b gene was first cloned into the bacterial expression plasmid (pET28a), using BamHI and SalI restriction sites, followed by cloning of the 663bp amplicon of linker-t2544 at SalI and XhoI restriction sites immediately downstream of ctx-b (**Fig. 1A).** To this end, 309 bp amplicon of *V. cholerae* ctx-b (cholera toxin B subunit) gene was amplified by PCR (**Fig. 1B**). In addition, ORF of *Salmonella* Typhi t2544 gene, along with the coding sequence of glycine-proline-glycine-proline (GPGP) linker at its NH2-terminus (total size 663bp) was PCR-amplified **(Fig. 1C**). Next, the fusion gene clone of ctx-b and t2544 was confirmed by colony PCR **(Fig. 1D**), restriction digestion (**Fig. 1E**) and finally by nucleotide sequencing.

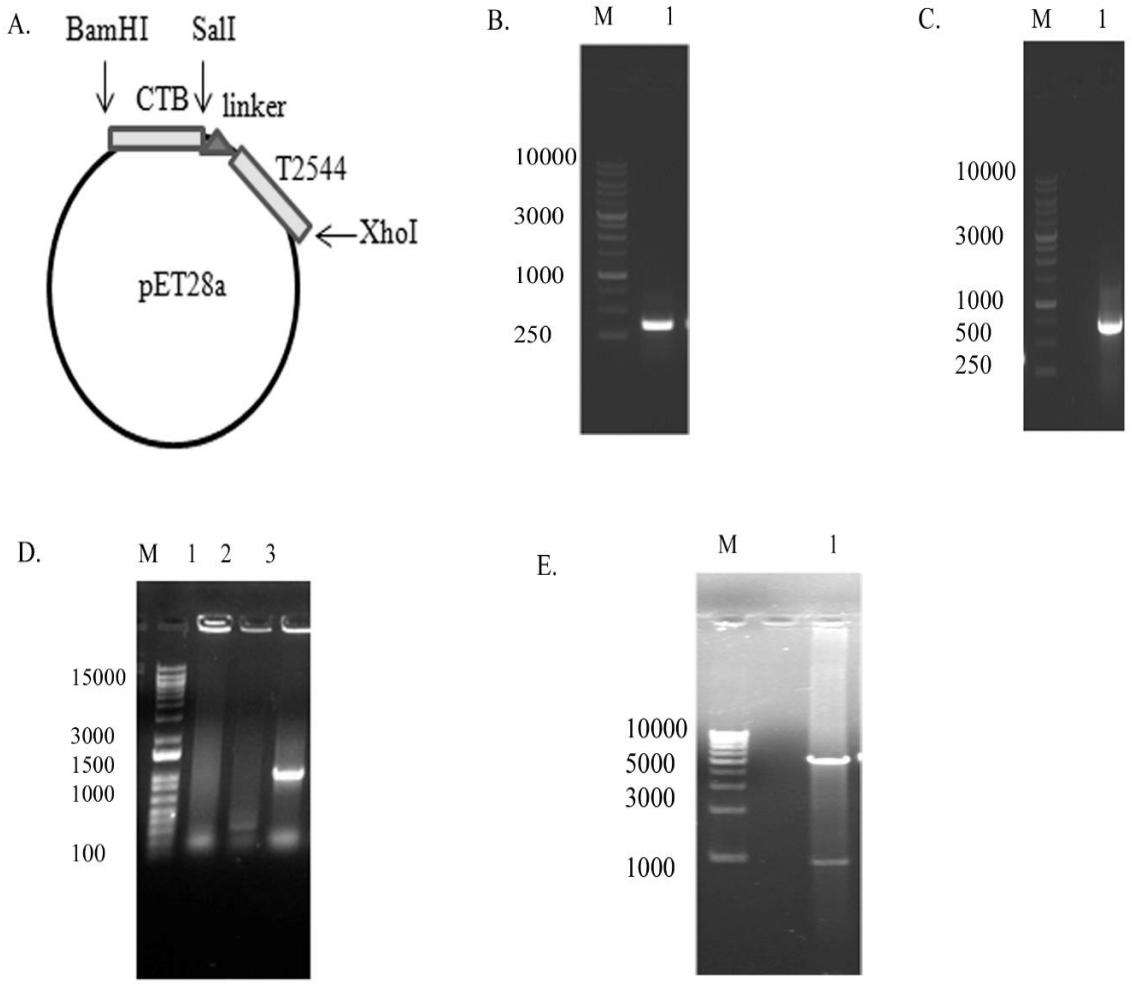

Fig 1. Cloning of rCTB-T2544. (A). Schematic representation of cloning ctx-b and t2544 genes in pET28a vector. (B). PCR amplification of ctx-b gene; Lane-M, 1Kb plus DNA ladder. (C). PCR amplification of t2544 gene (gene with GPGP linker); Lane-M, 1Kb plus DNA ladder. (D). Screening for positive clones of ctb-t2544 by PCR amplification after ligation into the pET28a vector, Lane-M, 1 Kb plus DNA ladder; Lane 1-3, ligated clones.

4.3.2. Expression and purification of recombinant proteins CTBT2544, rCTB and rT2544.

To develop the recombinant chimeric protein, pET28a plasmid construct carrying the ctx-b-t2544 fusion gene was transformed into the expression host *E. coli* BL21(DE3) and the expression of the recombinant chimeric protein (rCTBT2544) was induced by IPTG. Next, the chimeric rCTB-T2544 protein was extracted as an insoluble protein from inclusion bodies by sonication and solubilized with 8M urea in denaturing condition. Further, these denatured proteins were subjected to affinity chromatography using Ni2+conjugated agarose (Qiagen) and then renatured by gradual removal of urea by dialysis using a 10kD membrane (**Fig. 2A**) Similarly, rCTB and rT2544 were also purified using affinity chromatography (**Fig. 2B , 2C**).

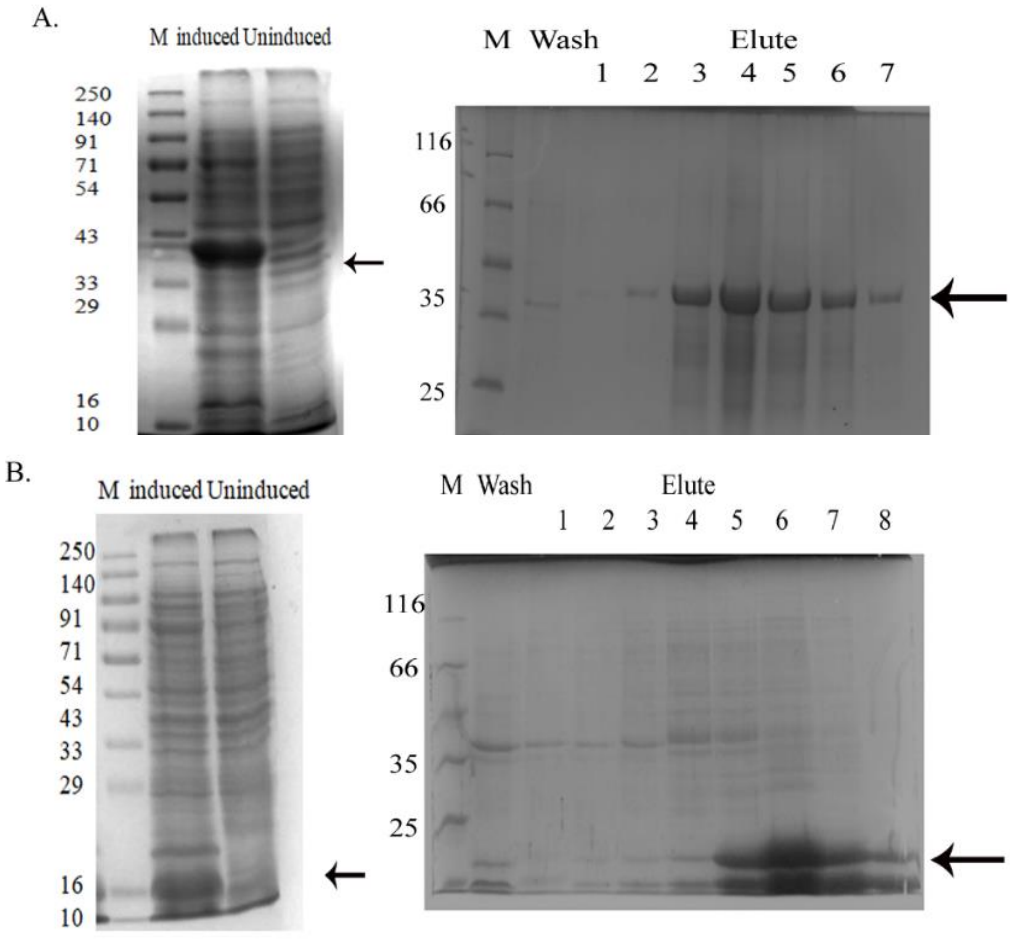

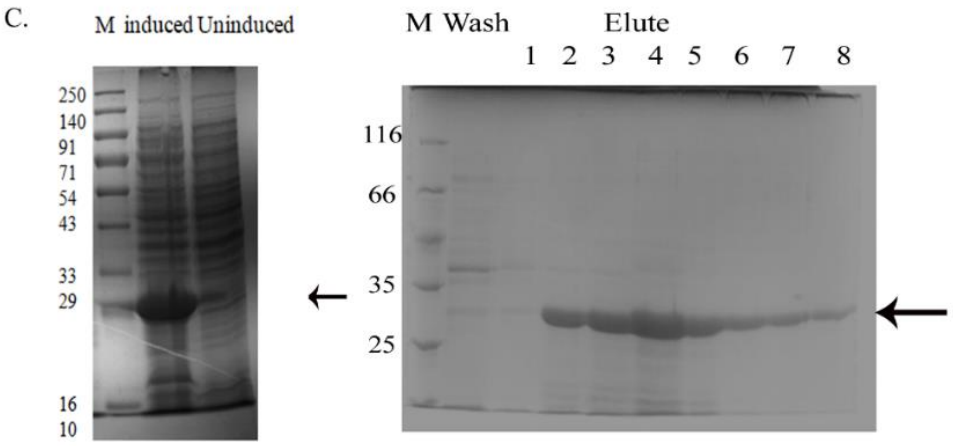

Fig 2. **Recombinant protein expression and purification.** A-C (left panel). SDS-PAGE profile of crude cell lysates showing recombinant protein expression induced by IPTG (1Mm). Lane M, Pre-stained protein marker; Lane Induced, cell lysates after protein induction by IPTG; Lane Uninduced, cell lysates of parallel culture without protein induction. Arrows indicate the respective induced proteins. (Right panel) SDS-PAGE profile of protein purified by Ni-column chromatography. Lane-M, Protein marker; Lane wash – flow through of column wash, Lane 1-8 - eluted fractions of purified proteins; Arrow indicates the respective purified proteins. A, B and C represent CTB-T2544, CTB and T2544, respectively.

4.3.3. Purity check and pentameric confirmation of rCTB-T2544.

The purity and the specificity of the chimeric protein was confirmed by SDS-PAGE (**Fig. 3A**) and western blots (**Fig. 3B**), respectively. The oligomeric structure of rCTB-T2544 was further investigated with gel electrophoresis. rCTB-T2544, when exposed to denaturing condition with boiling, migrated with a MW of 40 kDa, which is corresponded to the size of a chimera of T2544 and monomeric CTB. However, for the proper adjuvant functioning of CTB requires pentameric confirmation. To this end, we subjected our recombinant protein rCTB-T2544 in non-denaturing conditions without boiling. This time, it migrated to a higher molecular weight protein containing pentameric CTB (**Fig. 3C**). Further, we confirmed the presence of pentameric CTB in fusion chimera, we performed ELISA where we studied the binding affinity of the recombinant proteins (rCTB, rT2544 and rCTB-T2544) to the GM1 ganglioside receptor. The results suggesting the existence of CTB pentamer as both the recombinant proteins (rCTB and rCTB-T2544) bind to the receptor, in a dose-dependent manner, whereas, rT2544 could not (Fig. 3D). Next, secondary structure of these proteins (rCTB, rT2544 and rCTB-T2544)

were investigated from the Far-UV circular dichroism (CD) spectra. Data obtained were further analyzed using K2D2 software (http://cbdm-01.zdv.unimainz.de/~andrade/k2d2/). This analysis indicated that rCTB, rT2544 and rCTB-T2544 contained 79.93%, 6 4.22% and 72.38% α-helical structure, respectively. (**Fig. 3E**). The yields of the purified, rCTB, rT2544 and rCTB-T2544 were 30mg, 24mg and 18.75mg per liter of bacterial culture. Subsequently, using LAL assay, the level of endotoxin contaminations was detected for rCTB, rT2544, and rCTB-T2544 and found to be 0.015, 0.011, 0.008 EU/ml, respectively.

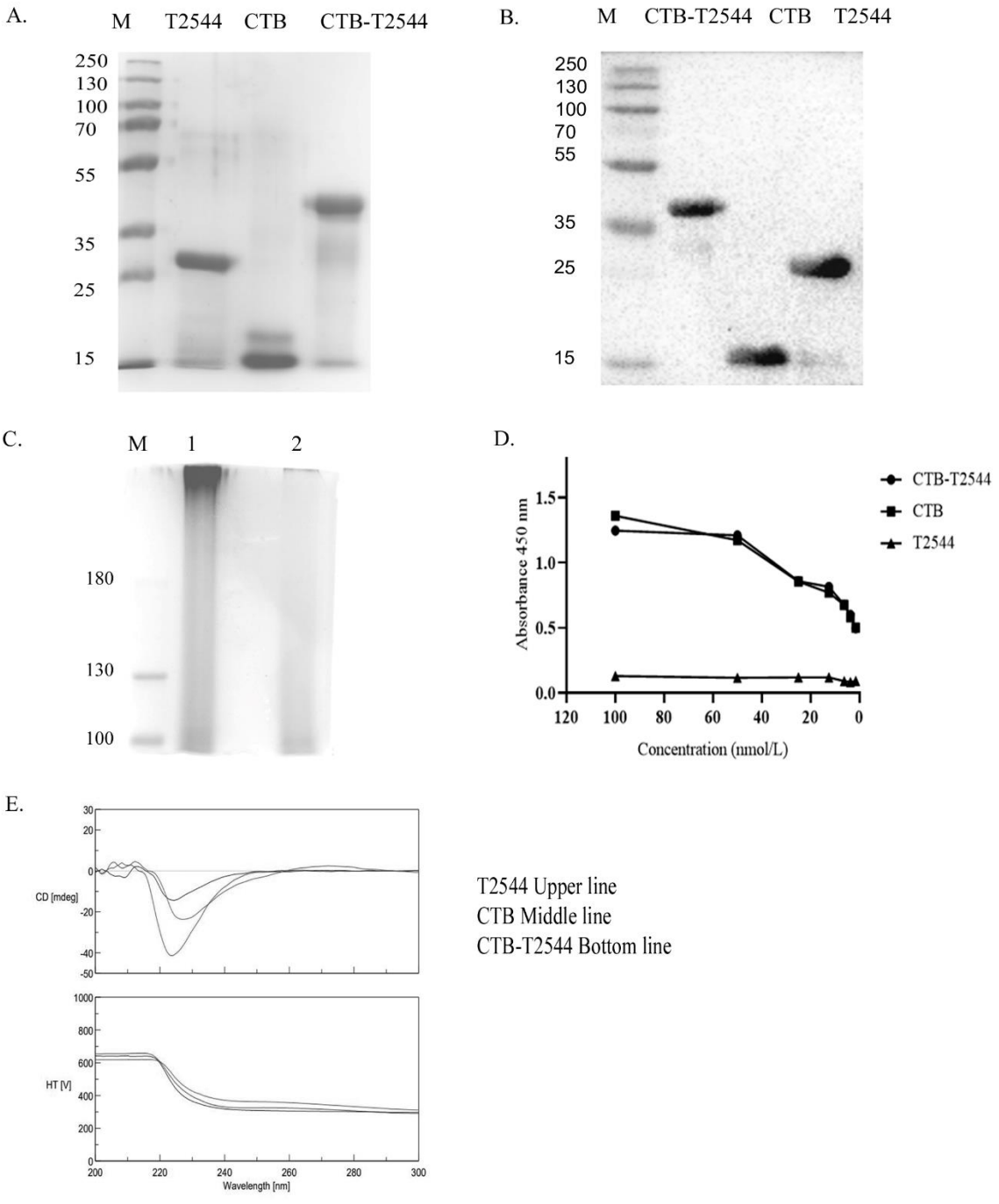

Fig 3. Purity and size of the recombinant proteins. A. Recombinant purified proteins (rT2544, rCTB , rCTB-T2544) were run in 10% SDS–PAGE, followed by staining with Coomassie brilliant blue; Lane-M is the pre-stained protein marker. B. Western blot analysis of purified recombinant proteins (rCTB-T2544, rCTB and rT2544); blot developed with anti-HIS monoclonal antibody; Lane-M is the pre-stained protein marker. C. rCTB-T2544 protein was subjected to non-denatured (unboiled) and denatured (boiled) conditions and resolved in 10% SDS PAGE, and stained with Coomassie brilliant blue. Lane-M is the Pre-stained protein marker, Lane-1 is the unboiled rCTB-T2544 and Lane-2 is the boiled rCTB-T2544. D.GM1-ELISA. Elisa plates were coated with GM1 ganglioside (1µg/well). Next recombinant proteins were added to the wells followed by developing with anti-HIS antiserum (1:2500). E. Far UV CD spectral analysis. Three purified recombinant proteins were subjected to Far UV CD spectral analysis. The minimum of three spectra for each of the protein sample were recorded at 25°C in the wavelength ranging from 200 to 300 nm, followed by smoothed, corrected, and virtually superimposed and analyzed. Simultaneous recording of High tension (HT) voltage of these three proteins indicated no noise.

4.3.4. Purification of rFliC.

The ORF of the gene fliC of 1500 bp from *S.* Typhimurium encoding FliC of 55 kDa recombinant protein was also cloned in pET28a vector separately. The ligated gene product corresponding to rFliC was transformed into BL21(DE3) cells. Positive clone is further confirmed the presence of rFliC gene by nucleotide sequencing. Positive clones were cultured and induced with 1mM IPTG and were grown for 5 hours. The expression profile of the induced recombinant protein rFliC was performed with SDS-PAGE (**Fig. 4A**). Next, the protein rFliC was extracted as a soluble protein from the supernatant by sonication and in native condition (**Fig. 4B**) and later dialyzed against PBS. SDS PAGE and Western blot analysis with anti-His tag antibody detected a 55kDa protein band (**Fig. 4C, 4D**). All these data together indicated successful isolation of purified flagellin protein.

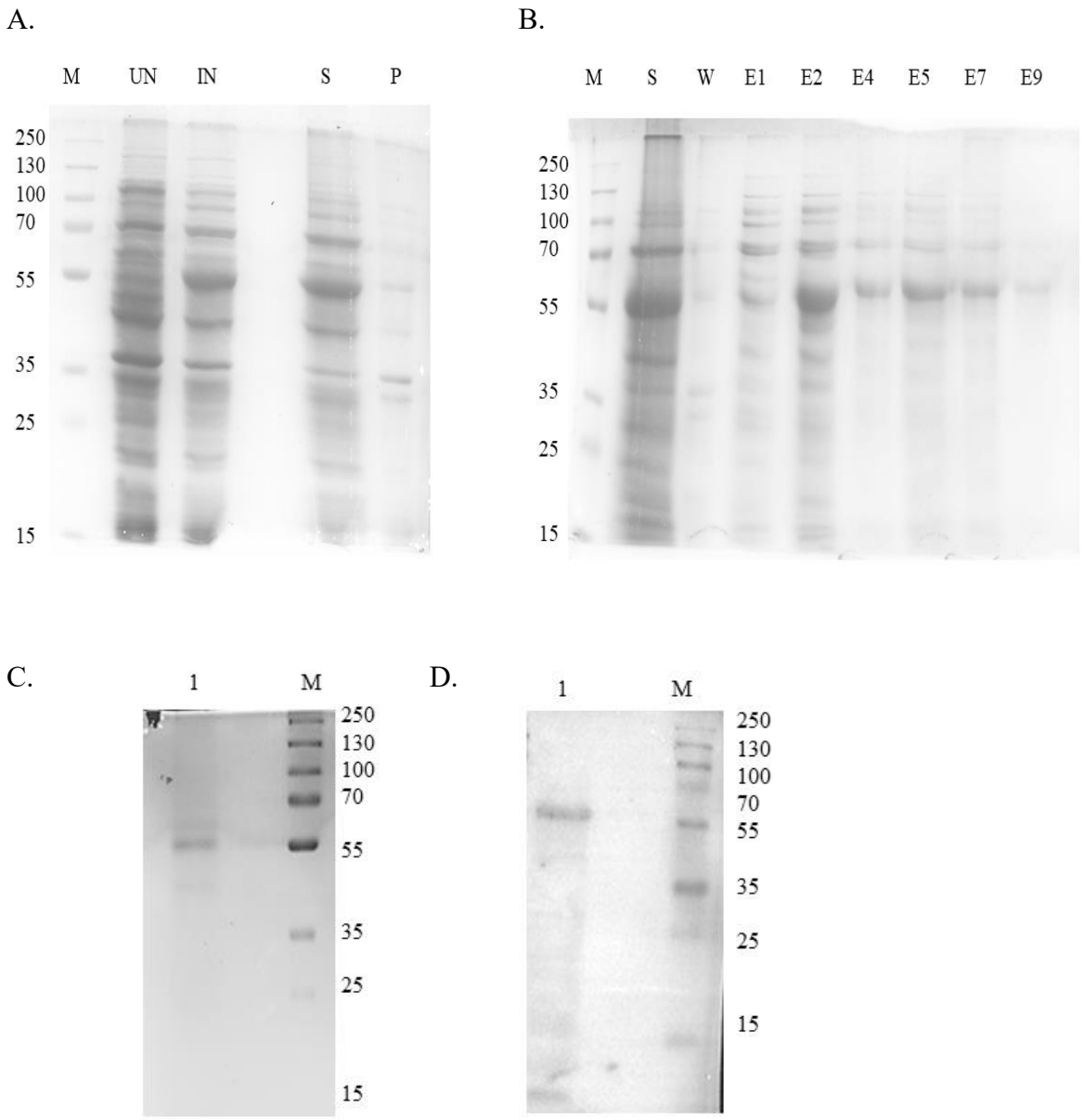

Fig 4. Expression profile and purification of rFliC. A. SDS-PAGE profile of crude cell lysates showing recombinant protein expression induced by IPTG (1Mm). Lane M, Pre-stained protein marker; Lane IN, cell lysates after protein induction by IPTG; Lane UN, cell lysates of parallel culture without protein induction, Lane S and P, cell lysate found in the supernatant and pellet of induced culture post sonication. B. Arrows indicate the induced protein. (Right panel) SDS-PAGE profile of protein purified in native condition Lane-M, Protein marker; Lane S contains cell lysate in supernatant after sonication, Lane W – flow through of column wash, Lane E1-E9 - eluted fractions of purified protein in native condition. C. SDS PAGE of rFliC and D. Western blot analysis of rFliC. Lane M is Pre-stain protein marker.

4.4 Result- Part II. Development of an iron overloaded mouse model for studying *Salmonella* Paratyphi A infection.

4.4.1. Characterizing the clinical isolates as *S*. Paratyphi A.

All the clinical isolates used in this study (hereby designated as C1 to C10) were screened for the presence of *fliC-a* gene, exclusively present in *S*. Paratyphi A, using PCR amplification of the genomic DNA for further characterizing them as *S*. Paratyphi A clinical isolates. A set of PCR primers amplifying the *fliC-a* gene were used in this study. One reference strain of *S*. Paratyphi A (ATCC 9150) was selected as positive control (designated as R) and *S*. Typhi Ty2 was used as negative control (designated as N). PCR products revealed the presence of 329 bp amplicon of *fliC-a* in all the clinical isolates when run on 1% Agarose gel electrophoresis (**Fig. 5**), characterizing all of them as *S*. Paratyphi A strains.

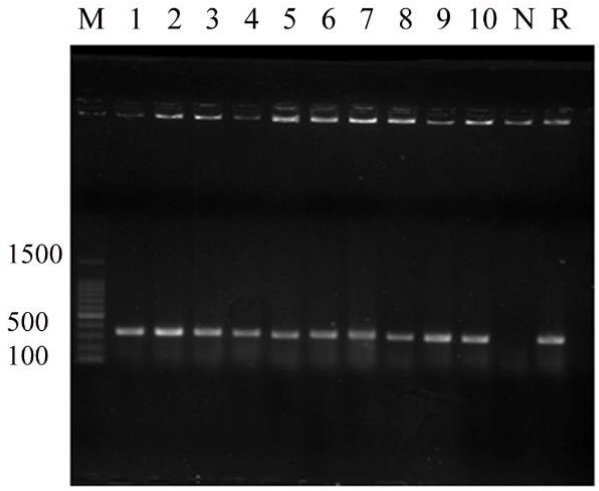

Fig. 5. Identification of clinical isolates of *Salmonella enterica* serovar Paratyphi A. The clinical strains were identified by PCR amplification of the fliC-a gene. PCR products were separated by 1% agarose gel electrophoresis. M is 100bp DNA ladder. Lane 1 to 10 clinical isolates. N is negative control *S.* Typhi Ty2 and R is reference strain *S*. Paratyphi A 9150.

4.4.2. *S*. Paratyphi A Clinical isolates exhibit differential infectivity and pathogenesis.

Next, pathogenic potential of all these clinical isolates of *S.* Paratyphi A was studied by invasion of non-phagocytic cells and their replicative potential within professional phagocytes. Out of 10 clinical isolates, two (named C1 and C2) showed maximum potency in invading murine intestinal epithelial cell line (**Fig. 6A**). Also, C1 survived and replicated significantly in murine macrophage cell line RAW264.7 compared to the reference strain ATCC 9150 (**Fig. 6B**). As motility was previously reported to contribute as one of the major virulence factors for

Salmonella Paratyphi A (Cohen et al. 2022; Scharte, Franzkoch, and Hensel 2024), we assessed relative motility by the soft agar assay. Clinical isolates (C1 and C2) showed higher motility (**Fig. 6C, 6D**) compared to the reference strain ATCC 9150, indicating a possible explanation of their increased pathogenicity.

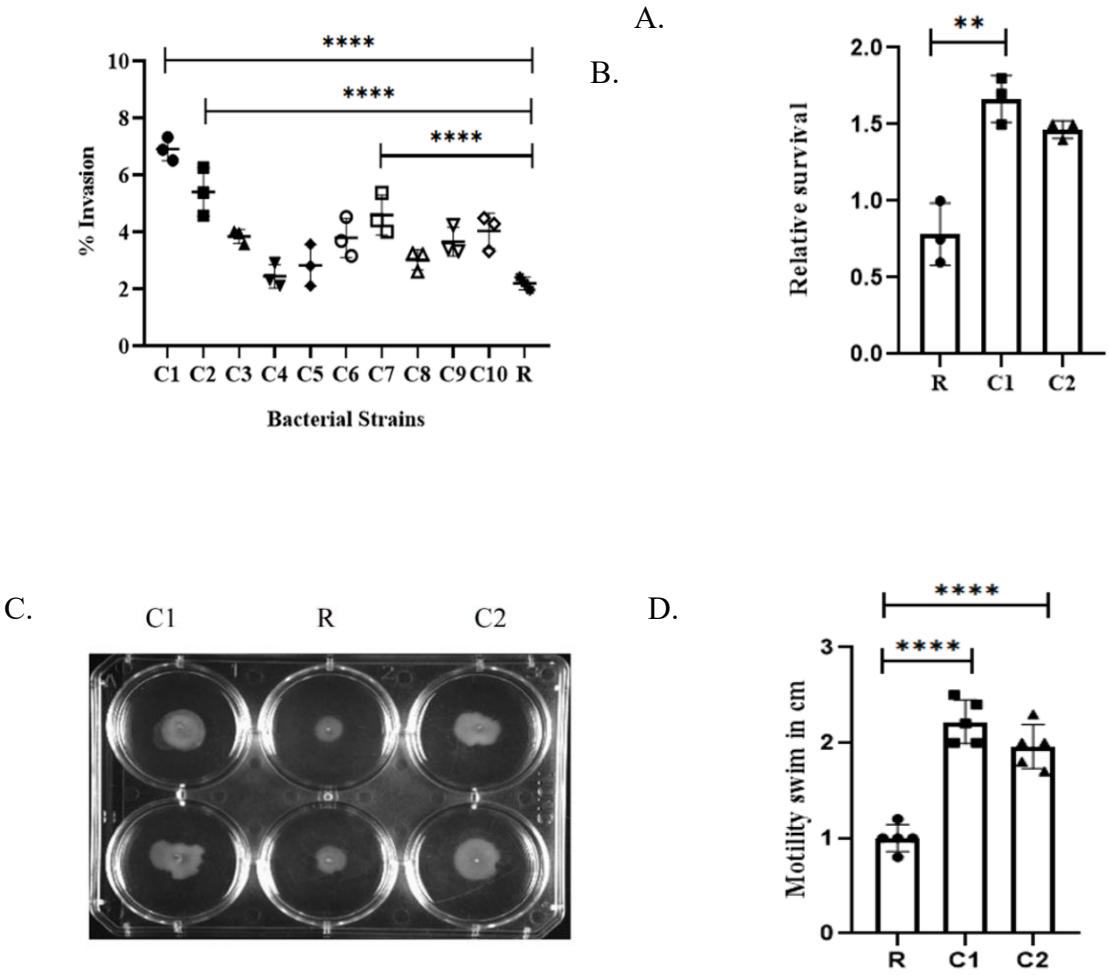

Fig. 6. Pathogenic potential of clinical isolates of *S*. Paratyphi A. A. Monolayers of murine IEC cells (5 x 10^5 cells/well) were infected with all the isolated clinical strains and reference strains at 1:100 MOI for 30 mins. Intracellular CFU counts after gentamicin protection assay were plotted as percentage of bacteria recovered after 90 min post infection with respect to the initial inoculum. B. The clinical isolates (C1, C2) and reference bacteria were inoculated to the RAW264.7 cells (5 x 10^5 cells/well) at a ratio of 10:1 for 1 hr. The extracellular bacteria were eliminated in the presence of 100µg/ml gentamicin for 1 h. At the indicated time 0 hr and 24 hr post inoculation, intracellular bacteria were released by addition of 1% Trition X-100, plated and intracellular survival was calculated as no of bacteria recovered at 24 hr divided by no of

bacteria recovered on 0 hr. C. 10ul of the overnight grown bacterial cultures (C1, C2 and R) were placed onto LB plate containing 0.4% agar. The plates were kept 6 h at 37°C without being inverted. The diameters of the concentrically growing bacterial cultures were measured and plotted. Unpaired t tests were performed to calculate the significance of the differences between the compared data. Error bars denote SD. *p:0.3332,**p:0.0021***p:0.0002,****p<0.0001.

4.4.3. In vivo infection with the selected strains.

As we observed highest infectivity and survival of the clinical isolate of *S.* Paratyphi A. named, C1, we proceeded with this strain for the development of animal model of infection. To this end, mice were injected intraperitoneally with desferoxamine and ferric chloride, as described in the Methods section. Four hours later, different doses (5 x 10^4, 5 x 10^5, 5 x 10^6) of *S.* Paratyphi A strains (C1 or R) were fed by oral gavage after neutralizing the gastric acid with 5% sodium bicarbonate. Fifty percent of the mice survived the challenge with 5 x 10^4 dose of the C1 strain, despite all of them developing moderate diarrhea within the first three days. In contrast, all the mice that received the higher doses of infection manifested severe diarrhea and succumbed to infection within 7 days. R strain required much higher dose to kill 50% of the mice. (**Fig. 7A**). We found significant reduction in the body weight of the mice post infection with the C1 strain (**Fig. 7B**). In addition, we also checked for bacterial shedding in the feces on d2, d4 and d8 for C1 strain (5 x 10^4 CFU dose). Bacteria recovered from the feces on d2. Bacterial shedding in feces increased on d4, but drastically dropped on D8 (**Fig. 7C**). All these suggested successful colonization of the bacterial in intestine.

A.

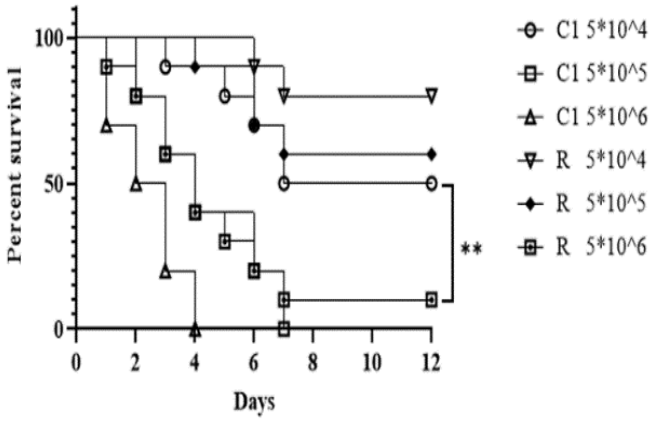

Strain	Dose CFU/Mouse	Mortality/ Total mice
C1	5*10^4	5/10
	5*10^5	10/10
	5*10^6	10/10
R	5*10^4	2/10
	5*10^5	4/10
	5*10^6	9/10

B. C.

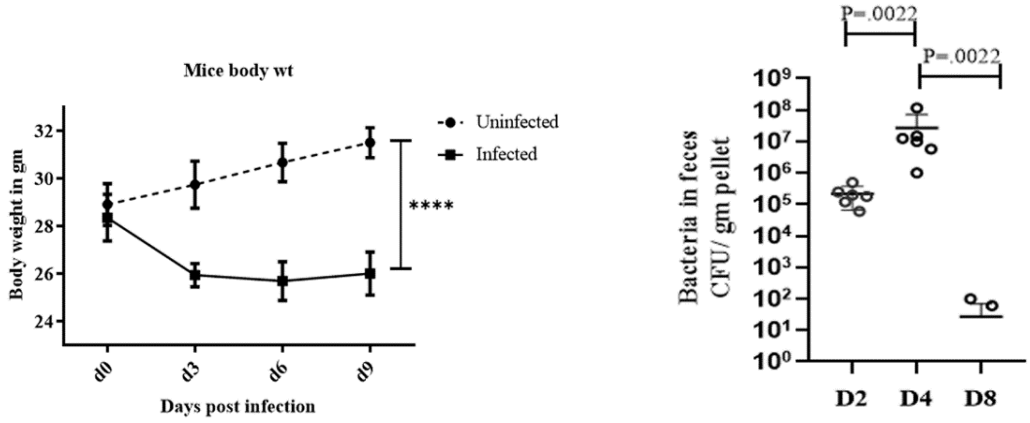

Fig. 7. Oral infection of iron overloaded BALB/c mice with *S.* Paratyphi A: A The LD50 of *S.* Paratyphi A reference strain (R) and clinical strain (C1) were assessed in an iron overload mouse model. Iron overloaded Balb/c mice (n= 10/group) were challenged with bacteria through orogastric route at 5 x 10^4, 5 x 10^5, 5 x 10^6 doses. Deaths of mice were monitored upto 12 days and Kaplan-Meyer survival curve was plotted and compared. Tabular form of LD50 dose of C1 and reference *S.* Paratyphi A strain are noted. B. Changes in the total body weight of the infected (infection dose 5 x 10^4 CFU mice (n=6/group) were monitored over time and plotted. C. Fecal shedding of *S.* Paratyphi on day 2, 4 and 8 post infection (5 x 10^4 CFU) were evaluated. Significance was calculated using unpaired t test. Error bars denote SD. *p:0.3332,**p:0.0021***p:0.0002,****p<0.0001.

4.4.4. Bacterial dissemination in the intestine and visceral organ.

To study successful colonization of *S.* Paratyphi A in the intestinal tissues and internal organs after oral infection, mice were infected with the C1 strain (dose: 5 x 10^4) and euthanized on d2, d4 and d6 and the bacteria were recovered from the tissue and organ lysates. The results demonstrated higher colonization in the intestinal tissues initially, which was later on replaced by more bacteria recovering from the internal organs possibly due to dissemination from the intestine (**Fig. 8A-C**).

A

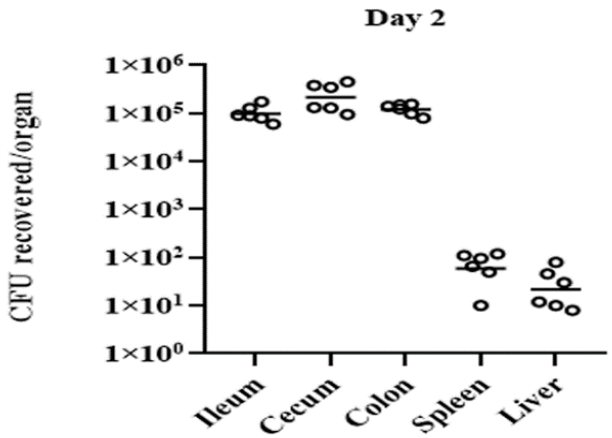

B.

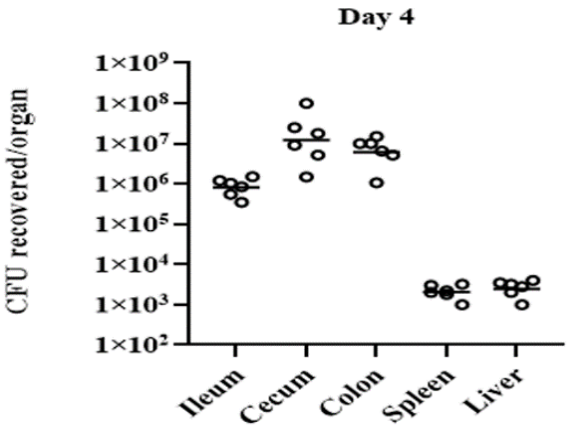

C.

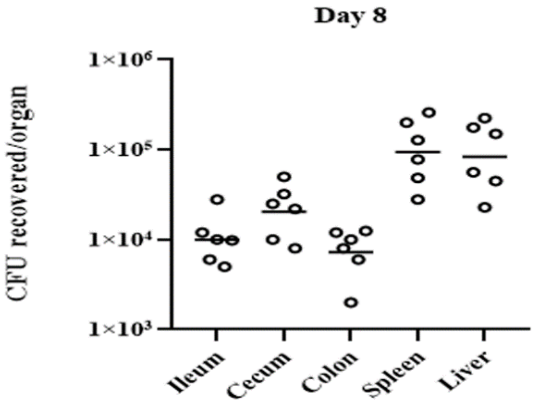

Fig 8. Bacterial colonization in the intestine and internal organs: Iron overload mice (n= 6/ time points) were infected with *S.* Paratyphi A- C1 at 5 x 10^4 CFU dose via the orogastric route. Bacterial load in the intestine and internal organs were plotted on day 2 (A) , 4 (B) and 8 (C) post infection. Geometric mean of each group was plotted.

4.4.5. Intestinal pathology of the *Salmonella* Paratyphi A -C1 infected mice.

4.4.5.1. Pathology of Ileal sections.

As we observed increased bacterial colonization in the intestine, we further investigated the intestinal pathology of those infected mice. Ileal sections of the uninfected mice maintained the normal mucosal epithelium with villi and glandular and lobular crypts, containing goblet cells (**Fig. 9A**). Post desferol and $FeCl_3$ treatment, the crypt architecture showed focal edema and condensed inflammatory aggregates at d3 (**Fig. 9B**) and D8 (**Fig. 9D**). Later, when we infected these iron overload mice with *S.* Paratyphi A, the epithelium layer of ileum showed

disintegration along with effacement in underlying glandular crypt architecture with presence of inflammatory infiltrates, edema and hemorrhage (**Fig. 9C, 9E**). Histopathological scoring of infected mice were higher than uninfected ileal sections as measured and plotted in **Fig. 9F.**

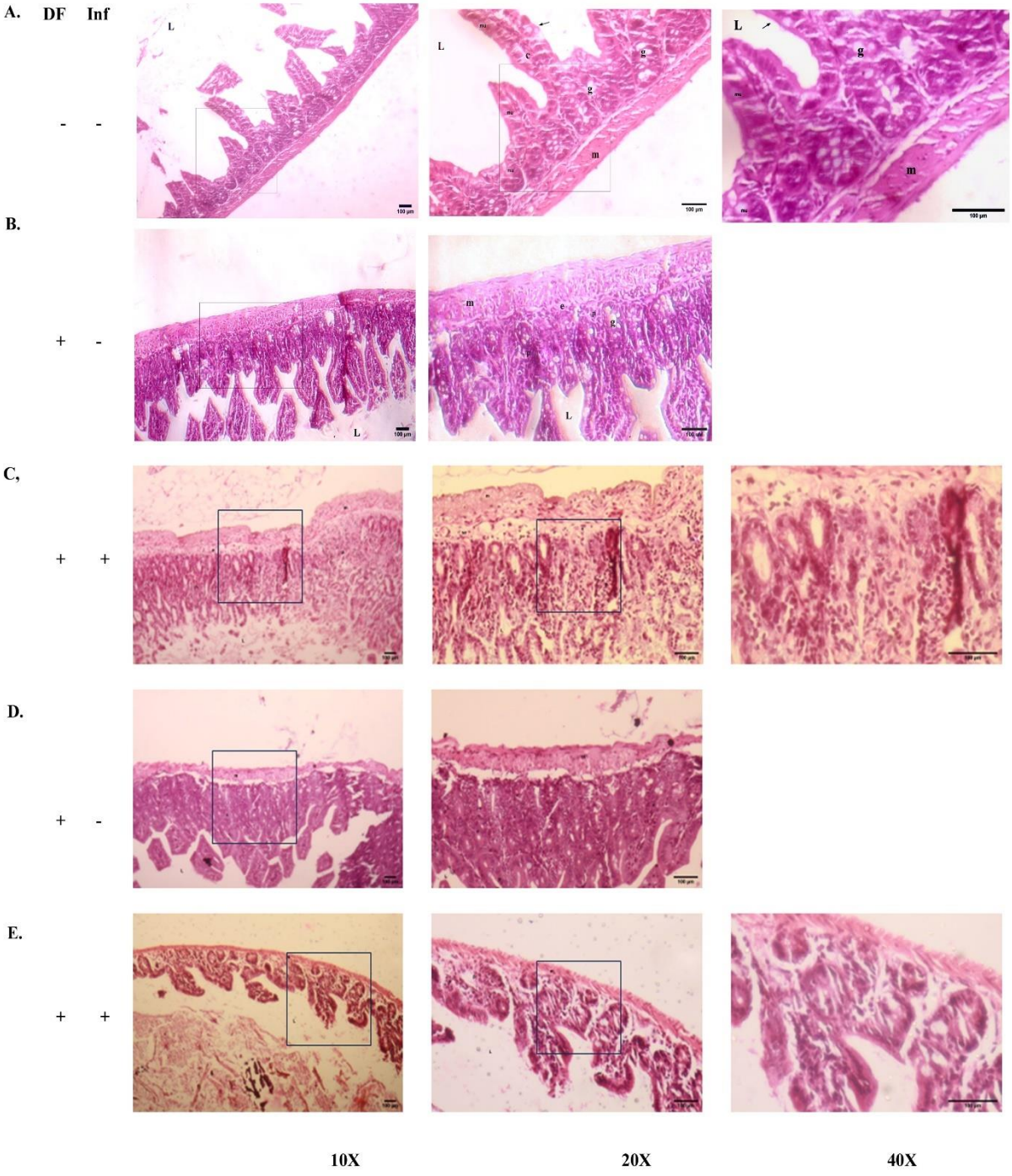

F.

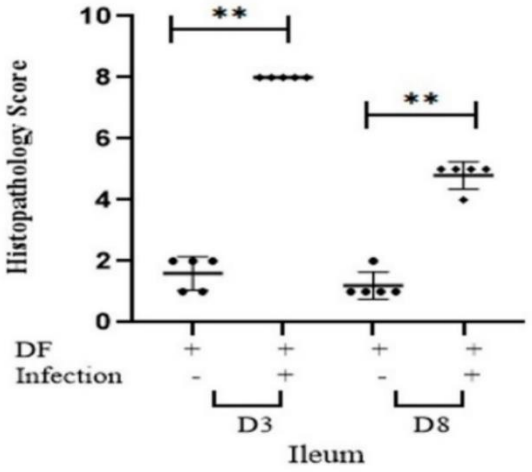

Fig 9: Intestinal pathology of BALB/c mice after *S.* Paratyphi A infection - Microscopic changes of Ileal section. A. Representative image of intestinal histopathological features of uninfected mice were shown. Next, mice (n=12) were treated with desferol and FeCl3 (DF). Half (n=6) of the mice were infected with *S.* Paratyphi A, whereas another half (n=6) remain uninfected. Ileal sections were collected from DF treated but not infected mice on day 3(B) and on day 8 (D) post infection. Simultaneously, another set of DF treated mice were infected with bacteria and ileal section were collected on day 3(C) and on day 8 (E) post infection. Later, collected tissue were fixed, embedded in paraffin, and 5-um thin sections were stained with H&E and were analysed at day 3 and at day 8 post infection. Images were captured at 10X, 20X and 40X. The pathological changes were mentioned in the image as L- lumen, m - mucosa, sa – submucosa, p - PMN infiltration, e - edema, er – epithelial erosion, u – ulceration, c – crypt. Histopathological scoring (F) of *S.* Paratyphi A infected group was evaluated by the extent of inflammatory cell infiltrate with epithelial changes compared with DF treated but not infected group.

4.4.5.2. Pathology of Cecal sections.

The cecal lining of the uninfected mice showed proper maintenance of columnar epithelium underlying properly integrated glandular and ductal architecture, containing goblet cells (**Fig. 10A**). Cecum sections showed loss of goblet cells with mild edematous changes in mice treated with desferol and FeCl3 (**Fig. 10B,10D**), while post-infection, marked disintegration in the underlying crypts with diffusely intense inflammatory infiltrates and areas of edema, and hemorrhage with profound loss of goblet cells were observed (**Fig. 10C, 10E**).

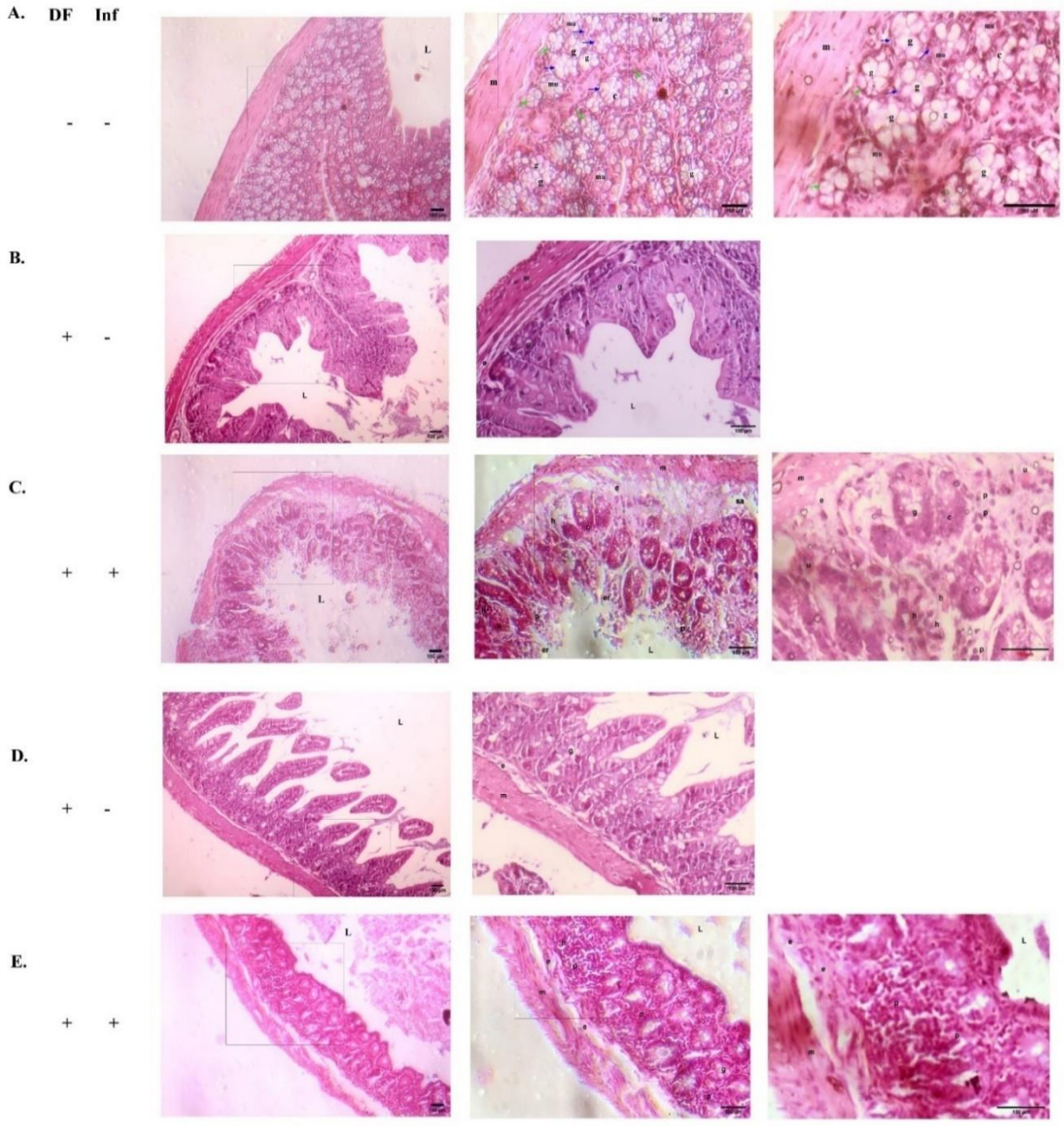

Fig 10: Intestinal pathology of BALB/c mice after *S*. Paratyphi A infection - Microscopic changes of ceeal section. A. Representative image of intestinal histopathological features of uninfected mice were shown. Next, mice (n=12) were treated with desferol and FeCl3 (DF). Half (n=6) of the mice were infected with *S*. Paratyphi A, whereas another half (n=6) remain uninfected. Cecal sections were collected from DF treated and PBS infected mice on day 3(B) and on day 8 (D) post infection. Simultaneously, another set of DF treated mice were infected with bacteria and cecal section were collected on day 3(C) and on day 8 (E) post infection. Later, collected tissue were fixed, embedded in paraffin, and 5-um thin sections were stained with H&E and were analysed at day 3 and at day 8 post infection. Images were captured

at 10X, 20X and 40X. The pathological changes were mentioned in the image as L- lumen, m - mucosa, sa – submucosa, p - PMN infiltration, e - edema, er – epithelial erosion, u – ulceration, c – crypt.

4.4.5.3. Pathology of Colonic sections. The colonic mucosa of uninfected mice possessed ciliated and stratified epithetlial lining showing prominent goblet cells, separated by bands of fibrous septa (**Fig. 11A**). While desferol and Fecl3 treatment led to occasional areas of inflammatory infiltrate in the colonic mucosa (**Fig. 11B, 11D),** it showed moderate inflammatory infiltrates interspersed with areas of edema and hemorrhage after *S.* Paratyphi infection (**Fig. 11C, 11E**). Histopathological scoring of cecal and colonic (**Fig. 11F**) tissue sections, adapted from the scoring of inflammation in IBD mouse models was performed where severity of infection was divided into four stages (Table 3.5). Sections from bacteria infected mice were significantly higher from the group who did not receive the infection. Additionally, MPO levels were found to be higher in infected group as compared to uninfected counterparts. All these data together suggested a successful colonization of the *S.* Paratyphi A in the mouse intestine.

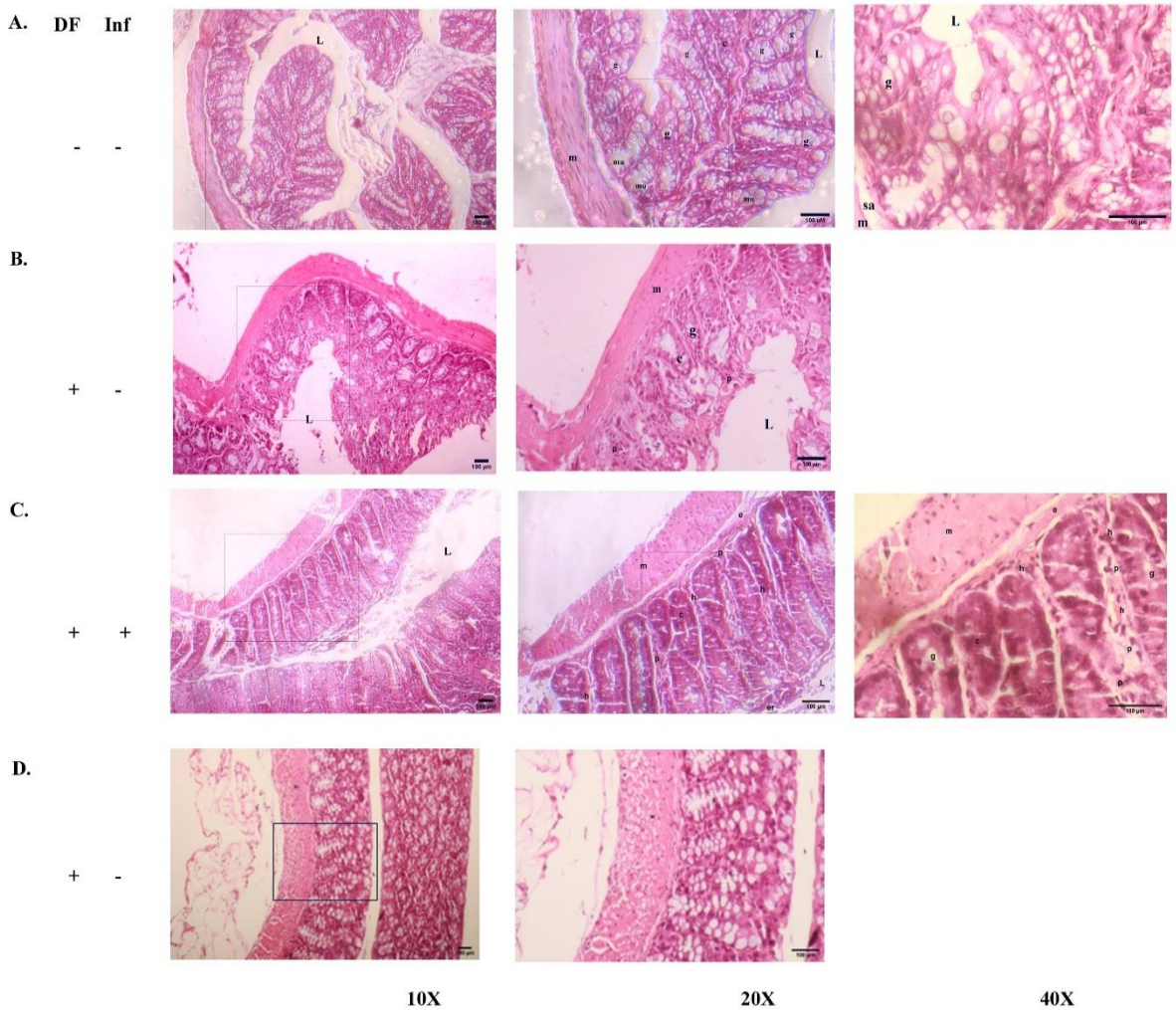

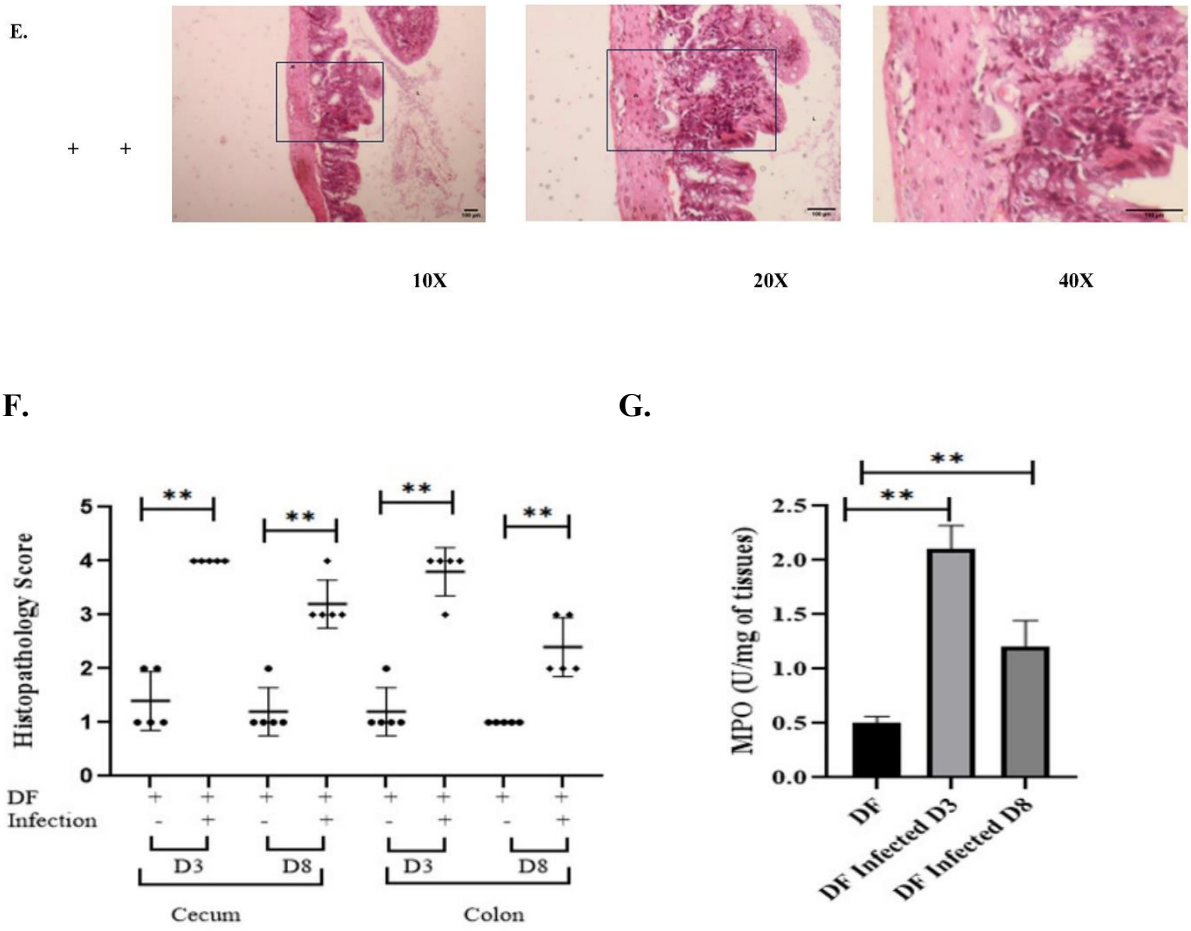

Fig.11. Intestinal pathology of BALB/c mice after *S.* Paratyphi A infection - Microscopic changes of colonic section. A. Representative image of intestinal histopathological features of uninfected mice were shown. Next, mice (n=12) were treated with desferol and FeCl3 (DF). Half (n=6) of the mice were infected with *S.* Paratyphi A, whereas another half (n=6) remain uninfected. Colonic sections were collected from DF treated but not infected mice on day 3(B) and on day 8 (D) post infection. Simultaneously, another set of DF treated mice were infected with bacteria and colonic section were collected on day 3(C) and on day 8 (E) post infection. Later, collected tissue were fixed, embedded in paraffin, and 5-um thin sections were stained with H&E and were analysed at day 3 and at day 8 post infection. Images were captured at 10X, 20X and 40X. The pathological changes were mentioned in the image as L- lumen, m - mucosa, sa – submucosa, p - PMN infiltration, e - edema, er – epithelial erosion, u – ulceration, c – crypt. G. Biochemical changes: MPO levels in the colonic tissue lysate as measured by spectrophotometry.

4.5. Results- Part- III. The adaptive immune response and protective efficacy of these vaccine candidates against *Salmonella* infection.

4.5.1 Intranasal immunization with rCTB-T2544 protects against oral *S*. Typhi.

Immunization through any of the mucosal route generates immune response at nearby mucosa at greater degree alongside of the immune response at a distal mucosa with a varibale degree- this existing concept of "Common mucosal immune system"(Holmgren and Czerkinsky 2005) inspired us to check whether intranasal immunization with rCTB-T2544 generates protective immune response at the intestine**.** To this end, Balb/c mice were intranasally immunized, thrice, with 60ug of rCTB-T2544, rCTB and rT2544 at 12 days interval (**Fig. 12A).** PBS immunized mice were taken as control. 12 days after the third immunization, all the immunized mice were subjected to lethal *S.* Typhi infection (10X LD50 dose: 5 x 10^7 CFU). An iron overloaded model described in the method section in chapter 2 were used as prototype. Mice were monitored for 10 days. 70% mice from the rCTB-T2544-immunized group survived the lethal challenge with *Salmonella* Typhi, whereas all the mice from other group gradually succumbed to the infection (**Fig. 12B**).

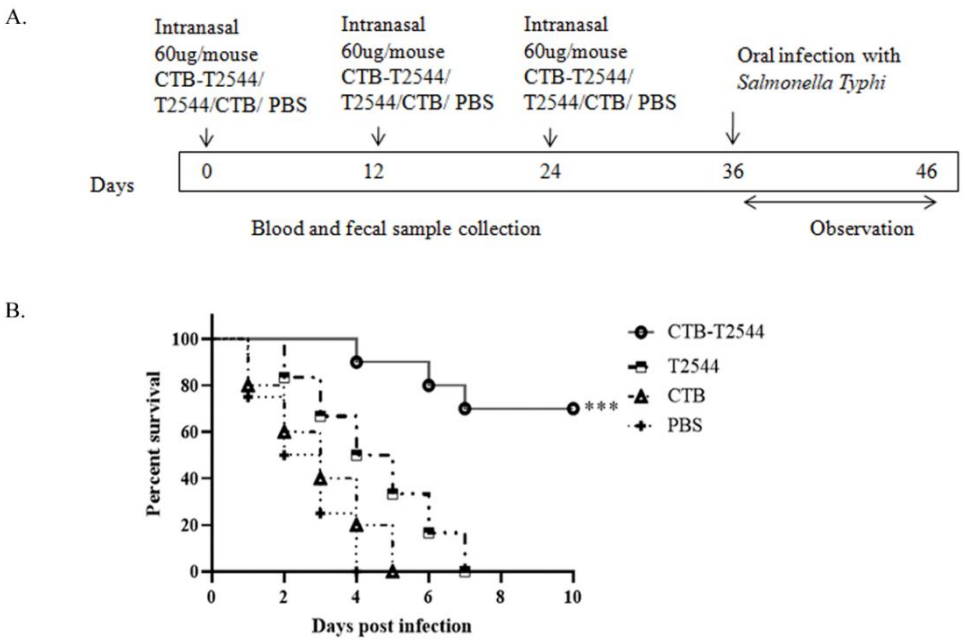

Fig 12. Immunization scheme and protective efficacy of rCTB-T2544. A. Schematic representation of the immunization schedule, sample collection and bacterial infection. B. cumulative mortality of immunized mice from different immunized group were plotted using Kaplan-Meyer survival curve analysis. 12 days after the third immunization, all the immunized

mice (n=10 in each group) were challenged with lethal *S*. Typhi infection. Mice were monitored for10 days. Significance was calculated by comparing the survival of the mice immunized by rCTB-T2544 with T2544 by Log-Rank Mantel Cox test. ***p=0.0001.

4.5.2. Intranasal immunization with rCTB-T2544 generates humoral immune response.

To investigate whether cholera toxin B subunit could augment the humoral immune response, specific to the co-administered antigen rT2544, end-point titers of the serum antibodies were determined using ELISA**.** Endpoint titer is defined as the reciprocal of the antibody titer, at which the absorbance of the experimental sample was the nearly similar as those from PBS-immunized mice. T2544-specific serum antibody titers (serum IgG, IgG1, IgG2a, and IgA) were found to be significantly increased in the rCTBT2544 immunized mice, as compared to the rT2544-immunized mice (**Fig. 13A**). These findings were in alignment with the substantial recovery of the rT2544 specific antibody-secreting cells (ASCs) in the MLN, spleen and Peyer's Patches (PP) of the rCTBT2544 immunized mice. ELISpot assay showed significantly elevated number of t2544 specific IgA and IgG ASC as a blue and red spot if the figure **13B** and further these data were presented as bar diagram in Fig. **13C** and **13D**. ASCs in other groups were very few in number.

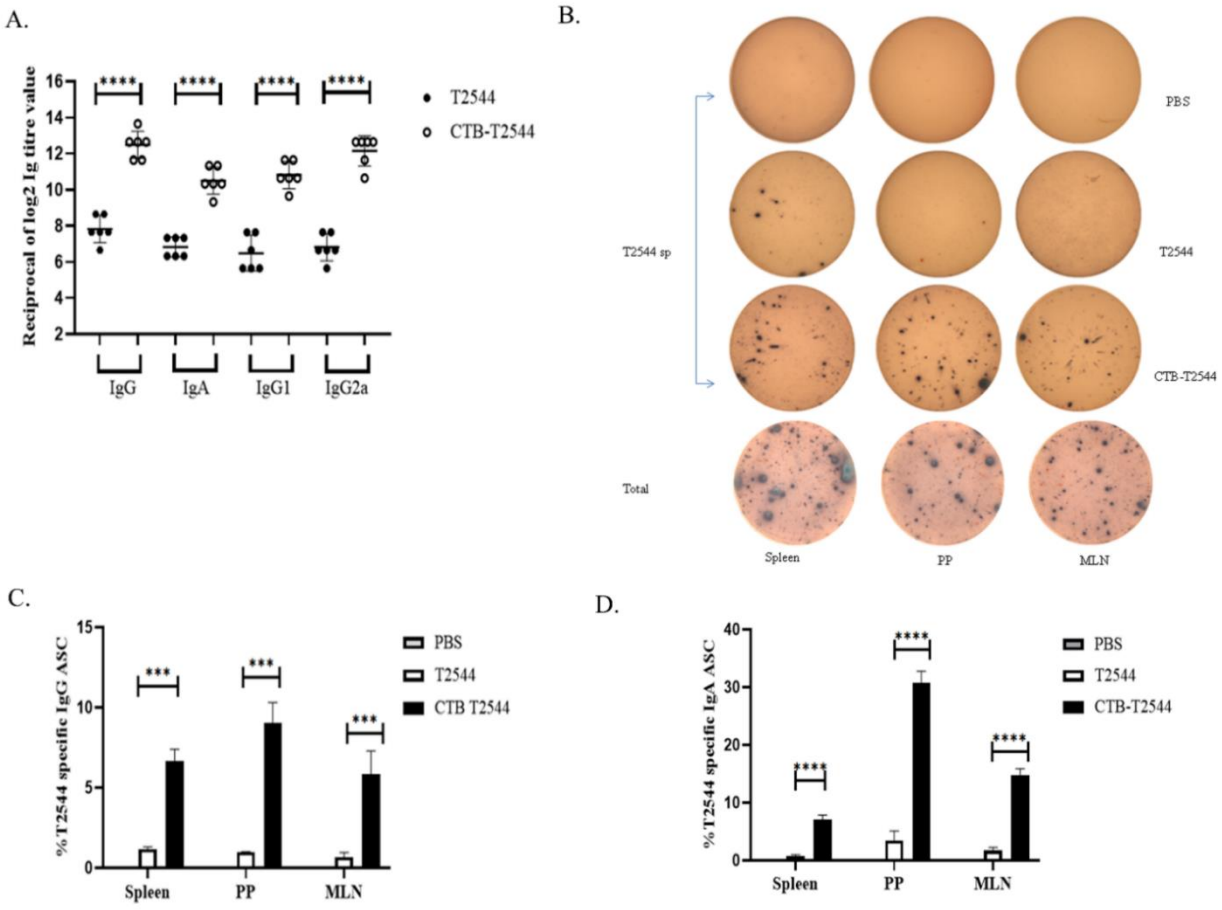

Fig 13. **Intranasal rCTBT2544 immunization induces humoral immune response.** A. Serum samples were collected from rCTBT2544 and rT2544 immunized mice (n=6/group) on 12 days after third immunization. ELISA plates were coated with rT2544 overnight. Serum samples were gradually half diluted (For IgG- dilution starts from 1:200 to1:25600 and for IgA it starts from 1:20 to1:2560) and rT2544-specific antibody titers were determined. Optical density at 450nm was recorded. The endpoint titer was calculated and was plotted in log 2 scale. B. Two weeks after the third immunization, all the immunized mice were euthanized. Cells from the spleen, MLN and Peyer's Patches (PP) were isolated and ELISPOT assay was performed. Spots were counted with ELISPOT reader. The numbers were plotted as percentages of rT2544-specific IgG and IgA ASCs out of the respective total Ig ASCs. Significance was calculated with similar cell populations isolated from PBS-immunized mice using unpaired t test (13C, 13D).

4.5.3. Intranasal immunization with rCTBT2544 generates mucosal immune response.

Intestinal sIgA antibody contributed a pivotal role in imparting protection against *S*. Typhi. We measured T2544-specific sIgA titers in the fecal and intestinal wash 12 days after third immunization. A strong T2544-specific sIgA response were observed in the rCTB-T2544 immunized mice (**Fig. 14**).

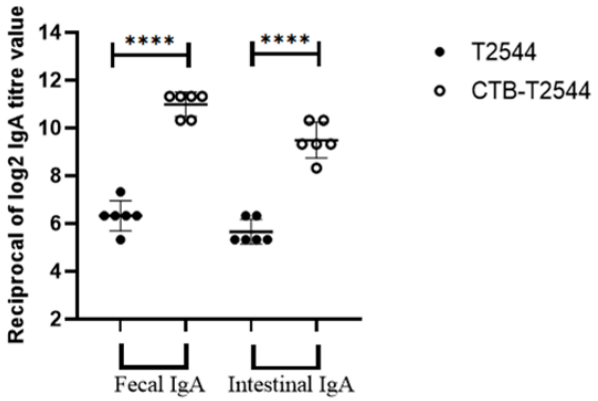

Fig 14. Intranasal rCTBT2544 immunization induces mucosal antibody. T2544-specific IgA antibodies in the fecal and intestinal contents were quantified 12 days after the third immunization (n=6/group). The endpoint titer was calculated and was plotted in log 2 scale. ****$p<0.0001$.

4.5.4. Intranasal immunization with CTB-T2544 protects against *S*. Paratyphi A infection.

An intranasal vaccine candidate, rCTB-T2544, showed to elicit protective immune responses against *S*. Typhi in an iron overload mouse model (**Fig. 12**). Next, we investigated the protective efficacy of this vaccine candidate against *S*. Paratyphi A infection. To this end, rCTB-T2544 immunized mice were challenged with 10xLD50 dose (5 x 10^5 CFU) of C1 strain and survival was monitored over next 10 days (**Fig. 15A**). 80 percent of the rCTB-T2544-immunized mice survived the lethal bacterial challenge, whereas all the animals immunized with rT2544 or PBS succumbed to the infection (**Fig. 15B**).

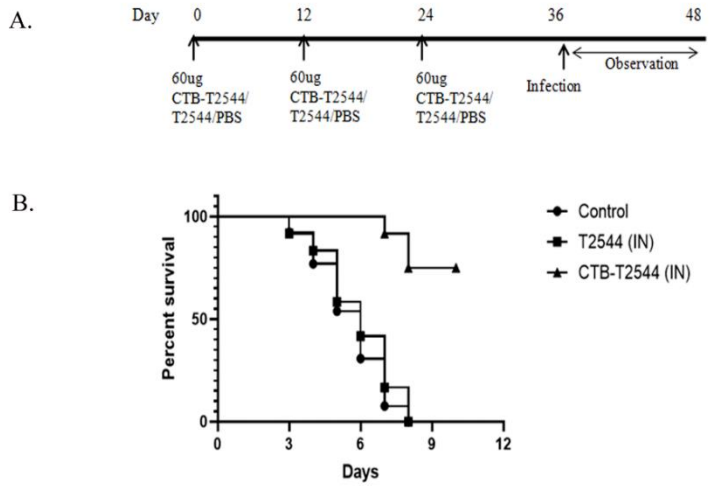

Fig. 15. rCTB-T2544 immunization protects from *Salmonella* Paratyphi A infection. A. Mice (n=10/group). were immunized intranasally thrice with rCTB-T2544, rT2544 and PBS following the scheme shown. B. immunized mice were iron overloaded and challenged with the 10XLD50 dose (5 x10^5 CFU) of *S*. Paratyphi. Kaplan-meyer survival curve for the mice were plotted and compared with rT2544. *p:0.3332,**p:0.0021***p:0.0002,****p<0.0001.

4.5.5. Intranasal immunization with CTB-T2544 protects against *Vibrio cholerae*.

In the newly generated vaccine candidate rCTB-T2544, CTB not only used as an adjuvant but also acted as an antigen while administering in mice. We observed CTB- specific IgG and IgA in serum (**Fig. 16A**) and in mucosal secretions (Feces and Intestinal contents) (**Fig. 16B**). As we observed increased CTB specific antibodies in mice, we subjected immunized mice into an ileal loop experiment where we administered cholera toxin (Satitsri et al. 2016). 8 hours after this surgery, we euthanized the mice and the fluid accumulation in the loops was noted as measuring loop weight/ length ratio. We observed significantly less fluid accumulation in

rCTB- and rCTB-T2544-immunized group compared to those received T2544 or the vehicle (**Fig. 16C,16D**).

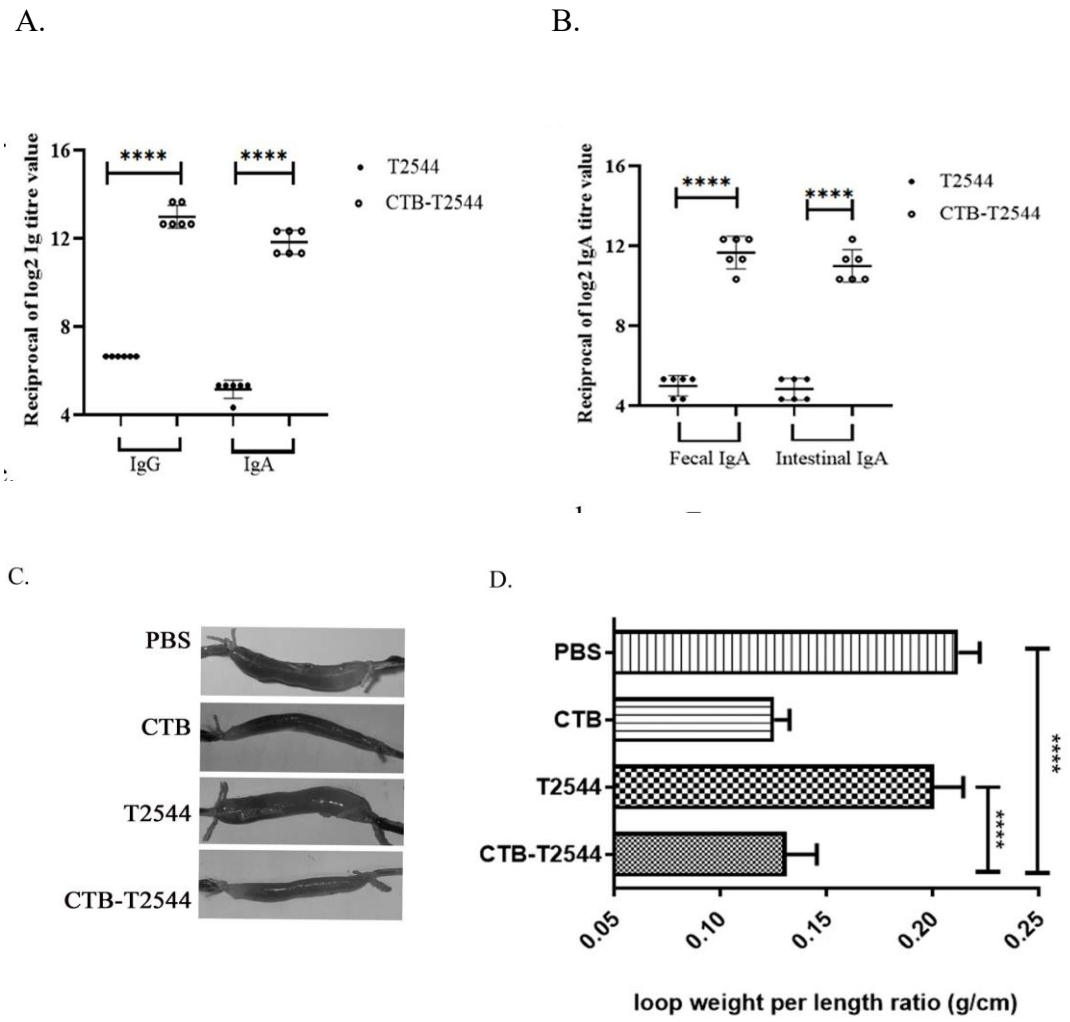

Fig. 16. rCTB-T2544 immunization protects from *Vibrio cholerae* infection. A. 12 days after post immunization, CTB specific IgG and IgA was measured in serum (A) and mucosal secretions (B) of all the immunized mice (n=6/group). In an ileal loop assay, immunized mice (n=6/group) were undergone surgery where cholera toxin were administered in the loops. 8 hr after the surgery, fluid accumulation was measured by quantifying the weight divided by the length of the individual loops in each group. Significance was calculated by comparing this loop weight/ length ratio of CTB-T2544 group with the rT2544 and PBS immunized group, using one-way ANOVA with post hoc analysis using Tukey's multiple comparison test. Data represented as mean with SD; ****p value<0.0001 vs. T2544 and PBS. Error bars represent SD.

4.5.6. Subcutaneous administration of rT2544 coadministered with rFliC generates increased humoral antibody.

Previously, we showed that our vaccine candidate, rT2544, alone could induce immunogenicity and confer protection against lethal challenge of mixed with *Salmonella* Typhi (Ghosh et al. 2011). We assessed immunogenicity of rT2544 at much lower doses than before with or without an adjuvant, rFliC. To this end, we immunized six weeks old balb/c mice with 5 and 12.5 ug of rT2544 co-admixed with or without rFliC (2.5ug) four times at 7 days intervals. We isolated serum from the blood of these immunized mice, 7 days after the last immunization. We observed that rT2544 showed immunogenicity alone at lower doses (both at 5ug and 12.5ug) but at a variable degree. These immune responses were boosted to a much higher magnitude in presence of 2.5ug of rFliC, supporting self-adjuvating nature of *Salmonella* flagellin (**Fig.17A**). Both the doses of rT2544 with rFliC generated similar magnitude of immune response. As we observed enhanced antigen specific antibody titer with 5ug of rT2544 admixed with 2.5ug of rFliC, we proceed our next experiments with this dose. Another set of immunization studies further confirmed enhanced rT2544-specific IgG and IgA antibodies in the serum of the mice that received both rT2544 and rFliC compared to the one that received rT2544 alone (**Fig.17B**). Similarly, we noted an enhanced rT2544 specific IgG isotypes in the serum of the mice treated with both the proteins (**Fig.17C**). These findings were in alignment with the recovery of significant numbers of rT2544 specific antibody-secreting cells (ASCs) from the splenocytes of the immunized mice that received rT2544 with or without rFliC. ELISpot assay showed significantly elevated number of rT2544 specific IgA and IgG ASC, marked in blue and red spots, respectively in the group receiving both rT2544 and rFliC(figure **17D, 17E)**. ASCs in the group that received rT2544 were very few in number.

A.

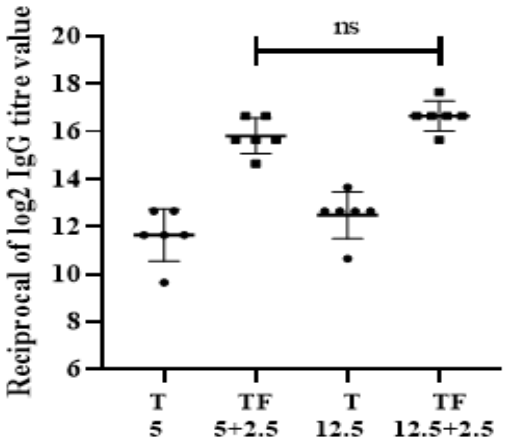

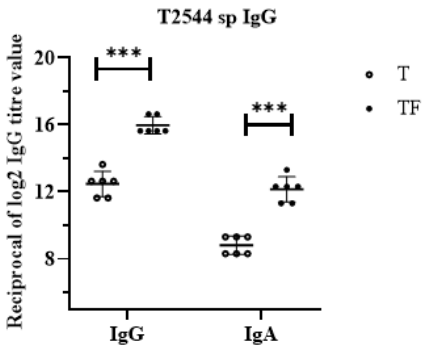

B.

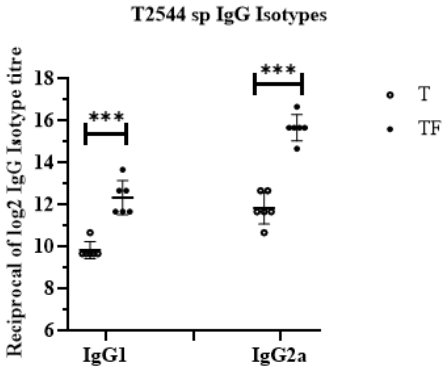

C.

D.

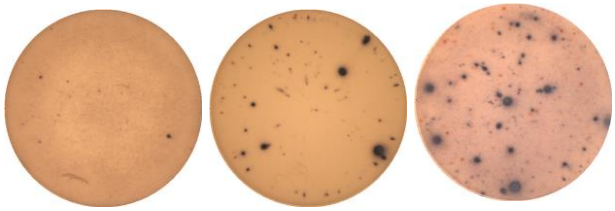

E.

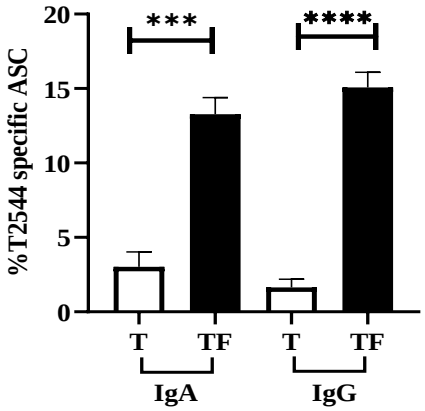

Fig. 17. Systemic rT2544 co-administered with rFliC induces humoral antibody. Seven days after the fourth immunization, serum was isolated from the blood of immunized mice (n=6/group). Endpoint titer value of serum IgG (A) at variable dose were assessed. B. Next, serum antibody (IgG and IgA) and IgG subtypes (C) were determined and plotted for each group and compared with rT2544 group. D. Representative image of splenocytes underwent ELSIPOT analysis; Red spots IgG, Blue spots IgA. E. Bar diagram of the % antigen specific ASC present in total number of ASC were plotted. Significance was calculated using two tailed unpaired t test. Error bars denote SD. *p:0.3332,**p:0.0021***p:0.0002,****p<0.0001.

4.5.7. Subcutaneous administration of rT2544 coadministered with rFliC generates mucosal antibody. Parenteral immunization does not induce higher mucosal secretory antibodies. Here in our study, we noted an elevated IgA response specific to rT2544 in fecal extract and intestinal contents of the mice immunized with rT2544 and rFliC compared to the mice that received rT2544 alone (**Fig. 18**)

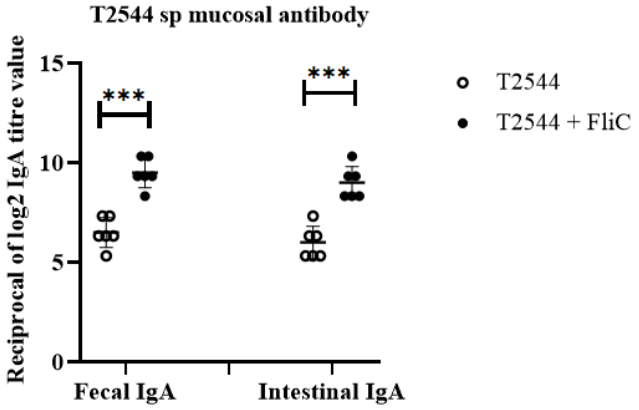

Fig.18. Systemic rT2544 co-administered with rFliC induces mucosal antibody. 7 days after the last immunization, fecal extract and intestinal contents were collected from all the immunized mice from all the groups (n=6/group). Endpoint titer value was determined and plotted for each group and compared with rT2544 group. Significance was calculated using unpaired t test. Error bars denote SD. *p:0.3332,**p:0.0021***p:0.0002,****p<0.0001.

4.5.8 Immunization with rT2544 and rFlic elicited an enhanced protective response against both *S*. Typhi and *S*. Paratyphi A.

To further investigate the potential of the vaccine candidates, we challenged the immunized mice with 10 x LD50 of *S*. Typhi. As a comparator we used Vi-TT. All the experimental mice were monitored for 10 days. 83% of the rT2544+rFliC (TF) immunized mice survived the lethal challenge whereas rT2544 (T) alone and Vi-TT immunized mice were conferred 50% and 61% protection, respectively (**Fig.19A**). No protection against *S*. Typhi infection were observed in the PBS control group. Similarly, we assessed the protective response with these candidates against *S*. Paratyphi A infection and found 91% and 58% protection in the rT2544+rFliC (TF) and rT2544 (T) group respectively, whereas PBS and Vi-TT conferred no protection (**Fig. 19B**). In a separate experiment, rFliC was subcutaneously injected in C57BL/6 mice at seven days interval for four weeks. This immunization scheme imparted only 30% protection from lethal

Salmonella Typhimurium challenge, indicating lower dose of rFliC alone is incapable of generating protective response in mice.

A.

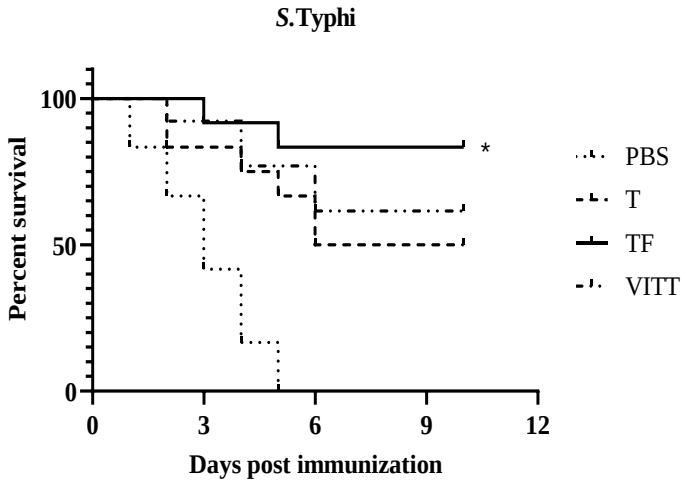

B.

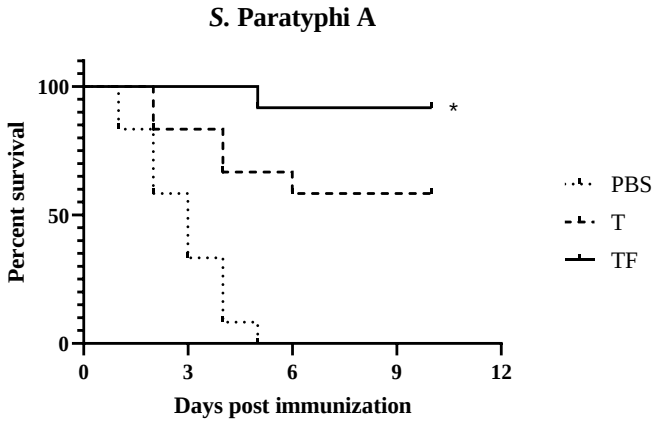

Fig.19. Immunization with rT2544 and rFlic protects mice from typhoidal Salmonella infection. Seven days after the fourth immunization, all the experimental mice (n=10/group) were challenged with 10 times lethal dose of *S.* Typhi (infection dose: 5 x 10^7) (A) or *S.* Paratyphi A (infection dose: 5 x 10^5) (B) through the orogastric route. Infected mice were monitored for 10 days. Death was recorded and significance was calculated by comparing survival of T2544 immunized and rT2544+rFliC immunized mice by Log-Rank Mantel Cox test.

4.6. Take-home message:

Here in this chapter,

We expressed and purified the recombinant fusion protein construct rCTB-T2544. Structural conformation of the purified protein was evaluated by GM1 ELISA and Far UV circular dichroism spectroscopy. Simultaneously, rFliC was also cloned, expressed and purified. Later, Western blot analysis confirmed the size of the purified protein.

Ten clinical bacterial isolates were PCR screened for characterizing them as *S*. Paratyphi A**.** Further, their pathogenic potential was evaluated using in vitro invasion study and assessing their ability to replicate intracellularly. Next, we proceeded with the clinical isolate that showed maximum infectivity (C1 strain). An iron overloaded mouse model was developed to study the infectivity and pathogenesis of *S.* Paratyphi A.

Next, we immunized mice with our formulated vaccine candidates and found increased immunogenicity and protective efficacy against both the Typhoidal *Salmonella* strains (*S.*Typhi and *S.*Paratyphi). rCTB-T2544, when administered intranasally, generated serum and mucosal antibody and 70% of the immunized mice survived the challenge, whereas a different formulation with rT2544 (rT2544 co-administered with rFliC: TF) augmented antigen specific immune response when administered through the subcutaneous route. 83% and 91% of TF immunized mice survived the lethal *Salmonella* Typhi and Paratyuphi challenge, respectively. 2.5ug of purified recombinant rFliC could not generate protective response against *S.* Typhimurium infection.

Chapter 5.

Objective 2

Augmentation of the immune response by adjuvants

5.1. Introduction.

Development of modern vaccination strategies includes inclusion of adjuvants to boost up both the immune arms (innate immune response and adaptive immune response). Adjuvant, a Latin word meaning “to help”, are the components of vaccine which improves the magnitude and durability of the induced immune response. Adjuvants have been used to improve the efficacy of the vaccine candidates since the early 1920s. They expedite antigen delivery to antigen presenting cells (APCs), enhances their processing and presentation by APCs. Additionally, it modulates antibody avidity and stimulates cell mediated immune responses (Awate, Babiuk, and Mutwiri 2013). Several diverse classes of compounds such as mineral salts, cytokines, microbial products, bacterial antigens, saponins, polymers and liposomes have been investigated as adjuvants (Guy 2007). Here in this study, we used cholera toxin B (CTB) from *Vibrio cholerae* and flagellin (FliC) from *Salmonella* Typhimurium as both vaccine antigens and adjuvants.

CTB was reported to have significant potential as vaccine adjuvant through multiple routes of administration, especially for oral and nasal vaccines. Oral adjuvanticity was better observed with live attenuated vaccines (Lopez et al. 2008), whereas nasal immunization worked well for subunit vaccines (Stratmann 2015). This was assumed to be refereed by the increased activation of dendritic cells (DCs) and T and B cell responses, thereby, reducing the antigenic dose requirement by five to tenfold. Study with the IFN-γ ELISPOT assay showed that 10μg DNA co-administered with CTB augmented the cellular immune responses to the magnitude of 50μg DNA used alone (Hou et al. 2014). Another study indicated that the adjuvant potential of CTB is due to direct stimulation of CD4+ and CD8+ T cells. These antigen primed T cells further improve the production of IL-2, IL-4, and IFN-γ cytokines (Wang, Bregenholt, and Petersen 2003). Primarily, CTB was reported to induce Th2-predominant immune response, whereas a Th1 type response was also observed in several studies (Stratmann 2015; Wiedinger, Pinho, and Bitsaktsis 2017; Lee et al. 2015).

CTB was shown previously to activate TLR signaling in BMDCs, resulting in proinflammatory cytokine production (Hou et al. 2014). In vivo and ex-vivo experiments with subcutaneous KLH immunization showed that CTB can also function as a potent adjuvant through direct stimulation of antigen-primed CD4+ and CD8+ T cells and stimulates IL-2, IL-4, and IFN-γ production (Wang, Bregenholt, and Petersen 2003).

The flagellin (FliC) protein of Gram-negative bacteria is a potential adjuvant. It binds to cell surface TLR-5 receptors and IpaF intracellular receptors, ultimately eliciting a pro-inflammatory signalling pathway (Hayashi et al., 2001) and stimulating the host immune system to eliminate bacterial infections. Since bacterial flagellin is involved in cell adhesion (Haiko and Westerlund-Wikström, 2013), the presence of flagellin on the cell surface promotes antigen uptake and presentation into antigen-presenting cells, eliciting robust immune response. Anti-FliC antibodies were reported to enable phagocyte dependent killing and also diminish the bacterial motility (Simon et al. 2013).

Here in this chapter, we will investigate the augmentation of immune responses induced by adjuvants.

5.2. Methods used:

Functional potential of the induced humoral and mucosal secretory antibodies after successful mucosal and systemic immunization, were investigated by assessing their ability to inhibit *S.* Typhi adherence to the epithelial cell monolayers, their respective potential to facilitate opsonophagocytosis and finally by investigating the impairment of the bacterial motility in presence of these antibodies. All the detailed methodologies are described in the material method section **3.2.15.3, 3.2.15.4**, **3.2.15.6.**

Later, we assessed the augmentation in the cytokine response in presence of an adjuvant. We also assessed the cytokine response in the immunized mice for gaining an insight for the cell mediated immune response augmented by the adjuvants used along with the antigen and were discussed in **3.2.7.4.** T cells secreting IFNγ and IL-17 cytokine was enumerated in immunized mice using IFNγ and IL-17 ELISPOT assay and were discussed in **3.2.8**.

All the experimental mice were infected with *S.*Typhi and *S.* Paratyphi A. Bacterial load determination in intestine, visceral organs and feces were discussed in **3.2.6.4, 3.2.6.5.** Further, histopathological changes in the intestinal segments, pathological scoring and MPO assay were **3.2.6.6, 3.2.14.**

5.3. Results:

5.3.1. Intranasal rCTB-T2544 immunization induces immunoglobulins with enhanced adhesion inhibition capacity.

Intranasal rCTB-T2544 immunization induces humoral and mucosal immunoglobulins in serum and fecal extract and intestinal contents, respectively. To investigate the functional potentiality of these antibodies, we studied whether the antibody-mediated blocking could prevent bacterial adhesion to epithelial cells. To this end, *S*. Typhi expressing green fluorescent protein were preincubated with heat inactivated sera, fecal and intestinal contents for 30 mins at 1:50 dilution. Further, these were used to infect HT-29 cell suspensions at 1:10 MOI. Adhesion of the bacteria, undergoing different pre-incubation treatment, to HT-29 cell monolayer were assessed with CFU counts and confocal microscopy. Antibodies from different immunized groups showed inhibition in bacterial adhesion to the HT-29 cells, out of all these, the maximum inhibition was found for the samples collected from rCTB-T2544 immunized mice (**Fig. 20A, 20B**).

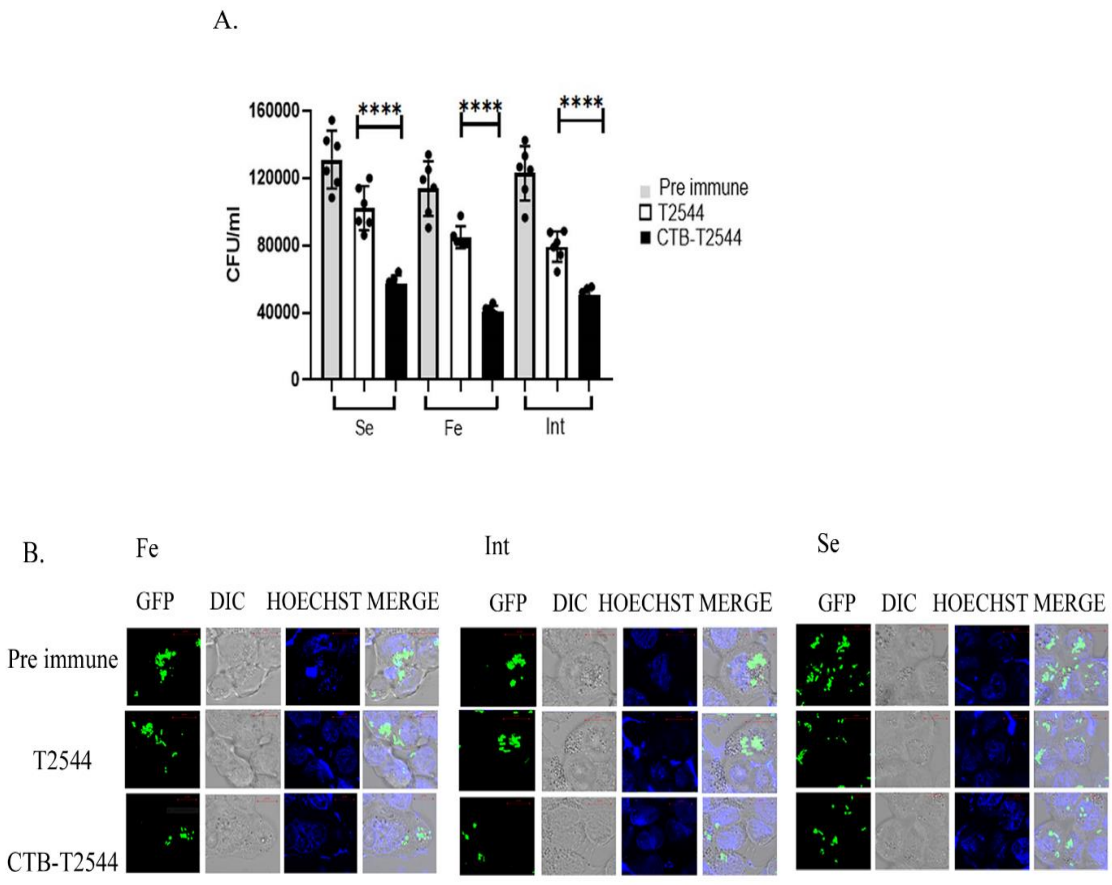

Fig 20. Immunoglobulins pose abilities to inhibit adhesion of bacterium to HT-29 cell. Serum, fecal extract and intestinal contents were collected from the immunized mice and pre-incubated with the *Salmonella* Typhi Ty2 expressing green fluorescent protein at 1:50 dilution for 30 mins. These suspensions were infected HT-29 cells (at M.O.I 1:10) and infection continued for 30 mins. A. Post infection, adherent bacteria were quantified by CFU counts recovered in LA plates after cell lysis with 1% triton-X100. B. Post infection, cells were washed and subjected to Hoechst staining. The cells were viewed under confocal microscope. Nucleus of the cells and adhered bacteria appear blue and green, respectively. Significance was evaluated using two tailed unpaired t test, comparing CTB-T2544 group with the corresponding T2544 group. ****$p<0.0001$.

5.3.2. Magnitude of adhesion inhibition capacity of immunoglobulins generated in rCTB-T2544 immunized mice.

We evaluated the magnitude of the functional potentiality of the induced immunoglobulins in rCTB-T2544 immunized mice by an extended adhesion inhibition assay. Here the bacteria were pre-incubated with the sera, fecal extract and intestinal contents for 30 mins at various dilutions (1:50,1:500,1:5000). We observed that 1:5000 dilutions of antibodies from rCTB-T2544 group achieved the similar magnitude of adhesion inhibition as observed in 1:50 dilution of the pre-immunization samples. This suggested that the former retained 100-fold more competency for the similar function (**Fig. 21**).

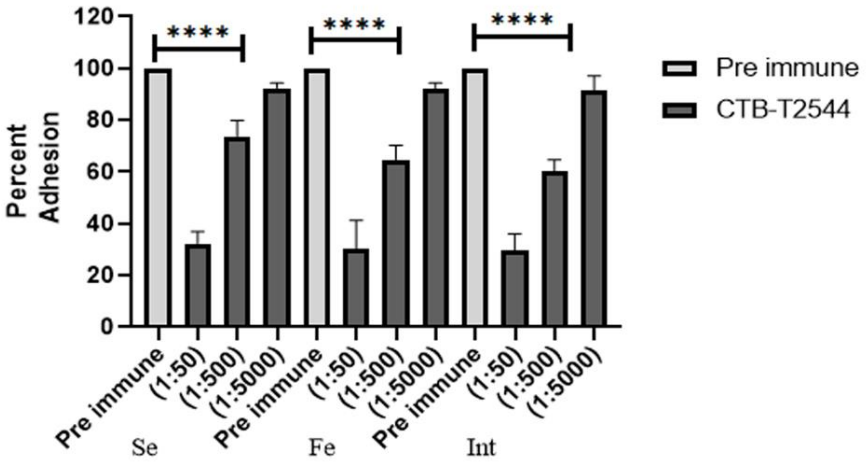

Fig 21. Pretreatment with immunoglobulins prevents percent adhesion of bacteria in HT-29 cells. Bacteria (*S*.Typhi) were pre-incubated with different dilutions of the serum and secretory antibodies for 30 min, followed by infection of HT-29 cells. Bacterial adhesion was calculated by CFU counts, recovered from the infected cells after overnight culture on Luria Agar plates, containing streptomycin (50 μg/ml). Percent adhesion for CTB-T2544 immunized samples was calculated with respect to adhesion for the corresponding pre-immune samples, considering it as 100 percent. Significance was calculated using unpaired t test between CTB-T2544 and pre immune sample.

5.3.3. Intranasal rCTB-T2544 immunization induces immunoglobulins with enhanced opsanophagocytic ability.

Functional validation of the induced immunoglobulins was determined by comparing the bacterial opsanophagocytosis by THP-1 cells in presence and absence of immunoglobulins. To this end, *S*. Typhi bacterial cell suspension was pre-incubated with 1:50 dilutions of serum, fecal extract and intestinal content for 30 mins and the suspension was used to infect THP-1 cell line at M.O.I 10. Opsanophagocytosis activity was checked by plating the internalized bacteria on appropriate agar plate. The mean peak fold increase of bacterial phagocytosis was found to be significantly higher following opsonization of the bacteria with the immunoglobulins generated in rCTB-T2544-immunized mice compared with the other immunized groups (**Fig. 22A**). This was also visualized when the infected THP-1 cells subjected to confocal microscopy. The bacteria appear green as it expressed green fluorescent protein and the nucleus appeared blue due to the Hoechst staining (**Fig. 22B**).

A.

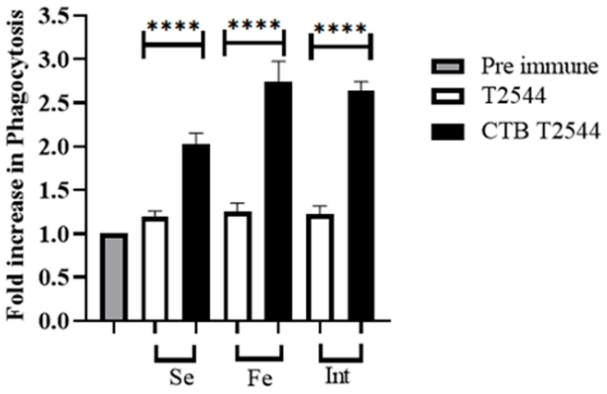

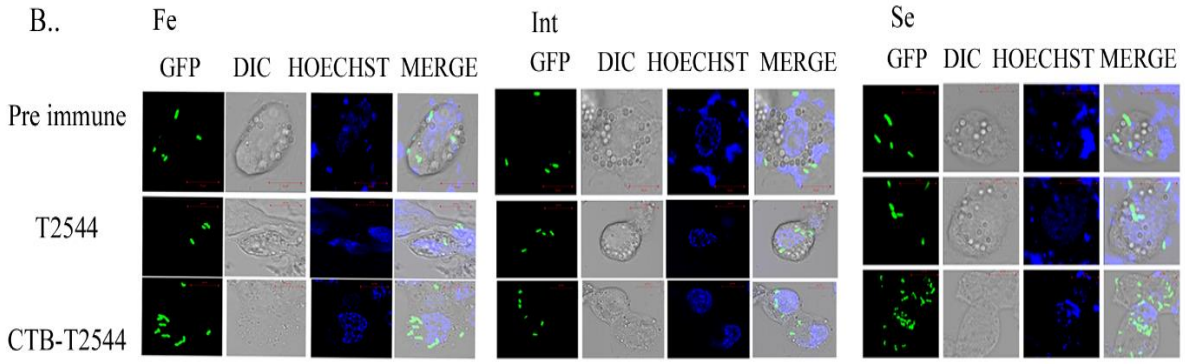

Fig.22. Opsanophagocytosis assay. *Salmonella* Typhi Ty2 expressing GFP, were pre-incubated with 1:50 dilution of the sera, fecal extract and intestinal content, followed by infection of the THP-1 cell monolayer. A. Phagocytosed bacteria for each treatment were quantified after cell lysis. The mean fold increase in the immunized samples were compared with the pre-immune counter parts. B. Post infection, cells were washed and subjected to Hoechst staining. The cells were viewed under confocal microscope. Nucleus of the cells and adhered bacteria appear blue and green, respectively. Significance was calculated using unpaired t test between CTB-T2544 and pre immune sample.

5.3.4. Soft agar motility inhibition assay.

Another experiment for determining functional potentiality of the induced immunoglobulins post immunization was bacterial motility inhibition by the immunoglobulins. 10 mL semi-solid medium was prepared with LB containing 0.4% agar, mixed with 5% of sera, and r the fecal extracts or intestinal contents of the immunized mice. Subsequently, 10 µL of *S.* Typhi cell suspension (OD600 = 0.2) was loaded on the center of each plate. Plates were then incubated at 37 °C for 6 hours. The progression of bacterial movement was measured by the diameter of the zone of inhibition which was presented in the graph (**Fig. 23A**). The representative image of the motiliy inhibition assay was captured (**Fig. 23B**)

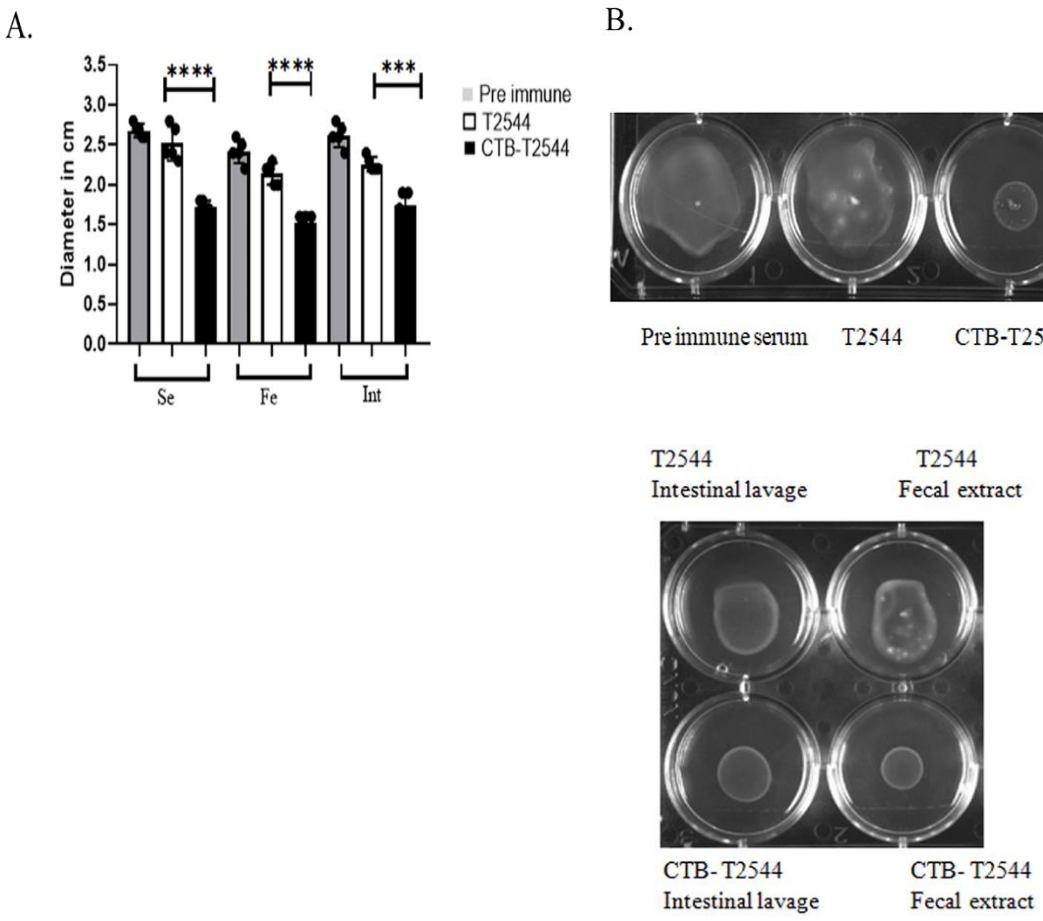

Fig 23. Motility inhibition assay. Motility of *Salmonella* Typhi Ty2 in LB +0.4% agar plate containing serum, fecal extract and intestinal content of immunized mice was observed till 6 hr. A.The zone diameters of bacterial growth were recorded and plotted. B. Representative images from each group is shown. Significance was evaluated using two tailed unpaired t test, comparing CTB-T2544 group with the corresponding T2544 group. ****p<0.0001, ***p=0.0002.

5.3.5. Relative contribution of mucosal antibodies imparting protection against *S.* Typhi infection.

To further characterize the relative contributions of the induced humoral and mucosal antibodies post rCTB-T2544-immunization, we performed two experiments simultaneously. In the first experiment, pooled immune sera from the rCTB-T2544-immunized mice were adoptively transferred to the naïve mice, followed by a lethal *S.* Typhi infection. 25% of the mice which received the sera, survived the challenge dose. This indicated a relatively minor role contributed by the serum antibodies (**Fig. 24A**). Next, to investigate the relative

contribution of mucosal antibodies in overall protection, we pre-incubated the bacteria (*S.* Typhi) with intestinal lavage and fecal extracts from the rCTB-T2544 immunized mice for 30 minutes. These pre-treated bacterial suspensions were used to infect the naïve mice. A lethal dose of these pre-treated bacteria killed 50% of the infected mice, while a sublethal dose of these pre-treated bacterial suspensions showed substantial reduction in the intestinal (ileum, cecum and colon) colonization (**Fig.24B–D**) and subsequent dissemination to the internal organs (MLN, spleen and liver) (**Fig.24E–G**) compared with the similar dose of un-treated bacteria. Together all these findings highlighted a significant role of mucosal antibodies in imparting protection.

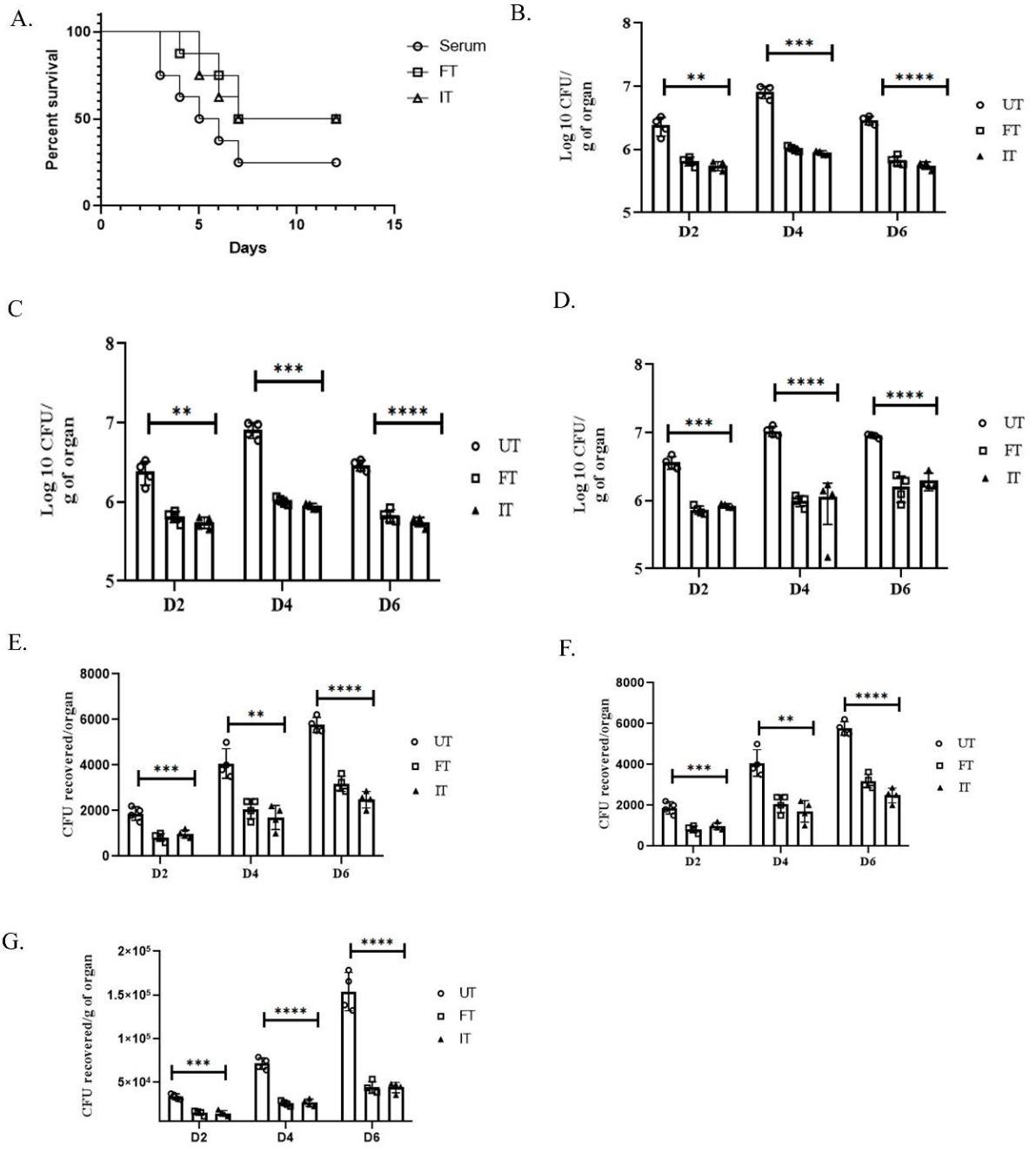

Fig.24. CTB-T2544 immunization induces protection from *S.* Typhi challenge. A. Pooled sera from rCTB-T2544-immunized BALB/c mice (n = 8) were adoptively transferred to naïve mice (n=8), followed by challenge with 5 × 10^6 CFU of *S.* Typhi through orogastric route. Similar experiments were performed in parallel by infecting naïve mice (n=8/group) with *S.* Typhi, pre-incubated with fecal extracts or intestinal lavage from rCTB-T2544 immunized mice. Animals were monitored for the next 12 days and percent death was calculated. B-G. In separate experiments, three groups of naive BALB/c mice (n= 12/groups; UT, FT and IT) were challenged with 10^4 CFU of *S.* Typhi Ty2, pre-incubated with or without fecal extracts and intestinal lavage from CTB-T2544 immunized mice. Mice were euthanized at days 2, 4, and 6. Bacterial load in the intestinal tissues (Ileum B, Cecum C colon D), Mesenteric lymph nodes (MLN, E) and visceral organs (Spleen F and liver G) were determined by culturing organ homogenates on LB Agar plates with streptomycin selection (50 μg/ml). Significance was calculated by comparing recovered CFU of bacteria from FT and IT group with UT group using unpaired t tests. UT- untreated bacteria, FT- bacteria treated with fecal extracts, IT- bacteria treated with intestinal lavage samples.

5.3.6. Analysis of Th Cell Response upon CTB-T2544 immunization. Th1 response is reported to be effective for elimination of *Salmonella*, whereas Th2 and Th17 majorly promote generation of humoral and mucosal antibodies. To gain partial insight into the nature of cell mediated immune responses induced by intranasal immunization with rCTB-T2544, we collected serum after 12 days of last immunization and assessed the cytokine response in serum. We observed an enhanced IL12 and IFNγ response with increased IL-4, IL-5, IL-10 cytokines in rCTB-T2544-immunized mice as compared to rT2544immunized groups (**Fig. 25A**). Additionally, the number of IFNγ- and IL-17A-secreting T cells in the Peyer's Patches was also augmented markedly after CTB-T2544 immunization (**Fig. 25B**).

A.

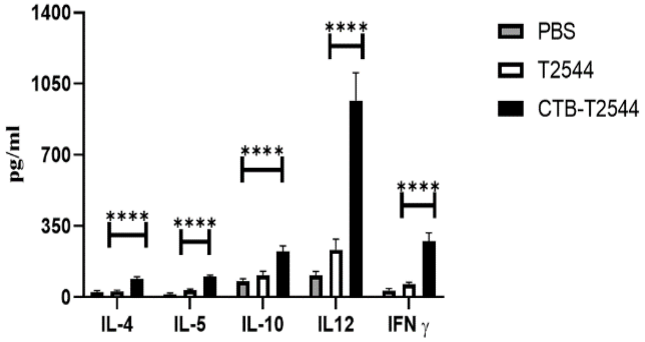

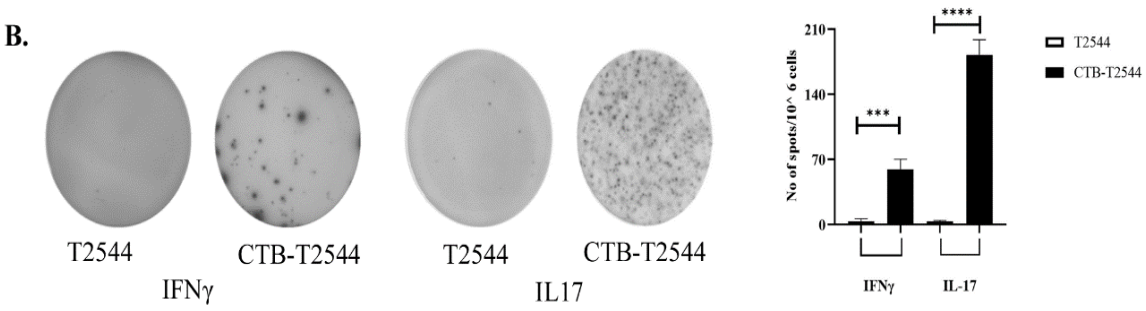

Fig. 25. Cell mediated response upon mucosal immunization. A. Different cell cytokines including Th1 (IL-12, IFN-γ) , Th2 (IL-4, IL-5), and Treg (IL-10) in the serum samples of different immunized mice were measured by ELISA. B. Cells from the Peyer's Patches of the mice from different group were isolated and incubated with rT2544 (10µg) for 24h. An ELISpot assay was performed to enumerate cytokine-secreting cells and data were represented as spot forming cells/ 10^6 total cells analyzed.

5.3.7. Intranasal rCTB-T2544 protects immunized mice from *S*. Paratyphi challenge by reducing bacterial colonization.

To further investigate if the protection (described in 4.4.3.4) was due to reduced colonization and systemic dissemination of *S*. Paratyphi, immunized mice were infected with 5 x 10^4 CFU of the bacteria. A significant reduction of intestinal colonization with fewer bacteria invading the systemic circulation was observed and compared with the mice that received rT2544, suggesting protection by the fusion protein vaccine (**Fig. 26A, 26B, 26C**).

A.

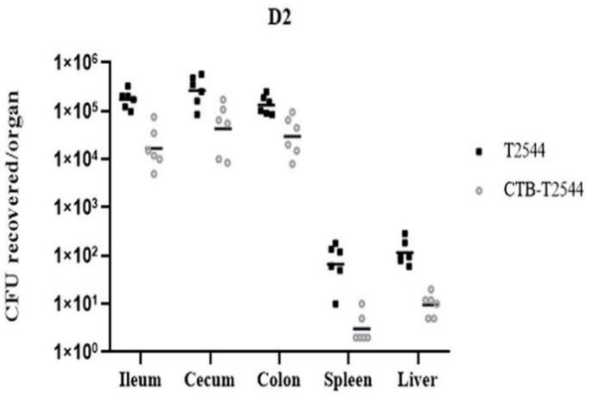

B.

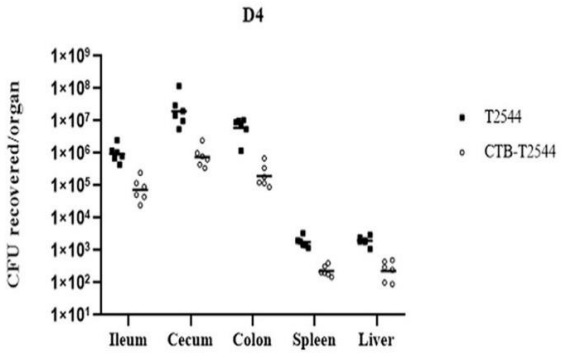

C.

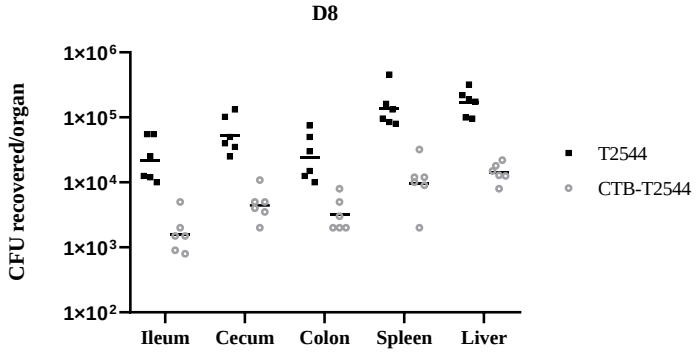

.

Fig 26. Reduced bacterial colonization leads to protection against *S*. Paratyphi A infection. Mice were intranasally immunized with rCTB-T2544, thrice at 12 days interval. 12 days after the last immunization mice were challenged with 5 x 10^4 CFU of the bacteria. Mice were euthanized on day 2(A), 4(B) and 6(C) post infection and bacteria were recovered from intestinal tissues and internal organs. Geometric mean of each group was plotted.

5.3.8. Comparative insights into the intestinal pathology of rCTB-T2544 and rT2544 immunized mice.

Since we observed reduced bacterial colonization upon intranasal CTB-T2544 immunization, we further investigated the intestinal pathology of these experimental mice. Vaccine-induced protection was further studied by histopathological analysis of the ileal, cecal and colonic tissues.

5.3.8.1. Pathology of Ileal sections.

On day 3 post infection, ileum of rT2544 immunized mice showed ulcerated epithelial lining with gradual effacement of glandular/ ductal crypt architecture through intense inflammatory infiltrates, hemorrhagic areas, edematous changes along with epithelial erosion (**Fig. 27A**). On Day 8, although focal hemorrhagic areas are present, gradually progressive restoration of the glandular/lobular and cryptic pattern can be seen. But inflammatory infiltrate is still evident **(Fig.27C).** On the contrary, CTB-T2544 immunized mouse ileal epithelium shows relatively fewer inflammatory infiltrate cascading in between the glandular fronds, hemorrhagic areas are also lesser (**Fig. 27B, 27D**).

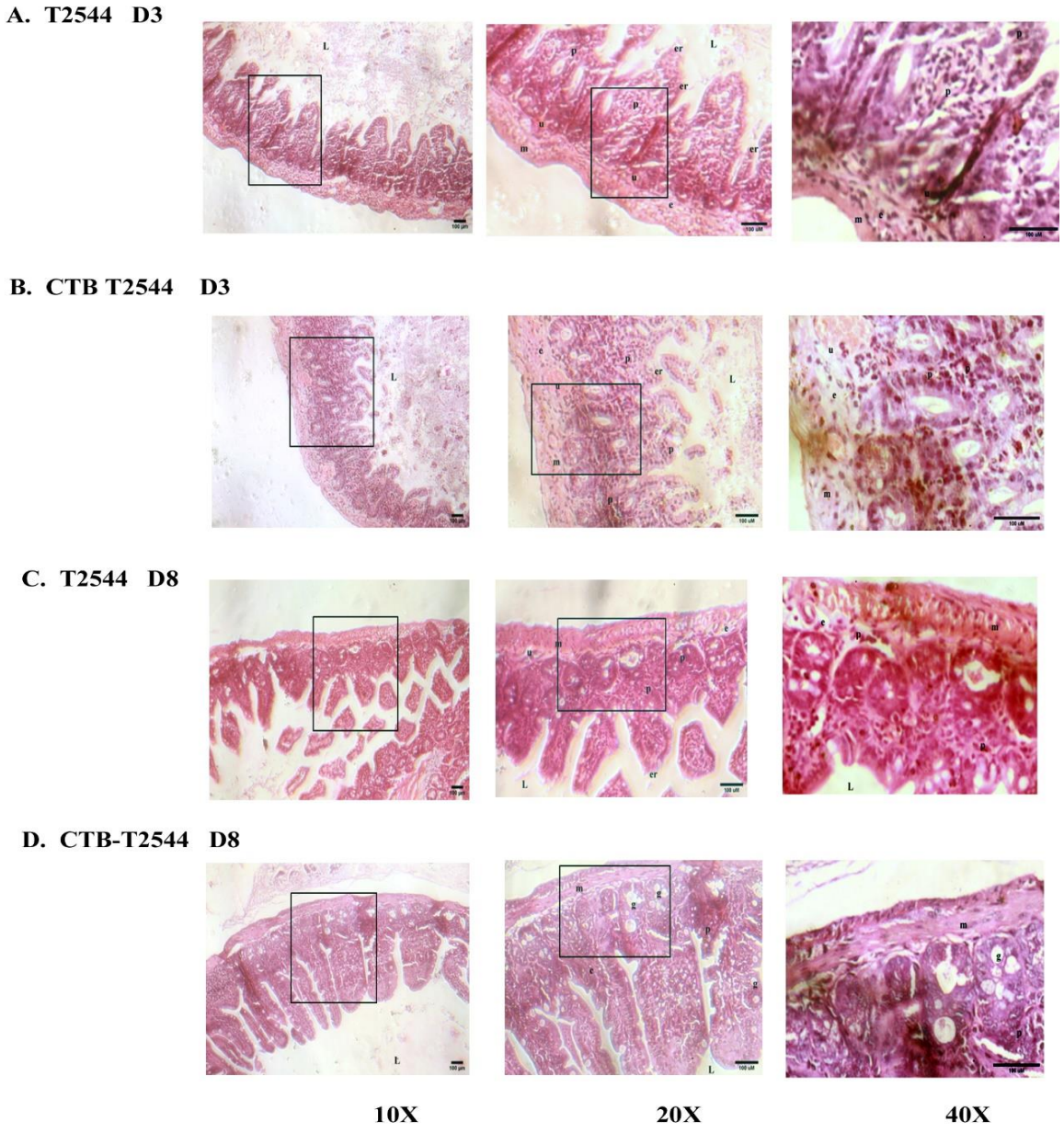

Fig. 27: Intestinal pathology of rT2544 and rCTB-T2544 immunized mice -Microscopic changes of ileal sections. rT2544 and rCTB-T2544 immunized mice were infected with 5 × 10^4 *S.* Paratyphi A. Ileal sections of rT2544 immunized mice on day 3 (A) and day 8 (C) post infection were fixed, embedded in paraffin, and 5 µm thin sections were stained with H&E and were analyzed. Similarly, ileal sections of rCTB-T2544 immunized mice on day 3 (B) and day 8 (D) post infection were processed. Images were captured at 10X, 20X and 40X. The pathological changes were mentioned in the image as L- lumen, m - mucosa, sa – submucosa, p - PMN infiltration, e - edema, er – epithelial erosion, u – ulceration, c – crypt.

5.3.8.2. Pathology of Cecal sections.

Similarly, cecal mucosa of t2544 group showed subepithelial hemorrhage, sprinkling of inflammatory infiltrates on glandular crypt architecture along with ulceration and edematous areas (**Fig. 28A**). Epithelial stratification is better maintained in CTB-T2544 immunized mice along with comparatively lesser inflammatory infiltrates and hemorrhagic areas, although edematous areas are still evident (**Fig. 28B**). On day 8, although epithelium is still associated with inflammation, it is reduced to some extent along with lesser edematous and hemorrhagic zones (**Fig.28C**), especially apparent in CTB-T2544 group (**Fig. 28D**).

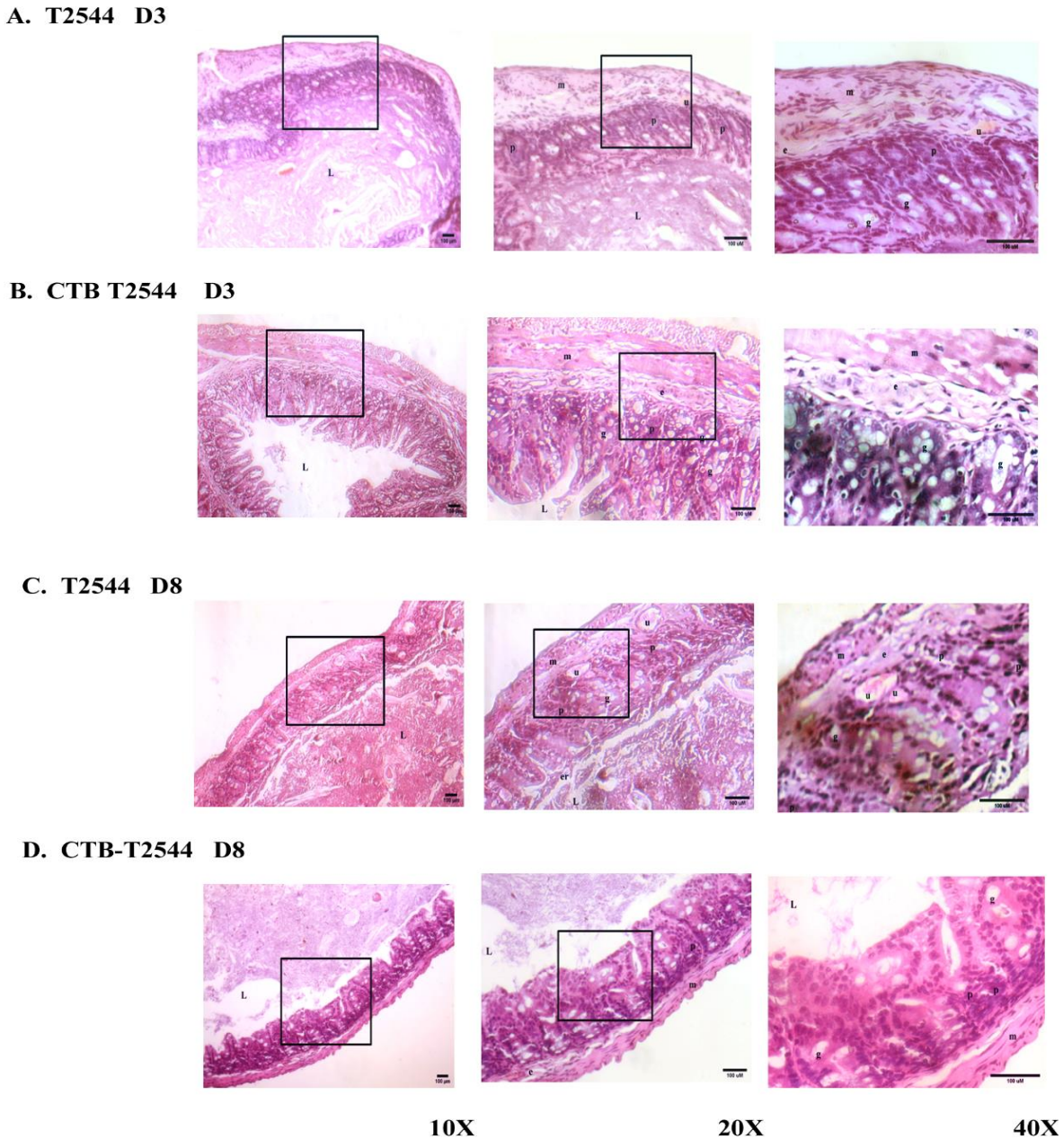

Fig 28: Intestinal pathology of rT2544 and rCTB-T2544 immunized mice -Microscopic changes of cecal sections. rT2544 and rCTB-T2544 immunized mice were infected with 5 × 10^4 *S.* Paratyphi A. Cecal sections of rT2544 immunized mice on day 3 (A) and day 8 (C) post infection were fixed, embedded in paraffin, and 5 µm thin sections were stained with H&E and were analyzed. Similarly, cecal sections of rCTB-T2544 immunized mice on day 3 (B) and day 8 (D) post infection were processed. Images were captured at 10X, 20X and 40X. The pathological changes were mentioned in the image as L- lumen, m - mucosa, sa – submucosa, p - PMN infiltration, e - edema, er – epithelial erosion, u – ulceration, c – crypt.

5.3.8.3. Pathology of Colonic sections.

On day 3 colonic mucosa of T2544 group showed periglandular moderate inflammatory infiltrate along with hemorrhagic areas (**Fig.29A**), whereas CTBT2544 showed an almost intact epithelial, glandular/ cryptic architecture with markedly lesser inflammation (**Fig. 29B**). On day 8 T2544 group showed reduced inflammatory infiltrates and edematous changes (**Fig. 29C**). CTB-T2544 showed better preserved epithelial integrity along with robust maintenance of glandular ductal architecture with very lesser inflammation (**Fig. 29D**). Histopathological scoring of ileal, cecal and colonic segments of rCTB-T2544 immunized group showed lesser inflammatory score compared to rT2544 group. Together all these data suggest rCTB-T2544 immunization confer protection against *S.* Paratyphi A infection using our iron overloaded mice model.

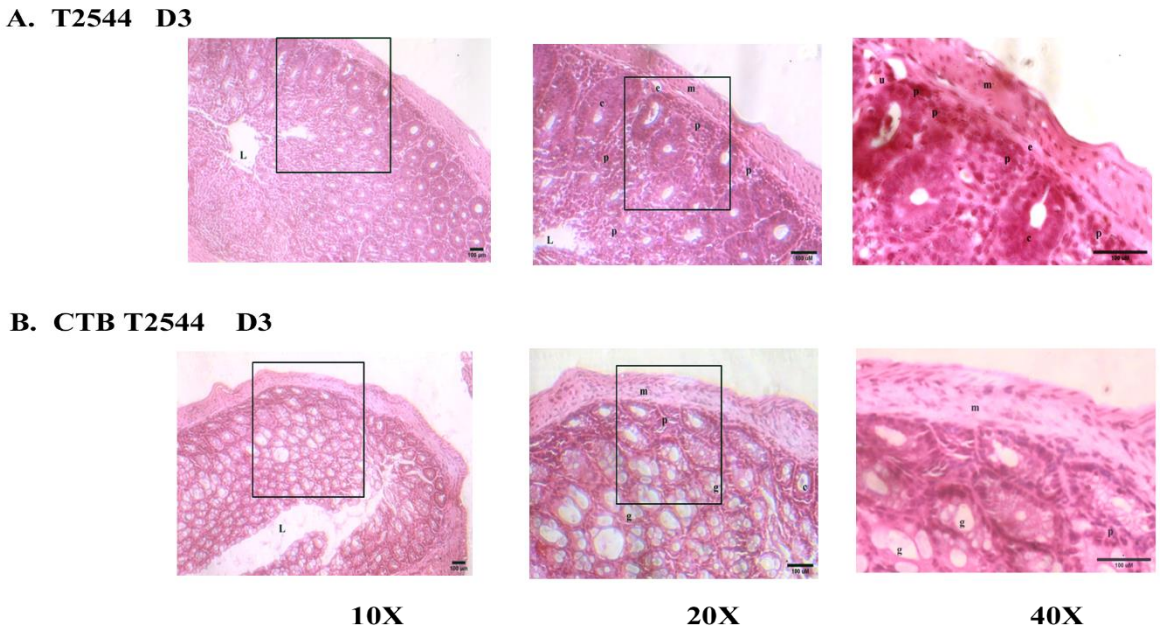

C. T2544 D8

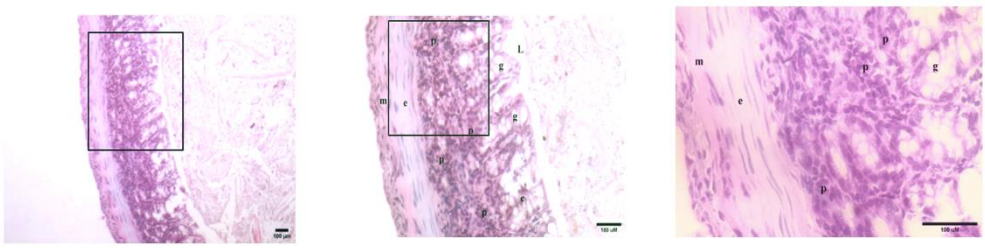

D. CTB-T2544 D8

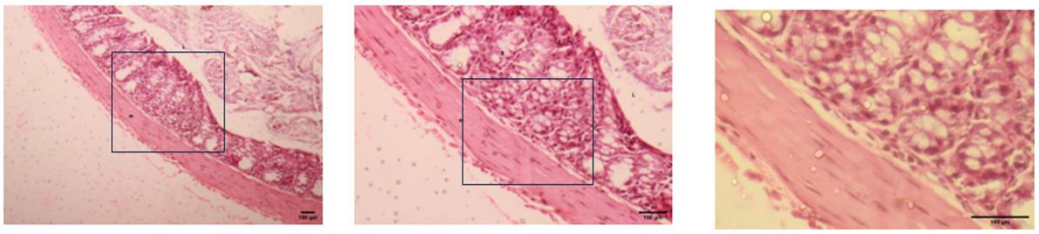

10X 20X 40X

E.

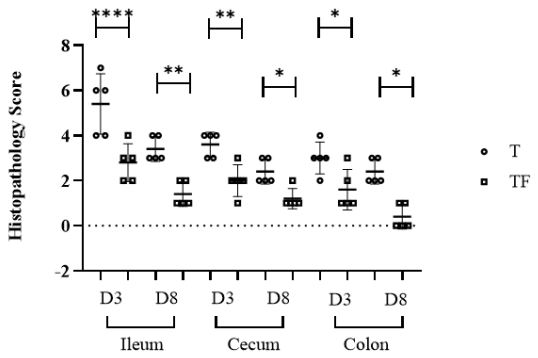

Fig 29: Intestinal pathology of rT2544 and rCTB-T2544 immunized mice -Microscopic changes of colonic sections. rT2544 and rCTB-T2544 immunized mice were infected with 5 × 10^4 *S.* Paratyphi A. Colonic sections of rT2544 immunized mice on day 3 (A) and day 8 (C) post infection were fixed, embedded in paraffin, and 5-µm thin sections were stained with H&E and were analyzed. Similarly, colonic sections of rCTB-T2544 immunized mice on day 3 (B) and day 8 (D) post infection were processed. Images were captured at 10X, 20X and 40X. The pathological changes were mentioned in the image as L- lumen, m - mucosa, sa – submucosa, p - PMN infiltration, e - edema, er – epithelial erosion, u – ulceration, c – crypt. Histopathological scoring of ileum, cecal and colonic sections of (E) CTB-T2544 group was evaluated by the extent of inflammatory cell infiltrate with epithelial changes compared with T2544 infected group. One way anova was performed to calculate significance of the various group. Error bars denote SD. *p:0.3332,**p:0.0021***p:0.0002,****p<0.0001.

5.3.9. Intranasal CTB-T2544 induces memory responses.

Next, to investigate the recall of cell mediated immunity, we isolated CD4+ T-cells from the spleenocytes of the experimental mice and were cocultured with *S*. Typhi-pulsed BMDCs derived from naïve mice and IFNγ release were quantified in the culture supernatants. The level was significantly higher for the rCTB-T2544 as compared to rT2544 and PBS group suggesting an augmentation of the memory response by CTB (**Fig. 30A**). Further, the percentages of both central memory (T_{CM}: $CD62L^{high}CD44^{high}$) and effector memory (T_{EM}: $CD62L^{low}CD44^{high}$) T cells (MacLeod et al. 2009) were observed to be increased in rCTB-T2544 group compared with rT2544 group **(Fig. 30B).** To assess the generation of memory B cells, a booster dose was administered on 108th day post first immunization and 12 days later, the level of serum anti-T2544 antibodies were quantified**.** A steeper increase in humoral antibody titers was observed in the rCTB-T2544 group compared to the rT2544 (**Fig. 30C**). Later, we measured the avidity index of these anti-T2544 IgG antibodies. The immune complexes were washed with or without 4M urea containing buffer and the respective absorbance were read. A significantly high avidity index (60–65%) was observed after the primary rCTB-T2544 immunization, which further increased up to the 70–78% following the booster immunization (**Fig. 30D**). In contrast, we found lower avidity index after rT2544 immunization (<35%), indicating poor priming in this group. These results together indicated an induction of long-term immune response against *S*. Typhi infection in intranasal rCTB-T2544 group compared to rT2544 group.

A.

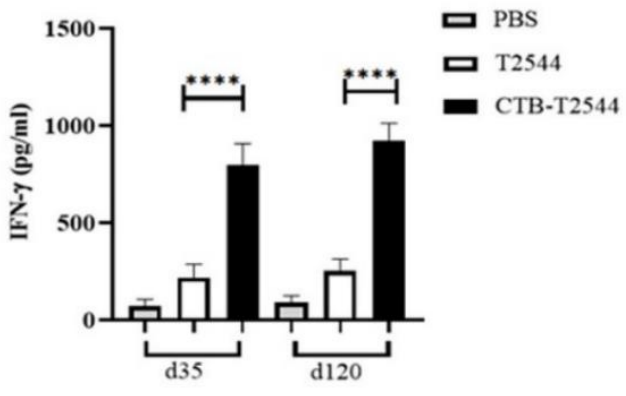

B.

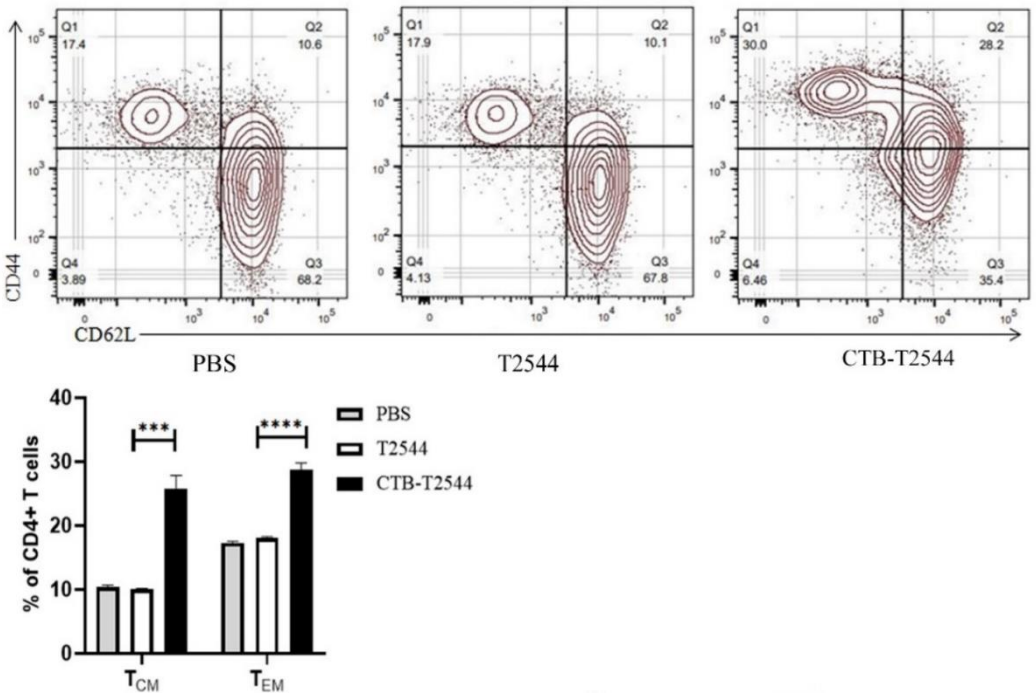

C.

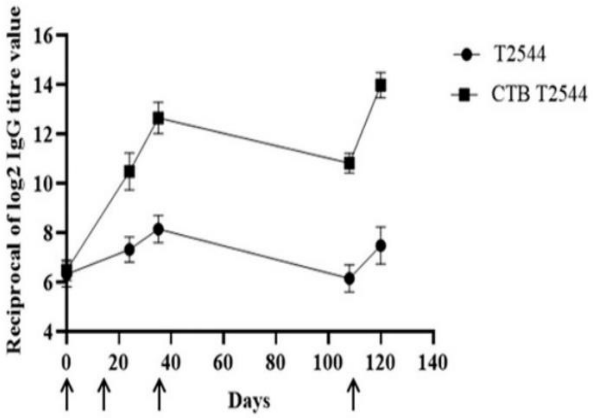

D.

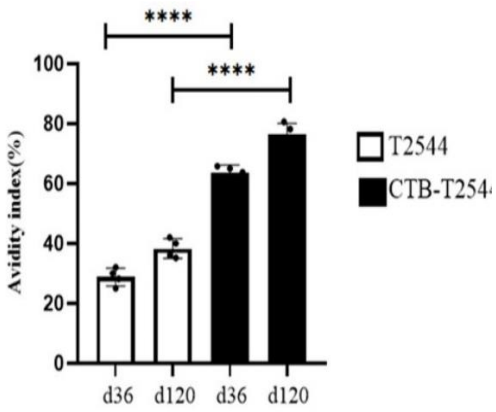

Fig 30. Immunological memory response upon intranasal CTB-T2544 immunization. A. Memory T cells were quantified using ELISA by measuring the IFN-γ release in the culture supernatants of CD4+ T cells (harvested from the spleenocytes of the experimental mice) and co-cultured with BMDCs, pulsed with rT2544. Data represents mean(±SD) of three independent experiments. B. The percentages of TEM (CD4+CD44hiCD62Llo) and TCM (CD4+CD44hiCD62Lhi) cells from the spleenocytes of the experimental mice were measured with flow cytometry. Representative images from one of the experiments and statistical analysis of the data from all three experiments are shown. C. Serum antibody titer (mean± SD) measured in the immunized mice (n=6) at the indicated time points are shown. Arrows indicate primary (3 doses at 0, 12 and 24th day) and booster (108th day) immunization. Mean± SD were

plotted for CTB-T2544 and T2544. D. Avidity assay. Anti-T2544 avidity index was measured by ELISA and represented as the ratio of IgG bound to T2544 in the presence and absence of 4M urea, multiplied by 100. Significance was calculated using one way (A,D) and two-way (B) ANOVA with post hoc analysis using Tukey's multiple comparison test. Error bars represent SD. ****p<0.0001.

5.3.10. Systemic immunization with rT2544 and rFliC (TF) induced humoral and mucosal antibodies with enhanced opsanophagocytic ability and increased adhesion inhibition capacity.

To validate functional activity of induced antibodies upon systemic immunization of T (T2544) and TF (T2544 and FliC), we investigated bacterial adhesion to the HT-29 cells at a fixed dilution of the different mucosal antibodies (fecal and intestinal extract) and humoral antibodies (serum). We noted significant inhibition in bacterial attachment with the antibodies collected from TF immunized mice compared to other groups (**Fig. 31A**). Similarly, upon opsonization of the bacteria from TF immunized mice, mean peak fold increase of bacterial phagocytosis by THP-1 cells was significantly higher as compared to other groups (**Fig. 31B**). These data together indicated induction of an improved functional potency in humoral and mucosal antibodies collected from TF immunized mice.

A.

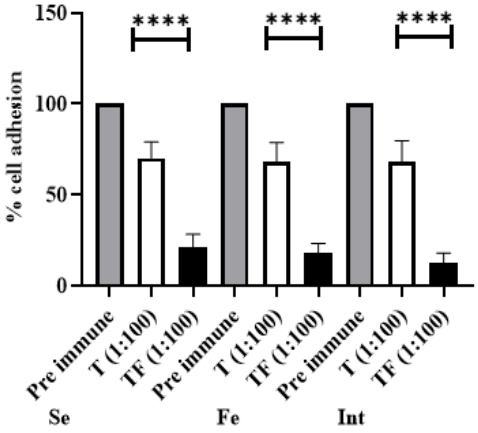

B.

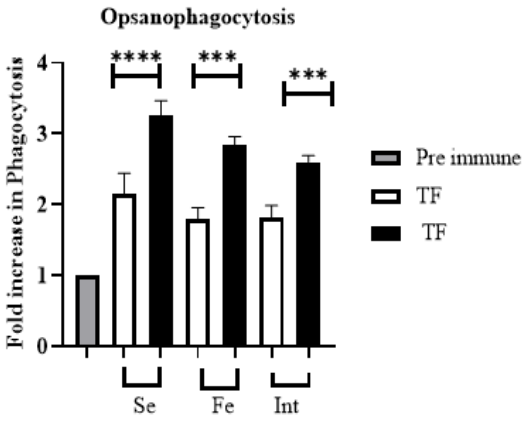

Fig. 31. TF potentiate induction of functionally active humoral and mucosal antibodies. A. Serum, fecal extract and intestinal contents were collected from the immunized mice and pre-incubated with the *Salmonella* Typhi Ty2 expressing green fluorescent protein at 1:50 dilution for 30 mins. These suspensions were infected HT-29 cells (at M.O.I 1:10) and infection continued for 30 mins. A. Post infection, adherent bacteria were quantified by CFU counts recovered in LA plates after cell lysis with 1% triton-X100. B. *Salmonella* Typhi Ty2 expressing GFP, were pre-incubated with 1:50 dilution of the sera, fecal extract and intestinal content, followed by infection of the THP-1 cell monolayer. A. Phagocytosed bacteria for each treatment were quantified after cell lysis. The mean fold increase in the immunized samples were compared with the pre-immune counter parts. One way anova was performed to calculate significance of the various group. Error bars denote SD. *p:0.3332,**p:0.0021***p:0.0002,****p<0.0001.

5.3.11. Reduced bacterial colonization upon TF immunization.

Since we observed TF immunized mice conferred protection against lethal *Salmonella* Typhi and *Salmonella* Paratyphi infection, we further assessed whether it was due to reduced bacterial load in the intestinal and visceral organs. Mice were infected with a sub-lethal dose of S. Typhi (104 CFU) and Paratyphi A (5 X 103 CFU). A significantly reduced bacterial colonization was observed in intestinal (**Fig. 32A**) and as well as visceral organs such as liver (**Fig. 32B**) and spleen (**Fig. 32C**). Together these results suggested that TF conferred significant protection of mice against *S.* Typhi and *S.* Paratyphi A challenge.

A.

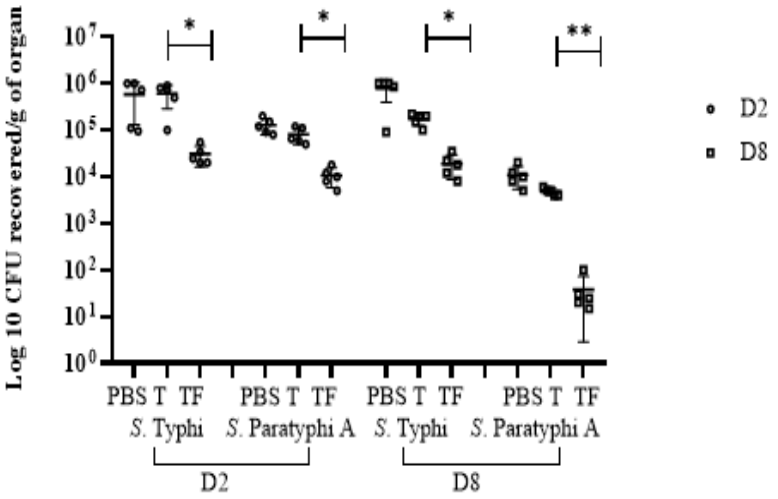

B.

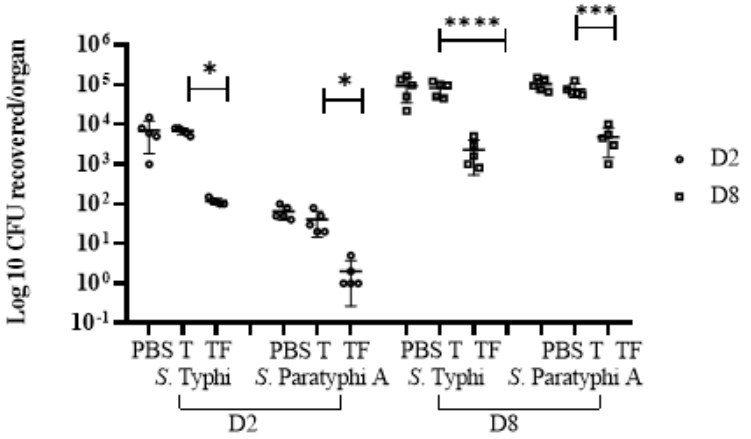

C.

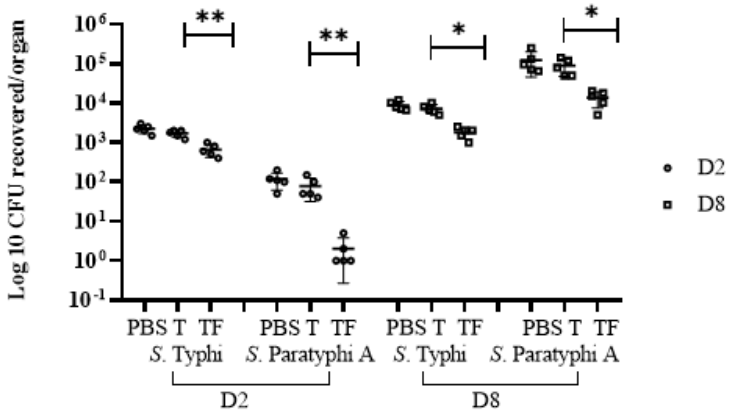

Fig. 32. TF immunization reduces bacterial colonization in intestine and subsequent dissemination to visceral organs. BALB/c mice (n=6/ group /time point) were immunized with PBS, T and TF and challenged with a sub-lethal dose of *S.* Typhi (104 CFU) and Paratyphi A (103 CFU). Mice were euthanized at the indicated time-points and intestinal segments and visceral organs were collected. Bacterial loads in the intestinal segments (A) and visceral organs including liver (B) and spleen (C) were determined by spreading the organ homogenates on HEA plates. Significance was calculated by comparing CFU of bacteria from TF immunized and T immunized mice using two way anova with Tukey's post hoc analysis. Experiments were repeated 3 times and data from one representative experiment is shown.

5.3.12. Cell mediated immune response (CMIR) upon TF immunization.

Cell mediated immune response (CMIR) contributes an essential role for complete clearance of intracellular bacterial like *Salmonella* (Kirimanjeswara et al. 2008). To investigate if TF immunization augments CMIR, splenocytes were isolated from the spleen of all the various immunized mice and stimulated with PBS or rT2544 for 72 hours. ELISA was performed to quantify the level of IFN-γ, IL-4 and IL-17 in the culture supernatant of the stimulated splenocytes. T and TF immunized mice both secrete comparatively higher cytokines to PBS immunized group; but the addition of rFliC produced statistically much higher IL-4, IFN-γ and IL-17 levels (**Fig. 33A).** Additionally, we observed markedly increased IFNγ- and IL-17A-secreting CD4+ T cells in the Peyer's Patches of the TF immunized mice (**Fig. 33B)**. All these data suggest that adjuvanted vaccine, FliC potentiates a mixed systematic Th1/Th2/Th17 immune response.

A.

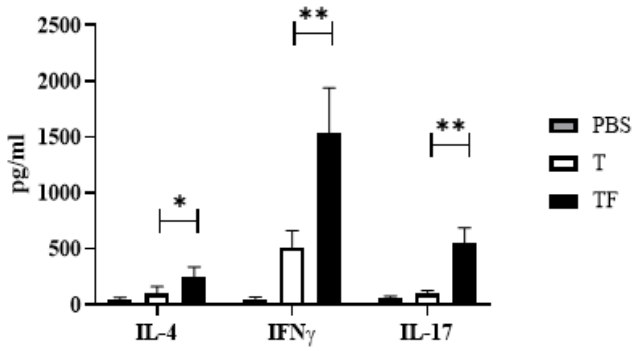

B.

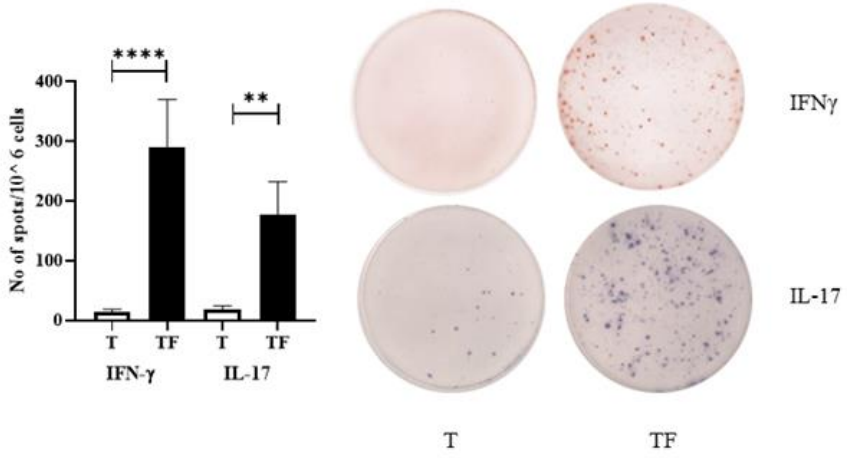

Fig. 33. TF immunization induces cell mediated immune response. A. Seven days after fourth immunization, splenocytes were isolated from all the immunized groups and were cultured in presence of PBS and 10ug of T and TF proteins for 24 h. IL-4, IFN-γ and IL-17 cytokines secretion in the culture supernatants were quantified using ELISA. B. Similarly, cells from peyer's patches were isolated and stimulated with PBS and 10ug of T and TF proteins for 24 h**.** IFN-γ and IL-17 cytokine-secreting cells were enumerated by ELISpot assays and data presented as spot forming cells/ 10^6 total cells analyzed**.** Significance was calculated by two-way (A) and one way (B) ANOVA with post hoc analysis using Tukey's multiple comparison test. The experiment was repeated three times and representative images from one experiment are shown. Bar diagram represents the statistical data from all three experiments. Error bars represent SD. ****p< 0.0001, ***p = 0.0006.

5.3.13. Immunization of mice with rT2544 generates immunological memory.

To investigate the recall of cell mediated immunity, we isolated CD4+ T-cells from the spleenocytes of the experimental mice on 30^{th} and 120^{th} days of post immunization and were cocultured with *S.* Typhi-pulsed BMDCs derived from naïve mice and IFNγ release were quantified in the culture supernatants. The levels were significantly higher at both the time points for TF group compared to T and unstimulated, supporting generation of durable T cell memory response in presence of FliC (**Fig. 34A**).

Next, splenocytes were isolated from T and TF immunized group and cultured in presence of B cell mitogens. T2544-specific memory IgA- and IgG-secreting ASCs were calculated using ELISPOT assay. The number of spots in unstimulated samples were subtracted from the number of mitogen stimulated samples, and the finally difference was presented as percentage of total number of ASCs found (**Fig. 34B**).

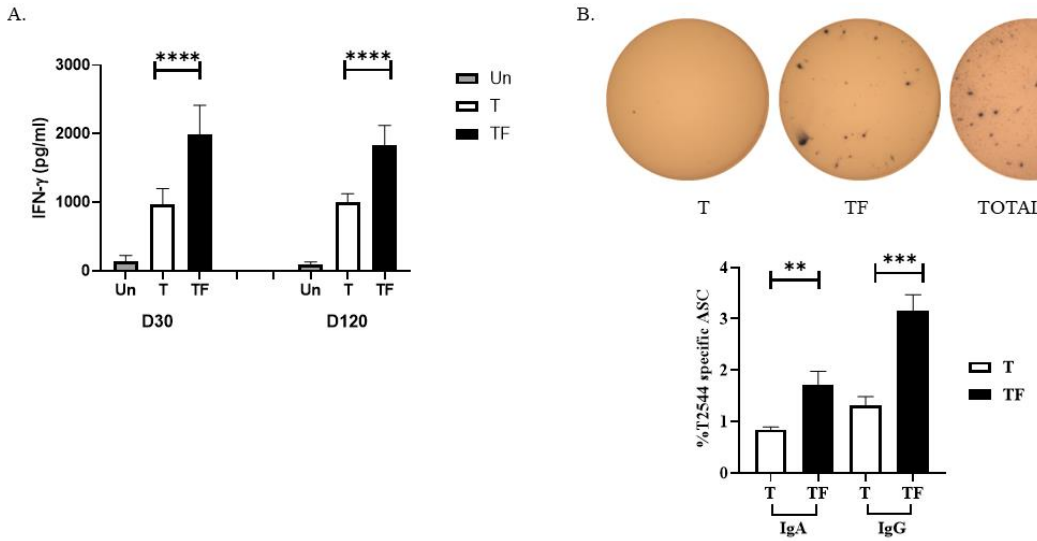

Fig. 34. TF immunization generates memory responses. A. Memory T cells were quantified using ELISA by measuring the IFN-γ release in the culture supernatants of CD4+ T cells (harvested from the spleenocytes of the experimental mice) and co-cultured with BMDCs, pulsed with rT2544. Data represents mean(±SD) of three independent experiments. B. For memory B cell response, splenocytes isolated from mice (n = 6) immunized with T, and TF were cultured in the presence of mitogens and the percentage of cells secreting T2544-specific IgG and IgA were calculated by ELISPOT assay. Significance was calculated w.r.t. the respective T-immunized group.

5.4. Take home messages.

- Here in this chapter, we assessed the functional potency of the induced humoral and mucosal antibodies upon rCTB-T2544 and T2544 with FliC immunization. Both the immunizations induced functionally active humoral and mucosal antibodies which greatly reduced the bacterial attachment to the host epithelial cells in a dose dependent manner. They greatly promote opsanophagocytosis of the bacteria by the macrophage cell line. Additionally, bacterial motility was found to be hindered in presence of these antibodies.
- Both the vaccine candidates generated a mixed Th1/Th 2/Th17 immune response in immunized mice, which is essential for effective elimination of *Salmonella.*
- We noted reduced bacterial colonization in rCTB-T2544 immunized group, whereas intranasally rT2544 immunized mice, which failed to confer protection against lethal bacterial challenge, showed higher colonization in the intestine and visceral organs. Additionally, lesser histopathological changes were observed with rCTB-T2544 immunized mice.
- All these data together suggested induction of a protective response against typhoidal *Salmonella* infection.

CHAPTER 6

Objective 3

Exploration of the mechanisms underlying the augmentation of immune response by adjuvants

6.1. Introduction.

Adjuvanticity of CTB was best observed with conjugated fusion proteins, either by genetically-conjugating the vaccine antigen or by coupling chemically to it, followed by nasal mucosal delivery to the host. CTB, owing to non-toxic nature and ease and reproducibility of recombinant protein production in large quantity, is one of the most popular mucosal adjuvants to-date (Sassone-Corsi et al. 2016; Kim et al. 2019). It can bind to the GM1 ganglioside receptor, which is expressed by multiple immune and non-immune cells such as B cells, macrophages, dendritic cells, epithelial cells. When CTB binds to GM1 ganglioside, it also targets the co-administered or chimeric antigen to the desired cell populations, resulting into increased antigen uptake and their presentation (Stratmann 2015; Lavelle and Ward 2022). Several other studies suggest direct antignen delivery through mucosal route often induce tolerance, most notably in the intestinal mucosa. CTB, on the contrary, was reported to break the oral tolerance due to unknown reasons, and was efficiently used as an oral adjuvant, such as with oral cholera vaccine (Dukoral), which is already commercially available and licensed for use (Clements and Freytag 2016). On the other hand, CTB delivered through non-oral mucosal routes improved antigen specific humoral and cell-mediated immunity, not only at the local site, but also at distal mucosa, a phenomenon called “common mucosal immunity”(Holmgren and Czerkinsky 2005).

Flagellin has shown to exert adjuvanticity as fusion protein partner and also by co-administering with other antigens. Literatures have established that the amount of flagellin required to induce maximal antigen-specific antibody response is much less than the dose necessary for maximal innate immunity (Honko and Mizel 2004; Honko et al. 2006), indicating a non-linear relationship between antibody response and degree of induced innate immune response. It can stimulate induction of proinflammatory cytokines and chemokines crucial for activation and developing antigen specific adaptive immunity. The activation of dendritic cells and other non-immune cells like epithelial and lymph node stromal cells by flagellin-based vaccines results into induction of cytokines and chemokines. This further promotes a significant recruitment of B and T lymphocytes to draining lymph nodes and thereby maximizing the development of antigen-specific lymphocytes (Hajam et al. 2017). All these mechanisms contribute to the overall potency of CTB and flagellin-based vaccines.

In this chapter, we will study the underlying mechanism to gain insight into how rCTB and rFliC are augmenting the host immune response, upon immunization with rCTB-T2544 and rT2544 and rFliC in our vaccine formulation.

6.2. Methods.

Confirming Dendritic cells (DCs) recruitment in the MLN and their migration was studied with flowcytometry. Next, the gut homing receptor expression on lymphocytes were quantified. Further, to investigate the percentage of induced follicular helper T cells along with the subset of memory T cells (T_{EM} and T_{CM}) were analyzed using flow cytometry. Data were analyzed with Flow Jo software. All the detailed methodologies were discussed in the material method section **3.2.10, 3.2.11**. Avidity index which measures the strength of the antibody- antigen interaction was discussed in **3.2.7.3.** Realtime PCR was performed to investigate the expression levels of IgA inducing factors from the different immunized groups. The detailed methodologies were discussed in the material method section **3.2.9.** In vitro bactericidal assay and cytotoxic T lymphocytes (CTL) assay were discussed in detail in the section **3.2.12** and **3.2.13.**

6.3. Result:

6.3.1. Intranasal immunization with rCTB-T2544 prompts DC recruitment in the MLN.

Upon intranasal immunization, lung dendritic cells imprint gut homing receptors on to the naïve B and CD4+ T cells in the mediastinal lymph node. It also directs class switch recombination of B cells which further induces generation of IgG+ and IgA+ cells. To address this, we investigated whether the presence of CTB upon intranasal immunization augments recruitment of dendritic cells (DCs) to the MLN. A four-time increase in the percentage of CD11c+ DCs was observed in the CTB-T2544 group compared to the T2544 (26.7% vs 7.0%) counterparts (**Fig. 35A, 35B**). This finding indicated that intranasal CTB promote DC migration to the downstream draining node at intestine. To further address this DC migration, we checked for the migratory DC markers (MHChiCD11CintCD103+) in the MLN. We observed 3-fold rise in the percentage of migratory DC in the CTB-T2544 group (**Fig. 35C**).

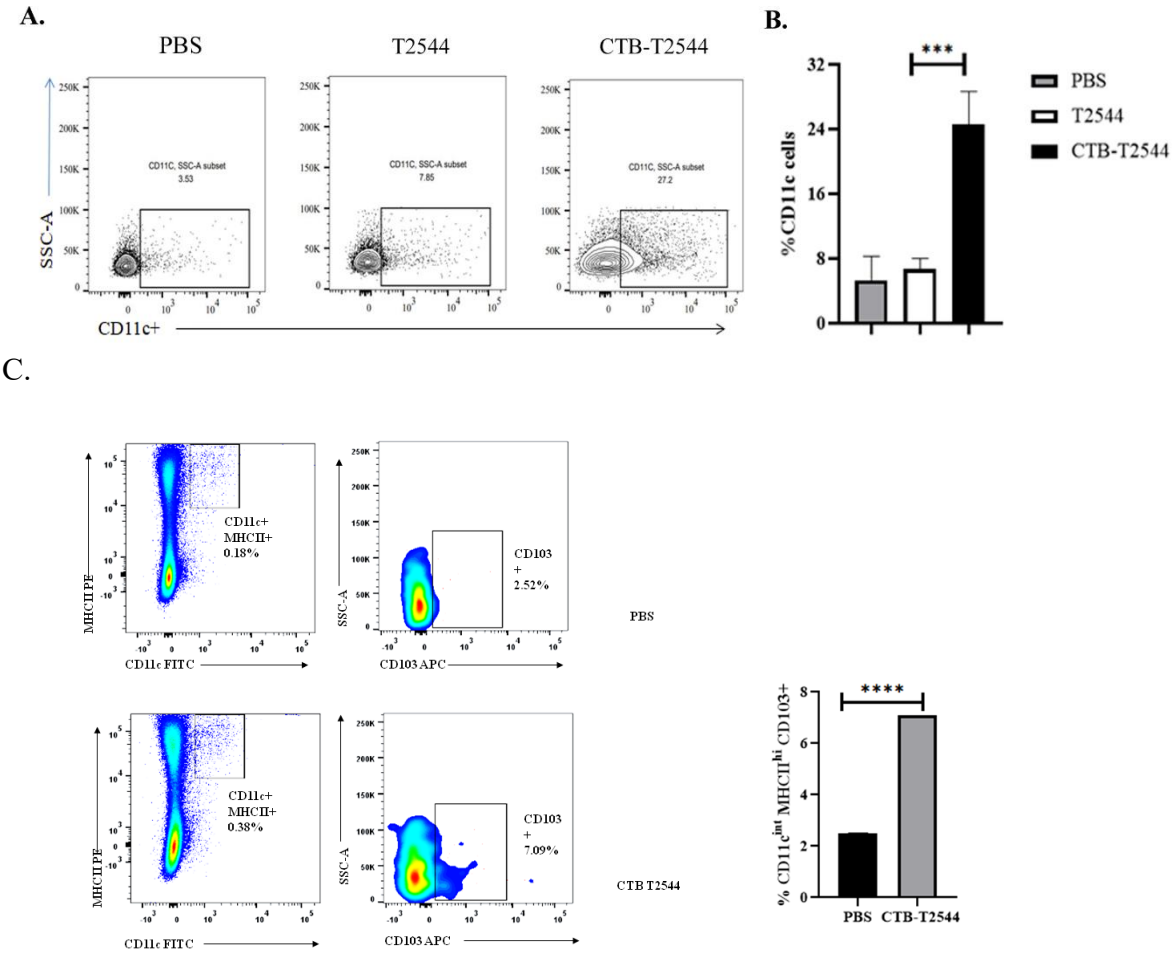

Fig. 35. Intranasal rCTB-T2544 immunization directs dendritic cell recruitment to the MLN. A. 12 days after last immunization, MLN cells were isolated from the immunized mice. Later MLN cells were stained with CD11c and analyzed with the flow cytometer. B. the percentage of the CD11c+ cells from all the groups were presented as bar diagram. C. MLN cells from CTB-T2544 and PBS immunized mice were stained with CD11c, $MHCII^{hi}$ and CD103+ cells. CD103+ cells were quantified in the cell population gated for $CD11c^{int}$ and $MHCII^{hi}$ expression. Significance was calculated using unpaired t test between CTB-T2544 and PBS groups. Representative flow images are provided here.

6.3.2. Intranasal immunization with rCTB-T2544 induces gut homing receptor expression.

As we observed an increase in the number of MLN DCs, it could lead into a greater population of lymphocytes which expresses gut homing receptors. Next, we investigated gut homing receptor expression in the lymphocytes isolated from the immunized mice. We found a substantial number of B and T cells in MLN and spleen expressing α4β7 and CCR9 receptors in the CTB-T2544 immunized group compared to the T2544 and PBS immunized group using flow cytometry. The representative image from MLN was shown in **Figs. 36A, 36B**, and from spleen was shown in **Figs. 36C, 36D.** Their respective population from MLN and spleen was presented in bar diagram in **Figs. 36E, 36F.**

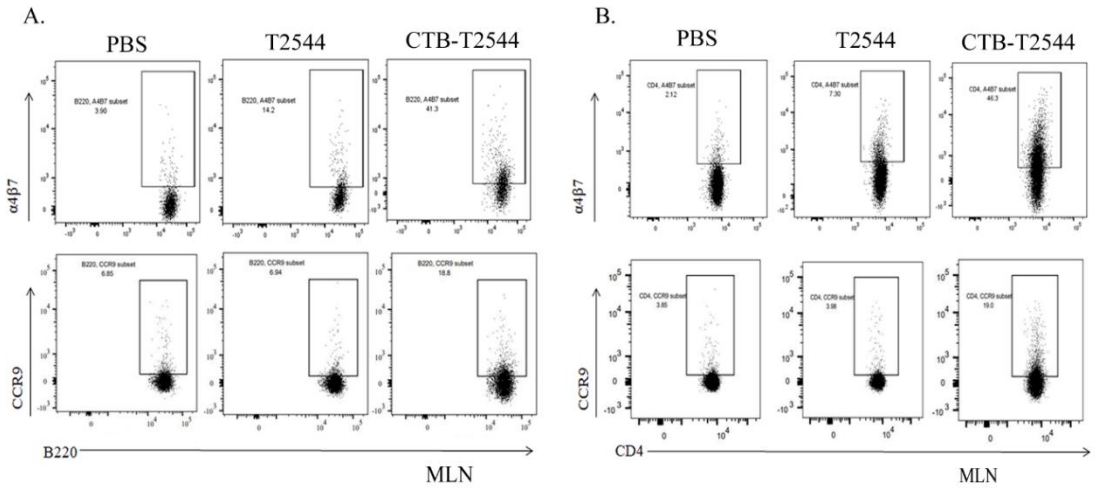

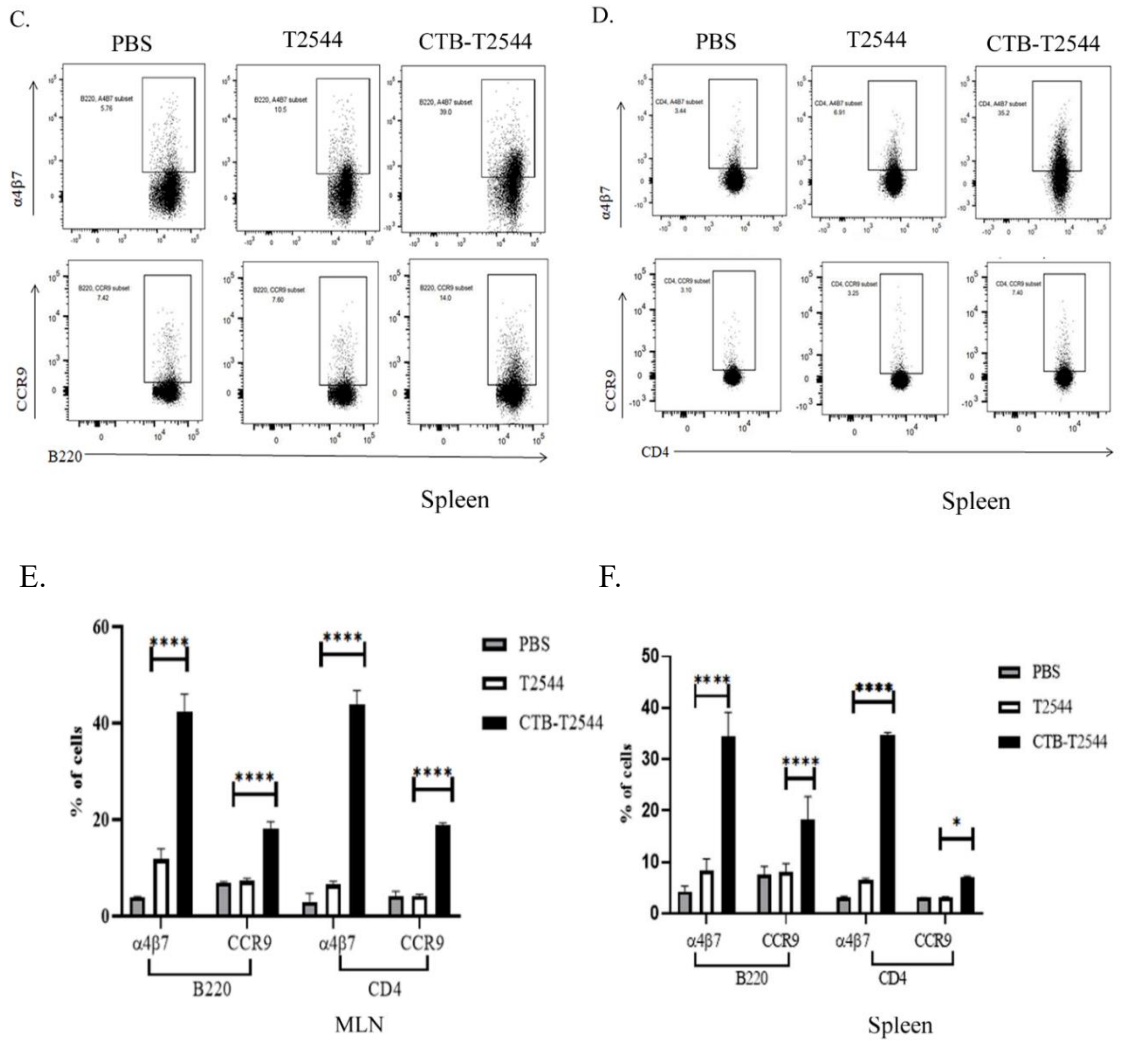

Fig 36. CTB-T2544 increases gut homing markers in the lymphocytes isolated from MLN and spleen. Twelve days after the last immunization, mice were euthanized and cells from MLN and spleen was isolated from the all the experimental groups (n=6/group). Cells were further stained with anti-mouse B220 and anti-mouse CD4 antibody for identification of B and T cells respectively, Additonally, cells were stained with flurochrome tagged gut homing markers (anti mouse α4β7 and CCR9 antibodies) and quantified using flow cytometer. Significance was calculated using unpaired t test between CTB-T2544 and T2544 groups. Representative flow images of MLN (A, B) and from spleen (C, D) are provided here. The population from MLN (E) and spleen (F) was further represented in bar diagram.

6.3.3. Intranasal CTB-T2544 immunization induces IgA inducing factors in the MLN.

Literatures reported that dendritic cells (DCs) impart a crucial role in mucosal sIgA production. Sevaral IgA inducing factors like (BAFF, APRIL, RALDH1, iNOS, IL-6 and TGF-β) were induced by DCs (Tezuka and Ohteki 2019). As we observed increased DC recruitment and migration to MLN with a strong mucosal antibody response in the intestine, we next explored whether an increased IgA inducing factor was increased by the DCs present in MLN. We found an augmented expression of the IgA inducing factors by the DCs present in MLN (**Fig. 37**)

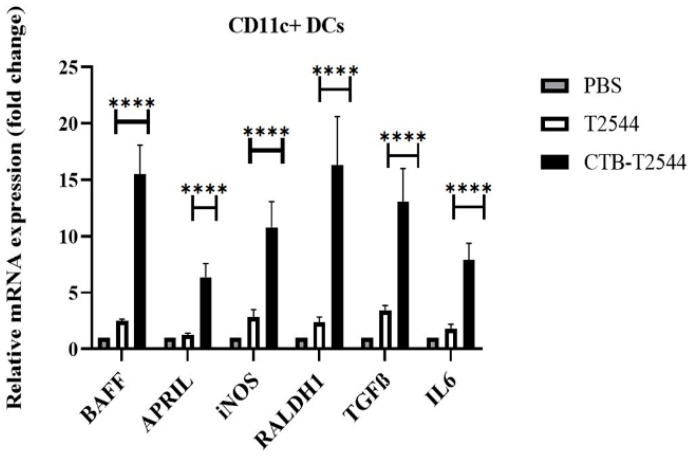

Fig. 37. Intranasal CTB-T2544 induced increased IgA inducing factors. Twelve days after the third immunization, all the experimental mice of CTB-T2544, T2544 and PBS immunized group (n=6/ group) were euthanized. MLN DCs were FACS sorted with anti-mouse CD11C antibody. mRNA was isolated from the sorted dendritic cells and the expression of IgA inducing factors were investigated using real time qPCR. Significance was calculated using unpaired t test between CTB-T2544 and T2544 groups.

6.3.4. Intranasal CTB-T2544 immunization induces increased generation of follicular helper T cells (T_{FH}).

T follicular helper cells (T_{FH}), a specialized subset of CD4+ T cells, were reported to play an essential role in germinal center formation, B cell proliferation and the development of high-affinity antibodies and memory B cells (Crotty 2014). Since we noted an increased antibody response with memory B cells, we next investigated whether CTB induced follicular helper T (T_{FH}) cells in the immunized mice and were found to be double in CTB-T2544 group compared to T2544 group (6.03% vs 3.16%) (**Fig. 38A,38B**).

A.

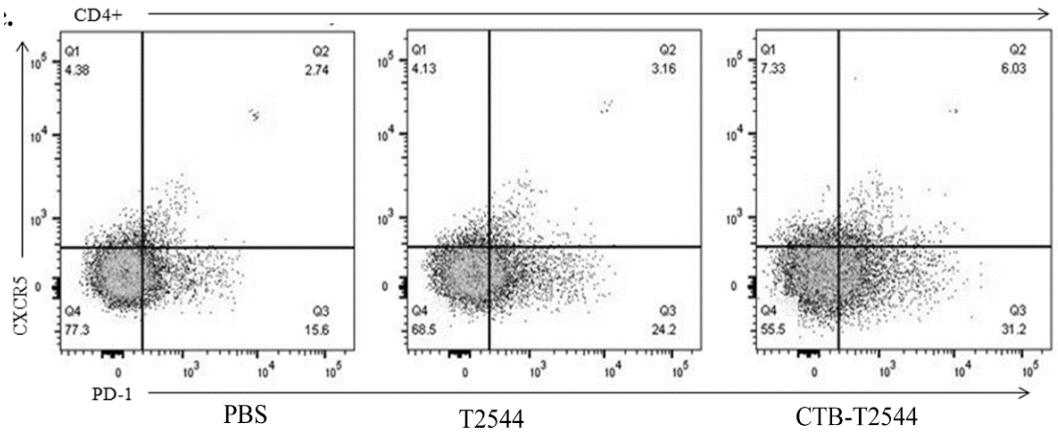

B.

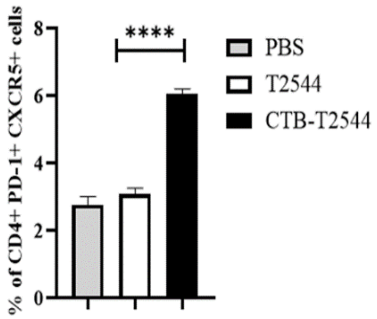

Fig. 38. Intranasal immunization increased Tfh induction in the MLN. Twelve days after the third immunization, all the experimental mice of CTB-T2544, T2544 and PBS immunized group (n=6/ group) were euthanized. Cells were isolated from MLN and stained with flurochrome tagged anti mouse CD4, CXCR5 and PD-1 and quantified using flow cytometer. A. Representative flow cytometric image. B. The CD4+ CXCR5+ and PD-1+ population was presented in bar diagram. Significance was calculated using unpaired t test between CTB-T2544 and T2544 groups.

6.3.5. TF immunization generates antigen-specific cytotoxic T lymphocytes (CTLs).

CTLs respond to viral and bacterial infections by recognizing the pathogen-derived peptides, presented by the major histocompatibility complex class I molecules on the surface of the antigen presenting cells (Germain 1994). Post CTL mediated lysis of infected macrophage, it eventually releases bacteria from their protective shell to the cytosol where it encounters soluble immune effectors (opsonic antibodies). This facilitates antibody dependent cell cytotoxicity and activate complement, thereby inducing bacterial killing and subsequent antigen presentation (Vazquez-Torres and Fang 2001).

To investigate if rT2544 and rFliC co-administration mounts any cellular immunity against typhoidal *salmonella* infection, we isolated cytotoxic T Lymphocytes or CTLs (CD8+ T cells)

from the spleenocytes of the immunized mice and expanded them by antigenic stimulation and co-cultured with the unpulsed or rT2544-pulsed EL4 cells (target cells). Next, we found a stoichiometric increase in percent specific lysis by incubating target and effector cells in the ratio of 1:5, 1:50 and 1:100. 55% specific lysis of rT2544-pulsed EL4 cells was found at 1:50 ratio, as opposed to minimal lysis of the T2544 stimulated cells (**Fig. 39A**), indicating a strong CTL response post rT2544+rFliC immunization. In a separate experiment, isolated splenic CD8+ T cells from the different immunized groups were stimulated in vitro by co-culturing with rT2544-pulsed bone marrow derived dendritic cells. We quantified released IFN-γ in the culture supernatants using ELISA. We observed a significant increase in the IFN-γ levels in rT2544 + rFliC-stimulated compared with the rT2544 CD8+ CTLs (**Fig. 39B**).

A. B.

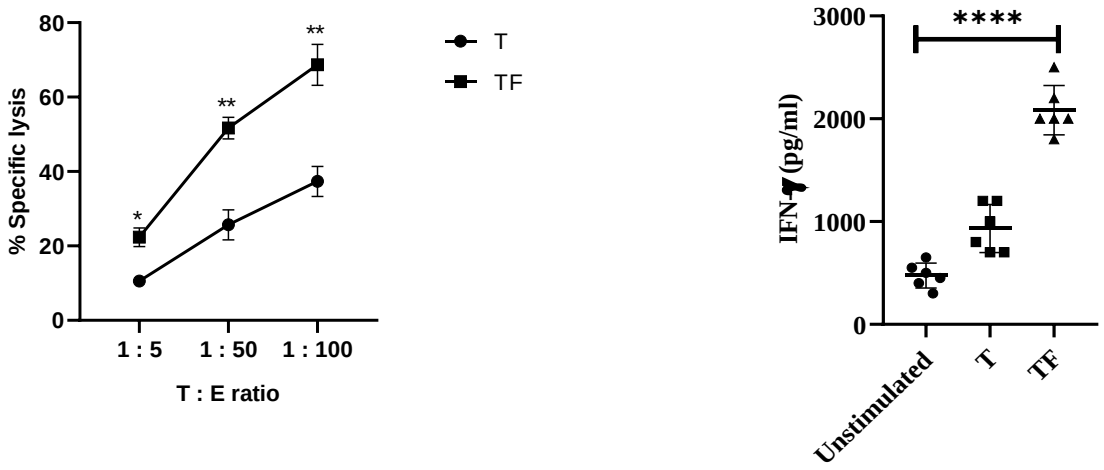

Fig. 39. T2544 co administered with FliC improved the CTL response. A. Cytotoxic T Lymphocyte Assay. CD8+ T lymphocytes, isolated from the spleenocytes of T and TF immunized mice with, were used as effector cells. rT2544 pulsed EL4 cells were used as Target cells. Different ratios (1:5, 1:50, 1:100) of target and effector cells were incubated and percent specific lysis were measured using LDH assay. Significance of percent lysis was further calculated by comparing the percent specific lysis of the TF and T. B. CD8+ T cells were isolated from the spleens of T and TF immunized mice and were co-cultured for 24 h with rT2544-pulsed BMDCs. IFN-γ released in the culture supernatants was measured by ELISA. Significance was calculated by comparing IFN-γ release by TF and T co-cultured with PBS stimulated cells.

6.3.6. Antibodies generated after rT2544 and rFliC co-administration showed enhanced bactericidal potential.

Literatures states that the enhanced bactericidal potency of an immune serum contributes towards improved functional efficacy. Both the *Salmonella* serovar Typhi and Paratyphi A were incubated with the heat inactivated different immune sera (experimental and commercial *S*. Typhi and *S*. Paratyphi immune serum) along with the guinea pig complement. Pre immune serum was used as comparator. Percent lysis of each bacterium was noted. Significant lysis for both the bacteria opsonized with the respective immune serum found to be comparable to the lysis induced by commercial antiserum, whereas a minimal lysis was observed with pre-immune serum. Bactericidal effects of 1:100 dilution of TF antiserum on *S*. Typhi (**Fig. 40A**) and *S*. Paratyphi A (**Fig. 40B**) reached almost 80% after an hour of incubation and was even higher with longer incubation periods. The above results suggested strong complement activation after immunization with rT2544 co-administered with rFliC, which might contribute to anti-bacterial immunity.

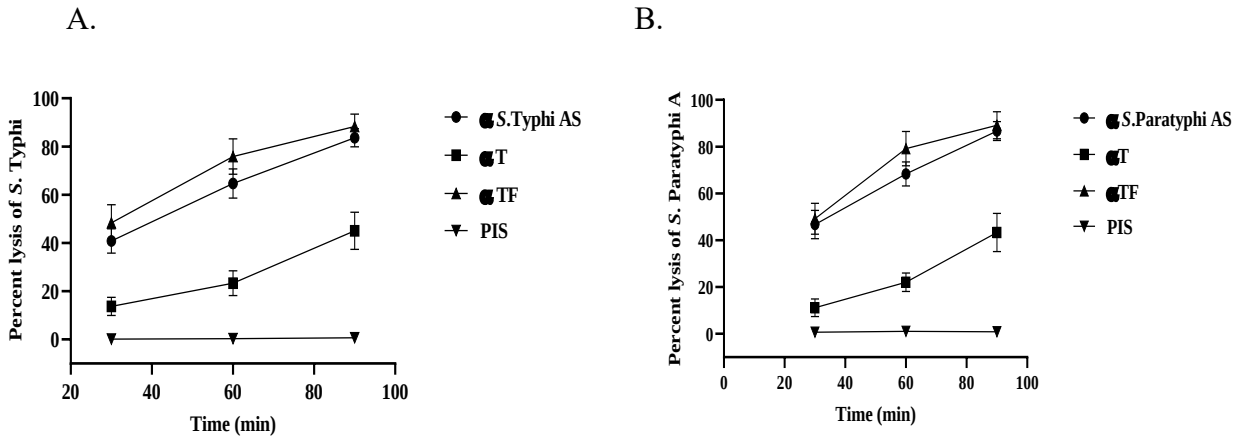

Fig. 40. TF serum contains bactericidal potency. Serum antibodies of T and TF immunized mice and pre-immune serum (PIS) was heat inactivated and incubated with *S*. Typhi (A) or *S*. Paratyphi A (B) at 1:100 dilution in the presence of guinea pig complement for different time points (30 min, 60 min and 90 min). Live bacteria were enumerated by plating on LB Agar with streptomycin selection (50 µg/ml; for *S*. Typhi) or HEA (*S*. Paratyphi A). Significance was calculated by comparing lysis by pre-immune and TF antiserum. Experiments were repeated 3 times and data from one representative experiment is shown.

6.4. Key points of this study-

- Together all these data have indicated an upregulation of IgA-inducing factors on local dendritic cells promoting their migration to mesenteric lymph node (MLNs). The MLN DCs further imprint gut homing receptors on the B and T lymphocytes which later migrate to intestinal mucosa to execute the proper functioning of secretory IgA and cytokine.
- Follicular helper T cells (T_{FH}), which play an essential role in germinal center formation, B cell proliferation and the development of high-affinity antibodies and memory B cells, were found to be double the number after rCTB-T2544 immunization.
- Serum bactericidal potency and cytotoxic T lymphocytes (CTL) were found to be increased in rT2544-FliC group. These further indicated a strong humoral response together with CTL mediated lysis of the infected macrophage cells. These CTL mediated cell lysis releases the intracellular bacteria from the protective niche, thereby rendering them susceptible to killing by immune effectors.
- Memory B and T lymphocytes were higher upon rCTB-T2544 and rT2544-FliC immunization, suggesting successful generation of sustained and durable immune response.

Additional Work.

CHAPTER. 7

Immunogenecity after Heterologus Prime boost immunization against Salmonella infection

7.1. Introduction:

Upon mucosal immunization, all the mucosal defense barriers get armored against infection by generating antigen-specific secretory IgA (SIgA) antibodies in the near or distant mucosa to variable degrees, representing hallmarks of immune response for that particular pathogen. Secretory IgA (SIgA) contributes to protection and the regulation of homeostasis in the mucosal epithelia. This eventually prevents various pathogens or toxins to bind to or invade the epithelial cells. Additionally, the antigen stimulated B cells and T cells exit the draining lymph nodes cells and go into the circulation for final 'seeding' into the various mucosal sites for an effective reinforcement of their barrier functions. But mucosal immunization could not generate strong humoral immune response (Lycke 2012).

All the available commercial Typhoidal vaccines work through anti-Vi antibodies, hence could not cross protect *S.* Paratyphi A. Additionally, it generate lesser degree of sIgA in the immunized individuals. Ty21a, an oral live attenuated vaccine generates sIgA in the gut mucosa of immunized individuals, but poorly confers protection from *S.* Paratyphi A infection. Hence, a vaccine candidate is urgently needed which would generate a balanced mucosal and systemic immune response against both the Typhoidal strains, *S.* Typhi and *S.* Paratyphi A.

In the study described previously in chapter 4, we showed that intranasal (IN) immunization with rCTB-T2544 prompted an elevated level of antigen specific fecal and intestinal secretory IgA (SIgA). This immunization scheme efficiently reduces the bacterial colonization in the intestinal tissues and subsequent systemic spread. However, this regimen induced comparatively lower antigen specific systemic antibody responses than the subcutaneous route, previously reported from our lab (Ghosh et al. 2011) . Here in this chapter, we proposed to generate a balanced long term immune response against Typhoidal Salmonella infection in mucosal and systemic compartments by introducing a combinatorial prime-boost immunization schedule using both IN and SC routes. We hypothesized that this combinatorial approach would induce more potent and durable immune response against Typhoidal Salmonella infection.

7.2. Method:

Six weeks old female BALB/c mice were primed intranasally with 60ug rCTB-T2544 on day 0. Later, 15ug of rT2544 was subcutaneously injected twice on 12 days interval. Another group received 60ug of rT2544 through intranasal route thrice on 12days interval. Immunogenicity

and protective efficacy of this heterologous prime boost immunization schedule were investigated against *salmonella* infection using Iron overloaded mice as prototype.

7.3. Result:

7.3.1. IN priming and SC boosting induce higher humoral antibody responses.

Mice were initially primed with rCTB-T2544 through intranasal route followed by subcutaneous boosting with rT2544 twice at 12 days interval. The intranasal vaccine regimen of rCTB-T2544, described in chapter 4 part 3, were taken as comparator. 12 days after the last immunization, mice were bled and serum was isolated. We observed an enhanced rT2544 specific IgG, IgA and IgG isotype response in the serum of IN/SC/SC immunized mice compared to IN/IN/IN group (**Fig 41A, 41B, 41C**).

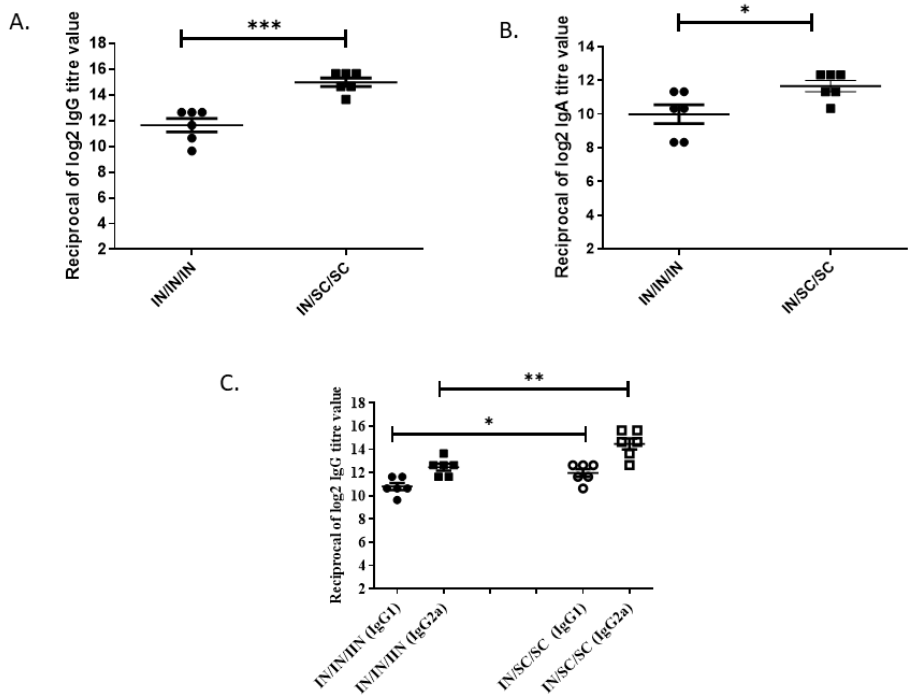

Fig. 41. Induction of rT2544 specific humoral antibodies in serum. Mice were immunized rCTB-T2544 mucosally and boosted with rT2544 twice at 12 days intervals. 12 days after the last immunization, sera were isolated from the collected blood of immunized mice. rT2544 specific IgG(A), IgA (B) and IgG isotypes (C) were measured using ELISA. The endpoint titer values were plotted and compared with serum antibody titers in the mice immunized intranasally with rCTB-T2544 thrice at 12 days interval. Significance was plotted using unpaired t test and the error bar denotes SD. ***p=0.0003, *p=0.0281(IgA), 0.0271 (IgG1), **P=0.0055.

7.3.2. IN priming and SC boosting induces higher mucosal antibody responses.

Twelve days after the last immunization, we investigated whether prime boost regimen prompted an elevated mucosal antibody compared to the intranasally immunized mice. We observed a significant increase in mucosal antibodies in the fecal extract (**Fig. 42A**) and intestinal contents (**Fig. 42B**) of the immunized mice undergone with prime boost regimen. Altogether, these findings indicated that IN priming with SC boost is better in priming systemic immune responses with enhanced SIgA production in the the mucosal compartment.

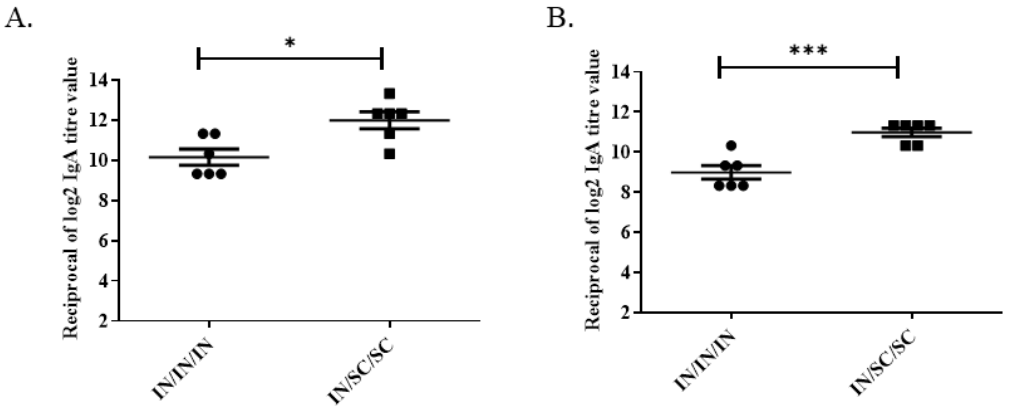

Fig 42. Induction of rT2544 specific mucosal antibody in fecal extract and intestinal content. Mice were immunized rCTB-T2544 mucosally and primed with rT2544 twice at 12 days interval. 12 days after the last immunization, fecal extract and intestinal contents were collected. rT2544 specific Fecal IgA(A) and intestinal IgA (B) were measured using ELISA. The endpoint titer value was plotted and compared with mucosal antibody titer collected from the mice immunized intranasally with rCTB-T2544 thrice at 12 days interval. Significance was plotted using unpaired t test and the error bar denotes SD.*p=0.0103,***p=0.0005.

7.3.3. IN priming and SC boosting elicits a greater degree of protection.

Previously, intranasal immunization regimen of rCTB-T2544 imparted 70% and 80% protective efficacy against 10 times lethal challenge dose of *S.* Typhi and *S.* Paratyphi A (Chapter 4). In this extended study, we investigated whether elevated antibody response in prime boost immunization regimen conferred improved immune protection. To this end, we initially primed Balb/c mice with rCTB-T2544 through intranasal route followed by two subcutaneous boosting with rT2544 twice at 12 days interval. 12 days after last immunization, mice were challenged with 20 times lethal dose of *S.* Typhi and *S.* Paratyphi A respectively. We observed 80% and 90% protection in prime boost immunized mice for infection with *S.* Typhi

and *S*. Paratyphi A, respectively, whereas, 55% and 60% of the intranasally immunized mice survived the 20 times lethal challenge with *S.* Typhi and *S*. Paratyphi A.

A. B.

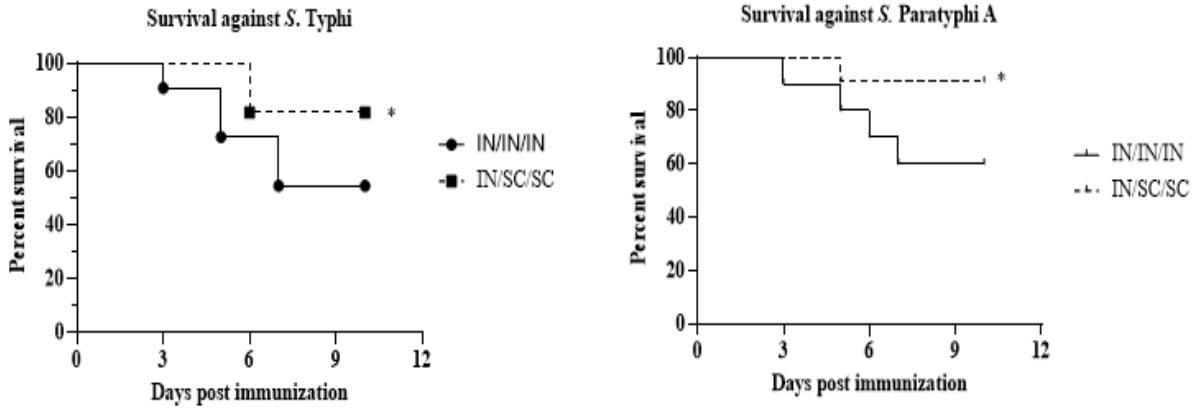

Fig. 43. Mucosally primed with rCTB-T2544 and systematically boost with rT2544 elicited greater degree of protection. Mice were immunized mucosally with rCTB-T2544 and boosted with rT2544 twice at 12 days interval. 12 days after the last immunization, mice were challenged with the 20 times LD 50 Dose of *S*. Typhi and *S*. Paratyphi A infection. Cumulative mortality of immunized mice from different immunized group were plotted using Kaplan-Meyer survival curve analysis against *S*. Typhi (A) and *S*. Paratyphi A (B) infection.

7.4. Take home message.

In previous chapters, mucosal administration of rCTB-T2544 induced enhanced mucosal antibody response with reduced magnitude of humoral antibody titers. On the other hand, rT2544-FliC (TF) prompted elevated humoral antibodies but with a lesser level of mucosal antibodies. Here in this chapter, we combined both the routes of administration in our vaccine regimen. Intranasal priming with subcutaneous boosting induced a balanced increase of antigen specific humoral and mucosal antibodies. We found improved protective efficacy with prime boost regimen even at a higher challenge dose. Further studies are required to establish the mechanism underlying this augmentation of immune responses.

Chapter 8

General Discussion

Salmonella enterica serovar Typhi and serovar Paratyphi A, both human restricted pathogens, cause enteric fever, encompassing Typhoid and Paratyphoid fevers, respectively and pose severe health concerns in the low and low-middle income countries where health, hygiene and sanitation are compromised. The traditional way to control the severity of the typhoidal *Salmonella* infection is based on the antibiotic treatment, either by killing or preventing the bacterial growth. However, several investigations documented the emergence of bacteria, which developed resistance to first line antibiotics, including ampicillin, chloramphenicol and cotrimoxazole (Wain et al. 1999; Sheorey et al. 1993; Kumar, Rizvi, and Berry 2008). Later, an alternate treatment with fluoroquinolones and cephalosporins was further reported to be ineffective in various cases from India, Bangladesh, Nepal and Pakistan (Barkume et al. 2018). Infections caused by these multi drug resistant strains are particularly becoming difficult to treat in low resource setting of developing countries. Mass vaccination has been suggested to be the most promising way to control *Salmonella* infection.

Generation of protective immune response upon typhoid infection was reported in few cases (Sztein, Salerno-Goncalves, and McArthur 2014), correlating with induction of modest immune response upon multiple doses of Ty21a immunization (Syed et al. 2020). On the other hand, typhoid conjugate vaccines, most notably Vi-TT, induced a sustained and durable immune protection. Yet an attack rate of 35% was found in a Controlled Human Infection Model (CHIM). Few reports indicated that serum antibody may not be solely sufficient for protection, as patients who recovered from typhoid fever, despite having an increased antibody titer against bacterial H, O, Vi-PS and porins, remain susceptible to reinfection (Das et al. 2017). Available reports with chronic biliary carriers from the endemic populations were documented with high anti-Vi IgG titers (Pulickal et al. 2009), underscoring an essential role played by the mucosal and cell-mediated immune responses for overall protection. Literatures documented that systemic administration of vaccine candidates induced weaker mucosal response which is found to be critical in conferring protection against typhoid and cholera infection (Lavelle and Ward 2022), thereby raising concern for developing mucosal vaccines. Additionally, animal studies revealed that *Salmonella*-specific T cells were mandatory for late clearance of intracellular bacteria (MacLennan 2014). This suggested that protection against typhoidal infection is not based on single component, rather necessitates a balanced cooperation between mucosal, humoral and cell mediated immune response.

Previously, we reported from our lab that a conserved outer membrane adhesion protein, rT2544 from *S*. Typhi, when administered subcutaneously induced bactericidal antibodies in

mice as well as naturally infected humans and also protects from lethal salmonella challenge (Ghosh et al. 2011) (Das et al. 2017). A subsequent study with the homologous protein PagN from *S*. Typhimurium exhibited protective immunity in mice (Bumann 2014). Additionally, no Typhoid subunit vaccine developed so far cross protects against paratyphoid infection. Since rT2544 was found to be present in multiple clinical isolates of *S*. Paratyphi A, we proposed an improved vaccine with somatic antigens like T2544 to cross protect against *S*. Paratyphi A infection. In this study, we investigated the whole spectrum of adaptive immune responses generated after mucosal and systemic immunization with our *Salmonella* antigen, rT2544 in presence of two extensively used adjuvants, rCTB and rFliC. Considering the significance of intestinal immunity against *Salmonella* infection in mind, we explored rCTB-T2544 for its immunogenicity and protective efficacy through intranasal route. A mucosal vaccine with easy production using bacterial expression of chimeric construct and simple administration significantly reduces the cost, which is not the case with TCVs, as they require complex chemical coupling process with probability of batch-to-batch variations and an increased production cost. Further, we proposed an iron overloaded murine model to study the pathogenesis of *S*. Paratyphi A. Additionally, in a separate work, we improved the immunogenicity of this vaccine candidate, rT2544 by the addition of another vaccine adjuvant rFliC as an initial step towards a goal to optimize the minimum immunogenic dose of different antigens from different enteric pathogen so that a multivalent subunit systemic vaccine can be developed against enteric diseases.

Mucosal Immunization with rCTB-T2544 prompts a robust T2544 specific gut mucosal immune response, in the form of sIgA and gut homing lymphocytes. This experimental formulation in mice had three intranasal doses of 60 ug each of rCTB-T2544. As literature confirmed the best pentameric fusion formation with C-terminus conjugation (Stratmann 2015) and reported a 10-fold rise in the immune response to co-administered antigens, suggesting C terminus chimera to be more immunogenic (Eriksson et al. 2003), we genetically fused t2544 to the C-terminus of *ctx-b* gene, using a non-furin (GPGP) linker sequence. Further, efficient binding of our recombinant fusion protein rCTB-T2544 to the GM1 receptor in an ELISA established appropriate retention of its pentameric structure upon purification. This study detected 70% protection to mice immunized intranasally with rCTB-T2544 against lethal challenge of *S*. Typhi. However, when we used 3-fold higher dose of rT2544 alone, through mucosal route, it failed to generate protection.

A conventional way of measuring efficacy of typhoid vaccines is monitoring serum antibodies, especially IgG titer. Despite inducing higher level of antibody titer and durable protection, TyVAC trial with TCV failed to establish a protective IgG and IgA titers. Controlled human infection model (CHIM) studies too poorly correlated protection against *S.* Typhi with serum IgG and SBA (Jones et al. 2021). On the other hand, serum IgA titers found to correlate significantly with Vi-PS-induced protection (Dahora et al. 2019)**,** underscoring a protective role for mucosal sIgA. Besides, oral vaccines documented the role of stool sIgA titer correlating with protection, However, studies could not establish a direct relation of sIgA with protection against typhoidal infection. CTB delivered through non-oral mucosal routes significantly boosted antigen specific humoral and cell-mediated immunity at both the local and distal mucosa, albeit to a variable degree (Holmgren and Czerkinsky 2005). Previous reports stated that intranasally immunized AIEC siderophore enterobactin conjugated to CTB elicited a strong mucosal antibody response in the small and large intestine and thereby reduced the bacterial colonization in the gut (Guo et al. 2014). Another study exhibited that intestinal mucosal antibodies induced after intranasal CTB-siderophore administration could significantly reduce *Salmonella* colonization of the inflamed gut (Sassone-Corsi et al. 2016). We reported a markedly raised IgG1 and IgG2a titer, specific to rT2544, in the serum in presence of CTB as compared to T2544 alone. This, followed by an elevated sIgA titers, along with increased number of IgA ASCs in the intestine of mice was observed upon intranasal CTB-T2544 immunization. The increased functional potential of the induced humoral and mucosal secretory antibodies was observed *in-vitro* by assessing their ability to inhibit *S.* Typhi adherence to the epithelial cell monolayers, their respective potential to facilitate opsonophagocytosis and finally by investigating the impairment of the bacterial motility in presence of these antibodies. These further correlated with *in vivo* challenge study, where S. Typhi pre-incubated with intestinal lavage and fecal extracts from the immunized mice were used to infect naïve mice. A lethal dose killed only 50% mice, while a sublethal dose of the pre-incubated bacteria showed significant reduction in the colonization of the intestinal and visceral organs. All these findings highlighted a more significant role of mucosal antibodies in imparting protection. Upon CTB-T2544 immunization, induced mucosal immunity increased bacterial shedding in feces, reducing their stay inside the host. This resulted into herd protection against *S.* Typhi, which was not yet observed with TCVs in the clinical trials (Khanam et al. 2023).

Most of the investigations reported induction of Th2 predominant immunity by CTB, while a Th1 type response was also observed with CTB conjugated vaccines depending on the antigen type, dose and route of administration studies (Stratmann 2015; Wiedinger, Pinho, and Bitsaktsis 2017; Lee et al. 2015). Genetic fusion of *t2544* with *ctxb* resulted into a balanced Th1/Th2/Th17 immune response, which was previously found to be essential for effective against *Salmonella* in the infection studies (Stratmann 2015; Wiedinger, Pinho, and Bitsaktsis 2017; Lee et al. 2015).

In addition to the humoral and mucosal antibodies, our study showed marked increase in B cell population, which express gut homing receptors (α4β7 and CCR9) in the MLNs and spleen of the rCTB-T2544 immunized mice. Previous investigations with intranasal administration of inactivated CT holotoxin prompted lung conventional dendritic cells to promote IgA class switch of B cells in the regional lymph nodes. Thereby, it imprinted gut homing markers α4β7 and CCR9 on IgA ASCs, leading their migration to the intestine (Ruane et al. 2013). Here, our study with mucosal immunization, for the first time, showed marked expansion of CD11c+ dendritic cells, expressing IgA inducing factors in the MLNs. Additionally, gut homing receptor expression on MLN B cells were found to be significantly elevated together with increased number of IgA+ ASCs in the Peyer's Patches and sIgA in the intestine. This indicated an essential role of CTB in inducing DC migration from the lungs to the MLN, thereby orchestrating B cell class switch with gut homing of IgA+ B cells (Tezuka and Ohteki 2019). Migratory DC (mDC) markers (MHChiCD11CintCD103+) were also found to be threefold higher in the MLN DCs of CTB-T2544 immunized mice, as compared with the PBS-immunized group**.** However, a possibility of induction of gut-homing lymphocyte in the lung-draining lymph nodes can't be excluded.

Memory B and T cell responses were previously reported to be associated with maintaining sustained protection against typhoidal infection. A durable connection between the antigen specific memory B cells and antibody titers was established before (Crotty 2014)**.** Conjugated chimeric formulation showed increase of higher antigen-specific serum antibody compared to the co-administered antigens used alone (Eriksson et al. 2003; Miyata et al. 2010), whereas another study reported weaker adjuvant function of cholera toxin B conjugated to streptococcal surface protein antigen (AgI/II) than to separate administration (Wu and Russell 1993). Besides, booster dose only improved AgI/II specific IgM and IgA antibody titer, but not IgG. In contrast, in our study, we noted a strong adjuvant effect of cholera toxin B (CTB) for primary and booster immunization with robust IgG induction**.** As opposed to the former study where

AgI/II was chemically coupled to CTB, we used genetic fusion of our protein antigen rT2544 with CTB and found enhanced adjuvanticity in our study. Follicular T helper (T_{FH}) cells are known to support memory B cell generation together with T cell-dependent affinity maturation of antibodies, leading into higher avidity of secondary antibodies. This was substantiated by our data, which showed doubling of the T_{FH} cell number in the MLN together with augmented avidity of anti-T2544 antibodies upon a recall response. Furthermore, great proportion of MLN and splenic CD4+ T cells expressed gut-homing receptors**.** A previous study with intranasal delivery of CTB imprinted homing receptors on T cells by lung DCs (Ruane et al. 2013). A quick insight of cytokine generation by intestinal CD4+ T cells into our study upon mucosal immunization further verified the generation of mixed Th1 and Th17 cytokines. Th1 cytokines are reported to be critical for effective clearance of the intracellular bacteria, whereas Th17 cytokine promotes induction of sIgA (Lavelle and Ward 2022; Cao et al. 2012)**.** An earlier report with human volunteers who received oral Ty21a vaccine displayed predominant induction of IL-17A by the CD8+ T cells in the peripheral circulation, indicating an essential contribution of mucosal protection against *S.* Typhi infection (Sztein, Salerno-Goncalves, and McArthur 2014)**.** Oral Ty21a immunization of volunteers reported an induction of monofunctional CD4+ T_{EM} (T effector memory) or T_{EMRA} (T Effector Memory Re-expressing CD45RA) cells, producing high levels of IL-17A or TNF-α and an increased population of polyfunctional CD8+ T cells, showing T_{EM} (T effector memory) phenotype and produced triple cytokines (Salerno-Goncalves et al. 2020)**.** Reports with intradermal immunization with porins (Ontiveros-Padilla et al. 2021) and aroA-attenuated live vaccine strain (Weil et al. 2009) showed circulating memory CD4+ and CD8+ T cells, secreting TNF-α and IFN-γ for protection against *Salmonella*. Here, in our study, we showed an increased T2544-specific memory CD4+ T cell response (T_{EM} and T_{CM}), which upregulated IFN-γ production.

Here, we reported that an intranasal vaccine candidate, rCTB-T2544 was protective against oral *S.* Typhi infection. The chimeric vaccine antigen comprised of cholera toxin B subunit (CTB) and outer membrane protein rT2544, augmented (i) secretory IgA (sIgA) in feces which inhibited bacterial motility and bacterial attachment to the host epithelial cells *in vitro*; (ii) Affinity maturation of antibodies with sustained and strong recall response; (iii) gut homing receptor expression lymphocytes which also produced Th1 and Th17 cytokines, and (iv) increased number of follicular helper T cells and CD4+ effector memory cells. All these results indicated that CTB-T2544 is a promising candidate for the development of an intranasal vaccine against human *S.* Typhi infection.

Next, we aimed to assess whether intranasal CTB-T2544 immunization protect from *S.* Paratyphi A infection. But, *S.* Paratyphi, being a human-restricted pathogen, non-availability of suitable animal models of infection is a major bottleneck for vaccine development. Although few studies utilized infant mice and rabbits as preclinical models of Paratyphoid infection, they failed to demonstrate bacterial pathogenicity and thereby poorly correlated with vaccine efficacy. We proposed an iron overloaded model based on the studies suggesting iron as one of the critical micronutrients for bacteria including *Salmonella.* Previously we reported the iron overloaded mice model for studying *S.* Typhi infection (Ghosh et al. 2011). Studies previously showed that systemic overload with iron (administered through the parenteral route) renders mouse susceptible to *S.* Typhi infection (Powell et al. 1980; O'Brien 1982). However, large dose requirement for iron that markedly suppresses the immune system could be circumvented by co-administration of iron chelator desferoxamine that makes iron available to the phagosomal bacteria and inhibits NADPH oxidase activity, promoting intracellular survival and growth and significantly reducing the lethal dose. We administered iron and iron chelator, desferoxamine, followed by bacterial infection with different doses of the bacteria. Since the *S.* Paratyphi A reference strain showed little colonization in the intestinal tissues of the streptomycin pretreated mice as compared to several clinical strains (Suar et al. 2006), we screened ten clinical isolates of *S.* Paratyphi A strains for improved pathogenicity. Our study for the first time showed that clinical isolates of *S.* Paratyphi A could invade murine epithelial cells and its subsequent intracellular replication in mouse macrophages. We further moved with the clinical strain C1 which showed maximum infectivity and improved bacterial colonization in the intestinal tissues of the challenged mice, especially in cecum, which further disseminates into visceral organs in due course of time. Another study demonstrated that *S.* Paratyphi A, expressing lower levels of SPI-1 genes and secreting lesser amounts of effector proteins eventually led to reduced colonization (Elhadad et al. 2016). This intestinal colonization was further improved by overexpression of SPI-1 activator, HilA in *S.* Paratyphi A, imparting moderately higher pathological changes and intestinal inflammation using streptomycin pretreated mice (Elhadad et al. 2016). However, this study did not show gradual pathological changes with passage of time, in the intestine. We observed mild to moderate diarrhoea upto D3 post infection which gradually resolved, yet pathological changes were persistent up to 8 days post infection. Our proposed murine model mimicked natural route of bacterial infection which was lacking in case of previous intraperitoneal hog gastric mucin model and infant mouse model. In addition, systemic spread of bacteria was also observed, which led to

comparable colonization with hog gastric mucin model, thereby providing a better platform to study potential vaccine candidates against *S.* Paratyphoid infection. One study with iron overloaded, monocyte-derived dendritic cells facilitated undisturbed growth of *S.* Typhi by upregulating the genes responsible for iron uptake (TFRC, STEAP3, SLC25A37) and storage (FTH1) with a downregulation in antioxidant genes (TXNIP, TXNRD1) and induction of genes involved in ROI and RNI formation (NCF1B, SOD2), indicating a unique strategy to reduce the oxidative and nitrosative stresses (Aulicino et al. 2022). However, the mechanisms underlying iron availability modulating immune cell interactions in the gut upon infection or during health is yet to be explored. Similarly, future studies are required to investigate whether the genes responsible for iron storage and transportation are regulated to establish successful colonization during paratyphoid infection Additionally, genetic characterization of clinical isolate C1 will add valuable insight into confirming the reason behind enhanced pathogenesis. Upon rCTB-T2544 immunization, we observed 80% protection against lethal challenge of *S.* Paratyphi A C1.

The new generation typhoid vaccines are aimed at ensuring greater protection and better safety profiles over the existing ones. Next, to investigate adaptive immune responses upon systemic immunization, we chose to optimize the minimum dose required for rT2544 to induce improved immune response. Here, flagellin (rFliC) was used as adjuvant to augment systemic as well as mucosal immune response. Flagellin was shown to exert adjuvanticity as fusion protein partner and also by co-administration with other antigens. Literatures have established that the amount of flagellin required to induce maximal antigen specific antibody response is much lower than the dose necessary to reach the maximal innate immunity (Honko and Mizel 2004; Honko et al. 2006), indicating a non-linear relationship between antibody response and degree of induced innate immune response. Here we evaluated dose-dependent immune response specific for rT2544 with or without rFliC. We lowered the amount of the required antigen to induce significantly improved immunogenicity at 5ug of rT2544 in presence of 2.5ug rFliC. Although few reports considered Vi antibodies to be protective, but no correlation with the functional potential and antibody titer was established yet. In our study, similar dose of Vi-TT imparted 60% protection against lethal *Salmonella* Typhi challenge as opposed to TF immunization that conferred 83% protection. However, we did not observe increased protective efficacy against *Salmonella* Typhimurium infection. Studies with Vi-TT further documented an elevated level of antigen specific serum antibodies. However, the susceptibility for reinfection had not been declined yet.

Previously, we had shown opsaonophagocytosis by T2544 specific antiserum, resulting in bacterial killing by macrophage and complement (Ghosh et al. 2011). Similar observations were reported with live attenuated vaccine candidates (Wahid et al. 2014). Considering plasma cells as improved predictor of humoral immune response, we analysed them in systemic circulation and found increased T2544-specific IgA and IgG ASCs in the splenocytes of the TF immunized mice. Simultaneously, literatures showed that sIgA contributes in imparting protection against enteric infections. We also noted a rise in T2544 specific sIgA in fecal and intestinal wash of the TF immunized mice, indicating induction of mucosal immune responses upon systemic TF immunization. Since bacterial flagellin is involved in cell adhesion (Haiko and Westerlund-Wikström, 2013), the presence of flagellin on the cell surface promotes antigen uptake and presentation into antigen-presenting cells, promoting robust immune response. Anti-FliC antibodies were reported to enable phagocyte-dependent killing and also diminish bacterial motility (Simon et al. 2013). We also assessed functional potential of the humoral and mucosal antibodies generated upon TF immunization. We observed significant reduction in bacterial attachment to the epithelial cells with increased opsanophagocytosis of the bacteria with antibodies collected from TF immunized mice. In agreement to the above results, heightened bactericidal titer was also observed with TF immunized mice. All these data suggested a strong complement activation after immunization with TF, which might contribute to anti-bacterial immunity.

Published articles suggested both the antibody mediated immune response and CMIR to play crucial role for optimal protection of susceptible host against *salmonella* infection. Like various other intracellular bacteria such as Legionella and Mycobacteria, type 1 CMIR is critical for protection against typhoidal salmonella infection (MacLennan 2014). Mice lacking CD4+ TCRαβ+ Tbet+ T cells or IFNγ receptor failed to recover salmonella infection (Pham and McSorley 2015). We observed splenic T cells to secrete IL-4, IFNγ and IL-17 cytokines. But the predominant secretion of IFN-γ confirmed a mixed type Th1/Th2/Th17 response. IL-17 contributes to the early stage of protection against *Salmonella* infection, especially at intestinal mucosa. Commercially available Vi-PS vaccine does not induce a memory T cell response (MacLennan 2014). Another licensed vaccine, Ty21a, encounters the mucosal tolerogenic environment leading to hindered immune response. No *Salmonella* specific T cell responses were generated upon Vi-conjugate vaccine immunization, The carrier protein used in conjugate vaccines are not of *Salmonella* origin (Mitra et al., 2016). However, Earlier report with Ty21a vaccine, recorded the induction of pathogen-specific CD8+ CTLs response. CTLs respond to

viral and bacterial infections by recognizing the pathogen-derived peptides, presented by the major histocompatibility complex class I molecules on the surface of the professional and non-professional antigen presenting cells (Germain, 1994). In the present study, we observed antigen specific enhanced CTL response upon systemic TF immunization. A profound cytotoxic effect was observed against S. Typhi infected lymphoma cell line (EL4) in vitro. Besides, CD8+ T cells from immunized mice secreted IFN-γ. Both these results indicated activation of macrophages, which further results into enhanced bacterial killing and efficient antigen presentation by activated B and T cells (Vazquez-Torres and Fang, 2001). Previous reports with *S*. Typhi flagella demonstrated it as a dominant antigen for CTL generation. A positive correlation was established between IFNγ production and cytotoxicity of the infected cells (Wahid et al. 2014; Salerno-Goncalves, Wahid, and Sztein 2010; Salerno-Goncalves et al. 2003).

The protein antigens such as flagella, sseB, porin, OmpD from *Salmonella* are poorly conserved among serovars and induce Th2 type response. In contrast, rT2544 is a conserved gene among *Salmonella* serovars, including *S.* Typhi and *S*. Paratyphi A strains. This underscores the potential of TF as a successful vaccine candidate. It previously reported to induce protective Th1 type immune response with a strong CTL and antibody response. This further bestowed this vaccine candidate to be used for assessing cross protection studies against multiple serovars and found to be 90% effective in conferring protection against *Salmonella* Paratyphi A. On the contrary, Vi was reported to suppress pro inflammatory response, while the carrier protein TT, evoked Th2 cytokines (Livingston, Jiang, and Stephensen 2013). Significant protection reported with Vi-TT resulted from systemic antibody in the circulation. However, Vi-CRM197 could not achieve the similar efficacy (MacLennan 2014). Several other complications were reported with Vi conjugate vaccines such as long-term inflammation leading to metabolic disorder (Balaji, Kevinkumar, and Aravindhan 2017); inadequate vigilance and maintenance during conjugate production resulting in batch to batch variations (Szu 2013) and futility against Vi-negative strains (Pulickal et al. 2009). Live attenuated vaccines were often reported with profuse systemic infections in T cell deficient mice; and may impose dangerous risk to chronic granulomatous disease (CGD) patients or HIV-1 infected individuals. On the other hand, our subunit vaccine TF induced a balanced cell mediated immune response and antibody response. In current study, the dose optimization avoids induction of any long-term inflammatory responses.

TF also induced long term protection against *Salmonella*. An effective humoral response was measured by rapid differentiation and antibody production by memory B cell. T-dependent and -independent memory response were earlier reported with Ty21a and CVD-909. We found 1.5% and 3.16% rT2544 specific IgG and IgA secreting memory B cells using ELISPOT assay. Literatures reported rapid proliferation of memory T cells with increased sensitivity to antigens as an added advantage of memory T cells. In our study, we observed enhanced secretion of IFN-γ from memory T cells up to 120 days upon antigen re-stimulation.

Additionally, being a recombinant protein-based subunit vaccine, it would be inexpensive to manufacture, which coupled with the ease of co-administration makes it safer than the live vaccine for younger children and immunocompromised individuals. We hereby showed that rT2544 admixed with rFliC significantly improved the proportion of antigen specific IgA and IgG secreting plasma and memory B cells. This is further accompanied with strong cell mediated immune response (CMIR) including cytotoxic T lymphocytes and effector and memory T cell responses. Addition to the previous reports from our lab, this TF co-administration establishes its protective potency and improved immunogenicity at relatively lower doses. The efficacy can further be improved by conjugating O-specific polysaccharide from *S.* Typhimurium and other potentially immunogenic proteins such as CTB from *Vibrio* and IpaB from *Shigella* to formulate a multivalent subunit vaccine.

Moreover, the present study suggested a higher relative contribution from the intestinal secretory antibodies compared with the serum antibodies for protection against S. Typhi following nasal immunization with CTB-T2544. This question may be further addressed in future studies by infecting immunized, polymeric immunoglobulin receptor (pIgR) knock-out (pIgR−/−) mice, which will be devoid of sIgA from the intestinal secretions. Both the vaccine formulation efficiently protects against typhoidal and paratyphoidal infection.

Chapter 9

Highlights of this study

Commercialized Typhoid vaccines are modestly effective and work through the induction of systemic antibody response, whereas efficacy of licensed oral vaccine is compromised for oral tolerance. However, considering the entry of the pathogen through the intestinal route, mucosal immune response in the intestine, in addition to the humoral immune response, is highly desirable.

- Here in this study, we reported that an intranasal vaccine candidate, purified recombinant CTB-T2544 was protective against oral *S.* Typhi.

  The chimeric vaccine antigen comprised of cholera toxin B subunit (CTB) and outer membrane protein rT2544, augmented (i) secretory IgA (sIgA) in feces which contain the potential to inhibit bacterial motility and bacterial attachment to the host epithelial cells in vitro; (ii) affinity maturation of antibodies with sustained and strong recall response; (iii) gut homing receptor expression on lymphocytes which also produced Th1 and Th17 cytokines, and (iv) increased number of follicular helper T cells and CD4+ effector memory cells. All these results indicated that CTB-T2544 is a promising candidate for the development of an intranasal vaccine against human *S.* Typhi infection (**Fig. Summary Image 1**).

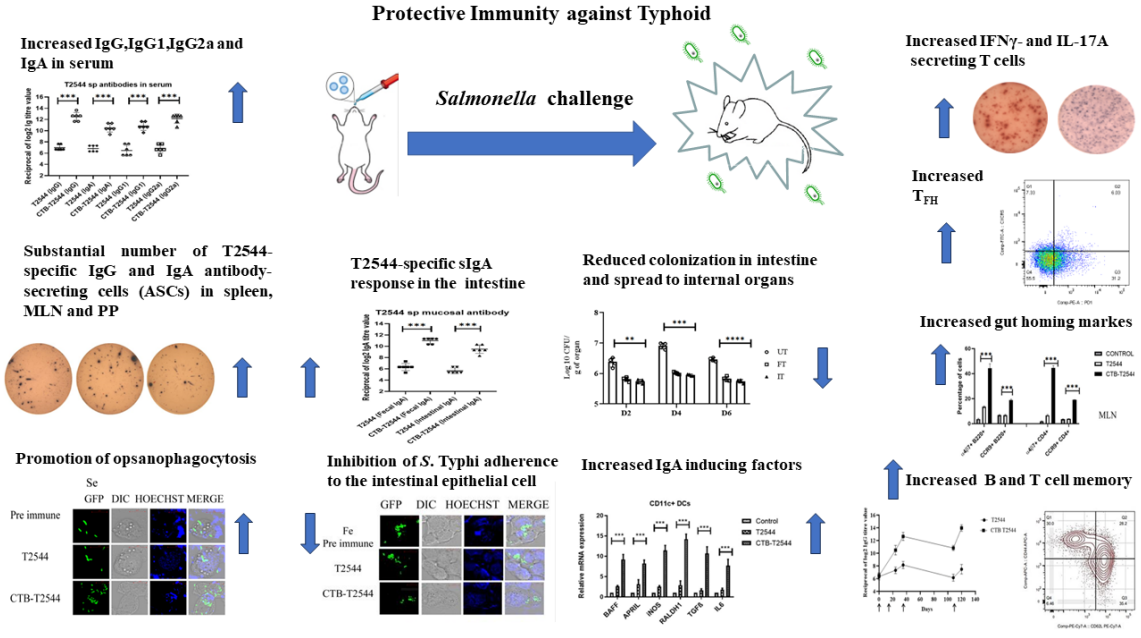

Fig. Summary Image 1. An image summarizing the study with intranasal administration of rCTB-T2544 against typhoidal infection is shown .

Reports with Vi negative multi drug resistant and extensive drug resistant *salmonella* strains further complicate the problem. This had happened owing to the spontaneous mutations in the regulatory region of the polysaccharide used. A possible threat associated with mass immunization program with Vi conjugate vaccine lies in the selection pressure favouring the existing Vi negative salmonella strains (Simon and Levine 2012). Additionally, non-availability of suitable animal models of infection is major bottleneck for studying pathogenesis of human restricted bacteria *S.* Paratyphi. Vi conjugate vaccine utilize anti-Vi antibodies, hence it did not confer any protection to such Vi negative *S.* Paratyphi A infection.

Aiming to develop future vaccines conferring protection against both the serovars, *S.* Typhi and *S.* Paratyphi A, somatic antigens like rT2544, which is conserved across serovars, provide the best opportunity to work with. In this regard, we first developed an iron overloaded mice model, to study the pathogenesis of *S.* Paratyphi A.

- We successfully established *S.* Paratyphi A infection in the iron overloaded mice. We noted bacterial colonization in the murine intestine which gradually disseminates to the visceral organs. Histopathological analysis further confirmed pathological changes upon bacterial infection.

- Next, using the iron overloaded mice, we found that 80% of the rCTB-T2544 immunized mice survived the lethal bacterial challenge. To further assess whether this protection is due to reduced bacterial colonization in the intestinal tissues and lesser dissemination in the visceral organ, we also found lower bacterial load in the rCTB-T2544 immunized group compared to rT2544, indicating this to be a promising bivalent vaccine candidate.

Next, to formulate multivalent vaccines, we hypothesized to incorporate immunogenic protein and peptides from various enteric pathogens. In this regard, our initiation step was to avoid generation of excessive proinflammatory cytokine stimulation due to the presence of the vaccine antigens and further to optimize the dose of the proteins. In this work, we utilized another mucosal adjuvant rFliC from *S.* Typhimurium in the vaccine formulation together with rT2544.

- We hereby showed that rT2544 admixed with rFliC significantly improved the proportion of antigen specific IgA and IgG secreting plasma and memory B cells. This is further accompanied with strong cell mediated immune response (CMIR) including cytotoxic T lymphocytes ansd effector and memory T cell responses. Addition to the previous reports from our lab, this TF co administration establishes its protective potency and improved immunogenicity at very lower doses (**Fig. Summary Image 2**).

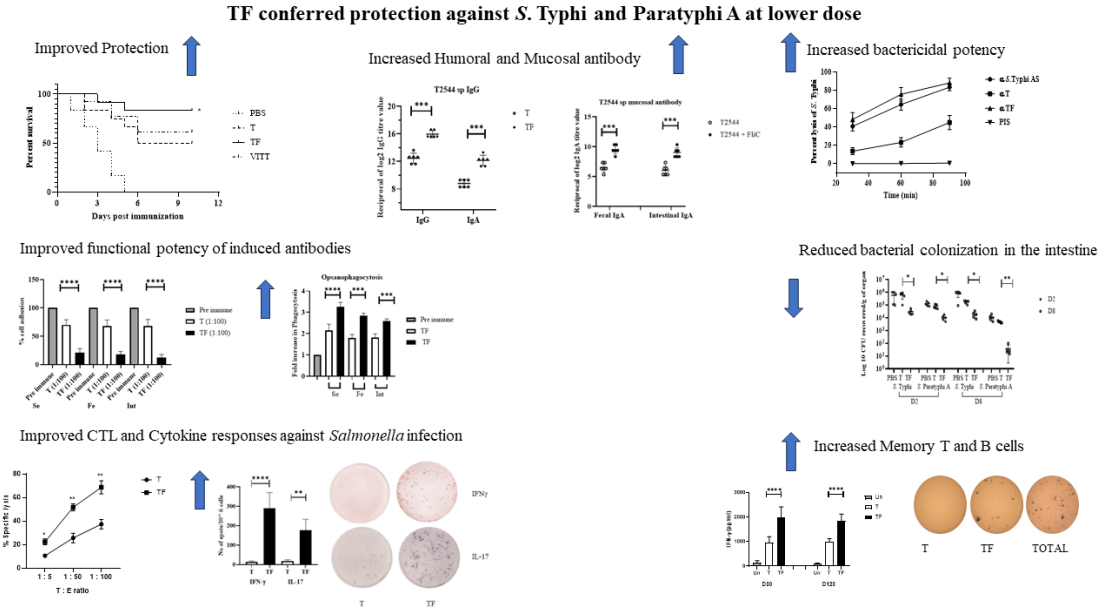

Fig. Summary Image 2. An image summarizing the investigation with subcutaneous administration of rT2544 + rFliC against typhoidal and paratyphoidal infection is shown.

Chapter 10

Future Directions

- Intranasal rCTB-T2544 immunization induced CTB-specific serum and mucosal antibodies in mice. Furthermore, upon challenge with cholera toxin, markedly reduced fluid accumulation in the ileal loops were observed. Intranasal and subcutaneous rCTB administration was previously known to impart protection against *Vibrio* infection. (Price, McFann, and Holmes 2013; Kundu et al. 2009). Future studies are needed to evaluate how CTB-T2544 performs vis-à-vis other cholera vaccines and if the former can boost immune response to other vaccines against *V. cholerae* infection.

- Literatures found mucosal vaccine to be more effective against mucosal infections. No vaccines are currently available against *S.* Paratyphi and NTS. Intranasal rCTB-T2544 immunization protects from *Salmonella* Typhi and *Salmonella* Paratyphi A infection. To formulate a broad-spectrum mucosal vaccine against typhoidal (*S*. Typhi and *S*. Paratyphi A) and non-typhoidal *Salmonella* (*S*. Typhimurium and *S*. Enteritidis) infections, we further planned to conjugate O-specific polysaccharide of *Salmonella* Typhimurium to rCTB-T2544.

- Studies may also be designed by comparing different routes of immunization and/or their combinations to establish the immune correlates of protection against *S*. Typhi infection after CTB-T2544. Such studies could be useful to formulate a prime-boost regimen (intranasal priming and boosting through other routes) with our candidate vaccine. Intranasal priming with subcutaneous boosting induced increased generation of antigen specific humoral and mucosal antibodies. We found improved protective efficacy with prime boost regimen even at a higher challenge dose. Further studies are required to establish the mechanism underlying this augmentation of immune responses.
- A study with rT2544 co-admixed with rFliC was found to be effective in imparting protection against typhoidal *Salmonella.* Next, we aim to include other immunogenic proteins such as IpaB from *Shigella* and CTB from *Vibrio.*

Chapter 11

References

'Aberdeen typhoid outbreak of 1964'. 1966. *Br Med J*, 2: 601-2.
Achtman, M., J. Wain, F. X. Weill, S. Nair, Z. Zhou, V. Sangal, M. G. Krauland, J. L. Hale, H. Harbottle, A. Uesbeck, G. Dougan, L. H. Harrison, S. Brisse, and S. Enterica MLST Study Group. 2012. 'Multilocus sequence typing as a replacement for serotyping in Salmonella enterica', *PLoS Pathog*, 8: e1002776.
Ahmed, D., A. Hoque, R. Mazumder, K. Nahar, N. Islam, S. A. Gazi, and M. A. Hossain. 2012. 'Salmonella enterica serovar Typhi strain producing extended-spectrum beta-lactamases in Dhaka, Bangladesh', *J Med Microbiol*, 61: 1032-33.
Alugupalli, K. R. 2024. 'TLR4 Ligands in Typhoid Vi Polysaccharide Subunit Vaccines Contribute to Immunogenicity', *Immunohorizons*, 8: 29-34.
Asadi Karam, M. R., M. Oloomi, M. Mahdavi, M. Habibi, and S. Bouzari. 2013. 'Vaccination with recombinant FimH fused with flagellin enhances cellular and humoral immunity against urinary tract infection in mice', *Vaccine*, 31: 1210-6.
Aulicino, A., A. Antanaviciute, J. Frost, A. Sousa Geros, E. Mellado, M. Attar, M. Jagielowicz, P. Hublitz, J. Sinz, L. Preciado-Llanes, G. Napolitani, R. Bowden, H. Koohy, H. Drakesmith, and A. Simmons. 2022. 'Dual RNA sequencing reveals dendritic cell reprogramming in response to typhoidal Salmonella invasion', *Commun Biol*, 5: 111.
Awate, S., L. A. Babiuk, and G. Mutwiri. 2013. 'Mechanisms of action of adjuvants', *Front Immunol*, 4: 114.
Ayub, A., M. Usman, A. Ihsan, Q. Ain, A. B. Awan, M. Wajid, A. Ali, A. Haque, M. Iqbal, and Y. Sarwar. 2022. 'Immunological characterization of chitosan adjuvanted outer membrane proteins of Salmonella enterica serovar Typhi as multi-epitope typhoid vaccine candidate', *Mol Biol Rep*, 49: 7377-87.
Balaji, C., V. Kevinkumar, and V. Aravindhan. 2017. 'Long term persistence of inflammation in children vaccinated with Salmonella conjugate vaccine is associated with augmented Th9-Th17 cytokine', *Cytokine*, 91: 128-31.
Bargieri, D. Y., D. S. Rosa, C. J. Braga, B. O. Carvalho, F. T. Costa, N. M. Espindola, A. J. Vaz, I. S. Soares, L. C. Ferreira, and M. M. Rodrigues. 2008. 'New malaria vaccine candidates based on the Plasmodium vivax Merozoite Surface Protein-1 and the TLR-5 agonist Salmonella Typhimurium FliC flagellin', *Vaccine*, 26: 6132-42.
Barkume, C., K. Date, S. K. Saha, F. N. Qamar, D. Sur, J. R. Andrews, S. P. Luby, M. I. Khan, A. Freeman, M. T. Yousafzai, and D. Garrett. 2018. 'Phase I of the Surveillance for Enteric Fever in Asia Project (SEAP): An Overview and Lessons Learned', *J Infect Dis*, 218: S188-S94.
Baumler, A. J. 1997. 'The record of horizontal gene transfer in Salmonella', *Trends Microbiol*, 5: 318-22.
Bhutta, Z. A., M. R. Capeding, A. Bavdekar, E. Marchetti, S. Ariff, S. B. Soofi, A. Anemona, M. A. Habib, E. Alberto, S. Juvekar, R. M. Khan, R. Marhaba, N. Ali, N. Malubay, A. Kawade, A. Saul, L. B. Martin, and A. Podda. 2014. 'Immunogenicity and safety of the Vi-CRM197 conjugate vaccine against typhoid fever in adults, children, and infants in south and southeast Asia: results from two randomised, observer-blind, age de-escalation, phase 2 trials', *Lancet Infect Dis*, 14: 119-29.
Blanc-Potard, A. B., and E. A. Groisman. 1997. 'The Salmonella selC locus contains a pathogenicity island mediating intramacrophage survival', *EMBO J*, 16: 5376-85.
Bouvet, J. P., N. Decroix, and P. Pamonsinlapatham. 2002. 'Stimulation of local antibody production: parenteral or mucosal vaccination?', *Trends Immunol*, 23: 209-13.
Buckle, G. C., C. L. Walker, and R. E. Black. 2012. 'Typhoid fever and paratyphoid fever: Systematic review to estimate global morbidity and mortality for 2010', *J Glob Health*, 2: 010401.

Bumann, D. 2014. 'Identification of Protective Antigens for Vaccination against Systemic Salmonellosis', *Front Immunol*, 5: 381.
Byerly, C. R. 2010. 'The U.S. military and the influenza pandemic of 1918-1919', *Public Health Rep*, 125 Suppl 3: 82-91.
Campodonico, V. L., N. J. Llosa, L. V. Bentancor, T. Maira-Litran, and G. B. Pier. 2011. 'Efficacy of a conjugate vaccine containing polymannuronic acid and flagellin against experimental Pseudomonas aeruginosa lung infection in mice', *Infect Immun*, 79: 3455-64.
Cancellieri, V., and G. M. Fara. 1985. 'Demonstration of specific IgA in human feces after immunization with live Ty21a Salmonella typhi vaccine', *J Infect Dis*, 151: 482-4.
Cao, A. T., S. Yao, B. Gong, C. O. Elson, and Y. Cong. 2012. 'Th17 cells upregulate polymeric Ig receptor and intestinal IgA and contribute to intestinal homeostasis', *J Immunol*, 189: 4666-73.
Carey, M. E., N. S. McCann, and M. M. Gibani. 2022. 'Typhoid fever control in the 21st century: where are we now?', *Curr Opin Infect Dis*, 35: 424-30.
Cartee, R. T., A. Thanawastien, T. J. Griffin Iv, J. J. Mekalanos, S. Bart, and K. P. Killeen. 2020. 'A phase 1 randomized safety, reactogenicity, and immunogenicity study of Typhax: A novel protein capsular matrix vaccine candidate for the prevention of typhoid fever', *PLoS Negl Trop Dis*, 14: e0007912.
Chakraborty, K., P. C. Maity, A. K. Sil, Y. Takeda, and S. Das. 2009. 'cAMP stringently regulates human cathelicidin antimicrobial peptide expression in the mucosal epithelial cells by activating cAMP-response element-binding protein, AP-1, and inducible cAMP early repressor', *J Biol Chem*, 284: 21810-27.
Chakraborty, S., P. Dutta, A. Pal, S. Chakraborty, G. Banik, P. Halder, A. Gope, S. I. Miyoshi, and S. Das. 2024. 'Intranasal immunization of mice with chimera of Salmonella Typhi protein elicits protective intestinal immunity', *NPJ Vaccines*, 9: 24.
Chiu, T. W., C. J. Peng, M. C. Chen, M. H. Hsu, Y. H. Liang, C. H. Chiu, J. M. Fang, and Y. C. Lee. 2020. 'Constructing conjugate vaccine against Salmonella Typhimurium using lipid-A free lipopolysaccharide', *J Biomed Sci*, 27: 89.
Chowdhury, R., R. S. Mandal, A. Ta, and S. Das. 2015. 'An AIL family protein promotes type three secretion system-1-independent invasion and pathogenesis of Salmonella enterica serovar Typhi', *Cell Microbiol*, 17: 486-503.
Clements, J. D., and L. C. Freytag. 2016. 'Parenteral Vaccination Can Be an Effective Means of Inducing Protective Mucosal Responses', *Clin Vaccine Immunol*, 23: 438-41.
Coburn, B., G. A. Grassl, and B. B. Finlay. 2007. 'Salmonella, the host and disease: a brief review', *Immunol Cell Biol*, 85: 112-8.
Cohen, H., C. Hoede, F. Scharte, C. Coluzzi, E. Cohen, I. Shomer, L. Mallet, S. Holbert, R. F. Serre, T. Schiex, I. Virlogeux-Payant, G. A. Grassl, M. Hensel, H. Chiapello, and O. Gal-Mor. 2022. 'Intracellular Salmonella Paratyphi A is motile and differs in the expression of flagella-chemotaxis, SPI-1 and carbon utilization pathways in comparison to intracellular S. Typhimurium', *PLoS Pathog*, 18: e1010425.
Crosa, J. H., D. J. Brenner, W. H. Ewing, and S. Falkow. 1973. 'Molecular relationships among the Salmonelleae', *J Bacteriol*, 115: 307-15.
Cross, D. L., M. K. Verheul, M. D. Leipold, G. Obermoser, C. Jin, E. Jones, J. S. Starr, I. Mohorianu, C. J. Blohmke, H. T. Maecker, G. Napolitani, J. Hill, and A. J. Pollard. 2020. 'Vi-Vaccinations Induce Heterogeneous Plasma Cell Responses That Associate With Protection From Typhoid Fever', *Front Immunol*, 11: 574057.
Crotty, S. 2014. 'T follicular helper cell differentiation, function, and roles in disease', *Immunity*, 41: 529-42.

Crump, J. A., S. P. Luby, and E. D. Mintz. 2004. 'The global burden of typhoid fever', *Bull World Health Organ*, 82: 346-53.
Crump, J. A., and E. D. Mintz. 2010. 'Global trends in typhoid and paratyphoid Fever', *Clin Infect Dis*, 50: 241-6.
Cui, B., X. Liu, Y. Fang, P. Zhou, Y. Zhang, and Y. Wang. 2018. 'Flagellin as a vaccine adjuvant', *Expert Rev Vaccines*, 17: 335-49.
Dahora, L. C., C. Jin, R. L. Spreng, F. Feely, R. Mathura, K. E. Seaton, L. Zhang, J. Hill, E. Jones, S. M. Alam, S. M. Dennison, A. J. Pollard, and G. D. Tomaras. 2019. 'IgA and IgG1 Specific to Vi Polysaccharide of Salmonella Typhi Correlate With Protection Status in a Typhoid Fever Controlled Human Infection Model', *Front Immunol*, 10: 2582.
Das, S., R. Chowdhury, S. Ghosh, and S. Das. 2017. 'A recombinant protein of Salmonella Typhi induces humoral and cell-mediated immune responses including memory responses', *Vaccine*, 35: 4523-31.
Dorsey, C. W., M. C. Laarakker, A. D. Humphries, E. H. Weening, and A. J. Baumler. 2005. 'Salmonella enterica serotype Typhimurium MisL is an intestinal colonization factor that binds fibronectin', *Mol Microbiol*, 57: 196-211.
Dougan, G., and S. Baker. 2014. 'Salmonella enterica serovar Typhi and the pathogenesis of typhoid fever', *Annu Rev Microbiol*, 68: 317-36.
Dupont, H. L., R. B. Hornick, M. J. Snyder, A. T. Dawkins, G. G. Heiner, and T. E. Woodward. 1971. 'Studies of immunity in typhoid fever. Protection induced by killed oral antigens or by primary infection', *Bull World Health Organ*, 44: 667-72.
Earle, C. 1979. 'Environment, disease and mortality in early Virginia', *J Hist Geogr*, 5: 365-90.
Edsall, G., S. Gaines, M. Landy, W. D. Tigertt, H. Sprinz, R. J. Trapani, A. D. Mandel, and A. S. Benenson. 1960. 'Studies on infection and immunity in experimental typhoid fever. I. Typhoid fever in chimpanzees orally infected with Salmonella typhosa', *J Exp Med*, 112: 143-66.
Elhadad, D., P. Desai, G. A. Grassl, M. McClelland, G. Rahav, and O. Gal-Mor. 2016. 'Differences in Host Cell Invasion and Salmonella Pathogenicity Island 1 Expression between Salmonella enterica Serovar Paratyphi A and Nontyphoidal S. Typhimurium', *Infect Immun*, 84: 1150-65.
Erben, U., C. Loddenkemper, K. Doerfel, S. Spieckermann, D. Haller, M. M. Heimesaat, M. Zeitz, B. Siegmund, and A. A. Kuhl. 2014. 'A guide to histomorphological evaluation of intestinal inflammation in mouse models', *Int J Clin Exp Pathol*, 7: 4557-76.
Eriksson, K., M. Fredriksson, I. Nordstrom, and J. Holmgren. 2003. 'Cholera toxin and its B subunit promote dendritic cell vaccination with different influences on Th1 and Th2 development', *Infect Immun*, 71: 1740-7.
Fabrega, A., and J. Vila. 2013. 'Salmonella enterica serovar Typhimurium skills to succeed in the host: virulence and regulation', *Clin Microbiol Rev*, 26: 308-41.
Garcia-del Portillo, F., J. W. Foster, and B. B. Finlay. 1993. 'Role of acid tolerance response genes in Salmonella typhimurium virulence', *Infect Immun*, 61: 4489-92.
Gasperini, G., R. Alfini, V. Arato, F. Mancini, M. G. Aruta, P. Kanvatirth, D. Pickard, F. Necchi, A. Saul, O. Rossi, F. Micoli, and P. Mastroeni. 2021. 'Salmonella Paratyphi A Outer Membrane Vesicles Displaying Vi Polysaccharide as a Multivalent Vaccine against Enteric Fever', *Infect Immun*, 89.
Germain, R. N. 1994. 'MHC-dependent antigen processing and peptide presentation: providing ligands for T lymphocyte activation', *Cell*, 76: 287-99.
Ghosh, S., K. Chakraborty, T. Nagaraja, S. Basak, H. Koley, S. Dutta, U. Mitra, and S. Das. 2011. 'An adhesion protein of Salmonella enterica serovar Typhi is required for

pathogenesis and potential target for vaccine development', *Proc Natl Acad Sci U S A*, 108: 3348-53.
Gonzalez-Escobedo, G., J. M. Marshall, and J. S. Gunn. 2011. 'Chronic and acute infection of the gall bladder by Salmonella Typhi: understanding the carrier state', *Nat Rev Microbiol*, 9: 9-14.
Guo, L., R. Yin, K. Liu, X. Lv, Y. Li, X. Duan, Y. Chu, T. Xi, and Y. Xing. 2014. 'Immunological features and efficacy of a multi-epitope vaccine CTB-UE against H. pylori in BALB/c mice model', *Appl Microbiol Biotechnol*, 98: 3495-507.
Guy, B. 2007. 'The perfect mix: recent progress in adjuvant research', *Nat Rev Microbiol*, 5: 505-17.
Guzman, C. A., S. Borsutzky, M. Griot-Wenk, I. C. Metcalfe, J. Pearman, A. Collioud, D. Favre, and G. Dietrich. 2006. 'Vaccines against typhoid fever', *Vaccine*, 24: 3804-11.
Hajam, I. A., P. A. Dar, I. Shahnawaz, J. C. Jaume, and J. H. Lee. 2017. 'Bacterial flagellin-a potent immunomodulatory agent', *Exp Mol Med*, 49: e373.
Hanabuchi, S., M. Koyanagi, A. Kawasaki, N. Shinohara, A. Matsuzawa, Y. Nishimura, Y. Kobayashi, S. Yonehara, H. Yagita, and K. Okumura. 1994. 'Fas and its ligand in a general mechanism of T-cell-mediated cytotoxicity', *Proc Natl Acad Sci U S A*, 91: 4930-4.
Hancuh, M., J. Walldorf, A. A. Minta, C. Tevi-Benissan, K. A. Christian, Y. Nedelec, K. Heitzinger, M. Mikoleit, A. Tiffany, A. D. Bentsi-Enchill, and L. Breakwell. 2023. 'Typhoid Fever Surveillance, Incidence Estimates, and Progress Toward Typhoid Conjugate Vaccine Introduction - Worldwide, 2018-2022', *MMWR Morb Mortal Wkly Rep*, 72: 171-76.
Hansen-Wester, I., and M. Hensel. 2002. 'Genome-based identification of chromosomal regions specific for Salmonella spp', *Infect Immun*, 70: 2351-60.
Haraga, A., M. B. Ohlson, and S. I. Miller. 2008. 'Salmonellae interplay with host cells', *Nat Rev Microbiol*, 6: 53-66.
Hensel, M., J. E. Shea, C. Gleeson, M. D. Jones, E. Dalton, and D. W. Holden. 1995. 'Simultaneous identification of bacterial virulence genes by negative selection', *Science*, 269: 400-3.
Herath, H. M. 2003. 'Early diagnosis of typhoid fever by the detection of salivary IgA', *J Clin Pathol*, 56: 694-8.
Hess, J., C. Ladel, D. Miko, and S. H. Kaufmann. 1996. 'Salmonella typhimurium aroA- infection in gene-targeted immunodeficient mice: major role of CD4+ TCR-alpha beta cells and IFN-gamma in bacterial clearance independent of intracellular location', *J Immunol*, 156: 3321-6.
Higginson, E. E., R. Simon, and S. M. Tennant. 2016. 'Animal Models for Salmonellosis: Applications in Vaccine Research', *Clin Vaccine Immunol*, 23: 746-56.
Hohmann, E. L., C. A. Oletta, K. P. Killeen, and S. I. Miller. 1996. 'phoP/phoQ-deleted Salmonella typhi (Ty800) is a safe and immunogenic single-dose typhoid fever vaccine in volunteers', *J Infect Dis*, 173: 1408-14.
Holmgren, J., and C. Czerkinsky. 2005. 'Mucosal immunity and vaccines', *Nat Med*, 11: S45-53.
Honda-Okubo, Y., R. T. Cartee, A. Thanawastien, J. Seung Yang, K. P. Killeen, and N. Petrovsky. 2022. 'A typhoid fever protein capsular matrix vaccine candidate formulated with Advax-CpG adjuvant induces a robust and durable anti-typhoid Vi polysaccharide antibody response in mice, rabbits and nonhuman primates', *Vaccine*, 40: 4625-34.
Honko, A. N., and S. B. Mizel. 2004. 'Mucosal administration of flagellin induces innate immunity in the mouse lung', *Infect Immun*, 72: 6676-9.

Honko, A. N., N. Sriranganathan, C. J. Lees, and S. B. Mizel. 2006. 'Flagellin is an effective adjuvant for immunization against lethal respiratory challenge with Yersinia pestis', *Infect Immun*, 74: 1113-20.

Hornick, R. B., S. E. Greisman, T. E. Woodward, H. L. DuPont, A. T. Dawkins, and M. J. Snyder. 1970. 'Typhoid fever: pathogenesis and immunologic control. 2', *N Engl J Med*, 283: 739-46.

Hou, J., Y. Liu, J. Hsi, H. Wang, R. Tao, and Y. Shao. 2014. 'Cholera toxin B subunit acts as a potent systemic adjuvant for HIV-1 DNA vaccination intramuscularly in mice', *Hum Vaccin Immunother*, 10: 1274-83.

Humphries, A. D., S. M. Townsend, R. A. Kingsley, T. L. Nicholson, R. M. Tsolis, and A. J. Baumler. 2001. 'Role of fimbriae as antigens and intestinal colonization factors of Salmonella serovars', *FEMS Microbiol Lett*, 201: 121-5.

Ivanoff, B., M. M. Levine, and P. H. Lambert. 1994. 'Vaccination against typhoid fever: present status', *Bull World Health Organ*, 72: 957-71.

Jones, E., C. Jin, L. Stockdale, C. Dold, A. J. Pollard, and J. Hill. 2021. 'A Salmonella Typhi Controlled Human Infection Study for Assessing Correlation between Bactericidal Antibodies and Protection against Infection Induced by Typhoid Vaccination', *Microorganisms*, 9.

Kagi, D., B. Ledermann, K. Burki, R. M. Zinkernagel, and H. Hengartner. 1996. 'Molecular mechanisms of lymphocyte-mediated cytotoxicity and their role in immunological protection and pathogenesis in vivo', *Annu Rev Immunol*, 14: 207-32.

Kantele, A. 1996. 'Peripheral blood antibody-secreting cells in the evaluation of the immune response to an oral vaccine', *J Biotechnol*, 44: 217-24.

Kantele, A., H. Arvilommi, J. M. Kantele, L. Rintala, and P. H. Makela. 1991. 'Comparison of the human immune response to live oral, killed oral or killed parenteral Salmonella typhi TY21A vaccines', *Microb Pathog*, 10: 117-26.

Kantele, A., S. H. Pakkanen, R. Karttunen, and J. M. Kantele. 2013. 'Head-to-head comparison of humoral immune responses to Vi capsular polysaccharide and Salmonella Typhi Ty21a typhoid vaccines--a randomized trial', *PLoS One*, 8: e60583.

Kantele, A., M. Westerholm, J. M. Kantele, P. H. Makela, and E. Savilahti. 1999. 'Homing potentials of circulating antibody-secreting cells after administration of oral or parenteral protein or polysaccharide vaccine in humans', *Vaccine*, 17: 229-36.

Khanam, F., D. R. Kim, X. Liu, M. Voysey, V. E. Pitzer, K. Zaman, A. J. Pollard, F. Qadri, and J. D. Clemens. 2023. 'Assessment of vaccine herd protection in a cluster-randomised trial of Vi conjugate vaccine against typhoid fever: results of further analysis', *EClinicalMedicine*, 58: 101925.

Kim, C., G. R. Goucher, B. T. Tadesse, W. Lee, K. Abbas, and J. H. Kim. 2023. 'Associations of water, sanitation, and hygiene with typhoid fever in case-control studies: a systematic review and meta-analysis', *BMC Infect Dis*, 23: 562.

Kim, C. L., L. M. Cruz Espinoza, K. S. Vannice, B. T. Tadesse, E. Owusu-Dabo, R. Rakotozandrindrainy, I. V. Jani, M. Teferi, A. Bassiahi Soura, O. Lunguya, A. D. Steele, and F. Marks. 2022. 'The Burden of Typhoid Fever in Sub-Saharan Africa: A Perspective', *Res Rep Trop Med*, 13: 1-9.

Kim, M. S., E. J. Yi, Y. I. Kim, S. H. Kim, Y. S. Jung, S. R. Kim, T. Iwawaki, H. J. Ko, and S. Y. Chang. 2019. 'ERdj5 in Innate Immune Cells Is a Crucial Factor for the Mucosal Adjuvanticity of Cholera Toxin', *Front Immunol*, 10: 1249.

Kingsley, R. A., R. L. Santos, A. M. Keestra, L. G. Adams, and A. J. Baumler. 2002. 'Salmonella enterica serotype Typhimurium ShdA is an outer membrane fibronectin-binding protein that is expressed in the intestine', *Mol Microbiol*, 43: 895-905.

Kirimanjeswara, G. S., S. Olmos, C. S. Bakshi, and D. W. Metzger. 2008. 'Humoral and cell-mediated immunity to the intracellular pathogen Francisella tularensis', *Immunol Rev*, 225: 244-55.

Kirkpatrick, B. D., R. McKenzie, J. P. O'Neill, C. J. Larsson, A. L. Bourgeois, J. Shimko, M. Bentley, J. Makin, S. Chatfield, Z. Hindle, C. Fidler, B. E. Robinson, C. H. Ventrone, N. Bansal, C. M. Carpenter, D. Kutzko, S. Hamlet, C. LaPointe, and D. N. Taylor. 2006. 'Evaluation of Salmonella enterica serovar Typhi (Ty2 aroC-ssaV-) M01ZH09, with a defined mutation in the Salmonella pathogenicity island 2, as a live, oral typhoid vaccine in human volunteers', *Vaccine*, 24: 116-23.

Kirkpatrick, B. D., K. M. Tenney, C. J. Larsson, J. P. O'Neill, C. Ventrone, M. Bentley, A. Upton, Z. Hindle, C. Fidler, D. Kutzko, R. Holdridge, C. Lapointe, S. Hamlet, and S. N. Chatfield. 2005. 'The novel oral typhoid vaccine M01ZH09 is well tolerated and highly immunogenic in 2 vaccine presentations', *J Infect Dis*, 192: 360-6.

Konadu, E., J. Shiloach, D. A. Bryla, J. B. Robbins, and S. C. Szu. 1996. 'Synthesis, characterization, and immunological properties in mice of conjugates composed of detoxified lipopolysaccharide of Salmonella paratyphi A bound to tetanus toxoid with emphasis on the role of O acetyls', *Infect Immun*, 64: 2709-15.

Kumar, S., M. Rizvi, and N. Berry. 2008. 'Rising prevalence of enteric fever due to multidrug-resistant Salmonella: an epidemiological study', *J Med Microbiol*, 57: 1247-50.

Kundu, J., R. Mazumder, R. Srivastava, and B. S. Srivastava. 2009. 'Intranasal immunization with recombinant toxin-coregulated pilus and cholera toxin B subunit protects rabbits against Vibrio cholerae O1 challenge', *FEMS Immunol Med Microbiol*, 56: 179-84.

Lavelle, E. C., and R. W. Ward. 2022. 'Mucosal vaccines - fortifying the frontiers', *Nat Rev Immunol*, 22: 236-50.

Lee, J., J. K. Yoo, H. J. Sohn, H. K. Kang, D. Kim, H. J. Shin, and J. H. Kim. 2015. 'Protective immunity against Naegleria fowleri infection on mice immunized with the rNfa1 protein using mucosal adjuvants', *Parasitol Res*, 114: 1377-85.

Levine, M. M., C. Ferreccio, P. Abrego, O. S. Martin, E. Ortiz, and S. Cryz. 1999. 'Duration of efficacy of Ty21a, attenuated Salmonella typhi live oral vaccine', *Vaccine*, 17 Suppl 2: S22-7.

Levine, M. M., C. O. Tacket, and M. B. Sztein. 2001. 'Host-Salmonella interaction: human trials', *Microbes Infect*, 3: 1271-9.

Liang, Y., A. J. Driscoll, P. D. Patel, S. Datta, M. Voysey, N. French, L. P. Jamka, M. Y. R. Henrion, L. Ndeketa, M. B. Laurens, R. S. Heyderman, M. A. Gordon, and K. M. Neuzil. 2023. 'Typhoid conjugate vaccine effectiveness in Malawi: evaluation of a test-negative design using randomised, controlled clinical trial data', *Lancet Glob Health*, 11: e136-e44.

Libby, S. J., M. A. Brehm, D. L. Greiner, L. D. Shultz, M. McClelland, K. D. Smith, B. T. Cookson, J. E. Karlinsey, T. L. Kinkel, S. Porwollik, R. Canals, L. A. Cummings, and F. C. Fang. 2010. 'Humanized nonobese diabetic-scid IL2rgammanull mice are susceptible to lethal Salmonella Typhi infection', *Proc Natl Acad Sci U S A*, 107: 15589-94.

Livingston, K. A., X. Jiang, and C. B. Stephensen. 2013. 'CD4 T-helper cell cytokine phenotypes and antibody response following tetanus toxoid booster immunization', *J Immunol Methods*, 390: 18-29.

Lockner, J. W., L. M. Eubanks, J. L. Choi, J. M. Lively, J. E. Schlosburg, K. C. Collins, D. Globisch, R. J. Rosenfeld-Gunn, I. A. Wilson, and K. D. Janda. 2015. 'Flagellin as carrier and adjuvant in cocaine vaccine development', *Mol Pharm*, 12: 653-62.

Lopez, A. L., J. D. Clemens, J. Deen, and L. Jodar. 2008. 'Cholera vaccines for the developing world', *Hum Vaccin*, 4: 165-9.

Lundin, B. S., C. Johansson, and A. M. Svennerholm. 2002. 'Oral immunization with a Salmonella enterica serovar typhi vaccine induces specific circulating mucosa-homing CD4(+) and CD8(+) T cells in humans', *Infect Immun*, 70: 5622-7.

Lycke, N. 2012. 'Recent progress in mucosal vaccine development: potential and limitations', *Nat Rev Immunol*, 12: 592-605.

MacLennan, C. A. 2014. 'Antibodies and protection against invasive salmonella disease', *Front Immunol*, 5: 635.

MacLeod, M. K., E. T. Clambey, J. W. Kappler, and P. Marrack. 2009. 'CD4 memory T cells: what are they and what can they do?', *Semin Immunol*, 21: 53-61.

Marineli, F., G. Tsoucalas, M. Karamanou, and G. Androutsos. 2013. 'Mary Mallon (1869-1938) and the history of typhoid fever', *Ann Gastroenterol*, 26: 132-34.

Martin, L. B., R. Simon, C. A. MacLennan, S. M. Tennant, S. Sahastrabuddhe, and M. I. Khan. 2016. 'Status of paratyphoid fever vaccine research and development', *Vaccine*, 34: 2900-02.

McArthur, M. A., and M. B. Sztein. 2012. 'Heterogeneity of multifunctional IL-17A producing S. Typhi-specific CD8+ T cells in volunteers following Ty21a typhoid immunization', *PLoS One*, 7: e38408.

Medise, B. E., S. Soedjatmiko, I. Rengganis, H. Gunardi, R. Sekartini, S. Koesno, H. I. Satari, S. R. Hadinegoro, J. S. Yang, J. L. Excler, S. Sahastrabuddhe, M. Puspita, R. M. Sari, and N. S. Bachtiar. 2019. 'Six-month follow up of a randomized clinical trial-phase I study in Indonesian adults and children: Safety and immunogenicity of Salmonella typhi polysaccharide-diphtheria toxoid (Vi-DT) conjugate vaccine', *PLoS One*, 14: e0211784.

Meloni, E., A. M. Colucci, F. Micoli, L. Sollai, M. Gavini, A. Saul, V. Di Cioccio, and C. A. MacLennan. 2015. 'Simplified low-cost production of O-antigen from Salmonella Typhimurium Generalized Modules for Membrane Antigens (GMMA)', *J Biotechnol*, 198: 46-52.

Mittrucker, H. W., B. Raupach, A. Kohler, and S. H. Kaufmann. 2000. 'Cutting edge: role of B lymphocytes in protective immunity against Salmonella typhimurium infection', *J Immunol*, 164: 1648-52.

Miyata, T., T. Harakuni, T. Tsuboi, J. Sattabongkot, H. Kohama, M. Tachibana, G. Matsuzaki, M. Torii, and T. Arakawa. 2010. 'Plasmodium vivax ookinete surface protein Pvs25 linked to cholera toxin B subunit induces potent transmission-blocking immunity by intranasal as well as subcutaneous immunization', *Infect Immun*, 78: 3773-82.

Mizel, S. B., and J. T. Bates. 2010. 'Flagellin as an adjuvant: cellular mechanisms and potential', *J Immunol*, 185: 5677-82.

Moorhead, R. 2002. 'William Budd and typhoid fever', *J R Soc Med*, 95: 561-4.

Mora, J. R., M. Iwata, B. Eksteen, S. Y. Song, T. Junt, B. Senman, K. L. Otipoby, A. Yokota, H. Takeuchi, P. Ricciardi-Castagnoli, K. Rajewsky, D. H. Adams, and U. H. von Andrian. 2006. 'Generation of gut-homing IgA-secreting B cells by intestinal dendritic cells', *Science*, 314: 1157-60.

Nossal, G. J., G. L. Ada, and C. M. Austin. 1964. 'Antigens in Immunity. Ii. Immunogenic Properties of Flagella, Polymerized Flagellin and Flagellin in the Primary Response', *Aust J Exp Biol Med Sci*, 42: 283-94.

O'Brien, A. D. 1982. 'Innate resistance of mice to Salmonella typhi infection', *Infect Immun*, 38: 948-52.

Ontiveros-Padilla, L., A. Garcia-Lozano, A. Tepale-Segura, T. Rivera-Hernandez, R. Pastelin-Palacios, A. Isibasi, L. A. Arriaga-Pizano, L. C. Bonifaz, and C. Lopez-Macias. 2021. 'CD4+ and CD8+ Circulating Memory T Cells Are Crucial in the Protection Induced by Vaccination with Salmonella Typhi Porins', *Microorganisms*, 9.

Pakkanen, S. H., J. M. Kantele, and A. Kantele. 2014. 'Cross-reactive immune response induced by the Vi capsular polysaccharide typhoid vaccine against Salmonella Paratyphi strains', *Scand J Immunol*, 79: 222-9.

Pakkanen, S. H., J. M. Kantele, Z. Moldoveanu, S. Hedges, M. Hakkinen, J. Mestecky, and A. Kantele. 2010. 'Expression of homing receptors on IgA1 and IgA2 plasmablasts in blood reflects differential distribution of IgA1 and IgA2 in various body fluids', *Clin Vaccine Immunol*, 17: 393-401.

Papagrigorakis, M. J., C. Yapijakis, P. N. Synodinos, and E. Baziotopoulou-Valavani. 2006. 'DNA examination of ancient dental pulp incriminates typhoid fever as a probable cause of the Plague of Athens', *Int J Infect Dis*, 10: 206-14.

Pasetti, M. F., J. K. Simon, M. B. Sztein, and M. M. Levine. 2011. 'Immunology of gut mucosal vaccines', *Immunol Rev*, 239: 125-48.

Perez-Shibayama, C., C. Gil-Cruz, R. Pastelin-Palacios, L. Cervantes-Barragan, E. Hisaki, Q. Chai, L. Onder, E. Scandella, T. Regen, A. Waisman, A. Isibasi, C. Lopez-Macias, and B. Ludewig. 2014. 'IFN-gamma-producing CD4+ T cells promote generation of protective germinal center-derived IgM+ B cell memory against Salmonella Typhi', *J Immunol*, 192: 5192-200.

Pham, O. H., and S. J. McSorley. 2015. 'Protective host immune responses to Salmonella infection', *Future Microbiol*, 10: 101-10.

Powell, C. J., Jr., C. R. DeSett, J. P. Lowenthal, and S. Berman. 1980. 'The effect of adding iron to mucin on the enhancement of virulence for mice of Salmonella typhi strain TY 2', *J Biol Stand*, 8: 79-85.

Price, G. A., K. McFann, and R. K. Holmes. 2013. 'Immunization with cholera toxin B subunit induces high-level protection in the suckling mouse model of cholera', *PLoS One*, 8: e57269.

Pulickal, A. S., S. Gautam, E. A. Clutterbuck, S. Thorson, B. Basynat, N. Adhikari, K. Makepeace, S. Rijpkema, R. Borrow, J. J. Farrar, and A. J. Pollard. 2009. 'Kinetics of the natural, humoral immune response to Salmonella enterica serovar Typhi in Kathmandu, Nepal', *Clin Vaccine Immunol*, 16: 1413-9.

Raymond, M., M. M. Gibani, N. P. J. Day, and P. Y. Cheah. 2019. 'Typhoidal Salmonella human challenge studies: ethical and practical challenges and considerations for low-resource settings', *Trials*, 20: 704.

Rhee, J. H., S. E. Lee, and S. Y. Kim. 2012. 'Mucosal vaccine adjuvants update', *Clin Exp Vaccine Res*, 1: 50-63.

Roland, K. L., S. A. Tinge, S. K. Kochi, L. J. Thomas, and K. P. Killeen. 2010. 'Reactogenicity and immunogenicity of live attenuated Salmonella enterica serovar Paratyphi A enteric fever vaccine candidates', *Vaccine*, 28: 3679-87.

Rosselin, M., I. Virlogeux-Payant, C. Roy, E. Bottreau, P. Y. Sizaret, L. Mijouin, P. Germon, E. Caron, P. Velge, and A. Wiedemann. 2010. 'Rck of Salmonella enterica, subspecies enterica serovar enteritidis, mediates zipper-like internalization', *Cell Res*, 20: 647-64.

Ruane, D., L. Brane, B. S. Reis, C. Cheong, J. Poles, Y. Do, H. Zhu, K. Velinzon, J. H. Choi, N. Studt, L. Mayer, E. C. Lavelle, R. M. Steinman, D. Mucida, and S. Mehandru. 2013. 'Lung dendritic cells induce migration of protective T cells to the gastrointestinal tract', *J Exp Med*, 210: 1871-88.

Ruby, T., L. McLaughlin, S. Gopinath, and D. Monack. 2012. 'Salmonella's long-term relationship with its host', *FEMS Microbiol Rev*, 36: 600-15.

Salazar-Gonzalez, R. M., C. Maldonado-Bernal, N. E. Ramirez-Cruz, N. Rios-Sarabia, J. Beltran-Nava, J. Castanon-Gonzalez, N. Castillo-Torres, J. A. Palma-Aguirre, M. Carrera-Camargo, C. Lopez-Macias, and A. Isibasi. 2004. 'Induction of cellular immune response and anti-Salmonella enterica serovar typhi bactericidal antibodies in healthy

volunteers by immunization with a vaccine candidate against typhoid fever', *Immunol Lett*, 93: 115-22.

Salerno-Goncalves, R., M. Fernandez-Vina, D. M. Lewinsohn, and M. B. Sztein. 2004. 'Identification of a human HLA-E-restricted CD8+ T cell subset in volunteers immunized with Salmonella enterica serovar Typhi strain Ty21a typhoid vaccine', *J Immunol*, 173: 5852-62.

Salerno-Goncalves, R., M. F. Pasetti, and M. B. Sztein. 2002. 'Characterization of CD8(+) effector T cell responses in volunteers immunized with Salmonella enterica serovar Typhi strain Ty21a typhoid vaccine', *J Immunol*, 169: 2196-203.

Salerno-Goncalves, R., and M. B. Sztein. 2009. 'Priming of Salmonella enterica serovar typhi-specific CD8(+) T cells by suicide dendritic cell cross-presentation in humans', *PLoS One*, 4: e5879.

Salerno-Goncalves, R., H. Tettelin, D. Luo, Q. Guo, M. T. Ardito, W. D. Martin, A. S. De Groot, and M. B. Sztein. 2020. 'Differential functional patterns of memory CD4(+) and CD8(+) T-cells from volunteers immunized with Ty21a typhoid vaccine observed using a recombinant Escherichia coli system expressing S. Typhi proteins', *Vaccine*, 38: 258-70.

Salerno-Goncalves, R., R. Wahid, and M. B. Sztein. 2005. 'Immunization of volunteers with Salmonella enterica serovar Typhi strain Ty21a elicits the oligoclonal expansion of CD8+ T cells with predominant Vbeta repertoires', *Infect Immun*, 73: 3521-30.

2010. 'Ex Vivo kinetics of early and long-term multifunctional human leukocyte antigen E-specific CD8+ cells in volunteers immunized with the Ty21a typhoid vaccine', *Clin Vaccine Immunol*, 17: 1305-14.

Salerno-Goncalves, R., T. L. Wyant, M. F. Pasetti, M. Fernandez-Vina, C. O. Tacket, M. M. Levine, and M. B. Sztein. 2003. 'Concomitant induction of CD4+ and CD8+ T cell responses in volunteers immunized with Salmonella enterica serovar typhi strain CVD 908-htrA', *J Immunol*, 170: 2734-41.

Sallusto, F., J. Geginat, and A. Lanzavecchia. 2004. 'Central memory and effector memory T cell subsets: function, generation, and maintenance', *Annu Rev Immunol*, 22: 745-63.

Sallusto, F., D. Lenig, R. Forster, M. Lipp, and A. Lanzavecchia. 1999. 'Two subsets of memory T lymphocytes with distinct homing potentials and effector functions', *Nature*, 401: 708-12.

Samanta, P., R. S. Mandal, R. N. Saha, S. Shaw, P. Ghosh, S. Dutta, A. Ghosh, D. Imamura, M. Morita, M. Ohnishi, T. Ramamurthy, and A. K. Mukhopadhyay. 2020. 'A Point Mutation in carR Is Involved in the Emergence of Polymyxin B-Sensitive Vibrio cholerae O1 El Tor Biotype by Influencing Gene Transcription', *Infect Immun*, 88.

Santander, J., and R. Curtiss, 3rd. 2010. 'Salmonella enterica Serovars Typhi and Paratyphi A are avirulent in newborn and infant mice even when expressing virulence plasmid genes of Salmonella Typhimurium', *J Infect Dev Ctries*, 4: 723-31.

Sassone-Corsi, M., P. Chairatana, T. Zheng, A. Perez-Lopez, R. A. Edwards, M. D. George, E. M. Nolan, and M. Raffatellu. 2016. 'Siderophore-based immunization strategy to inhibit growth of enteric pathogens', *Proc Natl Acad Sci U S A*, 113: 13462-67.

Satitsri, S., P. Pongkorpsakol, P. Srimanote, V. Chatsudthipong, and C. Muanprasat. 2016. 'Pathophysiological mechanisms of diarrhea caused by the Vibrio cholerae O1 El Tor variant: an in vivo study in mice', *Virulence*, 7: 789-805.

Scharte, F., R. Franzkoch, and M. Hensel. 2024. 'Flagella-mediated cytosolic motility of Salmonella enterica Paratyphi A aids in evasion of xenophagy but does not impact egress from host cells', *Mol Microbiol*, 121: 413-30.

Shakya, M., K. M. Neuzil, and A. J. Pollard. 2021. 'Prospects of Future Typhoid and Paratyphoid Vaccines in Endemic Countries', *J Infect Dis*, 224: S770-S74.

Shakya, M., M. Voysey, K. Theiss-Nyland, R. Colin-Jones, D. Pant, A. Adhikari, S. Tonks, Y. F. Mujadidi, P. O'Reilly, O. Mazur, S. Kelly, X. Liu, A. Maharjan, A. Dahal, N. Haque, A. Pradhan, S. Shrestha, M. Joshi, N. Smith, J. Hill, J. Clarke, L. Stockdale, E. Jones, T. Lubinda, B. Bajracharya, S. Dongol, A. Karkey, S. Baker, G. Dougan, V. E. Pitzer, K. M. Neuzil, S. Shrestha, B. Basnyat, A. J. Pollard, and V. A. C. Nepal Team Ty. 2021. 'Efficacy of typhoid conjugate vaccine in Nepal: final results of a phase 3, randomised, controlled trial', *Lancet Glob Health*, 9: e1561-e68.

Sheorey, H. S., D. V. Kaundinya, V. S. Hulyalkar, and A. K. Deshpande. 1993. 'Multi drug resistant Salmonella typhi in Bombay', *Indian J Pathol Microbiol*, 36: 8-12.

Simon, R., and M. M. Levine. 2012. 'Glycoconjugate vaccine strategies for protection against invasive Salmonella infections', *Hum Vaccin Immunother*, 8: 494-8.

Simon, R., J. Y. Wang, M. A. Boyd, M. E. Tulapurkar, G. Ramachandran, S. M. Tennant, M. Pasetti, J. E. Galen, and M. M. Levine. 2013. 'Sustained protection in mice immunized with fractional doses of Salmonella Enteritidis core and O polysaccharide-flagellin glycoconjugates', *PLoS One*, 8: e64680.

Song, J., T. Willinger, A. Rongvaux, E. E. Eynon, S. Stevens, M. G. Manz, R. A. Flavell, and J. E. Galan. 2010. 'A mouse model for the human pathogen Salmonella typhi', *Cell Host Microbe*, 8: 369-76.

Stratmann, T. 2015. 'Cholera Toxin Subunit B as Adjuvant--An Accelerator in Protective Immunity and a Break in Autoimmunity', *Vaccines (Basel)*, 3: 579-96.

Stuart, B. M., and R. L. Pullen. 1946. 'Typhoid; clinical analysis of 360 cases', *Arch Intern Med (Chic)*, 78: 629-61.

Suar, M., J. Jantsch, S. Hapfelmeier, M. Kremer, T. Stallmach, P. A. Barrow, and W. D. Hardt. 2006. 'Virulence of broad- and narrow-host-range Salmonella enterica serovars in the streptomycin-pretreated mouse model', *Infect Immun*, 74: 632-44.

Sundquist, M., A. Rydstrom, and M. J. Wick. 2004. 'Immunity to Salmonella from a dendritic point of view', *Cell Microbiol*, 6: 1-11.

Sundstrom, P., S. B. Lundin, L. A. Nilsson, and M. Quiding-Jarbrink. 2008. 'Human IgA-secreting cells induced by intestinal, but not systemic, immunization respond to CCL25 (TECK) and CCL28 (MEC)', *Eur J Immunol*, 38: 3327-38.

Sur, D., R. L. Ochiai, S. K. Bhattacharya, N. K. Ganguly, M. Ali, B. Manna, S. Dutta, A. Donner, S. Kanungo, J. K. Park, M. K. Puri, D. R. Kim, D. Dutta, B. Bhaduri, C. J. Acosta, and J. D. Clemens. 2009. 'A cluster-randomized effectiveness trial of Vi typhoid vaccine in India', *N Engl J Med*, 361: 335-44.

Syed, K. A., T. Saluja, H. Cho, A. Hsiao, H. Shaikh, T. A. Wartel, V. Mogasale, J. Lynch, J. H. Kim, J. L. Excler, and S. Sahastrabuddhe. 2020. 'Review on the Recent Advances on Typhoid Vaccine Development and Challenges Ahead', *Clin Infect Dis*, 71: S141-S50.

Sztein, M. B., and J. S. Booth. 2022. 'Controlled human infectious models, a path forward in uncovering immunological correlates of protection: Lessons from enteric fevers studies', *Front Microbiol*, 13: 983403.

Sztein, M. B., R. Salerno-Goncalves, and M. A. McArthur. 2014. 'Complex adaptive immunity to enteric fevers in humans: lessons learned and the path forward', *Front Immunol*, 5: 516.

Sztein, M. B., S. S. Wasserman, C. O. Tacket, R. Edelman, D. Hone, A. A. Lindberg, and M. M. Levine. 1994. 'Cytokine production patterns and lymphoproliferative responses in volunteers orally immunized with attenuated vaccine strains of Salmonella typhi', *J Infect Dis*, 170: 1508-17.

Szu, S. C. 2013. 'Development of Vi conjugate - a new generation of typhoid vaccine', *Expert Rev Vaccines*, 12: 1273-86.

Szu, S. C., K. P. Klugman, and S. Hunt. 2014. 'Re-examination of immune response and estimation of anti-Vi IgG protective threshold against typhoid fever-based on the efficacy trial of Vi conjugate in young children', *Vaccine*, 32: 2359-63.
Tacket, C. O., C. Ferreccio, J. B. Robbins, C. M. Tsai, D. Schulz, M. Cadoz, A. Goudeau, and M. M. Levine. 1986. 'Safety and immunogenicity of two Salmonella typhi Vi capsular polysaccharide vaccines', *J Infect Dis*, 154: 342-5.
Tacket, C. O., D. M. Hone, G. A. Losonsky, L. Guers, R. Edelman, and M. M. Levine. 1992. 'Clinical acceptability and immunogenicity of CVD 908 Salmonella typhi vaccine strain', *Vaccine*, 10: 443-6.
Tacket, C. O., M. F. Pasetti, M. B. Sztein, S. Livio, and M. M. Levine. 2004. 'Immune responses to an oral typhoid vaccine strain that is modified to constitutively express Vi capsular polysaccharide', *J Infect Dis*, 190: 565-70.
Tacket, C. O., M. B. Sztein, S. S. Wasserman, G. Losonsky, K. L. Kotloff, T. L. Wyant, J. P. Nataro, R. Edelman, J. Perry, P. Bedford, D. Brown, S. Chatfield, G. Dougan, and M. M. Levine. 2000. 'Phase 2 clinical trial of attenuated Salmonella enterica serovar typhi oral live vector vaccine CVD 908-htrA in U.S. volunteers', *Infect Immun*, 68: 1196-201.
Tagliabue, A., L. Villa, M. T. De Magistris, M. Romano, S. Silvestri, D. Boraschi, and L. Nencioni. 1986. 'IgA-driven T cell-mediated anti-bacterial immunity in man after live oral Ty 21a vaccine', *J Immunol*, 137: 1504-10.
Takemori, T., T. Kaji, Y. Takahashi, M. Shimoda, and K. Rajewsky. 2014. 'Generation of memory B cells inside and outside germinal centers', *Eur J Immunol*, 44: 1258-64.
Tarlinton, D., A. Radbruch, F. Hiepe, and T. Dorner. 2008. 'Plasma cell differentiation and survival', *Curr Opin Immunol*, 20: 162-9.
Tezuka, H., and T. Ohteki. 2019. 'Regulation of IgA Production by Intestinal Dendritic Cells and Related Cells', *Front Immunol*, 10: 1891.
Thiem, V. D., F. Y. Lin, D. G. Canh, N. H. Son, D. D. Anh, N. D. Mao, C. Chu, S. W. Hunt, J. B. Robbins, R. Schneerson, and S. C. Szu. 2011. 'The Vi conjugate typhoid vaccine is safe, elicits protective levels of IgG anti-Vi, and is compatible with routine infant vaccines', *Clin Vaccine Immunol*, 18: 730-5.
Tran, T. H., T. D. Nguyen, T. T. Nguyen, T. T. Ninh, N. B. Tran, V. M. Nguyen, T. T. Tran, T. T. Cao, V. M. Pham, T. C. Nguyen, T. D. Tran, V. T. Pham, S. D. To, J. I. Campbell, E. Stockwell, C. Schultsz, C. P. Simmons, C. Glover, W. Lam, F. Marques, J. P. May, A. Upton, R. Budhram, G. Dougan, J. Farrar, V. V. Nguyen, and C. Dolecek. 2010. 'A randomised trial evaluating the safety and immunogenicity of the novel single oral dose typhoid vaccine M01ZH09 in healthy Vietnamese children', *PLoS One*, 5: e11778.
Tritama, E., C. Riani, I. Rudiansyah, A. Hidayat, S. A. Kharisnaeni, and D. S. Retnoningrum. 2018. 'Evaluation of alum-based adjuvant on the immunogenicity of salmonella enterica serovar typhi conjugates vaccines', *Hum Vaccin Immunother*, 14: 1524-29.
Uchiya, K., M. A. Barbieri, K. Funato, A. H. Shah, P. D. Stahl, and E. A. Groisman. 1999. 'A Salmonella virulence protein that inhibits cellular trafficking', *EMBO J*, 18: 3924-33.
Vagene, A. J., A. Herbig, M. G. Campana, N. M. Robles Garcia, C. Warinner, S. Sabin, M. A. Spyrou, A. Andrades Valtuena, D. Huson, N. Tuross, K. I. Bos, and J. Krause. 2018. 'Salmonella enterica genomes from victims of a major sixteenth-century epidemic in Mexico', *Nat Ecol Evol*, 2: 520-28.
van Asten, A. J., and J. E. van Dijk. 2005. 'Distribution of "classic" virulence factors among Salmonella spp', *FEMS Immunol Med Microbiol*, 44: 251-9.
van Damme, P., F. Kafeja, A. Anemona, V. Basile, A. K. Hilbert, I. De Coster, S. Rondini, F. Micoli, R. M. Qasim Khan, E. Marchetti, V. Di Cioccio, A. Saul, L. B. Martin, and A. Podda. 2011. 'Safety, immunogenicity and dose ranging of a new Vi-CRM(1)(9)(7)

conjugate vaccine against typhoid fever: randomized clinical testing in healthy adults', *PLoS One*, 6: e25398.

Vazquez-Torres, A., and F. C. Fang. 2001. 'Oxygen-dependent anti-Salmonella activity of macrophages', *Trends Microbiol*, 9: 29-33.

Waddington, C. S., T. C. Darton, C. Jones, K. Haworth, A. Peters, T. John, B. A. Thompson, S. A. Kerridge, R. A. Kingsley, L. Zhou, K. E. Holt, L. M. Yu, S. Lockhart, J. J. Farrar, M. B. Sztein, G. Dougan, B. Angus, M. M. Levine, and A. J. Pollard. 2014. 'An outpatient, ambulant-design, controlled human infection model using escalating doses of Salmonella Typhi challenge delivered in sodium bicarbonate solution', *Clin Infect Dis*, 58: 1230-40.

Wahid, R., K. L. Kotloff, M. M. Levine, and M. B. Sztein. 2019. 'Cell mediated immune responses elicited in volunteers following immunization with candidate live oral Salmonella enterica serovar Paratyphi A attenuated vaccine strain CVD 1902', *Clin Immunol*, 201: 61-69.

Wahid, R., M. F. Pasetti, M. Maciel, Jr., J. K. Simon, C. O. Tacket, M. M. Levine, and M. B. Sztein. 2011. 'Oral priming with Salmonella Typhi vaccine strain CVD 909 followed by parenteral boost with the S. Typhi Vi capsular polysaccharide vaccine induces CD27+IgD-S. Typhi-specific IgA and IgG B memory cells in humans', *Clin Immunol*, 138: 187-200.

Wahid, R., R. Salerno-Goncalves, C. O. Tacket, M. M. Levine, and M. B. Sztein. 2007. 'Cell-mediated immune responses in humans after immunization with one or two doses of oral live attenuated typhoid vaccine CVD 909', *Vaccine*, 25: 1416-25.

———. 2008. 'Generation of specific effector and memory T cells with gut- and secondary lymphoid tissue- homing potential by oral attenuated CVD 909 typhoid vaccine in humans', *Mucosal Immunol*, 1: 389-98.

Wahid, R., R. Simon, S. J. Zafar, M. M. Levine, and M. B. Sztein. 2012. 'Live oral typhoid vaccine Ty21a induces cross-reactive humoral immune responses against Salmonella enterica serovar Paratyphi A and S. Paratyphi B in humans', *Clin Vaccine Immunol*, 19: 825-34.

Wahid, R., S. J. Zafar, M. A. McArthur, M. F. Pasetti, M. M. Levine, and M. B. Sztein. 2014. 'Live oral Salmonella enterica serovar Typhi vaccines Ty21a and CVD 909 induce opsonophagocytic functional antibodies in humans that cross-react with S. Paratyphi A and S. Paratyphi B', *Clin Vaccine Immunol*, 21: 427-34.

Wain, J., T. T. Hien, P. Connerton, T. Ali, C. M. Parry, N. T. Chinh, H. Vinh, C. X. Phuong, V. A. Ho, T. S. Diep, J. J. Farrar, N. J. White, and G. Dougan. 1999. 'Molecular typing of multiple-antibiotic-resistant Salmonella enterica serovar Typhi from Vietnam: application to acute and relapse cases of typhoid fever', *J Clin Microbiol*, 37: 2466-72.

Wang, M., S. Bregenholt, and J. S. Petersen. 2003. 'The cholera toxin B subunit directly costimulates antigen-primed CD4+ T cells ex vivo', *Scand J Immunol*, 58: 342-9.

Wang, M., I. H. Qazi, L. Wang, G. Zhou, and H. Han. 2020. 'Salmonella Virulence and Immune Escape', *Microorganisms*, 8.

Weil, A. A., M. Arifuzzaman, T. R. Bhuiyan, R. C. LaRocque, A. M. Harris, E. A. Kendall, A. Hossain, A. A. Tarique, A. Sheikh, F. Chowdhury, A. I. Khan, F. Murshed, K. C. Parker, K. K. Banerjee, E. T. Ryan, J. B. Harris, F. Qadri, and S. B. Calderwood. 2009. 'Memory T-cell responses to Vibrio cholerae O1 infection', *Infect Immun*, 77: 5090-6.

Wiedinger, K., D. Pinho, and C. Bitsaktsis. 2017. 'Utilization of cholera toxin B as a mucosal adjuvant elicits antibody-mediated protection against S. pneumoniae infection in mice', *Ther Adv Vaccines*, 5: 15-24.

Wu, H. Y., and M. W. Russell. 1993. 'Induction of mucosal immunity by intranasal application of a streptococcal surface protein antigen with the cholera toxin B subunit', *Infect Immun*, 61: 314-22.

Xiong, K., C. Zhu, Z. Chen, C. Zheng, Y. Tan, X. Rao, and Y. Cong. 2017. 'Vi Capsular Polysaccharide Produced by Recombinant Salmonella enterica Serovar Paratyphi A Confers Immunoprotection against Infection by Salmonella enterica Serovar Typhi', *Front Cell Infect Microbiol*, 7: 135.

Zhang, F., E. M. Boerth, J. Gong, N. Ma, K. Lucas, O. Ledue, R. Malley, and Y. J. Lu. 2022. 'A Bivalent MAPS Vaccine Induces Protective Antibody Responses against Salmonella Typhi and Paratyphi A', *Vaccines (Basel)*, 11.

Zhang, X. L., I. S. Tsui, C. M. Yip, A. W. Fung, D. K. Wong, X. Dai, Y. Yang, J. Hackett, and C. Morris. 2000. 'Salmonella enterica serovar typhi uses type IVB pili to enter human intestinal epithelial cells', *Infect Immun*, 68: 3067-73.

Zhu, C., K. Xiong, Z. Chen, X. Hu, J. Li, Y. Wang, X. Rao, and Y. Cong. 2015. 'Construction of an attenuated Salmonella enterica serovar Paratyphi A vaccine strain harboring defined mutations in htrA and yncD', *Microbiol Immunol*, 59: 443-51.

Chapter 12

Publications and Patents

Publications-

Research Articles-

1. **Suparna Chakraborty**, Pujarini Dutta, Ananda Pal, Swarnali Chakraborty, George Banik, Prolay Halder, Animesh Gope, Shin-Ichi Miyoshi, Santasabuj Das. Intranasal Immunization of Mice with a Chimeric Antigen of Cholera Toxin B and Salmonella Typhi outer membrane protein T2544 elicits protective antibodies and T cell response at the intestinal mucosa**. (2024). NPJ Vaccines (IF 9.2)** DOI: 10.21203/rs.3.rs-3061923/v1
2. Risha Haldar, Amlanjyoti Dhar , Debayan Ganguli, **Suparna Chakraborty**, Ananda Pal, George Banik, Shin-ichi Miyoshi, Santasabuj Das.. A candidate glycoconjugate vaccine induces protective antibodies in the serum and intestinal secretions, antibody recall response and memory T cells and protects against both typhoidal and nontyphoidal Salmonella serovars. **(2024). Frontiers in Immunology** (**IF 5.7**). doi: 10.3389/fimmu.2023.1304170
3. Debayan Ganguli, Swarnali Chakraborty, **Suparna Chakraborty**, Ananda Pal, Anim esh Gope, Santasabuj Das. Macrophage Cell Lines and Murine Infection by Salmonella enterica Serovar Typhi L-Form Bacteria. **(2022). Infection And Immunity (IF 3.3).** : https://doi.org/10.1128/iai.00119-22.

Review Article-

1. Asim Biswas, Rahul Shubhra Mandal, **Suparna Chakraborty**, George Maiti. Tapping the immunological imprints to design chimeric SARS-CoV-2 vaccine for elderly population. **(2021). International Reviews of Immunology** (**IF 4.4**). doi.org/10.1080/08830185.2021.1925267.

Book Chapter-

1. **Suparna Chakraborty**, Santasabuj Das. Murine Models to Study Acute and Chronic Bacterial Infections. In: Siddhardha B., Dyavaiah M., Syed A. (eds) Model Organisms for Microbial Pathogenesis, Biofilm Formation and Antimicrobial Drug Discovery. **(2020). Springer,** Singapore. DOI: 10.1007/978-981-15-1695-5_24.

Under Revision-

1. **Review paper:** Manuscript entitled 'Typhoid and paratyphoid vaccine development in the lab and beyond the laboratory: a case study in trial and tribulations' **(communicated).**
2. **Research Paper:** Manuscript entitled 'Improving Typhoid Vaccination: rT2544 and rFliC Adjuvant Synergy in Multivalent Vaccine Development'. **(Communicated).**
3. Manuscript entitled 'Development of a mouse model of *S.* Paratyphi A infection and study of protective efficacy of a novel candidate vaccine' (under preparation).

Patents:

1. Patent entitled with 'A Recombinant Fusion Protein Containing Salmonella Typhi Outer Membrane Protein, Vaccine And Uses Thereof' (Patent application number is 202211039222, submitted on July 7, 2022).
   Santasabuj Das. **Suparna Chakraborty**,

2. Patent entitled with 'A Glycoconjugate Vaccine Composition Against Salmonella sp.' (Patent application no. is 202311070211. submitted on 16th Oct, 2023).
   Santasabuj Das, Risha Haldar, Amlanjyoti Dhar, **Suparna Chakraborty**.

CHAPTER 13

List of Oral/Poster presentation at international conferences

Conferences

1. Presentation mode- **Oral.**

   Title: **Assessing the protective efficacy of an Intranasal vaccine candidate, rCTB-T2544, against Typhoid and Paratyphoid infection using Iron overloaded murine model**

   Conference- **13th International Conference on Typhoid and other Invasive Salmonelloses** from 5th -7th Dec, 2023 at **Kigali, Rwanda.**

   Authors- **Suparna Chakraborty**, Pujarini Dutta, Ananda Pal, Swarnali Chakraborty, Shin-Ichi Miyoshi, Santasabuj Das.

   Trvael award- **Sabin Vaccine Institute.**

2. Presentation mode- **Oral.**

   Title: **Evaluating the efficacy of an intranasal Vaccine Candidate, rCTB-T2544, against Paratyphoid Infection using iron overloaded murine model.**

   Conference**- Golden Jubilee Conference of Indian Immunology Society** from 5th – 8 th Oct, 2023 at **AIIMS, New Delhi.**

   Authors- **Suparna Chakraborty**, Pujarini Dutta, Ananda Pal, Swarnali Chakraborty, Santasabuj Das.

   Travel award- **Immunocon 50.**

3. Presentation mode- **Poster.**

   Title: **Development of iron-overloaded mouse model to study the pathogenicity and infectivity of Salmonella Paratyphi A infection.**

   Conference-2023 Salmonella Biology and Pathogenesis **Gordon Research Conference** organized at Renaissance Tuscany Il Ciocco in **Lucca (Barga), Lucca, Italy** during 23/07/2023 – 28/07/2023.

   Authors- **Suparna Chakraborty**, Pujarini Dutta, Ananda Pal, Risha Haldar, Santasabuj Das.

   Travel award- **International Travel scheme by SERB and Immunology foundation.**

4. Presentation mode- **Oral.** (Online)

   Title: **Protection against Salmonella and Vibrio infection by intranasal immunization with a fusion construct containing recombinant cholera toxin B subunit fused with Salmonella outer membrane protein T2544**.

Conference- 4th World Congress on Infectious Diseases & Antibiotics – 2023 on 22.01.2023

Authors- **Suparna Chakraborty**, Pujarini Dutta, Ananda Pal, Santasabuj Das.

5. Presentation mode- **Poster.**

Title- **Mucosal immunization with recombinant cholera toxin B fused to outer membrane protein T2544 protects against Salmonella infection**.

Conference- **16th Asian Conference on Diarrhoeal Disease and Nutrition (ASCODD)** in Kolkata, from 11th to 13th Nov,2022.

Authors- **Suparna Chakraborty**, Pujarini Dutta, Ananda Pal, George Banik, Swarnali Chakraborty, Shin-Ichi Miyoshi, Santasabuj Das.

Seminar

1. Presentation mode- **Poster.**

Title: **Investigating the pathogenicity and infectivity of *Salmonella* Paratyphi A infection using an iron overloaded mice model.**

Seminar - *Salmonella* Biology and Pathogenesis **Gordon Research Seminar** from 22/07/2023 – 23/07/2023 at Renaissance Tuscany Il Ciocco in **Lucca (Barga), Lucca, Italy.**

Authors- **Suparna Chakraborty**, Pujarini Dutta, Ananda Pal, Risha Haldar, Santasabuj Das.

Travel award- **International Travel scheme by SERB and Immunology foundation.**

npj | vaccines

www.nature.com/npjvaccines

ARTICLE OPEN

Intranasal immunization of mice with chimera of *Salmonella* Typhi protein elicits protective intestinal immunity

Suparna Chakraborty[1], Pujarini Dutta[1,2], Ananda Pal[1], Swarnali Chakraborty[1], George Banik[3], Prolay Halder[4], Animesh Gope[1], Shin-ichi Miyoshi[5,6] and Santasabuj Das[1,7]✉

Development of safe, highly effective and affordable enteric fever vaccines is a global health priority. Live, oral typhoid vaccines induce strong mucosal immunity and long-term protection, but safety remains a concern. In contrast, efficacy wears off rapidly for injectable, polysaccharide-based vaccines, which elicit poor mucosal response. We previously reported *Salmonella* Typhi outer membrane protein, T2544 as a potential candidate for bivalent (*S.* Typhi and *S.* Paratyphi A) vaccine development. Here, we show that intranasal immunization with a subunit vaccine (chimera of T2544 and cholera toxin B subunit) induced strong systemic and intestinal mucosal immunity and protection from *S.* Typhi challenge in a mouse model. CTB-T2544 augmented gut-homing receptor expression on lymphocytes that produced Th1 and Th17 cytokines, secretory IgA in stool that inhibited bacterial motility and epithelial attachment, antibody recall response and affinity maturation with increased number of follicular helper T cells and CD4+ central and effector memory cells.

npj Vaccines (2024)9:24; https://doi.org/10.1038/s41541-024-00812-4

INTRODUCTION

Salmonella enterica serovar Typhi (*S.* Typhi), a Gram-negative, intracellular pathogen and the etiological agent of typhoid fever, is a global threat to public health. The organism spreads through the faeco-oral route, causing significant morbidities and mortalities in the developing countries, especially of the south-east Asian region. As per Global Burden of Disease data, 9.24 million new typhoid fever cases occurred worldwide in 2019 (females 4.17 million and males 5.07 million), leading to 110,000 deaths and 8.05 million (3.86–13.9) disability adjusted life years (DALYs). Incidences in males and females were 7.3 (4.5–11.1) and 8.6 (5.4–12.9), respectively per 100,000 populations[1]. After crossing the intestinal barrier, *Salmonella* Typhi, being carried by the infected macrophages, spreads to the distant body sites like the liver, spleen, bone marrow and lymph nodes. As an obligate intracellular pathogen, the bacterium creates a niche for replication within the phagosomes of the infected macrophages, rendering it difficult for the host to eliminate it from the body[2]. The problem of *S.* Typhi infection is further complicated by the emergence and spread of multi-drug resistant and extensively drug-resistant (XDR) strains across continents[3]. While the mortality in untreated typhoid fever reaches nearly 20%, an incompletely cured acute infection may be followed by an asymptomatic chronic carrier state, which poses an increased risk for the development of adenocarcinoma of the gall bladder[4].

Improvement of sanitation, potable water supply and food hygiene is considered essential for elimination of *S.* Typhi. However, vaccination may play a significant role in decreasing the incidence in the endemic countries in the short run. Two vaccines, namely a live, attenuated *S.* Typhi Ty21a strain for oral administration and an injectable preparation, containing purified Vi polysaccharide (Vi-PS) are widely available commercially. Despite high seroconversion rates with good short term protection, they are at best modestly efficacious in the long run[5]. Oral typhoid vaccine induces systemic and intestinal secretory antibodies as well as good T cell response, but requires at least three to four doses for optimum protection. Further, it is not recommended for children below 6 years of age due to difficulty in swallowing large capsules of the vaccine formulation. Live typhoid vaccine has also raised safety concerns because of occasional reports of bacteremia[6]. To escalate immunogenicity with a single dose of vaccine administration, several research groups have developed alternative attenuated strains in the *S.* Typhi Ty2 background. Several mutant vaccine strains, such as Ty800 with the deletion of the global regulator phoP/phoQ, M01ZH09/ZH09 lacking aroC and ssaV genes and double mutant (aroC and aroD) strain CVD908 have passed Phase II trials and showed good mucosal and serum antibody response in the volunteers. However, CVD 908 resulted in vaccinemia with a single oral dose of 10^7 viable organisms, and was later on modified by the deletion of another stress protein, htrA that prevented vaccinemia, but retained both humoral and cellular immune responses. To ensure more consistent serum anti-Vi antibodies, Vi was constitutively expressed in CVD 908 strain, generating CVD909. A prime boost regimen with orally administered CVD 909, followed by an injection of Vi-polysaccharide vaccine failed to induce strong Vi-specific antibody response, but instead, significantly raised Vi-specific IgA^+ B memory cells. However, the need for pre-administration of buffer to neutralize stomach acid renders a potential delivery challenge for live attenuated vaccines[5]. None of the vaccine strains was shown to be effective against Paratyphoid infection.

[1]Division of Clinical Medicine, ICMR- National Institute of Cholera and Enteric Diseases, P-33, C.I.T. Road, Scheme XM, Beliaghata, Kolkata 700 010, India. [2]Department of Pediatrics, Steele Children's Research Center, University of Arizona, Tuscon, AZ, USA. [3]BD Biosciences, INDIA, Smart works Business Center, Victoria Park, 37/2 GN Block, Sector 5, Saltlake City, Kolkata 700091, India. [4]Division of Bacteriology, ICMR- National Institute of Cholera and Enteric Diseases, P-33, C.I.T. Road, Scheme XM, Beliaghata, Kolkata 700 010, India. [5]Graduate School of Medicine, Dentistry and Pharmaceutical Sciences, Okayama University, Okayama, Japan. [6]Collaborative Research Center of Okayama University for Infectious Diseases at Indian Council of Medical Research—National Institute of Cholera and Enteric Diseases, Kolkata 700010, India. [7]ICMR-National Institute of Occupational Health, Meghaninagar, Ahmedabad 3800016 Gujarat, India. ✉email: santasabujdas@yahoo.com

Published in partnership with the Sealy Institute for Vaccine Sciences

Vi-polysaccharide vaccine, on the other hand, primarily works through the serum antibodies, but is poorly immunogenic with modest long-term efficacy, especially in children, because of T-cell-independent antibody response. Given the success of subunit vaccines for other bacterial infections, hunt for a highly efficacious typhoid vaccine, especially for smaller children (<2 years) that is safe and at the same time, capable of inducing durable protection is focused on developing typhoid conjugate (Vi-conjugate) vaccines (TCVs). A glycoconjugate vaccine (Vi-PS conjugated to tetanus toxoid, called Vi-TT), recently licensed in India has been reported to mount considerably high levels of durable protection through induction of memory B and T-cells[7,8]. The landmark TyVAC trial in Nepal, Malawi, and Bangladesh had shown protective efficacy of Typbar TCV to the extent of 79%, 84%, 85%, respectively[9–11]. However, protection conferred by Vi-TT and other TCVs, such as Vi-rEPA (polysaccharide conjugated to *Pseudomonas aeruginosa* exotoxin A), Vi-CRM197 and Vi-DT (diphtheria toxoid) would be exclusively mediated by the circulating anti-Vi antibodies due to the absence of intrinsic *Salmonella* proteins in these preparations[12]. Consequently, the emerging Vi-negative MDR (multidrug resistant) and XDR (extensive drug resistant) strains that were developed due to spontaneous genomic mutations in the regulatory regions of Vi polysaccharide of *S.* Typhi have evoked concerns[12]. There is a distinct threat that mass vaccination drive targeting Vi polysaccharide may exert a selection pressure for the existing Vi-negative *S.* Typhi and *S.* Paratyphi A and B strains, eventually rendering the vaccines to lose their protective efficacy. This has sparked an interest to generate future vaccines with universally present somatic antigens like T2544, which are immunogenic as well as essential for virulence of the bacteria. Antigen-specific, cytotoxic T cells, which were previously found to significantly augment anti-*S.* Typhi immunity through the elimination of intracellular bacteria were induced by recombinant T2544, as shown by our previous study, but not by the existing Vi conjugate vaccines[13]. Further, antibody secreting cells (ASCs), generated by Vi-PS and the TCVs will be primarily targeted to the systemic circulation, and not to the intestine[14], whereas secretory antibodies, especially secretory IgA (sIgA) is believed to play a critical role in reducing systemic invasion of the luminal *S.* Typhi, thereby augmenting protection[15].

Cholera toxin B subunit (CTB) has been extensively used as a vaccine adjuvant, especially for the protein antigens, owing to its nontoxic nature, ease of production of recombinant CTB and its fusion proteins in large quantities in *E. coli* and rapid renaturation of the recombinant proteins to the pentameric form of the native counterpart, enabling CTB to bind to its cognate GM1 ganglioside receptor[16,17]. This receptor is widely expressed by multiple, non-immune and immune cells (epithelial cells, macrophages, DCs and B cells), and CTB-binding to the receptor targets the antigens, co-administered or delivered as chimera to the desired cell populations, leading to augmented antigen uptake and presentation[16,17]. Other proposed mechanisms for the co-stimulatory effects of rCTB include direct lymphocyte activation[18] and activation of the Toll-like receptors, although the identity of the TLRs remains unclear[19]. Adjuvanticity was most prominent when CTB was used as a genetically-fused partner of the vaccine antigen or chemically coupled to it, and delivered through the mucosal route. Indeed, CTB is one of the most potent mucosal adjuvants available to-date that attracted great attention[20,21]. Most antigens are poorly immunogenic when administered through the mucosal route, and tend to induce tolerance, especially at the intestinal mucosa. CTB often breaks the oral antigenic tolerance, but due to unknown reasons, significant oral adjuvanticity of CTB was only observed for live vaccines, such as oral cholera vaccine (Dukoral) that is already licensed for use[22]. In contrast, CTB administered through non-oral mucosal routes significantly enhanced antigen-specific humoral and cell-mediated immunity, not only at the local site, but also at distal mucosa, a phenomenon called "common mucosal immunity"[23]. Chemical and genetic conjugations of CTB with heterologous antigens from the simian immunodeficiency virus and *Schistosoma mansoni* have been proved to be potential vaccine candidates[24,25]. Adherent-invasive *Escherichia coli* (AIEC) tends to colonize the gut of patients with Crohn's disease and exacerbate inflammation. Intranasal immunization with AIEC siderophore enterobactin, conjugated to CTB induced robust mucosal antibody response against the siderophore in the small intestine and colon, thus reducing gut colonization of AIEC and colitis severity[26]. However, an earlier study showed that intestinal mucosal antibodies elicited against siderophores after intranasal CTB-siderophore conjugate administration could significantly reduce *Salmonella* colonization of the inflamed gut, but failed to reduce inflammation[20].

We had previously reported that an outer membrane protein of *S.* Typhi Ty2 strain (T2544) is strongly immunogenic in mouse and naturally-infected humans[27]. A candidate vaccine formulation based on T2544 induced high levels of serum antibodies as well as robust effector and memory T cell responses, when administered into mice through the subcutaneous route, and protected them against *S.* Typhi challenge[13,27]. T2544 was present in multiple clinical isolates of *S.* Typhi and *S.* Paratyphi, while T2544-specific antibodies were detected in the acute and convalescent sera of patients infected with *S.* Typhi[27].

Here, we report that intranasal immunization with purified CTB-T2544 was also protective against oral *S.* Typhi infection. The chimeric antigen augmented (i) secretory IgA in stool which inhibited bacterial motility and epithelial attachment (ii) affinity maturation of antibodies with strong recall response, (iii) gut-homing receptor expression on lymphocytes that produced Th1 and Th17 cytokines, and (iv) the number of follicular helper T cells and CD4+ effector memory cells. These results suggested that CTB-T2544 is a promising candidate for the development of an intranasal vaccine against human *S.* Typhi infection.

RESULTS

Cloning, expression and purification of recombinant CTB-T2544 chimeric protein

To generate a gene chimera of *ctx-b* and *t2544*, 309 bp open reading frame (ORF) of *V.cholerae ctx-b* (cholera toxin B subunit) gene was amplified by PCR (Fig. S1a). In addition, ORF of *Salmonella* Typhi *t2544* gene, along with the coding sequence of glycine-proline-glycine-proline (GPGP) linker at its NH2-terminus (total size 663 bp) was PCR-amplified (Fig. S1b). The amplicon of the *ctx-b* gene was cloned into the prokaryotic expression plasmid pET28a, using BamHI and SalI restriction sites, followed by cloning of the 663 bp amplicon of linker-*t2544* at SalI and XhoI restriction sites immediately downstream of *ctx-b* (Fig. 1a). Confirmation of the fusion gene clone of *ctx-b* and *t2544* was done by colony PCR (Fig. S1c), restriction digestion (Fig. 1b) and finally nucleotide sequencing (Fig. S1d). To generate the recombinant chimeric protein, pET28a plasmid construct carrying the *ctx-b-t2544* fusion gene was transformed into the expression host *E. coli* BL21 (DE3) and the expression of the recombinant chimeric protein (rCTB-T2544) was induced by IPTG. rCTB-T2544 was purified by affinity chromatography using Ni-NTA agarose and the purity and specificity of the chimeric protein was confirmed by SDS-PAGE and western blots, respectively (Fig. 1c, d). Secondary structure of rCTB-T2544 derived from the analysis of the Far-UV circular dichroism (CD) spectra, using K2D2 (http://cbdm-01.zdv.uni-mainz.de/~andrade/k2d2/) indicated α-helical structure (72.38%) (Fig. S1e). Secondary structure of the other two proteins (rT2544 and rCTB) indicated 64.22% and 79.93% of α-helical structures, respectively. The yields of the purified rCTB-T2544, rCTB and rT2544 were 18.75 mg, 30 mg and 24 mg per liter of bacterial

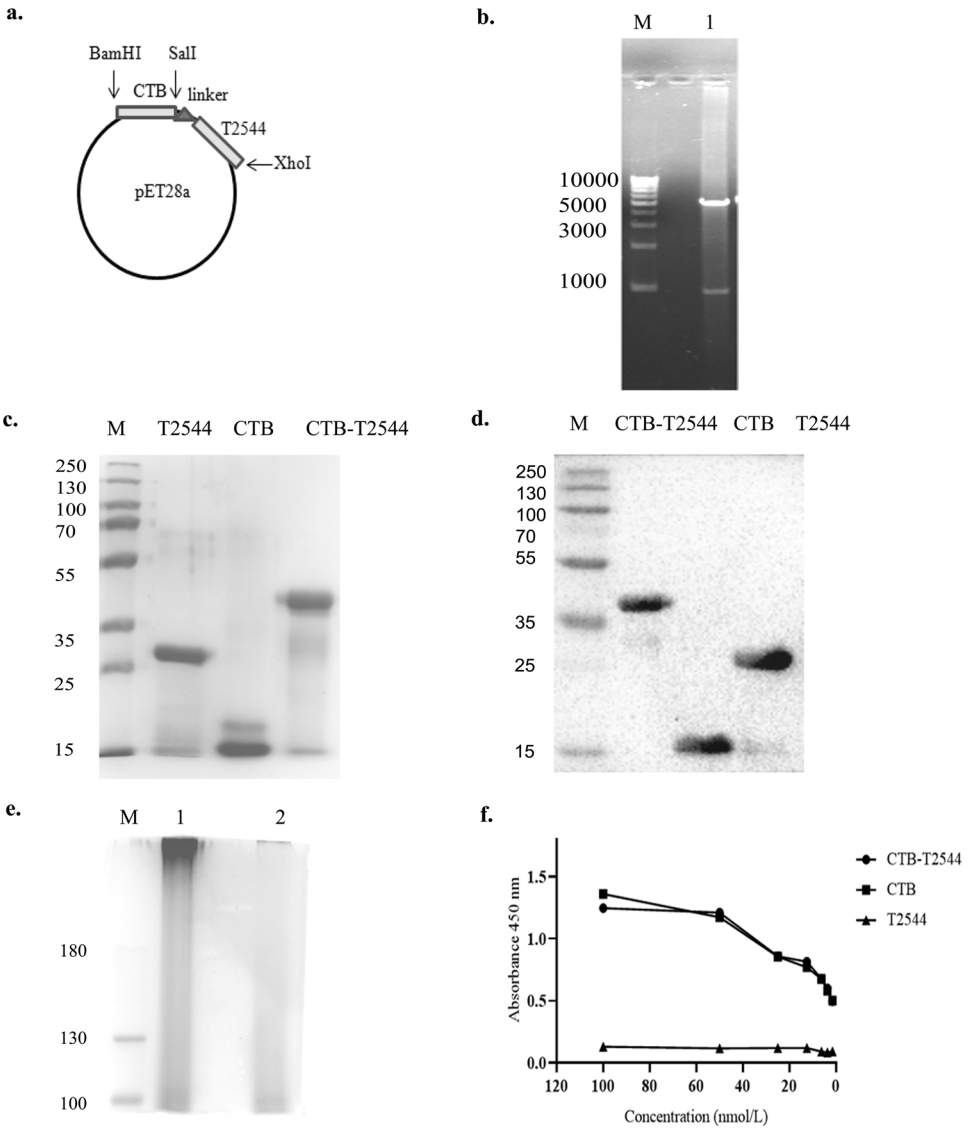

Fig. 1 Purified antigen preparation and characterization. a Schematic diagram of cloned *ctx-b* and *t2544* genes in pET28a vector. **b** 1% Agarose gel electrophoresis of pET28a-ctb-t2544 after restriction digestion with BamHI and XhoI in Lane 1; Lane-M shows 1 Kb plus DNA ladder. **c** Recombinant purified proteins run in 10% SDS–PAGE, followed by Coomassie blue staining; Lane-M, pre-stained protein marker. **d** Western blot analysis of purified recombinant proteins; the blot was developed using anti-HIS monoclonal antibody; Lane-M, pre-stained protein marker. **e** Denatured (boiled) and non-denatured (un-boiled) rCTB-T2544 protein, resolved in 10% SDS PAGE, followed by Coomassie blue staining of the gel. Lane M, Pre-stained protein marker, Lane 1, unboiled rCTB-T2544; Lane 2, rCTB-T2544 after boiling. All the blots or gels were derived from the same experiment and were processed in parallel. **f** GM1-ELISA after coating the plates with GM1 ganglioside (1 μg/well), followed by the addition of purified proteins as indicated. Plates were developed using anti-HIS antiserum (1:2500).

cultures, respectively. The endotoxin contaminations were found to be 0.015, 0.011, 0.008 EU/ml for rCTB, rT2544, and rCTB-T2544, respectively. Recombinant CTB-T2544, denatured by boiling, migrated in SDS-PAGE with the molecular weight marker that corresponded to the size of a chimera of T2544 and monomeric CTB (Fig. 1c**;** all the uncropped and unprocessed gel images are provided in Fig. S9**)**. However, the role of CTB as an adjuvant requires a pentamer that is capable to bind to its cognate cell surface receptor, GM1 ganglioside. The size of the non-denatured rCTB-T2544, resolved in SDS-PAGE corresponded to a higher molecular weight protein containing pentameric CTB (Fig. 1e). To check if the native chimera indeed contained a CTB pentamer, we studied by ELISA the binding of rCTB-T2544 to the GM1 ganglioside receptor. The results showed that both the recombinant CTB and CTB-T2544 were able to bind to the receptor in a dose-dependent manner, suggesting the existence of CTB pentamer (Fig. 1f).

Immunization with rCTB-T2544 through the intranasal route protects against oral *S.* Typhi and *Vibrio cholerae* infections

The existence of the so-called "Common mucosal immune system"[23] allows immunization through any mucosal route to induce immune response at the distant mucosal sites, albeit to a variable degree, due to migration of the activated immune cells. Intranasal immunization was earlier reported to elicit secretory IgA (sIgA) at the genital mucosa and salivary secretions[24–26]. To investigate if intranasal immunization with rCTB-T2544 induced protective immunity in the intestine, BALB/c mice were immunized with three doses of rCTB-T2544, rT2544, rCTB or the vehicle (PBS) at 12-day intervals (Fig. 2a). Twelve days after the 3rd dose,

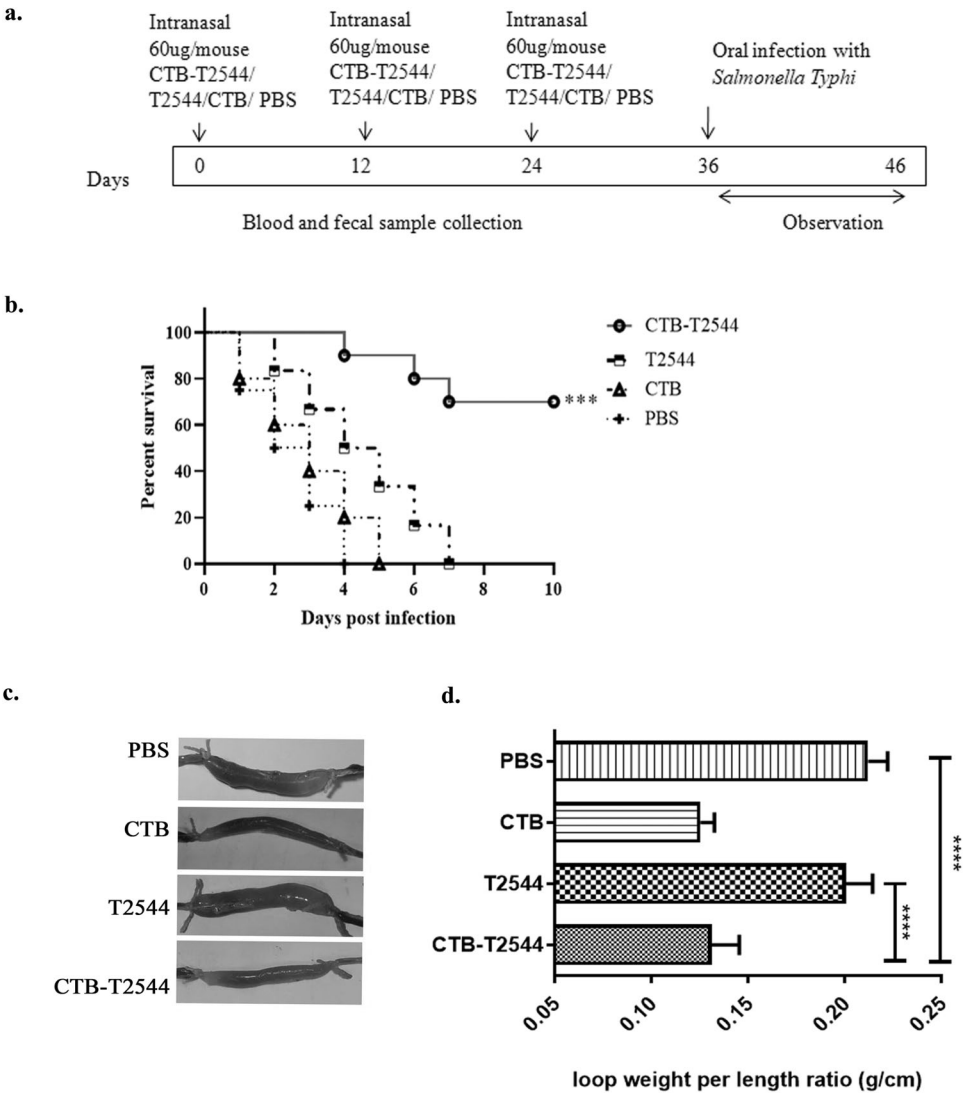

Fig. 2 Protective efficacy of the recombinant antigens after intranasal immunization of mouse. a Immunization schedule, sample collection, and bacterial challenge of BALB/c mice. Blood and stool samples were collected before each immunization dose and 12 days after the last immunization. **b** Mouse survival assay. Kaplan-Meyer plot of cumulative mortality of mice immunized intranasally with the vehicle or the recombinant protein antigens. Mice ($n = 10$/group) were challenged with *S.* Typhi 12 days after the last immunization dose and were monitored for 10 days. Significance was calculated by comparing the survival of the mice immunized by rCTB-T2544 with T2544 by Log-Rank Mantel Cox test. ***$p = 0.0001$ **c** In parallel experiments, mice immunized as above were subjected to ileal loop assay by injecting 100 ng of cholera toxin into each loop. The animals ($n = 8$/group) were checked for fluid accumulation in the ileal loops after 8 hours. **d** Fluid accumulation was measured by calculating the weight divided by the length of individual loops. Significance was calculated by comparing the loop weight/ length ratio of CTB-T2544 group with the T2544 and PBS immunized group, using one-way ANOVA with *post hoc* analysis using Tukey's multiple comparison test. Data represented as mean with SD; ****p value < 0.0001 vs. T2544 and PBS. Error bars represent SD.

mice were challenged with $5 \times 10\text{^}7$ CFU ($10 \times LD_{50}$) of *S.* Typhi Ty2 strain through oral gavage (as mentioned under *Methods* section). An iron-overload mouse model of oral *S.* Typhi infection, established previously in our laboratory was used for the challenge experiment[27]. The results showed death of all the mice in the vehicle (PBS)-, rCTB- and rT2544- immunized groups within a period of 8 days, while 70% of mice that received CTB-T2544 were alive after 30 days of infection (Fig. 2b). Further, when the immunized animals were subjected to an ileal loop experiment with the administration of cholera toxin[28], fluid accumulation in the loops was significantly less, resulting in lower loop weight/ length ratio for rCTB- and rCTB-T2544-immunized animals compared with the ones that received T2544 or the vehicle (Fig. 2c, d). Together, the above results underscored the efficacy of rCTB-T2544 as a candidate bivalent vaccine for *S.* Typhi and *V. cholerae* infections.

Intranasal immunization with rCTB-T2544 induces protective serum and mucosal antibody response

To check if CTB could augment humoral immune response to the co-administered antigen T2544, antibody end-point titers (The reciprocal of the titer, at which the absorbance of the sample was the same as those from PBS-immunized mice) were determined by ELISA 12 days after completion of primary immunization dose. Markedly raised titers of T2544-specific serum IgG, IgG1, IgG2a, and IgA antibodies were observed in the mice immunized with rCTB-T2544, as compared with the rT2544-immunized mice (Fig. 3a). Similarly, CTB-specific IgG and IgA antibody titers were also raised in

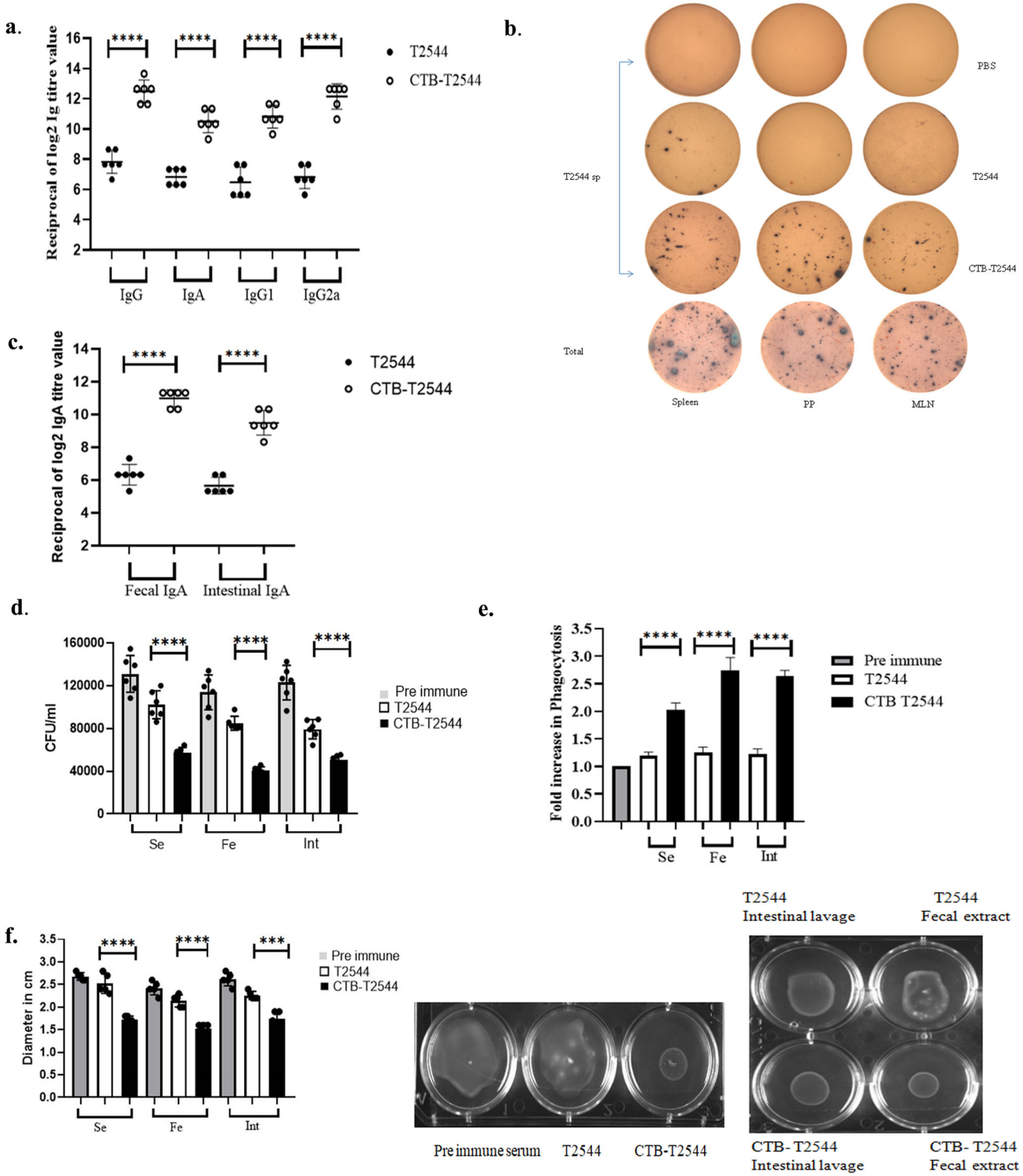

the serum (Fig. S3a). These results were in agreement with the recovery of substantial numbers of T2544-specific IgG and IgA antibody-secreting cells (ASCs) in the spleen, MLN, and Peyer's Patches (PP) after intranasal rCTB-T2544, as analyzed by the enzyme-linked immunosorbent spot (ELISpot) assays, while ASCs were much fewer in the other groups of mice (Figs. 3b, S3b).

Intestinal sIgA antibody could significantly contribute to the protection against *S.* Typhi, an enteric pathogen. We measured antigen-specific sIgA titers in the stool and intestinal contents and found strong T2544-specific sIgA response only in the mice immunized with rCTB-T2544 (Fig. 3c), which also mounted CTB-specific sIgA (Fig. S3c). Protective efficacies of the serum and secretory antibodies were revealed by the inhibition of *S.* Typhi adherence to the intestinal epithelial cell monolayers, impairment of bacterial motility in the soft agar and the promotion of opsanophagocytosis. Sera, fecal extracts and intestinal contents

Fig. 3 Intranasal immunization with rCTB-T2544 ($n = 6$) as above induces antigen-specific humoral and mucosal antibodies. a ELISA plates were coated with rT2544 protein and serum T2544-specific antibody titers were determined. Samples were serially half-diluted, from 1:200 to 1:25600 for IgG and 1:20 to 1:2560 for IgA. Optical density at 450 nm was recorded. The reciprocal of the titer, at which the absorbance of the sample was the same as the unimmunized mice samples was plotted in log2 scale. **b** Two weeks after the primary immunization, mice were sacrificed and cells were isolated from the spleen, MLN and Peyer's Patches (PP). ELISPOT assay was performed with anti-mouse IgG, IgA and total immunoglobulin. **c** T2544-specific IgA antibodies in the fecal extracts and intestinal contents were quantified two weeks after the primary immunization. **d** Adhesion Inhibition Assay. Bacteria were preincubated with 1:50 dilution of the serum, fecal extracts or intestinal wash samples of the unimmunized and immunized mice for 30 min and used for adhesion assay as described under Methods. Mean CFU recovered from the lysed cells were plotted. **e** Opsonophagoctosis assay. Bacteria were pre-incubated with 1:50 dilution of the serum, fecal contents or intestinal lavage, followed by infection of the THP-1 cell monolayer. Opsonophagocytosis assay was performed as described under Methods. Phagocytosed bacteria were calculated after cell lysis and mean fold increase for the immunized samples compared with the pre-immune counterparts was plotted. **f** Motility inhibition assay. Motility of *Salmonella* Typhi Ty2 in LB agar (0.4%), containing 5% serum, fecal extract or intestinal contents from the immunized mice was measured by the zone diameter of bacterial growth after 6 h. The above experiments were repeated three times and mean of the values from all three experiments were plotted. Error bars represent SD. A representative picture from the motility assays is shown. Significance was calculated using two tailed unpaired *t* test, comparing CTB-T2544 group with the corresponding T2544 group. **** $p < 0.0001$, ***$p = 0.0002$.

from the experimental mice were pre-incubated with *S.* Typhi, which was subsequently used to infect HT-29 and THP-1 cell monolayers. Adhesion of the bacteria to HT-29 cell monolayer was studied by CFU counts and confocal microscopy. Bacterial adhesion to the cells was inhibited by the antibodies present in different samples, out of which maximum inhibition was found for the samples collected from rCTB-T2544 immunized mice (Figs. 3d, S3d). We also observed that a 1:5000 dilution of the rCTB-T2544 antibodies had comparable adhesion to 1:50 dilution of the pre-immunization samples, indicating that the former had 100-fold higher functional competence for adhesion inhibition (Fig. S6). Similarly, in the opsanophagocytosis assay, mean peak fold increase of bacterial phagocytosis by THP-1 cells was significantly higher following opsonization of the bacteria with antibodies from rCTB-T2544-immunized mice compared with the other groups of animals (Figs. 3e, S3e). Finally, we evaluated soft agar motility inhibition of *S.* Typhi after incubation with the above antibodies and found much greater inhibition when antibodies from the mice immunized with the chimeric protein were used (Fig. 3f). Together, the above results suggested that intranasal immunization with a CTB chimera of *S.* Typhi antigen (T2544) induced greater number of ASCs specific to the antigen in the secondary lymphoid tissues and higher levels of antigen-specific circulating and mucosal antibodies with greater protective efficacies against *S.* Typhi infection, when compared with the antigen administered without CTB. To further dissect relative contribution of the serum and mucosal antibodies, we performed adoptive transfer of pooled immune sera from rCTB-T2544-immunized mice to naïve mice, followed by a lethal bacterial challenge. This resulted in a 25% survival rate, suggesting a relatively minor role played by the serum antibodies in overall protection (Fig. S5a). To study the contribution from mucosal antibodies in the protection, we pre-incubated *S.* Typhi with intestinal lavage and fecal extracts from the immunized mice for 30 minutes before infecting the naïve mice. A lethal dose killed only 50% mice, while with a sublethal dose of the pre-incubated bacteria showed significant reduction in the colonization of the intestine (ileum, cecum, colon Fig. S5 b–d) and spread to the internal visceral organs (MLN, spleen and liver Fig. S5e–g) compared with the similar dose of bacteria that were not pre-incubated with mucosal antibodies. These findings highlighted a more significant role of mucosal antibodies in imparting protection.

Intranasal immunization with rCTB-T2544 increased the recruitment of DCs and lymphocytes expressing gut-homing receptors to the MLN

Lung DCs were previously reported to imprint gut homing receptors on naïve (IgM^+) B cells and $CD4^+$ T cells in the local (mediastinal) lymph nodes after intranasal antigen administration, in addition to class switch recombination of B cells, generating IgG^+ and IgA^+ cells[29]. However, other studies had suggested that tissue homing of naïve lymphocytes is coupled with their site of activation by the DCs, and only the lymphocytes primed in the MLNs express α4β7 receptor that is required for migration to the intestine, although splenic lymphocytes show promiscuity with regard to tissue homing[30]. To address this issue in our study, we checked for DC recruitment to the MLNs of the immunized mice. The percentage of $CD11c^+$ DCs in the MLNs after rCTB-T2544 immunization was nearly four times higher than after immunization with rT2544 (26.7% vs 7.0%) (Fig. 4a), indicating that intranasal CTB promotes DC migration to the draining nodes of the intestine. Next, to address DC migration, migratory DC (mDC) markers ($MHC^{hi}CD11C^{int}CD103^+$) expression in the MLN DCs was assessed and found to be 3-fold higher (Fig. S7) in the MLN of the rCTB-T2544 immunized mice compared with the vehicle-immunized mice. Increased number of MLN DCs could result in greater number of lymphocytes expressing gut homing receptors. Indeed, we found significantly higher number of B and T cells, not only in the MLNs, but also from the spleen expressing α4β7 and CCR9 receptors (Figs. 4b, c, S4). DCs play a critical role in mucosal sIgA production by expressing several factors like BAFF, APRIL, iNOS, RALDH1, TGF-β and IL-6[31]. Given increased DC migration to the MLNs and strong sIgA response in the intestine after intranasal immunization with CTB-T2544, we studied for the IgA-inducing factor expression by the MLN DCs. The results showed augmented expression of the factors as above by the MLN DCs (Fig. 4d). Together the above results suggested that intranasal CTB upregulates the expression of IgA-inducing factors on the local DCs and promotes their migration to the MLNs. These MLN DCs imprint gut homing receptors on the lymphocytes, which then migrate to the intestinal mucosa to execute the effector function by sIgA and cytokines production.

CTB-T2544 immunization induces a balanced T helper cell response

Th1 response is required for the clearance of intracellular pathogens like *Salmonella*[32], while Th2 and Th17 cells promote serum antibodies and sIgA production, respectively. We found significantly elevated, circulating Th1 (IL12 and IFNγ) and Th2 (IL-4, IL-5, IL-10) cytokines in rCTB-T2544-immunized mice as opposed to only modest elevation in the comparator immunized groups (Fig. 5a). In addition, the number of IFNγ- and IL-17A-secreting $CD4^+$ T cells (Th1 and Th17 cells, respectively) in the Peyer's Patches was also increased markedly after CTB-T2544 immunization (Fig. 5b). We also checked if CTB induced follicular helper T (T_{FH}) cells, which play a crucial role in the germinal center formation and the development of high-affinity antibodies and memory B cells[33]. T_{FH} cell number in MLN after immunization with rCTB-T2544 was doubled compared with rT2544 or no immunization (6.03% vs 3.06% vs 2.74%, respectively) (Fig. 5c). Together,

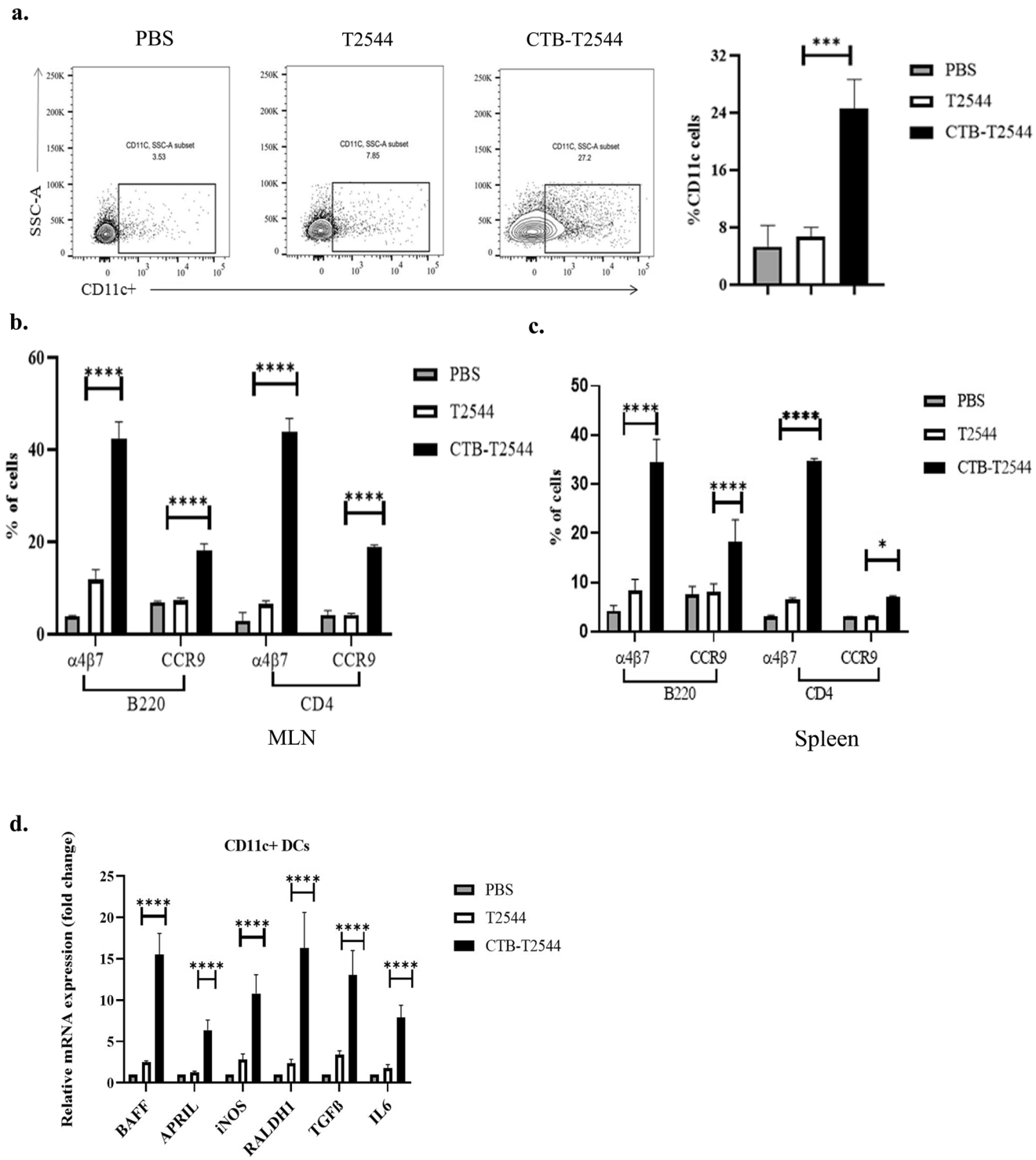

Fig. 4 Intranasal immunization with CTB-T2544 directs DC and lymphocyte migration. a Twelve days after the primary immunization, MLN cells were surface-stained with CD11c and analyzed by flow cytometry. **b, c** Gut homing receptor expression on B and T lymphocytes. Twelve days after the primary immunization, lymphocytes isolated from the MLN (**b**) and spleen (**c**) of the experimental mice were stained with fluorochrome-tagged antibodies against cell lineage markers (CD4 and B220) and gut homing receptors (α4β7 and CCR9) and analyzed by flow cytometry. Data presented as percentages of cells out of the total T and B cells, expressing the homing receptors. **d** RT-qPCR analysis of gene expressions in DCs, isolated from the MLN of experimental mice were plotted. GAPDH-normalized expression of all the genes was represented as fold changes of the PBS-immunized group. All experiments were repeated three times, and data from a representative one are presented in (**a**) and mean (± SD) of the data from all three experiments are shown under (**b**–**d**). Significance was calculated using one way ANOVA (**a**) and two-way ANOVA (**b**,**c**) with *post hoc analysis using* Tukey's multiple comparison test. Error bar represents SD. *$p = 0.0281$, ***$p = 0.0008$ and ****$p < 0.0001$ (T2544 vs. CTB-T2544).

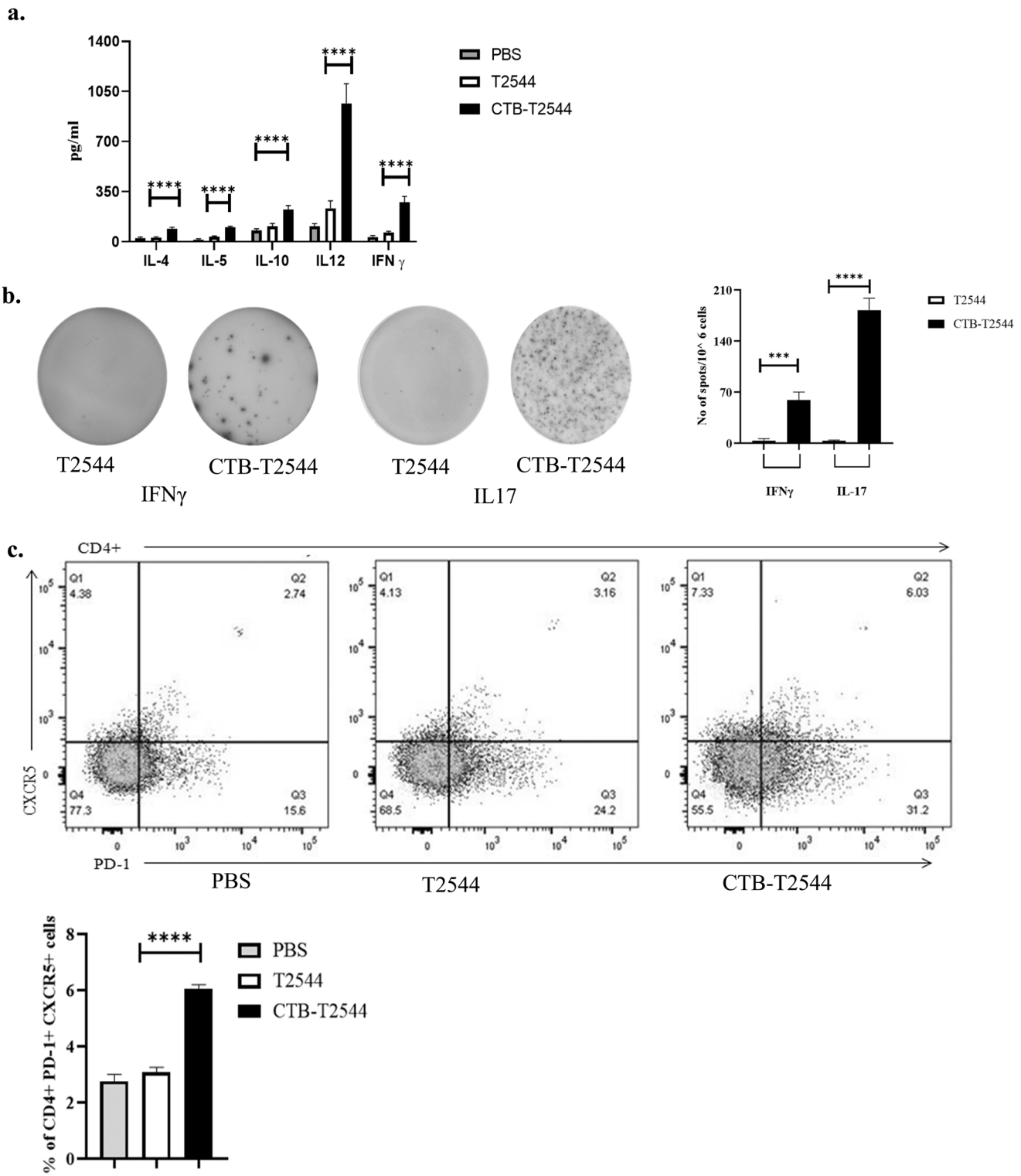

Fig. 5 T cell response measured after 12 days of primary immunization. a Th1 (IL-12, IFN-γ), Th2 (IL-4, IL-5), and Treg (IL-10) cell cytokines in the serum samples of the unimmunized and immunized mice were measured by ELISA. **b** Cells from the PP of the experimental mice were incubated with 10 μg of T2544 for 24 h. Cytokine-secreting cells were enumerated by ELISpot assays and data presented as spot forming cells/ 10^6 total cells analyzed. **c** Analysis of T_{FH} (T follicular helper) cells in the MLN. Cells were detected by measuring the expression of CXCR5 and PD-1 on $CD4^+$ cells using flow cytometer. Significance was calculated by one way (**b**, **c**) and two-way (**a**) ANOVA with *post hoc* analysis using Tukey's multiple comparison test. The experiment was repeated three times and representative images from one experiment are shown. Bar diagram represents the statistical data from all three experiments. Error bars represent SD. ****$p < 0.0001$, ***$p = 0.0006$.

these results suggested that rCTB-T2544 chimera helped to create a protective milieu in the intestine through the induction of T cell subsets and cytokines.

CTB-T2544 immunization elicits memory response

Antigen-specific memory T cell response was evaluated by co-culture of the $CD4^+$ T-cells, isolated from the spleen of the experimental mice with *S.* Typhi-pulsed bone marrow dendritic cells (BMDCs) derived from naïve mice. IFNγ release measured in the culture supernatants was significantly higher for the $CD4^+$ cells recovered from the mice immunized with rCTB-T2544 as compared with the animals that received rT2544 or left unimmunized, suggesting augmentation of the memory response by CTB (Fig. 6a). With respect to specific memory cell subsets, percentages of both central memory ($CD62L^{high}CD44^{high}$) and effector memory ($CD62L^{low}CD44^{high}$) T cells (T_{CM} and T_{EM})[34] were increased after immunization with the chimeric antigen containing CTB (Fig. 6b). In contrast, these mice had half the number of naïve $CD4^+$ cells in the spleen as compared with the other immunized groups. To compare the induction of memory B cells after immunization, a booster dose was administered on 108th day of experiment and serum anti-T2544 antibodies were measured 12 days later. A steeper rise of antibody production with significantly higher titers was observed after rCTB-T2544 immunization as compared with the immunization using rT2544 alone (Fig. 6c), suggesting the critical role played by CTB in antigen-induced differentiation of memory B cells into the plasma cells, producing IgG. Avidity index of anti-T2544 IgG antibodies was assessed by measuring the OD of the ELISA plates after washing the immune complexes with or without 4 M urea-containing buffer. We observed significantly high avidity index (60–65%) after the primary immunization, which further went up to 70–78% following the booster immunization (Fig. 6d), suggesting successful priming. In contrast, intranasal T2544 immunization resulted in poor priming (avidity index < 35%). These results together suggest that intranasal rCTB-T2544 may elicit long-term immunity against *S.* Typhi infection.

DISCUSSION

Typhoid is a systemic febrile illness, caused by an intracellular pathogen, acquired through the intestine. Protective immunity following typhoid occurs in minority of the cases[35]. This correlates with rather modest immune response after oral immunization with live Ty21a vaccine and the requirement of multiple doses[5]. In contrast, injectable TCVs, especially Vi-TT demonstrated a high level of durable protection in clinical trials, but an attack rate of 35% was observed in a CHIM (Controlled Human Infection Model) studies. However, several challenges related to the TCVs still persist that merit immediate attention. Available studies suggest that serum antibodies may not be sufficient for protection, since patients recovered from typhoid fever remain susceptible to re-infection despite elevated levels of circulating antibodies against multiple *S.* Typhi antigens (H, O, Vi-PS, porins etc)[13]. High anti-Vi IgG titers were also present in the chronic biliary carriers from the endemic populations[36]. This perhaps underscores a critical role played by the mucosal and cell-mediated immunity for overall protection against typhoid infection. Parenteral vaccination is considered a poor method for inducing mucosal immune response that was previously reported to confer protection against cholera and typhoid fever[17]. A mucosal vaccine will be highly desirable also for the ease of administration without technical assistance. Further, mouse infection studies found that *Salmonella*-specific T cells were required for late clearance of intracellular bacteria[37]. This suggests that no single component of the immune response is sufficient to provide complete protection against *S.* Typhi. We had earlier shown that T2544 induces antigen-specific cytotoxic T lymphocytes (CTLs) in mice in addition to serum antibodies[13]. In the present study, we demonstrated that a strong gut mucosal immune response in the form of protective secretory antibodies (sIgA) and gut homing lymphocytes (ASCs and Th1/Th17 cells), induced by the CTB-T2544 chimera may significantly contribute to the protection of mouse against oral *S.* Typhi challenge. The tested vaccination regimen for CTB-T2544 in mice had three intranasal doses, as opposed to single intramuscular (IM) dose of TCVs in humans. It is usual to administer multiple doses of candidate vaccines for animal studies, while single dose regimens of these formulations are often developed during clinical trials[38–40]. Mucosal immunity following CTB-T2544 will increase bacterial shedding and reduce their stay inside the body. This might provide herd protection, since *S.* Typhi does not survive long outside the human system. Herd protection was not observed with Vi-TT in the clinical trials conducted so far[11]. Another concern related to TCV, especially for low- and middle-income countries, is its relatively high cost of production, because of the requirement of complex chemical conjugations and significant batch-to-batch variations. In contrast, bacterial expression of recombinant CTB-T2544 will substantially reduce the cost and eliminate batch variations. Finally, like Vi-TT, CTB-T2544 is expected to be compatible with other vaccines, given that T2544 is absent outside the genus *Salmonella*. Because CTB functions as adjuvants to the co-administered antigens as well, CTB-T2544 may augment immunogenicity of other childhood vaccines.

CTB-T2544 chimeric antigen was generated by genetic fusion of *t2544* to the C-terminus of *ctx-b* gene, using a non-furin (GPGP) linker sequence[41]. CTB promotes immune response to both the co-administered antigens and antigens delivered as CTB chimera, but the chimeric formulations are perhaps more immunogenic, since conjugated CTB elicited 10-fold higher immunogenicity to ovalbumin than co-administered CTB[42]. Also, CTB C-terminus fusion led to the best pentamer formation, with strongest binding affinity to the GM1 receptor[16]. We observed similar binding for CTB-T2544 and CTB pentamer to the GM1 receptor, indicating that pentameric structure of CTB was retained in the chimera. However, we did not observe significantly lower expression levels of CTB-T2544 compared with CTB alone, as was reported earlier for recombinant CTB chimera.

CTB showed efficacy as vaccine adjuvant after administration through multiple routes, most notably for oral and nasal vaccines. While oral adjuvanticity was largely limited to the live vaccines[43], nasal administration worked well for subunit vaccines as well[16]. This was proposed to be mediated by increased DC activation and T and B cell responses, leading to five to tenfold reduction in antigenic dose requirement. For example, 10 µg DNA co-administered with CTB induced cellular immune responses to the magnitude of 50 µg DNA used alone in the IFN-γ ELISPOT assay[19]. In the present study, T2544 conferred over 70% protection to mice against *S.* Typhi challenge ($10 \times LD_{50}$ dose) when administered as CTB chimera, but immunization with a 3-fold higher dose of T2544 alone was non-protective. CTB was shown previously to activate TLR signaling in BMDCs, resulting in pro-inflammatory cytokine production[19]. In vivo and ex-vivo experiments with subcutaneous KLH immunization showed that CTB can also function as a potent adjuvant through direct stimulation of antigen-primed $CD4^+$ and $CD8^+$ T cells and stimulates IL-2, IL-4, and IFN-γ production[18]. However, most investigators had reported a Th2-predominant immune response with CTB and tolerization to the co-administered antigens in vivo, while either a Th1 or a more balanced T-helper (Th1/Th2) and T-regulatory (Treg) response was observed by others[16,44,45]. CTB-T2544 also displayed a mixed T cell response (both Th1/pro-inflammatory and Th-2/anti-inflammatory cytokines) (Fig. 5a, b). Published literature and the current study suggest that the nature of the immune response might depend on multiple factors, including the antigen type, dose and route of administration.

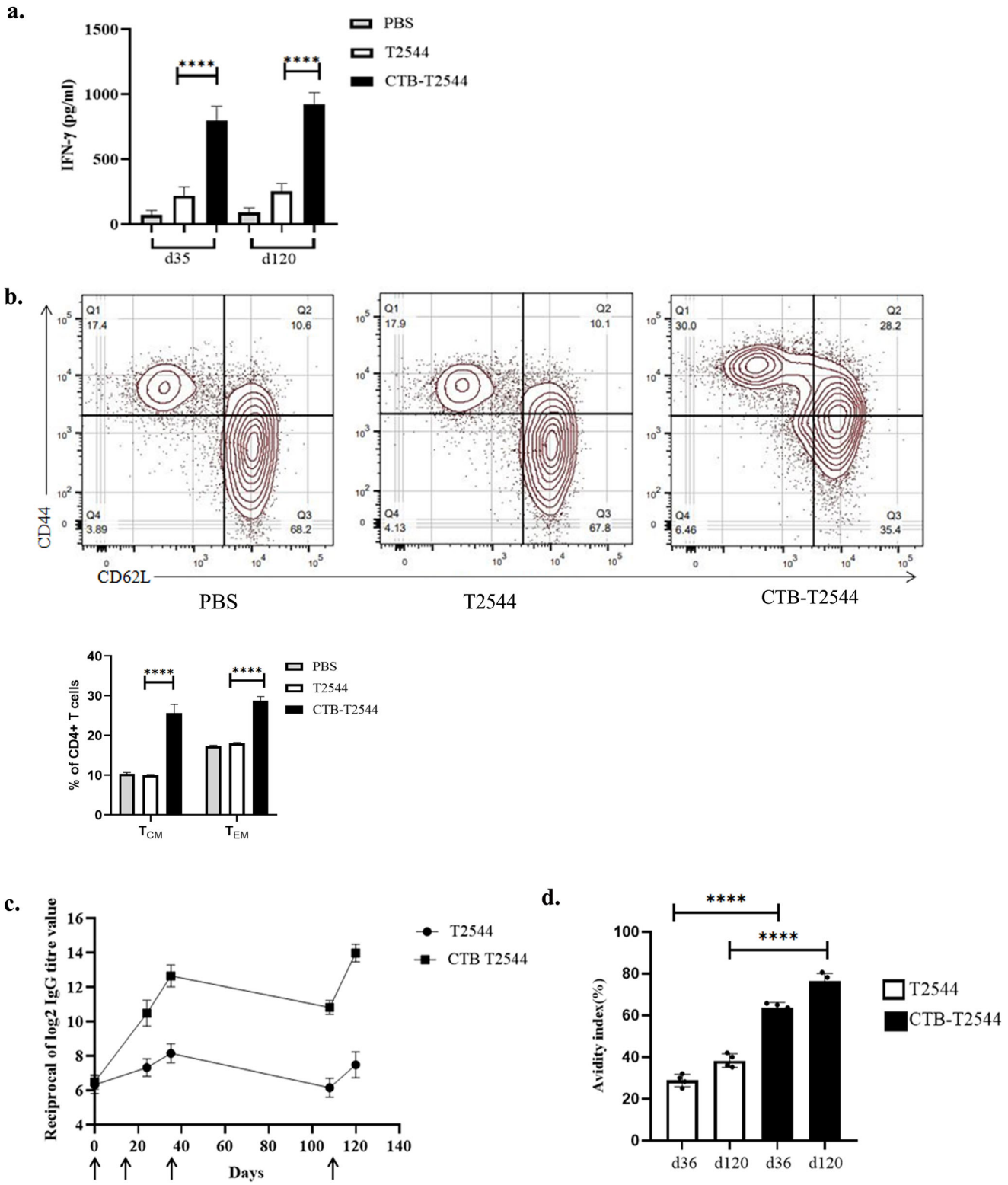

Fig. 6 Immunological memory response. a Memory T cells were analyzed by ELISA for IFN-γ release in the culture supernatants of $CD4^+$ T cells, isolated from the spleen of the experimental mice and co-cultured with BMDCs, pulsed with rT2544. Data represents mean(±SD) of three independent experiments. **b** The percentages of T_{EM} ($CD4^+CD44^{hi}CD62L^{lo}$) and T_{CM} ($CD4^+CD44^{hi}CD62L^{hi}$) cells from the spleens of different experimental groups were quantified using flow cytometry. Representative images from one of the experiments and statistical analysis of the data from all three experiments are shown. **c** Serum antibody titers (mean ± SD) measured in the immunized mice ($n = 6$) at the indicated time points are shown. Arrows indicate primary (3 doses at 0, 12 and 24th day) and booster (108th day) immunization. Mean ± SD were plotted for CTB-T2544 and T2544. **d** Avidity assay. Anti-T2544 avidity index was measured by ELISA and represented as the ratio of IgG bound to T2544 in the presence and absence of 4 M urea, multiplied by 100. Significance was calculated using one way (**a**, **d**) and two-way (**b**) ANOVA with *post hoc* analysis using Tukey's multiple comparison test. Error bars represent SD. ****$p < 0.0001$.

Efficacy of typhoid vaccines is traditionally monitored by serum antibodies, especially antigen-specific IgG titers. CTB significantly raised the titers of both IgG1 and IgG2a specific to T2544 in the serum (Fig. 3a), indicating humoral as well as cell-mediated immune responses. However, TCV under TyVAC trial failed to establish protective IgG and IgA titers despite inducing high levels of durable protection. In the controlled human infection model (CHIM) studies, serum IgG and SBA titers at the time of challenge after vaccination with Vi-PS or Vi-TT poorly matched with the protection against *S.* Typhi[46]. Instead, serum IgA titers showed significant correlation with Vi-PS-induced protection[47], underscoring potential role for intestinal sIgA. Stool sIgA titer is also believed to correlate with protection conferred by oral vaccines[48]. However, direct demonstration of protection by sIgA for typhoid vaccines is lacking in the literature. We reported here high sIgA titers, along with increased number of IgA ASCs in the intestine of mice after intranasal CTB-T2544 immunization (Fig. 3b). Further, we demonstrated functionality of the secretory antibodies by in vitro assays, such as adhesion and motility inhibition and their in vivo protective role by infecting mice with *S.* Typhi, preincubated with fecal extracts and intestinal washes (Figs. 3, S5). The above results also suggest that intranasal CTB-T2544 may potentially confer herd protection to the vaccinated community by increasing bacterial shedding from the intestine, which was not found with TCVs[11,49].

Our study found marked increase in the percentages of B cells, expressing gut homing receptors (α4β7 and CCR9) in the mouse MLNs and spleen (Fig. 4b, c). Earlier reports showed that intranasal immunization with inactivated CT holotoxin stimulates lung conventional DCs (cDCs) to promote IgA class switch of B cells in the regional lymph nodes and imprint α4β7 and CCR9 on IgA ASCs, resulting in their migration to the intestine[29]. However, we found significant expansion of $CD11c^+$ DCs, expressing IgA-inducing factors in the MLNs, which was not described earlier after intranasal immunization (Fig. 4d). This coupled with gut homing receptor expression on MLN B cells and increased number of IgA^+ ASCs in the Peyer's Patches, along with sIgA in the intestine suggests that CTB might have induced DC migration from the lungs to the MLN where they orchestrated B cell class switch and gut homing of IgA^+ B cells[31]. To address DC migration, we checked for migratory DC (mDC) markers ($MHC^{hi}CD11C^{int}CD103^+$) expression in the MLN DCs. The results showed threefold higher number of mDCs in the MLN (Fig. S7) in the mice immunized with CTB-T2544 compared with the vehicle-immunized animals. However, we did not rule out gut-homing lymphocyte generation in the lung-draining lymph nodes as well. Although in vitro experiments conducted previously suggested that CTB might require LPS to stimulate dendritic cells to promote IgA production by B cells[50], recombinant CTB-T2544 contained negligible amounts of LPS.

Memory B (B_M) cells are required for long term protection against typhoid fever. A strong association between the antigen-specific B_M cells and antibody titers were reported in the literature[33]. Several studies had reported significantly higher antigen-specific serum antibody response with chimeric CTB compared with CTB co-administration with the antigens[42,51]. In contrast, a separate study suggested weaker adjuvant function of CT or CTB, conjugated to streptococcal surface protein antigen AgI/II than to simultaneous, but separate administration with the antigen for recall antibody response to booster intranasal immunization[52]. Moreover, booster dose only enhanced AgI/II specific IgM and IgA, but not IgG. In contrast, we observed strong adjuvant effects of CTB for both the primary and booster immunization with robust IgG induction (Fig. 6c). The difference in the outcome of CTB adjuvanticity between the above two studies might be due to the fact that the authors from the earlier report used chemical conjugation of CTB and Streptococcal antigens as opposed to genetic fusion of CTB and T2544 in our study. T_{FH} cells were reported to support B_M cell generation and T cell-dependent affinity maturation of antibodies, resulting in higher avidity secondary antibodies. This was corroborated by our results that showed doubling of the T_{FH} cell number in the MLN and significantly increased avidity of anti-T2544 antibodies after a recall response (Figs. 5c, 6d).

In addition to B cells, large proportion of $CD4^+$ T cells from the spleen and MLNs expressed gut homing receptors. Imprinting of homing receptors on T cells by lung DCs was reported previously following intranasal immunization with CTB[53]. Intestinal $CD4^+$ cells in our study expressed Th1 and Th17 cytokines, both of which are critical for clearing of the intracellular bacteria, while Th17 also promotes sIgA production[17,54]. A previous study with human volunteers who received oral Ty21a vaccine showed that IL-17A, predominantly produced by the $CD8^+$ T cells in the peripheral circulation, contributes to mucosal protection against *S.* Typhi infection[55].

Circulating as well as tissue-resident memory T cells provide protection against *S.* Typhi. Oral vaccination of volunteers with Ty21a generated largely monofunctional $CD4^+$ T_{EM} or T_{EMRA} (T Effector Memory Re-expressing CD45RA) cells that produced high levels of IL-17A or TNF-α. In contrast, $CD8^+$ T cells were predominantly polyfunctional, 80% of which showed T_{EM} phenotype and produced triple cytokines[56]. The requirement of circulating memory $CD4^+$ and $CD8^+$ T cells as well as TNF-α and IFN-γ for protection against *Salmonella* was shown in mice after oral immunization with aroA-attenuated live vaccine strain or intradermal immunization with porins[57,58]. Here, we show that mice that received intranasal CTB as a chimeric partner augmented T2544-specific memory $CD4^+$ response, which upregulated IFN-γ production and were constituted by equal numbers of T_{EM} and T_{CM} (Fig. 6a, b).

There are some limitations of the current study. Immunogenicity and protective efficacy of CTB as an antigen was revealed by the induction of CTB-specific serum and mucosal antibodies in the mice immunized with CTB-T2544 as well as markedly reduced fluid accumulation in the ileal loops after challenge with cholera toxin. Previous studies with intranasal immunization with rCTB conferred 70% protection to rabbits against *V. cholerae* challenge, while co-administration of purified CTB and TcpA was 100% protective[59]. Another study showed intranasal, intraperitoneal, and subcutaneous immunization of mothers with rCTB alone provided high level protection to the pups against lethal challenge with *Vibrio*[60]. However, further studies are needed to evaluate how CTB-T2544 performs vis-à-vis other cholera vaccines and if the former can boost immune response to other vaccines against *V. cholerae* infection.

The present study suggested a higher relative contribution from the intestinal secretory antibodies for protection against *S.* Typhi following nasal immunization with CTB-T2544 (Fig. S5). This question may be further addressed in future studies by infecting immunized, polymeric immunoglobulin receptor (pIgR) knock-out ($pIgR^{-/-}$) mice, which will be devoid of sIgA from the intestinal secretions. Studies may also be designed by comparing different routes of immunization and/or their combinations to establish the immune correlates of protection against *S.* Typhi infection after CTB-T2544. Such studies could be useful to formulate a prime-boost regimen (intranasal priming and boosting through other routes) with our candidate vaccine. Another important aspect of future studies could be the vaccine efficacy against MDR and XDR strains of *S.* Typhi.

Given that mucosal vaccines are more desirable than the injectable preparations for mucosal infections and polysaccharides have limited immunogenicity as mucosal antigens, further investigations need to be carried out to exploit the conserved, immunogenic protein antigens of *Salmonella* for the development of highly efficacious mucosal vaccines. Another desirable goal is to design multivalent vaccines that can simultaneously protect

against typhoidal and non-typhoidal *Salmonella* infections, since no vaccines are currently available against *S.* Paratyphi and NTS. We have developed a multivalent vaccine containing T2544 and O-specific polysaccharide of *S.* Typhimurium that confers protection against *Salmonella* Typhi/Paratphi/Typhimurium with cross protection against *S.* Enteritidis [61].

Overall, we studied the adjuvant function of CTB to the protein subunit vaccine candidate T2544 for intestinal mucosal immune response after immunization through the intranasal route. Recombinant CTB-T2544 chimera induced high titers of antigen-specific and protective serum IgG and mucosal sIgA antibodies. sIgA response was mediated by CTB-elicited migration of DCs, expressing IgA-inducing factors to the MLN and imprinting of gut homing receptors on the lymphocytes over there. This study also highlighted the role of CTB in inducing a balanced T helper cell response, including the Th1, Th2, Th17, and T_{FH} cells. This, accompanied by augmented, antigen-specific memory B and T cell response after intranasal CTB elicited a strong and durable mucosal immunity at the intestine, leading to protection against oral *S.* Typhi infection.

METHODS

Cells, strains, growth condition, and plasmid

HT-29 and THP-1 cells used in this study were purchased from the American Type Culture Collection (ATCC, UDA). HT-29 cells were maintained in Dulbecco's modified Eagle's medium, supplemented with 10% fetal bovine serum (FBS). THP-1 cells were grown in RPMI 1640, supplemented with 10% FBS and 0.05 mM 2-mercapto ethanol. *Salmonella* Typhi Ty2, a gift from J. Parkhill (Sanger Institute, Hinxton, UK) was grown in Hektoen enteric agar (BD Difco). *Escherichia coli* strain BL21, a kind gift from Dr. Rupak k. Bhadra (Indian Institute of Chemical Biology) was maintained in Luria–Bertani agar at 37 °C. Liquid cultures of the bacterial strains were grown in Luria-Bertani broth (BD Difco). pET-28a was purchased from Addgene, USA.

Cloning, expression, and purification of recombinant rCTB-T2544 protein

A 309 bp coding sequence of *ctx-b* gene was PCR amplified (CTB fus Prot FP: CGCGGATCCACACCTCAAAATATTACTGATTTGTG; CTB fus Prot RP: GCCGTCGACATTTGCCATACTAATTGCGGC) from *V. Cholerae* and cloned in pET28a vector between BamHI and SalI restriction sites. Later on, *t2544* along with an upstream linker sequence (*ggaccaggacca* is the gene codon of a non-furin linker containing glycine and proline amino acids) (total sequence length 663 bp) was PCR amplified and the PCR product was cloned between SalI and XhoI restriction enzymes of pET28a-CTB plasmid (Fus T2544 FP: GCCGTCGACGGACCAGGACCAGAAGGGATCTATATCACCGGG; Fus T2544 RP: GCCCTCGAGTTAAAAGGCGTAAGTAATGCCGAG). The newly generated construct was transformed into the expression host *E. coli* BL21 (DE3) and the recombinant fusion protein (rCTB-T2544) expression was induced with 1 mM Isopropyl β-D-1-thiogalactopyranoside (IPTG, SIGMA) by culturing the bacteria in LB medium at 37 °C. rCTB-T2544 was extracted as an insoluble protein from inclusion bodies by sonication and solubilized by denaturing with 8 M urea. Denatured protein was purified by affinity chromatography using Ni^{2+}-conjugated agarose (Qiagen) and then renatured by gradual removal of urea by dialysis using a 10 kD membrane. Purified protein was quantified by Bradford Reagent and the purity was confirmed by SDS-PAGE, stained with Coomassie Brilliant Blue.

Immunoblot and pentamer analysis assay

Aliquotes of the protein samples were subjected to SDS-PAGE and transferred to PVDF membrane (Millipore). After blocking with 5% BSA in PBS containing 0.05% Tween 20 for 1 h, membranes were incubated with anti-His antiserum (1:2500 dilution) overnight at 4 °C. After washing, the membrane was incubated with HRP-conjugated anti-rabbit IgG (1:10,000) for another 1 h. Then, the membrane was developed by adding chemiluminescent substrates (SuperSignal West Pico, Thermo Scientific) using ChemiDoc.

To assess whether CTB-T2544 folds into pentameric state during SDS-PAGE, samples were subjected to non-denaturing and denaturing conditions. In the former conditions, samples were not boiled, and the sample buffer used did not contain β-mercaptoethanol and DTT. All the uncropped and unprocessed gel images are provided in Fig. S9.

Endotoxin detection assay

We measured the endotoxin level according to the Pierce™ Chromogenic Endotoxin Quant Kit. Briefly, 50 µl of different dilutions of endotoxin standard and test samples (1 mg/ml) were added to the plate which was pre equilibrated with heat at 37 °C. Next 50 µl of Amebocyte lysate reagent was added to each well and gently mixed. Further it was incubated for 30 min. Later, 100 µl of pre-warmed chromogenic substrate were added and incubated for 6 min followed by addition of 50 µl of stop solution (25% acetic acid) to each well and absorbance were measured at 405 nm. A standard curve was prepared from the absorbance of the endotoxin standard solutions. The endotoxin contaminations in each protein were calculated using the standard curve.

Circular dichroism

Circular dichroism (CD) spectra were recorded on Jasco-1500 spectrophotometer in the wavelength ranging from 200 to 300 nm at 25 °C. A 1.0 ml sample (150 µg/ml) of each protein was loaded into a quartz cell. Minimum of three spectra for each sample were recorded, smoothed and corrected, and analyzed.

Animals housing, immunization, and sample collection

All animal experiments were carried out as per the ethical approval (PRO/176/-MAY 2023, dt. 14.05.2020) accorded by the animal ethical committee of ICMR- National Institute of Cholera and Enteric Diseases (NICED), Kolkata, India. All the animals were taken from in house animal facility of NICED (registration number. 68/GO/ReBi/S/99/CPCSEA) and maintained at 25 °C and 45-55% humidity with 12-h alternate light and dark cycles. Immunogenicity was studied by intranasal administration of 60 µg of the recombinant proteins into female BALB/c mice (~5 weeks old) for three times at 12 days intervals. Mice were bled from the tail vein to collect blood on days 0, 11, 23, 35, 108, and 120 without sacrificing them. Stool was also collected prior to each immunization dose and 12 days after the last immunization dose. In a separate experiment, serum, stool, and intestinal wash were collected from the experimental mice twelve days after the last immunization. The mice were euthanized in a euthanasia chamber following the gradual carbon dioxide filling method from a compressed CO_2 gas cylinder followed by decapitation as per the American Veterinary Medical Association (AVMA) guidelines approved by IAEC. Samples were collected and stored at −20 °C.

Animal infection and protective efficacy

Four hours prior to the bacterial challenge of the immunized mice with *S.* Typhi Ty2, an iron-overload condition was created by intraperitoneal injection of Fe^{3+} as $FeCl_3$ (SRL) in 10^{-4} N HCl (0.32 mg per gm of body weight) along with Desferoxamine (Novartis) (25 mg/kg body weight). Mice were orally challenged with 5×10^7 *S.* Typhi bacteria and monitored for 10 days. In a separate experiment, mice from different immunized groups were subjected to an ileal loop experiment. To this end, mice were

anaesthetized by intraperitoneal injection of a mixture of ketamine (35 mg kg^{-1} body weight; Sterfil Laboratories Pvt. Ltd, India) and xylazine (5 mg kg^{-1} body weight, AstraZeneca Pharma Ltd, India). A small abdominal incision was made and a loop (2–3 cm in length) in the distal ileum was created by suture. The closed ileal loop was instilled with 100 ng of cholera toxin (Sigma). After 8 h of the surgery, mice were euthanized by gradual carbon dioxide inhalation as described above. The loop weight/length ratio was quantified 8 h later.

Enzyme linked immunosorbent assay (ELISA)

The binding affinity of the recombinant proteins, rCTB–T2544, rT2544, and rCTB for the GM1-ganglioside was measured by GM1-ELISA.To this end, ELISA plates were coated with 1 µg/well of GM1 ganglioside at 4 °C overnight. After washing of the wells with PBS-T (Phosphate buffer saline containing 0.05% Tween 20), blocking was done with 5% BSA in PBS for 1 h at 37 °C. Later on, the wells were incubated for 2 h at 37 °C with 100 µL of the recombinant proteins, serially diluted in PBS, and then washed again. Anti-His antibody (Cell Signaling Technology) (1:2500 dilution) was added to the plates and incubated for additional 1 h at 37 °C, followed by repeated washing with PBS-T. The wells were incubated with HRP-conjugated, goat anti-rabbit IgG for 1 h at 37 °C and developed by adding tetramethylbenzidine (TMB) (BD) substrate at room temperature. The absorbance was measured at 450 nm using a microplate reader.

To estimate antibody titers at days 0, 12, 24, 36, 108, 120, 96 well microtitre plates were coated with purified proteins (10 ng/well) overnight at 4 °C. After blocking the wells with 1% BSA in PBS to prevent nonspecific binding, they were incubated with the samples (serum, fecal extract, or intestinal wash contents) obtained from the immunized mice and serially diluted in PBS for 2 h. HRP-conjugated, goat anti-mouse IgG (1:10000) and goat anti-mouse IgA (1:5000) antibody was added to the respective wells and incubated for 1 h at 37 °C. The plates were developed using TMB substrate and the absorbance was measured using a microplate reader at 450 nm.

To test the avidity of IgG antibody against T2544, the sera (diluted 1:100) from CTB-T2544 and T2544 immunized mice after primary and booster immunization were allowed to react with T2544 coated wells for 2 h at 37 °C. The wells were washed three times for 5 min with PBS-Tween 20 with or without 4 M urea, followed by adding HRP-conjugated, goat anti-mouse IgG antibody to the wells and incubating for 1 h at 37 °C. The plates were developed using TMB substrate and the absorbance was measured using a microplate reader at 450 nm. The avidity index was represented as the ratio of the absorbance of the wells washed with and without 4 M Urea containing buffer and multiplying the value by 100.

Enzyme-linked Immunospot (ELISpot) assay

Mixed cellulose ester membrane-bottom plates (Millipore) were coated with rT2544 or anti-mouse total immunoglobulin overnight at 4 °C. Wells were blocked with 1% BSA and incubated for 2 h at 37 °C. Cells isolated from mesenteric lymph nodes (MLN), Peyer's Patches (PP), and spleen of immunized mice was added to blocked wells for 5 h, followed by washing with PBST. The plate was incubated with enzyme-conjugated anti-mouse IgG and IgA (Southern Biotech) overnight at 4 °C and developed with substrate. The number of spots was counted separately for each well. In a separate experiment, IFN-γ (ELISpot set from BD Bioscience) and IL-17 (ELISpot kit from R&D) pre coated mixed cellulose ester membrane-bottom plates were incubated with cells isolated from Peyer's Patches (PP) stimulated with rT2544 for 24 h. The plate was incubated with enzyme-conjugated anti-mouse IFN-γ and IL-17 antibodies and developed with substrate. The number of spots was counted separately for each well.

Bacterial adhesion inhibition assay

Bacterial cell suspensions were pre-incubated for 30 min with 1:50, 1:500, 1:5000 dilutions of the heat-inactivated immune serum, fecal extracts or intestinal contents. HT-29 Cell monolayers (5 × 10^5 cells/ml) were infected with bacteria at 1:10 M.O.I (multiplicity of infection) and synchronized by centrifugation at 400 × *g* for 5 min. Infected cells were incubated for 30 min and non-adhering bacteria were washed off with 1X PBS. Adherent bacteria were quantified by CFU counts after cell lysis with 1% triton-X100 and spreading over the lysates on LA agar plates containing Streptomycin 50 µg/ml. In a separate experiment, naïve mice were infected with or without bacteria pretreated with mucosal antibody present in fecal extract and intestinal wash. mice were euthanized by gradual carbon dioxide inhalation as described under "Methods" section on day 2, 4, 6 post-infection, and bacterial colonization was assessed in intestinal tissues and visceral organs.

Opsonophagocytosis assay

Bacterial cell suspensions were pre-incubated for 30 min with 1:50 dilution of the heat inactivated immune serum, fecal extracts, or intestinal contents at 37 °C to allow for opsonization. The opsonized bacteria were then added to the THP-1 cell-derived macrophage monolayers (5 × 10^5 cells/ml), cultured in antibiotic-free complete medium at a multiplicity of infection of 1:10 (cell/bacteria) and centrifuged at 400 × *g* for 5 min to allow adhesion. The plates were incubated for 30 min at 37 °C. Following incubation, plates were washed three times with PBS. Extracellular bacteria were killed by incubating the plates with complete medium containing gentamicin (200 µg/ml) for 60 min. After washing the plates thrice with PBS, cells were lysed with 1% Triton X-100 for 15 min at 37 °C. The lysates were diluted in PBS and plated onto LA agar plates containing Streptomycin 50 µg/ml.

Motility inhibition assay

For soft agar motility assay, 0.4% Bacto agar and 5% serum, fecal, or intestinal extracts were added to LB medium, which was poured on plates and allowed to settle at room temperature for 30 min. Bacterial culture was inoculated on the center of the plates and placed at 37 °C. The diameters of the concentrically growing bacterial cultures were measured for 6 h.

RNA Isolation and quantitative real-time PCR

Dendritic cells (DCs) were separated from the other cells of the MLN of the PBS-immunized and experimental immunized mice using $CD11c^+$ magnetic beads (Miltenyi Biotech). Total RNA was extracted from the DCs, and cDNA was prepared using a cDNA synthesis kit according to the manufacturer's instructions. Transcript levels were determined by quantitative real-time PCR, using SYBR Green PCR Master Mix (Applied Biosystem) on StepOnePlus real time PCR system (Applied Biosystem). GAPDH levels were taken for normalization, fold changes were calculated using $2^{-\Delta\Delta Ct}$. In a separate experiment, CTB-T2544 and PBS immunized mice were euthanized by gradual carbon dioxide inhalation as described under *Methods* section after 12 days of three successful immunization and $CD11c^{int}MHCII^{hi}CD103^+$ cells were stained with fluorochrome-tagged antibody and evaluated using flow cytometer.

Flow cytometry

Twelve days after the last immunization, the PBS and experimental immunized mice were euthanized by gradual carbon dioxide inhalation as described under Methods section. B and T cell subsets were isolated and stained with fluorochrome-conjugated antibodies (BD Biosciences) against specific surface markers. After

staining, the cells were washed and analyzed by flow cytometry (BD FACS ARIA II) following standard protocol. The gating strategy is provided in Fig. S8. All the used antibodies are listed in Supplementary Table 1 (Table S1).

Memory T cell assay

Dendritic cells were generated from bone marrow (BM) cells collected from the femurs and tibias of BALB/c mice. Briefly, BM cells, after collection, were cultured in 90 mm dish in complete RPMI 1640 medium supplemented with murine recombinant GM-CSF (20 ng/ml). Sixty percent of the culture medium was replaced every 3rd day with fresh medium. Cells were collected on day 7 and starved by culturing in RPMI 1640 containing 1% FBS for 12 h, before treatment with rT2544 for 24 h. To generate memory T cells, immunized mice were euthanized by gradual carbon dioxide inhalation as described under *Methods* section. $CD4^+$ T lymphocytes were isolated from the immunized mice after 120 days and co-cultured for 5 days with antigen-pulsed BMDCs at 37 °C and in the presence of 5% CO_2. Memory T cells ($CD4^+CD62L^{low}CD44^{hi}$, $CD4^+CD62L^{hi}CD44^{hi}$) were studied by flow cytometry and the culture supernatants were assayed for IFN-γ by ELISA. All the used ELISA and ELISPOT kits are listed in the Supplementary Table 2 (Table S2).

Statistical analyses

Statistical analyses of data were performed using GraphPad Prism 8.0.1.244. Log rank Mantel-Cox test was performed to analyze survival curves. Unpaired *t* test was used to compare between two groups, while one-way and two-way ANOVA with *post hoc* Tukey's multiple comparison tests were performed to compare amongst more than two groups. A *P* value of <0.05 was considered significant; **p*: 0.3332, ***p*: 0.0021 ****p*: 0.0002, *****p* < 0.0001. Data represented as mean ± SD. Error bars represent SD.

Reporting summary

Further information on research design is available in the Nature Research Reporting Summary linked to this article.

DATA AVAILABILITY

Data will be made available upon request from the corresponding author (Santasabuj Das; email id- santasabujdas@yahoo.com).

Received: 14 June 2023; Accepted: 26 January 2024;
Published online: 06 February 2024

REFERENCES

1. Hancuh, M. et al. Typhoid fever surveillance, incidence estimates, and progress toward typhoid conjugate vaccine introduction—worldwide, 2018–2022. *MMWR Morb. Mortal. Wkly Rep.* **72**, 171–176 (2023).
2. Dougan, G. & Baker, S. Salmonella enterica serovar Typhi and the pathogenesis of typhoid fever. *Annu. Rev. Microbiol.* **68**, 317–336 (2014).
3. Carey, M. E., McCann, N. S. & Gibani, M. M. Typhoid fever control in the 21st century: where are we now? *Curr. Opin. Infect. Dis.* **35**, 424–430 (2022).
4. Gonzalez-Escobedo, G., Marshall, J. M. & Gunn, J. S. Chronic and acute infection of the gall bladder by Salmonella Typhi: understanding the carrier state. *Nat. Rev. Microbiol.* **9**, 9–14 (2011).
5. Syed, K. A. et al. Review on the recent advances on typhoid vaccine development and challenges ahead. *Clin. Infect. Dis.* **71**, S141–S150 (2020).
6. Guzman, C. A. et al. Vaccines against typhoid fever. *Vaccine* **24**, 3804–3811 (2006).
7. Carey, M. E. Gateway to typhoid conjugate vaccine introduction in India and beyond - programmatic effectiveness of a public sector typhoid conjugate vaccine campaign in Navi Mumbai. *Clin. Infect. Dis.* **77**, 145–147 (2023). p.ciad134.
8. Cross, D. L. et al. Vi-vaccinations induce heterogeneous plasma cell responses that associate with protection from typhoid fever. *Front. Immunol.* **11**, 574057 (2020).
9. Shakya, M. et al. Efficacy of typhoid conjugate vaccine in Nepal: final results of a phase 3, randomised, controlled trial. *Lancet Glob. Health* **9**, e1561–e1568 (2021).
10. Liang, Y. et al. Typhoid conjugate vaccine effectiveness in Malawi: evaluation of a test-negative design using randomised, controlled clinical trial data. *Lancet Glob. Health* **11**, e136–e144 (2023).
11. Khanam, F. et al. Assessment of vaccine herd protection in a cluster-randomised trial of Vi conjugate vaccine against typhoid fever: results of further analysis. *EClinicalMedicine* **58**, 101925 (2023).
12. Simon, R. & Levine, M. M. Glycoconjugate vaccine strategies for protection against invasive Salmonella infections. *Hum. Vaccin Immunother.* **8**, 494–498 (2012).
13. Das, S., Chowdhury, R., Ghosh, S. & Das, S. A recombinant protein of Salmonella Typhi induces humoral and cell-mediated immune responses including memory responses. *Vaccine* **35**, 4523–4531 (2017).
14. Kantele, A., Pakkanen, S. H., Karttunen, R. & Kantele, J. M. Head-to-head comparison of humoral immune responses to Vi capsular polysaccharide and Salmonella Typhi Ty21a typhoid vaccines-a randomized trial. *PLoS One* **8**, e60583 (2013).
15. Davitt, C. J. & Lavelle, E. C. Delivery strategies to enhance oral vaccination against enteric infections. *Adv. Drug Deliv. Rev.* **91**, 52–69 (2015).
16. Stratmann, T. Cholera toxin subunit B as adjuvant—an accelerator in protective immunity and a break in autoimmunity. *Vaccines* **3**, 579–596 (2015).
17. Lavelle, E. C. & Ward, R. W. Mucosal vaccines—fortifying the frontiers. *Nat. Rev. Immunol.* **22**, 236–250 (2022).
18. Wang, M., Bregenholt, S. & Petersen, J. S. The cholera toxin B subunit directly costimulates antigen-primed CD4+ T cells ex vivo. *Scand. J. Immunol.* **58**, 342–349 (2003).
19. Hou, J. et al. Cholera toxin B subunit acts as a potent systemic adjuvant for HIV-1 DNA vaccination intramuscularly in mice. *Hum. Vaccin. Immunother.* **10**, 1274–1283 (2014).
20. Sassone-Corsi, M. et al. Siderophore-based immunization strategy to inhibit growth of enteric pathogens. *Proc. Natl Acad. Sci. USA* **113**, 13462–13467 (2016).
21. Kim, M. S. et al. ERdj5 in innate immune cells is a crucial factor for the mucosal adjuvanticity of cholera toxin. *Front Immunol.* **10**, 1249 (2019).
22. Clements, J. D. & Freytag, L. C. Parenteral vaccination can be an effective means of inducing protective mucosal responses. *Clin. Vaccin. Immunol.* **23**, 438–441 (2016).
23. Holmgren, J. & Czerkinsky, C. Mucosal immunity and vaccines. *Nat. Med.* **11**, S45–S53 (2005).
24. Kang, S. M., Yao, Q., Guo, L. & Compans, R. W. Mucosal immunization with virus-like particles of simian immunodeficiency virus conjugated with cholera toxin subunit B. *J. Virol.* **77**, 9823–9830 (2003).
25. Lebens, M. et al. A mucosally administered recombinant fusion protein vaccine against schistosomiasis protecting against immunopathology and infection. *Vaccine* **21**, 514–520 (2003).
26. Guo, L. et al. Immunological features and efficacy of a multi-epitope vaccine CTB-UE against H. pylori in BALB/c mice model. *Appl. Microbiol. Biotechnol.* **98**, 3495–3507 (2014).
27. Ghosh, S. et al. An adhesion protein of Salmonella enterica serovar Typhi is required for pathogenesis and potential target for vaccine development. *Proc. Natl Acad. Sci. USA* **108**, 3348–3353 (2011).
28. Satitsri, S., Pongkorpsakol, P., Srimanote, P., Chatsudthipong, V. & Muanprasat, C. Pathophysiological mechanisms of diarrhea caused by the Vibrio cholerae O1 El Tor variant: an in vivo study in mice. *Virulence* **7**, 789–805 (2016).
29. Ruane, D. et al. Microbiota regulate the ability of lung dendritic cells to induce IgA class-switch recombination and generate protective gastrointestinal immune responses. *J. Exp. Med.* **213**, 53–73 (2016).
30. Fu, H., Ward, E. J. & Marelli-Berg, F. M. Mechanisms of T cell organotropism. *Cell Mol. Life Sci.* **73**, 3009–3033 (2016).
31. Tezuka, H. & Ohteki, T. Regulation of IgA production by intestinal dendritic cells and related cells. *Front. Immunol.* **10**, 1891 (2019).
32. O'Donnell, H. & McSorley, S. J. Salmonella as a model for non-cognate Th1 cell stimulation. *Front. Immunol.* **5**, 621 (2014).
33. Crotty, S. T follicular helper cell differentiation, function, and roles in disease. *Immunity* **41**, 529–542 (2014).
34. MacLeod, M. K., Clambey, E. T., Kappler, J. W. & Marrack, P. CD4 memory T cells: what are they and what can they do? *Semin. Immunol.* **21**, 53–61 (2009).
35. Sztein, M. B., Salerno-Goncalves, R. & McArthur, M. A. Complex adaptive immunity to enteric fevers in humans: lessons learned and the path forward. *Front. Immunol.* **5**, 516 (2014).
36. Pulickal, A. S. et al. Kinetics of the natural, humoral immune response to Salmonella enterica serovar Typhi in Kathmandu, Nepal. *Clin. Vaccin. Immunol.* **16**, 1413–1419 (2009).
37. MacLennan, C. A. Antibodies and protection against invasive salmonella disease. *Front. Immunol.* **5**, 635 (2014).

38. Micoli, F. et al. Vi-CRM 197 as a new conjugate vaccine against Salmonella Typhi. *Vaccine* **29**, 712–720 (2011).
39. Haque, S. et al. Immune response of S. Typhi-derived Vi polysaccharide and outer membrane protein a conjugate in mice. *Pediatr. Neonatol.* **64**, 518–527 (2023).
40. Tritama, E. et al. Evaluation of alum-based adjuvant on the immunogenicity of salmonella enterica serovar typhi conjugates vaccines. *Hum. Vaccin. Immunother.* **14**, 1524–1529 (2018).
41. Matoba, N. et al. A mucosally targeted subunit vaccine candidate eliciting HIV-1 transcytosis-blocking Abs. *Proc. Natl Acad. Sci. USA* **101**, 13584–13589 (2004).
42. Eriksson, K., Fredriksson, M., Nordstrom, I. & Holmgren, J. Cholera toxin and its B subunit promote dendritic cell vaccination with different influences on Th1 and Th2 development. *Infect. Immun.* **71**, 1740–1747 (2003).
43. Lopez, A. L., Clemens, J. D., Deen, J. & Jodar, L. Cholera vaccines for the developing world. *Hum. Vaccin.* **4**, 165–169 (2008).
44. Wiedinger, K., Pinho, D. & Bitsaktsis, C. Utilization of cholera toxin B as a mucosal adjuvant elicits antibody-mediated protection against S. pneumoniae infection in mice. *Ther. Adv. Vaccines* **5**, 15–24 (2017).
45. Lee, J. et al. Protective immunity against Naegleria fowleri infection on mice immunized with the rNfa1 protein using mucosal adjuvants. *Parasitol. Res.* **114**, 1377–1385 (2015).
46. Jones, E. et al. A *Salmonella Typhi* controlled human infection study for assessing correlation between bactericidal antibodies and protection against infection induced by typhoid vaccination. *Microorganisms* **9**, 1394 (2021).
47. Dahora, L. C. et al. IgA and IgG1 specific to Vi polysaccharide of Salmonella Typhi correlate with protection status in a typhoid fever controlled human infection model. *Front. Immunol.* **10**, 2582 (2019).
48. Holmgren, J. et al. Correlates of protection for enteric vaccines. *Vaccine* **35**, 3355–3363 (2017).
49. Mantis, N. J., Rol, N. & Corthesy, B. Secretory IgA's complex roles in immunity and mucosal homeostasis in the gut. *Mucosal Immunol.* **4**, 603–611 (2011).
50. Gloudemans, A. K. et al. The mucosal adjuvant cholera toxin B instructs non-mucosal dendritic cells to promote IgA production via retinoic acid and TGF-beta. *PLoS One* **8**, e59822 (2013).
51. Miyata, T. et al. Plasmodium vivax ookinete surface protein Pvs25 linked to cholera toxin B subunit induces potent transmission-blocking immunity by intranasal as well as subcutaneous immunization. *Infect. Immun.* **78**, 3773–3782 (2010).
52. Wu, H. Y. & Russell, M. W. Induction of mucosal immunity by intranasal application of a streptococcal surface protein antigen with the cholera toxin B subunit. *Infect. Immun.* **61**, 314–322 (1993).
53. Ruane, D. et al. Lung dendritic cells induce migration of protective T cells to the gastrointestinal tract. *J. Exp. Med.* **210**, 1871–1888 (2013).
54. Cao, A. T., Yao, S., Gong, B., Elson, C. O. & Cong, Y. Th17 cells upregulate polymeric Ig receptor and intestinal IgA and contribute to intestinal homeostasis. *J. Immunol.* **189**, 4666–4673 (2012).
55. McArthur, M. A. & Sztein, M. B. Heterogeneity of multifunctional IL-17A producing S. Typhi-specific CD8+ T cells in volunteers following Ty21a typhoid immunization. *PLoS One* **7**, e38408 (2012).
56. Salerno-Goncalves, R. et al. Differential functional patterns of memory CD4(+) and CD8(+) T-cells from volunteers immunized with Ty21a typhoid vaccine observed using a recombinant Escherichia coli system expressing S. Typhi proteins. *Vaccine* **38**, 258–270 (2020).
57. Ontiveros-Padilla, L. et al. CD4+ and CD8+ circulating memory T cells are crucial in the protection induced by vaccination with Salmonella Typhi porins. *Microorganisms* **9**, 770 (2021).
58. Weil, A. A. et al. Memory T-cell responses to Vibrio cholerae O1 infection. *Infect. Immun.* **77**, 5090–5096 (2009).
59. Kundu, J., Mazumder, R., Srivastava, R. & Srivastava, B. S. Intranasal immunization with recombinant toxin-coregulated pilus and cholera toxin B subunit protects rabbits against Vibrio cholerae O1 challenge. *FEMS Immunol. Med. Microbiol.* **56**, 179–184 (2009).
60. Price, G. A., McFann, K. & Holmes, R. K. Immunization with cholera toxin B subunit induces high-level protection in the suckling mouse model of cholera. *PLoS One* **8**, e57269 (2013).
61. Haldar, R. et al. A candidate glycoconjugate vaccine induces protective antibodies in the serum and intestinal secretions, antibody recall response and memory T cells and protects against both typhoidal and non-typhoidal *Salmonella* serovars. *Front Immunol.* **14**, 1304170 (2024).

ACKNOWLEDGEMENTS

This work was supported by the Japan Agency for Medical Research and Development (AMED; Grant No. JP23wm0125004) and an extramural grant (58/17/2020/PHA/BMS) from Indian Council of Medical Research, Government of India. Suparna Chakraborty is the recipient of senior research fellowship provided by the Department of Science and Technology DST-INSPIRE, Government of India.

AUTHOR CONTRIBUTIONS

S.D., S.M. and S.C. had conceptualized the work. S.C. performed all experimental work. S.C., P.D., A.P., and P.H. carried out the animal experiment. A.G. helped to capture confocal images. Sw.C. performed the cell culture. G.B. helped in flow cytometric image analysis. S.D. and S.C. wrote the paper. S.M. critically read the paper and made final edits. All authors revised the manuscript and have approved the final version and accountable for all aspects of the work. Suparna Chakraborty is the first author.

COMPETING INTERESTS

G.B. was employed by company BD Biosciences; rest declared that the research was conducted in the absence of any financial or non-financial relationships which could be construed as a potential conflict of interest.

ADDITIONAL INFORMATION

Supplementary information The online version contains supplementary material available at https://doi.org/10.1038/s41541-024-00812-4.

Correspondence and requests for materials should be addressed to Santasabuj Das.

Reprints and permission information is available at http://www.nature.com/reprints

Publisher's note Springer Nature remains neutral with regard to jurisdictional claims in published maps and institutional affiliations.

Murine Models to Study Acute and Chronic Bacterial Infections

24

Suparna Chakraborty and Santasabuj Das

Contents

S. Chakraborty · S. Das (✉)
Division of Clinical Medicine, ICMR National Institute of Cholera and Enteric Diseases, Kolkata, India
e-mail: dasss.niced@gov.in

B. Siddhardha et al. (eds.), *Model Organisms for Microbial Pathogenesis, Biofilm Formation and Antimicrobial Drug Discovery*,
https://doi.org/10.1007/978-981-15-1695-5_24

Abstract

Despite spectacular advances in gaining insights into the biology of bacterial pathogens and the human host and the availability of different classes of antibiotics, bacterial diseases continue to be a major killer around the world, affecting both the developing and developed nations. The latter half of the last century had witnessed a revolution in biomedical sciences and health science research, including research in infectious diseases. Although the discovery of antibiotics dates back to the late 1920s, little was known about the specific mechanisms underlying host–pathogen interactions that involve microbial pathogenesis and host immune responses before the introduction and widespread use of molecular techniques. In fact, the vast majority of knowledge in the field is generated in the last four decades, primarily through the experiments involving gene-modified host and pathogenic microorganisms. An expanding number of disease models have greatly helped the cause of better understanding of infectious diseases and development of novel therapeutics, including drugs and vaccines. However, murine models have remained invaluable to study human infections, including those caused by bacterial pathogens, because of the genetic, anatomical, and physiological similarities between the human and mouse and the ease of genetic and other manipulations (construction of transgenic, knockout, and humanized animals) of mouse. Laboratory-bred mice with homogeneous genetic backgrounds are cheap, easily available, and amenable to experimental interventions. This review discusses the current trends of the use of murine models to study different bacterial infections of the human and contrasts the traditional and more recent mouse models. A better understanding of various murine models, along with the advantages and limitations of each of them will offer new insights into the pathogenesis of acute and chronic bacterial infections and pave the way for better control of these diseases.

Keywords

Murine model · Acute infection · Chronic infection · Bacterial pathogen

24.1 Introduction

Human is exposed to numerous pathogenic bacteria in the environment throughout their course of life. But the infection only takes place when the host's immune system fails to contain the invading bacteria. Persistent infections may go asymptomatic or result in clinically noticeable symptoms. Certain bacterial pathogens, such as *Mycobacterium tuberculosis* and *Salmonella enterica* serovar Typhi (*S*. Typhi), adapt the art of escaping the host defense machinery and persist within the host for decades without showing any symptoms (Gomez and McKinney 2004; Monack et al. 2004). On the other hand, *Pseudomonas aeruginosa* and *Escherichia coli* develop symptomatic acute or chronic infections.

24.1.1 Importance of Animal Models to Study Bacterial Infections

The fundamental rationale behind using a model organism to study disease pathogenesis lies in the anatomical and physiological relatedness of the affected species. This holds true for infectious diseases, including bacterial infections as well where the same tissues are infected with similar disease manifestations for the model host and the natural hosts. Animal experimentations are extensively used to study human diseases, especially the bacterial infections to elucidate their interactions with the host immune system and for assessing novel therapeutics. Studies involving animal models help us to understand the disease pathogenesis, host immune responses against the invading pathogens and most importantly, to evaluate the efficacy of antibiotics and potential vaccine candidates. Hence, a suitable animal model bridges the gap between the characterization of a pathogen in vitro and the clinical disease to address cure of the infection. Finch and Crimmins (2004) proposed that early age infections burden the patients with "cohort morbidity phenotype," which persists throughout their lives (Finch and Crimmins 2004). Even after the acute bacterial infection is resolved by the standard treatment, an "immunologic scar" persists. Currently, heightened concerns about antimicrobial resistance have led the researchers to develop optimized dosing regimens, using animals. Animal models, especially mouse models have been widely employed for quantitative and qualitative study of the host immune response and also to translate this knowledge at the clinic.

24.1.2 Mouse Models of Bacterial Infections

The choice of proper animals is one of the most important things to be considered while studying any disease. *Mus musculus* has remained a much favored model to study infectious bacterial diseases and the subsequent host immune response. The similarities between the human and the mouse in their genetic makeup, anatomical structures, and physiological functions have made the murine model invaluable to study bacterial diseases that affect human beings. Numerous inbred and outbred mouse strains are currently available to establish infectious disease models. Inbred mouse strains provide a uniform response to infections as well as investigational treatments and novel vaccine candidates, whereas an outbred strain maintains heterogeneity. Inbred mouse strains include BALB/c, C57BL/6, DBA, and CBA, whereas MF1, CD-1(Swiss), Swiss-Webster, and NMRI fall under the category of outbred strains. With the help of genome engineering, mouse can be genetically manipulated with relative ease to create transgenic, knockout, and knockin animals. Immunodeficient mouse models are useful to dissect bacterial infections and their interactions with the host immune system. Nude mice (nu) have mutation at *Foxn1* (winged-helix/forkhead transcription factor) gene and lack T cells due to athymia, which blocks the development of thymus-derived T cells. Severe combined immunodeficiency (SCID) strains have mutation at *Prkdc/scid* (protein kinase, DNA activated, catalytic polypeptide) protein. The latter is essential to join the nonhomologous ends of double-stranded DNA. The *Rag1* or *Rag2* (recombination activating genes)

gene deletions in mice result in the arrest of rearrangement of B and T cell receptors and differentiation of the cells. Although mice have been extensively used to study disease pathogenesis, host–pathogen interactions, identify the virulence factors critical for establishing infections, and test the potential of drug and vaccine candidates, there are limitations of using mouse models while studying human biology. Unlike humans, absence of functional TLR10 and the presence of other innate immune responders, such as TLR11, TLR12, and TLR13 in mice made mouse models somewhat incongruent. Some pathogenic bacteria are restricted to the humans and are difficult to mimic in mouse models. To overcome these limitations, immunodeficient mice were engrafted with human tissues or cells to generate mouse/human chimera, which became increasingly popular to study human restricted pathogens. In this review, we will discuss various mouse models used to study acute and chronic bacterial infections.

24.2 Mouse Models to Study Acute Bacterial Infections

Table 24.1 summarizes the mouse models that were used to study acute bacterial infections affecting humans.

24.2.1 Cholera

Cholera is manifested by acute watery diarrhea and caused by *Vibrio cholerae*, a Gram-negative bacterium. If the circulatory volume loss is not replenished immediately, dehydration, leading to hypovolemic shock rapidly ensues. Genes encoding the two major virulence determinants of *V. cholerae*, cholera toxin (CT) and toxin co-regulated pilus (TCP) are parts of the *ToxR* regulon. Their expressions are regulated by the transcriptional regulators, encoded by *toxRS*, *tcpPH*, and *toxT* genes (Bina et al. 2003). The rabbit ileal loop model has been extensively used to study the pathogenesis of toxigenic *V. cholerae* strains as well as purified CT (Ritchie et al. 2010). However, the only physiologically relevant model of cholera developed to date is the RITARD model. We had improvised a mouse ileal loop model to test the functions of CT as well as infection with the live organisms. We demonstrated that CT suppresses cathelicidin and human beta-defensin 2, two endogenously produced cationic antimicrobial peptides that are abundant at the intestinal mucosal surface and aid in immune evasion (Chakraborty et al. 2008). However, *V. cholerae* fails to colonize the adult mouse intestine. Instead, a suckling mouse model has been widely used to study intestinal colonization of *V. cholerae* and the role of TCP in this process. This model was tested for therapeutic interventions against *V. cholerae* infection. In an intriguing set of experiments, researchers had shown that *E. coli* Nissle, expressing the *V. cholerae* quorum sensing molecules, autoinducer-2 (AI-2) and cholera autoinducer-1 (CAI-1) suppresses virulence genes (CT and TCP) expression by *V. cholerae*. An 80% reduction in CT production led to >90% survival of the mice (Duan and March 2010). Phage

Table 24.1 Mouse models of acute bacterial infections

Disease	Organism	Mouse strain	Aim of study	Major questions addressed/ finding	References
Cholera	*Vibrio cholerae* 569B inaba	Swiss mice; ICR (outbred)	Disease pathophysiology	Fluid accumulation in ileal loops inoculated with bacteria and toxin	Basu and Pickett (1969), Sawasvirojwong et al. (2013)
	Vibrio cholerae	Suckling CD-1 mice	Disease model	Colonization studies and virulence factor	Klose (2000), Duan and March (2010)
	Vibrio cholerae	BALB/c	Streptomycin-pretreated mouse model	Colonization studies and protective antibody response	Nygren et al. (2009)
	Vibrio cholerae	Mouse ileal loop model	Disease pathogenesis	Immune evasion	Chakraborty et al. (2008)
	V. cholerae E1 tor INABA	Balb/c	Pulmonary infection model	Colonization studies and virulence factor	Fullner et al. (2002), Pineyro et al. (2010)
	Vibrio cholerae	Infant mouse model	Infant mouse model	Phage therapy	Yen et al. (2017)
Pneumonia	*S. pneumoniae*	C57BL/6	Disease pathogenesis	Efficacies of different antibiotics	Azoulay-Dupuis et al. (1991)
	S. pneumoniae	MF1	Disease pathogenesis	Evaluating the role of pneumolysin and autolysin	Canvin et al. (1995)
	S. pneumoniae	Infant NMRI mice	Disease model description	Early-life immunization	Jakobsen et al. (2002)
	L. pneumophila	A/J	Disease model description	Acute pneumonia	Yamamoto et al. (1988), Yoshida et al. (1991), Brieland et al. (1994)
	L. pneumophila	C57BL/6	Disease model description	Study of flagellin mutants	Archer et al. (2009), Archer et al. (2010), Berrington et al. (2010)

(continued)

Table 24.1 (continued)

Disease	Organism	Mouse strain	Aim of study	Major questions addressed/ finding	References
Acute bacterial meningitis	*S. pneumoniae*	C57BL/6	Elucidate the role of nitric oxide synthase	To study innate immune response	Koedel et al. (2001)
	S. pneumoniae	CD-1	Therapeutic efficacy of drugs	Infection induced via intracerebral route	Shapiro et al. (2000)
	S. pneumoniae	BALB/c, C57BL/6, CD-1	Disease pathogenesis	Model of brain damage in pneumococcal meningitis	Grandgirard et al. (2007)
	S. pneumoniae	Swiss mice, C57/129	Disease pathogenesis	Infection through intranasal route and intraperitoneal route	Tan et al. (1995), Zwijnenburg et al. (2001)
	Neisseria meningitidis	CD46 transgenic mouse expressing human CD46	Model to study disease pathophysiology	To study bacterial load, quantification of antibody titers and cytokine response	Johansson et al. (2003), Johansson et al. (2005)
	N. meningitidis	Transgenic mice expressing human factor(fH)	Model to study disease pathophysiology	Antibiotic susceptibility testing	Belkacem et al. (2016)
	L. monocytogenes	C57BL/6	Oral model description	Disease pathogenesis	Czuprynski et al. (2003), Bergmann et al. (2013)
	L. monocytogenes	C57BL/6	Intracerebral model description	Immunomodulation and study the function of TNF and IL10	Schluter et al. (1996), Deckert et al. (2001), Virna et al. (2006)
Shigellosis	*S. flexneri*	SCID-HU-INT chimeric mouse	Disease pathogenesis	Immune evasion	Zhang et al. (2001)
	S. flexneri	Newborn BALB/c mice	Model description and disease pathogenesis	Mucosal inflammatory process	Siegrist (2001), Fernandez et al. (2003)
	S. flexneri	C57BL/6	Intraperitoneal disease model	Evaluating vaccine candidates	Yang et al. (2013)
	S. flexneri	Balb/c	Intraperitoneal disease model	Therapeutic efficacy of Toll-like receptor 3	Ta et al. (2017)

Salmonellosis: systemic infection	*S.* Typhi	C57/BL6	tlr11−/− mice model	Disease pathogenesis	Mathur et al. (2012)
	S. Typhi	B6.C3Pde6b^{rd1} Hsp4^{le}/J	Model description	Colonization study and Virulence factor	Spano et al. (2016)
	S. Typhi	Swiss mice; C57BL/6	Disease pathogenesis	Protective antibody responses	Ghosh et al. (2011), Das et al. (2017)
Salmonella-associated enterocolitis	*S. enterica* typhimurium	C57BL/6	Streptomycin-pretreated colitis mouse model	Molecular mechanisms of enteric salmonellosis	Barthel et al. (2003), Coburn et al. (2005)
	S. enterica typhimurium	C57BL/6	Streptomycin-pretreated colitis mouse model	Colonization studies and virulence factor	Hapfelmeier et al. (2004), Stecher et al. (2004)
Campylobacter infection	*Campylobacter jejuni*	BALb/c	Model description and disease pathophysiology	Colonization studies	McCardell et al. (1986a, b), Stanfield et al. (1987)
	Campylobacter jejuni	C57BL/6	Model description	Influence of diet and antibiotics in alterations of gut microflora	Giallourou et al. (2018)
	Campylobacter jejuni	C3H mice with limited gut flora (LF)	Model description	Colonization determinants and host immune response	Chang and Miller (2006)
Sepsis	*Streptococcus pneumoniae*	CBA/N, DBA/2, BALB/c	Disease pathogenesis	Drug efficacy and virulence study	Briles et al. (1981)
	Streptococcus pneumoniae, Klebsiella pneumoniae	CD-1	Model description and disease pathogenesis	Immune response	Wang et al. (2001)

(continued)

Table 24.1 (continued)

Disease	Organism	Mouse strain	Aim of study	Major questions addressed/ finding	References
Skin infection	*Staphylococcus aureus, MSSA, MRSA*	ICR	Burnt skin model	Efficacy of antibiotics	Akiyama et al. (1994), Yamakawa et al. (2002)
	Staphylococcus aureus and *Streptococcus pyogenes*	MF1	Skin suture-wound model	Efficacy of antibiotics	Boon and Beale (1987), Gisby and Bryant (2000)
Polymicrobial infection	*Escherichia coli*, *Bacteroides fragilis*, and *Clostridium perfringens*	Diabetic mouse strain BKS.Cg-m +/+ Leprdb/J	Disease progression	Influence of diabetes on polymicrobial infection	Mastropaolo et al. (2005)
	P. gingivalis, *T. denticola*, and *T. forsythia*	ApoE$^{-/-}$ B6.129P2-*Apoe*^{tm1Unc}/J	Model description	Relations between periodontal disease and associated atherosclerosis	Rivera et al. (2013), Chukkapalli et al. (2015), Chukkapalli et al. (2017)
	Candida albicans, *Pseudomonas aeruginosa*	C3H/HeN	Neutropenic mouse model	*To study fungal secreted products that inhibit bacterial colonization*	Lopez-Medina et al. (2015)
	Candida albicans, Pseudomonas aeruginosa	Cr1 CF1 BR non-Swiss mice	Model description	Sequential infection of a burned mouse model and disease	Neely et al. (1986), Peters and Noverr (2013)
Anaerobic infection	*Fusobacterium necrophorum*	Swiss mice; Balb/c	Disease pathogenesis	Efficacy of antibiotics	Wilkins and Smith (1974), Maestrone et al. (1975), Nagaoka et al. (2013)
	Fusobacterium necrophorum	A/J; CF1	Model description	Disease pathogenesis, efficacy on antibiotics	Abe et al. (1976), Hill (1977)
	Escherichia coli	Streptomycin-treated CD1 mice	Model description	Colonization studies	Jones et al. (2011)

Colitis in mice	*C. rodentium*	C57BL/6	Disease pathophysiology	Role of MyD88 signaling	Gibson et al. (2008), Lebeis et al. (2008); Bhinder et al. (2014)
	C. rodentium	C57BL/6-*Igh*-6^{tm1Cgn} mice	Disease pathophysiology	Role of B cells and T cell subsets	Simmons et al. (2003), Maaser et al. (2004)
	C. rodentium	C57BL/6J	Disease pathophysiology	Host responses to A/E lesion	Higgins et al. (1999), Newman et al. (1999), Gonçalves et al. (2001)
	EPEC	C57BL/6J	Model description	Disease pathophysiology	Savkovic et al. (2005)
	EPEC and EHEC	BALB/c mice	Model description	Cross-reactive protection	Calderon Toledo et al. (2011)

therapy for cholera was also successfully tested in the infant mouse model. Orogastric administration of a cocktail of three lytic phages 3 h prior to *V. cholerae* infection resulted in 2-log decrease in the number of surviving *V. cholerae* in the small intestine (Yen et al. 2017). Innate immune response to *V. cholerae* infection was studied using both infant and adult mice. At the peak of infection (24–30 h post-infection), several pro-inflammatory mediators, such as KC, MIP-2, NOS-2, IL-6, and IL-17a, were upregulated in the neonatal intestinal tissues (Bishop et al. 2014). This was in contrast to adult mice (streptomycin treatment model), which showed only modest increase in KC, MIP-2, and IL-6 expression. In the ketamine-dependent adult mouse model, IL-6 and MIP-2 were increased, but not the levels of NOS-2 and IL-17a. While no changes in TNF-α and IL-1β expressions were observed in any of the above models, IL-10 was induced only in the adult mice. Intriguingly IL-10 expression displayed strain specificity to *V. cholerae* infection, with C57/BL6 being more efficiently colonized than BALB/c or CD-1 strain. Inflammation in the infant mouse model is dependent on CT, and the accessory toxins like RtxA and HlyA play a minor role in CTX positive *V. cholerae* strain. In contrast, RtxA appears to be more important than CT for inflammation in the adult mouse model. Innate immune response to *V. cholerae* is also characterized by the recruitment of neutrophils and appearance of neutrophil extracellular traps (NETs), but secreted DNAses from *V. cholerae* disrupt the NETs (Bishop et al. 2014).

24.2.2 Acute Bacterial Meningitis

Acute bacterial meningitis, a life-threatening bacterial infection, is characterized by inflammation of the meninges and the subarachnoid space. This infection is fatal in 5–40% of patients, while 30% of the survivors develop serious neurological sequelae, such as seizures, deafness, and impairment of learning and memory (Leib and Tauber 1999; Koedel et al. 2002). The most common bacterial pathogens involved are *Streptococcus pneumoniae*, *N. meningitidis,* and *Listeria monocytogenes*. After the introduction of the Hib vaccine, *S. pneumoniae* became the major bacteria responsible for acute bacterial meningitis in all age groups. After colonizing the nasopharynx, the bacteria reach the lungs and from there, invades the bloodstream to effectively cross the blood–brain barrier (Leib and Tauber 1999). Rat and rabbit models were previously used to study meningitis, but two different types of mouse models have been established recently. Direct inoculation of the bacterium into the CNS through the intracerebral or the intracisternal route is useful to study host–pathogen interactions after the infection is established. Blood and brain homogenate levels of KC, IL6, and MIP-2 were elevated. Brain histology uniformly showed meningeal inflammation, characterized by neutrophilic infiltration, microglial activation, and hippocampal apoptosis. Parenchymal, subarachnoidal, and cortical hemorrhages were also seen in some mice (Mook-Kanamori et al. 2012). On the other hand, intranasal and intraperitoneal inoculation aids to study disease progression from colonization to establishment of the disease (Tan et al. 1995; Zwijnenburg et al. 2001). A female transgenic mouse model of intraperitoneal infection with

bioluminescent *N. meningitidis* was demonstrated to be particularly useful for antibiotic susceptibility testing (AST) (Belkacem et al. 2016).

24.2.3 *Salmonella* Infection

Salmonella serotypes can cause enteritis, enteric (typhoid and paratyphoid) fever, and bacteremia in humans. Enteric fever caused by *Salmonella enterica* serovar Typhi (*S*. Typhi) and *S. enterica* serovar Paratyphi (*S.* Paratyphi) A and B is a human restricted, potentially life-threatening illness. The infections spread by the fecal–oral route via contaminated food and water and result in similar clinical illnesses. Annually, 26.9 and 5.9 million cases of typhoid and paratyphoid fevers, respectively, are reported (Crump et al. 2004; Buckle et al. 2012). Upper small intestinal biopsy of patients reveals diffuse enteritis, caused by infiltration of mononuclear cells. Mucosal thickening of the ileum and enlargement of the mesenteric lymph nodes, spleen, and liver are also observed. Bacterial colonization often leads to capillary thrombosis in the Peyer's patches of the terminal ileum, which further results in hemorrhage, necrosis, ulceration, and intestinal perforation (Sprinz et al. 1966; Bitar and Tarpley 1985; Kraus et al. 1999). Acute enteritis due to *S. enterica* serotypes, Typhimurium and Enteritidis infection represents the second most common cause of bacterial food-borne disease in the USA (Mead et al. 1999) and is characterized by mucosal edema and infiltration of PMN leukocytes (Day et al. 1978). In the mouse, *S. enterica* serotypes Typhimurium (previously known as *Bacillus* Typhi) causes human typhoid-like illness. Since the tissue lesions of mice infected with *S.* Typhimurium are similar to those of the patients suffering from typhoid, murine typhoid model has been extensively used to study human typhoid fever. However, despite ~98% overall identity of the *S*. Typhimurium and *S.* Typhi genomes, the pathogenicity islands of the two serotypes contain ~11% non-homologous genes that account for different host specificity and disease manifestations. The use of knockout mice has offered new insights into the pathogenesis of typhoid. A study reported that deletion of TLR11, which is expressed in mice, but not in humans results in the establishment of *S.* Typhi infection in mice after oral administration (Mathur et al. 2012). Mice lacking Rab32 (Rab family GTPase) and BLOC-3 (Nucleotide exchange factor) was also shown to be susceptible to *S*. Typhi infection. *S*. Typhimurium blocks this pathway by delivering two effector molecules, namely SopD2 (Rab32 GAP) and GtgE (Rab32 protease). A mutant strain of *S*. Typhimurium devoid of these two effector molecules showed reduced virulence in mice (Spano et al. 2016). O'Brien (1982) first reported that mice become more prone to *S.* Typhi infection when administrated intraperitoneally with iron alone or with an iron chelator (O'Brien 1982). Based on this, we developed an iron overload mouse model for systemic *S.* Typhi infection through the natural route. Swiss Albino mice were intraperitoneally injected with Fe^{3+} and desferrioxamine 4 h before the bacterial challenge. We observed that outer membrane proteins of *S.* Typhi, such as T2544 and T2942 play a major role in bacterial adhesion and/or invasion of the intestinal epithelial cells and disease development in the mice (Ghosh et al. 2011;

Chowdhury et al. 2015). This model was also successfully used to study the protective immune responses induced by T2544 (Ghosh et al. 2011; Das et al. 2017). *S.* Typhimurium-induced enterocolitis was modeled in streptomycin-pretreated mice. Streptomycin eliminates the commensal microflora, allowing intestinal colonization of mice with *S.* Typhimurium. Mutant *S.* Typhimurium strains with defective SPI-1 type III secretion system fail to cause systemic infection, but successfully colonize the lower intestinal tract of streptomycin pretreated mice (Barthel et al. 2003; Hapfelmeier et al. 2004; Stecher et al. 2004; Coburn et al. 2005).

24.2.4 Shigellosis

Bacillary dysentery or shigellosis is an acute invasive disease caused by a Gram-negative, facultative bacteria that belong to the *Shigella* sp. Broadly, four different species of *Shigella,* namely *Shigella flexneri*, *Shigella sonnei*, *Shigella dysenteriae*, and *Shigella boydii* cause Shigellosis, which remains a major threat to public health in the developing world. The age group primarily affected is 0-5 years and accounts for more than one million deaths every year (Kotloff et al. 1999). Patients with shigellosis develop fever, intestinal cramps, and discharge of mucopurulent and bloody feces. *Shigella* invades the intestinal epithelial layer of the human and nonhuman primates and causes infiltration of the inflammatory cells into it, resulting in tissue edema and areas of epithelial erosions (Mathan and Mathan 1991). Numerous in vivo models, such as the macaque monkey, rabbit, guinea pig, and mouse models have been developed to mimic human shigellosis. Among these models, macaque monkey is the most relevant to assess immunogenicity and protection by vaccine administration (Phalipon and Sansonetti 2007). Guinea pigs, resistant to both natural and experimental infections of the intestine by *Shigella* were used to demonstrate acute inflammation, characterized by keratoconjunctivitis following bacterial infection of the eye (Sereny test) (Sereny 1957). Adult mouse fails to establish intestinal *Shigella* infection due to the lack of IL-8, a key player of the human immune system, which recruits neutrophils to the site of infection (Singer and Sansonetti 2004). However, a mouse model of pulmonary infection developed by intranasal administration of *Shigella* showed acute bronchopneumonia due to massive neutrophilic infiltration. This model is still used to assess immunization efficacy and protection against bacterial challenge (Sharma et al. 2016). Zhang et al. (2001) established successful colonization of the bacterium in human intestinal xenografts in severe combined immunodeficient mice (SCID-HU-INT mice) (Zhang et al. 2001). Another group reported a 4-days old neonatal mouse model to study the pathogenesis of *Shigella* infection (Fernandez et al. 2003). Yang et al. (2013) had established shigellosis in adult mice by intraperitoneal (i.p.) infection (Yang et al. 2013). The model mimics human shigellosis in many respects and was used to study protective efficacy of potential vaccine candidates. High doses (10^8 CFU) of *S. flexneri* cause severe dysentery with massive destruction of the mucosal tissues and reduced colon length, leading to 100% mortality within 18 h of infection. In contrast, low dose (~10^6 CFU) infection induces diarrhea and mild inflammatory

response. CFU counts in the stool and infected colon support bacterial colonization of the intestinal tissues. We have used the intraperitoneal model of shigellosis to study therapeutic efficacy of Toll-like receptor 3 ligand, poly(I;C) that functions by inducing cationic antimicrobial peptide cathelicidin in the colonic epithelium (Ta et al. 2017).

24.2.5 *Citrobacter rodentium* Infection

Infection pattern of *Citrobacter rodentium,* a Gram-negative, mouse restricted, mucosal pathogen provides a robust model to study bacteria-induced colitis in mice. Upon infection, it injects several effector proteins into the host cells to subverts the innate immune system of the host and leads to the formation of characteristic attaching and effacing lesions. Studies reported the role of B cells (Maaser et al. 2004), T cell subsets (Simmons et al. 2003) and MyD88 signaling (Gibson et al. 2008; Bhinder et al. 2014) in the development of immunity toward *Citrobacter rodentium*-induced colitis in vivo. *Citrobacter rodentium* is also used as a surrogate model to study the disease pathogenesis of two diarrheagenic pathogens of the human, namely EPEC (enteropathogenic *E. coli*) and EHEC (enterohemorrhagic *E. coli*).

24.2.6 *Campylobacter jejuni* Infection

Absence of animal models, especially the mouse models that replicate the human disease has long been a major bottleneck in the study of *C. jejuni* pathogenesis. In chickens and most other animals, the bacteria reside as a commensal microbe within the intestine, while causing severe diarrhea and gastroenteritis in humans (Walker et al. 1986; Wassenaar and Blaser 1999; Enocksson et al. 2004). A large number of studies reported intestinal colonization in both the neonatal and adult mice, which increases after antibiotic pre-treatment. However, reports of diarrhea and deaths in non-manipulated adult mice are rare (Baqar et al. 1999). Vancomycin pre-treatment of mice deficient in Single IgG IL-1 Related Receptor (SIGIRR), a negative regulator of MyD88-dependent signaling resulted in widespread and extensive colonization of *C. jejuni*, accompanied by severe gastroenteritis involving high levels of Th1/Th17 cytokines. SIGIRR−/− mice showed increased susceptibility to infection by *Citrobacter rodentium* and *Salmonella enterica* serovar Typhimurium, the two natural enteric bacterial pathogens of mice. However, Tlr4−/−/Sigirr−/− mice were largely unresponsive to infection by *C. jejuni* despite heavy colonization, while Tlr2−/−/Sigirr−/− mice developed exaggerated inflammation and pathology. This indicates that TLR4 signaling is mainly responsible for enteritis seen in this model, whereas TLR2 signaling is protective (Stahl et al. 2014). A weaned mouse model of *C. jejuni* infection was developed that replicated the two widely recognized clinical manifestations of the human disease, namely, enteropathy with growth failure and overt bloody diarrhea. The animals were fed Zn-deficient or protein-deficient diet and treated with vancomycin to disrupt the commensal microflora before *C. jejuni*

infection. The Zn-deficiency model showed severe enteropathy with bloody diarrhea, fecal shedding of bacteria for more than 2 weeks and growth failure. In contrast, protein-deficient diet modeled a milder disease with modest enteropathy, but no overt diarrhea as observed for childhood infection in the developing world (Giallourou et al. 2018).

24.2.7 Skin Infections

Human skin primarily provides a physical barrier to the invading organisms. It can secrete antimicrobial peptides, which aid the host defense system to fight off the pathogen. Methicillin-sensitive and -resistant *Staph. aureus* (MSSA and MRSA) and *Streptococcus pyogenes* are the major causal agents of primary skin and soft tissue infections, leading to a wide range of dermatological diseases, including atopic dermatitis, psoriasis, and skin cancers. Burnt skin model (Akiyama et al. 1994; Yamakawa et al. 2002) and skin suture-wound model (Boon and Beale 1987; Gisby and Bryant 2000) were used to assess the efficacy of the antibiotics.

24.2.8 Bacteremia and Sepsis

Bacteremia and sepsis pose major threats to public health. Bone et al. (1989) defined the term sepsis as a host systemic response to infection measured by several clinical parameters, such as blood leukocyte count, heart and respiratory rates, and the body temperature (Bone et al. 1989). In contrast, bacteremia denotes the bacterial load in the blood. *S. pneumoniae*, *P. aeruginosa*, and *L. penumophilia* are the most common bacteria associated with acute bacteremic pneumonia in humans (Whitney 2016). These pathogens frequently colonize the upper respiratory tract and often lead to the secondary pneumonia following a viral infection (Morens et al. 2008). Mouse models of pneumonia allow the evaluation of the bacterial load in the lungs and the blood, histological analysis of lung tissue inflammation, quantification of antibody titers, and screening of antimicrobials. Despite intensive studies, murine models of sepsis have remained a topic of debate. A comparison of the complex physiology of the human with a single genetic strain of mouse may be inappropriate. Inoculation of bacteria through the intraperitoneal or intravenous route induces sepsis in mice, but the disease is usually short lived, with either death of the animal or clearing of the bacteria. Inclusion of fibrin clots impregnated with standardized number of bacteria into the peritoneal cavity added an advantage to the bacterial injection model of sepsis. This fibrin clot, serving as a reservoir of inoculums, allows monitoring the rate of bacterial clearance and titrating the mortality rate. This model showed the importance of early antibiotic treatment over delayed administration in sepsis (Kumar et al. 2006). The cecal slurry method is based on injecting cecal contents intraperitoneally, which is quantified as a fecal mass and resuspended in liquid, whereas cecal ligation and puncture (CLP) model involves ligation of a part of the cecum in conjunction with cecal colotomies via needle puncture. Due to incomplete

intestinal development of neonatal mice and small organ size, the cecal slurry model is advantageous over CLP method to study sepsis. Studies on cecal slurry model of sepsis showed distinctive genetic and cytokine responses (Gentile et al. 2014).

24.2.9 Polymicrobial and Anaerobic Infections

Animal models are the key to our current knowledge about the pathogenesis of human infections and the therapeutic advancement to combat them. However, the reductionist approach of using one infectious agent at a time has limitations and fails to capture the complexities of human infections that often occur with more than one pathogen, infecting simultaneously or sequentially. Concomitant infection(s) could change the outcome of infectious diseases, due to either synergistic or antagonistic interactions between the pathogens or by modulating the host immune response.

Periodontal infection is a classic example of polymicrobial infection caused by several early colonizer pathogens, including *Prevotella, Peptostreptococcus, Campylobacter*, and *F. nucleatum* and some late colonizers, such as *Treponema denticola, Porphyromonas gingivalis*, and *Bacteroides forsythus*. There are numerous reports of an association between periodontal infection and atherosclerotic vascular disease, and epidemiological studies have suggested that periodontal infection is a risk factor for coronary artery disease (CAD). Causative association between the two was addressed in two widely used mouse models of accelerated atherosclerosis, namely the ApoE−/− and LDLR−/− mice (Rivera et al. 2013; Chukkapalli et al. 2015; Chukkapalli et al. 2017). Simultaneous or sequential infection of the mouse oral cavity with periodontal pathogens proved polymicrobial synergism in the aggravation of the pre-existing aortic atherosclerotic lesions. This may be contributed by the activation of aortic TLR and inflammasome signaling pathways and increase in the local aortic oxidative stress (Velsko et al. 2015). The models demonstrated hematogenous dissemination of the periodontal pathogens to distant tissues, including the heart and the aorta. The ApoE−/− mice also showed unique changes in the inflammatory response to polymicrobial infection with the progression of the atherosclerotic disease (Chukkapalli et al. 2015). The intestine is host to a vast number and varieties of microorganisms, including bacteria and fungi. Thus, bacterial–fungal interactions are likely to have significant implications for human health and disease. Using polymicrobial infection of a neutropenic mouse strain, Lopez-Medina and colleagues showed that co-colonization with *Candida albicans* significantly inhibits *P. aeruginosa* virulence without interference of the colonization ability of either organism. *C. albicans* inhibits the expression of *P. aeruginosa* siderophores, pyochelin and pyoverdine through fungal secreted products (Lopez-Medina et al. 2015). In contrast, sequential infection of a burned mouse model with sublethal doses of elastase-producing *P. aeruginosa* strain and *C. albicans* exhibited a mortality rate of 60% as opposed to less than 10% mortality of unburned mice challenged in the same way or burned mice receiving a single organism or elastase-negative *P. aeruginosa* (Neely et al. 1986). While monomicrobial infection with *C.*

albicans or *Staphylococcus aureus* is nonlethal in a mouse peritonitis model, coinfection caused ~40% mortality that was perhaps precipitated by increased proinflammatory cytokine secretion (Peters and Noverr 2013). Similarly, nonlethal intravenous infection of *E. coli* or administration of *E. coli* lipopolysaccharide (LPS) accelerated death due to lethal doses of *C. albicans* given through the intravenous route (Akagawa et al. 1995).

24.3 Mouse Models to Study Chronic Bacterial Infections

More than half of the world population is affected by chronic bacterial infections. Chronicity may result from incomplete cure of an acute infection. However, certain bacterial pathogens have evolved with specific mechanisms to survive within the host for a long time despite antimicrobial treatment. Various mouse models used to study chronic bacterial infections are summarized in Table 24.2.

24.3.1 *Helicobacter pylori* Infection

Helicobacter pylori, a Gram-negative bacterium colonizes the gastroduodenal epithelium and persists over there for decades by escaping the host defense mechanisms. The infection may be asymptomatic or may cause mild gastritis to gastric and duodenal ulcers (Nomura et al. 1994) and gastric adenocarcinoma (Wotherspoon et al. 1991). Since the natural *H. pylori* infection is restricted to humans, establishing a mouse model was initially challenging. An earlier study reported colonization of *H. pylori* in the nude mice (Karita et al. 1991; Karita et al. 1995; Marchetti et al. 1995). Later on, *H. pylori* and *H. felis* infections were established in several wild-type and gene-modified mouse strains to model different outcomes of human infections (Zhang and Moss 2012). C57BL/6 mice were extensively used to study gastric carcinogenesis. However, high-grade dysplasia was observed with *H. felis*, but not with *H. pylori* infection (Kim et al. 2003). Recently, INS-GAS mouse that overexpress human gastrin gene under the control of an insulin promoter was used to investigate the synergistic role of *Helicobacter* infection and hypergastrinemia in gastric carcinogenesis (Wang et al. 2000) C57BL/6 mice also develop severe gastritis; but unlike human disease, which shows both neutrophil and mononuclear cell infiltration into the lesion, mouse gastritis is predominantly infiltrated by the mononuclear cells (Sakagami et al. 1996). In contrast, BALB/c mice exhibit a Th2-predominant response to *Helicobacter* infection, characterized by fewer epithelial lesions, but larger number of intralesional bacteria (Mohammadi et al. 1996). These mice were also used as a model for *Helicobacter*-induced MALT lymphoma (Thompson et al. 2004). *H. pylori* infection in cytokine knockout mice shed light on the underlying mechanisms of the development of gastritis and gastric carcinoma. IFN-γ was found to play a critical role in *Helicobacter*-induced gastric inflammation and epithelial cell damage (Sawai et al. 1999), while *Helicobacter* infection and IL-1β synergistically promote gastric neoplasia (Tu et al. 2008). Similarly, IL-10

deficiency in the 129/EvSv background leads to severe hyperplastic gastritis when infected with *H. felis* (Berg et al. 1998). Mice deficient in p27 tumor suppressor gene developed metaplasia, dysplasia, and finally gastric cancer after *H. pylori* infection (Kuzushit et al. 2005).

24.3.2 Chronic Respiratory Infections

A common mouse model for chronic lung infection is cystic fibrosis (CF), an autosomal recessive disorder. It is caused by mutations in the cystic fibrosis transmembrane conductance regulator (CFTR) gene that is located on human chromosome 7 and encodes a cAMP-regulated chloride channel (Guilbault et al. 2007). The multiorgan exocrine dysfunction observed in CF patients is difficult to replicate in mouse. However, several CF mouse models have been generated, either by disruption of the CFTR gene or by introduction of frequently occurring mutations, such as F508 and G551D mutations in the ES cells (Semaniakou et al. 2018). Human patients with

Table 24.2 Mouse models of chronic bacterial infections

Disease	Organism	Mouse strain	Aim of study	Major questions addressed/ finding	References
H. pylori infection	*H. pylori*	Athymic and euthymic BALB/c	Model description	Immune response	Karita et al. (1991), Karita et al. (1995), Marchetti et al. (1995), Rabelo-Goncalves et al. (2005)
	Mouse adapted *H. pylori*	CD1	Disease pathogenesis	Colonization and vaccine studies	Dorer et al. (2013)
Chronic respiratory infection	*S. pneumoniae*	CBA/J	Intranasal aerosol pneumonia model	Effectively mimic the episode of pneumonia in humans	Iizawa et al. (1996)
	Pseudomonas aeruginosa	C57BL/6	Chronic infection by mucoid strain	Dose-dependent response	Bragonzi et al. (2005)
	Mycobacterium tuberculosis	Chimeric IFNγR1-deficient mouse	Disease pathogenesis and cellular response	Role of IFNγ, cellular response during early life infection	Saito et al. (2001), Desvignes and Ernst (2009)

(continued)

Table 24.2 (continued)

Disease	Organism	Mouse strain	Aim of study	Major questions addressed/ finding	References
Chronic *Salmonella* infection	*S.* Typhimurium	129X1/SvJ Nramp1+/+ mouse	Chronic *Salmonella* infection model	Colonization and persistence inside host	Monack et al. (2004)
	S. Typhimurium	129X1/SvJ Nramp1+/+ mouse	Chronic *Salmonella* infection model	Bacterial colonization in the gall bladder tissue	Crawford et al. (2010)
	S. Typhi	Immuno-deficient Rag2(−/−) γc(−/−) mice	Chronic *Salmonella* infection model	Bacterial pathogenesis and therapeutic strategies	Song et al. (2010), Firoz Mian et al. (2011)
UTI	*E. coli*	BALB/c	Disease pathophysiology	Comparing the route of inoculation	Schaeffer et al. (1987); Hopkins et al. (1995)
	E. coli	C57BL/6	Disease pathophysiology	Host immune response	Gunther et al. (2001), Lane et al. (2007)
Chronic colitis infection	*C. difficile*	C57BL/6	Disease pathophysiology	Prophylactic effects of *B. fragilis in a CDI mouse model*	Deng et al. (2018)
	C. difficile	C57BL/6	Mouse relapse CDI model	Host immune response	Sun et al. (2011)
	C. difficile	C57BL/6	Mouse model of antibiotic-induced CDAD	Disease pathogenesis	Chen et al. (2008)
Chronic wound infection	*MRSA, Pseudomonas aeruginosa*	FVB/N	Disease model description with bioluminescent bacteria	Enhancement of antimicrobial photodynamic therapy	Fila et al. (2016)
	Staphylococcus aureus Staphylococcus epidermidis	C57Bl6/J	Murine cutaneous wound model	Wound healing and biofilm visualization	Schierle et al. (2009)
	Pseudomonas aeruginosa	Diabetic mice	Disease model description	Wound healing and antibiotic tolerance	Zhao et al. (2010), Watters et al. (2013)

CF are frequently colonized by *P. aeruginosa* and *S. aureus*, whereas spontaneous colonization with the typical CF pathogens was not found in CF mice. Administration of free *P. aeruginosa* causes acute, not chronic, lung infection, and specific techniques such as intranasal inoculation with agar beads laden with *P. aeruginosa* revealed defects in bacterial clearance, resulting an inflammatory response in CFTR mutant mice (Heeckeren et al. 1997). Shah et al. demonstrated that overexpression of ATP12A in CF mice airways leads to impaired airway host defense and increased bacterial load (Shah et al. 2016). Very recently, a G542XCF mouse model was generated with CRISPR/Cas9 gene editing method (McHugh et al. 2018). These mice have decreased CFTR expression and lack CFTR functions in the airways and intestine.

Inbred mouse strains CBA, C3HeB/FeJ, DBA/2, and 129SvJ are susceptible to chronic *Mycobacterium tuberculosis*, whereas C57BL/6 J and BALB/c are resistant (Medina and North 1998). In vivo studies help us to understand the mechanisms of disease progression as well as cellular response mediated by the host to combat the infection.

24.3.3 Chronic *Salmonella* Infection

Regardless of adequate treatment of acute typhoid fever, *S*. Typhi persists in the gallbladder of 3–5% of the affected individuals, resulting in an asymptomatic and chronic infection. They shed bacteria in their stools and urine, which can further infect other individuals, leading to a major public health hazard. There are cases of asymptomatic carriers who developed adenocarcinoma of the gall bladder (Gonzalez-Escobedo et al. 2011). Monack et al. (2004) studied the chronic infection of *S*. Typhimurium by infecting 129X1/SvJ Nramp1+/+ mouse through oral route and found detectable presence of the bacterium in the gall bladder for one year post-infection (Monack et al. 2004). Using this model, another study was conducted where mice were fed with lithogenic diet for 6–8 weeks, which facilitates the formation of cholesterol gallstones in mice. Subsequent *S*. Typhimurium infection resulted in enhanced bacterial colonization in the gall bladder tissue and bile of the mice. Electron microscopic analysis showed bacterial biofilms on the gallstones (Crawford et al. 2010). A separate study suggested that an immunodeficient Rag2(−/−)γc(−/−) mice, engrafted with human fetal liver hematopoietic stem and progenitor cells effectively support *S*. Typhi infection and is very useful to elucidate bacterial pathogenesis (Song et al. 2010). Another study with humanized mouse model, where a lymphoid RAG-2-(−/−) γ(c)(−/−) mouse was engrafted with human leukocytes demonstrated that intravenous administration of *S*. Typhi was able to establish successful infection. A significant bacterial load was found in the liver, spleen, blood, and bone marrow of these mice (Firoz Mian et al. 2011).

24.3.4 Chronic Colitis Model

An increased incidence of morbidity and mortality of patients infected with *Clostridium difficile* are observed due to the emergence of hypervirulent, antibiotic-resistant strains. This Gram-positive, spore-forming bacillus causes nosocomial antibiotic-associated diarrhea and colitis, which are collectively referred to as CDI. Numerous in vivo models including hamsters, rabbits, guinea pigs, and rats were used to study the pathogenesis of CDI. However, a recently developed mouse CDI model closely resembled the human infection (Chen et al. 2008). Invading bacterium releases two exotoxins, TcdA and TcdB to establish successful colonization of the host. One study reported that vancomycin treatment of mice delays disease recurrence and generate neutralizing polysera against bacterial exotoxins (Sun et al. 2011). Another study showed that short-chain fatty acids, such as butyrate protects intestinal epithelial cells of CDI mouse from tissue damage by the activation and stabilization of HIF-1 transcription factor (Fachi et al. 2019). Clinical cases reported significant decrease of *Bacteroides fragilis* in patients infected with *Clostridium difficile,* leading to the study prophylactic role of *Bacteroides fragilis* in CDI mouse model. *Bacteroides fragilis* confers protection by modulating the gut microbiota of the infected mice (Deng et al. 2018).

24.3.5 Urinary Tract Infection

Urinary tract infection is another severe bacterial infection, frequently caused by uropathogenic *Escherichia coli*. Though it primarily affects women, young boys and elderly men are also at risk. Upper UTI involves bladder and kidney, which are known as cystitis and pyelonephritis, respectively. There are many murine models to study the pathophysiology of UTI. Hopkins et al. (1995) effectively introduced bacteria into the bladder through intraurethral and transurethral routes, with the induction of vesicoureteral reflux (VUR) (Hopkins et al. 1995). Most studies with mouse models used polyethylene plastic catheter tubes, fitted over needles for the administration of bacteria through it. This method reduces induction of VUR. There are reports of similar mouse models to study several other uropathogenic bacteria, such as *Enterococcus faecalis* and *Klebsiella pneumoniae* (Rosen et al. 2008a, b).

24.3.6 Chronic Wound Infections

Chronic infections with multispecies biofilms are a major problem in the diabetic population. In an obese diabetic mouse (BKS.Cg-m+/+ Lepr(db)/J) model for human type 2 diabetes, inner thigh abscess was induced by subcutaneous injection of mixed cultures containing *Escherichia coli*, *Bacteroides fragilis*, and *Clostridium perfringens*. Synergy, as determined by statistically significant increase in the number of bacterial pathogens following coinfection as opposed to infection with the individual pathogens was found between *E. coli* and *B. fragilis*, but *C. Perfringens*

was antagonistic (Mastropaolo et al. 2005). Biofilm-associated chronic wound infection was also modeled in *db/db* mice (diabetic mice that have a spontaneous mutation in the leptin receptor, resulting in insulin tolerance). A full thickness, excision wound was transferred and infected over time with bacterial species of the mouse normal skin flora, such as *S. aureus,* coagulase-negative *Staphylococcus* sp., *Enterococcus* sp., *Enterobacter cloacae*, and *Pseudomonas* sp. (Dhall et al. 2014). In an elegant experiment, Dalton et al. (2011) demonstrated "biofilm transplant" from an infected wound and showed that the transfer of planktonic cultures would instead allow growth of only one species (Dalton et al. 2011).

24.4 Bystander Infection

In most intances, mice being used in studying the host's immune system in response to bacterial infection are housed in specific pathogen-free conditions in the laboratories. Humans and mice both are exposed to the various pathogens in the environment throughout their lives. This has shaped their immune system to fight against those disease-causing pathogens. Specific pathogen-free conditions lead to immature immune system in mice. This could be less representative of the real life infections. Previous history of microbial exposure would be helpful to recapitulate the disease and immune response (Beura et al. 2016; Reese et al. 2016). A recent work reported that significant colonization of a novel protist, residing in the mouse intestine, protected mice from *Salmonella* Typhimurium infection (Chudnovskiy et al. 2016). Pathogen-free animals did not develop colitis. C57L/J mice infected with *Helicobacter* species and on lithogenic diet developed gallstones (Maurer et al. 2005) and enhanced colitis (Ward et al. 1996). Bystander infections could alter the basal immune activation of the host. A study reported significant increase in lymphatic leakage into the mesenteric adipose tissue and reduced number of migratory dendritic cells were observed with *Yersinia pseudotuberculosis* infection in mice. However, although the bacterial infection is resolved with antibiotic treatment, it results in alterations of the intestinal microbiota, which persists for long time after pathogen clearance. Similar observations were seen with *Yersinia enterocolitica* infection in Toll-like receptor 1-deficient mice. These studies explain that acute infections drive changes in intestinal microflora which eventually lead to chronic illness (Fonseca et al. 2015, Kamdar et al. 2016).

24.5 Conclusion

Murine models are attractive tools for researchers. They are extensively used in biomedical studies. They can be easily manipulated genetically to mimic human physiological conditions and disease states, which further aid in studying disease pathophysiology. Although mice and humans differ in the disease response to a particular pathogen, genetic engineering solves the issues by creating desired mutations to reflect the human infection and study disease progression. The mouse model

indeed allows unbiased approaches to screen various drug targets and potential vaccine candidates.

References

Abe PM, Lennard ES, Holland JW (1976) *Fusobacterium necrophorum* infection in mice as a model for the study of liver abscess formation and induction of immunity. Infect Immun 13(5):1473–1478

Akagawa G, Abe S, Yamaguchi H (1995) Mortality of *Candida albicans*-infected mice is facilitated by superinfection of *Escherichia coli* or administration of its lipopolysaccharide. J Infect Dis 171(6):1539–1544

Akiyama H, Kanzaki H, Abe Y, Tada J, Arata J (1994) *Staphylococcus aureus* infection on experimental croton oil-inflamed skin in mice. J Dermatol Sci 8(1):1–10

Archer KA, Alexopoulou L, Flavell RA, Roy CR (2009) Multiple MyD88-dependent responses contribute to pulmonary clearance of *Legionella pneumophila*. Cell Microbiol 11(1):21–36

Archer KA, Ader F, Kobayashi KS, Flavell RA, Roy CR (2010) Cooperation between multiple microbial pattern recognition systems is important for host protection against the intracellular pathogen *Legionella pneumophila*. Infect Immun 78(6):2477–2487

Azoulay-Dupuis E, Bedos JP, Vallée E, Hardy DJ, Swanson RN, Pocidalo JJ (1991) Antipneumococcal activity of ciprofloxacin, ofloxacin, and temafloxacin in an experimental mouse pneumonia model at various stages of the disease. J Infect Dis 163(2):319–324

Baqar S, Burg EF, Murphy JR (1999) Chapter 26 - mouse models of *Campylobacter jejuni* infection. In: Zak O, Sande MA (eds) Handbook of animal models of infection. Academic, London, pp 223–239

Barthel M, Hapfelmeier S, Quintanilla-Martínez L, Kremer M, Rohde M, Hogardt M, Pfeffer K, Rüssmann H, Hardt W-D (2003) Pretreatment of mice with streptomycin provides a *Salmonella enterica* serovar Typhimurium colitis model that allows analysis of both pathogen and host. Infect Immun 71(5):2839–2858

Basu S, Pickett MJ (1969) Reaction of *Vibrio cholerae* and choleragenic toxin in ileal loop of laboratory animals. J Bacteriol 100(2):1142–1143

Belkacem N, Hong E, Antunes A, Terrade A, Deghmane A-E, Taha M-K (2016) Use of animal models to support revising meningococcal breakpoints of β-lactams. Antimicrob Agents 60(7):4023–4027

Berg DJ, Lynch NA, Lynch RG, Lauricella DM (1998) Rapid development of severe hyperplastic gastritis with gastric epithelial dedifferentiation in *Helicobacter felis*-infected IL-10(-/-) mice. Am J Pathol 152(5):1377–1386

Bergmann S, Beard PM, Pasche B, Lienenklaus S, Weiss S, Gahan CG, Schughart K, Lengeling A (2013) Influence of internalin A murinisation on host resistance to orally acquired listeriosis in mice. BMC Microbiol 13:90

Berrington WR, Iyer R, Wells RD, Smith KD, Skerrett SJ, Hawn TR (2010) NOD1 and NOD2 regulation of pulmonary innate immunity to *Legionella pneumophila*. Eur J Immunol 40(12):3519–3527

Beura LK, Hamilton SE, Bi K, Schenkel JM, Odumade OA, Casey KA, Thompson EA, Fraser KA, Rosato PC, Filali-Mouhim A, Sekaly RP, Jenkins MK, Vezys V, Haining WN, Jameson SC, Masopust D (2016) Normalizing the environment recapitulates adult human immune traits in laboratory mice. Nature 532:512

Bhinder G, Stahl M, Sham HP, Crowley SM, Morampudi V, Dalwadi U, Ma C, Jacobson K, Vallance BA (2014) Intestinal epithelium-specific MyD88 signaling impacts host susceptibility to Infectious colitis by promoting protective goblet cell and antimicrobial responses. Infect Immun 82(9):3753–3763

Bina J, Zhu J, Dziejman M, Faruque S, Calderwood S, Mekalanos J (2003) ToxR regulon of *Vibrio cholerae* and its expression in vibrios shed by cholera patients. Proc Natl Acad Sci U S A 100(5):2801–2806

Bishop AL, Patimalla B, Camilli A (2014) *Vibrio cholerae*-induced inflammation in the neonatal mouse cholera model. Infect Immun 82(6):2434–2447

Bitar R, Tarpley J (1985) Intestinal perforation in typhoid fever: a historical and state-of-the-art review. Rev Infect Dis 7(2):257–271

Bone RCC, Fisher CJ, Clemmer TP, Slotman GJ, Metz CA, Balk RA (1989) Sepsis syndrome: a valid clinical entity. Crit Care Med 17(5):389–393

Boon RJ, Beale AS (1987) Response of *Streptococcus pyogenes* to therapy with amoxicillin or amoxicillin-clavulanic acid in a mouse model of mixed infection caused by *Staphylococcus aureus* and *Streptococcus pyogenes*. Antimicrob Agents Chemother 31(8):1204–1209

Bragonzi A, Worlitzsch D, Pier GB, Timpert P, Ulrich M, Hentzer M, Andersen JB, Givskov M, Conese M, Doring G (2005) Nonmucoid *Pseudomonas aeruginosa* expresses alginate in the lungs of patients with cystic fibrosis and in a mouse model. J Infect Dis 192(3):410–419

Brieland J, Freeman P, Kunkel R, Chrisp C, Hurley M, Fantone J, Engleberg C (1994) Replicative *Legionella pneumophila* lung infection in intratracheally inoculated A/J mice. A murine model of human Legionnaires' disease. Am J Pathol 145(6):1537–1546

Briles DE, Nahm M, Schroer K, Davie J, Baker P, Kearney J, Barletta R (1981) Antiphosphocholine antibodies found in normal mouse serum are protective against intravenous infection with type 3 Streptococcus pneumoniae. J Exp Med 153(3):694–705

Buckle GC, Walker CLF, Black RE (2012) Typhoid fever and paratyphoid fever: systematic review to estimate global morbidity and mortality for 2010. J Glob Health 2(1):010401

Calderon Toledo C, Arvidsson I, Karpman D (2011) Cross-reactive protection against enterohemorrhagic *Escherichia coli* infection by enteropathogenic *E. coli* in a mouse model. Infect Immun 79(6):2224–2233

Canvin JR, Marvin AP, Sivakumaran M, Paton JC, Boulnois GJ, Andrew PW, Mitchell TJ (1995) The role of pneumolysin and autolysin in the pathology of pneumonia and septicemia in mice infected with a type 2 pneumococcus. J Infect Dis 172(1):119–123

Chakraborty K, Ghosh S, Koley H, Mukhopadhyay AK, Ramamurthy T, Saha DR, Mukhopadhyay D, Roychowdhury S, Hamabata T, Takeda Y, Das S (2008) Bacterial exotoxins downregulate cathelicidin (hCAP-18/LL-37) and human beta-defensin 1 (HBD-1) expression in the intestinal epithelial cells. Cell Microbiol 10(12):2520–2537

Chang C, Miller JF (2006) *Campylobacter jejuni* colonization of mice with limited enteric flora. Infect Immun 74(9):5261–5271

Chen X, Katchar K, Goldsmith JD, Nanthakumar N, Cheknis A, Gerding DN, Kelly CP (2008) A mouse model of *Clostridium difficile*-associated disease. Gastroenterology 135(6):1984–1992

Chowdhury R, Mandal RS, Das S (2015) An AIL family protein promotes type three secretion system-1-independent invasion and pathogenesis of *Salmonella enterica* serovar Typhi. Cell Microbiol 17(4):486–503

Chudnovskiy A, Mortha A, Kana V, Kennard A, Ramirez JD, Rahman A, Remark R, Mogno I, Ng R, Gnjatic S, Amir ED, Solovyov A, Greenbaum B, Clemente J, Faith J, Belkaid Y, Grigg ME, Merad M (2016) Host-protozoan interactions protect from mucosal infections through activation of the inflammasome. Cell 167(2):444–456

Chukkapalli SS, Velsko IM, Rivera-Kweh MF, Zheng D, Lucas AR, Kesavalu L (2015) Polymicrobial oral infection with four periodontal bacteria orchestrates a distinct inflammatory response and atherosclerosis in ApoE null mice. PLoS One 10(11):e0143291

Chukkapalli SS, Easwaran M, Rivera-Kweh MF, Velsko IM, Ambadapadi S, Dai J, Larjava H, Lucas AR, Kesavalu L (2017) Sequential colonization of periodontal pathogens in induction of periodontal disease and atherosclerosis in LDLR null mice. Pathog Dis 75(1):ftx003

Coburn B, Li Y, Owen D, Vallance BA, Finlay BB (2005) *Salmonella enterica* serovar Typhimurium pathogenicity island 2 is necessary for complete virulence in a mouse model of Infectious enterocolitis. Infect Immun 73(6):3219–3227

Crawford RW, Rosales-Reyes R, de Ramirez-Aguilar ML, Chapa-Azuela O, Alpuche-Aranda C, Gunn JS (2010) Gallstones play a significant role in *Salmonella* spp. gallbladder colonization and carriage. Proc Natl Acad Sci U S A 107(9):4353–4358

Crump J, Luby SP, Mintz ED (2004) The global burden of typhoid fever. Bull World Health Organ 82(5):346–353

Czuprynski CJ, Faith NG, Steinberg H (2003) A/J mice are susceptible and C57BL/6 mice are resistant to *Listeria monocytogenes* infection by intragastric inoculation. Infect Immun 71(2):682–689

Dalton T, Dowd SE, Wolcott RD, Sun Y, Watters C, Griswold JA, Rumbaugh KP (2011) An in vivo polymicrobial biofilm wound infection model to study interspecies interactions. PLoS One 6(11):e27317

Das S, Chowdhury R, Ghosh S, Das S (2017) A recombinant protein of *Salmonella Typhi* induces humoral and cell-mediated immune responses including memory responses. Vaccine 35(35 Pt B):4523–4531

Day DW, Mandal BK, Morson BC (1978) The rectal biopsy appearances in *Salmonella colitis*. Histopathology 2(2):117–131

Deckert M, Soltek S, Geginat G, Lütjen S, Montesinos-Rongen M, Hof H, Schlüter D (2001) Endogenous interleukin-10 is required for prevention of a hyperinflammatory intracerebral immune response in *Listeria monocytogenes* meningoencephalitis. Infect Immun 69(7):4561–4571

Deng H, Yang S, Zhang Y, Qian K, Zhang Z, Liu Y, Wang Y, Bai Y, Fan H, Zhao X, Zhi F (2018) *Bacteroides fragilis* prevents *Clostridium difficile* infection in a mouse model by restoring gut barrier and microbiome regulation. Front Microbiol 9:2976

Desvignes L, Ernst JD (2009) Interferon-gamma-responsive nonhematopoietic cells regulate the immune response to *Mycobacterium tuberculosis*. Immunity 31(6):974–985

Dhall S, Do DC, Garcia M, Kim J, Mirebrahim SH, Lyubovitsky J, Lonardi S, Nothnagel EA, Schiller N, Martins-Green M (2014) Generating and reversing chronic wounds in diabetic mice by manipulating wound redox parameters. J Diabetes Res 2014:18

Dorer MS, Cohen IE, Sessler TH, Fero J, Salama NR (2013) Natural competence promotes Helicobacter pylori chronic infection. Infect Immun 81(1):209–215

Duan F, March JC (2010) Engineered bacterial communication prevents *Vibrio cholerae* virulence in an infant mouse model. Proc Natl Acad Sci U S A 107(25):11260–11264

Enocksson A, Lundberg J, Weitzberg E, Norrby-Teglund A, Svenungsson B (2004) Rectal nitric oxide gas and stool cytokine levels during the course of infectious gastroenteritis. Clin Diagn Lab Immunol 11(2):250–254

Fachi JL, Felipe JDS, Pral LP, da Silva BK, Correa RO, de Andrade MCP, da Fonseca DM, Basso PJ, Camara NOS, de Sales e Souza EL, dos Santos Martins F, Guima SES, Thomas AM, Setubal JC, Magalhães YT, Forti FL, Candreva T, Rodrigues HG, de Jesus MB, Consonni SR, Farias ADS, Varga-Weisz P, Vinolo MAR (2019) Butyrate protects mice from *Clostridium difficile*-Induced colitis through an HIF-1-dependent mechanism. Cell Rep 27(3):750–761

Fernandez MI, Thuizat A, Pedron T, Neutra M, Phalipon A, Sansonetti PJ (2003) A newborn mouse model for the study of intestinal pathogenesis of shigellosis. Cell Microbiol 5(7):481–491

Fila G, Kasimova K, Arenas Y, Nakonieczna J, Grinholc M, Bielawski MP, Lilge L (2016) Murine model imitating chronic wound infections for evaluation of antimicrobial photodynamic therapy efficacy. Front Microbiol 7:1258

Finch CE, Crimmins EM (2004) Inflammatory exposure and historical changes in human lifespans. Science 305(5691):1736–1739

Firoz Mian M, Pek EA, Chenoweth MJ, Ashkar AA (2011) Humanized mice are susceptible to *Salmonella typhi* infection. Cell Mol Immunol 8(1):83–87

Fonseca DM, Hand TW, Han SJ, Gerner MY, Glatman Zaretsky A, Byrd AL, Harrison OJ, Ortiz AM, Quinones M, Trinchieri G, Brenchley JM, Brodsky IE, Germain RN, Randolph GJ, Belkaid Y (2015) Microbiota-dependent sequelae of acute infection compromise tissue-specific immunity. Cell 163(2):354–366

Fullner KJ, Boucher JC, Hanes MA, Haines GK, Meehan BM, Walchle C, Sansonetti PJ, Mekalanos JJ (2002) The contribution of accessory toxins of *Vibrio cholerae* O1 El Tor to the proinflammatory response in a murine pulmonary cholera model. J Exp Med 195(11):1455–1462

Gentile LF, Nacionales DC, Lopez MC, Vanzant E, Cuenca A, Szpila BE, Cuenca AG, Joseph A, Moore FA, Leeuwenburgh C, Baker HV, Moldawer LL, Efron PA (2014) Host responses to sepsis vary in different low-lethality murine models. PLoS One 9(5):e94404

Ghosh S, Chakraborty, Nagaraja T, Basak S, Koley H, Dutta S, Mitra U, Das S (2011) An adhesion protein of *Salmonella enterica* serovar Typhi is required for pathogenesis and potential target for vaccine development. Proc Natl Acad Sci U S A 108(8):3348–3353

Giallourou N, Medlock GL, Bolick DT, Medeiros PH, Ledwaba SE, Kolling GL, Tung K, Guerry P, Swann JR, Guerrant RL (2018) A novel mouse model of *Campylobacter jejuni* enteropathy and diarrhea. PLoS Pathog 14(3):e1007083

Gibson DL, Ma C, Bergstrom KS, Huang JT, Man C, Vallance BA (2008) MyD88 signalling plays a critical role in host defence by controlling pathogen burden and promoting epithelial cell homeostasis during *Citrobacter rodentium*-induced colitis. Cell Microbiol 10(3):618–631

Gisby J, Bryant J (2000) Efficacy of a new cream formulation of mupirocin: comparison with oral and topical agents in experimental skin infections. Antimicrob Agents Chemother 44(2):255–260

Gomez JE, McKinney JD (2004) *M. tuberculosis* persistence, latency, and drug tolerance. Tuberculosis 84(1):29–44

Gonçalves NS, Ghaem-Maghami M, Monteleone G, Frankel G, Dougan G, Lewis DJM, Simmons CP, MacDonald TT (2001) Critical role for tumor necrosis factor alpha in controlling the number of lumenal pathogenic bacteria and immunopathology in Infectious colitis. Infect Immun 69(11):6651–6659

Gonzalez-Escobedo G, Marshall JM, Gunn JS (2011) Chronic and acute infection of the gall bladder by *Salmonella Typhi*: understanding the carrier state. Nat Rev Microbiol 9(1):9–14

Grandgirard D, Steiner O, Tauber MG, Leib SL (2007) An infant mouse model of brain damage in pneumococcal meningitis. Acta Neuropathol 114(6):609–617

Guilbault C, Saeed Z, Downey GP, Radzioch D (2007) Cystic fibrosis mouse models. Am J Respir Cell Mol Biol 36(1):1–7

Gunther NWT, Lockatell V, Johnson DE, Mobley HL (2001) In vivo dynamics of type 1 fimbria regulation in uropathogenic *Escherichia coli* during experimental urinary tract infection. Infect Immun 69(5):2838–2846

Hapfelmeier S, Ehrbar K, Stecher B, Barthel M, Kremer M, Hardt WD (2004) Role of the *Salmonella* pathogenicity island 1 effector proteins *SipA*, *SopB*, *SopE*, and *SopE2* in *Salmonella enterica* subspecies 1 serovar Typhimurium colitis in streptomycin-pretreated mice. Infect Immun 72(2):795–809

Heeckeren A, Walenga R, Konstan MW, Bonfield T, Davis PB, Ferkol T (1997) Excessive inflammatory response of cystic fibrosis mice to bronchopulmonary infection with *Pseudomonas aeruginosa*. J Clin Invest 100(11):2810–2815

Higgins LM, Frankel G, Douce G, Dougan G, MacDonald TT (1999) *Citrobacter rodentium* infection in mice elicits a mucosal Th1 cytokine response and lesions similar to those in murine inflammatory bowel disease. Infect Immun 67(6):3031–3039

Hill GB (1977) Therapeutic evaluation of minocycline and tetracycline for mixed anaerobic infection in mice. Antimicrob Agents Chemother 11(4):625–630

Hopkins WJ, Hall JA, Conway BP, Uehling DT (1995) Induction of urinary tract infection by intraurethral inoculation with *Escherichia coli*: refining the murine model. J Infect Dis 171(2):462–465

Iizawa Y, Kitamoto N, Hiroe K, Nakao M (1996) *Streptococcus pneumoniae* in the nasal cavity of mice causes lower respiratory tract infection after airway obstruction. J Med Microbiol 44(6):490–495

Jakobsen H, Bjarnarson S, Del Giudice G, Moreau M, Siegrist CA, Jonsdottir I (2002) Intranasal immunization with pneumococcal conjugate vaccines with LT-K63, a nontoxic mutant of

frontiers | Frontiers in Immunology

TYPE Original Research
PUBLISHED 09 January 2024
DOI 10.3389/fimmu.2023.1304170

OPEN ACCESS

EDITED BY
Malick Mahdi Gibani,
Imperial College London, United Kingdom

REVIEWED BY
Ugo D'Oro,
GlaxoSmithKline, Italy
Prashant Kumar,
University of Kansas, United States

*CORRESPONDENCE
Santasabuj Das
santasabujdas@yahoo.com;
dasss.niced@gov.in

RECEIVED 29 September 2023
ACCEPTED 18 December 2023
PUBLISHED 09 January 2024

CITATION
Haldar R, Dhar A, Ganguli D, Chakraborty S, Pal A, Banik G, Miyoshi S-i and Das S (2024) A candidate glycoconjugate vaccine induces protective antibodies in the serum and intestinal secretions, antibody recall response and memory T cells and protects against both typhoidal and non-typhoidal *Salmonella* serovars. *Front. Immunol.* 14:1304170. doi: 10.3389/fimmu.2023.1304170

A candidate glycoconjugate vaccine induces protective antibodies in the serum and intestinal secretions, antibody recall response and memory T cells and protects against both typhoidal and non-typhoidal *Salmonella* serovars

Risha Haldar[1], Amlanjyoti Dhar[2], Debayan Ganguli[3], Suparna Chakraborty[1], Ananda Pal[1], George Banik[4], Shin-ichi Miyoshi[5] and Santasabuj Das[1,6]*

[1]Division of Clinical Medicine, Indian Council of Medical Research (ICMR)-National Institute of Cholera and Enteric Diseases, Kolkata, India, [2]Division of Molecular Biology and Genomics, International Institute of Innovation and Technology (I3T), Kolkata, India, [3]Department of Infectious Diseases, Washington University School of Medicine at St. Louis, St. Louis, MO, United States, [4]BD Biosciences, Kolkata, India, [5]Division of Medicine, Dentistry and Pharmaceutical Sciences, Graduate School of Medicine, Dentistry and Pharmaceutical Sciences, Okayama University, Okayama, Japan, [6]Division of Biological Science, Indian Council of Medical Research (ICMR)-National Institute of Occupational Health, Ahmedabad, India

Human *Salmonella* infections pose significant public health challenges globally, primarily due to low diagnostic yield of systemic infections, emerging and expanding antibiotic resistance of both the typhoidal and non-typhoidal *Salmonella* strains and the development of asymptomatic carrier state that functions as a reservoir of infection in the community. The limited long-term efficacy of the currently licensed typhoid vaccines, especially in smaller children and non-availability of vaccines against other *Salmonella* serovars necessitate active research towards developing a multivalent vaccine with wider coverage of protection against pathogenic *Salmonella* serovars. We had earlier reported immunogenicity and protective efficacy of a subunit vaccine containing a recombinant outer membrane protein (T2544) of *Salmonella* Typhi in a mouse model. This was achieved through the robust induction of serum IgG, mucosal secretory IgA and *Salmonella*-specific cytotoxic T cells as well as memory B and T cell response. Here, we report the development of a glycoconjugate vaccine, containing high molecular weight complexes of *Salmonella* Typhimurium O-specific polysaccharide (OSP) and recombinant T2544 that conferred simultaneous protection against *S.* Typhi, *S.* Paratyphi, *S.* Typhimurium and cross-protection against *S.* enteritidis in mice. Our findings corroborate with the published studies that suggested the potential of *Salmonella* OSP as a vaccine antigen. The role of serum antibodies in vaccine-mediated protection is suggested by rapid seroconversion with high titers of serum IgG and IgA, persistently elevated titers after primary immunization along with a strong

10.3389/fimmu.2023.1304170

antibody recall response with higher avidity serum IgG against both OSP and T2544 and significantly raised SBA titers of both primary and secondary antibodies against different *Salmonella* serovars. Elevated intestinal secretory IgA and bacterial motility inhibition by the secretory antibodies supported their role as well in vaccine-induced protection. Finally, robust induction of T effector memory response indicates long term efficacy of the candidate vaccine. The above findings coupled with protection of vaccinated animals against multiple clinical isolates confirm the suitability of OSP-rT2544 as a broad-spectrum candidate subunit vaccine against human infection due to typhoidal and non-typhoidal *Salmonella* serovars.

KEYWORDS

glycoconjugate vaccine, O-specific polysaccharide (OSP), typhoidal and non-typhoidal *Salmonella* serovars, secretory IgA (sIgA), serum bactericidal assay (SBA), soft agar motility inhibition assay, antibody avidity, memory response

Introduction

Gram-negative enteric pathogen *Salmonella* is a significant contributor to infectious disease-associated morbidity and mortality of the populations around the world. Among different serovars that cause human infections; enteric fever, manifested by an acute febrile illness with mild to moderate gastrointestinal symptoms is caused by the typhoidal *Salmonella* strains, such as *S.* Typhi and *S.* Paratyphi and is more common in South-East Asia (1). *Salmonella* Typhimurium and *Salmonella* Enteritidis, in particular, are among the most common non-typhoidal *Salmonella* (NTS) strains causes gastroenteritis without spread of the bacteria to the blood or visceral organs in other parts of the world, such as US, UK and Africa. However, invasive NTS (non-typhoidal *Salmonella*) disease is not uncommon, especially among immunocompromised individuals with case fatality rate reaching as high as 15% (2). On the other hand, around 20% of untreated enteric fever patients die of complications like intestinal perforation or encephalopathy (2). According to estimates from the Global Burden of Disease (GBD) 2019 report by the Institute of Health Metrics and Evaluation, typhoid, paratyphoid and invasive non-typhoidal infection were responsible for 40%, 9%, and 29% of all *Salmonella* mortality with 17%, 2% and 45% deaths, respectively in under 5 children (3). Further, gallstone disease has shown an association with *Salmonella* carriage that may lead to adenocarcinoma of the gall bladder.

Vaccination remains the most attractive and immediate solution for the prevention of transmission of human *Salmonella* infections. A live attenuated (*S.* Typhi Ty21a strain) and a subunit (Vi-polysaccharide) vaccine against *S.* Typhi are globally available in different countries. However, available vaccines are of only modest efficacy in the long run, while safety and efficacy remain major concerns for the live and Vi-based vaccines, respectively in the small children (4). Recent development of Vi-polysaccharide based glycoconjugate vaccines (Vi-tetanus toxoid, Vi-diphtheria toxoid, Vi-rEPA, Vi-CRM197 etc) has generated considerable hope, but their long-term efficacy in typhoid endemic areas need further proof (5). Moreover, protection induced by the available Vi-conjugate vaccines would still depend on systemic anti-Vi antibodies (6) due to the absence of intrinsic *Salmonella* proteins and would confer little protection against *S.* Paratyphi A and B and Vi-negative *S.* Typhi strains. However, cross-protection against *S.* Paratyphi B was reported with the live typhoid vaccine (7).

In contrast to the available typhoid vaccines, no vaccine against *S.* Paratyphi and NTS (non-typhoidal *Salmonella*) infections has been licensed so far. Phase 1 studies were conducted to investigate the effectiveness of the oral, live-attenuated *S.* Paratyphi A vaccine (CVD 1902), while preclinical studies evaluated oral vaccines against *S.* Typhimurium (CVD 1921 and CVD 1941) (8). Phase 1 trial with the live vaccine WT05 against iNTS resulted in prolonged stool shedding in volunteers, leading to its abandonment. The major challenge in the development of live-attenuated vaccines is the optimal degree of attenuation without reducing the immunogenicity. While the GMMA (Generalized Modules for Membrane Antigens) vaccines against *S.* Typhimurium and *S.* Enteritidis are safer than the live vaccines and induced *Salmonella*-specific B and T cell immunity, an optimal balance between the reactogenicity and immunogenicity in humans is yet to be established (8).

Recombinant *Salmonella* proteins like flagellin and outer membrane proteins (Omp C, F, and D) were examined in the vaccination strategy that generated *Salmonella*-specific B and T cells. However, proteins having multiple membrane-spanning domains have problems maintaining their structure, leading to the induction of antibodies with poor functions. Further, such vaccines are not always accessible to simple production methods and may require a laborious procedure associated with increased risk of contamination, particularly with lipopolysaccharide (LPS) (9). In addition, FliC was reported by other studies to cause significant toxicities in mice, such as liver injury, acute cardiac

dysfunction, pro-apoptotic signaling and sepsis-like systemic inflammatory response (10–12). Few published reports suggested the conserved type 3 secretion system tip and translocator proteins of NTS (non-typhoidal *Salmonella*) and their chimera as vaccine candidates for serotype-independent protection (13). In contrast, several other protein subunit vaccines provided limited protection only against the homologous NTS (non-typhoidal *Salmonella*) serovar. Overall, subunit vaccines developed against the NTS (non-typhoidal *Salmonella*) strains to-date are at best modestly efficacious, for other (14, 15).

Bacterial membrane polysaccharides have been successfully incorporated in different candidate vaccines against different pathogenic strains (16–18). *Salmonella* O-antigen (O-specific polysaccharide or OSP) is a component of the outer membrane of Gram-negative bacteria which forms the distal portion of LPS. Clinical studies have implicated it as a target for protective immunity against non-Typhi serotypes as anti-OSP antibody was able to mediate serum bactericidal activity in healthy adults and children in the United States (19). Other studies showed that OSP-specific antibodies were found to kill *Salmonella in vivo* by lowering the bacterial loads in blood, liver, and spleen following passive immunization in mice and *in vitro* studies showed complement-mediated and phagocytosis mediated bacterial killing (20). Although *Salmonella* OSP molecules in their unconjugated state have limited immunogenicity, covalent attachment to proteins significantly enhances the immune response and allows their incorporation into OSP-based vaccines (21). Several formulations with different carrier proteins (TT, DT, CRM197, FliC), chemically conjugated to OSP showed considerable promise in mouse experiments. However, the side chains attached to the common backbone of the O-antigens from different serovars make them antigenically unique (22, 23). For example, O:2 antigen is characteristic of *S.* Paratyphi A, whereas O:4 and O:4,5 is for *S.* Typhimurium. *S.* Enteritidis and *S.* Typhi share the O:9 antigen (24). As a result, different monovalent glycoconjugate vaccine formulations were combined for wider vaccine coverage against multiple serovars. For example, *S.* Paratyphi OSP-DT + *S.* Typhi Vi-DT, *S.* Typhimurium OSP-CRM_{197} + *S.* typhi Vi- CRM_{197} were evaluated in preclinical studies (25) while others were tested in phase I (*S.* Typhimurium COPS-FliC + *S.* Enteritidis COPS-FliC + *S.* Typhi Vi-TT) or phase II (OSP-TT + Vi-TT) trials (3). Despite the potential of broader protective coverage, combined glycoconjugate vaccine has several inherent limitations. Administration of multiple conjugate vaccine formulations with the same or different carrier proteins may increase the chance of carrier-specific epitope suppression (CIES) or bystander interference, as reviewed by various authors (26–28). The mechanisms related to the CIES describe the pre-existing immunity to a Carrier protein may inhibit the hapten or saccharide specific immune response connected to the same carrier. However, monovalent combination of OSP-TT examined in phase 2 study against *Salmonella* Paratyphi A showed significantly increased antibody titer against OSP (3-4-fold rise at day 180) (29). Besides this, preparation of a multi-glycoconjugate vaccine is time-consuming and costly. This underscores the need for the development of single formulation carrying multivalency (multivalent vaccines) that could offer protection against a variety of *Salmonella* serovars, both typhoidal and nontyphoidal.

Use of novel carrier proteins could overcome the limitations mentioned above and enable further development of vaccine formulations. A single vaccine formulation of *Salmonella*-specific antigens that covers different *Salmonella* serovars would be preferred. We report here the development of a glycoconjugate candidate vaccine where OSP from *S.* Typhimurium is chemically linked to the recombinant outer membrane protein rT2544 from *S.* Typhi. Previous studies from our laboratory reported strong immunogenic potential of rT2544, generating antigen-specific, opsonic antibodies and cytotoxic T cells that led to protection from bacterial challenge in mice (30). In addition to antigenicity of rT2544 and its protective efficacy against *S.* Typhi and *S.* Paratyphi, we observed strong adjuvanticity to OSP, leading to augmented anti-OSP antibody response. Thus, this study creates an opportunity to use rT2544 as a carrier protein in the glycoconjugate platform. Given that no vaccines with combined protective efficacies against typhoidal and non-typhoidal *Salmonella* are currently under clinical trials, development of an OSP-based trivalent vaccine containing rT2544 as the carrier protein could be a key step forward toward the development of a broad-specificity as well as safe and effective glycoconjugate vaccine.

Materials and methods

Bacterial strains, growth conditions and plasmid

Salmonella Typhi Ty2 and *Salmonella* Typhimirium LT2 were generous gifts from J. Parkhill, Sanger Institute, Hinxton, UK. Clinical isolates of *Salmonella* Typhimurium and *Salmonella* Enteritidis were gifted by A. Mukhopadhyay (ICMR-NICED, Kolkata, India), while clinical isolates of *Salmonella* Typhi and *Salmonella* Paratyphi A were received from IMTECH, Chandigarh. All *Salmonella* strains were grown in Hektoen enteric agar and *Escherichia coli* BL21, a kind gift from Dr. Rupak K. Bhadra (CSIR-IICB, Kolkata, India) was cultured in Luria–Bertani agar at 37°C. Liquid cultures of the bacterial strains were grown in Luria Broth. Bacterial culture media and pET-28a plasmid were purchased from BD Difco and Addgene (USA), respectively. The oligonucleotides used in this study were synthesized from IDT.

Cloning and expression, of recombinant T2544

t2544 ORF with four arginine coding sequences inserted at the NH2 terminus was PCR amplified, using *Salmonella* Typhi Ty2 genomic DNA as the template and the following forward and reverse primers:

FP-5'TTCGCCATGGAACGCCGCGGGATCTATATCACCGGG-3',

RP-5' GCCCTCGAGTTAGCGGCGAAAGGCGTAAGTAATGCC-3'.

The PCR product was cloned into pET28a at the NCoI and XhoI restriction enzymes (New England Biolabs) sites. After clone confirmation by restriction digestion, followed by sequencing (AgriGenome, India), the recombinant plasmid was transformed into *E. coli* BL21 (DE3). Transformed bacteria were inoculated into LB (BD Difco) broth (300 ml) and incubated until the OD_{600} reached 0.5. Recombinant T2544 expression was inducted by 1mM IPTG for 4h at 37°C, followed by centrifugation at 5000 g. The induction was confirmed by SDS-PAGE, stained with Coomassie Blue.

Extraction of rT2544 from bacterial inclusion bodies and purification by ion exchange chromatography

To isolate the inclusion bodies, induced bacterial cells were resuspended in sonication buffer (30 ml) and subjected to 5 cycles of sonication on ice, with each cycle consisting of 5 pulses of 1 sec each followed by 1-minute incubation. The power output was designed to deliver a maximum of 30 watts at a frequency of 20 kHz. The sonicated pellet was collected following centrifugation at 15000 rpm for 20 min at 4°C, and washed three times with protein extraction wash buffer (20 ml). After centrifugation, recombinant T2544 was extracted from the inclusion bodies using protein extraction buffer [10 mM Tris-HCL (pH 12.0), 5ml] and analyzed by 12% SDS-PAGE. The extracted rT2544 was purified by ion exchange chromatography using UNO sphere Q resin (Bio-rad), according to the manufacturer's protocol. A Glass econo-column (1.0 x 10 cm, Bio-Rad) was packed 50% with the resin, followed by washing with 5 column volumes (CV) of water and equilibration with 10 CV (column volume) of equilibration buffer (1X PBS, pH 7.4). The equilibrated resin was admixed with the recombinant protein (rT2544, 5ml) and kept for binding up to 3h at room temperature. The mixture was passed through the column and after washing with 3 CV (column volume) of ion exchange wash buffer, column-bound rT2544 was eluted using ion exchange elution buffer with Nacl gradient. Briefly, 1 ml of elution buffer containing 1M NaCl was inserted to the protein bound column that already had 40% of wash buffer and 1ml of eluted volume was collected. Eluted rT2544 was quantitated by Bradford Reagent (Sigma) and protein purity was determined by 12% SDS-PAGE. Protein extraction and IEC buffer compositions are mentioned in Supplementary Table 1.

Extraction and purification of OSP

Lipopolysaccharide (LPS) was purified from *S.* Typhimurium, using the hot phenol method as reported earlier (31). Briefly, *Salmonella* Typhimurium LT2 strain was cultured in Luria Broth (1L) at 37°C for 10h (OD 1.8). Formalin-inactivated cells were collected by centrifugation at 5000 g and washed twice with PBS. After resuspension in PBS (30 ml), 90% phenol (HiMedia) was used for 30 min at 68°C to extract crude LPS from the cell pellet. The suspension was centrifuged at 7,300 × g at 10°C for 1 h. The aqueous layer (60 ml) was precipitated with ethanol (final concentration 75%), and the precipitate was treated with DNAse (1 µg/mL), RNase (1 µg/mL) and Proteinase K (100 µg/mL) (all purchased from Roche), followed by dialysis overnight against PBS (pH 7.4) at 4°C. Extracted LPS was used to further extract O-specific polysaccharide (OSP). to this end, LPS was incubated with 1% acetic acid (HiMedia), pH 3.0, and 100°C for 1.5 hours, followed by ultracentrifugation at 64,000 ×g for 5h at 10°C, using a WX+ Ultra series centrifuge (Thermo Scientific). The supernatant was dialyzed for 48h against PBS (pH 7.4) and OSP was purified by size exclusion chromatography.

Conjugation of OSP and rT2544

Conjugation was performed as described earlier (31). Briefly, purified OSP (1.2 mg/ml in PBS, pH 8.5-9.0) was activated with an equal volume of cyanogen bromide (CnBr, SRL), prepared as 1.2 mg/ml in acetonitrile (Fluka). The reaction mixture was kept for 6 min on ice and the pH was maintained with 0.1M NaOH. The activated mixture was derivatized with 0.8M ADH (Sigma), dissolved in 5M $NaHCO_3$ (SRL). For this reaction, the pH was adjusted to 8-8.5 with 0.1M HCl. The reaction mixture was stirred at 4°C overnight and dialyzed against 1x PBS, pH 7.4 at the same temperature for 16 h. ADH derivatized OSP was then mixed with 3 ml of recombinant T2544 (1.25 mg/ml), followed by the addition of EDAC (0.05M) to the mixture and incubated for 4h on ice. The pH of this protein-polysaccharide mixture was maintained at 5.1 to 5.5 with 0.1 M HCl. Finally, the mixture was dialyzed against 1x PBS (pH 7.4) for 48 hours at 4°C.

Circular dichroism

Circular dichroism was performed as described earlier (32). Briefly, 1.0 ml of rT2544 (180 µg/ml) was filtered through a 0.45 µm pore-size filter to remove suspended particles, and taken in a 0.1 mm path-length quartz cuvette. Circular dichroism (CD) spectrum of the protein sample was captured at the wavelength range of 200 to 300 nm at 25°C on the Jasco-1500 spectrophotometer. A minimum of three spectra were recorded at 1 nm steps at a speed of 50 nm per minute. Baselines were subtracted and data was recorded as ellipticity (CD [mdeg]).

Fast-performance liquid chromatography

FPLC was performed as described earlier (33). Briefly, rT2544, OSP and OSP-rT2544 (conjugate) samples in normal saline (pH 7.4) were filtered through 0.22 µm syringe filters (HiMedia) and run in a Hiload 16/60 Sephacryl S300 size exclusion column (Cytiva Life Sciences) at a flow rate of 0.5 mL/min at 4°C using Biorad NGC chromatography system. The column was previously equilibrated with normal saline (pH 7.4). The buffer solution was degassed and filtered through 0.22 µm cellulose acetate membrane filters (Millipore). The polysaccharide and the protein were detected at λ =215 nm and 280 nm, respectively.

Dynamic light scattering

DLS was performed as described earlier (34, 35). Briefly, 1 ml of Protein, polysaccharide and conjugate samples at a concentration of 0.8-1 mg/ml were filtered through a 0.45 µm pore-size filter to remove particles, if any prior to the measurement. Hydrodynamic sizes of the samples were calculated using ZEN 3600 Malvern Zetasizer with 5 mW HeNe laser at 25°C. The dispersed light is gathered at 173° in this system, which employs backscatter detection.

Fourier transform infrared spectroscopy

FTIR was performed as described earlier (36). Briefly, functional groups of lyophilized samples were monitored using potassium bromide (KBr) pellet method (1:100 w/w). To create translucent 1 mm pellets, potassium bromide was combined with lyophilized samples (0.8–1.0 mg) and pressed with 7500 kg for 30 seconds. Spectra were recorded using the translucent pellet in Perkin Elmer Spectrum 100 system in the spectral region of 4000–400/cm.

Proton NMR

^{1}H NMR was performed as described earlier (34). Briefly, Lyophilized samples, dissolved in 0.5 mL of D_2O (Sigma, 99.9%) were analyzed in a 400 MHz NMR spectrometer (JOEL 400 YH) at 25°C using NMR Pipe on Mac OS X workstation. A sodium salt, TSP-D4 (0.38%) was used as a standard. The spectrometer was arranged with a 5 mm triple-resonance z-axis gradient cryogenic probe head and four frequency channels. Initial delays in the indirect dimensions were intended to provide -180° and 90° first-order phase corrections at zero and first order, respectively. States-TPPI phase cycling was used to achieve quadrature detection in the indirect dimensions with a one-second relaxation delay.

Western blot

Western blot was performed as described earlier (37). Briefly, OSP, rT2544 and OSP-rT2544 (8 µg each), resolved in 10% SDS-PAGE were transferred to a PVDF membrane (Millipore). After blocking with 5% BSA for 1 h at room temperature, membranes were incubated overnight at 4°C with polyclonal anti-rT2544 antibody (1:5000 dilutions), raised in-house. Membranes were washed with TBS-T [Tris Buffered Saline pH 7.5, containing 0.1% Tween-20 (v/v)] for 5 times and incubated with goat anti-mouse IgG antibody (1:10000 dilutions), conjugated to horseradish peroxidase (HRP) for 1 h at room temperature. After 3 washes with TBS-T in an orbital shaker, membranes were developed by chemiluminescent reagents(SuperSignal West Pico, Thermo Fisher) and the signals were captured in ChemiDoc ^{TM} MP imaging system (Bio Rad).

Animal breeding, immunization, and infection

Animal breeding and experimentation were approved by the institutional animal ethical committee (PRO/192/-June 2022-25). Female, inbred C57BL/6 and BALB/c mice (5-6 weeks old) were immunized subcutaneously with OSP (8µg), rT2544 (24 µg), or OSP-rT2544 (8µg of OSP and 24 µg of rT2544) at 2-weeks intervals for 3 times. Blood samples were taken from the immunized mice on days 0, 14, 28, 38, 110, and 120 by tail snip and incubated for 30 min at 37°C and centrifuged at 1,200 × g at 4°C for 15 min and stored at −80°C. Fecal samples were collected on days 0, 14, 28, and 38, weighed, and carefully dissolved in 100 mg/ml of PBS, containing 1% BSA (SRL), centrifuged at 15,000 × g at 4°C for 10 min, and protease inhibitor cocktails (Sigma-Aldrich) were added to the supernatants before storage at −80°C. Intestinal washes were collected after sacrifice of the C57BL/6 mice (on day 38). To this end, the small intestine was removed and washed three times with 1 ml of PBS-1% BSA (BSA, SRL). Samples were centrifuged at 10,000 × g at 4°C for 10 min, and protease inhibitor cocktails (Sigma-Aldrich) were added to the supernatants before storage at −80°C. Fourteen days after the last immunization (day 42), iron-overload BALB/c mice were infected with *Salmonella* Typhi or *Salmonella* Paratyphi A, while streptomycin pre-treated C57BL/6 mice were infected with *Salmonella* Typhimurium and *Salmonella* Enteritidis as described earlier (37–39). Briefly, BALB/c mice were treated with intraperitoneal injection of $Fe3^{+}$ as $FeCl_3$ in 10^{-4} N HCl (0.32 mg per gm of body weight) along with Desferoxamine (25 mg/Kg body weight) four hours prior to the bacterial challenge. Mice were orally infected with 5 x 10^7 CFU of *S.* Typhi or 5 x 10^5 CFU of *S.* Paratyphi A and monitored for 10 days. C57BL/6 mice were treated with streptomycin (20 mg/mouse) orally as a beverage for 24 h. At 20 h after streptomycin treatment, water and food were withdrawn for 4 h before the mice were infected orally with 5 x 10^6 CFU of *S.* Typhimurium or *S.* Enteritidis and monitored for 30 days.

Enzyme-linked immunosorbent assay

ELISA was performed as described earlier (37, 40). Microtiter plates were coated with 5 µg/ml of OSP or 2 µg/ml of rT2544 and incubated at 4°C overnight. After rinsing with PBS-T (Phosphate buffer saline, containing 0.05% Tween 20), the wells were blocked using PBS, containing 1% BSA (SRL) for 1 hour at room temperature. Following further washes, plates were incubated with serum, feces, or intestinal lavage samples, diluted serially (1:200 to 1: 102400 for IgG and 1:20 to 1:20480 for IgA) for 2 hours at room temperature. Subsequently, Goat anti-mouse IgG (1:10000) or IgA (1:5000) antibodies conjugated to HRP were added to the wells and incubated for 1 h at room temperature. The immune complex was developed using tetramethyl benzidine (TMB) substrate (BD OptEIA^{TM}) and OD_{450} of the mixture was measured in a spectrophotometer (Shimadzu, Japan).

Avidity test was performed as described earlier (41). Briefly, after overnight incubation with the respective antigens (OSP, rT2544), microtiter plates were incubated with OSP-rT2544 antisera with a dilution of 1:100 in PBS-T. To test for the avidity of serum IgG antibody, respective antigen-antibody complexes in the wells were washed (3 times) with PBS-T, containing 6M urea before the addition of HRP-conjugated anti-mouse IgG. The avidity index was calculated by multiplying the ratio of the absorbances of the wells that were washed with and without 6M urea-containing buffer by 100.

Serum cytokines (IL-4, IL-6, IFN- γ, IL-10 and TNF-α) (Invitrogen, USA) as well as IFN-γ (Krishgen biosystem) in the co-culture supernatants of T cells and BMDCs were measured using the commercial ELISA kits following the manufacturer's protocol.

Serum bactericidal assay

Serum bactericidal assay was performed according to an earlier described method (38, 42). Sera collected from the immunized C57BL/6 and BALB/c mice on day 38 of first immunization were heat-inactivated at 56°C for 20 min and serially diluted in PBS (1:100 to 1:102400). A mixture comprising of 25µl of guinea pig complement (25% final concentration) and 15 µl of PBS, 50 µl of diluted heat-inactivated serum and 10 µl of diluted bacteria (310 CFU, T_0) was prepared. The mixture was incubated for three hours (T_{180}) at 37°C with gentle agitation (130 rpm). The mixtures were plated on LB agar and the plates were incubated overnight at 37°C. Bactericidal titer of the complement-containing antisera was expressed as the dilution of the serum required for the reduction of bacterial growth by 50% at T_{180} compared with T_0. Data was analyzed using GraphPad Prism 8.0.1.244 software.

Soft agar motility inhibition assay

A motility assay was performed as described earlier (43). Briefly, soft agar (LB medium with 0.4% Bacto agar, BD Difco) was mixed with 5% intestinal lavage from the experimental mice (collected on day 38 after the first immunization dose) and left at room temperature to dry. Bacteria (1×10^6 CFU) were plated on top of the dried plates, which were incubated for 10 hours at 37°C. Bacterial motility was measured by the diameter (mm) of the clearing zones and the data was analyzed using GraphPad Prism 8.0.1.244 software.

Memory T cell assay

Myeloid precursor cells from mouse bone marrow (BM) were used to generate dendritic cells as described earlier (30). Briefly, bone marrow cells from the femur and tibia of naïve C57BL/6 mice were cultured in RPMI 1640 medium, supplemented with murine Granulocyte-Macrophage Colony Stimulating Factor (mGM-CSF, 20 ng/mL) for 7 days. On day 7, cells were harvested and starved for 12 h in RPMI 1640 containing 1% FBS, followed by stimulation with OSP or OSP-rT2544 for 24h. $CD4^+$ T cells were isolated from the spleens of the immunized mice on day 120 of the first immunization using magnetic beads (BD IMag™ anti-mouse CD4 Magnetic Particles, USA). $CD4^+$ T Cells were co-cultured for 24h at 37°C in presence of 5% CO2 with antigen-pulsed BMDCs at 1:1 ratio. IFN-γ concentration was estimated in the culture supernatants by ELISA (Krishgen biosystem), while the$CD4^+$ T cells were analyzed by flow cytometry for T-effector memory cell determination markers ($CD4^+CD62L^{low}$ $CD44^{hi}$).

Flow cytometry

Cells were stained with fluorochrome-conjugated anti-mouse antibodies following the standard protocol. Briefly, $CD4^+$ T Cells co-cultured with antigen-pulsed BMDCs were harvested and subjected to F_c blocking in FACS buffer (1:50 ratio) for 20 min on ice. Following centrifugation at 1500 rpm for 5 min at 4°C, cells were stained with fluorochrome-conjugated antibodies (BD Biosciences) against specific surface markers (CD4-Percp Cy5.5, CD44- FITC, and CD62L-PE Cy7) for 30 min at 4°C in the dark. After staining, the cells were washed three times in FACS buffer and fluorescent signals were measured by FACS ARIA-II (BD Bioscience). Data were analyzed by FlowJo (version V10.8.1).

Data analysis

Data related to CD, FPLC, DLS and FTIR were analyzed using ORIGIN software (2019b). NMR data were processed in MestReNova -9.0.1-13254 software. Antibody titers were represented as reciprocal of the log 2 values. Statistical analysis was performed using GraphPad Prism 8.0.1.244. Comparison between two groups was calculated by student t-test, while two-way ANOVA with Tukey's *post-hoc* test was performed for multiple comparisons. Statistical significance was measured at *P <0.05, **P < 0.01, ***P < 0.001, ****P < 0.0001).

Results

Purification and characterization of recombinant T2544

Cloning of pET28a-*t2544* was confirmed by restriction digestion, followed by agarose gel electrophoresis of the digested product that showed migration of *t2455* amplicon along the predicted size of 663bp (Figure 1A). Nucleotide sequencing of the clone showed in-frame cloning and correct orientation of *t2544* gene (Supplementary Figure 1A). Recombinant T2544 (rT2544) extracted from the inclusion bodies of *E. coli* BL21 (DE3) migrated along the size of 30 kDa in SDS-PAGE (Supplementary Figure 1B) and ion exchange chromatography yielded a highly purified protein of the same size (Figure 1B). Further purification by size exclusion chromatography generated a smaller peak near 104.8 ml and a major peak near 112.8 ml fractions (Figure 1C). The secondary

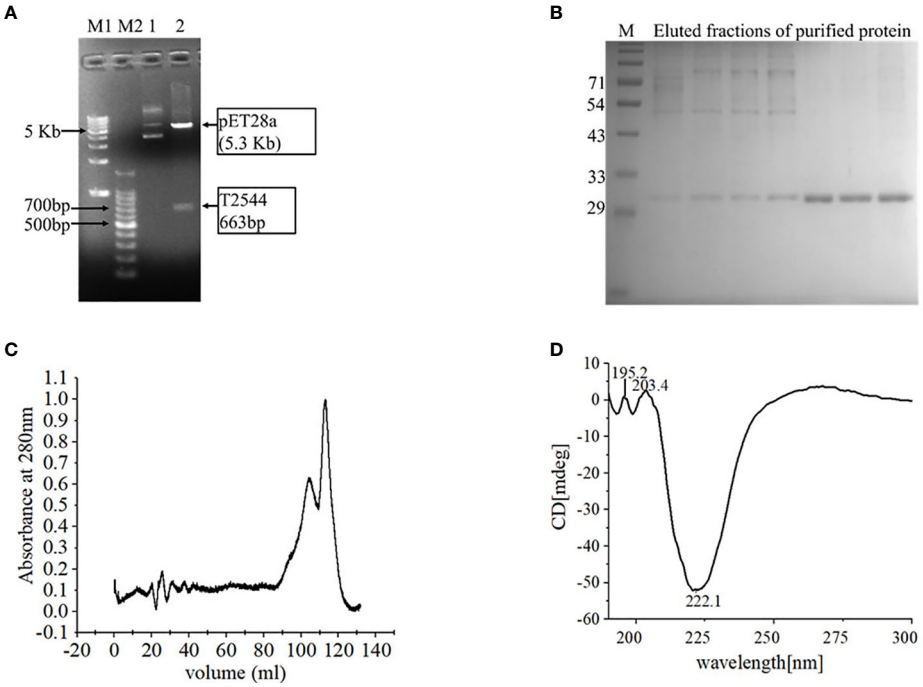

FIGURE 1
Purification and characterization of recombinant T2544. **(A)** 1% Agarose gel electrophoresis of pET28A-*t2544* after restriction digestion with XhoI and NcoI. Lane M1: 1 kb DNA ladder, M2: 100bp DNA ladder, 1: Undigested pET28A-*t2544* clone, 2: pET28A-*t2544* clone digested by XhoI and NcoI. **(B)** 12% SDS-PAGE showing the elution profile of rT2544 (3.5 µg) after ion exchange chromatography (IEC). rT2544 extracted from the inclusion bodies of E.coli was admixed with UNO sphere Q ion-exchange resin (Bio-rad), followed by binding to the Glass econo-column, 1.0 x 10 cm (Biorad) **(C)** Elution profiles of rT2544 (0.8 mg/ml) from the size exclusion chromatography column (Hiload 16/60 Sephacryl S300, Cytiva), detected at 280 nm. **(D)** Far-UV circular dichroism spectra of rT2544 (180 µg/ml) captured at the wavelength range of 200 to 300 nm at 25°C in PBS (pH 7.4) on the Jasco-1500 spectrophotometer. Data presented as ellipticity (CD [mdeg]) after subtracting the baseline values. For each analysis, experiment was replicated three times, and data from a representative experiment are shown.

structure of rT2544 detected by Far-UV CD spectra showed one negative band at 222.1 nm, indicating alpha helix, and two positive bands at 195.2 nm and 203.4 nm, suggesting β helical structures (Figure 1D). Dynamic light scattering measured the hydrodynamic radius of rT2544 as 22.16 nm (Supplementary Figure 1C).

Purification and characterization of OSP

Lipopolysaccharide extracted from *S.* Typhimurium LT2 and resolved in SDS-PAGE showed multiple higher molecular weight bands and a smear corresponding to lower molecular weights upon silver staining. Acid hydrolysis of LPS removed the smear, suggesting their origin from the lipid A component, while the core oligosaccharide bands were left behind in the gel (Figure 2A). The gel filtration profile of OSP showed two peaks near 109.23 ml and 117.9 ml fractions that corresponded to their average K_d values of ~ 22.75 kDa (Figure 2B; Supplementary Table 2). ^{1}H NMR analysis showed signals between 2.0 and 2.2 ppm, arising from the O-acetyl groups at C-2 of Abequose that confirmed the presence of the characteristic sugar of *S.* Typhimurium OSP. Signals between 1.79 and 1.97 ppm and 3.50 and 3.94 ppm of NMR spectra were generated from the protons bound to C-3 of Abequose and C-5 of Rhamnose and Abequose, respectively (Supplementary Figure 2A). Molecular radius of OSP was 4.42 nm, as calculated by DLS (Figure 2C). FTIR analysis disclosed the characteristic wave patterns of active OSP. Waves near 1650 cm^{-1} indicated carbonyl group (C=O), while those in the region of 1413-1261 cm^{-1} represented the deformation of C-H and C-OH groups. In contrast, waves near 1095 cm^{-1} and 1022 cm^{-1} corresponded to the characteristic peaks of the glycosidic linkage and the bands in the 936–800 cm^{-1} region, which is called the anomeric region, indicated the α and β configuration of the anomeric carbon (Supplementary Figure 2B).

OSP and rT2544 conjugation, purification and characterization of the conjugate

Conjugates of OSP and rT2544 displayed a smear tail in the western blots, probed with T2544 antibody, indicating heterogeneity of size and mass-to-charge ratios (Supplementary Figure 3). FPLC analysis showed the major peak of OSP-r2544 elution after the calculated void volume (41.66 ml), as opposed to the elution peaks of OSP at 109.23 ml and 117.9 ml and rT2544 at 112.8 ml (Figure 3A). Higher hydrodynamic diameter of OSP-rT2544 (57.45 nm) compared with OSP (4.42 nm) and rT2544 (22.16 nm) suggested the formation of higher-order complex formation between the polysaccharide (OSP) and the protein (rT2544) (Figure 3B). However, we observed different molar

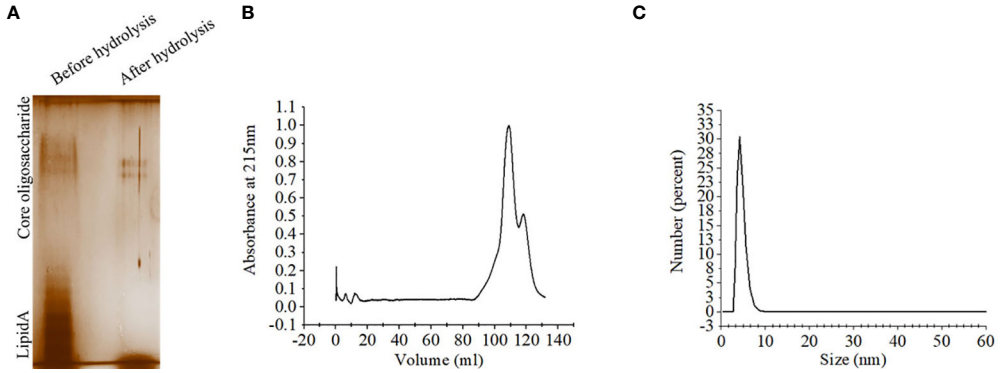

FIGURE 2
Extraction and purification of OSP. **(A)** Visualization of LPS and OSP resolved in 10% SDS-PAGE, stained by silver staining. LPS was extracted from *S.* Typhimurium LT2 strain by hot-phenol method and subjected to acid hydrolysis to isolate OSP. Lane 1: purified LPS (8 µg), Lane 2: purified OSP (8 µg). **(B)** Elution profiles of OSP (1mg/ml in normal saline, pH 7.4) eluted at a flow rate of 0.5 mL/min at 4°C from a size exclusion chromatography column (Hiload 16/60 Sephacryl S300, Cytiva), pre-equilibrated with normal saline, pH 7.4. The OSP was detected at λ =215 nm using Bio-Rad NGC chromatography system. **(C)** Dynamic light scattering (DLS) showing hydrodynamic radius (R_h) of OSP (0.88 mg/ml, PBS, pH 7.4), determined at 25°C using ZEN 3600 Malvern Zetasizer. For each analysis, experiment was replicated three times, and data from a representative experiment are shown.

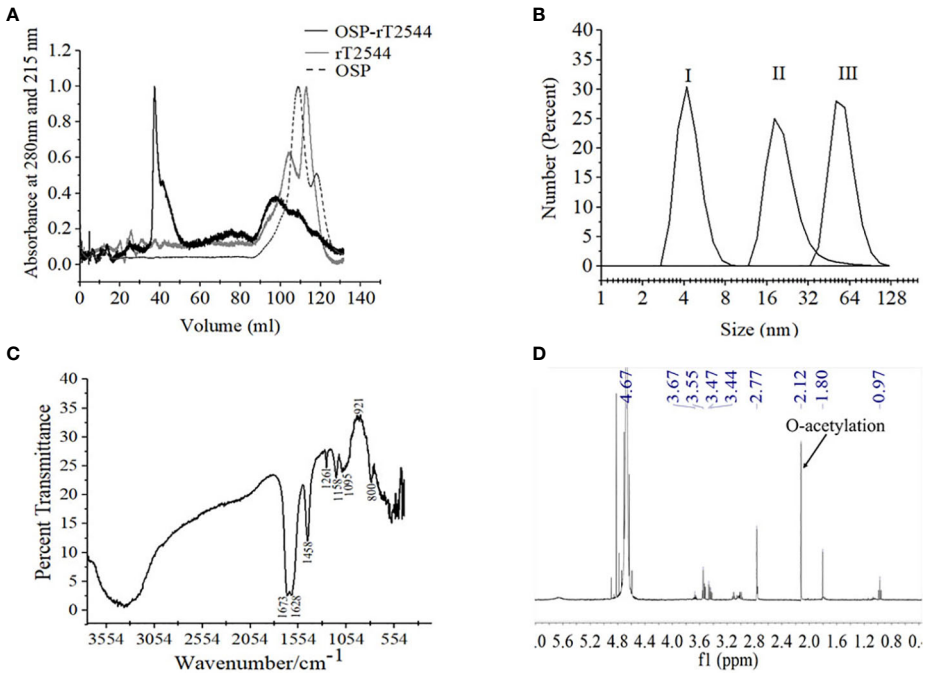

FIGURE 3
Characterization of OSP-rT2544 conjugate. **(A)** Gel filtration chromatography. OSP-rT2544 conjugate containing 1.83 mg of total protein and 0.59 mg of total sugar in normal saline (pH 7.4) was injected into Hiload 16/60 Sephacryl S300 column (Cytiva). The column was pre-equilibrated with normal saline, pH 7.4 and the flow rate was maintained at 0.5 mL/min. The conjugate (OSP-rT2544) and T2544 were observed (eluted at 41.66 ml and 112.8 ml) at 280 nm, while OSP (eluted at 109.23 ml and 117.9 ml) was observed at 215 nm at 4°C using Bio-Rad NGC chromatography system. **(B)** Dynamic light scattering (DLS) showing hydrodynamic radius (R_h) of (I) OSP (0.88 mg/ml); (II) rT2544 (0.8 mg/ml); (III) OSP-rT2544 (1 mg/ml), dissolved in PBS (pH 7.4) at 25°C using ZEN 3600 Malvern Zetasizer. **(C)** Fourier Transform Infrared (FTIR) spectrum of the lyophilized conjugated sample (OSP-rT2544) was monitored using potassium bromide (KBr) pellet method (1:100 w/w). Spectra recorded in the Perkin Elmer Spectrum 100 system in the spectral region of 4000–400/cm indicating different functional groups of OSP-rT2544: carbonyl group (C=O) (1673 cm^{-1}), C-H and C-OH groups (1458-1261 cm^{-1}), glycosidic linkage (1095 and 1158 cm^{-1}), aldehyde and ketone groups (921 and 800 cm^{-1}) and amide bond of the protein (1628 cm^{-1}). **(D)** ^{1}H NMR of lyophilized OSP-rT2544, dissolved in 0.5 mL of D_2O showing the characteristic peak of O-acetylation of OSP at C-2 of Abequose (2.12 ppm) in a 400 MHz NMR spectrometer (JOEL 400 YH) at 25°C. Additional peaks indicate protons bound to C-5 (3.4-3.6 ppm) and C-3 (1.8 ppm) of monosaccharides, the protein peaks (0.97 and 2.77 ppm) and the D2O solvent (4.67 ppm). For each analysis, experiment was replicated three times, and data from a representative experiment are shown.

ratios of OSP and rT2544 in the glycoconjugate molecules (Supplementary Table 3). To find out the functional groups in the purified OSP-rT2544 conjugate, FTIR analysis was performed. FTIR showed one additional functional group in the conjugate (OSP-rT2544), the strong amide bond of protein at 1628 cm^{-1}, which was absent in OSP. On the other hand, similar functional groups in OSP-rT2544 and OSP corresponded to different wave lengths. Thus, carbonyl groups (C=O) were detected at 1673 cm-^{1}, deformation of C-H, C-OH groups appeared near region 1458-1261 cm^{-1} and glycosidic linkage emerged at 1095 cm^{-1} and 1158 cm^{-1} in OSP-T2544. In addition, α and β configurations of the anomeric carbon were detected near the regions 921 cm^{-1} and 800 cm^{-1} (Figure 3C). However, O-acetylation pattern at C-2 of Abequose between 2.0 and 2.2 ppm was similar in OSP and OSP-T2544 in ^{1}H NMR study (Figure 3D). But, two different peaks of the OSP-rT2544 molecule that corresponded to the aliphatic region of the protein and observed near 0.97 ppm and 2.77 ppm were absent from OSP. Total sugar and protein contents and the molecular weights of the conjugate and the un-conjugated preparations used for immunization are shown in Supplementary Table 4.

Vaccination with OSP-rT2544 conferred a broad range of protection against typhoidal and non-typhoidal *Salmonella*

To investigate broad range efficacy of our candidate vaccine, BALB/c and C57BL/6 mice were immunized s.c. with three doses of OSP-rT2544, rT2544, OSP, or PBS (vehicle) at 14 days intervals (Figure 4A; Supplementary Table 5). Protective efficacy of the vaccines was evaluated in BALB/c mice for *S.* Typhi and *S.* Paratyphi A and in C57BL/6 mice for *S.* Typhimurium and *S.* Enteritidis strains, as mentioned under Materials and Methods (Supplementary Table 6). A 10xLD_{50} dose killed all the BALB/c mice within a period of 5-6 days in the vehicle- and OSP-treated groups, while 75-77% of mice that received either OSP-rT2544 or rT2544 were alive at 10 days post-infection and beyond (Figures 4B, C). On the other hand, OSP-rT2544 and OSP immunization protected 70-80% and 20% of C57BL/6 mice, respectively against *S.* Typhimurium infection, while all the mice that received rT2544 or the vehicle only died within 25 days (Figure 4D). Interestingly, 55-60% of latter mouse strain immunized with OSP-rT2544 also survived *S.* Enteritidis challenge (Figure 4E). Protection of the immunized mice was observed for both the reference as well as clinical strains, strongly suggesting the potential of OSP-rT2544 as a candidate quadrivalent vaccine for typhoidal and non-typhoidal *Salmonella* infections.

OSP-rT2544 induces protective humoral immune response against *S.* Typhi and *S.* Paratyphi A

We had earlier reported protective humoral response in mice against *S.* Typhi upon s.c. immunization with recombinant T2544. To check if rT2544 present in the conjugate vaccine is equally immunogenic, serum antibody endpoint titers (The reciprocal of the titer (1/Y) at which the absorbance of the immune sera was the same as the control (PBS immunized sera)) were measured by ELISA, 10 days after completion of the primary immunization series as well as 110 days after the first immunization dose of BALB/c mice, immunized with OSP-rT2544 or the unconjugated vaccine formulations (Figure 5A; Supplementary Table 5). The results

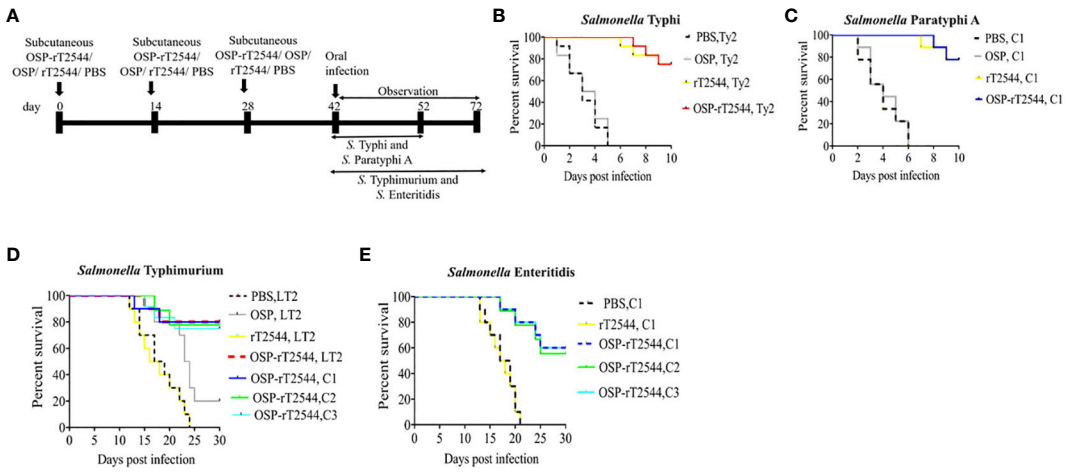

FIGURE 4
Protection of mice after subcutaneous immunization with OSP-rT2544. **(A)** Experimental scheme of mouse subcutaneous immunization with the vehicle (PBS), conjugate (OSP-rT2544) (8 µg of OSP or 24 µg of rT2544 in conjugate), or unconjugated vaccines (OSP 8 µg, rT2544 24 µg)), followed by oral bacterial challenge. **(B–E)** Kaplan-Meyer plot of cumulative mortality of the infected mice. BALB/c mice were orally challenged with *S.* Typhi Ty2 (5 x 10^{7} CFU, n= 12) **(B)** or *S.* Paratyphi A (5 x 10^{5} CFU, n=9) **(C)** and monitored for 10 days. For NTS strains, C57BL/6 mice were orally challenged with *S.* Typhimurium (5 x 10^{6} CFU of the LT2 strain (n=10), clinical strain 1 (C1, n=10), clinical strain 2 (C2, n=9) and clinical strain 3 (C3, n=12)) **(D)** or *S.* Enteritidis (5 x 10^{6} CFU of C1 (n=10), C2 (n=9) or C3 (n=10)) **(E)** and monitored for 30 days. The color scheme used to mark different experimental groups are shown in Table 1.

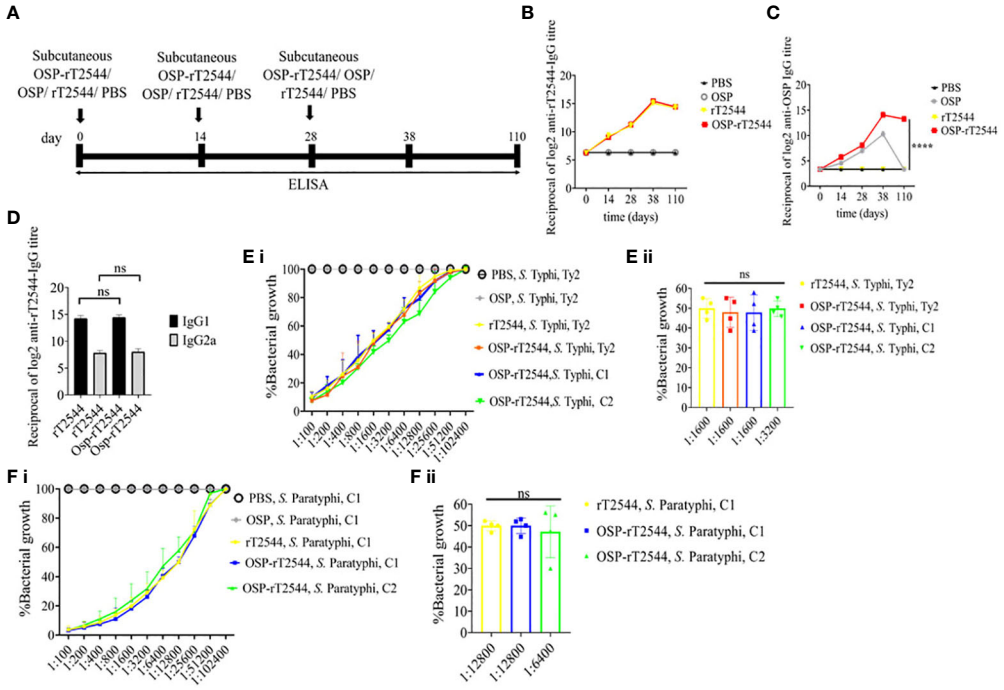

FIGURE 5
Protective antibody response against *S.* Typhi and *S.* Paratyphi A by OSP-rT2544 immunization. **(A)** Scheme of subcutaneous immunization of BALB/c mice as described under Figure 4. Mouse tissue samples were collected before each immunization dose and on day38 and day110 of the start of immunization. **(B, C)** Time kinetics of antigen-specific total IgG in the mouse serum as measured by ELISA. Data represent mean ± SEM values from different mice samples (n=5). X-axis indicate the time points after the start of the immunization when samples were collected. Statistical significance between the titer values from OSP-rT2544 and unconjugated OSP vaccine recipients is shown. Statistical analysis was performed using two-way ANOVA and Tukey's post-test for multiple comparisons. *P < 0.05, **P < 0.01, ***P < 0.001. **(D)** rT2544 specific serum IgG isotypes measured by ELISA at day 38. Data represent mean ± SEM values from different mice samples (n=5). Statistical analysis was performed using two-tailed Student's *t*-test. **(E, F)** Serum bactericidal assay. Serial dilutions of heat-inactivated antisera, collected from different groups of the immunized mice at 38 d of immunization were mixed with 25% guinea pig complement and incubated for 3h with the *S.* Typhi or *S.* Paratyphi A strains as indicated in the figure. Percentages of each live bacterial strain out of the original counts remaining at the end of the experiment for the individual serum dilutions are plotted **(E i, F i)**. Bactericidal activity was expressed as the serum dilutions at which 50% of the live bacterial loads are recovered after 3h of incubation **(E ii, F ii)**. C1, C2 are clinical isolates; bars represent the mean percent of growth reduction ± SEM of quadruplicate samples. The color scheme used are the same as above.

TABLE 1 Color scheme for different experimental groups.

Immunogen (no infection)	Color code
Vehicle (PBS)	**Black**
OSP	**Grey**
rT2544	**Yellow**
OSP-rT2544	**Orange**
Immunogen (with infection)	**Color code**
Vehicle (PBS)	**Black**
OSP	**Grey**
rT2544	**Yellow**
OSP-rT2544 (infection with reference strains)	**Orange**
OSP-rT2544 (infection with C1)	**Blue**
OSP-rT2544 (infection with C2)	**Green**
OSP-rT2544 (infection with C3)	**Sky**

showed similar anti-rT2544 IgG responses at both the above time points, following vaccination with rT2544 and OSP-rT2544 (Figure 5B). In contrast, anti-OSP IgG titer remained significantly elevated 110 days after immunization with OSP-rT2544 only, while it touched the baseline for the mice that received unconjugated OSP, suggesting that rT2544 acted as a vaccine adjuvant to OSP (Figure 5C). Anti-rT2544 IgG was comprised of IgG1 and IgG2a isotypes, indicating the induction of both Th1 and Th2 type responses; however, IgG1 was the predominant isotype (Figure 5D). To determine the functional activities of the immune sera, bactericidal assay was performed by incubating *S.* Typhi and *S.* Paratyphi A with heat-inactivated, serially-diluted sera collected from the immunized mice, supplemented with guinea pig complement. Both OSP-rT2544 and rT2544 immune sera from BALB/c mice reduced the growth of *S.* Typhi and *S.* Paratyphi A by 50% at dilutions between 1:1600 and 1:3200 and 1:6400 and 1:12800, respectively after 3h of incubation, while unconjugated OSP immune sera displayed no growth inhibition (Figures 5E, F; Supplementary Table 7). Similar growth inhibition of *S.* Typhi and *S.* Paratyphi A was obtained for OSP-rT2544 anti-sera collected from C57BL/6 mice as well (Supplementary Figure 4).

Protective humoral immune response against *S.* Typhimurium by OSP-rT2544 immunization

Given the persistently elevated, serum anti-OSP IgG titer in BALB/c mice after immunization with OSP-rT2544, we sought to investigate antisera-mediated protection against *S.* Typhimurium in similarly-immunized C57BL/6 mice by measuring antibody endpoint titers as well as SBA titers (Figure 6A; Supplementary Table 5). Like the BALB/c mice, anti-OSP IgG titer was significantly higher in OSP-rT2544 antisera than OSP antisera at day 38 of immunization and remained elevated at day 110, while OSP antisera reached the baseline (Figure 6B). This corroborated with correspondingly higher SBA titer of OSP-rT2544 antisera (1:6400 versus 1:200) against *S.* Typhimurium (Figure 6E; Supplementary Table 7). Similar titer values were found for OSP-rT2544 antisera from BALB/c mice to induce 50% growth reduction of *S.* Typhimurium (Supplementary Figure 4). As expected, there was no difference in the magnitudes of serum anti-rT2544 antibodies between the animals vaccinated with OSP-rT2544 conjugate and unconjugated rT2544 (Figure 6C). Markedly raised titers of OSP-specific serum IgG1 and IgG2a antibodies were observed in C57BL/6 mice immunized with OSP-rT2544, as compared with the OSP immunized mice, indicating induction of both Th1 and Th2 type responses, albeit to a significantly higher level for the later as observed for anti-rT2544 IgG isotype (Figure 6D). Together the above results suggested the potential for significant protection against both typhoidal and non-typhoidal Salmonellae by OSP-rT2544 antisera.

OSP-rT2544 provides cross-protection against *S.* Enteritidis

To evaluate cross-protection against *S.* Enteritidis after immunization with OSP-rT2544 candidate vaccine, reactivity of the antisera with OSPs extracted from different *S.* Enteritidis strains was studied by measuring the titers of anti-OSP antibodies. The results showed significant cross-reactivity of OSP-rT2544 antisera with the OSPs of several clinical *S.* Enteritidis strains (Figure 7A). To investigate cross-protection of the antisera against *S.* Enteritidis, SBA titers were estimated as described above. The results showed 50% growth inhibition of *S.* Enteritidis by OSP-rT2544 antisera dilution of 1:800 to 1:1600 versus 1:200 dilution of OSP antisera (Figure 7B; Supplementary Table 7). Similar result was observed for the 50% growth reduction of *S.* Enteritidis when OSP-rT2544 antisera from BALB/c mice was used to perform serum bactericidal assay (Supplementary Figure 4). This result suggested broad range of protection against NTS strains after vaccination with OSP-rT2544 antigen.

OSP-rT2544 candidate vaccine generates functional sIgA response, a hallmark of mucosal immunity

To study the mucosal immune response after OSP-rT2544 immunization, anti-OSP and anti-rT2544 sIgA antibodies were measured in the intestinal washes and fecal samples of the immunized mice and the titers were compared with the serum

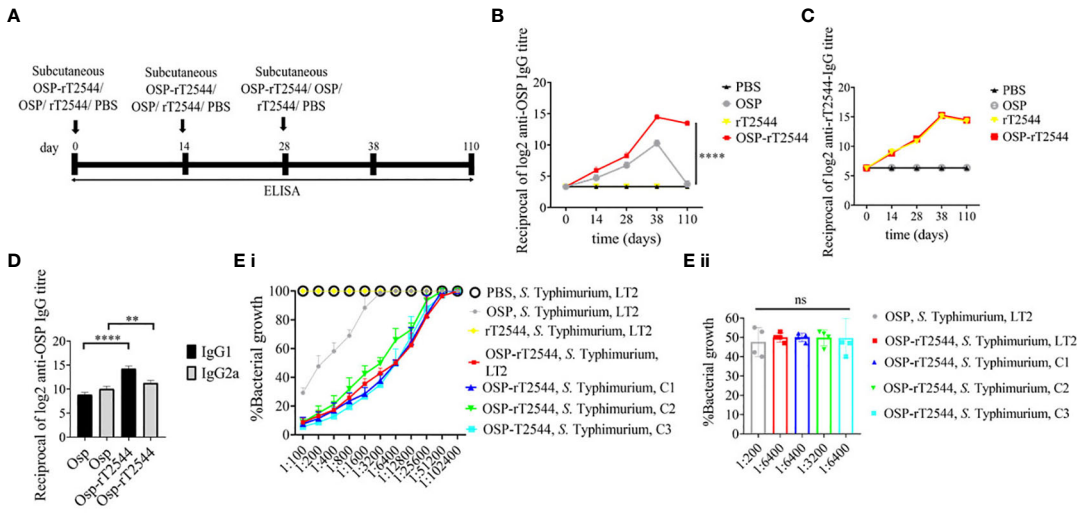

FIGURE 6
OSP-rT2544 immunization generates protective antibodies against *S.* Typhimurium. **(A)** Scheme of subcutaneous immunization of C57BL/6 mice and tissue sample collection. The scheme is similar to that described for BALB/c mice under Figure 5. **(B, C)** Time kinetics of antigen-specific total IgG in the mouse serum as measured by ELISA. Data presented and statistical significance calculated as under Figure 5. **(D)** OSP-specific serum IgG isotypes measured by ELISA at day 38. Data represent mean ± SEM values from different mice samples (n=5). Statistical analysis was performed using two-tailed Student's *t*-test (**P < 0.01; ****P < 0.0001). **(E)** Serum bactericidal assay. SBA was performed with *S.* Typhimurium, LT2 strain or the clinical isolates, as indicated in the figure, using serial dilutions of heat-inactivated antisera and guinea pig complement as described under Figure 5. Bactericidal activity was expressed as above. C1, C2 and C3 are clinical isolates and bars represent the mean percent of growth reduction ± SEM of quadruplicate samples. The color scheme used are the same as above.

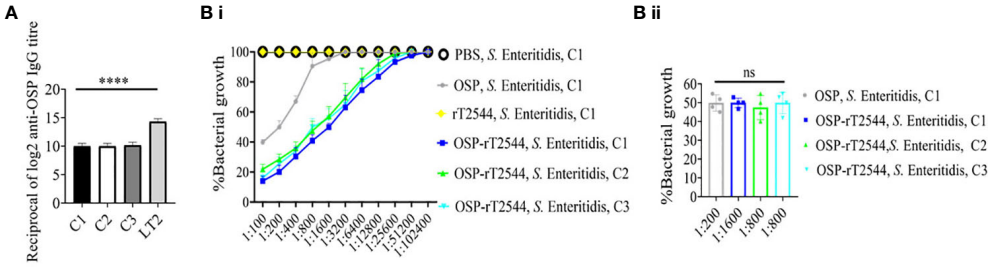

FIGURE 7
OSP-rT2544 immunization generates cross-protective antibodies against *S.* Enteritidis. **(A)** OSP was isolated from *S.* Typhimurium (LT2) and different *S.* Enteritidis (clinical isolates, C1-C3) strains and coated on the microtiter plate. Cross-reactive antibody titer was measured in OSP-rT2544 sera (38d) by ELISA. *S.* Typhimurium (LT2) OSP was used as a positive control. Data represent mean ± SEM values from different mice samples (n=6). Statistical analysis was performed using two-tailed Student's *t*-test (****P< 0.0001). **(B)** Serum bactericidal assay. Serial dilutions of heat-inactivated antisera, collected from differentially immunized mice at 38 d of immunization were mixed with 25% guinea pig complement and incubated with the *S.* Enteritidis or clinical isolates as indicated in the figure **(B i)** Bactericidal activity was expressed as the serum dilution at which 50% growth inhibition of the bacteria was noted at T_{180} (3h incubation) compared with T_0. Specific serum dilutions showing 50% growth reduction with individual immunogens are indicated in the figure **(B ii)**. C1, C2 and C3 are clinical isolates and bars represent the mean percent of growth reduction ± SEM of quadruplicate samples. Color scheme used is same as above.

IgA titers (Figure 8A). Anti-OSP IgA titer was increased four times in the mice immunized with the conjugate OSP-rT2544 compared with the unconjugated OSP (Figure 8B). On the other hand, anti-rT2544 IgA titers were comparable for the conjugated and unconjugated vaccine recipients (Figure 8C). To study the functionality of intestinal secretory antibodies, inhibition of bacterial motility in soft agar motility assay by intestinal lavage from the immunized mice was performed. Motility was determined by measuring the diameter of the bacterial zones after 10 hours of incubation at 37°C (Figures 8D–G; Supplementary Figure 5). Motility inhibition of *S.* Typhi and *S.* Paratyphi A was comparable for OSP-rT2544 and rT2544 immunization. In contrast, intestinal lavage from the mice immunized with OSP-rT2544 inhibited the motility of *S.* Typhimurium significantly more (~2.5 times) than similar samples collected from OSP-immunized mice. Similar difference was observed between the two immunization groups for soft agar motility of *S.* Enteritidis (33-36% vs 15.4% inhibition). Together these results suggested that OSP-rT2544 induced functional sIgA response in the intestine against both typhoidal and non-typhoidal *Salmonella* strains.

OSP-rT2544 induces both Th1 and Th2 serum cytokine response

Salmonella clearance requires a Th1 response, whereas Th2 cells support the generation of sIgA and serum antibodies. To determine the serum cytokine response, sera were collected from the OSP-rT2544 immunized C57BL/6 mice on day 38 and cytokine

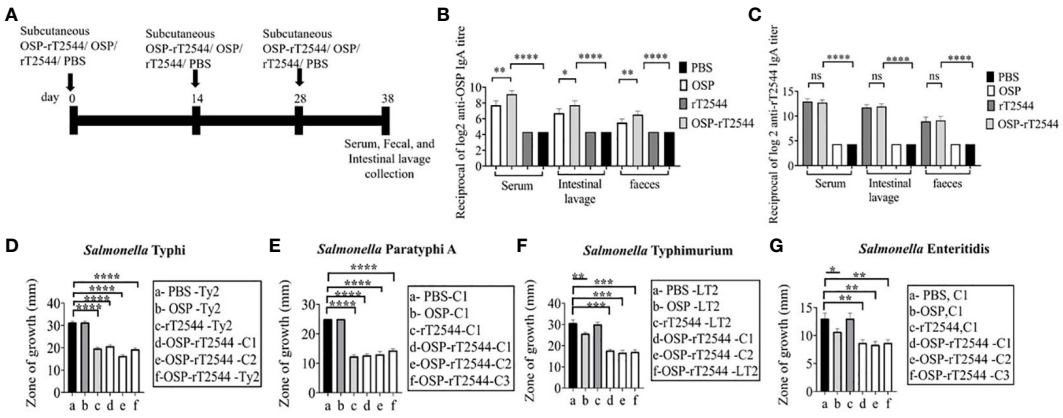

FIGURE 8
Induction of protective mucosal antibodies by OSP-rT2544 immunization. **(A)** Schedule of subcutaneous immunization of C57BL/6 mice at days 0, 14, and 28 with vehicle (PBS), conjugate (OSP-rT2544) (8μg of OSP in conjugate), or unconjugated vaccines (OSP (8 μg), rT2544 (24 μg)). Mice were sacrificed on day 38 and samples were collected. **(B, C)** ELISA showing OSP- and rT2544-specific serum IgA and intestinal sIgA titers in the groups of mice (n=5/group) after immunization with different antigens. Data represent mean ± SEM values from different mice samples (n=5). Statistical analysis was performed using two-tailed Student's *t*-test (**P < 0.01; ***P < 0.001; ****P < 0.0001). **(D–G)** Soft agar motility assay. Bacteria were spotted at the center of the soft agar (LB medium with 0.4% Bacto agar) containing intestinal wash (5%) from the immunized mice collected on day 38. Bacterial migration from the inoculation point to the periphery of the plate was measured after 10h incubation at 37°C. Experiments were repeated three times and mean (± SEM) of the values from all three experiments were plotted. Statistical analysis was performed using two-tailed Student's *t*-test (*p<0.05; **P < 0.01; ***P < 0.001; ****P < 0.0001). Color scheme used is same as above.

concentrations were measured by ELISA. We found significantly elevated, circulating pro-inflammatory/Th1 (IFNγ, TNF-α) and anti-inflammatory/Th2 (IL-4, IL-10, IL-6) cytokines in OSP-rT2544-immunized mice as opposed to only modest elevation in the comparator immunized groups (Figure 9). This result suggested that OSP-rT2544 immunization induces both Th1 and Th2 cytokine response in serum with the latter being predominant.

Immunization with OSP-rT2544 generates protective memory response

To study antigen-specific memory T cells, bone marrow derived dendritic cells (BMDCs) were isolated from the naïve C57BL/6 mice and pulsed *in vitro* with OSP or OSP-rT2544 antigen for 24h. Antigen-pulsed BMDCs were then co-cultured with the experimental mice splenocytes containing $CD4^+$ T cells. IFNγ release in the co-culture supernatants was estimated to be >10 folds higher for the splenocytes from OSP-rT2544 immunized mice compared with the animals that received OSP alone or left unimmunized (13.5 pg/ml), suggesting significant augmentation of T cell memory response by rT2544 when conjugated to OSP (Figure 10A). To determine memory T cell subsets, co-cultured $CD4^+$ T cells, as mentioned above were analyzed by flow cytometry after staining for the surface expression of 'Cluster of differentiation' (CD) markers ($CD4^+CD62L^{low}CD44^{hi}$). Cell subset analysis showed that augmented memory response was largely contributed by the effector memory T cells ($CD62L^{low}CD44^{high}$) (Figure 10B). Further, to analyze memory B cell response, a booster dose was administered to the immunized mice on day 110 of the first immunization and anti-OSP and anti-rT2544 serum antibodies were measured ten days later. A significantly higher secondary antibody response (day 120) compared with the primary response (day 38) was observed (four times for anti-OSP, and eight times for anti-rT2544 antibodies) (Figures 10C, D), suggesting differentiation of memory B cells into plasma cells, producing IgG at the latter time point. Given that the avidity of antibodies for the secondary response is higher than the primary response, anti-rT2544 and anti-OSP IgG immune complexes collected at days 38 and 120 were washed (3 times) with PBS-T, containing 6M urea before the addition of HRP-conjugated secondary antibodies. The avidity index was calculated by multiplying the ratio of the absorbances of the wells that were washed with and without 6M urea-containing buffer by 100. The result showed significantly high avidity indices (60-62%) of the secondary antibodies after booster immunization compared with the primary immunization (18-22%), suggesting a strong memory B cell response (Figures 10E, F). To corroborate functional activities of the higher avidity antibodies, we performed serum bactericidal assay (SBA) with these antibodies and different *Salmonella* strains (Supplementary Table 6). The results showed 50% growth inhibition at dilutions of secondary OSP-rT2544 antisera compared with the dilutions of the primary antisera as follows, 1:3200 vs. 1:1600 for *S.* Typhi Ty2, 1:25600 vs. 1:12800 for *S.* Paratyphi A, 1:12800 vs. 1:6400 for *S.* Typhimurium LT2, 1:3200 vs. 1:1600 for *S.* Enteritidis. The result suggested that inhibition dilution of the secondary OSP-rT2544 antisera was significantly higher than inhibition accompanied by antisera collected on day 38 (Figure 10G; Supplementary Table 8). These results suggested that immunization with OSP-rT2544 might elicit potent, long-lived protective immunity against *Salmonella* infection.

Discussion

We report here development of a glycoconjugate containing O-specific polysaccharide (OSP) from *S.* Typhimurium and an outer membrane protein (T2544) of *S.* Typhi/*S.* Paratyphi that displayed strong potential as a candidate multivalent vaccine against typhoidal and non-typhoidal *Salmonella* serovars in mouse infection models. Subcutaneous immunization of mice with OSP-rT2544 induced rapid seroconversion with high titers of protective antibodies in the serum and intestinal secretions, in addition to memory B and T cell response, conferring high protection of vaccinated animals against *Salmonella* infection.

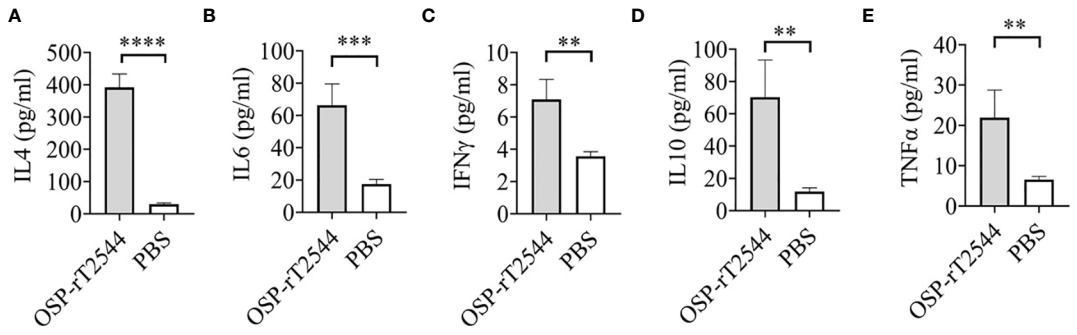

FIGURE 9
OSP-rT2544 induces both Th1 and Th2 serum cytokine response. **(A–E)** C57BL/6 mice were subcutaneously immunized with OSP-rT2544 (8μg of OSP in conjugate) or PBS (vehicle) on days 0, 14, and 28. Ten days after the last immunization (day 38), sera were collected from the immunized mice and cytokine levels in the serum were measured by ELISA. Briefly, Precoated ninety-six well plates were incubated with serum samples along with biotin-conjugate for 2h at room temperature. After three subsequent washes, plates were further incubated for one hour at room temperature with streptavidin-HRP. Following the addition of the TMB substrate, color development was evaluated using spectrophotometry at 450 nm. Statistical analysis was performed using two-tailed Student's *t*-test (**P < 0.01; ***P < 0.001; ****P < 0.0001).

Previous studies reported serotype independent protection against NTS (non-typhoidal *salmonella*) by S. Typhimurium type 3 secretion system tip and translocator proteins and their chimera. However, protection conferred was modest at best (13) as opposed to up to 80% protective efficacy for OSP-T2544. Bacterial surface polysaccharides are attractive candidates for vaccine development and presently constitute many commercially available vaccines. While polysaccharides, being T-independent antigens are poorly immunogenic by themselves and fail to induce immunological memory, they have been efficiently conjugated with carrier proteins to augment immunogenicity (44). Synthesis of glycoconjugate vaccines with a covalent bond between the saccharide and the carrier protein molecules and using different conjugation chemistries were described previously (45–48). The approaches taken fall into two main categories, namely the 'random linkage' along the polysaccharide (PS) chain and 'selective attachment' at the PS terminus. High molecular weight (MW), cross-linked, and generally undefined heterogeneous structures are produced by random chemistry, whereas selective chemistry generates better-defined structures while avoiding chemical alteration of the saccharide chain (45, 49–51). Immunogenicity of glycoconjugate vaccines is significantly influenced by the conjugation chemistry. Studies with OSP from different *Salmonella* strains coupled to multiple carrier proteins, using different chemical methods and diverse linkers suggested that important antigenic epitopes may be sterically protected by the bulky protein when polysaccharides are directly connected to the carrier protein (52). Instead, when a linker joins the polysaccharide to a carrier protein, steric shielding may be reduced and the polysaccharide externally presented to the immune cells, increasing the number of antigenic epitopes that are available to activate antigen-presenting cells (52). In this study, we developed the OSP-rT2544 conjugate using random linkage method where hydroxyl groups along the saccharide were randomly activated by CnBr (cyanogen bromide) chemistry (53–56). Cyanylation is a time-tested method and a simple and quick workflow for sugar-protein conjugation, as described previously for OSP-TT (31), Hib-protein conjugate (56), V. cholerae O:1 serotype Inaba (57), V. cholerae O:1 serotype Ogawa (58), and *Francisella tularensis* (59). Following cyanylation reaction, cyanate esters are formed that further interact with the hydroxyl groups to create cyclic imidocarbonates that can effectively couple to the carboxyl groups

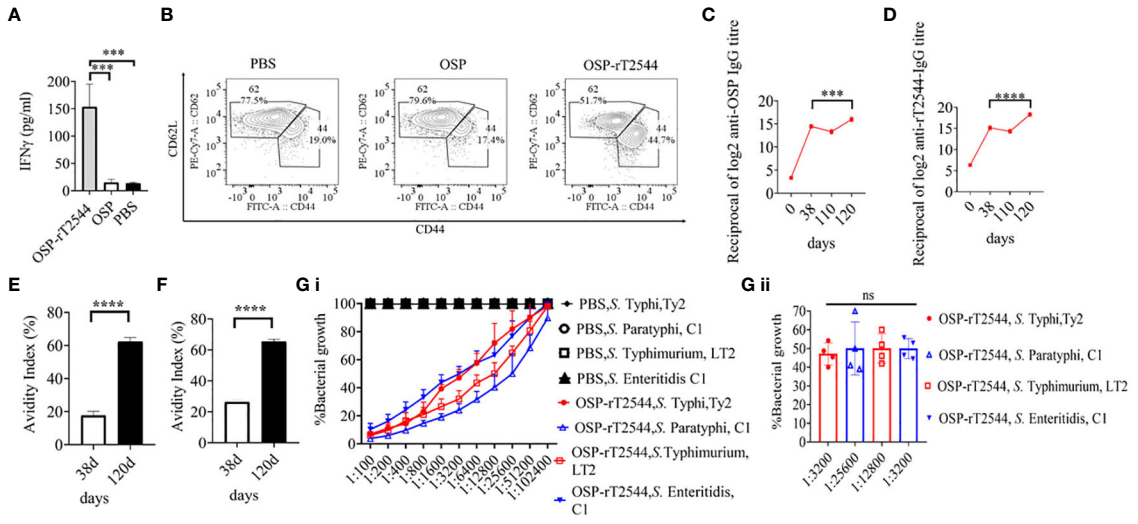

FIGURE 10
Induction of protective memory response. **(A)** C57BL/6 mice were subcutaneously immunized as described above with the antigens indicated in the Figure 6. Antigen-primed memory CD4+ T cells were isolated from the splenocytes of the mice 120 days of the start of the immunization. To evaluate the memory T cells response, cells were converted to effector T cells by presenting the respective antigens to them in association with MHC Class II. To this end, bone marrow derived dendritic cells (BMDCs), isolated from the naïve C57BL/6 mice were pulsed with OSP or OSP-rT2544 for 24h, followed by co-culturing of the cells with the memory T cells. Memory response was analyzed by the quantification of IFNγ released in the co-culture supernatants using ELISA. Statistical analysis was performed using two-tailed Student's *t*-test (***P < 0.001; ****P < 0.0001). Data represents mean (± SEM) of four independent experiments. **(B)** $CD4^+$ T cells, co-cultured with antigen-pulsed BMDCs for 24h, as mentioned under 'Figure 10 A', were analyzed by flow cytometry after staining for the surface expression of 'Cluster of differentiation' (CD) markers for T-effector memory cell determination ($CD4^+CD62L^{low}$ $CD44^{hi}$). Representative images from one out of four experiments are shown. **(C, D)** C57BL/6 mice were subcutaneously immunized on days 0, 14, and 28 with OSP-rT2544 (8µg of OSP and 24 µg of rT2544 in conjugate) and a booster was given with the same antigen on day 110 **(C)** OSP and **(D)** rT2544-specific serum IgG titers were measured by ELISA at the indicated time points. Data represent mean ± SEM values from different mice samples (n=6). Statistical analysis was performed using two-tailed Student's *t*-test (***P < 0.001; ****P < 0.0001). **(E, F)** Antibody avidity assay. Anti-rT2544 **(E)** and anti-OSP **(F)** avidity index were determined in the OSP-rT2544 serum (diluted 1:100 in PBS-T), collected at the indicated time points after washing the immune complex with 6M urea buffer by ELISA. The avidity index was calculated by multiplying the ratio of the absorbances of the wells that were washed with and without urea-containing buffer by 100. Data represent mean ± SEM values from different mice samples (n=3). Statistical analysis was performed using two-tailed Student's *t*-test (****P < 0.0001). **(G)** Serum bactericidal assay. Serial dilutions of heat-inactivated antisera, collected from differentially immunized mice at 120 d of immunization were mixed with 25% guinea pig complement and incubated with the *S.* Typhi, *S.* Paratyphi A, *S.* Typhimurium, LT2 and *S.* Enteritidis as indicated in the figure **(G i)** Bactericidal activity was expressed as the serum dilution at which 50% growth inhibition of the bacteria was noted at T_{180} (3h incubation) compared with T_0. Immunogens that have a 50% growth reduction at a specific serum dilution are indicated in the figure **(G ii)**. Bars represent the percent mean (± SEM) of growth reduction of quadruplicate samples. Color scheme used is same as above.

of the carrier proteins, following 1-ethyl-3-(3-dimethy laminopropyl) carbodiimide (EDC)-mediated condensation (60). For several other glycoconjugates, CDAP replaced CnBr to activate polysaccharides (31, 61). Primary mechanism of CDAP-mediated activation is the creation of isourea linkages between the cyanoesters on the activated carbohydrate and the lysine residues on the carrier protein (55, 58). However, one major drawback associated with CDAP chemistry is over-crosslinking, leading to reduced immunogenicity of the glycoconjugates due to gelling of the carbohydrates and peptides (52). In vaccine production, CnBr activation is commonly accompanied by the use of ADH linker. It was previously reported that conjugation chemistry using ADH linker is more reactive due to shorter reaction time and higher derivatization yield, as was found with the glycoconjugate vaccine for meningococcal serogroup X (62). Similar to OSP-TT (31), Vi-CRM197 (48) and Hib-protein (56) conjugates, we used ADH linker to create a covalent linkage between OSP and T2544 by carbodiimide chemistry.

Several factors, including the molecular weight (MW) of the conjugate and the molar ratio of the sugar and the carrier protein influence vaccine immunogenicity. In our study, very high molecular weight, crosslinked conjugate with partition coefficient (kd) of 0.02 was formed, as there are multiple activation points within OSP and multiple linkage points on the protein (T2544). It was previously reported that immunization with higher MW glycoconjugates results in greater anti-PS antibody response. Thus, larger and more cross-linked Vi-DT and GBS type III-TT conjugate vaccines induced higher anti-Vi and anti-saccharide IgG response, respectively (63, 64). The saccharide-to-protein ratio has a direct relationship with the immunogenicity of glycoconjugates; a larger ratio leads to improved cross-linking and activation of saccharide-specific B cells with increased polysaccharide loading.

For OSP-rT2544 conjugate containing ADH linker and generated by random activation, PS to protein molar ratio of 1.53 elicited significantly higher anti-OSP antibodies compared with OSP alone after three doses of mouse immunization. These features are in agreement with *Salmonella* Typhimurium OSP-TT conjugate with ADH linker and a saccharide to protein ratio of 0.6, produced by random activation. This conjugate was more immunogenic than the molecule generated by selective chemistry with the saccharide to protein ratio (w/w) of 0.1 (61). Further, using ADH linker rather than cystamine or SPDP increased the immunogenicity of *Salmonella* Typhi Vi conjugates, when it was coupled to recombinant Pseudomonas aeruginosa exotoxin A (rEPA) by random chemistry (65). Similar results were obtained with *S.* aureus type 8 capsular PS linked via random chemistry to rEPA or DT, where use of ADH linker yielded higher PS to protein ratio compared with cystamine or SPDP (66, 67). A study using deacylated lipopolysaccharides (LPS) from *Vibrio cholerae* O1 serotype Inaba and cholera toxin (CT) reported that random chemistry and ADH linker produced conjugates with LPS to CT ratio of 0.8 as opposed to 0.72 for single-point attachment using SPDP linker with the former being more immunogenic (68). However, *Salmonella* Enteritidis OSP directly conjugated to flagellin monomers, polymers, or CRM197 by random activation without linkers or with selective aminooxyoxime thioether chemistry using diaminooxy cysteamine and N-(γ-maleimidobutyloxy)- sulfosuccinimide ester linker induced similar IgG response and confers protection against bacterial challenge in mice (65, 69).

Carrier proteins used in the glycoconjugate preparations augment the immune response against the covalently attached polysaccharides, while the immune response specific to the protein largely remains unaltered. T2544 functions as an adjuvant to increase the serum anti-OSP antibody titer by 32 times after subcutaneous immunization of mice, keeping the levels of anti-T2544 antibodies unchanged (Figures 5B, C, 6B, C). Flagellin in a conjugate formulation with *Salmonella* Enteritidis OSP enhanced anti-OSP antibody titers by 10-fold in mice after 3 intramuscular immunization doses, while anti-flagellin antibody response against the conjugate was similar to that of unconjugated flagellin (69). Similar results were observed for *Salmonella* Typhimurium when OSP was conjugated to FliC or CRM197 by random chemistry (42, 70), although anti-CRM197 antibody titer was 100-fold elevated with the conjugate. Surprisingly, much higher anti-OSP antibody response was reported here when conjugation was performed using selective chemistry. This is contrary to most other studies that reported higher antibody response with glycoconjugates developed by random chemistry rather than selective conjugation (61, 65, 68). Intraperitoneal immunization with *S.* Typhimurium OSP-porin conjugate resulted in anti-OSP and anti-porin end-points titers of 1/600 and 1/8500, respectively after 3 doses (71). This contrasts with anti-OSP and anti-T2544 end-point titers of 1/25600 and 1/51200, respectively in our study.

Salmonella conjugate vaccines, including the licensed products and those at the advanced stage of clinical development are largely monovalent, specifically acting against single *Salmonella* serovar. A Vi-TT conjugate vaccine has been licensed for local distribution in India (4–6). For *S.* Typhimurium, 90-100% protection was conferred by OSP-FliC, OSP-CRM197 and OSP-porin conjugates (70, 71) against clinical and reference strains of *Salmonella*. In contrast, OSP-T2544 candidate vaccine conferred 75-80% of protection against *S.* Typhi, *S.* Paratyphi, and *S.* Typhimurium and 55-60% cross-protection against *S.* Enteritidis (Figure 4). While the cause of cross-reactivity to S. Enteritidis is still under investigation, antibodies against common O-Ag epitopes like O:1 and O:12 or the shared core region are most likely to account for (42).

OSP- and rT2544-specific serum antibodies were comprised of both IgG1 and IgG2a sub-classes (Figures 5D, 6D). Polysaccharide antigens have been found to induce IgG2 class switch in the absence of T cell engagement (72). In contrast, T cell-dependent (TD) protein antigens elicit antibodies of IgG1 subclass. Anti-polysaccharide antibodies shifted towards the IgG1 subclass in mice following conjugation to a carrier protein (73, 74). Similarly, OSP-rT2544 conjugate induced higher titers of anti-OSP IgG1 than IgG2a compared with unconjugated OSP (Figure 6D). This corroborates with the other published studies that reported

predominantly IgG1 antibodies specific to OSP in the conjugate immunized group (42, 75). The elevated IgG1 response in conjugate compared to the unconjugated form of saccharide supports the concept that two forms of the saccharide may activate different regulating mechanisms or select B cell clones with different isotype-specificity (30). We also found increased IL4 concentrations in the conjugate antisera (Figure 9) that was previously reported for other glycoconjugate vaccines (29). IL-4 plays an important role in humoral immunity by inducing differentiation of Th0 into Th2 cells and mediating IgG1 antibody release, which may activate the classical complement pathway and provide long-term protection.

We measured protective efficacy of vaccine antigen-specific antibodies by serum bactericidal assay (SBA) titer and soft agar motility inhibition assay using intestinal sIgA. SBA is accepted as an *in vitro* surrogate of vaccine immunogenicity. SBA measured functional *Salmonella*-specific antibodies capable of complement-mediated bacterial killing, resulting in 50% decrease in bacterial count. OSP-rT2544 antisera displayed SBA titer of 1:1600 against *S.* Typhi and *S.* Enteritidis, while similar titers for *S.* Paratyphi A and *S.* Typhimurium attained the values of 1:12800 and 1:6400, respectively (Figures 5E, F, 6E, 7B). Published studies reported comparatively lower values of serum bactericidal titers for OSP-TT (against *S.* Typhi) and OSP-CRM197 (against *S.* Typhimurium and *S.* Enteritidis) (42, 76). We found significant inhibition of bacterial motility in soft agar by intestinal secretory antibodies, but failed to find similar studies in the published literature with other glycoconjugate vaccines. However, 3-fold increased titers of sIgA were reported after immunization with OSP-CRM197 (42) as opposed to 2-fold increase after OSP-rT2544 in the present study (Figures 8D-G). This might correlate with decreased motility of *Salmonella*, pre-incubated with the intestinal wash from the vaccinated mice, as was previously reported for *S.* Typhi and *S.* Paratyphi A ghost cell-based bivalent vaccine candidate (77).

In some studies, functional assays with the conjugate sera was performed by passive transfer into mice. Passive protection conferred by OSP-TT antisera administered through intraperitoneal route suggested functional serum antibodies against *S.* Typhimurium (61), where passively transferred IgM (80-100%) was more protective than IgG (20-30%). However, passive administration of rabbit antisera against OSP-porin conjugate through intravenous route showed 100% protection of mice against intraperitoneal challenge with *S.* Typhimurium (71). In other studies, opsonophagocytosis was performed to determine the functionality of the conjugate antisera. For *S.* Enteritidis COPS-FliC conjugate, pre-incubation with antisera resulted in 5% increase of opsonophagocytosis compared with the vehicle immune sera (69). We, however, did not evaluate OSP-rT2544 antisera by passive immunization or opsonophagocytosis assay.

The ability to generate robust and enduring immune memory is the hallmark of a successful vaccine and critical for the intended public health impact. An antibody recall response was demonstrated with tetrasaccharide-CRM_{197} conjugate after a booster on day 260 when the primary antibody response was reduced by two-fold compared with the titers achieved after the third dose of immunization (day 36) (78). In contrast, following vaccination with OSP-rT2544, sustained OSP- and rT2544-specific primary antibody response was observed at day 110, which further increased after the administration of a booster dose with the production of higher avidity antibodies which is a marker for T-cell dependent affinity maturation. A separate study evaluated B cell memory response by ELISPOT assay after human volunteers received a conjugate vaccine containing *Vibrio Cholerae* O1 Inaba and tetanus toxoid and reported 3.5 OSP-specific and 5 carrier protein-specific IgG spots per 10^5 splenocytes at day 56 day (18).

To further corroborate the antibody recall response, we checked for $CD4^+$ effector memory cells producing IFN-γ in the OSP-rT2544 immunized mice. Generation of recombinant T2544-specific $CD4^+$ T cells was earlier reported earlier by our laboratory (30). Elevated levels of IFN-γ production was found following antigen restimulation of mouse splenocytes in the recipients of OSP-rT2544 (Figures 10A, B). However, similar studies were not reported earlier for glycoconjugate vaccines containing OSP.

Despite convincingly demonstrating activation of different arms of the immune system with protective serum and mucosal antibody response, conferring broad spectrum protection against typhoidal and non-typhoidal *Salmonella* serovars, this study has several limitations. We did not compare immunogenicity of candidate glycoconjugate vaccines, developed using different conjugation chemistries and having diverse linker molecules between OSP and T2544. Given that T2544 is an intrinsic *Salmonella* protein, head-to-head comparison with a different preparation, comprising of OSP linked to a non-*Salmonella* protein would provide further insights into the mechanisms underlying immune activation by glycoconjugate vaccines. Further elaboration of T cell response, including activation of different $CD4^+$ cell subsets (Th9, Th17, follicular helper T cell, resident memory and central memory T cells) as well as cytotoxic T cells (central and effector memory cell) would better characterize the immune response. Finally, studies elaborating the relative contributions of different compartments of the immune system (humoral, cellular and mucosal) would help to develop newer vaccines with improved efficacies.

Data availability statement

The original contributions presented in the study are included in the article/Supplementary Material. Further inquiries can be directed to the corresponding author.

Ethics statement

The animal study was approved by ICMR-National Institute of Cholera and Enteric Diseases. The study was conducted in accordance with the local legislation and institutional requirements.

Author contributions

RH: Conceptualization, Data curation, Formal analysis, Investigation, Methodology, Software, Visualization, Writing – original draft, Writing – review & editing. AD: Methodology,

Writing – review & editing. DG: Methodology, Writing – review & editing. SC: Methodology, Writing – review & editing. AP: Methodology, Writing – review & editing. GB: Methodology, Writing – review & editing. S-iM: Funding acquisition, Writing – review & editing. SD: Conceptualization, Data curation, Formal Analysis, Funding acquisition, Investigation, Methodology, Project administration, Resources, Software, Supervision, Validation, Visualization, Writing – original draft, Writing – review & editing.

Funding

The author(s) declare financial support was received for the research, authorship, and/or publication of this article. This work was supported by extramural grants from Indian Council of Medical Research, Government of India (58/17/2020/PHA/BMS) and the Japan Agency for Medical Research and Development (AMED; Grant No. JP23wm0125004).

Acknowledgments

RH acknowledges the University Grant Commission (UGC) (student ID-191620094970) to get the fellowship for this study. All other authors acknowledge Indian Council of Medical Research (ICMR), National Institute of Cholera and Enteric Diseases (NICED) and Japan Agency for Medical Research and Development (AMED; Grant No. JP23wm0125004).

Conflict of interest

Author GB was employed by company BD Biosciences.

The remaining authors declare that the research was conducted in the absence of any commercial or financial relationships that could be construed as a potential conflict of interest.

Publisher's note

Supplementary material

The Supplementary Material for this article can be found online at: https://www.frontiersin.org/articles/10.3389/fimmu.2023.1304170/full#supplementary-material

References

1. Deen J, von Seidlein L, Andersen F, Elle N, White NJ, Lubell Y. Community-acquired bacterial bloodstream infections in developing countries in south and southeast Asia: a systematic review. *Lancet Infect Dis* (2012) 12(6):480–7. doi: 10.1016/S1473-3099(12)70028-2

2. Marchello CS, Birkhold M, Crump JAVacc-iNTS consortium collaborators. Complications and mortality of non-typhoidal salmonella invasive disease: a global systematic review and meta-analysis. *Lancet Infect Dis* (2022) 22(5):692–705. doi: 10.1016/S1473-3099(21)00615-0

3. MacLennan CA, Stanaway J, Grow S, Vannice K, Steele AD. *Salmonella* combination vaccines: moving beyond typhoid. *Open Forum Infect Dis* (2023) 10 (Suppl 1):S58–66. doi: 10.1093/ofid/ofad041

4. Patel PD, Patel P, Liang Y, Meiring JE, Misiri T, Mwakiseghile F, et al. Safety and efficacy of a typhoid conjugate vaccine in Malawian children. *N Engl J Med* (2021) 385 (12):1104–15. doi: 10.1056/NEJMoa2035916

5. Qadri F, Khanam F, Liu X, Theiss-Nyland K, Biswas PK, Bhuiyan AI, et al. Protection by vaccination of children against typhoid fever with a Vi-tetanus toxoid conjugate vaccine in urban Bangladesh: a cluster-randomised trial. *Lancet* (2021) 398 (10301):675–84. doi: 10.1016/S0140-6736(21)01124-7

6. Shakya M, Voysey M, Theiss-Nyland K, Colin-Jones R, Pant D, Adhikari A, et al. Efficacy of typhoid conjugate vaccine in Nepal: final results of a phase 3, randomised, controlled trial. *Lancet Glob Health* (2021) 9(11):e1561–8. doi: 10.1016/S2214-109X(21)00346-6

7. Black RE, Levine MM, Ferreccio C, Clements ML, Lanata C, Rooney J, et al. Efficacy of one or two doses of Ty21a Salmonella typhi vaccine in enteric-coated capsules in a controlled field trial. *Chilean Typhoid Commit Vaccine* (1990) 8(1):81–4. doi: 10.1016/0264-410x(90)90183-m

8. MacLennan CA, Martin LB, Micoli F. Vaccines against invasive Salmonella disease: current status and future directions. *Hum Vaccin Immunother* (2014) 10 (6):1478–93. doi: 10.4161/hv.29054

9. Kumar VS, Gautam V, Balakrishna K, Kumar S. Overexpression, purification, and immunogenicity of recombinant porin proteins of Salmonella enterica serovar Typhi (S. Typhi). *J Microbiol Biotechnol* (2009) 19(9):1034–40. doi: 10.4014/jmb.0812.675

10. Rolli J, Rosenblatt-Velin N, Li J, Loukili N, Levrand S, Pacher P, et al. Bacterial flagellin triggers cardiac innate immune responses and acute contractile dysfunction. *PloS One* (2010) 5(9):e12687. doi: 10.1371/journal.pone.0012687

11. Xiao Y, Liu F, Yang J, Zhong M, Zhang E, Li Y, et al. Over-activation of TLR5 signaling by high-dose flagellin induces liver injury in mice. *Cell Mol Immunol* (2015) 12(6):729–42. doi: 10.1038/cmi.2014.110

12. Rolli J, Loukili N, Levrand S, Rosenblatt-Velin N, Rignault-Clerc S, Waeber B, et al. Bacterial flagellin elicits widespread innate immune defense mechanisms, apoptotic signaling, and a sepsis-like systemic inflammatory response in mice. *Crit Care* (2010) 14(4):R160. doi: 10.1186/cc9235

13. Martinez-Becerra FJ, Kumar P, Vishwakarma V, Kim JH, Arizmendi O, Middaugh CR, et al. Characterization and Protective Efficacy of Type III Secretion Proteins as a Broadly Protective Subunit Vaccine against Salmonella enterica Serotypes. *Infect Immun* (2018) 86(3):e00473–17. doi: 10.1128/IAI.00473-17

14. Lee SJ, Benoun J, Sheridan BS, Fogassy Z, Pham O, Pham QM, et al. Dual immunization with sseB/flagellin provides enhanced protection against salmonella infection mediated by circulating memory cells. *J Immunol* (2017) 199(4):1353–61. doi: 10.4049/jimmunol.1601357

15. Jneid B, Rouaix A, Féraudet-Tarisse C, Simon S. SipD and IpaD induce a cross-protection against Shigella and Salmonella infections. *PloS Negl Trop Dis* (2020) 14(5): e0008326. doi: 10.1371/journal.pntd.0008326

16. Phalipon A, Tanguy M, Grandjean C, Guerreiro C, Bélot F, Cohen D, et al. A synthetic carbohydrate-protein conjugate vaccine candidate against Shigella flexneri 2a infection. *J Immunol* (2009) 182(4):2241–7. doi: 10.4049/jimmunol.0803141

17. Desalegn G, Kapoor N, Pill-Pepe L, Bautista L, Yin L, Ndungo E, et al. A novel shigella O-polysaccharide-ipaB conjugate vaccine elicits robust antibody responses and confers protection against multiple shigella serotypes. *mSphere* (2023) 8(3):e0001923. doi: 10.1128/msphere.00019-23

18. Sayeed MA, Bufano MK, Xu P, Eckhoff G, Charles RC, Alam MM, et al. A Cholera Conjugate Vaccine Containing O-specific Polysaccharide (OSP) of V. cholerae O1 Inaba and Recombinant Fragment of Tetanus Toxin Heavy Chain (OSP:rTTHc)

Induces Serum, Memory and Lamina Proprial Responses against OSP and Is Protective in Mice. *PloS Negl Trop Dis* (2015) 9(7):e0003881. doi: 10.1371/journal.pntd.0003881

19. Trebicka E, Jacob S, Pirzai W, Hurley BP, Cherayil BJ. Role of antilipopolysaccharide antibodies in serum bactericidal activity against Salmonella enterica serovar Typhimurium in healthy adults and children in the United States. *Clin Vaccine Immunol* (2013) 20(10):1491–8. doi: 10.1128/CVI.00289-13

20. Goh YS, Clare S, Micoli F, Saul A, Mastroeni P, MacLennan CA. Monoclonal antibodies of a diverse isotype induced by an O-antigen glycoconjugate vaccine mediate *in vitro* and *in vivo* killing of African invasive nontyphoidal salmonella. *Infect Immun* (2015) 83(9):3722–31. doi: 10.1128/IAI.00547-15

21. Simon R, Levine MM. Glycoconjugate vaccine strategies for protection against invasive Salmonella infections. *Hum Vaccin Immunother* (2012) 8(4):494–8. doi: 10.4161/hv.19158

22. Micoli F, Ravenscroft N, Cescutti P, Stefanetti G, Londero S, Rondini S, et al. Structural analysis of O-polysaccharide chains extracted from different Salmonella Typhimurium strains. *Carbohydr Res* (2014) 385:1–8. doi: 10.1016/j.carres.2013.12.003

23. Ravenscroft N, Cescutti P, Gavini M, Stefanetti G, MacLennan CA, Martin LB, et al. Structural analysis of the O-acetylated O-polysaccharide isolated from Salmonella Paratyphi A and used for vaccine preparation. *Carbohydr Res* (2015) 404:108–16. doi: 10.1016/j.carres.2014.12.002

24. World Health Organization. *Antigenic formulae of the Salmonella serovars* (2007). Available at: https://www.pasteur.fr/sites/default/files/veng_0.pdf (Accessed 6 November 2022).

25. Perera SR, Sokaribo AS, White AP. Polysaccharide vaccines: A perspective on non-typhoidal. *Salmonella* (2021) 25:691–714. doi: 10.3390/polysaccharides2030042

26. Borrow R, Dagan R, Zepp F, Hallander H, Poolman J. Glycoconjugate vaccines and immune interactions, and implications for vaccination schedules. *Expert Rev Vaccines* (2011) 10(11):1621–31. doi: 10.1586/erv.11.142

27. Findlow H, Borrow R. Interactions of conjugate vaccines and co-administered vaccines. *Hum Vaccin Immunother* (2016) 12(1):226–30. doi: 10.1080/21645515.2015.1091908

28. Dagan R, Poolman J, Siegrist CA. Glycoconjugate vaccines and immune interference: a review. *Vaccine* (2010) 28:5513–23. doi: 10.1016/j.vaccine.2010.06.026

29. Konadu EY, Lin FY, Hó VA, Thuy NT, Van Bay P, Thanh TC, et al. Phase 1 and phase 2 studies of Salmonella enterica serovar Paratyphi A O-specific polysaccharide-tetanus toxoid conjugates in adults, teenagers, and 2- to 4-year-old children in Vietnam. *Infect Immun* (2000) 68(3):1529–34. doi: 10.1128/IAI.68.3.1529-1534.2000

30. Das S, Chowdhury R, Ghosh S, Das S. A recombinant protein of Salmonella Typhi induces humoral and cell-mediated immune responses including memory responses. *Vaccine* (2017) 35(35 Pt B):4523–31. doi: 10.1016/j.vaccine.2017.07.035

31. Konadu E, Shiloach J, Bryla DA, Robbins JB, Szu SC. Synthesis, characterization, and immunological properties in mice of conjugates composed of detoxified lipopolysaccharide of Salmonella Paratyphi A bound to tetanus toxoid with emphasis on the role of O acetyls. *Infect Immun* (1996) 64(7):2709–15. doi: 10.1128/iai.64.7.2709-2715.1996

32. Bastos RC, Corrêa MB, de Souza IM, da Silva MN, da Silva Gomes Pereira D, Martins FO, et al. Brazilian meningococcal C conjugate vaccine: physicochemical, immunological, and thermal stability characteristics. *Glycoconj J* (2018) 35(1):3–13. doi: 10.1007/s10719-017-9787-2

33. Micoli F, Rondini S, Gavini M, Lanzilao L, Medaglini D, Saul A, et al. O:2-CRM (197) conjugates against Salmonella Paratyphi A. *PloS One* (2012) 7(11):e47039. doi: 10.1371/journal.pone.0047039

34. He W, Mazzuca P, Yuan W, Varney K, Bugatti A, Cagnotto A, et al. Identification of amino acid residues critical for the B cell growth-promoting activity of HIV-1 matrix protein p17 variants. *Biochim Biophys Acta Gen Subj.* (2019) 1863 (1):13–24. doi: 10.1016/j.bbagen.2018.09.016

35. Nguyen TK, Selvanayagam R, Ho KKK, Chen R, Kutty SK, Rice SA, et al. Co-delivery of nitric oxide and antibiotic using polymeric nanoparticles. *Chem Sci* (2016) 7 (2):1016–27. doi: 10.1039/c5sc02769a

36. Satpute SK, Banpurkar AG, Dhakephalkar PK, Banat IM, Chopade BA. Methods for investigating biosurfactants and bioemulsifiers: a review. *Crit Rev Biotechnol* (2010) 30(2):127–44. doi: 10.3109/07388550903427280

37. Das S, Chowdhury R, Pal A, Okamoto K, Das S. Salmonella Typhi outer membrane protein STIV is a potential candidate for vaccine development against typhoid and paratyphoid fever. *Immunobiology* (2019) 224(3):371–82. doi: 10.1016/j.imbio.2019.02.011

38. Ghosh S, Chakraborty K, Nagaraja T, Basak S, Koley H, Dutta S, et al. An adhesion protein of Salmonella enterica serovar Typhi is required for pathogenesis and potential target for vaccine development. *Proc Natl Acad Sci U S A.* (2011) 108(8):3348–53. doi: 10.1073/pnas.1016180108

39. Barthel M, Hapfelmeier S, Quintanilla-Martínez L, Kremer M, Rohde M, Hogardt M, et al. Pretreatment of mice with streptomycin provides a Salmonella enterica serovar Typhimurium colitis model that allows analysis of both pathogen and host. *Infect Immun* (2003) 71(5):2839–58. doi: 10.1128/IAI.71.5.2839-2858.2003

40. Rondini S, Micoli F, Lanzilao L, Gavini M, Alfini R, Brandt C, et al. Design of glycoconjugate vaccines against invasive African Salmonella enterica serovar Typhimurium. *Infect Immun* (2015) 83(3):996–1007. doi: 10.1128/IAI.03079-14

41. Hedman K, Rousseau SA. Measurement of avidity of specific IgG for verification of recent primary rubella. *J Med Virol* (1989) 27:288–92. doi: 10.1002/jmv.1890270406

42. Fiorino F, Rondini S, Micoli F, Lanzilao L, Alfini R, Mancini F, et al. Immunogenicity of a bivalent adjuvanted glycoconjugate vaccine against salmonella typhimurium and salmonella enteritidis. *Front Immunol* (2017) 8:168. doi: 10.3389/fimmu.2017.00168

43. Shippy DC, Eakley NM, Mikheil DM, Fadl AA. Role of StdA in adhesion of Salmonella enterica serovar Enteritidis phage type 8 to host intestinal epithelial cells. *Gut Pathog* (2013) 5(1):43. doi: 10.1186/1757-4749-5-43

44. MacLennan CA, Martin LB, Micoli F. Vaccines against invasive Salmonella disease. *Human Vaccines & Immunotherapeutics*. (2014) 10(6):1478–93. doi: 10.4161/hv.29054

45. Pozsgay V. Oligosaccharide-protein conjugates as vaccine candidates against bacteria. *Adv Carbohydr Chem Biochem* (2000) 56:153–99. doi: 10.1016/s0065-2318(01)56004-7

46. Frasch CE. Preparation of bacterial polysaccharide-protein conjugates: analytical and manufacturing challenges. *Vaccine* (2009) 27(46):6468–70. doi: 10.1016/j.vaccine.2009.06.013

47. Costantino P, Rappuoli R, Berti F. The design of semi-synthetic and synthetic glycoconjugate vaccines. *Expert Opin Drug Discovery* (2011) 6(10):1045–66. doi: 10.1517/17460441.2011.609554

48. Micoli F, Rondini S, Pisoni I, Proietti D, Berti F, Costantino P, et al. Vi-CRM 197 as a new conjugate vaccine against Salmonella Typhi. *Vaccine* (2011) 29:712–20. doi: 10.1016/j.vaccine.2010.11.022

49. Wang JY, Chang AH, Guttormsen HK, Rosas AL, Kasper DL. Construction of designer glycoconjugate vaccines with size-specific oligosaccharide antigens and site-controlled coupling. *Vaccine* (2003) 21(11-12):1112–7. doi: 10.1016/s0264-410x(02)00625-4

50. Jones C. Vaccines based on the cell surface carbohydrates of pathogenic bacteria. *Acad Bras Cienc* (2005) 77:293–324. doi: 10.1590/s0001-37652005000200009

51. Lucas AH, Apicella MA, Taylor CE. Carbohydrate moieties as vaccine candidates. *Clin Infect Dis* (2005) 41(5):705–12. doi: 10.1086/432582

52. Bröker M, Berti F, Costantino P. Factors contributing to the immunogenicity of meningococcal conjugate vaccines. *Hum Vaccin Immunother* (2016) 12(7):1808–24. doi: 10.1080/21645515.2016.1153206

53. Chu C, Schneerson R, Robbins JB, Rastogi SC. Further studies on the immunogenicity of Haemophilus influenzae type b and pneumococcal type 6A polysaccharide-protein conjugates. *Infect Immun* (1983) 40(1):245–56. doi: 10.1128/iai.40.1.245-256.1983

54. Lees A, Nelson BL, Mond JJ. Activation of soluble polysaccharides with 1 cyano-4-dimethylaminopyridinium tetrafluoroborate for use in proteinpolysaccharide conjugate vaccines and immunological reagents. *Vaccine* (1996) 14:190–8. doi: 10.1016/0264-410x(95)00195-7

55. Shafer DE, Toll B, Schuman RF, Nelson BL, Mond JJ, Lees A. Activation of soluble polysaccharides with 1-cyano-4-dimethylaminopyridinium tetrafluoroborate (CDAP) for use in protein-polysaccharide conjugate vaccines and immunological reagents. II. Selective crosslinking of proteins to CDAP-activated polysaccharides. *Vaccine* (2000) 18(13):1273–81. doi: 10.1016/s0264-410x(99)00370-9

56. Schneerson R, Barrera O, Sutton A, Robbins JB. Preparation, characterization, and immunogenicity of Haemophilus influenzae type b polysaccharide-protein conjugates. *J Exp Med* (1980) 152(2):361–76. doi: 10.1084/jem.152.2.361

57. Grandjean C, Wade TK, Ropartz D, Ernst L, Wade WF. Acid-detoxified Inaba lipopolysaccharide (pmLPS) is a superior cholera conjugate vaccine immunogen than hydrazine-detoxified lipopolysaccharide and induces vibriocidal and protective antibodies. *Pathog Dis* (2013) 67(2):136–58. doi: 10.1111/2049-632X.12022

58. Ftacek P, Nelson V, Szu SC. Immunochemical characterization of synthetic hexa-, octa- and decasaccharide conjugate vaccines for Vibrio cholerae O:1 serotype Ogawa with emphasis on antigenic density and chain length. *Glycoconj J* (2013) 30 (9):871–80. doi: 10.1007/s10719-013-9491-9

59. Stefanetti G, Okan N, Fink A, Gardner E, Kasper DL. Glycoconjugate vaccine using a genetically modified O antigen induces protective antibodies to *Francisella tularensis*. *Proc Natl Acad Sci U S A.* (2019) 116(14):7062–70. doi: 10.1073/pnas.1900144116

60. Zhu H, Rollier CS, Pollard AJ. Recent advances in lipopolysaccharide-based glycoconjugate vaccines. *Expert Rev Vaccines* (2021) 20(12):1515–38. doi: 10.1080/14760584.2021.1984889

61. Watson DC, Robbins JB, Szu SC. Protection of mice against Salmonella typhimurium with an O-specific polysaccharide-protein conjugate vaccine. *Infect Immun* (1992) 60(11):4679–86. doi: 10.1128/iai.60.11.4679-4686.1992

62. Micoli F, Romano MR, Tontini M, Cappelletti E, Gavini M, Proietti D, et al. Development of a glycoconjugate vaccine to prevent meningitis in Africa caused by meningococcal serogroup X. *Proc Natl Acad Sci U S A.* (2013) 110(47):19077–82. doi: 10.1073/pnas.1314476110

63. An SJ, Yoon YK, Kothari S, Kothari N, Kim JA, Lee E, et al. Physico-chemical properties of Salmonella typhi Vi polysaccharide-diphtheria toxoid conjugate vaccines affect immunogenicity. *Vaccine* (2011) 29(44):7618–23. doi: 10.1016/j.vaccine.2011.08.019

64. Wessels MR, Paoletti LC, Guttormsen HK, Michon F, D'Ambra AJ, Kasper DL. Structural properties of group B streptococcal type III polysaccharide conjugate vaccines that influence immunogenicity and efficacy. *Infect Immun* (1998) 66 (5):2186–92. doi: 10.1128/IAI.66.5.2186-2192.1998

65. Kossaczka Z, Lin FY, Ho VA, Thuy NT, Van Bay P, Thanh TC, et al. Safety and immunogenicity of Vi conjugate vaccines for typhoid fever in adults, teenagers, and 2- to 4-year-old children in Vietnam. *Infect Immun* (1999) 67(11):5806–10. doi: 10.1128/IAI.67.11.5806-5810.1999

66. Fattom A, Shiloach J, Bryla D, Fitzgerald D, Pastan I, Karakawa WW, et al. Comparative immunogenicity of conjugates composed of the Staphylococcus aureus type 8 capsular polysaccharide bound to carrier proteins by adipic acid dihydrazide or N-succinimidyl-3-(2-pyridyldithio)propionate. *Infect Immun* (1992) 60(2):584–9. doi: 10.1128/iai.60.2.584-589.1992

67. Fattom A, Li X, Cho YH, Burns A, Hawwari A, Shepherd SE, et al. Effect of conjugation methodology, carrier protein, and adjuvants on the immune response to Staphylococcus aureus capsular polysaccharides. *Vaccine* (1995) 13:1288–93. doi: 10.1016/0264-410x(95)00052-3

68. Gupta RK, Szu SC, Finkelstein RA, Robbins JB. Synthesis, characterization, and some immunological properties of conjugates composed of the detoxified lipopolysaccharide of Vibrio cholerae O1 serotype Inaba bound to cholera toxin. *Infect Immun* (1992) 60(8):3201–8. doi: 10.1128/iai.60.8.3201-3208.1992

69. Simon R, Tennant SM, Wang JY, Schmidlein PJ, Lees A, Ernst RK, et al. Salmonella enterica serovar enteritidis core O polysaccharide conjugated to H:g,m flagellin as a candidate vaccine for protection against invasive infection with S. enteritidis. *Infect Immun* (2011) 79(10):4240–9. doi: 10.1128/IAI.05484-11

70. Baliban SM, Yang M, Ramachandran G, Curtis B, Shridhar S, Laufer RS, et al. Development of a glycoconjugate vaccine to prevent invasive Salmonella Typhimurium infections in sub-Saharan Africa. *PloS Negl Trop Dis* (2017) 11(4):e0005493. doi: 10.1371/journal.pntd.0005493

71. Svenson SB, Nurminen M, Lindberg AA. Artificial Salmonella vaccines: O-antigenic oligosaccharide-protein conjugates induce protection against infection with Salmonella typhimurium. *Infect Immun* (1979) 25(3):863–72. doi: 10.1128/iai.25.3.863-872.1979

72. Vidarsson G, Dekkers G, Rispens T. IgG subclasses and allotypes: from structure to effector functions. *Front Immunol* (2014) 5:520. doi: 10.3389/fimmu.2014.00520

73. Mäkelä O, Péterfy F, Outschoorn IG, Richter AW, Seppälä I. Immunogenic properties of alpha (1-6) dextran, its protein conjugates, and conjugates of its breakdown products in mice. *Scand J Immunol* (1984) 19(6):541–50. doi: 10.1111/j.1365-3083.1984.tb00965.x

74. Seppälä I, Pelkonen J, Mäkelä O. Isotypes of antibodies induced by plain dextran or a dextran-protein conjugate. *Eur J Immunol* (1985) 15(8):827–33. doi: 10.1002/eji.1830150816

75. Sun P, Pan C, Zeng M, Liu B, Liang H, Wang D, et al. Design and production of conjugate vaccines against S. Paratyphi A using an O-linked glycosylation system in *vivo*. *NPJ Vaccines* (2018) 3:4. doi: 10.1038/s41541-017-0037-1

76. Saxena M, Di Fabio JL. Salmonella typhi O-polysaccharide–tetanus toxoid conjugated vaccine. *Vaccine* (1994) 12(10):879–84. doi: 10.1016/0264-410x(94)90029-9

77. Halder P, Maiti S, Banerjee S, Das S, Dutta M, Dutta S, et al. Bacterial ghost cell based bivalent candidate vaccine against Salmonella Typhi and Salmonella Paratyphi A: A prophylactic study in BALB/c mice. *Vaccine* (2023) 41(41):5994–6007. doi: 10.1016/j.vaccine.2023.08.049

78. Reinhardt A, Yang Y, Claus H, Pereira CL, Cox AD, Vogel U, et al. Antigenic potential of a highly conserved Neisseria meningitidis lipopolysaccharide inner core structure defined by chemical synthesis. *Chem Biol* (2015) 22(1):38–49. doi: 10.1016/j.chembiol.2014.11.016

AMERICAN SOCIETY FOR MICROBIOLOGY | Infection and Immunity®

CELLULAR MICROBIOLOGY: PATHOGEN-HOST CELL MOLECULAR INTERACTIONS

Macrophage Cell Lines and Murine Infection by *Salmonella enterica* Serovar Typhi L-Form Bacteria

Debayan Ganguli,[a] Swarnali Chakraborty,[a] Suparna Chakraborty,[a] Ananda Pal,[a] Animesh Gope,[a] Santasabuj Das[a]

[a]ICMR–National Institute of Cholera and Enteric diseases, Beleghata, Kolkata, West Bengal, India

Debayan Ganguli and Swarnali Chakraborty contributed equally to this article. The order was determined by the corresponding author after negotiation.

ABSTRACT Antibiotic resistance of pathogenic bacteria has emerged as a major threat to public health worldwide. While stable resistance due to the acquisition of genomic mutations or plasmids carrying antibiotic resistance genes is well established, much less is known about the temporary and reversible resistance induced by antibiotic treatment, such as that due to treatment with bacterial cell wall-inhibiting antibiotics such as ampicillin. Typically, ampicillin concentration in the blood and other tissues gradually increases over time after initiation of the treatment. As a result, the bacterial population is exposed to a concentration gradient of ampicillin during the treatment of infectious diseases. This is different from *in vitro* drug testing, where the organism is exposed to fixed drug concentrations from the beginning until the end. To mimic the mode of antibiotic exposure of microorganisms within host tissues, we cultured the wild-type, ampicillin-sensitive *Salmonella enterica* serovar Typhi Ty2 strain (*S.* Typhi Ty2) in the presence of increasing concentrations of ampicillin over a period of 14 days. This resulted in the development of a strain that displayed several features of the so-called L-form of bacteria, including the absence of the cell wall, altered shape, and lower growth rate compared with the parental form. Studies of the pathogenesis of *S.* Typhi L-form showed efficient infection of the murine and human macrophage cell lines. More importantly, *S.* Typhi L-form was also able to establish infection in a mouse model to the extent comparable to its parental form. These results suggested that L-form generation following the initiation of treatment with antibiotics could lead to drug escape of *S.* Typhi and cell to cell (macrophages) spread of the bacteria, which sustain the infection. Oral infection by the L-form bacteria underscores the potential of rapid disease transmission through the fecal-oral route, highlighting the need for new approaches to decrease the reservoir of infection.

KEYWORDS *Salmonella*, L-form, ampicillin, macrophage, antibiotic resistance

Around 26.9 million cases of typhoid fever are reported annually worldwide (1). Multidrug-resistant strains of *Salmonella enterica* serovar Typhi have been known of for several decades and were isolated in different parts of the globe. *S.* Typhi was earlier treated with ampicillin, chloramphenicol, and trimethoprim-sulfamethoxazole (2). The appearance of multidrug resistance to first line antibiotics during late the 1980s led fluoroquinolones, especially ciprofloxacin, becoming the drug of choice for typhoid fever (3). In 1991, an *S.* Typhi strain resistant to ciprofloxacin emerged, which led to an outbreak in 1997 (4). Subsequently, macrolides, 3rd-generation cephalosporins, and carbapenems were widely used to treat *S.* Typhi infection. In 2018 and 2019, extremely drug-resistant (XDR) *S.* Typhi strains, unresponsive to macrolides, fluoroquinolones, and 3rd-generation cephalosporins were reported from Hyderabad, Pakistan (5, 6). The WHO had recently announced 10,365 infections with XDR strains in Pakistan and travel-associated infections in China, the United States, Australia, Denmark, and Canada, thus making *S.* Typhi drug resistance a global threat (7). Interestingly, reversal of ampicillin sensitivity to *S.* Typhi was reported by studies carried out in different

Editor Igor E. Brodsky, University of Pennsylvania

Address correspondence to Santasabuj Das, santasabujdas@yahoo.com.

The authors declare no conflict of interest.

Received 25 March 2022
Accepted 20 April 2022
Published 19 May 2022

parts of India (8). Harish et al. reported that ampicillin-resistant strains in Chennai fell from 52% to 23% during the period of 2002 to 2009 (9). In another study, around 94.5% of *S. Typhi* clinical isolates collected from India were found to be ampicillin sensitive (10).

Antibiotic resistance of *S.* Typhi was believed to be plasmid-borne. Genome sequencing of CT18 and several other ampicillin-resistant *S.* Typhi strains revealed the presence of a *Salmonella*-associated transferable R plasmid, called pHCM1 (11). This plasmid was responsible for the resistance to all three first-line antibiotics. However, temporary and reversible ampicillin resistance may also be conferred by the formation of L-form bacteria. Ampicillin targets the bacterial cell wall machinery, and bacteria can overcome the lethal effects of the drug by shutting down the cell wall production temporarily. The bacterial L-form was first discovered in 1935 (12), and subsequent studies further characterized this form. However, most studies were carried out in the pre-molecular biology era, and thorough knowledge about the formation of the L-form is still lacking. Recently, Errington and others explored the mechanism underlying L-form transition of *Bacillus subtilis* (13–15). They discovered that deletion of the cell wall machinery genes (*murE* operon) was not sufficient to induce stable L-form growth. Inactivating mutation of *ispA* or a glycolytic or respiratory chain enzyme in addition to *murE* knockout was necessary for the L-form to survive (15). However, the transient and reversible nature of antibiotic resistance, associated with the L-form failing to attract much global attention, led to poor understanding about its significance in the pathogenesis and contribution to treatment failures associated with antimicrobial resistance. Notwithstanding, bacterial L-forms were shown to be responsible for recurrent and chronic infections, although their diagnosis as etiologic agents is frequently missed due to slow growth and the requirement for specialized culture medium. Back in 1965, the L-form was suggested to cause chronic staphylococcal infection (16). Gutman et al. isolated L-forms of *Escherichia coli*, *Klebsiella* spp., and *Enterococcus faecalis* from patients suffering from chronic bacteriuria or pyelonephritis (17).

E. faecalis L-forms persisted in rats infected with walled bacteria following treatment with penicillin (18). Cell wall-deficient L-forms of *Corynebacterium* and *Mycobacterium tuberculosis* were isolated from blood samples of patients suffering from subacute bacterial endocarditis and sarcoidosis, respectively, who received antibiotic treatment (19, 20). Similar observations were made for patients with chronic brucellosis (21) and rheumatic fever caused by group A *Streptococci* (22).

Salmonella was also reported to undergo L-form transition in the presence of cell wall-targeting drugs. Recent studies with *S. enterica* serovar Typhimurium showed that the L-form can be readily induced by cefazolin (23). These L-form bacteria were also resistant to 3rd-generation cephalosporins (23). Others envisaged L-form *Salmonella* to be responsible for the long-term effects of attenuated bacterial vaccines, indicating their nonpathogenic nature (24). On the contrary, several studies from 1970s suggested that L-form *Salmonella* was capable of causing disease. However, most of these publications were either not in English or unavailable in the databases. Development of L-form *Salmonella in vivo* and its role in pathogenesis require further elucidation.

In this study, we induced transition to the *S.* Typhi L-form *in vitro* by treating an ampicillin-sensitive strain (Ty2) with increasing concentrations of ampicillin over a period of 14 days. This exposure of a drug-sensitive *S.* Typhi strain to a gradient of ampicillin would mimic the *in vivo* condition during treatment of typhoid fever patients with antibiotics. We characterized the *S.* Typhi L-form generated and demonstrated its abilities to infect murine and human macrophage cell lines. Finally, we showed that L-form bacteria were capable of establishing productive infection in a mouse model. This study, for the first time, explored in detail the potential pathogenic role of the ampicillin-induced L-form of *S.* Typhi.

RESULTS

Generation of *S.* Typhi L-form and its characterization. Parental *S.* Typhi strain Ty2 was subjected to increasing concentrations of ampicillin over a period of 14 days as described under Materials and Methods. The bacterial strain obtained at the end of the cultures was called A_{200}, since the dose escalation of ampicillin was done up to 200 μg/mL.

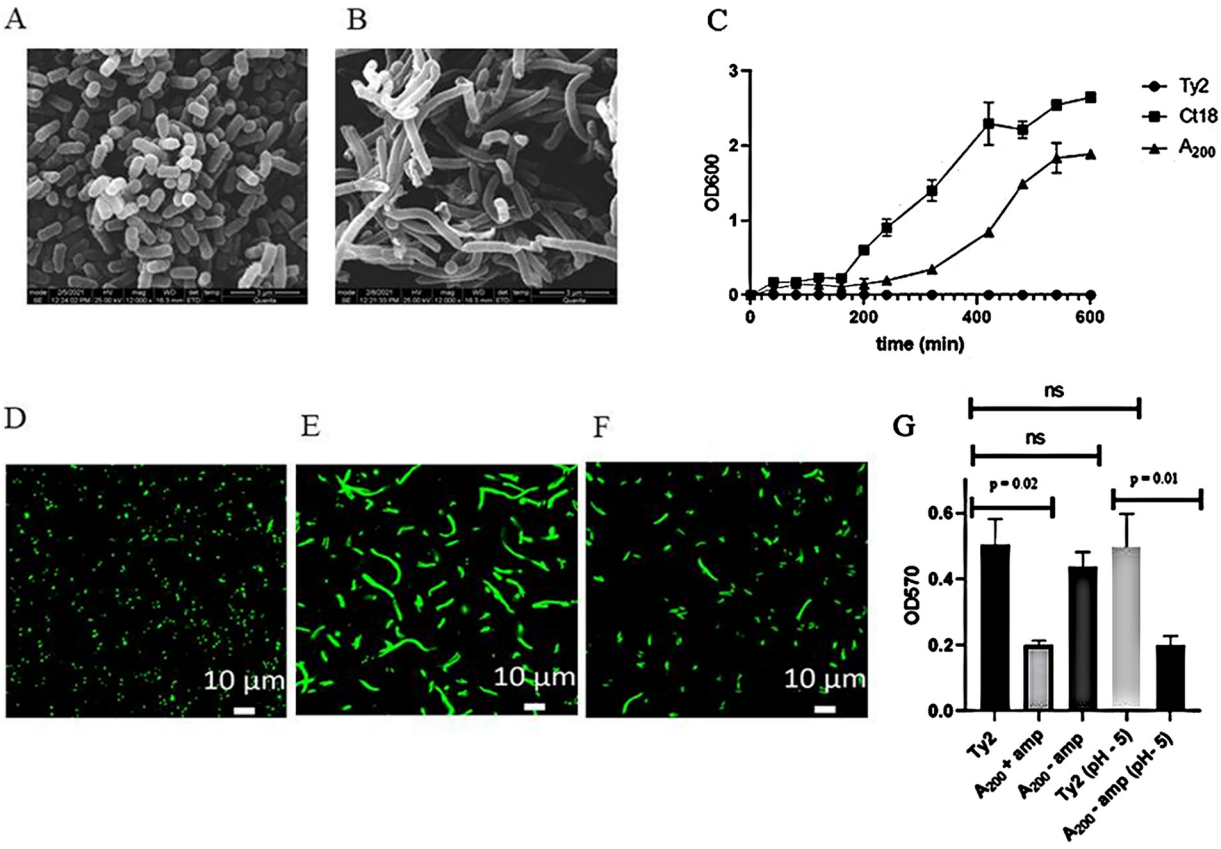

FIG 1 Characterization of A200. (A and B) Electron microscopic image of overnight cultures of parental Ty2 (A) and A_{200} (B). (C) Growth curves of ampicillin-sensitive (Ty2), ampicillin-resistant (CT18), and A_{200} strains. The data represent the mean of three independent experiments, with the standard deviation (SD) value indicated by the error bar. (D to F) Confocal microscopy of GFP-expressing bacteria cultured overnight in LB broth. (D) Ty2; (E) A_{200} in the presence of ampicillin; (F) A_{200} in the absence of ampicillin. (G) Quantification of total peptidoglycan extracted from 106 cells of Ty2 or A_{200} cultured at pH 7.0 or pH 5.0. A_{200} grown in the presence or absence of ampicillin. The data shown are the mean of three independent experiments, with the SD value shown by the error bar. Statistical significance was measured by Student's *t* test.

Visualization of A_{200} under a scanning electron microscope revealed gross morphological changes from parental Ty2 in the form of an elongated shape with a higher cytoplasmic to nuclear ratio (Fig. 1A and B). Each bacterial cell of A_{200} contained more than one nucleoid region, compared with the single-nucleoid parental bacteria (compare Fig. S1A and B at https://doi.org/10.6084/m9.figshare.19673022.v1), indicating compromised cell division of A_{200}. Furthermore, comparison of the growth curves of A_{200} and a naturally ampicillin-resistant strain, CT18, showed significantly reduced growth of the former bacterium (Fig. 1C). However, when A_{200} was allowed to grow in the absence of ampicillin, it resumed the growth kinetics of parental Ty2 (Fig. S1C at the URL mentioned above). In addition, most cells rapidly reverted back to the original morphology upon removal of ampicillin (compare Fig. 1D to F). Time kinetic studies revealed that the reversion of morphology and restoration of growth rate of the majority of A_{200} bacteria occurred within a period of 3 h of culture in the absence of ampicillin (see Fig. S1E at the URL mentioned above). However, this reversion was not observed when A_{200} was allowed to grow at low pH (~5.0). At this pH, A_{200} continued to grow at a lower rate than the parental Ty2 (see Fig. S1C at the URL mentioned above) and retained an elongated morphology (Fig. S1E, lower panel at the URL mentioned above) even in the absence of ampicillin. In agreement with the previous studies (25), A_{200} produced significantly reduced amounts of peptidoglycan (Fig. 1G) and LPS (Fig. S2A at the URL mentioned above) compared to the parental form. When grown without ampicillin, A_{200} regained the cell wall, as indicated by the larger amount of peptidoglycan production (Fig. 1G; S1D at the URL mentioned above). However, culture at low pH (~5.0) (without ampicillin) interfered with the process of restoration of peptidoglycan production by A_{200} (Fig. 1G), further indicating

slower reversion of the L-form at acidic pH. Similar to other L-form bacteria, the A_{200} strain was more resistant to several antibiotics (Fig. S2B at the URL mentioned above), further suggesting that it did not revert back to the parental form. Together, the above observations strongly suggested that the A_{200} strain was indeed the L-form *S.* Typhi.

***S.* Typhi L-form was capable of infecting macrophage cells.** To compare the infectivity of the parental Ty2 and A_{200} mouse macrophage cell line, RAW264.7 and human THP-1 cell-derived macrophages were infected with a multiplicity of infection (MOI) of 50, followed by a gentamicin protection assay. The results showed greater susceptibility of THP-1 cells to infection, resulting in a higher number of intracellular bacteria at the 0-h time point (see Fig. S3 at https://doi.org/10.6084/m9.figshare.19673022.v1). This may be due to the human origin of the THP-1 cell line and human-restricted pathogenesis of *S.* Typhi. However, the difference in intracellular bacterial counts between the two cell lines was obliterated after 24 h of infection, underscoring the robust oxidative killing mechanisms of these cells. On the other hand, a higher number of intracellular A_{200} than the parental Ty2 bacteria were recovered at the 0-h time point, indicating its greater infectivity (see Fig. S3A and B at the URL mentioned above). This may be explained by the absence of LPS in A_{200}, which inhibits phagocytosis. Alternatively, A_{200} might display higher activities of Type III Secretion System (T3SS-1), which promotes bacterium-mediated endocytosis, although this possibility was not investigated in the current study. However, T3SS-mediated uptake is more relevant for nonphagocytic cells such as epithelial cells. Then, 24 h later, the intracellular bacterial number increased for both parental Ty2 and A_{200}, with the latter still being more numerous. This underscores efficient survival and multiplication of A_{200} within the mouse and human macrophage cell lines (see Fig. S3A and B at the URL mentioned above). To gain further insights into the infectivity of A_{200}, infected cells were visualized under the confocal microscope. At both the 0-h and 24-h time points, intracellular parental and A_{200} bacteria colocalized with the acidic vacuoles (stained with Dextran-Alexa fluor 594) (Fig. 2 and 3). A_{200} isolated from the macrophage cells after 24 h of infection retained the ability to grow in the presence of 200 μg/mL ampicillin, indicating no or minimal reversal of parental Ty2 (see Fig. S4A and B at the URL mentioned above). Together, the above results indicated that the A_{200} strain efficiently infected macrophages and replicated within the acidic vacuoles of these cells, despite altered morphology and slower growth in the *in vitro* cultures. Given the higher infectivity of the A_{200} strain, we investigated if it resulted in more cell death. To this end, infected cells were stained with annexin-V and propidium iodide (PI), and apoptosis was studied by flow cytometry. We observed 65% apoptosis of the cells after 24 h of infection with Ty2, compared with only 11% apoptosis following A_{200} infection. At 48 h postinfection, apoptosis further increased for Ty2-infected cells (~70%), but not for A_{200}-infected cells (Fig. 4). These results indicated that A_{200} induced minimal cell death, although it was more efficient in causing infection *in vitro*.

Further, we observed altered morphology of the host cells 24 h postinfection of the parental Ty2 strain, which was not observed at the 0-h time point or after infection with A_{200}. This difference in cell shape was not due to dextran preloading, as it was noted even in the absence of dextran, while dextran preloading failed to induce any change of the uninfected or A_{200}-infected cells (see Fig. S5 at https://doi.org/10.6084/m9.figshare.19673022.v1). Taking these data together, it might be concluded that higher stress, as underscored by more pronounced apoptosis after Ty2 infection, was perhaps responsible for the changes in cellular morphology.

***S.* Typhi L-form established infection in mice.** The ability of A_{200} to infect macrophage cell lines prompted us to investigate if it was also capable of establishing infection *in vivo*. Mice were infected orally or through the intraperitoneal (i.p.) route with a sublethal dose of the parental Ty2 or A_{200}. For oral infection, an iron-overload mouse model, as described previously, was used (26). Bacterial load in the visceral organs was measured at 2, 4, and 8 days postinfection (dpi). Similar numbers of both types of bacteria were recovered from the liver, spleen, and gallbladder after 2 days of i.p. infection, indicating that A_{200} was as competent as the parental organisms to infect live animals (Fig. 5). Bacterial load further increased for both Ty2 and A_{200} at 4 dpi, underscoring their competence for survival and replication *in vivo*. However, there was drastic reduction of the load in the visceral organs at 8 dpi, which suggested pathogen clearance by the host immune system. Interestingly, the visceral load for

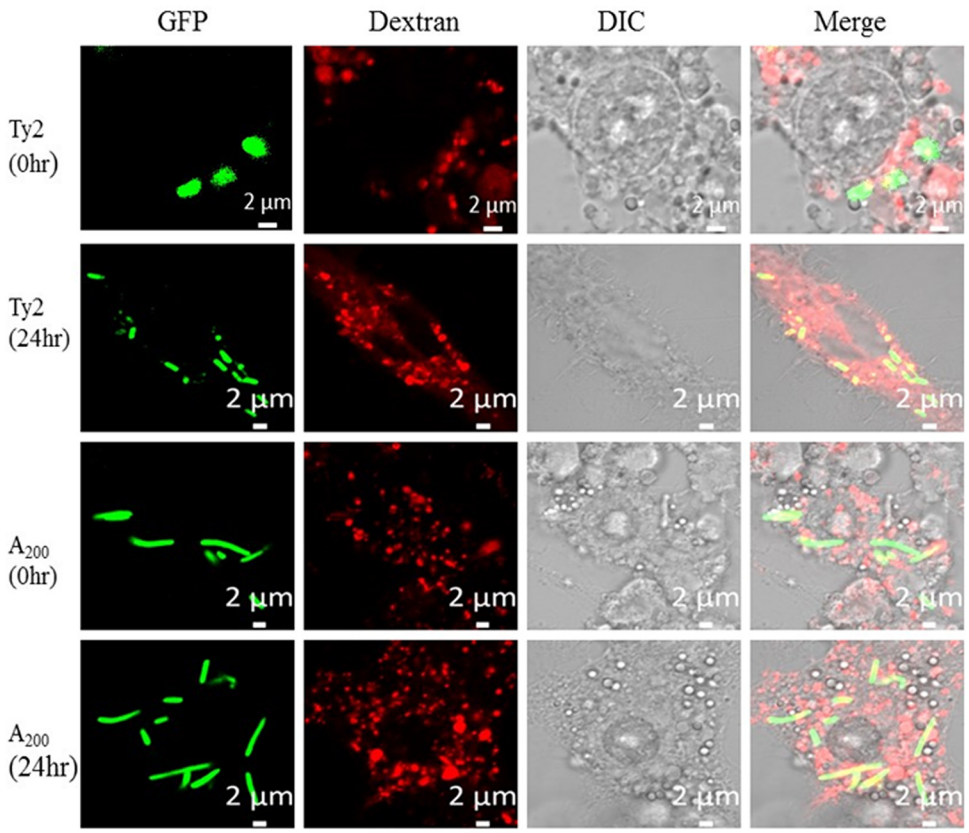

FIG 2 Infection of the RAW264.7 cell line with parental Ty2 and A_{200} strains. Representative confocal microscopy images of cells preloaded with dextran (red) and infected with 50 MOI of Ty2 or A_{200} bacteria expressing GFP (green). Intracellular localization of bacteria was studied by superimposition of red and green fluorescence (merged images). Scale bar = 2 μm.

A_{200} was significantly higher at this time point than with the parental bacteria. This observation indicated that A_{200} was perhaps more efficient in evading the host immune system. As opposed to i.p. infection, substantial bacterial recovery after oral administration was only observed at 4 dpi, suggesting a delay in systemic translocation following intestinal colonization (Fig. 6). Moreover, significantly fewer A_{200} bacteria than parental Ty2 were recovered from the internal organs at this time point. Given that both types of bacteria survived and replicated in the visceral organs with equal competence and that A_{200} was more efficient at resisting clearance by the host (Fig. 5), the above-described results suggested more efficient systemic invasion by parental *S.* Typhi from the intestine. However, higher resistance of A_{200} to host clearance led to minimization of the difference between the bacterial loads of the two strains in the internal organs at 8 dpi (Fig. 6). A_{200} isolated from the liver and spleen after 8 days of both peritoneal and oral infection was found to retain the ability to grow in the presence of ampicillin (200 μg/mL), indicating a lack of reversal to parental Ty2 (see Fig. S6A to D at https://doi.org/10.6084/m9.figshare.19673022.v1).

One mechanism of spread of the bacteria from the peritoneum to the bloodstream and visceral organs follows serosal colonization of the gut and subsequent invasion into the lamina propria, a process that requires lipopolysaccharide (LPS). That A_{200} was as competent as parental Ty2 to spread systemically from the peritoneum despite the absence of LPS indicates an alternative route of bacterial spread after i.p. infection. To address this question, bacterial load was measured in the blood, spleen, and gut 30 min postinfection. Significant numbers of bacteria were recovered from the blood and spleen, while the gut contained very few organisms (see Fig. S7 at https://doi.org/10.6084/m9.figshare.19673022.v1). This suggests direct spread of the bacteria from the peritoneum to the bloodstream and visceral organs, bypassing the gut. Our results corroborated the published studies that reported a

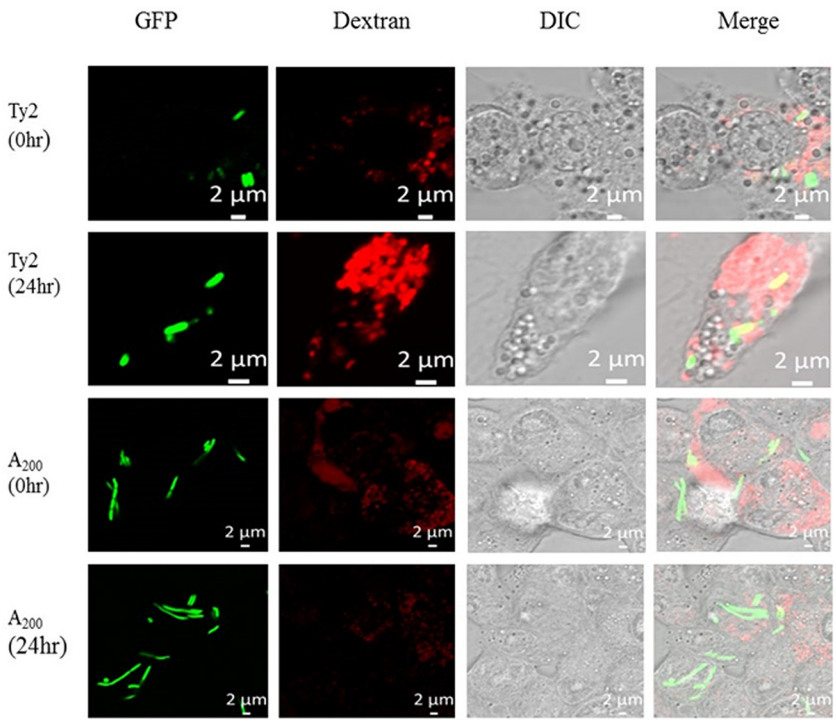

FIG 3 Infection of the THP-1 cell line with Ty2 and A_{200}. Representative confocal microscopy images of THP-1 cells preloaded with dextran and infected with *S. Typhi* strains as described for Fig. 2. Scale bar = 2 μm.

rapid spread of i.p. bacteria to the bloodstream through the thoracic duct lymph (27). This explain why A_{200}, despite having less LPS, was able to colonize the visceral organs when given i.p. Together, the above-described results suggested similar growth of the parental and L-form *S. Typhi* in the mouse peripheral blood and the visceral organs after oral and i.p. infection, in contrast to slower growth of A_{200} in the *in vitro* cultures. However, the L-form was less efficient in systemic translocation from the gut but resisted clearance by the host more efficiently once it entered the bloodstream.

DISCUSSION

Antibiotic treatment cures bacterial infection either by killing the pathogen or halting its growth, leading to clearance of bacteria by the host immune system. However, antibiotic concentration in the tissues does not reach the optimum level after the first dose of the drug; rather, it increases with time until it reaches the desired concentration. Thus, bacterial populations in different tissues are subjected to a progressively increasing gradient of antibiotics. In this study, we aimed to investigate the effects of an increasing concentration gradient of the antibiotic drug ampicillin on *S.* Typhi. Ampicillin inhibits transpeptidases and kills bacteria by blocking cell wall synthesis. When ampicillin-sensitive *S.* Typhi was subjected to progressively higher doses of the drug over a period of 14 days, the bacteria changed the morphology, shut down cell wall and LPS synthesis, and became able to grow in the presence of 200 μg/mL of ampicillin. This phenomenon was not observed when *S.* Typhi strain Ty2 was cultured in the presence of 200 μg/mL ampicillin from the beginning, which killed all the bacterial cells. This contrasts with *Salmonella* Typhimurium, where the L-form was induced by culturing antibiotic-sensitive bacteria with a cell wall-inhibiting drug, cefazolin, at a single dose (30 μg) (23). An increasing concentration gradient of ampicillin led to the transition of the *S.* Typhi Ty2 strain to L-form bacteria, as characterized by a drastic reduction of the cell wall and LPS production, an elongated shape with higher cytoplasmic volume and more than one nucleoid per cell, and significantly compromised growth in the *in vitro* cultures. However, characteristics of the parental strain were largely restored when ampicillin was removed from the culture medium, indicating that the changes were reversible. However, this

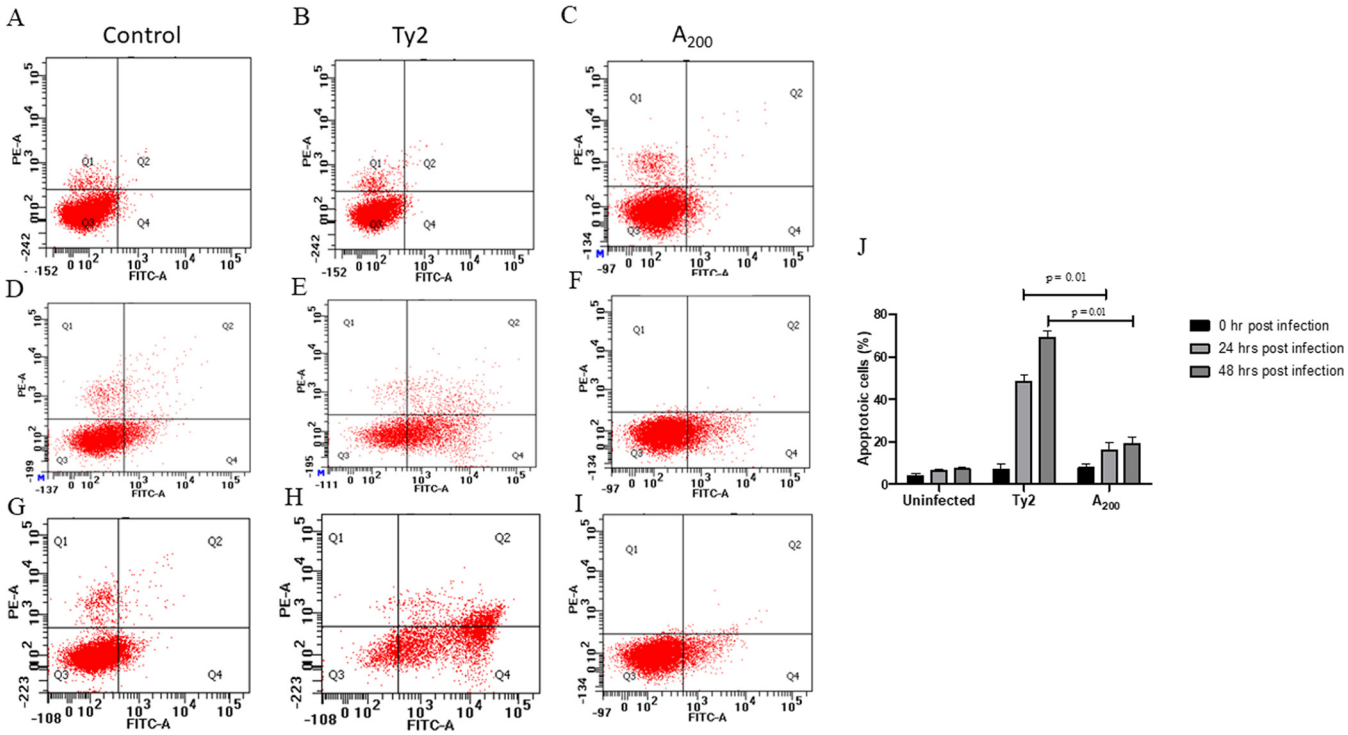

FIG 4 Apoptosis induction of THP-1 cells by Ty2 and A_{200}. (A to I) Representative flow cytometry images of THP-1 cells, either left uninfected or infected for different amounts of time with the Ty2 or A_{200} strain. Cells were harvested, washed with 1× PBS, and stained with annexin V and PI following the manufacturer's instructions. (A to C) 0 h infection; (D to F) 24 h of infection; (G to I) 48 h of infection. (J) Quantification of apoptotic cells as described for panels A to I. Data represent the mean of three independent experiments, with the SD value indicated by the error bar. Statistical significance was measured by Student's *t* test.

reversion greatly slowed down at an acidic pH. Since *Salmonella* resides in the acidic environment of phagosomes *in vivo*, the reversion to the parental Ty2 form would not readily happen. The morphological changes observed in this study were similar to those observed for cefazolin-induced L-form of *S.* Typhi (23). Similar phenotypic changes were reported by studies with multidrug-resistant (MDR) *E. coli* A9 strain, subjected to 20 times the MIC of ampicillin (28).

The L-form of several pathogenic species was isolated from different organs of individuals suffering from symptomatic infections and also from the carriers of the diseases (29). Isolation of the L-forms from the carriers particularly fascinated the microbiologists for several decades concerning the actual role of this form in the pathogenesis of a disease. *Streptococcus pyogenes* L-form was found to infect an animal model and persist over a longer period of time than the walled form. This L-form bacterium was phagocytosed by macrophages and survived and replicated inside these cells (30). On the contrary, the L-form of another Gram-positive bacterium, *Corynebacterium diphtheriae*, failed to cause productive infection and disease in the animal model. The authors concluded that defects in the cell wall formation abrogated diphtheria toxin production, leading to loss of infectivity (31). Unlike the Gram-positive bacteria, pathogenesis of Gram-negative bacterial L-forms remains largely unexplored.

In this study, the *S.* Typhi L-form was shown to infect murine as well as human macrophage cell lines. Gentamycin assay and confocal microscopic studies revealed active multiplication of the A_{200} strain inside these cells. Moreover, infectivity of the A_{200} strain was found to be higher than that of parental *S.* Typhi. This may be explained by reduced LPS synthesis by the A_{200} strain, since LPS was earlier reported to inhibit phagocytosis by macrophages. However, higher infectivity of the L-form did not result in more cell death, suggesting the potential for longer intracellular persistence.

A_{200} was as efficient as the parental *S.* Typhi Ty2 in establishing infection in a mouse model. When administered through the i.p. route, similar numbers of the two *S.* Typhi forms were isolated from different organs at 2 and 4 dpi, indicating that the two bacterial types

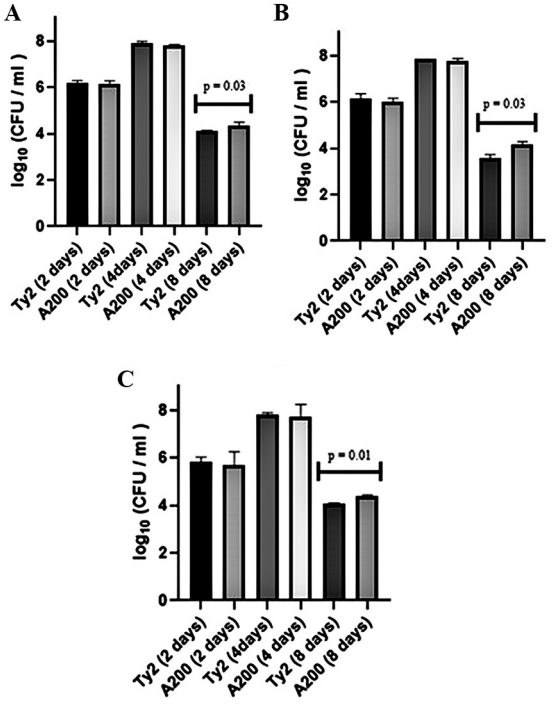

FIG 5 Intraperitoneal infection of mice by A_{200}. (A to C) Live bacteria were isolated from (A) liver, (B) spleen, and (C) gallbladder of BALB/c mice (n = 5) at the indicated time points of infection. CFU counts were done after growing the bacteria overnight on LB agar plates containing 50 μg/mL of streptomycin. Statistical significance was measured by Student's t test.

infected and multiplied with equal efficiency *in vivo*. However, despite a significant reduction in bacterial load at 8 dpi, suggesting clearance by the host immune system, the load for A_{200} in the host tissues remained considerably higher than that in parental Ty2. This suggested that A_{200} was more efficient in evading the host immune system. This is surprising given that the cell wall confers protection to bacteria against the host immune system. However, similar results were observed for *Streptococcus pyogenes* infection, where the L-form persisted for a longer period in the tissues and was thought to be responsible for recurrent bacterial infection (30). Perhaps the absence of the cell wall helped the L-form bacteria to avoid activation of the host immune system, thereby evading clearance by the host. We have also shown that after administration of bacteria through the i.p. route, the organisms directly enter the systemic circulation before invading the gut. This is in agreement with the previous studies where bacteria from the peritoneal cavity were found to migrate through the thoracic duct to the systemic circulation (27).

Surprisingly, A_{200} behaved differently inside the host upon oral delivery compared with the i.p. administration. Small but equal numbers of the parental and A_{200} strains were isolated from different organs of mice at 2 dpi, indicating equally efficient gut colonization and early translocation to the systemic sites. However, at 4 dpi, recovery of A_{200} was less than that of the parental bacteria. This was not due to slower replication of A_{200}, as reflected by the isolation of similar numbers of both forms of bacteria at different time points after i.p. infection (Fig. 5). This was not due to more rapid clearance of *S.* Typhi L-form from the systemic circulation either, since both parental Ty2 and A_{200} were isolated at higher numbers at 8 dpi than 4 dpi. Instead, cell wall-deficient A_{200} might be less efficient at colonizing the intestine, thus resulting in less systemic translocation at later time points. The exact mechanisms underlying the difference in relative recovery of the parental and L-form *S.* Typhi after oral infection requires further investigations.

S. Typhi was earlier shown to spontaneously convert to the L-form in the gallbladder (32). In our study, A_{200} was able to colonize the gallbladder after both oral and i.p. infections. Gallbladder colonization and fecal shedding are the most important factors behind *S.* Typhi

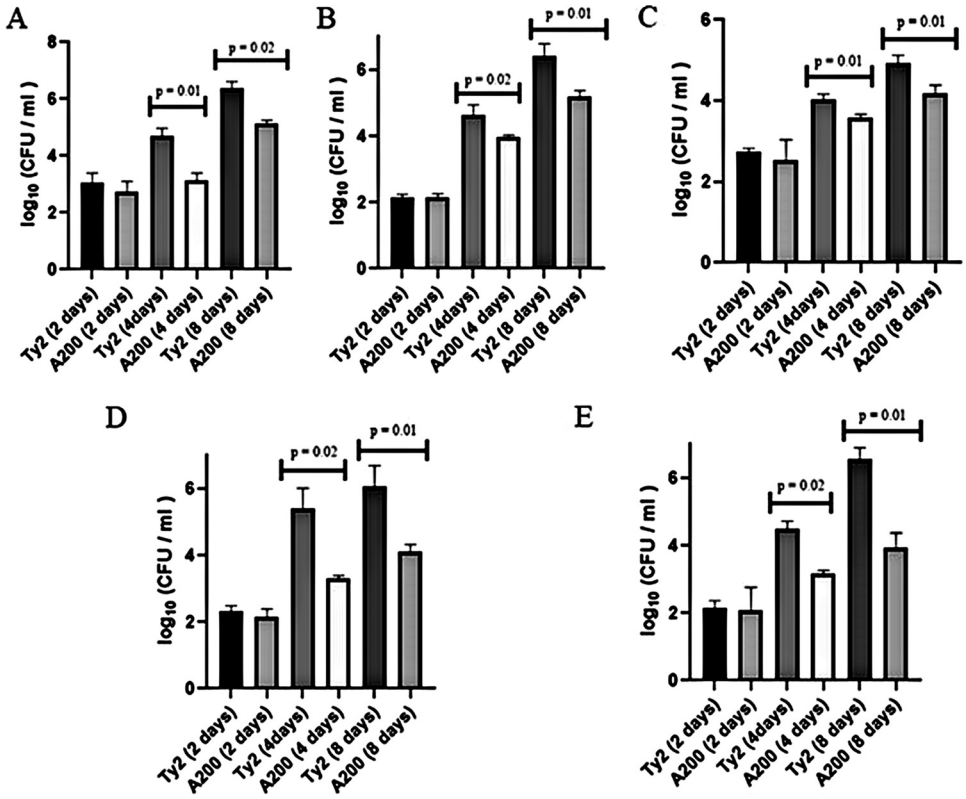

FIG 6 Oral infection of mice by A_{200}. Infection was done in iron-overload BALB/c mice (n = 5 per group) as described in Materials and Methods. (A to E) Bacteria isolated from (A) liver, (B) spleen, (C) gallbladder, (D) MLN, and (E) Peyer's patches at the indicated time points after the infection were enumerated as described for Fig. 4. Statistical significance was measured by Student's t test.

transmission from otherwise healthy carriers (33). The prevailing concept suggests that *S.* Typhi shed in the stool needs to revert back to the walled phenotype to infect a new host. Our study showed that *S.* Typhi L-form was equally capable of causing infection, which points toward more potent human to human transmission of *S.* Typhi.

Conclusions. No studies of the pathogenesis of the L-forms of *Salmonella* spp. are currently available. We studied pathogenesis of *S.* Typhi L-form after oral and i.p. infection for the first time. This study revealed that exposure of *S.* Typhi to an increasing concentration gradient of ampicillin during the treatment of human infection fails to clear the entire bacterial population from the host. Rather, it may render *Salmonella* resistant to the antibiotic without notable genetic mutations. In this state, cell wall-deficient and elongated bacteria infect macrophages and multiply efficiently *in vivo*.

MATERIALS AND METHODS

Cells and reagents. Cell lines (THP-1 and RAW) and cell culture reagents (RPMI, Dulbecco's modified Eagle's medium [DMEM], and fetal bovine serum [FBS]) were procured from the American Type Culture Collection (ATCC) and Invitrogen, respectively. Bacterial culture media (Luria-Bertani [LB] broth and LB agar) were purchased from HiMedia. *E. coli* DH5α and *Salmonella* Typhi Ty2 and CT18 strains were purchased from ATCC. All antibiotics used were procured from Sigma. pAKGFP1 plasmid (Addgene 14076) was modified by replacing the ampicillin resistance cassette with the kanamycin resistance gene (Kan^r).

Bacterial culture. *E. coli* DH5α, transformed with pAKGFP1 (Kan^r) was grown in LB broth containing 60 μg/mL of kanamycin at 37°C. Ty2 and CT18 strains were grown in LB broth in the presence of 50 μg/mL of streptomycin and 100 μg/mL of ampicillin, respectively, at 37°C. *S.* Typhi L-form (A_{200}) was grown in LB medium in the presence of 50 μg/mL of streptomycin and 200 μg/mL of ampicillin.

The GFP-Ty2 and GFP-A_{200} strains were generated by introducing the pAKGFP1 (Kan^r) plasmid into Ty2 and A_{200} by electroporation (5 pulses of 2,500 V each). Engineered bacterial strains, expressing green fluorescent protein (GFP) were grown in LB medium in the presence of streptomycin (50 μg/mL) and kanamycin (60 μg/mL) at 37°C. For GFP-A_{200}, ampicillin (200 μg/mL) was also added to the culture medium in addition to the other antibiotics.

Generation of *S.* Typhi L-form (A_{200}). Ampicillin-sensitive the *S.* Typhi Ty2 strain was sequentially exposed to increasing concentrations of ampicillin (0.05 μg/mL, 0.2 μg/mL, 0.8 μg/mL, 2 μg/mL, 10 μg/mL, 50 μg/mL, and 200 μg/mL) over a period of 14 days. Bacteria were allowed to grow for 2 days at each concentration of the drug until a saturated growth was obtained, and then they were transferred to fresh medium containing the next higher concentration of ampicillin.

***In vitro* growth assay.** About 105 cells were inoculated into 100 mL LB medium containing the appropriate antibiotic(s) (50 μg/mL streptomycin for Ty2, 50 μg/mL streptomycin and 200 μg/mL ampicillin for A200, 100 μg/mL ampicillin for CT18) and cultured at 37°C. For culture at low pH, 0.1 M HCl was added to the LB medium until the pH dropped to 5.0. Growth curves were obtained by plotting optical densities of the bacterial cultures, taken at 600-nm wavelength (OD_{600}) after different time intervals from the start of the culture.

LPS extraction and quantification. LPS was purified using hot phenol and quantified using the phenol-sulfuric acid method, as described previously (34). Briefly, bacteria were cultured for 18 h in LB medium at 37°C. The harvested cells ($\sim 10^{10}$ cells) were resuspended in distilled water and lysed by sonication (7 watts, 10-s pulse and 10-s interval for 20 min). The cell lysates produced were treated with DNase I (10 mg/mL) and RNase A (5 mg/mL), followed by proteinase K (20 mg/mL) at 60°C for 1 h. The lysate was then incubated with phenol at 65 to 70°C with vigorous shaking for 1 h, and the solution was allowed to cool down to 10°C before being centrifuged at 10,000 rpm for 10 min to separate the organic and aqueous phases. Finally, the aqueous phase was mixed with double the volume of ethanol, and the mixture was incubated overnight at −20°C for complete precipitation of LPS.

Purified LPS was quantified using the phenol-sulfuric acid method as described earlier (35). Briefly, LPS was incubated with 50% phenol at room temperature for 10 min. Then, 500 μL of concentrated sulfuric acid was added to the mixture, and the absorbance of the resulting yellow-colored solution was measured. The LPS concentration was finally determined using a standard curve, generated with commercially available LPS (Sigma).

Peptidoglycan estimation. Peptidoglycan was measured according to the standard protocol (36). Parental Ty2 and A_{200} were cultured in LB medium with or without ampicillin at pH 7.0 and pH 5.0 for 7 h at 37°C. About 10^6 bacterial cells from each culture were incubated with 50 μL of 1 M NaOH at 37°C for 30 min, followed by the addition of 1 mL of concentrated sulfuric acid, and kept in a boiling water bath for 3 min. The mixture was cooled down rapidly on ice for 1 min and treated with 10 μL of 0.16 M copper sulfate and 20 μL of 0.09 M p-hydroxy biphenyl at 30°C for 30 min. Peptidoglycan was estimated by measuring the absorbance at 570 nm using a spectrophotometer.

Cell culture. The human acute monocytic leukemia cell line, THP-1, was maintained in RPMI 1640 medium supplemented with 10% (vol/vol) heat-inactivated fetal bovine serum (FBS) and penicillin-streptomycin (50 μg/mL penicillin and 50 μg/mL streptomycin). Cells were maintained at a density of 5×10^5 to 1.0×10^6 cells/mL. To differentiate THP-1 cells into macrophages, they were cultured in the above-described medium in the presence of 100 nM phorbol 12-myristate 13-acetate (PMA) for 24 h, followed by a recovery phase culture of 24 h in the absence of PMA. Before every experiment, cells were cultured overnight in RPMI 1640 containing 10% FBS but no antibiotics. Mouse macrophage cell line RAW264.7 was cultured in Dulbecco's modified Eagle's medium (DMEM) supplemented with 10% FBS and penicillin-streptomycin. Cells were subcultured when 90% confluence was attained.

Gentamicin protection assay. This assay was done following the standard protocol (37). Briefly, THP-1 cells (5×10^5 cells/well of 24-well culture plates) were differentiated as described above and cultured overnight in complete RPMI without antibiotics. Ty2 and A_{200} bacterial cells were allowed to grow until the OD_{600} reached 1.0. Bacteria were harvested, washed repeatedly with phosphate-buffered saline (PBS), opsonized with the respective complete medium without antibiotics for 30 min, and added to the cell cultures at a multiplicity of infection (MOI) of 50 (10^9 and 10^8 bacterial cells were equal to OD 1.0 for the Ty2 and A_{200} strains, respectively). After synchronization of the bacteria and the cells by centrifugation at $400 \times g$ for 5 min, infection was continued for 30 min at 37°C in the presence of 5% CO_2. Extracellular bacteria were removed by repeated washing with 1× PBS, following which, the cells were cultured first in complete RPMI containing 100 μg/mL of gentamicin for 1 h and then in 15 μg/mL of gentamicin until the end of the experiment. Cells were lysed with 1× PBS containing 0.25% Triton X-100 (200 μL), and the lysates were plated on Luria-Bertani (LB) agar containing streptomycin (50 μg/mL). CFU counts were done after overnight growth of the bacteria on LB agar. For growth in the presence of ampicillin, bacteria were plated on LB agar containing 200 μg/mL ampicillin.

Confocal microscopy. THP1 and RAW264.7 cells were seeded on collagen-coated coverslips, placed in 24-well plates (5×10^5 cells per well), and cultured in antibiotic-free medium containing dextran-conjugated Alexa fluor 594 (5 mg/mL) (Thermo Fisher). Infection was done as described above under "Gentamicin Protection Assay." At the end of the experiment, cells were washed three times with 1× PBS, and the coverslips were mounted on clean glass slides with fluorophore mounting medium (Sigma). Dextran taken up into the acidic vacuoles of the cells emitted red fluorescence, which was visualized under a confocal microscope (Zeiss LSM710), and bacteria were counted manually.

***In vivo* experiments.** All animal experiments were carried out following the protocols approved by the Institutional Animal Ethics Committee of ICMR-National Institute of Cholera and Enteric Diseases (NICED), Kolkata, India (project license number PRO/103/May 2014-September 2017, date 11.03.1999). ICMR-NICED adheres to the animal handling protocols issued by the Committee for the Purpose of Control and Supervision of Experiments on Animals (CPCSEA), Ministry of Environment, Forest and Climate Change, Government of India. All mice were taken from an NICED in-house animal facility (registration [reg.] no. 68/GO/ReBi/S/99/CPCSEA). Mice were fed autoclaved chow and double-distilled water (ddH_2O) and kept at an ambient temperature of 25°C to 27°C with alternate light and dark cycles of 10 h and 14 h, respectively.

An iron-overload mouse model was used for oral *S.* Typhi infection as described previously (26). Briefly, 6- to 8-week-old female BALB/c mice were injected i.p. with desferrioxamine (Novartis, Switzerland;

0.025 mg/g of body weight) and Fe^{3+} (0.32 mg/g of body weight) 4 h prior to infection. Gastric acid was neutralized with 500 μL of 5% sodium bicarbonate, administered orally 20 min before the infection. Mice were infected with a sublethal dose (5×10^5 CFU) of log-phase cultures of *S.* Typhi, suspended in 100 μL of 1× PBS, and systemic infection was analyzed by the recovery of live bacteria from the liver, spleen, gallbladder, mesenteric lymph nodes (MLN) and Peyer's patches on 2, 4, and 8 days postinfection. To this end, single-cell suspensions of the above-mentioned organs were prepared, and the cells were lysed with 1 mL of 1× PBS containing 0.25% Triton X-100 (Sigma-Aldrich, USA). Cell lysates were plated on LB agar, supplemented with 50 μg/mL of streptomycin and, wherever needed, 200 μg/mL of ampicillin.

For i.p. infection, a sublethal dose (5×10^4 CFU) of *S.* Typhi in 1× PBS (100 μL) was injected into the peritoneum of 6- to 8-week-old BALB/c mice. Bacteria were recovered from the visceral organs (liver, spleen, and gallbladder) at the same time points as after the oral infection and plated on LB agar for CFU counting, as stated above.

ACKNOWLEDGMENTS

We declare that there is no conflict of interest regarding the publication of this article.

This work was partly funded by an extramural grant from ICMR (file number 2019-3127/Gen/ADHOC-BMS) and received intramural funding from ICMR.

REFERENCES

1. Wain J, Hendriksen RS, Mikoleit ML, Keddy KH, Ochiai RL. 2015. Typhoid fever. Lancet 385:1136–1145. https://doi.org/10.1016/S0140-6736(13)62708-7.
2. Rowe B, Ward LR, Threlfall EJ. 1997. Multidrug-resistant Salmonella typhi: a worldwide epidemic. Clinical Infectious Diseases 24:S106–S109. https://doi.org/10.1093/clinids/24.Supplement_1.S106.
3. Rowe B, Ward LR, Threlfall EJ, Wallace M, Yousif A. 1990. Spread of multiresistant Salmonella typhi. Lancet 8722:P1065–P1066.
4. Threlfall EJ, Ward LR, Skinner JA, Smith HR, Lacey S. 1999. Ciprofloxacin-resistant Salmonella typhi and treatment failure. Lancet 353:1590–1591. https://doi.org/10.1016/s0140-6736(99)01001-6.
5. Qamar FN, Yousafzai MT, Khalid M, Kazi AM, Lohana H, Karim S, Khan A, Hotwani A, Qureshi S, Kabir F, Aziz F, Memon NM, Domki MH, Hasan R. 2018. Outbreak investigation of ceftriaxone-resistant Salmonella enterica serotype Typhi and its risk factors among the general population in Hyderabad, Pakistan: a matched case-control study. Lancet Infect Dis 18:1368–1376. https://doi.org/10.1016/S1473-3099(18)30483-3.
6. Yousafzai MT, Qamar FN, Shakoor S, Saleem K, Lohana H, Karim S, Hotwani A, Qureshi S, Masood N, Rauf M, Khanzada JA, Kazi M, Hasan R. 2019. Ceftriaxone-resistant Salmonella Typhi outbreak in Hyderabad City of Sindh, Pakistan: high time for the introduction of typhoid conjugate vaccine. Clin Infect Dis 68:S16–S21. https://doi.org/10.1093/cid/ciy877.
7. Chatham-Stephens K, Medalla F, Hughes M, Appiah GD, Aubert RD, Caidi H, Angelo KM, Walker AT, Hatley N, Masani S, Nash J, Belko J, Ryan ET, Mintz E, Friedman CR. 2019. Emergence of extensively drug-resistant Salmonella Typhi infections among travelers to or from Pakistan—United States, 2016–2018. MMWR Morb Mortal Wkly Rep 68:11–13. https://doi.org/10.15585/mmwr.mm6801a3.
8. Krishnan P, Stalin M, Balasubramanian S. 2009. Changing trends in antimicrobial resistance of Salmonella enterica serovar Typhi and Salmonella enterica serovar Paratyphi A in Chennai. Indian J Pathol Microbiol 52:505–508. https://doi.org/10.4103/0377-4929.56140.
9. Harish BN, Menezes GA. 2011. Preserving efficacy of chloramphenicol against typhoid fever in a tertiary care hospital, India. WHO Offset Publ 15:92–96.
10. Kumar Y, Sharma A, Mani KR. 2011. Re-emergence of susceptibility to conventionally used drugs among strains of Salmonella Typhi in central west India. J Infect Dev Ctries 5:227–230. https://doi.org/10.3855/jidc.1310.
11. Parkhill J, Dougan G, James KD, Thomson NR, Pickard D, Wain J, Churcher C, Mungall KL, Bentley SD, Holden MT, Sebaihia M, Baker S, Basham D, Brooks K, Chillingworth T, Connerton P, Cronin A, Davis P, Davies RM, Dowd L, White N, Farrar J, Feltwell T, Hamlin N, Haque A, Hien TT, Holroyd S, Jagels K, Krogh A, Larsen TS, Leather S, Moule S, O'Gaora P, Parry C, Quail M, Rutherford K, Simmonds M, Skelton J, Stevens K, Whitehead S, Barrell BG. 2001. Complete genome sequence of a multiple drug resistant Salmonella enterica serovar Typhi CT18. Nature 413:848–852. https://doi.org/10.1038/35101607.
12. Klieneberger E. 1935. The natural occurrence of pleuropneumonia-like organisms in apparent symbiosis with Streptobacillus moniliformis and other bacteria. J Pathol 40:93–105. https://doi.org/10.1002/path.1700400108.
13. Kawai Y, Mercier R, Wu LJ, Domínguez-Cuevas P, Oshima T, Errington J. 2015. Cell growth of wall-free L-form bacteria is limited by oxidative damage. Curr Biol 25:1613–1618. https://doi.org/10.1016/j.cub.2015.04.031.
14. Gilpin RW, Young FE, Chatterjee AN. 1973. Characterization of a stable L-form of Bacillus subtilis 168. J Bacteriol 113:486–499. https://doi.org/10.1128/jb.113.1.486-499.1973.
15. Kawai Y, Mercier R, Mickiewicz K, Serafini A, de Carvalho LPS, Errington J. 2019. Crucial role for central carbon metabolism in the bacterial L-form switch and killing by β-lactam antibiotics. Nat Microbiol 4:1716–1726. https://doi.org/10.1038/s41564-019-0497-3.
16. Godzeski CW, Brier G, Griffith RS, Black HR. 1965. Association of bacterial L-phase organisms in chronic infections. Nature 205:1340–1340. https://doi.org/10.1038/2051340a0.
17. Gutman LT, Turck M, Petersdorf RG, Wedgwood RJ. 1965. Significance of bacterial variants in urine of patients with chronic bacteriuria. J Clin Invest 44:1945–1952. https://doi.org/10.1172/JCI105300.
18. Guze LB, Kalmanson GM. 1964. Persistence of bacteria in "protoplast" form after apparent cure of pyelonephritis in rats. Science 143:1340–1341. https://doi.org/10.1126/science.143.3612.1340.
19. Wittler RG, Malizia WF, Kramer PE, Tuckett JD, Pritchard HN, Baker HJ. 1960. Isolation of a Corynebacterium and its transitional forms from a case of subacute bacterial endocarditis treated with antibiotics. J Gen Microbiol 23:315–333. https://doi.org/10.1099/00221287-23-2-315.
20. Almenoff PL, Johnson A, Lesser M, Mattman LH. 1996. Growth of acid fast L forms from the blood of patients with sarcoidosis. Thorax 51:530–533. https://doi.org/10.1136/thx.51.5.530.
21. Nelson EL, Pickett MJ. 1951. The recovery of L forms of Brucella and their relation to Brucella phage. J Infect Dis 89:226–232. https://doi.org/10.1093/infdis/89.3.226.
22. Onwuamaegbu ME, Belcher RA, Soare C. 2005. Cell wall-deficient bacteria as a cause of infections: a review of the clinical significance. J Int Med Res 33:1–20. https://doi.org/10.1177/147323000503300101.
23. Yang C, Li H, Zhang T, Chu Y, Zuo J, Chen D. 2020. Study on antibiotic susceptibility of Salmonella Typhimurium L forms to the third and forth generation cephalosporins. Sci Rep 10:1–5. https://doi.org/10.1038/s41598-020-59456-8.
24. Kita E, Nishikawa F, Kamikaidou N, Oku D, Yasui K, Kashiba S. 1992. Mechanism of the protective immunity against murine typhoid: persistence of Salmonella L forms in the liver after immunization with live-cell vaccines. FEMS Microbiol Immunol 5:191–199.
25. Stepanova LK, Gorelov AL, Sergeeva NS, Levina GA, IuA B. 1983. Immunoelectrophoretic analysis of the antigenic composition of Salmonella Typhi in the process of L transformation and reversion. Zh Mikrobiol Epidemiol Immunobiol 28:29–32.
26. Theeya N, Ta A, Das S, Mandal RS, Chakrabarti O, Chakrabarti S, Ghosh AN, Das S. 2015. An inducible and secreted eukaryote-like serine/threonine kinase of Salmonella enterica serovar Typhi promotes intracellular survival and pathogenesis. Infect Immun 83:522–533. https://doi.org/10.1128/IAI.02521-14.
27. Wells HG, Johnstone OP. 1907. On the route of absorption of bacteria from the peritoneal cavity. J Infect Dis 4:582–594. https://doi.org/10.1093/infdis/4.4.582.
28. Uzoechi SC, Abu-Lail NI. 2020. Variations in the morphology, mechanics and adhesion of persister and resister E. coli cells in response to ampicillin: AFM study. Antibiotics 9:235. https://doi.org/10.3390/antibiotics9050235.

29. Errington J, Mickiewicz K, Kawai Y, Wu LJ. 2016. L-form bacteria, chronic diseases and the origins of life. Philos Trans R Soc B 371:20150494. https://doi.org/10.1098/rstb.2015.0494.
30. Michailova L, Markova N, Radoucheva T, Stoitsova S, Kussovski V, Jordanova M. 2000. Atypical behaviour and survival of Streptococcus pyogenes L forms during intraperitoneal infection in rats. FEMS Immunol Med Microbiol 28:55–65. https://doi.org/10.1111/j.1574-695X.2000.tb01457.x.
31. Yi X, Wang H. 2006. Effect of cell wall defect on pathogenicity of Corynebacterium diphtheriae. J Microbiol 26:57–60.
32. Wang DN, Wu WJ, Wang T, Pan YZ, Tang KL, She XL, Ding WJ, Wang H. 2015. Salmonella L-forms: formation in human bile in vitro and isolation culture from patients' gallbladder samples by a non-high osmotic isolation technique. Clin Microbiol Infect 21:470.e9. https://doi.org/10.1016/j.cmi.2014.12.016.
33. Khanam F, Darton TC, Meiring JE, Sarker PK, Biswas PK, Bhuiyan MAI, Rajib HN, Tonks S, Pollard AJ, Clemens JD, Qadri F. 2021. Salmonella Typhi stool shedding by patients with enteric fever and asymptomatic chronic carriers in an endemic urban setting. J Infectious Diseases 224:S759–S763. https://doi.org/10.1093/infdis/jiab476.
34. Hassan M, Ali A, Ahmad A, Saleemi MK, Wajid M, Sarwar Y, Iqbal M. 2021. Purification and antigenic detection of lipopolysaccharides of Salmonella enterica serovar Typhimurium isolate from Faisalabad, Pakistan. Pakistan Vet J 41:434–438.
35. Dubois M, Gilles KA, Hamilton JK, Rebers PT, Smith F. 1956. Colorimetric method for determination of sugars and related substances. Anal Chem 28:350–356. https://doi.org/10.1021/ac60111a017.
36. Maleehuan A, Ounjai P, Harnvoravongchai P, Janvilisri T, Chankhamhaengdecha S. 2021. Induction of Clostridioides difficile L-form. 7th International Conference on Biochemistry and Molecular Biology.
37. Dasgupta S, Das S, Biswas A, Bhadra RK, Das S. 2019. Small alarmones (p)ppGpp regulate virulence associated traits and pathogenesis of Salmonella enterica serovar Typhi. Cell Microbiol 21:e13034. https://doi.org/10.1111/cmi.13034.

INTERNATIONAL REVIEWS OF IMMUNOLOGY
https://doi.org/10.1080/08830185.2021.1925267

Taylor & Francis
Taylor & Francis Group

REVIEW

Tapping the immunological imprints to design chimeric SARS-CoV-2 vaccine for elderly population

Asim Biswas[a], Rahul Subhra Mandal[b], Suparna Chakraborty[c] and George Maiti

[a]Department of Ophthalmology, New York University Grossman School of Medicine, New York, NY, USA; [b]Department of Cancer Biology, Perelman School of Medicine, University of Pennsylvania, Philadelphia, PA, USA; [c]Division of Clinical Medicine, National Institute of Cholera and Enteric Diseases, Kolkata, India

ABSTRACT

The impact of SARS-CoV-2 and COVID-19 disease susceptibility varies depending on the age and health status of an individual. Currently, there are more than 140 COVID-19 vaccines under development. However, the challenge will be to induce an effective immune response in the elderly population. Analysis of B cell epitopes indicates the minor role of the stalk domain of spike protein in viral neutralization due to low surface accessibility. Nevertheless, the accumulation of mutations in the receptor-binding domain (RBD) might reduce the vaccine efficacy in all age groups. We also propose the concept of chimeric vaccines based on the co-expression of SARS-CoV-2 spike and influenza hemagglutinin (HA) and matrix protein 1 (M1) proteins to generate chimeric virus-like particles (VLP). This review discusses the possible approaches by which influenza-specific memory repertoire developed during the lifetime of the elderly populations can converge to mount an effective immune response against the SARS-CoV-2 spike protein with the possibilities of designing single vaccines for COVID-19 and influenza.

ARTICLE HISTORY
Received 16 February 2021
Accepted 23 April 2021

KEYWORDS
Immunosenescence; COVID-19; SARS-CoV-2; Influenza; vaccine; virus-like particle; memory cells; hemagglutinin

Highlights

- Immunosenescence aggravates COVID-19 symptoms in elderly individuals.
- Low immunogenicity of SARS-CoV-2 vaccines in elderly population.
- Tapping the memory T and B cell repertoire in elderly can enhance vaccine efficiency.
- Chimeric vaccines can mount effective immune response against COVID-19 in elderly.
- Chimeric vaccines co-express SARS-CoV-2 spike and influenza HA and M1 proteins.

Introduction

The appearance of novel coronavirus known as SARS-CoV-2 is accountable for the disease called COVID-19 which caused more than 2 million global deaths. Coronaviruses are widespread family of viruses existing in numerous species of animals, including camels, cattle, cats, bats, and birds. Zoonotic transmission of coronaviruses seldom transpires in the human population. The previous human to human transmission of coronaviruses occurred in 2003 and 2014 with SARS-CoV and the middle-eastern and the respiratory syndrome coronavirus (MERS-CoV), respectively. Current literature describes two types of the coronaviruses alphacoronaviruses (229E and NL63) and betacoronaviruses (OC43 and HKU1) that circulates in human causing common flu [1]. The pathogenic strains that infect human are SARS-CoV-1, MERS-CoV and SARS-CoV-2, all of which belong to betacoronaviruses [2]. SARS-CoV-2 has 29.9 kb single stranded positive sense RNA genome that encodes 29 viral genes. Around 16 of these elements codes for nonstructural proteins that are copied as pair of large polyproteins (Orf1a and Orf1b) that are further processed into different polypeptides via viral proteases. Other elements codes for several viral proteins that forms variety of accessory and structural components including the spike (S), envelope (E), membrane (M) and nucelocapsid (N) proteins. The interaction between the SARS-CoV-2 spike protein and the angiotensin-converting enzyme 2 (ACE2) receptor on host cell membrane helps the virus to penetrate the cell [3]. The trimeric S protein comprises of two subunits, S1 and S2, which mediates receptor binding and membrane fusion [4,5]. Hence the spike protein has been emphasized and used as a prime candidate for vaccine development globally [6,7].

CONTACT George Maiti George.Maiti@nyulangone.org

Development of vaccine is time consuming and challenging especially for the mutating RNA viruses. However, the mutation rate of SARS-CoV-2 is lower than other single stranded RNA viruses like influenza or HIV [8]. RNA viruses have the tendency to lose infectivity after acquiring mutation but few quasi-species retain infectivity and others become highly infective. These highly infective species bypass the existing immunity to establish themselves in the circulation as a new variant. The repeated viral mutation is well observed during flu season caused by influenza viruses. Every year new flu vaccine is developed based on the previous year's epidemiological data. SARS-CoV-2 rapid multiplication and infectivity allows the virus to acquire mutations such as D164G, A222V, L18F, P681H and N501Y mutations in the Spike (S) proteins, P323L in the NSP12 protein and R203K, G204R and A220V in the nucleocapsid proteins [9]. Current epidemiological studies have identified new variants in UK (B.1.1.7), South Africa (B.1.351) and Brazil (P.1) and all three have now been detected in the USA [10]. Current vaccines under use can neutralize emerging strains but to what extent they can protect elderly population remains a major concern.

Earlier reports by CDC indicated that older adults (≥ 65 years) comprising 9% of the global population accounted for more than 80% of COVID-19 related mortality [11]. This emphasizes the severity and vulnerability of the elderly individuals to SARS-CoV-2 infection. The SARS-CoV-2 infection can overwhelmingly excite the immune system in the elderly patients thereby leading to acute respiratory distress syndrome (ARDS) which is a natural outcome of immunopathological episodes and remains a critical reason for mortality [12]. The weakened immune system of older adults is characterized by steady decline of innate and adaptive immune responses poses a major challenge for developing a vaccine that will effectively work for people of all ages [13–15]. The bottleneck to developing such vaccines is the limited knowledge about the correlates of vaccine-induced protection in older adults. Previous studies have reported various physiological and immunological changes in the human body with aging [16,17]. Therefore, vaccination does not always ensure protection to an older individual due to their inherent loss of immune functions and heightened susceptibility to infectious diseases. Thus, we must consider additional safeguards while designing a vaccine for these groups. In this review, we emphasize on the elderly population (≥ 65 years age) and their immune correlation against vaccination based on previous and current studies. We further discuss the innovative approaches of hybrid vaccines containing influenza and SARS-CoV-2 motifs to overcome the suboptimal immune response during vaccination in elderly population.

Immunosenescence and aging aggravates COVID-19 disease

Multifaceted alterations in immune system are the hallmark of the aging process. Immunosenescence is defined as gradual decrease in immune function with age leading to augmented susceptibility to infectious diseases [18]. Studies have reported a systemic inflammatory state with aging, known as 'inflammaging' leading to a chronic low-grade inflammation in the lung of elderly people. The respiratory system undergoes a set of functional and structural changes with age. The progressive decline in lung functions including anatomical changes of the thoracic cage leading reduction in chest wall compliance, decreased strength of respiratory muscle affecting airway clearance are observed with aging [19,20]. Uncontrolled inflammation may impair lung, heart and kidney functions due to impeded resolution and presence of frailty in the older individuals [21]. Older individual has dysregulated innate immune cells lacking efficient phagocytosis and egress mechanism from the site of infection which further increases proinflammatory response by engaging with pathogen-associated molecular patterns (PAMPs) and damage-associated molecular patterns (DAMPs) resulting in further tissue damage [22,23]. Innate immune response is primarily responsible for initial inflammations leading to the accumulation of phagocytes (neutrophils and macrophages) at the site of infection. The phagocytes clear-up the virus infected cells and dead or apoptotic cells damaged due to viral multiplication [24,25]. Alveolar macrophages (Aφs) provide the first line defense against respiratory pathogen and plays a pivotal role maintaining tissue homeostasis [26]. In a resting state, Aφs binds to the alveolar type II epithelium and expresses regulatory ligands (CD200 and TGFβ) and anti-inflammatory cytokines, such as IL10 and TGF β [27,28]. Upon sensing any danger signals or insult, Aφs undergo molecular reprogramming to regulate a complex interaction between suppressive and activating signals [29,30]. Neutrophils from aged animals also show a similar reduced ability to mount an innate immune response like formation of neutrophil extracellular traps (NETs) [31,32]. Lower expression of Atg5 in aged mice leads to reduced autophagy mediated NET formation [33]. Innate immune responses promote adaptive immunity by

stimulating the antigen presenting cells (APCs) to capture and present antigen and by producing cytokines, chemokines and co stimulatory molecules that is required for optimum T helper cell response at the secondary lymphoid organs [34]. Antibodies and CD4+ T cells are essential to neutralize virus particles by opsonization and killing of virus infected cells by cytotoxic T cells [35,36]. Aging significantly influences thymic involution with a gradual declination of the structural integrity of the thymus in aged people resulting in a steady decrease in the T cell production [37]. Older individuals have reduced number of naïve T helper cell populations and distorted lymph node architecture critical to retain naïve cells which promote germinal center reaction after activation by APCs to produce affinity matured and class switched antibodies (Figure 1A) [38,39].

Outcome of any infectious disease depends on both the arm of the immune responses. Aging leads to gradual changes in every aspect of host immunity affecting both the innate and adaptive immune arm resulting in heightened inflammatory response or cytokines storms during robust viral replication and cell damage that defines the disease pathophysiology of COVID-19 [40,41]. Recent clinical studies have reported significant upregulation in proinflammatory cytokines (TNF-α, IL-1β, IL-6, IL-8, G-CSF and GM-CSF) and chemokines such as MCP1, IP10 and MIP1α in severely affected COVID-19 individuals [42–44]. Cytokines storms are characteristics for many viral diseases like SARS, MERS and H5N1 infection including the current COVID-19, providing them an inflammatory disease signature [45,46]. High SARS-CoV-2 replication in the type 2 pneumocytes causes it to differentiate from a quiescent state to a highly proliferating inflammatory state resulting in an impairment of suppressing signals [47].

Severely affected SARS-CoV-2 patients of all ages have very low number of T regulatory (Tregs) cells [48]. Patients severely suffering from COVID-19 were reported to have an uncontrolled inflammation associated with pneumonia, myocarditis and microvascular

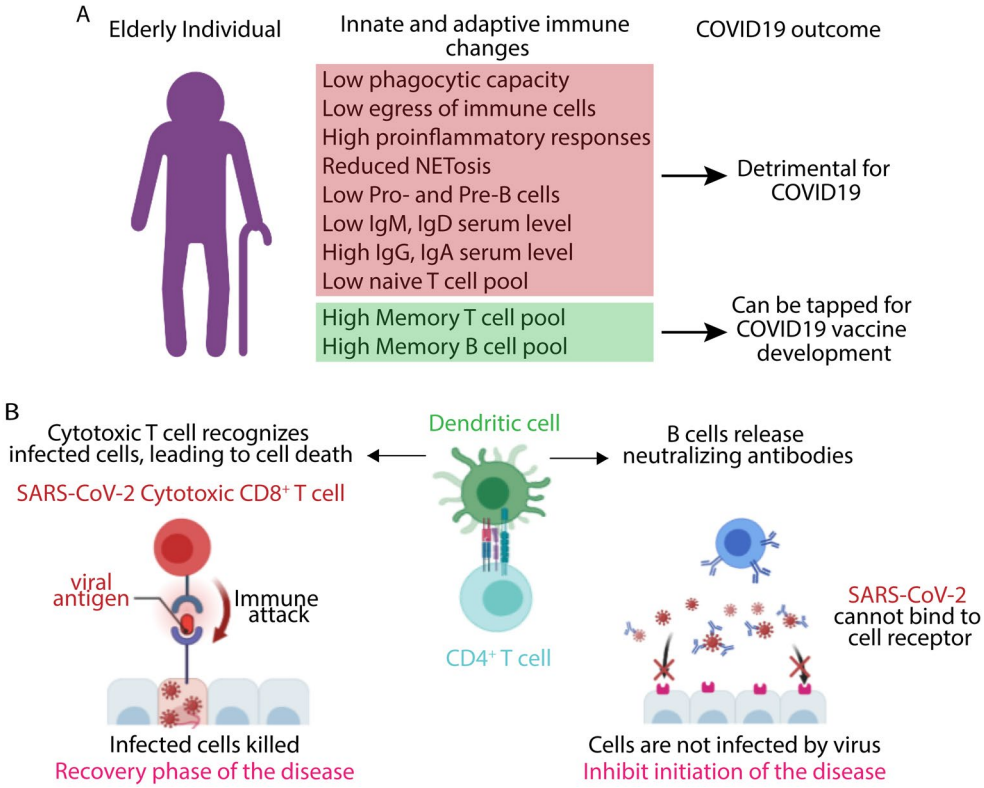

Figure 1. Factors influencing COVID-19 outcomes in the elderly population. **A.** Immunosenescence mediated changes in innate and adaptive immune response might affect the COVID19 disease outcome. The immunosenescence is characterized by thymic involution, modified T and B cell responses due to alteration in the naïve/memory lymphocyte population, and heightened serum levels of IgG and IgA with a lower level of IgM and IgD, and a weak response to newly encountered pathogens/antigens such as SARS-CoV2 or influenza or after vaccination which may lead to severe disease outcome specially within the elderly population. **B.** Both the humoral (mediated by SARS-CoV-2 specific neutralizing antibodies) and cellular immune response (mediated by CD8+T cells that kills virus infected cells) are indispensable for effective COVID-19 immune response. Diverse memory T and B cells in elderly individual might act as a reservoir that can be tapped to raise a strong adaptive immune response against SARS-CoV-2 by tweaking novel vaccine design.

thrombosis, and cytokine storms which can be effectively dealt with increased Tregs [49]. Several clinical studies with SARS-CoV-2 patients have reported the presence of proinflammatory cytokines including IL6, IL8 and IL12, IFN γ and IL-2 [50,51]. ACE2, the key receptor of SARS-CoV-2, is reported to be downregulated after SARS-CoV-2 infection, thereby leading to ARDS and cardiac injury due to increase accumulation of angiotensin II [52,53].

COVID-19 vaccination and immune response within the elderly population (≤65 years)

All the COVID-19 vaccines are designed to induce an effective antiviral response and the efficacy is analyzed by measuring the neutralizing antibody titer against the spike protein or receptors binding domain of spike [54]. The total number of CD4+ and CD8+ T cells were dramatically reduced in COVID-19 patients, especially among elderly and ICU patients. Moreover, T cells in these individuals shows high expression of PD-1 and Tim-3 expression compared to healthy controls, an indicative of T cell exhaustion [55]. A recent study compared T cell memory response in COVID-19 recovered patients (28 with mild disease and 14 with severe disease) and indicated that mild cases have higher proportions of SARS-CoV-2 specific CD8+ T cells whereas individual with severe COVID-19 have more SARS-CoV-2 specific antibody titer compared to mild case [48]. These finding suggest that humoral immune responses alone were unable to protect an individual from severity of the disease. Earlier study by Wang et al, have found that H7N9 infected influenza patients discharged within 2–3 weeks have early prominent H7N9-specific CD8+ T cell responses, while individuals with prolonged hospital stays have late recruitment of CD8+ or CD4+ T cells and antibodies simultaneously [56]. These studies suggest that recovery phases of acute viral infection are dependent on effective CD8+ T cell response. All these observations suggest an optimum T cell response is indispensable for the resolution of COVID-19 disease which may be lacking in elderly population and provide rationalization for vulnerability toward severe SARS-CoV-2 infection (Figure 1B). The use of spike as a vaccine candidate can be effective to induce effective CD8+ T cell responses, as new findings also suggest that during natural infection a significant number of CD8+ T cell responses were observed with spike derived peptide pool during ex vivo challenge [48,56,57].

Inovio pharmaceuticals had developed INO-4800, a novel DNA based vaccine candidate which is administered directly into the skin of the recipient through Cellectra 2000 [58,59]. As soon as the genetic sequence of the novel corona virus was published [60], Inovio constructed a DNA based vaccine without further delay utilizing their proprietary DNA medicine platform technology. It successfully prompted antigen specific robust T cell mediated immune response and neutralizing antibody production that effectively blocked the binding affinity of the spike protein to ACE2 receptor. Phase 1 clinical trial with INO-4800 exhibited excellent safety and tolerability and remained immunogenic in 100% (38/38) of the vaccinated individuals by evoking either or both humoral or cellular immune responses [59]. Currently a study with populations 51 years and older is underway (NCT04336410).

The mRNA vaccines are similar to DNA vaccines off late gaining much required attention due to their robust immunogenicity, easy production scale up, and the development of lipid nanoparticles for efficient delivery [61]. With this new technology viral antigen can be delivered as mRNA sequence within lipid nanoparticles (LNP) instead of viral protein molecules [62–64]. The antigen is then expressed in the recipient cells of the vaccinated individual to mount humoral and cell mediated immune responses (Figure 2). There are several mRNA vaccines that are under development or in trials for COVID-19 (Table 1).

Moderna in collaboration with the National Institute of Allergy and Infectious Diseases (NIAID) have developed a LNP encapsulated mRNA vaccine named mRNA-1273 that encodes full-length perfusion stabilized spike protein [65]. The perfusion form encompasses a transmembrane anchor and an unaltered S1-S2 cleavage site. The substitution mutation of two proline residues in the S2 region stabilizes the newly designed protein [66]. The genetic similarity of the MERS-CoV and SARS-CoV-2 lead to the development of a single synthetic viral RNA molecule as a vaccine candidate making it safer for human use. The phase 1 and phase 2 clinical trials were carried out to evaluate the safety, reactogenicity, and immunogenicity of the vaccine in human. Antigen-specific neutralizing antibody developed in a *Rhesus macaque* model also enhanced protection in the lung without any symptoms of pathological changes [67]. The participants in this trial were between the age group of 18–70 years. Vaccine trials have found mild adverse events of fatigue, chills, headache, and pain at the site of the injection area were observed. This study also reported the presence of neutralizing antibodies in the serum with strong CD4+ mediated T cell responses. The phase III trial had 25.3% population with 65 years and older age. The vaccine evoked

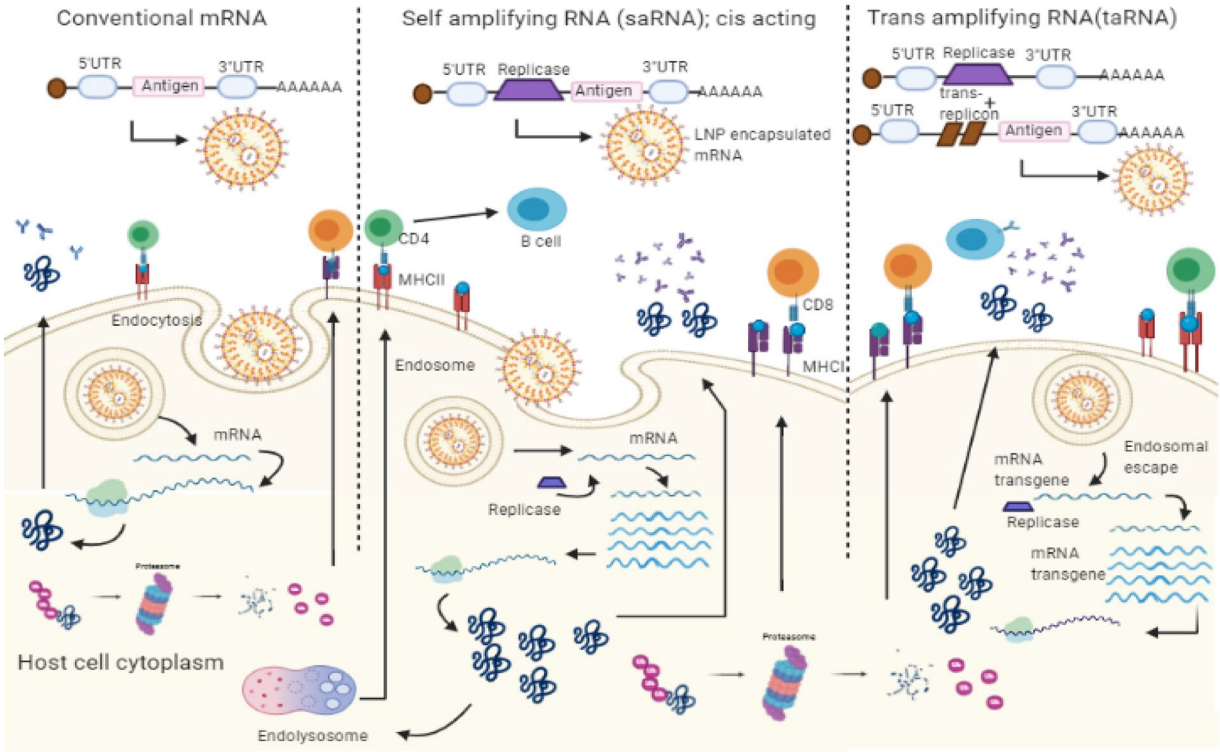

Figure 2. Overview of mRNA vaccines mediated immune responses. The mRNA incorporated in the lipid nanoparticles are delivered to host cells by intramuscular injection. Inside the cells, mRNA is translated into antigenic proteins which is subsequently processed into peptides by the proteasomal degradation or endosomal lysis and represented by MHC molecules on the plasma membrane to mount an immune response. There are some variations within mRNA vaccine architecture based on mRNA molecules either consisting of the only the target antigen (conventional mRNA vaccines) or target antigen along with replication machinery (self-amplifying or trans-amplifying mRNA vaccines) to amplify the mRNA molecules further after entering the host cells for a longer and higher amount antigen expression.

Table 1. Major COVID-19 vaccines available or under development.

Company/Institute	Vaccine name	Backbone	Target antigen	Age	Clinical status (Trial No.)
Inovio Pharmaceuticals	INO-4800	DNA-based	SARS-CoV-2 spike protein	≥19 to ≤64	Phase 2/3 (NCT04447781)
Codagenix/Serum Institute of India	CDX-005	Deoptimized live attenuated virus	Whole virus particle	No information	Preclinical/Phase 1 trial
Moderna/NIAID	mRNA-1273	mRNA	Stabilized spike protein	≥18	Phase1/2 /3 completed and under emergency use (NCT04470427)
BioNTech and Pfizer	BNT162	mRNA	Spike protein	≥18 to ≤55; 56 to ≤85	Phase1/2 /3 completed and under emergency use (NCT04380701)
Novavax	NVX-CoV2373	Protein Subunit	Full length S trimers/ nanoparticle + Matrix M	≥ 18 to 59 ≥ 18 to 84	Phase 2 (NCT04533399, NCT04368988). Phase 3 under trial
AstraZeneca	ChAdOx1 nCoV-19(AZD1222)	Non-replicating chimpanzee adenovirus	Spike protein	≥18 to ≤55 ≥18	In use (NCT04324606, NCT04516746)
Bharat Biotech	Covaxin (BBV152B)	Inactivated SARS-CoV-2 virus with 6 µg-Algel-IMDG	A whole virion	≥18	Phase III completed (NCT0464181)

elevated local and systemic adverse reactions compared to those in the placebo group during phase III trial, usually enduring a few days. The reactogenicity were commonly mild to moderate and generally less frequent in older adults (≥65 years) as compared to younger participants [68].

In USA, the BNT162 mRNA vaccine developed by BioNTech and Pfizer, encodes an optimized SARS-CoV-2 receptor-binding domain (RBD) antigen which is currently used for vaccination [69]. A prime-boost regimen strategy was explored with this vaccine and reported to be well tolerated during the early-stage human trial and elicited dose-dependent immunogenicity [70]. During December 2020, monitoring by the Vaccine Adverse Event Reporting System identified 21 cases of anaphylaxis (which is a severe,

life-threatening allergic reaction that occurs rarely after vaccination) following administration of a reported 1,893,360 primary doses of the Pfizer-BioNTech COVID-19 vaccine (11.1 cases per million doses); 71% of these appeared within 15 minutes of vaccination. Recent reports of 23 elderly patients death in Norway after having regular doses of Pfizer/BioNTech mRNA vaccines created panic in certain parts of the world about their safety and tolerability [71]. The higher dose of conventional mRNA vaccine can induce an adverse side effect in the vulnerable frail group. Health authorities are investigating the reason behind such deaths in the elderly population [71]. Both Moderna and Pfizer/BioNTech vaccines require two doses and the reactogenicity is typically higher after the booster dose.

Novavax investigated their proposed vaccine, NVX-CoV2373, full length S subunit protein, with or without Matrix-M^{TM} as an adjuvant. The anti-Spike IgG antibody was found to be present in the all-vaccine recipient right after the single dose and the presence of the adjuvant further augmented the polyfunctional CD4 + T cell responses [72]. In this study participants were between 18 to 59 years of age were divided in to multiple groups to carry out the immunogenicity of the vaccine. The phase 3 trial aimed in enrolling 30,000 people in the United States and Mexico with two cohorts: individuals 18 through 64 years old and those ≥ 65 years older, with a goal of enrolling at least 25% of all volunteers who are.

Live attenuated vaccines are produced by creating a genetically weakened variant of the virus that replicates to a constrained extent, causing no or mild disease but induces immune responses comparable to that induced by natural infection [73]. Codagenix, Inc. in collaboration with Serum Institute of India had developed CDX-005, an engineered live attenuated virus with the help of codon deoptimization software platform [74]. Although the amino acid sequence of the constructed mutated whole virus particle is structurally identical to the wild type SARS-CoV2, it is unable to replicate in the host. The newly designed nonpathogenic attenuated virus reported to generate strong humoral and T cell mediated immune responses in the preclinical studies with mice and guinea pigs and with non-human primates.

The ChAdOx1 nCoV-19 vaccine developed by the University of Oxford in collaboration with AstraZeneca and the Serum Institute of India, expresses a full-length, wild-type version of the Spike protein. The ChAdOx1 nCoV-19 vaccines are typically based on a modified adenovirus that has been engineered to express the Spike protein and has been disabled from replication in vivo by the deletion of parts of its genome. During safety and immunogenicity study with ChAdOx1 nCoV-19 the local and systemic reactions including pain, feeling feverish, colds, muscle ache, headache, and malaise were more frequent in the ChAdOx1 nCoV-19 groups which were lessened by the use of prophylactic paracetamol [75]. A recent study was conducted from four ongoing blinded, randomized, controlled trials done across the UK, Brazil, and South Africa. In this trial, in Britain, the registered population was predominantly white and, in younger age groups, incorporated more female participants due to the focus on recruitment of health-care workers whereas in Brazil, there was a larger proportion of nonwhite ethnicities. Study participants aged 18 years and older were randomly assigned to ChAdOx1 nCoV-19 vaccine or control. Overall vaccine efficacy across both groups was around 70·4% [76]. The phase 1/2 trial proposes two-dose regime where the booster dose induces a strong T cell response and anti-spike neutralizing antibody production and the vaccine is currently under phase 3 trial [77]. Recently many European countries halted the use of AstraZeneca's vaccine in March 2021 following the report of symptoms that led to at least 15 deaths. However, vaccination was resumed on European Medicines Agency (EMA) recommendation stating the benefits of vaccine outweighs its risks [78].

All these vaccines use various advanced technologies and are reported to mount a protective immune response by generating antigen specific neutralizing antibodies and an optimum T cell response. Most effective COVID-19 vaccine must induce an effective CD8+ T cell response with neutralizing antibody titer. However, current determinant of vaccine efficacy doesn't provide enough importance to CD8+ T cell response. Also, it is not known how long vaccine induced neutralizing antibody titer will provide protection from infection or reinfection. Current COVID-19 vaccine development must include the capability to efficiently induce CD8+ T cell memory response that will provide an additional layer of protection to avoid severe consequences during future reinfection. Vaccines developed using the whole virus not only induced CD8+ T cell response against Spike but also for other viral proteins like M, Nucleoprotein ORF3a, ORF6 and ORF7a [57,79–81]. Therefore, spike-based vaccines lack diversified CD8+ T cell responses, limiting the breadth of immune response which may play important role during resolution phase of the infection. Thus, all the next gen mRNA-based vaccines have an inherent drawback of lower capacity to induce diverse immune response particularly within

elderly individuals with low antigens specific naïve CD4+ or CD8+ T cells [82]. Although the current phase 3 trial results of mRNA-1273 vaccine suggests that it is safe and effective at preventing symptomatic COVID-19 in adults but its efficacy within elderly population (≥ 65 years) remains matter of concern. Recently, BioNTech and Pfizer have also expanded this study to determine vaccine efficacy within the elderly group but the data is yet to be public (NCT04368728) [70]. Gradual mutations in spike protein will make the current vaccines no longer effective similar to flu vaccines. However live attenuated SARS-CoV-2 strains can overcome such challenges by mounting an effective CD8+ T cell response to various relatively conserved proteins.

Lessons learned from earlier vaccination strategies for elderly population

New vaccines are being developed by modifying the antigen, the route of administration, higher dose administration and implementing adjuvants. Administering higher dose via parenteral route activates follicular DCs and subsequently antigen presentation and B cell activation in the older population [83]. Majority of the commercialized licensed vaccines imparts reduced immunogenicity and lesser protective efficacy among elderly population due to evident decrease in naïve T cell population, distorted lymphoid architecture whereas polyfunctional CD8+ T cell remain unaffected with aging [84]. The commercially available widely used vaccines for elderly people especially in the developing countries have recommended guidelines for vaccination in elderly people against infections like influenza, pneumonia, herpes zoster, and tetanus (Table 2). Waning immune system generates a weaker immune response toward vaccination in elderly population and requires repeated boosters.

Adjuvants are recognized to enhance the potency and endurance of specific immune responses generated to the administered antigen. However, live attenuated bacteria or viruses do not always require any adjuvants due to their structural components or genetic material that can induce the host's innate immune system. One such licensed attenuated vaccine, Zostavax, was reported to be 33% protective but can effectively reduce hospitalization suffering from herpes zoster and postherpetic neuralgia among the elderly [85], whereas TIV (trivalent inactivated influenza vaccine) contains two antigens from influenza A (H1N1, H3N2 strain) and one from influenza B strain (Victoria or Yamagata) along with MF59, is an oil in water emulsion based adjuvant composed of squalene, tween 20 and span 85. A cumulative effect of all of the components of MF59 was reported to impart enhanced immunogenicity by activating the genes supporting trans-endothelial cell migration, favoring antigen uptake and its transportation to the lymph node [86,87]. Matrix-MTM and ASO3 are also reported to enhance the antigen uptake and favor the augmentation of Th1 and Th2 responses which will be beneficial for elderly group as they have dysregulated T cell machinery [88]. ASO3 is an immuno-enhancing oil in water emulsion-based adjuvant, comprising of squalene, polysorbate 80 and α-tocopherol, used in the Influenza (H1N1/pdm2009) vaccine formulation [89]. It was reported to generate microneutralizing antibodies which can persist up to more than a year after immunization with a much lower dose of antigen whereas other non-adjuvanted vaccine required higher dose of antigen but showed a declination in antibody responses over this time [90]. Another liposome-based adjuvant, ASO1, comprises MPL (Lipid molecule named 3-*O*-desacyl-40-monophosphoryl lipid A obtained from *Salmonella minnesota*) and QS-21 (a lytic saponin fraction of QuilA) was used to enhance vaccine efficacy of a subunit zoster vaccine named Shingrix [78]. A significant increase in humoral as well as cellular immunity including cytotoxic T cell responses with a vaccine efficacy of more than 90% was observed compared to non-adjuvanted vaccine [91]. Influenza virosomes have also been used as an adjuvant and carrier system owing to its excellent antigen delivery mechanism to the target sites [92]. Structurally the modified virus is composed of unilamellar phospoholipid membrane incorporating surface hemagglutinin (HA) and neuraminidase (NA) antigen but lacks the viral inner core and genetic information making it replication deficient. Mimicking the natural infection, virosome adjuvanted influenza vaccine effectively induced humoral antibody and cytotoxic T cell activity in elderly people [93,94]. Microparticles of β-d-[2 ->1] poly(fructo-furanosyl)α-d-glucose (delta inulin) proved to be safe and nontoxic adjuvant for human use. It skewed immune responses to the Th1 or Th2 depending upon the type of antigen it is administered with, functioning as an amplifier. It is effectively used in Hepatitis B, influenza, and HIV [95–97]. The most extensively used adjuvant is Matrix-M, comprises cholesterol, phospholipids and saponin, augments humoral and cellular immune responses. Although, the mechanism underlying the potency of this adjuvant is not yet resolved but it creates a milieu of activated T and B lymphocytes, NK cells, neutrophils and monocytes at local lymph nodes [98,99]. Researchers had employed vector-based

Table 2. List of non-COVID-19 vaccines available for elderly population.

Vaccine name	Formulation	Immune response	Schedule	Refs
Pneumococcal polysaccharide vaccine (Pneumovac23)	T cell independent antigen response.	It generates IgM dominated antibody response but lacks immunological memory.	Suboptimal response of Pneumovac23 in the elder individual requires repeated booster.	[103]
Pneumococcal conjugate vaccine (Prevnar13)	Carrier protein conjugated with capsular polysaccharide.	T cell dependent response, opsanophagocytic antibody production.	A prime boost strategy by priming with Prevnar13 and boosting with pneumovac23 is recommended in elderly.	[104]
Shingles vaccine (Zostavax)	Comprising of at least 2000 PFU of highly potent live attenuated varicella zoster virus (oka strain)	Induces T cell and antibody response with moderate efficacy.	Cellular immunity increases with booster dose which was given more than 10 years after the first dose.	[130,131]
Shingles Subunit zoster vaccine (Shingrix)	Recombinant vaccine contains viral glycoprotein E along with ASO1 based liposomal adjuvant.	Generates T cell and humoral response and induces robust memory response.	Cellular immunity increases with booster dose which was given more than 10 years after the first dose.	[85,91]
Influenza trivalent inactivated influenza vaccine (TIV)	TIV contains antigens from two influenza A (H1N1 and H3N2) and one influenza B (Victoria/ Yamagata) strains and MF59 as adjuvant.	It efficaciously prevented hospitalizations due to flu and generates robust T cell response in elderly (≥ 65 years).	Due to antigenic drift, annual vaccination schedule was adapted.	[132,133]
Influenza (H1N1/ pdm2009)	Contains H1N1 antigen along with ASO3 as adjuvant.	Provides higher antigen-sparing capacity. It generates higher HAI titer values compared to whole-virion vaccine.	Two dose strategies were considered for older individuals.	[134]
Influenza vaccine (Inflexal-V)	Virosomal influenza vaccine containing surface antigen HA and neuraminidase (NA).	Mimics natural infection and reported to be efficacious especially in immune-compromised individuals.	Licensed for people of all age groups and adapted annually.	[135]
Hepatitis vaccine (Twinrix)	Contains combination of inactivated hepatitis A and B virus surface antigen.	It induced higher seropositive rates in people above 40 years compared to other monovalent vaccines.	Three doses over a span of 6 months.	[136]
Recombinant hepatitis B vaccine (Engerix-B)	DNA vaccine containing HBsAg surface antigen of hepatitis B.	Confers protective efficacy for up to 10 years and effectively immunogenic for diabetes mellitus patients.	Three doses over a span of 6 months.	[137]
Respiratory Syncytial Virus vaccine (RSV F)	Nanoparticles based vaccine contains recombinant F protein with aluminum phosphate and Matrix-M1 as adjuvant.	Induces strong neutralizing antibody titers in elderly between 60 and 80 years old compared to non-adjuvant vaccines.	Completed Phase-I and started Phase-II trial (NCT03026348). Single and two dose regimen were compared.	[138]
Multivalent vector-based RSV vaccine (MVA-BN-RSV)	Contains non-replicating modified vaccinia Ankara viral vector F and G antigens from both A and B subtypes and two internal proteins N and M2.	Induces Th1 type cell mediated immune responses in adults aged ≥55 years that can persist up to 6 months.	Completed Phase-II trial (NCT02873286); boosted annually.	[102]
Lipid based vaccine platform DepoVax (DPX-RSV[A]) vaccine	Contains the ectodomain of the small hydrophobic glycoprotein (SHe) of RSV subgroup A.	Highly immunogenic in healthy people between ages 50 and 64 years; IgG responses persisted over a year.	Completed Phase-I trial (NCT02472548)	[139]

vaccines with influenza nucleoprotein and matrix protein and reported to mount a robust immune response that compensates for annual influenza vaccination [100]. Non replicating viral vectors are also used to deliver potential vaccine candidate. Modified vaccinia Ankara viral vector containing five respiratory syncytical virus (RSV) proteins were being tested in a clinical trial and reported to induce Th1 type cell mediated immune responses among older adults [101,102].

A 23 valent polysaccharide based pneumococcal vaccine, containing a T cell independent antigen, elicites exclusively humoral immunity but fails to generate immunologic memory owing to its lack of direct recognition by T cells [103]. Nonetheless, chemical conjugation of polysaccharide to a carrier protein makes 13 valent conjugate pneumococcal vaccine into a T cell dependent antigen which eventually generates high affinity matured antibody and immunological memory [104]. A prime-boost regimen with Prevnar13 followed by Pneumovac23 further augmented the immune responses among elderly. This prime-boost strategy resulted in improved serotype specific IgG responses [105]. Much deeper perceptive is required to develop potential vaccine candidate for the elderly people to boost their immune system.

In addition to the appropriate selection of adjuvants and suitable modification of antigens, vaccine efficacy largely depends on several host factors. Considering the weaken immune system of the elderly people and several other co-morbid clinical conditions, effective vaccination must overcome these hurdles successfully. An aged immune system harbors multitude of changes especially a steady decline in naïve CD4+ T cell number due to inability of lymphocyte generation in the primary lymphoid organ. Parallelly, alternation of secondary lymphoid structure and function results in altered T cell trafficking and a restricted T cell repertoire [16,106]. Depletion of naïve CD4+ T cells during vaccination in elderly people significantly reduces the vaccine efficacy. The influenza specific memory T cells are directed toward conserved protein sequences across numerous influenza strains available. Therefore, these memory T cells can successfully confer cross protection against numerous strains of influenza and strategically bestows an alternative approach to treat elderly people with an added advantage. Older individuals have encountered several influenza strains throughout their life span and unknowingly carries diverse influenza specific memory CD4+ T cell populations [107].

SARS-CoV-2 mutations and vaccine effectiveness

Researchers around the world are toiling to develop targeted vaccines against COVID-19 in record time. The spike glycoprotein present on the surface of the coronavirus that helps in receptor binding and membrane fusion was proposed to be a potential vaccine candidate by various research groups [108]. The viral S protein consists of two subunits: S1 and S2. The S1 domain contains the receptor-binding domain (RBD) crucial for the initial attachment of the virus to the host cell, and S2 prompted viral fusion with the host cells to initiate the infection [109,110]. Numerous studies have identified the probable B cell epitopes from the spike protein which often acquires point mutations [111–114]. Further studies also indicate that the variable region is more prone to point mutations than the stalk region [115,116]. So, the efficacy of the spike-based vaccines can be compromised by acquired mutations over time. Numerous naturally occurring spike variants like Q414E, N439K, G446V, K458N, I472V, A475V, T478I, V483I, F490L, H519P, D614G and Q321L have been reported to decrease the sensitivity to neutralizing antibody and convalescent sera [117]. Most of these naturally occurring mutations found in RBD domain of variable region of spike protein. Our analysis of B cell epitopes and surface accessibility of spike protein, S1 region (S1: aa13 to aa685 and RBD: aa319 to aa514) and stalk domain (S2: aa686 to aa1273) shows that stalk directed B cells epitopes are less accessible (Figure 3). But accumulation of RBD mutations may influence vaccine effectiveness both in general as well as in the elderly populations. Consistent with our findings the RBD of spike is a target for 90% of the neutralizing SARS-CoV-2 immune sera indicating their immunodominance and the less accessible stalk B cell epitopes probably plays minor role in viral neutralization [113]. The E484K a receptor-binding-domain mutation, and 501V2 mutation N501Y was stated to be linked with escape mutant from neutralizing antibodies [118,119]. The current BNT162b2 vaccine elicited sera can neutralize N501Y variants [120]. However, convalescent sera from COVID-19 individual were unable to neutralize a novel bat coronavirus (W1V1–CoV) that is highly homologous to SARS-CoV-2 and uses ACE2 receptor for host cell entry indicating their pandemic potential in the future [121,122]. Immune selection of antigenic variants seldom occurs within immune-compromised or elderly populations due to their inadequate immune response or sustained pathogen presence [123]. Altogether these findings indicate that humoral response against spike-based vaccines may reduce their efficacy with the emergence of new antigenic variants inadequate immune response within the elderly population may facilitate such antigenic variant selection.

Strategies to induce SARS-CoV-2 specific immune response within elderly population

Researchers discovered constant regions of influenza virus trimeric HA especially in the stalk domain and utilized it to generate neutralizing antibodies which will impart universal protection against several influenza strains [124–126]. Analyzing and identifying the conserved region of the spike protein of SARS-CoV-2 can lead to generation of a hybrid or chimeric vaccine candidate harboring both the influenza and SARS-CoV-2 antigens part is possible. Our Vaxijen based prediction shows the presence of some B cell epitopes in the stalk region but due to their low surface accessibility stalk region, unlike influenza HA stalk may not be an appropriate vaccine candidate (Figure 3). A hybrid/chimeric protein can be generated by combining the HA and spike protein as the formation of the trimeric assembly largely depends on the residues present in the stalk region. The residues from the stalk region form numerous H-bond

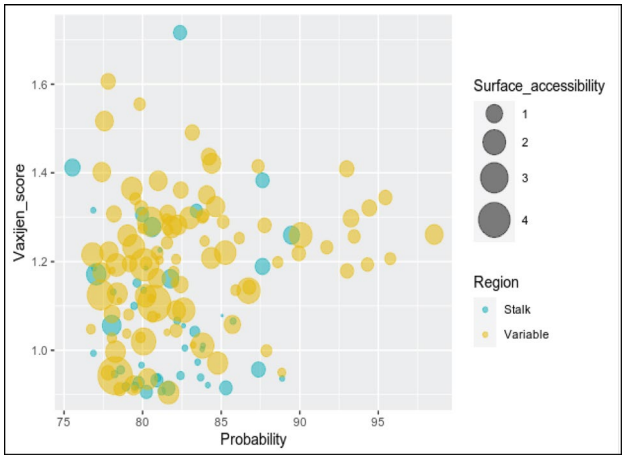

Figure 3. Bubble plot analysis of the SARS-CoV-2 spike protein. The plot shows the probable B cell epitopes from the variable (S1 domain: aa13 to aa685) and stalk region (S2 domain: aa686 to aa1273) of the Spike protein. The corresponding Vaxijen score and the percentage of candidate vaccine probability shown in *y* and *x* axis, respectively. The size of each bubble signifies the respective surface accessibility. The B cell epitopes from the stalk S2 domain have less surface accessibility making it a poor vaccine candidate compared to the highly accessible B cell epitopes in the variable S1 domain and RBD.

interaction to form the trimeric assembly of the Spike protein and the residues from the variable region also gets stabilized by interacting with the stalk region (Figure 4A) [109,127]. The baculovirus insect cell expression system can be used to produce hybrid and/or chimeric VLPs comprising the SARS-COV-2 spike protein, stalk region of HA and the influenza M1 protein (Figure 4B) [128,129]. Chimeric protein with intact stalk region for the HA protein and the Spike variable or RBD domain will allow utilization of influenza specific CD4+ T cell populations to mount an effective antibody response in germinal center reactions. Each VLP will have both Spike, HA and M1 capable of utilizing corresponding CD4+ T cells help during germinal center reaction with spike specific B cells subsequently promoting affinity maturation and class switching (Figure 4C). This influenza specific CD4+ T cells can interact with spike specific B cells when the same B cell clone portrays MHC II containing influenza specific peptides for T cell help during germinal center reaction in the secondary lymph node. This may overcome the lack of spike

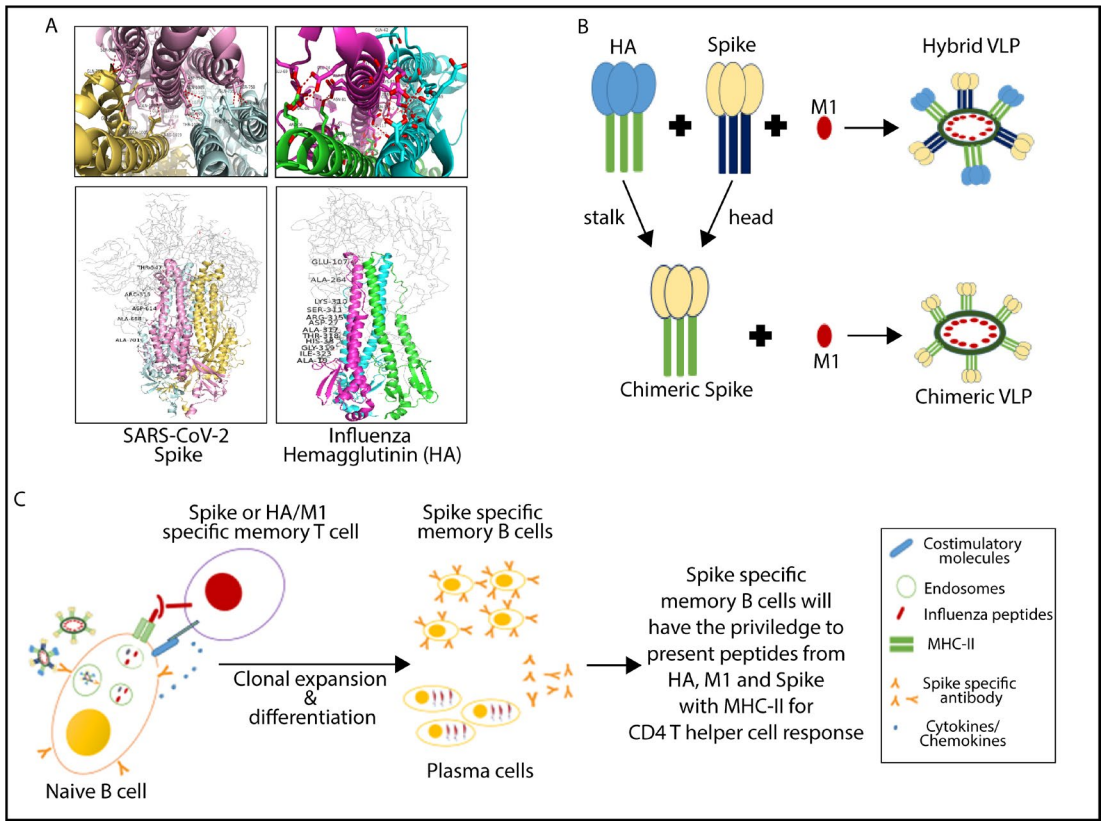

Figure 4. Structure and design of hybrid or chimeric VLP for SARS-CoV-2 vaccination. (**A**) The trimeric assembly of SARS-COV-2 Spike protein and Influenza HA. Residues from stalk region represented in a cartoon format, differnt colors signifies three different chains. The residues from the variable region those are making H-bond with the stalk are labeled (representative from a single chain) whereas all the other residues shown as a ribbon diagramme. Upper figure showing the H-bond interaction profile for a single chain stalk region (pink) within the trimeric assembly. (**B**) Influnza Hemagglutinin (HA) and SARS-CoV-2 Spike contain head and stalk domain. Matrix protein 1 (M1), either with chimeric Spike (stalk from HA with head from Spike). (**C**) Schematic diagram showing cooperation between influenza induced memory T cells and development of spike specific immune response.

antigen specific naïve or matured CD4+ T cells population which lack in aged individual due to age related defects. This strategy was explored widely against polysaccharide vaccines, where polysaccharide is attached directly to a protein molecule to mount strong T cell dependent immune responses to produce high affinity and class switched antibodies. The repetitive antigenic structure present on the surface of the VLPs makes it easier to be recognized and prompted a strong induction of humoral and cell mediated immune responses.

This novel approach of designing of chimeric or hybrid vaccine will give additional protection against influenza viruses responsible for thousands of deaths every year during seasonal flu. Recently phase 1 clinical trials were conducted with chimeric HA (consisting of constant stalk region with variable head domain of different strain of influenza viruses) inducing broadly protective HA stalk directed antibodies in vaccinated individuals [125]. Natural head domain of HA replaced with spike head can induce spike specific antibodies as well as antibodies directed against the HA stalk. This will further boost influenza specific immunity within vaccinated individual.

Conclusions

The terrific brunt of SARS-CoV-2 infection and the scarcity of available effective treatments specially to cure elderly individuals require more rational approach. Multifactorial changes in developing an appropriate cell mediated immune responses in elderly individual is of paramount need for designing an efficacious vaccine. The vaccines from Moderna, Pfizer and AstraZeneca, which are under emergency use in the USA and Europe will protect an individual from COVID-19 but the durability within normal or elderly population is unknown. The disease manifestation of COVID-19 has similarities with seasonal flu caused by influenza viruses. The ultimate goal is to design a universal vaccine for influenza, SARS-CoV-2 or other coronaviruses. In this article we highlighted the design of vaccine molecule having multiple antigens from different viruses can complement each other to mount an effective immune response especially in the elderly population with low naïve immune cell population. Stalk region of HA is relatively conserved and stalk directed antibodies can give protection to wide range of influenza strains. Therefore, chimeric vaccines for both influenza and SARS-CoV-2 will be a significant boost to deal global challenges against seasonal or pandemic flu viruses. Researchers should move forward with the idea of making a single chimeric molecule as vaccine candidates for both influenza and SARS-CoV-2. The idea of making chimeric molecules can be incorporated with mRNA, DNA, and adenovirus-based vaccine delivery system. This will have a significant impact on worldwide vaccination drive and their economic impact in the future to save human lives.

Funding sources

This research did not receive any specific grants from funding agencies in public, commercial, or not-for-profit sectors.

Disclosure statement

The authors declare no financial interest to disclose.

ORCID

George Maiti http://orcid.org/0000-0002-6701-5499

References

1. Cui J, Li F, Shi ZL. Origin and evolution of pathogenic coronaviruses. *Nat Rev Microbiol.* 2019;17:181–192. doi:10.1038/s41579-018-0118-9.
2. He G, Sun Z, Zhao Y, et al. Zhou Q: β-coronavirus infectious diseases: recommended strategies for the prevention and control of transmission. *Int J Clin Exp Pathol.* 2020;13:1060–1065.
3. Zhou P, Yang X-L, Wang X-G, et al. A pneumonia outbreak associated with a new coronavirus of probable bat origin. *Nature.* 2020;579:270–273. doi:10.1038/s41586-020-2012-7.
4. Astuti IY . Severe Acute Respiratory Syndrome Coronavirus 2 (SARS-CoV-2): an overview of viral structure and host response. *Diabetes Metab Syndr.* 2020;14:407–412. doi:10.1016/j.dsx.2020.04.020.
5. Kim D, Lee JY, Yang JS, et al. The architecture of SARS-CoV-2 transcriptome. *Cell.* 2020;181:914–921, e910. doi:10.1016/j.cell.2020.04.011.
6. Dong Y, Dai T, Wei Y, et al. A systematic review of SARS-CoV-2 vaccine candidates. *Signal Transduct Target Ther.* 2020;5:237. doi:10.1038/s41392-020-00352-y.
7. Funk CD, Laferrière C, Ardakani A. A snapshot of the global race for vaccines targeting SARS-CoV-2 and the COVID-19 pandemic. *Front Pharmacol.* 2020;11(937):1–17.
8. Callaway E. The coronavirus is mutating – does it matter?*Nature*. 2020;585:174–177. doi:10.1038/d41586-020-02544-6.
9. Vilar S, Isom DG. One year of SARS-CoV-2: how much has the virus changed?
10. Galloway SE, Paul P, MacCannell DR, et al. Emergence of SARS-CoV-2 B.1.1.7 Lineage - United States, December 29, 2020–January 12, 2021. *MMWR Morb Mortal Wkly Rep.* 2021;70:95–99. doi:10.15585/mmwr.mm7003e2.

11. O'Driscoll M, Ribeiro Dos SG, Wang L, et al. Age-specific mortality and immunity patterns of SARS-CoV-2. *Nature*. 2020 ;590(7844):140–145.
12. Chen Y, Klein SL, Garibaldi BT, et al. Aging in COVID-19: vulnerability, immunity and intervention. *Ageing Res Rev*. 2021;65:101205. doi:10.1016/j.arr.2020.101205.
13. Del Giudice G, Goronzy JJ, Grubeck-Loebenstein B, et al. Fighting against a protean enemy: immunosenescence, vaccines, and healthy aging. *NPJ Aging Mech Dis*. 2017;4:1. doi:10.1038/s41514-017-0020-0.
14. Gibson KL, Wu YC, Barnett Y, et al. B-cell diversity decreases in old age and is correlated with poor health status. *Aging Cell*. 2009;8:18–25. doi:10.1111/j.1474-9726.2008.00443.x.
15. Haq K, McElhaney JE. Immunosenescence: Influenza vaccination and the elderly. *Curr Opin Immunol*. 2014;29:38–42. doi:10.1016/j.coi.2014.03.008.
16. Weng NP. Aging of the immune system: how much can the adaptive immune system adapt?*Immunity*. 2006;24:495–499. doi:10.1016/j.immuni.2006.05.001.
17. Nikolich-Žugich J. The twilight of immunity: emerging concepts in aging of the immune system. *Nat Immunol*. 2018;19(1):10–19. doi:10.1038/s41590-018-0205-0.
18. Cambier J. Immunosenescence: a problem of lymphopoiesis, homeostasis, microenvironment, and signaling. *Immunol Rev*. 2005;205:5–6. doi:10.1111/j.0105-2896.2005.00276.x.
19. Campisi J. Cellular senescence and lung function during aging, Yin and Yang. *Ann Am Thorac Soc*. 2016;13 Suppl 5:S402–S406. doi:10.1513/AnnalsATS.201609-703AW.
20. Murray MA, Chotirmall SH. The impact of immunosenescence on pulmonary disease. *Mediators Inflamm*. 2015;2015:692546. doi:10.1155/2015/692546.
21. Rea IM, Gibson DS, McGilligan V, et al. Age and age-related diseases: role of inflammation triggers and cytokines. *Front Immunol*. 2018;9(586):1–28.
22. Wong CK, Smith CA, Sakamoto K, et al. Aging impairs alveolar macrophage phagocytosis and increases influenza-induced mortality in mice. *J Immunol*. 2017;199:1060–1068. doi:10.4049/jimmunol.1700397.
23. van Beek AA, Van den Bossche J, Mastroberardino PG, et al. Metabolic alterations in aging macrophages: ingredients for inflammaging?*Trends Immunol*. 2019;40:113–127. doi:10.1016/j.it.2018.12.007.
24. Nainu F, Shiratsuchi A, Nakanishi Y. Induction of apoptosis and subsequent phagocytosis of virus-infected cells as an antiviral mechanism. *Front Immunol*. 2017;8(1220):1–11.
25. Fujimoto I, Pan J, Takizawa T, et al. Virus clearance through apoptosis-dependent phagocytosis of influenza A virus-infected cells by macrophages. *J Virol*. 2000;74:3399–3403. doi:10.1128/jvi.74.7.3399-3403.2000.
26. Puttur F, Gregory LG, Lloyd CM. Airway macrophages as the guardians of tissue repair in the lung. *Immunol Cell Biol*. 2019;97:246–257. doi:10.1111/imcb.12235.
27. Snelgrove RJ, Goulding J, Didierlaurent AM, et al. A critical function for CD200 in lung immune homeostasis and the severity of influenza infection. *Nat Immunol*. 2008;9:1074–1083. doi:10.1038/ni.1637.
28. Yu X, Buttgereit A, Lelios I, et al. The cytokine TGF-β promotes the development and homeostasis of alveolar macrophages. *Immunity*. 2017;47:903–912.e904. doi:10.1016/j.immuni.2017.10.007.
29. Kulikauskaite J, Wack A. Teaching old dogs new tricks? The plasticity of lung alveolar macrophage subsets. *Trends Immunol*. 2020;41:864–877. doi:10.1016/j.it.2020.08.008.
30. Hussell T, Bell TJ. Alveolar macrophages: plasticity in a tissue-specific context. *Nat Rev Immunol*. 2014;14:81–93. doi:10.1038/nri3600.
31. Wenisch C, Patruta S, Daxböck F, et al. Effect of age on human neutrophil function. *J Leukoc Biol*. 2000;67(1):40–45. doi:10.1002/jlb.67.1.40.
32. Ortmann W, Kolaczkowska E. Age is the work of art? Impact of neutrophil and organism age on neutrophil extracellular trap formation. *Cell Tissue Res*. 2018;371:473–488. doi:10.1007/s00441-017-2751-4.
33. Xu F, Zhang C, Zou Z, et al. Aging-related Atg5 defect impairs neutrophil extracellular traps formation. *Immunology*. 2017;151:417–432. doi:10.1111/imm.12740.
34. Ruddle NH, Akirav EM. Secondary lymphoid organs: responding to genetic and environmental cues in ontogeny and the immune response. *J Immunol*. 2009;183:2205–2212. doi:10.4049/jimmunol.0804324.
35. Goronzy JJ, Fang F, Cavanagh MM, et al. Naive T cell maintenance and function in human aging. *J Immunol*. 2015;194:4073–4080. doi:10.4049/jimmunol.1500046.
36. Swain SL, McKinstry KK, Strutt TM. Expanding roles for $CD4^+$ T cells in immunity to viruses. *Nat Rev Immunol*. 2012;12:136–148. doi:10.1038/nri3152.
37. Palmer S, Albergante L, Blackburn CC, et al. Thymic involution and rising disease incidence with age. *Proc Natl Acad Sci USA*. 2018;115:1883–1888. doi:10.1073/pnas.1714478115.
38. Turner VM, Mabbott NA. Influence of ageing on the microarchitecture of the spleen and lymph nodes. *Biogerontology*. 2017;18:723–738. doi:10.1007/s10522-017-9707-7.
39. Dunn-Walters DK. The ageing human B cell repertoire: a failure of selection?*Clin Exp Immunol*. 2016;183:50–56. doi:10.1111/cei.12700.
40. Brodin P. Immune determinants of COVID-19 disease presentation and severity. *Nat Med*. 2021;27:28–33. doi:10.1038/s41591-020-01202-8.
41. Vellas C, Delobel P, de Souto Barreto P, et al. COVID-19, virology and geroscience: a perspective. *J Nutr Health Aging*. 2020;24:685–691. doi:10.1007/s12603-020-1416-2.
42. Liu J, Li S, Liu J, et al. Longitudinal characteristics of lymphocyte responses and cytokine profiles in the peripheral blood of SARS-CoV-2 infected patients. *EBioMedicine*. 2020;55:102763. doi:10.1016/j.ebiom.2020.102763.
43. Laing AG, Lorenc A, Del Molino Del Barrio I, et al. A dynamic COVID-19 immune signature includes associations with poor prognosis. *Nat Med*. 2020;26:1623–1635. doi:10.1038/s41591-020-1038-6.
44. Qin C, Zhou L, Hu Z, et al. Dysregulation of immune response in patients with coronavirus 2019 (COVID-19) in Wuhan, China. *Clin Infect Dis*. 2020;71:762–768. doi:10.1093/cid/ciaa248.
45. Biswas A, Bhattacharjee U, Chakrabarti AK, et al. Emergence of novel coronavirus and COVID-19: whether to stay or die out?*Crit Rev Microbiol*. 2020;46:182–193. doi:10.1080/1040841X.2020.1739001.
46. Zhang YY, Li BR, Ning BT. The comparative immunological characteristics of SARS-CoV, MERS-CoV, and

SARS-CoV-2 coronavirus infections. *Front Immunol.* 2020;11:2033. doi:10.3389/fimmu.2020.02033.
47. Li S, Jiang L, Li X, et al. Clinical and pathological investigation of patients with severe COVID-19. *JCI Insight.* 2020;5(12):5. doi:10.1172/jci.insight.138070.
48. Peng Y, Mentzer AJ, Liu G, et al. Broad and strong memory CD4(+) and CD8(+) T cells induced by SARS-CoV-2 in UK convalescent individuals following COVID-19. *Nat Immunol.* 2020;21:1336–1345. doi:10.1038/s41590-020-0782-6.
49. Johnstone J, Parsons R, Botelho F, et al. Immune biomarkers predictive of respiratory viral infection in elderly nursing home residents. *PLoS One.* 2014;9:e108481. doi:10.1371/journal.pone.0108481.
50. Conti P, Ronconi G, Caraffa A, et al. Induction of pro-inflammatory cytokines (IL-1 and IL-6) and lung inflammation by Coronavirus-19 (COVI-19 or SARS-CoV-2): anti-inflammatory strategies. *J Biol Regul Homeost Agents.* 2020;34:327–331. doi:10.23812/CONTI-E.
51. Huang C, Wang Y, Li X, et al. Clinical features of patients infected with 2019 novel coronavirus in Wuhan, China. *Lancet.* 2020;395:497–506. doi:10.1016/S0140-6736(20)30183-5.
52. Ciulla MM. SARS-CoV-2 downregulation of ACE2 and pleiotropic effects of ACEIs/ARBs. *Hypertens Res.* 2020;43:985–986. doi:10.1038/s41440-020-0488-z.
53. Cheng H, Wang Y, Wang GQ. Organ-protective effect of angiotensin-converting enzyme 2 and its effect on the prognosis of COVID-19. *J Med Virol.* 2020;92:726–730. doi:10.1002/jmv.25785.
54. Premkumar L, Segovia-Chumbez B, Jadi R, et al. The receptor binding domain of the viral spike protein is an immunodominant and highly specific target of antibodies in SARS-CoV-2 patients. *Sci Immunol.* 2020:5(48):eabc8413.
55. Diao B, Wang C, Tan Y, et al. Reduction and functional exhaustion of T cells in patients with Coronavirus Disease 2019 (COVID-19). *Front Immunol.* 2020;11:827. doi:10.3389/fimmu.2020.00827.
56. Wang Z, Wan Y, Qiu C, et al. Recovery from severe H7N9 disease is associated with diverse response mechanisms dominated by $CD8^+$ T cells. *Nat Commun.* 2015;6:6833. doi:10.1038/ncomms7833.
57. Grifoni A, Weiskopf D, Ramirez SI, et al. Targets of T cell responses to SARS-CoV-2 coronavirus in humans with COVID-19 disease and unexposed individuals. *Cell.* 2020;181:1489–1501. e1415. doi:10.1016/j.cell.2020.05.015.
58. Patel A, Walters J, Reuschel EL, et al. Intradermal-delivered DNA vaccine provides anamnestic protection in a rhesus macaque SARS-CoV-2 challenge model. *bioRxiv.* 2020. bioRxiv. doi:10.1101/2020.07.28.225649.
59. Tebas P, Yang S, Boyer JD, et al. Safety and immunogenicity of INO-4800 DNA vaccine against SARS-CoV-2: A preliminary report of an open-label, Phase 1 clinical trial. *EClin Med.* 2021;31:100689. doi:10.1016/j.eclinm.2020.100689.
60. Wu A, Peng Y, Huang B, et al. Genome composition and divergence of the novel coronavirus (2019-nCoV) originating in China. *Cell Host Microbe.* 2020;27:325–328. doi:10.1016/j.chom.2020.02.001.
61. Zhang C, Maruggi G, Shan H, et al. Advances in mRNA vaccines for infectious diseases. *Front Immunol.* 2019;10(594);1–13.
62. Kowalski PS, Rudra A, Miao L, et al. Delivering the messenger: advances in technologies for therapeutic mRNA delivery. *Mol Ther.* 2019;27:710–728. doi:10.1016/j.ymthe.2019.02.012.
63. Reichmuth AM, Oberli MA, Jaklenec A, et al. mRNA vaccine delivery using lipid nanoparticles. *Ther Deliv.* 2016;7:319–334. doi:10.4155/tde-2016-0006.
64. Bloom K, van den Berg F, Arbuthnot P. Self-amplifying RNA vaccines for infectious diseases. *Gene Ther.* 2020;28(3-4):117–129.
65. Anderson EJ, Rouphael NG, Widge AT, et al. Safety and immunogenicity of SARS-CoV-2 mRNA-1273 vaccine in older adults. *N Engl J Med.* 2020;383:2427–2438. doi:10.1056/NEJMoa2028436.
66. Corbett KS, Edwards DK, Leist SR, et al. SARS-CoV-2 mRNA vaccine design enabled by prototype pathogen preparedness. *Nature.* 2020;586:567–571. doi:10.1038/s41586-020-2622-0.
67. Corbett KS, Flynn B, Foulds KE, et al. Evaluation of the mRNA-1273 vaccine against SARS-CoV-2 in nonhuman primates. *N Engl J Med.* 2020;383(16):1544–1555. doi:10.1056/NEJMoa2024671.
68. Baden LR, El Sahly HM, Essink B, et al. Efficacy and safety of the mRNA-1273 SARS-CoV-2 vaccine. *N Engl J Med.* 2021;384(5):403–416. doi:10.1056/NEJMoa2035389.
69. Walsh EE, Frenck RW Jr., Falsey AR, et al. Safety and immunogenicity of two RNA-based covid-19 vaccine candidates. *N Engl J Med.* 2020;383:2439–2450. doi:10.1056/NEJMoa2027906.
70. Polack FP, Thomas SJ, Kitchin N, et al. Safety and efficacy of the BNT162b2 mRNA Covid-19 vaccine. *N Engl J Med.* 2020;383:2603–2615. doi:10.1056/NEJMoa2034577.
71. Torjesen I. Covid-19: Norway investigates 23 deaths in frail elderly patients after vaccination. *BMJ.* 2021;372:n149. doi:10.1136/bmj.n149.
72. Keech C, Albert G, Cho I, et al. Phase 1-2 trial of a SARS-CoV-2 recombinant spike protein nanoparticle vaccine. *N Engl J Med.* 2020;383:2320–2332. doi:10.1056/NEJMoa2026920.
73. Todorov G, Uversky VN. A possible path towards rapid development of live-attenuated SARS-CoV-2 vaccines: plunging into the natural pool. *Biomolecules.* 2020;10(10):1438. doi:10.3390/biom10101438.
74. https://www.pharmaceutical-technology.com/news/codagenix-sii-dosing-vaccine/.
75. Folegatti PM, Ewer KJ, Aley PK, et al. Safety and immunogenicity of the ChAdOx1 nCoV-19 vaccine against SARS-CoV-2: a preliminary report of a phase 1/2, single-blind, randomised controlled trial. *Lancet.* 2020;396(10249):467–478. doi:10.1016/S0140-6736(20)31604-4.
76. Voysey M, Clemens SAC, Madhi SA, et al. Safety and efficacy of the ChAdOx1 nCoV-19 vaccine (AZD1222) against SARS-CoV-2: an interim analysis of four randomised controlled trials in Brazil, South Africa, and the UK. *Lancet.* 2021;397:99–111. doi:10.1016/S0140-6736(20)32661-1.
77. Barrett JR, Belij-Rammerstorfer S, Dold C, et al. Phase 1/2 trial of SARS-CoV-2 vaccine ChAdOx1 nCoV-19 with a booster dose induces multifunctional antibody

responses. *Nat Med*. 2021;27(2):279–288. doi:10.1038/s41591-020-01179-4.
78. Graham F. Daily briefing: Oxford–AstraZeneca COVID vaccine is back on track. *Nature*. 2021.
79. Sattler A, Angermair S, Stockmann H, et al. SARS-CoV-2-specific T cell responses and correlations with COVID-19 patient predisposition. *J Clin Invest*. 2020;130:6477–6489. doi:10.1172/JCI140965.
80. de Candia P, Prattichizzo F, Garavelli S, et al. T cells: warriors of SARS-CoV-2 infection. *Trends Immunol*. 2021;42:18–30. doi:10.1016/j.it.2020.11.002.
81. Sekine T, Perez-Potti A, Rivera-Ballesteros O, et al. Robust T cell immunity in convalescent individuals with asymptomatic or mild COVID-19. *Cell*. 2020;183(1):158–168. doi:10.1016/j.cell.2020.08.017.
82. Saule P, Trauet J, Dutriez V, et al. Accumulation of memory T cells from childhood to old age: central and effector memory cells in CD4(+) versus effector memory and terminally differentiated memory cells in CD8(+) compartment. *Mech Ageing Dev*. 2006;127:274–281. doi:10.1016/j.mad.2005.11.001.
83. El Shikh ME, El Sayed RM, Sukumar S, et al. Activation of B cells by antigens on follicular dendritic cells. *Trends Immunol*. 2010;31:205–211. doi:10.1016/j.it.2010.03.002.
84. Lelic A, Verschoor CP, Ventresca M, et al. The polyfunctionality of human memory CD8+ T cells elicited by acute and chronic virus infections is not influenced by age. *PLoS Pathog*. 2012;8(12):e1003076. doi:10.1371/journal.ppat.1003076.
85. Izurieta HS, Wernecke M, Kelman J, et al. Effectiveness and duration of protection provided by the live-attenuated Herpes Zoster Vaccine in the Medicare population ages 65 years and older. *Clin Infect Dis*. 2017;64:785–793. doi:10.1093/cid/ciw854.
86. Calabro S, Tritto E, Pezzotti A, et al. The adjuvant effect of MF59 is due to the oil-in-water emulsion formulation, none of the individual components induce a comparable adjuvant effect. *Vaccine*. 2013;31:3363–3369. doi:10.1016/j.vaccine.2013.05.007.
87. Del Giudice G, Rappuoli R. Inactivated and adjuvanted influenza vaccines. *Curr Top Microbiol Immunol*. 2015;386:151–180. doi:10.1007/82_2014_406.
88. Magnusson SE, Reimer JM, Karlsson KH, et al. Immune enhancing properties of the novel Matrix-M™ adjuvant leads to potentiated immune responses to an influenza vaccine in mice. *Vaccine*. 2013;31:1725–1733. doi:10.1016/j.vaccine.2013.01.039.
89. De Serres G, Gariépy MC, et al. Short and long-term safety of the 2009 AS03-adjuvanted pandemic vaccine. *PLoS One*. 2012;7(7):e38563. doi:10.1371/journal.pone.0038563.
90. Chen WH, Jackson LA, Edwards KM, et al. Persistence of antibody to Influenza A/H5N1 vaccine virus: impact of AS03 adjuvant. *Clin Vaccine Immunol*. 2016;23:73–77. doi:10.1128/CVI.00475-15.
91. Lal H, Cunningham AL, Godeaux O, et al. Efficacy of an adjuvanted herpes zoster subunit vaccine in older adults. *N Engl J Med*. 2015;372(22):2087–2096. doi:10.1056/NEJMoa1501184.
92. Moser C, Amacker M, Zurbriggen R. Influenza virosomes as a vaccine adjuvant and carrier system. *Expert Rev Vaccines*. 2011;10:437–446. doi:10.1586/erv.11.15.
93. Conne P, Gauthey L, Vernet P, et al. Immunogenicity of trivalent subunit versus virosome-formulated influenza vaccines in geriatric patients. *Vaccine*. 1997;15(15):1675–1679. doi:10.1016/S0264-410X(97)00087-X.
94. Glück R, Mischler R, Finkel B, et al. Immunogenicity of new virosome influenza vaccine in elderly people. *Lancet*. 1994;344:160–163. doi:10.1016/S0140-6736(94)92758-8.
95. Saade F, Honda-Okubo Y, Trec S, et al. A novel hepatitis B vaccine containing Advax™, a polysaccharide adjuvant derived from delta inulin, induces robust humoral and cellular immunity with minimal reactogenicity in preclinical testing. *Vaccine*. 2013;31:1999–2007. doi:10.1016/j.vaccine.2012.12.077.
96. Honda-Okubo Y, Saade F, Petrovsky N. Advax™, a polysaccharide adjuvant derived from delta inulin, provides improved influenza vaccine protection through broad-based enhancement of adaptive immune responses. *Vaccine*. 2012;30:5373–5381. doi:10.1016/j.vaccine.2012.06.021.
97. Dolter KE, Evans CF, Ellefsen B, et al. Immunogenicity, safety, biodistribution and persistence of ADVAX, a prophylactic DNA vaccine for HIV-1, delivered by *in vivo* electroporation. *Vaccine*. 2011;29:795–803. doi:10.1016/j.vaccine.2010.11.011.
98. Reimer JM, Karlsson KH, Lövgren-Bengtsson K, et al. Matrix-M™ adjuvant induces local recruitment, activation and maturation of central immune cells in absence of antigen. *PLoS One*. 2012;7:e41451. doi:10.1371/journal.pone.0041451.
99. Bengtsson KL, Karlsson KH, Magnusson SE, et al. Matrix-M adjuvant: enhancing immune responses by 'setting the stage' for the antigen. *Expert Rev Vaccines*. 2013;12:821–823. doi:10.1586/14760584.2013.814822.
100. Antrobus RD, Lillie PJ, Berthoud TK, et al. A T cell-inducing influenza vaccine for the elderly: safety and immunogenicity of MVA-NP + M1 in adults aged over 50 years. *PLoS One*. 2012;7:e48322. doi:10.1371/journal.pone.0048322.
101. Altenburg AF, Kreijtz JH, de Vries RD, et al. Modified vaccinia virus Ankara (MVA) as production platform for vaccines against influenza and other viral respiratory diseases. *Viruses*. 2014;6:2735–2761. doi:10.3390/v6072735.
102. Jordan E, Lawrence SJ, Meyer TPH, et al. Broad antibody and cellular immune response from a phase 2 clinical trial with a novel multivalent poxvirus-based respiratory syncytial virus vaccine. *J Infect Dis*. 2021;223:1062–1072. doi:10.1093/infdis/jiaa460.
103. Suzuki M, Dhoubhadel BG, Ishifuji T, et al. Serotype-specific effectiveness of 23-valent pneumococcal polysaccharide vaccine against pneumococcal pneumonia in adults aged 65 years or older: a multicentre, prospective, test-negative design study. *Lancet Infect Dis*. 2017;17:313–321. doi:10.1016/S1473-3099(17)30049-X.
104. van Deursen AMM, van Houten MA, Webber C, et al. Immunogenicity of the 13-valent pneumococcal conjugate vaccine in older adults with and without comorbidities in the community-acquired pneumonia immunization trial in adults (CAPiTA). *Clin Infect Dis*. 2017;65:787–795. doi:10.1093/cid/cix419.
105. Nived P, Jönsson G, Settergren B, et al. Prime-boost vaccination strategy enhances immunogenicity com-

pared to single pneumococcal conjugate vaccination in patients receiving conventional DMARDs, to some extent in abatacept but not in rituximab-treated patients. *Arthritis Res Ther*. 2020;22(1):36. doi:10.1186/s13075-020-02256-2.
106. Weyand CM, Goronzy JJ. Aging of the immune system. Mechanisms and therapeutic targets. *Ann Am Thorac Soc*. 2016;13 Suppl 5:S422–S428. doi:10.1513/AnnalsATS.201602-095AW.
107. Crooke SN, Ovsyannikova IG, Poland GA, et al. Immunosenescence and human vaccine immune responses. *Immun Ageing*. 2019;16:25. doi:10.1186/s12979-019-0164-9.
108. Dai L, Gao GF. Viral targets for vaccines against COVID-19. *Nat Rev Immunol*. 2021;21:73–82. doi:10.1038/s41577-020-00480-0.
109. Cai Y, Zhang J, Xiao T, et al. Distinct conformational states of SARS-CoV-2 spike protein. *Science*. 2020;369:1586–1592. doi:10.1126/science.abd4251.
110. Huang Y, Yang C, Xu XF, et al. Structural and functional properties of SARS-CoV-2 spike protein: potential antivirus drug development for COVID-19. *Acta Pharmacol Sin*. 2020;41:1141–1149. doi:10.1038/s41401-020-0485-4.
111. Wang D, Mai J, Zhou W, et al. Immunoinformatic analysis of T- and B-cell epitopes for SARS-CoV-2 vaccine design. *Vaccines (Basel)*. 2020;8(3):355. doi:10.3390/vaccines8030355.
112. Shi R, Shan C, Duan X, et al. A human neutralizing antibody targets the receptor-binding site of SARS-CoV-2. *Nature*. 2020;584:120–124. doi:10.1038/s41586-020-2381-y.
113. Piccoli L, Park YJ, Tortorici MA, et al. Mapping neutralizing and immunodominant sites on the SARS-CoV-2 spike receptor-binding domain by structure-guided high-resolution serology. *Cell*. 2020;183(4):1024–1042. doi:10.1016/j.cell.2020.09.037.
114. Dearlove B, Lewitus E, Bai H, et al. A SARS-CoV-2 vaccine candidate would likely match all currently circulating variants. *Proc Natl Acad Sci USA*. 2020;117:23652–23662. doi:10.1073/pnas.2008281117.
115. Laha S, Chakraborty J, Das S, et al. Characterizations of SARS-CoV-2 mutational profile, spike protein stability and viral transmission. *Infect Genet Evol*. 2020;85:104445.
116. Pokhrel S, Kraemer BR, Mochly-Rosen D. Natural variants in SARS-CoV-2 S protein pinpoint structural and functional hotspots; implications for prophylaxis strategies. 2021.
117. Li Q, Wu J, Nie J, et al. The impact of mutations in SARS-CoV-2 spike on viral infectivity and antigenicity. *Cell*. 2020;182:1284–1294,e1289. doi:10.1016/j.cell.2020.07.012.
118. Weisblum Y, Schmidt F, Zhang F, et al. Escape from neutralizing antibodies by SARS-CoV-2 spike protein variants. *Elife*. 2020;9:9. doi:10.7554/eLife.61312.
119. Fratev F. The N501Y and K417N mutations in the spike protein of SARS-CoV-2 alter the interactions with both hACE2 and human derived antibody: a free energy of perturbation study. 2020. bioRxiv. doi:10.1101/2020.12.23.424283.
120. Xie X, Zou J, Fontes-Garfias CR, et al. Neutralization of SARS-CoV-2 spike69/70 deletion, E484K and N501Y variants by BNT162b2 vaccine-elicited sera. *Nature Medicine* 2021;27:620–621.
121. Krammer F, Pica N, Hai R, et al. Chimeric hemagglutinin influenza virus vaccine constructs elicit broadly protective stalk-specific antibodies. *J Virol*. 2013;87:6542–6550. doi:10.1128/JVI.00641-13.
122. Garcia-Beltran WF, Lam EC, Astudillo MG, et al. COVID-19-neutralizing antibodies predict disease severity and survival. *Cell*. 2021;184:476–488,e411. doi:10.1016/j.cell.2020.12.015.
123. Georgieva M, Buckee CO, Lipsitch M. Models of immune selection for multi-locus antigenic diversity of pathogens. *Nat Rev Immunol*. 2019;19:55–62. doi:10.1038/s41577-018-0092-5.
124. Krammer F, Pica N, Hai R, Tan GS, et al. Hemagglutinin stalk-reactive antibodies are boosted following sequential infection with seasonal and pandemic H1N1 Influenza Virus in mice. *J Virol*. 2012;86:10302–10307. doi:10.1128/JVI.01336-12.
125. Nachbagauer R, Feser J, Naficy A, et al. A chimeric hemagglutinin-based universal influenza virus vaccine approach induces broad and long-lasting immunity in a randomized, placebo-controlled phase I trial. *Nat Med*. 2021;27:106–114. doi:10.1038/s41591-020-1118-7.
126. Biswas A, Chakrabarti AK, Dutta S. Current challenges: from the path of "original antigenic sin" towards the development of universal flu vaccines. *Int Rev Immunol*. 2020;39:21–36. doi:10.1080/08830185.2019.1685990.
127. Xiong X, Qu K, Ciazynska KA, et al. A thermostable, closed SARS-CoV-2 spike protein trimer. *Nat Struct Mol Biol*. 2020;27:934–941. doi:10.1038/s41594-020-0478-5.
128. Mortola E, Roy P. Efficient assembly and release of SARS coronavirus-like particles by a heterologous expression system. *FEBS Lett*. 2004;576:174–178. doi:10.1016/j.febslet.2004.09.009.
129. Liu YV, Massare MJ, Barnard DL, et al. Chimeric severe acute respiratory syndrome coronavirus (SARS-CoV) S glycoprotein and influenza matrix 1 efficiently form virus-like particles (VLPs) that protect mice against challenge with SARS-CoV. *Vaccine*. 2011;29(38):6606–6613. doi:10.1016/j.vaccine.2011.06.111.
130. Levin MJ, Oxman MN, Zhang JH, et al. Varicella-zoster virus-specific immune responses in elderly recipients of a herpes zoster vaccine. *J Infect Dis*. 2008;197:825–835. doi:10.1086/528696.
131. Levin MJ, Schmader KE, Pang L, et al. Cellular and humoral responses to a second dose of herpes zoster vaccine administered 10 years after the first dose among older adults. *J Infect Dis*. 2016;213:14–22. doi:10.1093/infdis/jiv480.
132. Jefferson T, Rivetti D, Rivetti A, et al. Efficacy and effectiveness of influenza vaccines in elderly people: a systematic review. *Lancet*. 2005;366:1165–1174. doi:10.1016/S0140-6736(05)67339-4.
133. Ciabattini A, Nardini C, Santoro F, et al. Vaccination in the elderly: the challenge of immune changes with aging. *Semin Immunol*. 2018;40:83–94. doi:10.1016/j.smim.2018.10.010. Q11

134. Nicholson KG, Abrams KR, Batham S, et al. Immunogenicity and safety of a two-dose schedule of whole-virion and AS03A-adjuvanted 2009 influenza A (H1N1) vaccines: a randomised, multicentre, age-stratified, head-to-head trial. *Lancet Infect Dis*. 2011;11:91–101. doi:10.1016/S1473-3099(10)70296-6.
135. Herzog C, Hartmann K, Künzi V, et al. Eleven years of Inflexal V-a virosomal adjuvanted influenza vaccine. *Vaccine*. 2009;27:4381–4387. doi:10.1016/j.vaccine.2009.05.029.
136. Joines RW, Blatter M, Abraham B, et al. A prospective, randomized, comparative US trial of a combination hepatitis A and B vaccine (Twinrix) with corresponding monovalent vaccines (Havrix and Engerix-B) in adults. *Vaccine*. 2001;19(32):4710–4719. doi:10.1016/S0264-410X(01)00240-7.
137. Keating GM, Noble S. Recombinant hepatitis B vaccine (Engerix-B): a review of its immunogenicity and protective efficacy against hepatitis B. *Drugs*. 2003;63:1021–1051. doi:10.2165/00003495-200363100-00006.
138. https://clinicaltrials.gov/ct2/show/NCT03026348.
139. Langley JM, MacDonald LD, Weir GM, et al. A respiratory syncytial virus vaccine based on the small hydrophobic protein ectodomain presented with a novel lipid-based formulation is highly immunogenic and safe in adults: a first-in-humans study. *J Infect Dis*. 2018;218:378–387. doi:10.1093/infdis/jiy177.